NUREG/CP-0052

Proceedings of the U.S. Nuclear Regulatory Commission

NRC Nuclear Waste Geochemistry '83

Held at the
United States Geological Survey National Center
Reston, Virginia
August 30-31, 1983

Edited by D. H. Alexander and G. F. Birchard

Office of
Nuclear Regulatory Research

U.S. Nuclear Regulatory
Commission

GPO Printed copy price: $10.00

NUREG/CP-0052
RW

Proceedings of the U.S. Nuclear Regulatory Commission

NRC Nuclear Waste Geochemistry '83

Held at
United States Geological Survey National Center
Reston, Virginia
August 30-31, 1983

Manuscript Completed: April 1984
Date Published: May 1984

Edited by D. H. Alexander, G. F. Birchard

Division of Health, Siting and Waste Management
Office of Nuclear Regulatory Research
U.S. Nuclear Regulatory Commission
Washington, D.C. 20555

FOREWORD

This document summarizes papers and panel discussions presented at the Office of Nuclear Regulatory Research sponsored conference on "Nuclear Waste Management Research on Geochemistry of HLW Disposal". The conference was held at the United States Geological Survey Federal Center in Reston, Virginia on August 30-31, 1983.

The purpose of the meeting was to present results from NRC sponsored research and to identify regulatory research issues which need to be addressed prior to licensing a high level waste repository. Important summaries of technical issues and recommendations are included with each paper. The issues reflect areas of technical uncertainty addressed by the NRC Research program in geochemistry and are not intended to represent a comprehensive list of the important geochemistry issues which the Department of Energy and the Nuclear Regulatory Commission will need to consider during the licensing process.

The objectives of the NRC Research Program in geochemistry are to provide a technical basis for waste management rulemaking, to provide the NRC waste management licensing office with information that can be used to support sound licensing decisions, and to identify investigations that need to be conducted by DOE to support a license application. In order to achieve these objectives the Office of Nuclear Regulatory Research needs to communicate licensing concerns raised by our contractors to the scientific community through meetings and publications. The technical peer reviews and exchanges are essential in confirming our concerns and in providing feed-back for the future emphasis and direction of our program. Therefore, we encourage you to consider the findings and issues raised in this document and provide the Commission with comments.

TABLE OF CONTENTS

ACKNOWLEDGEMENTS

The editors would like to extend their gratitude to the many individuals who have made contributions to the publication of this document. Jack Robertson and Jane Kenney of the Office of Hazardous Waste Hydrology, U.S. Geologic Survey (USGS), deserve special thanks for making arrangements for the USGS conference facilities at Reston, Virginia. We thank Marlene Barbour, Office of Nuclear Regulatory Research (RES), U.S. Nuclear Regulatory Commission (NRC), who coordinated announcements and registered over 100 participants. Patricia Comella, RES, NRC, and Hubert Miller, Office of Nuclear Material Safety and Safeguards, provided necessary overviews of the regulatory perspective and explained NRC's mission at the conference.

We are especially grateful for the encouragement and guidance of Frank Arsenault and Jared Davis, RES, NRC, from conception to publication. Finally, we are most appreciative of the patience, helpful comments, and contributions of the authors who made this document possible.

1.0 INTRODUCTION: NRC NUCLEAR WASTE GEOCHEMISTRY '83

Donald H Alexander* and G. F. Birchard

Office of Nuclear Regulatory Research
United States Nuclear Regulatory Commission
Washington, D.C. 20555

*Now with the Office of Civilian Radioactive Waste Management
United States Department of Energy
Germantown, MD

1.1 INTRODUCTION

The objectives of this document are to: (1) present findings of the U.S. Nuclear Regulatory Commission's (NRC) sponsored research in high-level waste (HLW) geochemistry for 1983; (2) identify regulatory research issues which need to be addressed prior to licensing an HLW repository; (3) present recommendations for licensing; and (4) summarize geochemistry research efforts planned for 1984. The research issues have been contributed by the authors and reflect areas of technical uncertainty addressed by the NRC Research Program in geochemistry and are not intended to represent a comprehensive list of the important geochemistry issues which the Department of Energy (DOE) and NRC will need to consider during the licensing process. The findings of the NRC Research Program in geochemistry will be used to provide a technical basis for waste management rulemaking, to provide the NRC Waste Management Licensing Office with information that can be used to support sound licensing decisions and to identify investigations that need to be conducted by DOE to support a license application.

The Commission recently established regulatory framework for licensing disposal of high-level radioactive wastes in geologic repositories by DOE [46 FR 13971 and 48 FR 28194] which will be used to implement applicable Environmental Protection Agency (EPA) standards [40 CFR 191]. The regulations require numerical prediction of the overall repository system and several of its components in order to assess compliance with these standards. Mathematical models based on a risk assessment approach are being developed which will be used to assess uncertainties and demonstrate compliance with the regulatory criteria. A large contribution to overall uncertainty in performance prediction arises from uncertainties in assessing the long-term changes to baseline hydrological and geochemical conditions. A fundamental reason for the uncertainties is that the earth sciences are descriptive sciences which have not traditionally been applied to making long-term predictions.

Therefore, the NRC has established a research program with the objective of developing the capability to accurately assess compliance of DOE license submittals with regulatory criteria. Moreover, NRC has contracted for technical assistance to determine the reproducibility of site-specific data and the sensitivity of calculated discharges to measurement error. Because

existing models are highly uncertain in predicting performance as a result of difficulty in modeling hydrology and geochemistry, the NRC has committed a substantial portion of its waste management research effort in order to understand the processes that cause uncertainties. The NRC needs this research effort to assess DOE's claims of compliance with regulatory criteria.

The projects provide a basis for NRC review of site characterization reports, data produced by DOE laboratories, and in situ site characterization plans and environmental assessments and have been used extensively in the NRC Site Characterization Analysis (SCA) of the Basalt Waste Isolation Project (BWIP) Site Characterization Report (NUREG-0960).

1.2 ROLE OF GEOCHEMISTRY IN LICENSING RADIOACTIVE WASTE REPOSITORIES

1.2.1 Background and Objectives

Geochemistry is perhaps the single most important area of research for assessing whether proposed high level waste repository sites, low level waste repository sites, in situ uranium mines, and uranium mill tailings disposal sites will meet criteria for radionuclide releases. Geochemical considerations are important in assessment of: (1) site characterization; (2) engineered systems including waste form, waste container, and backfill; and (3) long term performance of the system to meet applicable safety criteria. Geochemical considerations are also important in repository development activities such as site selection, pre-closure and post-closure monitoring, and engineered systems design which are not the subjects of NRC research.

One of the major objectives of the NRC geochemistry research program is to provide a basis for assessing geochemical information collected by the applicant during site characterization. A number of current projects are studying the mobilities of radionuclides in natural systems. Research on the speciation and migration of radionuclides from weapons testing fall-out (Simpson et al., 4.2), power plant effluent (Robertson et al., 4.1), mill tailings ponds (Peterson et al., 5.6), and uranium ore body sources (Airey et al., 4.3) are providing the NRC with information on time dependent processes, natural conditions, and characteristics best suited for retention of radionuclides. Several programs are assessing techniques that may provide direct information on site suitability. For example, ground water age dating techniques (Davis et al., 4.4) are being researched to provide information on groundwater and isotope circulation. Isotope disequilibria techniques (Airey et al., 4.3) are being assessed as a means of directly evaluating the mobility of naturally occurring isotopes in proposed sites.

A second major objective of the NRC geochemistry research program is to provide a basis for assessing the source term and near-field migration of radionuclides released from engineered systems and to provide information on the geochemical environment which will affect the performance of those systems. The long term performance of waste forms is being assessed through laboratory studies of radionuclide doped glasses and naturally occurring basaltic glasses (Seitz et al., 5.5). Radionuclide releases from natural ore bodies (Airey et al., 4.3) may provide information on the performance of spent fuel waste forms. Research sponsored by the Australian Atomic Energy Commission (not supported by NRC) indicates that crystalline waste forms may be far superior

to either glass or spent fuel waste forms but at the moment NRC is not sponsoring research on alternatives to waste forms proposed by the DOE program. Studies on the performance of container materials are being covered by the NRC waste package research program. However, the geochemistry program is assessing the effects of radionuclide interactions with metallic containers (Perry et al., 2.2) and interactions between metallic components and backfill systems (Soudek et al., 3.1). The NRC is also conducting research on backfill which is considered to be an important major barrier because it can be engineered to control release rates (Soudek et al., 3.1) and it is relatively easy to test and to assess. Materials proposed for backfill such as smectite occur in natural hydrothermal systems which approximate very near-field repository conditions (Apps, 2.1). Significant attributes of backfill materials (Soudek et al , 3.1) and potential failure mechanisms (Couture and Seitz, 3.2; Peacor et al., 3.3) are being evaluated.

The third major objective of the geochemistry research program is to provide a basis for performance assessment. Codes are being applied to simulate laboratory systems (Carnahan et al., 5.1 in collaboration with Seitz et al., 5.5) and field systems (Peterson et al., 5.6). We are encouraging collaboration between lab and field research and modelers. Initial results (e.g., Carnahan et al., 5.1, Peterson et al., 5.6) indicate that both laboratory and field data collection and modeling techniques benefit. The NRC is also conducting research on mechanisms and processes such as speciation (Perry, 2.2) and precipitation/ dissolution (Silva, 2.3) to which performance assessment model results are most sensitive (Carnahan et al., 5.1).

Groundwater travel time and engineered systems are considered to be barriers to waste migration in HLW regulations. Serious limitations to the performance of these barriers which have often been overlooked are discussed in the following sections. These limitations are discussed to show that knowledge of the geochemistry of a site is necessary to surmount these limitations.

1.2.2 Limitations in the Role of Hydrology in Licensing Radioactive Waste Depositories

One of the major assumptions often made in waste management is that the pre-closure travel time along the fastest path between the disposal site and the accessible environment sets an upper limit on radionuclide transport rate. This assumption is often invalid at low level waste burial sites, and uranium mill tailings disposal sites because disturbance of the natural ground surface increases infiltration which can cause groundwater mounding at the site. However, the assumption is far worse for high level waste disposal because (1) the fastest pre-closure path cannot be identified with confidence; (2) the thermal perturbation due to the radioactive decay of wastes after closure may significantly accelerate flow due to thermal buoyancy; and (3) thermal-mechanical disturbances may generate new flow paths which short circuit pre-emplacement paths and provide a faster route to the accessible environment.

The NRC Draft Site Characterization Analysis (DSCA, 1983) of the Basalt Waste Isolation Project (BWIP) Site Characterization Report (SCR, 1983) provides an important regulatory assessment which illustrates the problem of trying to identify the fastest pre-closure groundwater path at an actual proposed HLW site. The applicant (Rockwell Hanford Operations, Department of Energy)

provides groundwater travel times of greater than 10,000 years (SCR, 1983). Confirmatory calculations of the DOE travel time estimates were made by Golder Associates (Appendix D, DSCA, 1983) on behalf of the NRC using the same data used by DOE. The results of the Golder Associates calculations range from 20 years to 43,547 years. The Golder Associates calculations are not surprising given that there are literally millions of possible pathways between the proposed repository horizon and the accessible environment. However, such disparity in results might not be resolved during licensing and could disrupt the licensing process.

Pre-emplacement travel times are only relevant for waste management applications in which little change in post-emplacement travel times can be assumed. Travel times are only important once radionuclides are no longer contained. High level waste containers are required to contain wastes for 300 to 1000 years after closure (Performance Objective 60.113(a)(ii)(B)) and releases are to be considered for 10,000 years after closure (EPA, 40 CFR 191). Numerous studies estimate that the repository near-field will experience a thermal maximum at 300 to 1000 years after emplacement, a time coincident with waste package failure (Wang et al., 1981; Runchal and Maini, 1980). An assessment by Runchal and Maini (1981) of thermal effects on flow velocities for saturated conditions in fractured granites indicate significant acceleration in flow due to thermal buoyancy. They assume a pre-emplacement travel time between the repository horizon and the surface of 2,400 years and a loading of 25 W/m^2. Their calculations suggest that the travel time can be reduced to 40 years at 1,000 years after waste emplacement and 50 years at 10,000 years after waste emplacement. Therefore, if travel times are to be considered in performance they must be estimated for the conditions which apply when wastes are released.

Pre-emplacement travel times are not applicable to high level waste management because new pathways may result from thermal-mechanical readjustments after closure. Maximum mechanical disturbance is likely to occur when peak temperatures in the host rock are reached, again at a time approximately coincident with release. Due to a combination of local stress build-up due to construction and heat, stress-relief fracturing is likely (e.g., Osnes et al., 1980; Ratigan et al., 1981). The orientation, extent and location of these fractures can only be predicted in qualitative terms. However, the stress-relief fractures may short circuit pre-emplacement paths and provide a faster route to the accessible environment.

1.2.3 Limitations in the Role of Engineering Systems in Licensing Radioactive Waste Repositories

The fundamental limitation in the role of engineered systems is that there is very little information for predicting their long term performance. Adjustments in technical regulatory criteria (Advance Notice vs. final rule, 10 CFR 60) to less restrictive levels reflects the lack of confidence in predicting their long term performance. Many of the recommended waste container materials are complex alloys (e.g., Ticode-12), low-carbon steel, and stainless steel which have not been subjected to repository conditions for extensive periods of time. Numerous mechanisms have been identified and studied which could result in container failure such as stress corrosion cracking, pitting corrosion and hydrogen embrittlement. Data and models are

not available for reliable prediction of time of failure for complex alloys because the mechanisms responsible for failure over long time periods is unknown. However, information is available from natural geochemical systems which indicate that under certain conditions, near pure end member metals such as copper and iron are stable in basalts for hundreds of millions of years (for this reason the Swedish program is considering copper containers). Likewise, data and models are not available for reliable prediction of waste form performance.

NRC research indicates that accelerated testing using fresh glasses is not conservative. Waste glasses which are artificially aged release wastes at much higher rates than the fresh material (Seitz et al., 5.5). Field studies indicate that glasses dissolve rapidly in geothermal systems in tuffaceous and basaltic hosts over a range of temperatures anticipated for the repository near-field. Backfill materials being considered by the DOE program can be shown to be stable for millions of years, through natural analogue programs. It is for this reason that the NRC geochemistry program is supporting confirmatory research on the mechanisms which could result in long term stability or failure of backfill systems (Soudek et al., 3.1; Couture and Seitz, 3.2; Peacor et al., 3.3).

1.3 APPROACH FOR SIMPLIFYING WASTE MANAGEMENT GEOCHEMISTRY

Waste management geochemistry programs have often been challenged because the issues and solutions appear to be complicated or unresolvable. Nevertheless, inherent limitations and uncertainties in the long-term performance of other major waste management barriers such as groundwater travel time and engineered systems neccessitate the use of geochemistry to reduce uncertainties in performance assessment analyses. In the remainder of this section we propose an approach to waste management geochemistry which involves prioritizing research by ranking radionuclides. The approach can greatly simplify resolution of the major question of whether or not important toxic radionuclides will be released to the accessible environment at levels which will exceed applicable regulatory criteria.

The number of important radionuclides of concern to high level waste management may be initially limited to approximately 12 as specified in Table 2 of the proposed EPA standard (EPA, 40 CFR 191, 1982). The important radioelements specified are Am, C, Cs, Np, Pu, Ra, Sr, Tc, Sn. Radionuclides which are individually unspecified but which are addressed by the standard include I, U, and Se. The list can be significantly reduced based on waste package and site specific information. For example, Cs-137 and Sr-90 are low priority because they have relatively short half lives compared to anticipated waste container life and they exhibit a simple and predicatable chemistry in natural systems. If the site exhibits strong reducing conditions then several of the multivalent transuranics such as Np, Pu, and U may be reduced and precipitated near the container. Similarly, under certain engineered or site specific conditions Tc, which persists in solution as the extremely mobile pertechnetate anion under oxidizing conditions may be removed by reduction and coprecipitation with iron near the waste package (Meyer et al., 1984; Swanson, 1984). Of course, for any given site the applicant must demonstrate that reduction precipitation reactions actually will control release. If the Pu forms a mobile polymer in a range of anticipated reducing or oxidizing environments

the precipitation mechanism may be aborted and standard release limits could be exceeded. Therefore, site specific studies need to establish which mechanisms are most important in retarding radionuclides for the anticipated range of conditions relevant to that site.

Uncertainties in performance assessment can be reduced by selectively evaluating the mechanisms which control the mobility of a radionuclide. For example the mobility of neptunium-237 may be controlled by a three stage process initiated by surface adsorption, followed by reduction, followed by long-term incorporation into the crystal structure of the solid. If adsorption alone reduces Np mobility to such an extent that meeting the EPA standard for Np seems probable then uncertainties in other areas of performance assessment such as hydrology can be obviated by study of the additional major geochemical process of reduction and incorporation into the solid phase. Minor geochemical processes can then be ignored. Next the need for additional site characterization research can be prioritized by conducting an assessment of the performance of the radionuclides which are most likely to exceed standards. Emphasis may then be placed on studies of geochemical processes, engineering designs, or further site characterization to increase confidence that the radionuclides most likely to exceed standards will not exceed standards. Therefore, geochemistry research, and waste management research in general should be prioritized by ranking the radionuclides that must be evaluated. Mechanisms which reduce the mobility of individual elements should be identified. Emphasis should then be placed on mechanisms which provide reproducible quantitative data. This approach can simplify the geochemical investigations and reduce uncertainties in performance assessment analyses.

REFERENCES

Airey, P. L., D. Roman, C. Golian, S. Short, T. Nightingale, and R. T. Lowson. 1984. "Radionuclide Migration Around Uranium Ore Bodies in the Aligator River Region of the Northern Territory, Australia-Analogue of Radioactive Waste Repositories". In NRC Nuclear Waste Geochemistry '83. NUREG/CP-0052.

Apps, J. 1984. "Hydrothermal Evolution of Repository Groundwaters in Basalt". In NRC Nuclear Waste Geochemistry '83. NUREG/CP-0052.

Carnahan, C. L., C. W. Miller, and J. S. Remer. 1984. "Verification and Improvement of Predictive Algorithms for Radionuclide Migration". In NRC Nuclear Waste Geochemistry '83. NUREG/CP-0052.

Couture, R. A. and M. G. Seitz. 1984. "Physical Response of Backfill Materials to Mineralogical Changes in a Basalt Environment". In NRC Nuclear Waste Geochemistry '83. NUREG/CP-0052.

Davis, S. N., H. W. Bentley, and R. Zito. 1984. "Dating Ground Water: An Evaluation of its Use in the Assessment of HLW Repositories". In NRC Nuclear Waste Geochemistry '83. NUREG/CP-0052.

Osnes, J. D., R. A. Wagner, and H. Waldman. 1980. "Parametric Thermal/ Thermoelastic Analyses of Nuclear Waste Repositories in Granite and Other Non-Salt Rock Types". 21st U.S. Rock Mechanics Symposium, RSI Publ. No. 80-11, pp. 73-85.

Peacor, D. R., E. J. Essene, J. H. Lee, and L. Kuo. 1984. "Long-term Stability of the Backfill-Host Rock System for High Level Waste Disposal: Experimental and Electron Microscopic Studies". In NRC Nuclear Waste Geochemistry '83. NUREG/CP-0052.

Peterson, S. R., R. J. Serne, A. R. Felmy, R. L. Erikson, K. M. Krupka and G. W. Gee. 1984. "Interactions of Acidic Solutions with Sediments" A Case Study". In NRC Nuclear Waste Geochemistry '83. NUREG/CP-0052.

Ratigan J. L., J. D. Osnes, and J. Brandshaug. 1981. "Temperature History for Candu Reprocessing Waste and Immobilized Fuel in an Underground Vault in Plutonic Rock". 22nd U.S. Rock Mechanics Symposium, pp. 157-161.

Robertson, D. 1984. "Speciation and Transport of Radionuclides in Natural Environments." In NRC Nuclear Waste Geochemistry '83. NUREG/CP-0052.

Runchal, A. and T. Maini, 1980. "The Impact of a High Level Nuclear Waste Repository on the Regional Ground Water Flow". Int. J. Rock Mech. Min. Sci. & Geomech. Vol. 17, pp. 253-264.

Seitz, M. G., G. F. Vandergrift, D. L. Bowers, and T. S. Gerding. 1984. "Effect of Aged Waste Package and Aged Basalt on Radioelement Release". In NRC Nuclear Waste Geochemistry '83. NUREG/CP-0052.

Silva, R. J. and H. Nitsche. 1984. "Thermodynamic Properties of Chemical Species of Waste Radionuclides". In NRC Nuclear Waste Geochemistry '83. NUREG/CP-0052.

Simpson, H. J., R. M. Trier, Y. -H. Li, and R. F. Anderson. 1984. "Field Experiment Determinations of Distribution Coefficients of Actinide Elements in Alkaline Lake Environments". In NRC Nuclear Waste Geochemistry '83. NUREG/CP-0052.

Soudek, A., F. M. Jahnke, and C. J. Radke. 1984. "Ion-Exchange Equilibria and Diffusion in Engineered Backfill". In NRC Nuclear Waste Geochemistry '83. NUREG/CP-0052.

Swanson, J. L. 1984. "Organic Complexant Enhanced Mobility of Toxic Elements in Low-Level Wastes". Interim Report, PNL-4965-2.

U.S. DOE Basalt Waste Isolation Project. 1983. "Site Characterization Report for the Basalt Waste Isolation Project". DOE/RL 82-3.

U.S. Environmental Protection Agency. 1982. "Environmental Standards for the Management and Disposal of Spent Nuclear Fuel, High Level and Transuranic Radioactive Waste," Federal Register, V-47, no. 250, pp. 58196-58206.

U.S. Nuclear Regulatory Commission. 1983. "Disposal of High Level Radioactive Wastes in Geologic Repositories, Technical Criteria," Federal Register, v. 46, no. 120, pp. 28194-282229.

U.S. Nuclear Regulatory Commission. 1983. "Draft Site Characterization Analysis of the Site Characterization Report for the Basalt Waste Isolation Project". NUREG-0960.

Wang, J. S. Y., Tsang, C. F., Cook, N. G. W. and P. A. Witherspoon. 1981. "A Study of Regional Temperature and Thermohydrological Effects of an Underground Repository for Nuclear Wastes in Hard Rock," Journal of Geophysical Research, Vol. 86, No. B5, p. 3759-3770.

2.0 SOURCE TERM AND NEAR-FIELD TRANSPORT

Performance assessment analyses of cumulative releases of radionuclides to the accessible environment will require an understanding of the geochemical mechanisms and processes which govern source term characteristics and near field transport. Highly aggregated empirical values used to describe release or retardation such as a constant distribution coefficient (k_D) cannot be relied upon to adequately account for changes of chemical composition of chemical components transported in ground water near the waste package (Carnahan, 5.1). The uncertainty introduced into licensing from these empirical terms can be greatly reduced by a better undertanding of important mechanisms and processes. The objective of the research reported in this chapter is to provide the NRC with a basis for assessing DOE analyses of source term characteristics and very near-field transport. Specifically, the research is assessing: (1) the importance of hydrothermal ground waters on corrosion, release rates, and very near-field retardation (Apps, 2.1); (2) the source term speciation of radionuclides released from the waste package (Perry, 2.2); (3) solubility constraints on the maximum concentrations of radionuclides (Silva, 2.3); (4) waste-water-rock interactions under near-field conditions (White and Yee, 2.6); and uncertainties resulting from themodynamic data (Schweitzer and Davis, 2.4), standard methods (Meyer et al., 2.5) and routine data collection (Kelmers et al., 2.7).

Numerous studies indicate that the form and valence of the chemical species released from the source will control the fate of the radionuclide during transport (Coles and Ramspott, 1982; Robertson et al., 1981; Robertson, et al., 1983; Moody, 1983; Perry, 2.2; Silva, 2.3; Robertson et al., 4.1). Colloids, anionic species, nonionic species, and organic species are potentially more mobile than positively charged simple ions and complexes because they tend to interact to a lesser degree with sorptive materials lining flow paths. The mobility of the nuclide is also controlled by the valence state of the species (Cleveland, 1983; Meyer, 2.5). In general, the more mobile species of actinicles and transuranics tend to be in a higher valence state (e.g., U^{IV} vs. U^{VI}). The speciation of radionuclides released from the waste package to the backfill must be determined in order to evaluate successive interactions of those species with solids and ground water between the origin and the accessible environment. The range of species likely to be released from the waste package can be assessed through a combination of hydrothermal laboratory studies and field studies. Given that different species of the same nuclide exhibit a wide range of mobility, performance assessment analyses must assess the rate of release and migration of individual species of a nuclide rather than treat all species of a nuclide as an average (Carnahan, 5.1; Robertson, 4.1).

The speciation and mobility of a radionuclide will be controlled by conditions at the time of release. Ground water composition, pH, Eh, temperature, and aging of near field components such as the waste form, container, backfill, and host rock affect release and transport rates. For example, aged glass waste forms may release radionuclides at significantly higher rates than fresh glass (Bates et al., 1982; Seitz, 5.5). Therefore, use of fresh

materials for conditions not representative of release conditions may result in unreliable results and should be carefully assessed or avoided in performance assessment analyses.

The evolution of nearfield ground water compositions should be established since ground water composition will have a major effect on container corosion, solubility, and speciation of migrating nuclides (A.2.1). The reaction of the ground water (or vapor) in the thermal environment near the package will chemically react with near-field solids. Some of these reactions such as precipitation or dissolution will affect local porosity and permeability, whereas hydrothermal mineral transformations will affect the sorptive capacity of substrates along transport paths.

A far-field source term, which has significantly different characteristics than the source term released from the waste package, may evolve as a result of near-field hydrothermal reactions involving radionuclides, evolved ground water, and solids. The characteristics of the far-field source term can be reliably determined only by establishing the source term released at the waste package backfill interface and assessing subsequent modification to that source term as it moves to the near-field/far-field boundary.

Following the breach of the waste container, the hydrothermally evolved ground water will begin to leach radionuclides from the waste form and transport them to the backfill. Radionuclides will initially react with the container walls where breaching due to corrosion mechanisms such as pitting or stress corrosion cracking have occurred. Initial experiments indicate that reactions between chemisorbed actinides such as uranium may accelerate the breakdown of the metallic container (Perry, 2.2). Uranium released from the breaching of the first container may attack adjacent containers and reduce their performance by accelerating corrosion. If this infant mortality scenario occurs it could have a domino effect on adjacent containers. On the other hand, reactions between radionuclides and corroded container components may result in precipitation or coprecipitation of nuclides. Therefore, corrosion studies should be conducted to assess the affect of nuclides and other ground water components on the performance of intact containers following breaching of the first container.

Solubility constraints will control the maximum concentrations of many radionuclides in the backfill and very near-field (Silva, 2.3). Above the solubility limit, a radionuclide precipitate begins to form so that increases in the concentrations in solution do not occur (provided that the rate of precipitation is sufficiently rapid and provided that metastable colloids do not form or that radiolysis does not alter the chemical conditions of the ground water). An upper bound on solution concentrations of radionuclides can be determined using the solubilities of specific compounds. Uncertainties in the thermodynamic data required to estimate solution concentrations need to be assessed to assure that the measurement errors are adequate for performance assessment (Schweitzer and Davis, 2.4). The effects of temperature and CO_2 fugacity must be considered to avoid large measurement errors (Silva, 2.3).

Significant quantities of radionuclides will be removed in the near-field due to fixation by mineral solids. The importance of a specific geochemical mechanism will be largely controlled by reaction kinetics. If the reaction is

rapid compared to the transport time, then it is important and should be assessed. Mechanisms which appear to be important to nuclide migration include precipitation, dissolution, ion exchange, sorption (without exchange), isotopic exchange, matrix diffusion, direct solid diffusion, dead end pore diffusion, ultrafiltration, and flow induced dispersion (Muller and Duda, 1982; Apps, 2.1; Silva and Nitsche, 2.3; Meyer et al., 2.5; White and Yee, 2.6). In order to confirm the adequacy and reliability of data collected by DOE that will be used in performance assessment analyses, the NRC is conducting comparative tests (Kelmers et al., 2.7).

REFERENCES

Apps, J. A. 1984. "Hydrothermal Evolution of Repository Groundwaters in Basalt." In NRC Nuclear Waste Geochemistry '83, NUREG/CP-0052.

Bates, J. K., L. J. Jardine, and M. J. Steinder, 1982. "Hydration Aging of Nuclear Waste Glass," Science, 218:51-54.

Carnahan, C. L., C. W. Miller, and J. S. Remer. 1984. "Verification of Improvement of Predictive Algorithms for Radionuclide Migration." In NRC Nuclear Waste Geochemistry '83, NUREG/CP-0052.

Cleveland, J. M. and T. F. Rees. 1981. "Characterization of Plutonium in Maxey Flats Radioactive Trench Leachates," Science, Vol. 112, 1506.

Coles, D. G. and L. D. Ramspott. 1982. "Ru Migration in a Deep Tuffaceous Alluvium Aquifer, Nevada Test Site: Discrepancy Between Field Observations and Prediction From Laboratory Measurements," Science, Vol. 215, pp. 1235-1237.

Kelmers, A. D., R. J. Clark, N. H. Cutshall, J. S. Johnson, and J. H. Kessler. 1984. "Evaluation of DOE Radionuclide Solubility Data and Selected Retardation Parameters: Description of Calculational and Confirmatory Experimental Activities." In NRC Nuclear Waste Geochemistry '83, NUREG/CP-0052.

Meyer, R. E., W. D. Arnold, F. I. Case. 1984. "Valence Effects on Sorption: Laboratory Control of Valence State." In NRC Nuclear Waste Geochemistry '83, NUREG/CP-0052.

Moody, J. B. 1982. "Radionuclide Migration/Retardation Research and Development Technology Status Report," ONWI-321, ONWI, Battelle Memorial Institute, Columbus, OH.

Perry, D. L. 1984. "Near Field Chemical Speciation: The Reaction of Uranium and Thorium With Hanford Basalt at Elevated pH." In NRC Nuclear Waste Geochemistry '83, NUREG/CP-0052.

Robertson, D. E., K. H. Abel, W. H. Rickard, and A. P. Toste. 1981. "Influence of the Physiochemical Forms of Radionuclides During Migration in Groundwaters." Annual Progress Report for 1981. Prepared for the U.S. Nuclear Regulatory Commission by PNL, Richland, WA.

Robertson, D. E., A. P. Toste, K. H. Abel, and R. L. Brodzinski. 1983. "Radionuclide Migration in Groundwater." NUREG/CR-3554, PNL-4773 RW.

Robertson, D. E., A. P. Toste, K. H. Abel, C. E. Cowan, E. A. Jenne, C. W. Thomas. 1984. "Speciation and Transport of Radionuclides in Groundwater." In NRC Nuclear Waste Geochemistry '83, NUREG/CP-0052.

Schweitzer, D. C. and M. S. Davis. 1984. "The Uncertainties in the Thermodynamics of Basalt-Oxygen and Basalt-Water Reactions." In NRC Nuclear Waste Geochemistry '83, NUREG/CP-0052.

Sietz, M. G., G. F. Vandegrift, D. L. Bowers, and T. J. Gerding. 1984. "Effect of Aged Waste Package and Aged Basalt on Radioelement Release." In NRC Nuclear Waste Geochemistry '83, NUREG/CP-0052.

Silva, R. J. and H. Nitsche. 1984. "Thermodynamic Properties of Chemical Species of Waste Radionuclides." In NRC Nuclear Waste Geochemistry '83, NUREG/CP-0052.

White, A. F. and A. Yee. 1984. "Surface Oxidation - Reduction Reactions in Columbia Plateau Basalts." In NRC Nuclear Waste Geochemistry '83, NUREG/CP-0052.

2. HYDROTHERMAL EVOLUTION OF REPOSITORY GROUNDWATERS IN BASALT

John A. Apps

The Lawrence Berkeley Laboratory
University of California
Berkeley, California 94720

ABSTRACT

The groundwaters in the near field of a radioactive waste repository in basalt will change their chemical composition in response to reactions with the basalt. These reactions will be promoted by the heat generated by the decaying waste. It is important to predict both the rate and the extent of these reactions , and the secondary minerals produced. This is because the alteration process controls the chemical environment affecting the corrosion of the canister, the solubility and complexation of migrating radionuclides, the reactivity of the alteration products to radionuclide sorption, and the porosity and permeability of the host rock.

A comprehensive review of the literature leads to the preliminary finding that hydrothermally altering basalts in geothermal regions such as Iceland lead to a secondary mineralogy and groundwater composition similar to that expected to surround a repository. Furthermore, laboratory experiments replicating the alteration conditions approximate those observed in the field and expected in a repository.

Preliminary estimates were made of the rate of hydration and devitrification of basaltic glass and the zero order dissolution rate of basaltic materials. The rates were compared with those for rhyolitic glasses and silicate minerals. Preliminary calculations were also made of mixed process alteration kinetics, involving pore diffusion and surface reaction. They suggest that at temperatures greater than 150^{o}C, alteration proceeds so rapidly as to become pervasive in normally fractured basalt exposed to higher temperatures in the field. However, laboratory experiments will be required to quantify these processes.

The paper ends with conclusions and recommendations pertaining to repository containment issues, and briefly describes planned research to resolve them.

2.1. Introduction

A candidate site for a geologic repository for high level radioactive waste is in a flood basalt host rock beneath the Hanford Reservation in Washington. If the repository is commissioned, the most likely horizon in the stratigraphic column is the Cohassett flow of the Grande Ronde formation. This flow is located between 2,000 feet and 3,000 feet below the water table. Therefore the host rock and engineered backfill barriers will be altered subsequent to closure by the groundwater due to heat generated by the decaying waste. Hydrothermal alteration raises a number of issues affecting repository integrity and radionuclide containment, and which require resolution. Otherwise it will be difficult to formulate technical guidelines regarding the design and integrity of such a repository, or to judge the significance of findings in planned environmental impact reports submitted by DOE in support of licensing applications.

2.2. Issues Addressed

In this report I will discuss the approach taken in attempting to resolve the issues raised by hydrothermal alteration in a basalt host rock repository. They include questions relating to:-

- The corrosion rates of the canister,
- The solubility and complexation of migrating radionuclides,
- The resulting mineral composition of the backfill and host rocks, and the role of secondary minerals acting as radioelement hosts,
- Porosity and permeability changes of backfill and host rocks affected by hydrothermal alteration,
- Chemical transport rates due to thermal gradients induced in the surrounding host rocks during radioactive decay.

It is clear that the most important issue at hand is to understand how chemical reactions between the rock and the surrounding groundwater will affect radionuclide containment. I will show that the nature of alteration of basalts and the chemical processes that take place are sufficiently well studied that most of the issues regarding the response of the repository host rocks to the thermal regime can at least be be understood if not quantified at the present time. Final resolution of some of the issues will require laboratory hydrothermal experiments, limited field measurements, and some theoretical calculations as input for mathematical models.

2.3. Background and Objectives

Previous research bearing directly on the issues is limited. D. Grandstaff, Temple University, and J. Holloway, Arizona State University, both under contract to Rockwell Hanford Operations, and Rockwell Hanford Operations staff together investigated interactions between pulverized basalt, simulated spent fuel, borosilicate glass and groundwater, with and without simulated high level waste, using Dickson type autoclaves at temperatures between 150 and 300°C, (Apted and Myers, 1982). Earlier, McCarthy et al., (1978a,b,c) and Komarneni et al., (1980), at the Pennsylvania State University, conducted waste-basalt-water interaction studies using sealed gold capsules in cold seal rod bombs, These, and independent studies undertaken by Pacific Northwest Laboratory are summarized in Smith, (1980). All of these earlier studies also used pulverized basalt as starting materials.

In the scientific literature, a number of papers report on laboratory experiments to characterize the hydrothermal alteration of basalt. Field studies of basalt alteration under hydrothermal conditions are also reported. Many of these papers are valuable contributions to our understanding of hydrothermal alteration under natural conditions. However, the research conducted so far does not allow us to quantify either the hydrothermal alteration kinetics of basalt or radionuclide transport from a repository at the temperatures of interest. Further research must therefore be conducted through a carefully designed series of experiments whose technical objectives would be to:-

(1) Determine the rates of host rock alteration between host rock ambient temperatures and 300°C.

(2) Find out how rock alteration will affect porosity and permeability.

(3) Determine the chemical composition of the coexisting fluid phase and how it may affect canister corrosion.

(4) Determine the effect of dissolved chemical constituents on the oxidation state and degree of complexing of toxic radionuclide elements being transported in the groundwater.

(5) Identify thermodynamic and kinetic controls on the rate of migration of selected toxic radionuclide elements in the hydrothermally altered environment.

(6) Obtain data to estiamte chemical transport rates due to thermal gradients induced in the surrounding host rocks during radioactive decay.

The technical objectives should also support mathematical models to predict alteration in the near field, where

the duration and spatial dimensions greatly exceed those attainable in the laboratory, or where laboratory experiments to predict chemical transport rates in the near field would be difficult to perform.

2.4. Scope of the Present Investigation

In this paper I wish to review what is known about the hydrothermal alteration of basalts and how this bears on the composition of the coexisting groundwater. The purpose is to refine the design of experiments to permit measurement of hydrothermal reaction rates and to find out how radionuclide containment will be affected by the changing composition of the reacting groundwater.

The findings are divided into two sections. The first covers field and experimental observations of basalt alteration under hydrothermal conditions. The second deals with the kinetics of rock-water interactions. The first section starts with a brief review of the petrographic characteristics of basalt and how they influence alteration. This is followed by comments on the effect on the secondary mineralogy of the ratio of total amount of water reacted with a given quantity of rock, and the relevance of natural alteration to repository alteration. Next follows a comparison between the observed secondary mineralogy with that predicted on the basis of equilibrium with groundwater, and that produced during laboratory experiment. The second section discusses what are probably the principal mechanisms leading to the alteration of natural glasses, including basalt:-

(1) Solid state diffusion through the glass mesostasis, followed by devitrification and recrystallization.

(2) Surface dissolution.

(3) Aqueous and/or grain boundary diffusion through pores and cracks in the rock, followed by surface attack and/or solid state diffusion.

The paper ends with conclusions, recommendations and a discussion of planned research.

2.5. Findings

2.5.1. Hydrothermal Alteration of Basalt

2.5.1.1. Introduction

Basalts are extrusive or locally intrusive mafic igneous rocks that have undergone relatively rapid cooling under subaerial or subaqueous conditions. In texture they range from vitreous to holocrystalline. They often contain phenocrysts of plagioclase and clinopyroxene (augite), with accessory titanomagnetite and apatite. Olivine and

orthopyroxene (pidgeonite) phenocrysts are also relatively common. Although the groundmass or mesostasis is normally aphanitic, small amounts of glass are commonly present in the interstices of the mesostasis minerals.

Field evidence shows that when a basalt undergoes hydrothermal alteration, the glassy mesostasis, if present, is the first constituent to be altered, usually to clay or clay precursors. The glass alters through solid state diffusion of cations, especially the hydronium ion, leading to devitrification and recrystallisation from the surfaces of major fractures. If the basalt contains an extensive network of microfractures and pores, glass alteration may be accelerated by aqueous and surface diffusion of reactive constituents along these channels to the exposed glass in the rock interior.

When the basalt is primarily cryptocrystalline or holocrystalline, with or without phenocrysts, microfractures and pores are sometimes extensive, and alteration proceeds primarily by aqueous and surface diffusion of reactants through these pores. The depth of penetration is much greater than displayed by basaltic glasses undergoing devitrification. Furthermore, the minerals alter at different rates. Titanomagnetite and olivine usually alter first, followed by plagioclase, and finally clinopyroxene. The alteration products are diverse, depending on duration of exposure to elevated temperature, the composition of the groundwater, and the ratio of water to rock altered.

Basalts, hydrothermally altered at temperatures over 150°C, show pervasive alteration. Mineral zoning is stratified in response to local hydrothermal gradients. Localized alteration zones adjacent to fractures having formed over 150°C, have not been described in the literature. The possible reason for this is that hydrothermal reaction rates above 150°C are normally so fast that secondary mineral formation is essentially complete during the period that the basalts are exposed to elevated temperatures. This will be discussed further in a later section of this paper. When pervasive alteration occurs, field studies are useful primarily in identifying the secondary mineral assemblages likely form at given temperatures rather than indicating reaction rates, although some estimates of conversion rates of metastable minerals to more stable forms might be made.

2.5.1.2. The Effect of Water/Rock Ratio

Hydrothermal alteration of a rock rarely takes place in the natural environment without some addition or removal of components by the aqueous phase. The secondary mineral assemblages could differ substantially depending on the quantity of water passing through the system during alteration. To compare field observations or laboratory experiments to repository conditions, we need to know how much

water is likely to pass through a repository, and how critical this volume is in affecting the secondary mineralogy.

A convenient, though non rigorous way of expressing this parameter is to define a water/rock ratio, i.e. the mass of water that affects a unit mass of rock over the period of alteration. A repository water/rock ratio should ideally be less than unity over the containment period, but will probably range between unity and ten, depending on regional groundwater flow rates, the porosity of the rock, and the changes in permeabilty of the host rock during hydrothermal alteration, convective dissolution and precipitation.

In natural systems, water/rock ratios range from very large, when submarine basalt is exposed to seawater, to ratios approximating the repository range. Field estimates of water/rock ratios are difficult to obtain. However, estimates have been made by several investigators in studying the alteration of basalts by seawater adjacent to sea floor spreading centers. These are based on the loss or gain of chemical components by the basalt. For basalts exposed to seawater at or near the sea floor, the ratio can be as high as 10^4, (Bohlke et al., 1980). Seyfried and his coworkers, (Seyfried and Bischoff, 1977; Seyfried, Mottl and Bischoff, 1978) estimated the water/rock ratio to vary between 10 and 62, whereas Wolery and Sleep (1976) estimated the ratio to be 9(v/v). Humphris and Thompson (1978) give 5-47 and 5-57 based on the uptake from seawater of magnesium and calcium respectively.

Mottl and Seyfried (1980) found from experiment that a seawater/rock ratio above 50 had a drastic effect, both on the composition of the seawater, and on the secondary mineralogy. i.e. the system becomes "seawater dominated" as opposed to "rock dominated" during hydrothermal alteration. This condition apparently holds between 150 and 350°C.

In the geothermal system at Reykjanes, Iceland, the groundwater is modified seawater and the water/rock ratio is estimated to be range from 0.1 to 3, (Mottl and Seyfried, 1980). Hence the groundwater composition of this system will be determined by the secondary mineralogy. It will be shown below that Icelandic geothermal systems, including Reykjanes, contain groundwaters whose chemical components all behave uniformly with temperature and salinity, (Arnorsson et al., 1983a). This implies that all are rock dominated and may have comparable water/rock ratios to Rekyanes. If the water/rock ratios of most Icelandic geothermal systems are similar in range to that expected in a basalt repository, they could serve as natural analogues of repository conditions during the post closure thermal period. In the following sections, I will discuss the mineralogical and chemical characteristics of these systems more fully, particularly in relation to repository

performance.

2.5.1.3. Secondary Mineralogy Resulting From Hydrothermal Alteration

The secondary mineralogy in the hydrothermally altered zone surronding the radioactive waste can be estimated with reasonable certainty as a result of several studies of the secondary mineralogy in piles of altered basaltic lavas and hyaloclastites, mostly from Iceland, (Benson and Teague, 1980; Keith and Barger, 1983; Gibson et al., 1966; Kristmannsdottir, 1979, 1982; Kristmannsdottir and Tomasson, 1978; Mehegan et al., 1982; Palmason et al., 1979; Sigvaldason, 1962; Tomasson and Kristmannsdottir, 1972; Viereck et al., 1982; Walker, 1959, 1960a,b). In these studies, the secondary mineralogy has been correlated with depth and often with contemporaneous or fossil geothermal gradients.

In Fig. 2.1, the normally observed occurrence of secondary minerals in geothermal wells from Iceland is graphed as a function of temperature. The information is drawn primarily from Kristmannsdottir (1979) and Kristmannsdottir and Tomasson (1978). A comparable distribution of minerals has been observed by Keith and Barger (1983) from a drill hole penetrating volcaniclastics and lavas filling the Newberry Caldera, near Bend, Oregon. The rocks are primarily basaltic towards the bottom of the hole where the temperature ranges between 200° and >250°C. The similarities between the two profiles are striking, and arise because the bulk chemical compositions of most basalts do not vary greatly. Minor variations will affect the relative amounts of the secondary phases rather than their identities.* Furthermore, because many basaltic systems, particularly those altered by fresh water, are rock dominated, the secondary mineral assemblages are controlled by the composition of the rock rather than by the dissolved constituents introduced by the water.

Of considerable interest to predictions of repository host rock alteration and radionuclide transport is the relative stability of the secondary minerals. For example, which minerals are metastable and which are thermodynamically stable, but are not observed because crystallization rates are too slow? Over what temperature ranges are given minerals metastable, stable, or unstable? Which minerals control the activities of various components in the aqueous phase at given temperatures and which minerals may act as hosts to migrating radionuclides? Some of these questions

---

*Differences in phase assemblages are sometimes observed. For example, Walker (1959, 1960a,b), and Gibson et al., (1966) note distinct variations in secondary mineralogy between olivine basalts and tholeiites.

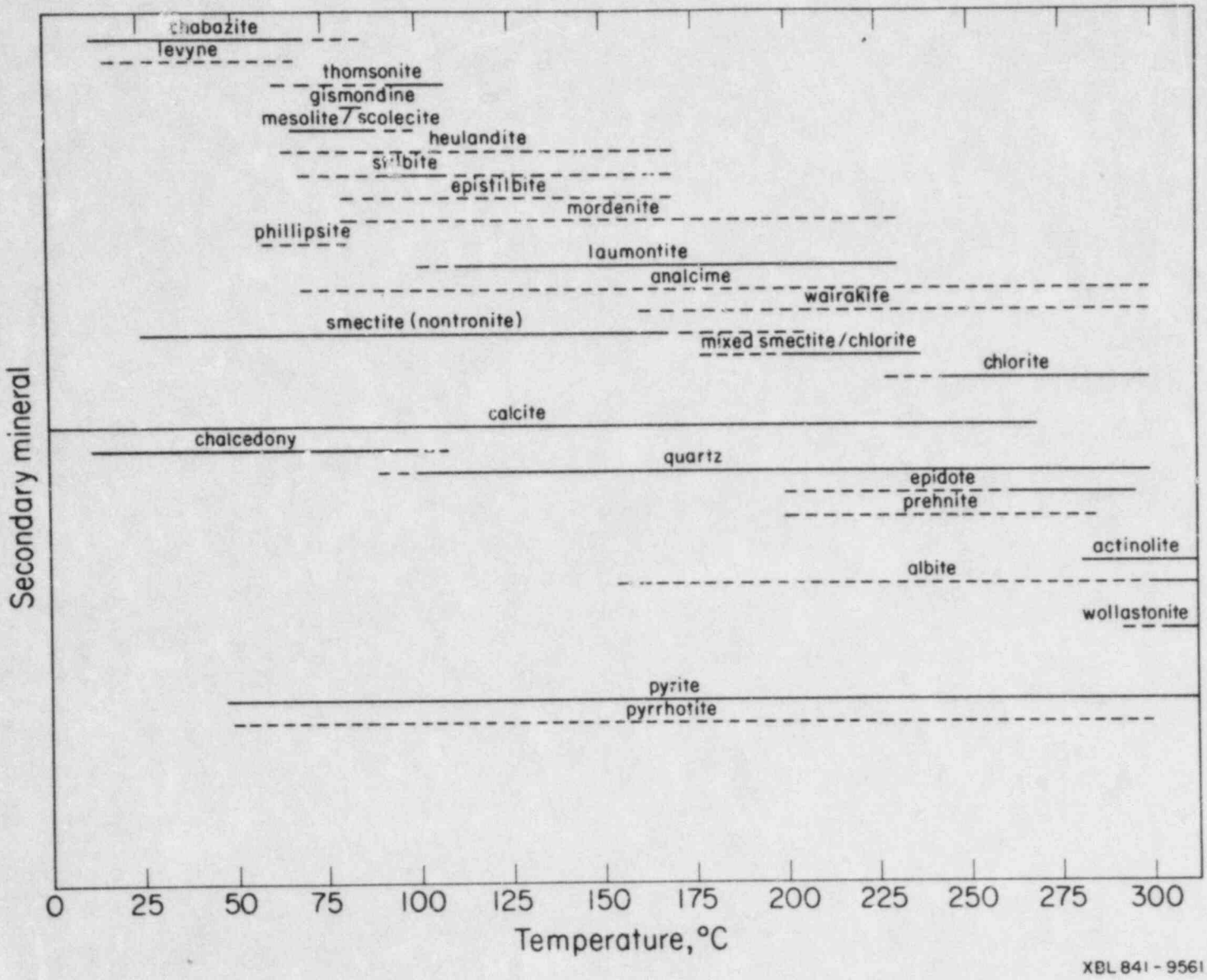

Figure 2.1. Observed stability ranges of secondary minerals in hydrothermally altered Icelandic basalts.

may be answered by four important papers in which the chemical behaviour of groundwaters from basaltic host rocks in Iceland is examined as a function of temperature (Arnorsson et al., 1983a,b; Gunnlaugsson and Arnorsson, 1982; Palmason et al., 1979). These investigators calculated the chemical potentials of the major rock forming oxide components and HF and H_2S in groundwaters from hot springs, hot water wells and wet steam wells as a function of ambient formation temperature. They found that most of the chemical potentials varied with temperature in a smooth regular fashion, regardless of the total dissolved solids in the solution, which ranged from about 100 to 39,000 ppm , or the site from which the sample was collected. Using available thermodynamic data, they calculated whether the aqueous samples were saturated with respect to a number of observed secondary minerals. Their findings have been graphed in Fig. 2.2 on the same scale and in a similar manner to those drawn from field observations.

Comparison of the graphs indicates that quartz, low albite, microcline, epidote, and to a lesser extent hematite, laumontite and pyrite all make their appearance in the field at higher temperatures than predicted on the basis of thermodynamic stability. Clearly, the kinetics of precipitation of these phases at lower temperatures is too slow to prevent significant supersaturation and the precipitation of competing metastable phases containing the same chemical components. For example, opal, beta cristobalite and chalcedony precipitate instead of quartz, and marcasite precipitates instead of pyrite below 100°C. Also, sodium, potassium and calcium zeolites form instead of albite, potash feldspar or epidote below 200°C. Other minerals, notably anhydrite, calcite and fluorite appear to precipitate sufficiently rapidly to be in equilibrium with the groundwater when present.

If mineral assemblages are kinetically controlled in the natural environment, where temperatures may have been maintained for periods of many thousands of years, then it is even more likely in the laboratory where experiments can rarely continue for more than two years. An important question is whether hydrothermal experiments simulating repository conditions will give meaningful data if the resulting phase assemblages differ significantly from those that will form in a repository.

Because of a growing interest in the hydrothermal alteration of oceanic crust adjacent to spreading plate boundaries, and the chemical processes leading to greenschist formation, many experimental studies in the past decade have been made that throw light on these processes, (Bischoff and Dickson, 1975; Hajash, 1975; Hajash and Archer, 1980; Hajash and Chandler, 1981; Moody et al., 1983; Mottl and Holland, 1978, Mottl et al., 1979; and Seyfried

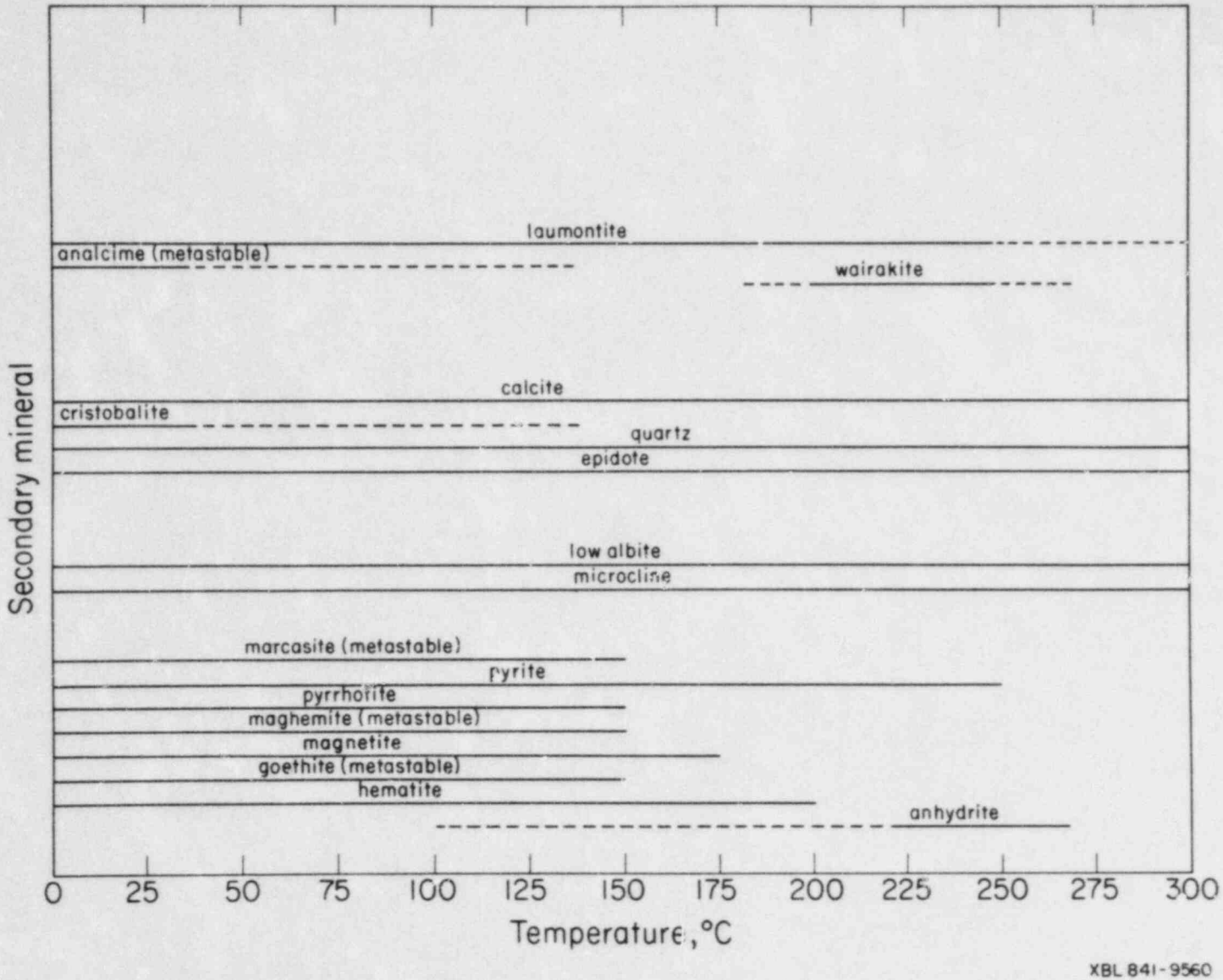

Figure 2.2. Predicted secondary mineral stability ranges based on the chemical composition of groundwaters in Icelandic geothermal systems.

and Bischoff, 1979, 1981), as well as basalt alteration studies for the Basalt Waste Isolation Project, (Apted and Myers, 1982). The temperatures at which these investigators conducted their experiments ranged from 70 to 500°C, although the majority were made between 200 and 300°C. Water/rock ratios ranged from 1 to 50. Most experiments used seawater as the aqueous reactant. The longest experiment lasted nearly 14,500 hours, although most ran for between 2,000 and 4,000 hours.

The secondary phases observed in all experiments below 400°C are summarized in Fig. 2.3. It is immediately apparent that kinetic restraints are severe, and that only smectite, analcime, magnetite, pyrite, amorphous silica and illite form in observable quantities below 300°C. However, the implications of this experimental limitation in predicting radionuclide containment may not be particularly significant as will be discussed in the next section.

It may be possible, using both laboratory and field data on the times and temperatures necessary to produce observable quantities of a given mineral, to compute the approximate rates of formation, i.e. precipitation, of these minerals as a function of temperature. This information would be valuable in estimating the formation of relative quantities of given secondary minerals around the repository and the final mineral mineral assemblages that would be produced. It would also permit initial calculations of alteration rates in mixed kinetic models. See section 2.5.2.4.

2.5.1.4. Composition of the Coexisting Groundwater

Arnorsson et al., (1983a), and Gunnlaugsson et al., (1982), on the basis of a thermodynamic analysis of 63 Icelandic geothermal waters, showed that the chemical potentials of major dissolved components in these waters all follow smooth trends as a function of temperature, even though the the chloride concentration varied between 100 and 19,000 ppm. Particularly good correlations were obtained from analyses of unmixed drillhole discharges, which are presumably most representative of subsurface waters. Those chemical components, here defined as activity ratios, showing smooth trends, include $[SiO_2]$, $[H_2CO_3]$, $[H_2S]$, $[H_2SO_4]$, [HF], $[Na^+]/[H^+]$, $[K^+]/[H^+]$, $[Fe^{2+}]/[H^+]^2$, $[Ca^{2+}]/[H^+]$, and $[Mg^{2+}]/[H^+]^2$.

An excellent correlation was even found between Eh/pH and temperature. The exception to this general behaviour occurred in the case of alumina, ($[Al(OH)_4]^-/[OH]^-$) where the correlation between was poor above 150°C. This is attributed to the inadequacy of thermodynamic data pertaining to aqueous aluminum speciation at elevated temperatures, thereby making the prediction of aluminosilicate

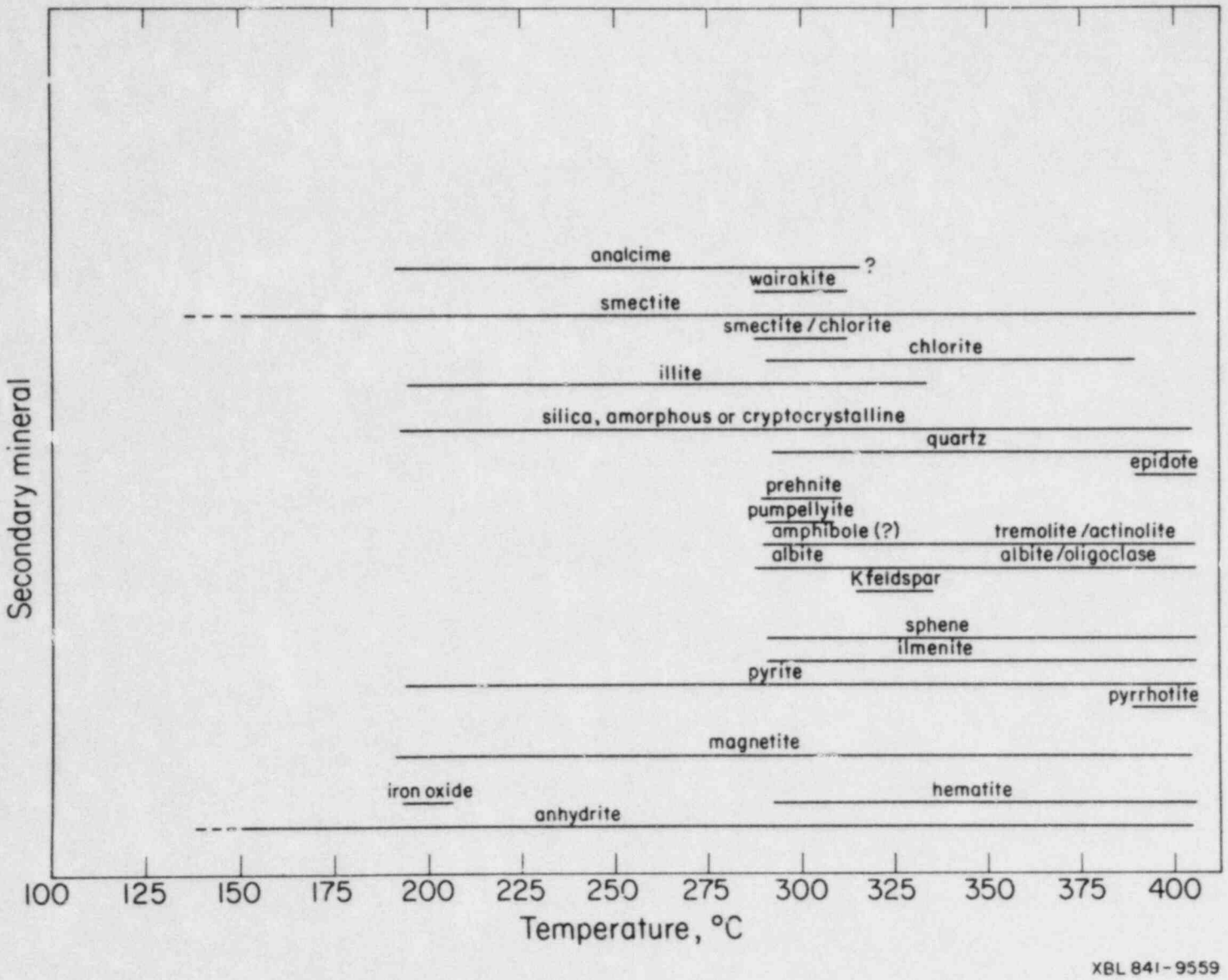

Figure 2.3. Secondary minerals produced during hydrothermal experiments, using basalt or basaltic glass as starting materials.

solubilities at elevated temperatures less certain.

The systematic behaviour of the thermodynamic properties of Icelandic geothermal waters arises because (a) secondary mineral assemblages are similar throughout the areas sampled, and control the chemical potentials of major components in the aqueous phase, (b) chemical constituents transported into the rock by the aqueous phase affect the bulk chemistry of the system to an insignificant degree, because the systems are probably rock dominated, (c) several of the secondary minerals persist over much of the observed temperature range, (d) metastable secondary minerals equilibrate with major chemical constituents in the aqueous phase at chemical potentials only incrementally higher than would their stable counterparts, and (e) phase transitions with changing temperature, either as a result of thermodynamic univariant reactions, or through kinetically controlled precipitation of a stable phase in place of a metastable one, will lead to minor groundwater compositional discontinuities that are probably within the limits of precision of chemical analyses. Arnorsson et al., (1983a) point out that all major chemical constituents with the exception of chloride are controlled by coexisting solid phases, and that the groundwater composition can be predicted by specifying only two independent variables or degrees of freedom: temperature and chloride content. The authors note that the number of secondary minerals observed in field assemblages is essentially in agreement with that predicted by Gibbs' phase rule for a system with two degrees of freedom.

Because groundwater composition and secondary mineralogy in the repository host rock can be predicted, it should also be possible to predict radioelement solubility in the groundwater, given the thermodynamic properties of the radioelement aqueous species and the solid phases. The required thermodynamic data for most radioelements is inadquate at the temperatures of interest. Therefore direct experimental measurements under simulated repository conditions appears to be the most efficacious route for obtaining the required information.

Two important dependent parameters in the system are pH and Eh. It is not clear from inspection, which of the heterogeneous reactions in the system controls the pH. It probably involves aluminosilicates although calcite cannot be discounted. The oxidation state of the system definately appears to be controlled by the precipitation of sulfides, primarily pyrite, or marcasite at lower temperatures. Reducing conditions may be induced by the hydrolysis of ferrous ion containing materials in the primary basalt mineral assemblage, leading to the reduction of sulfate to sulfide. Some evidence that this may be taking place, is provided by Floyd and Fuge, (1982) who note that the Fe_2O_3/FeO ratio in Icelandic basalts increases with depth and degree of

hydration. If the volume of water passing through the rock is small in relation to the mass of the rock, as suggested by the low water/rock ratio proposed for Reykjanes, then it could not have brought in sufficient oxygen to cause the observed oxidation. The ferrous iron oxidation must therefore have been coupled with a corresponding sulfate reduction.

In regard to canister corrosion, it appears that the relative stability of iron oxides or sulfides under repository conditions will be predictable thereby indicating whether a given canister material will be coated with a passive oxide layer, or be sulfidized. Specific alteration phenomena and rates can be determined only after selection of candidate materials, and testing with groundwater and altering rock under simulated conditions.

2.5.1.5. Dispersion of Elements During Hydrothermal Alteration

Hydrothermal alteration of basalts leads to the mobilization and redistribution of a wide range of elements. Some of these also have radionuclides that are fission products contained in high level waste; others have chemically similar propoerties. The extent of element mobililization, whether local or regional, and the host minerals which trap them, are important in predicting post closure repository behaviour.

It has been known for some time that many elements in unaltered basalts show systematic variations in concentration or coherence. Several hypotheses have been advanced to explain this phenomenon, the most popular proposing that it is due to processes occuring during progressive fusion of upper mantle rocks, (Bowman et al., 1975).

Dispersion of a given element due to hydrothermal alteration, can be estimated by measuring the loss of coherence between that element and a known immobile element such as zirconium or tantalum. Element dispersion can also be estimated through mineralogical and geochemical studies.

Chemical analyses of Eastern Icelandic basalts by Wood et al., (1976), show that the minor and trace elements Ti, P, Zr, Nb, Ta, Hf and some of the rare earths possess a high degree of coherence, indicating that these elements are relatively immobile. Of the major elements, total iron, Ca, Mn, Na, and P show good correlation when plotted against

*Note, however, that Viereck et al., (1982), observed significant iron oxidation in the upper volcanicalstic horizons of associated basalts, so the alteration may be due to oxygenated waters in the highly porous horizons.

stable incompatible elements.* In contrast, plots of K_2O, Rb and Sr concentrations versus Zr show poor correlation. Furthermore, SiO_2, MgO, K_2O, Rb, Sr and the light rare earths show greater variability in altered than in unaltered flows. The authors note that amygdale zeolites in Eastern Iceland lavas are high in Ba, K, Rb, and Sr. Rocks higher in H_2O and Fe_2O_3 are enriched in K and Rb, a feature also observed in basalts and basaltic glasses having undergone alteration by seawater, (Staudigel and Hart, 1983; Honnorez, 1981).

Floyd and Fuge, (1982), in their study of alkali and halogen distributions in basalt flows from a drill core in Eastern Iceland show that the differential mobility of these elements was Rb > K > Li > Na and Cl > F > I. In contrast to observations by Wood et al., (1976), they noted that only K and Rb show systematic decreases with progressive hydration, whereas Mg and Li show increases with progressive hydration in some lavas.

A parallel study conducted by Viereck et al., (1982) on associated volcaniclastics in the same drill hole showed them to be most strongly depleted in Ca, Na, Mg, and Si. Rocks less than 800 m deep showed pronounced losses in Si, but also showed gains in Fe and Ti. Drastic gains in K and Rb, due to illite formation was also noted, suggesting that these elements were drawn from neighboring basalt flows. Al, Fe and Ti showed smaller changes, although all showed gains in rocks of more basaltic composition. Sphene appeared to be a ubiquitous secondary mineral confirming the mobility of titanium. Zr and Nb concentrations were similar to the associated lavas, yet Y was enriched in rocks of basaltic composition. The mobility of the rare earths was shown by the presence of secondary allanite.

In summary, it can be shown that few elements remain immobile during hydrothermal alteration. The mobility of a given element is determined by many factors, some of which relate to the relative stabilities of the primary and secondary host minerals. A quantitative analysis of the mobility of specific radioelements can be made, but is likely to be laborious. Direct measurements in the laboratory combined with field observations and thermodynamic analyses appears to be the most promising avenue in establishing the limits of element migration in the near field of a repository.

Regarding radioelements, it would appear that cesium could be incorporated by secondary zeolites, following K and Rb. Actinides might follow the rare earths in

---

*However Palmason et al., (1978) observed Ca enrichment in groundwaters in the Reykjanes geothermal area, and Viereck et al., (1982) found that both Ca and Na is strongly depleted from volcaniclastics.

coprecipitating in allanite or epidote. However, the high temperatures required for their formation would suggest that actinides would probably be forced to enter other host minerals at lower temperatures. Among these might be phosphates, such as apatite or members of the monazite xenotime family. The reducing conditions prevalent in basalts undergoing hydrothermal alteration in a substantially closed system, suggest that technecium will be stable in the +4 state. Since both Tc^{4+} and Sn^{4+} have a similar radius to Ti^{4+}, both could follow titanium and coprecipitate in sphene, or titanium oxides. The decreased mobility of iodide with respect to chloride and fluoride is noteworthy and should be investigated further.

A secondary effect, that of changing porosity and permeability resulting from the dispersion of rock forming components and the formation of secondary minerals, has with one exception, been discussed in the literature only in qualitative terms. On the basis of measured cracks in submarine pillow and massive basalts and breccias in a hole drilled in the North Atlantic, Johnson (1980), calculated the permeability, density, and porosity profiles as a function of depth. The cracks were distinguished in terms of mineral filling, i.e. open, calcium carbonate filled or smectite filled. He found that while the intrinsic permeability of unfractured basalt ranged around 10^{-15} cm^2, the permeability due to cracks averaged 10^{-4} cm^2. The filling of some cracks caused the permeability to drop half an order of magnitude. However, Johnson did not comment on the effect on bulk permeability that filling all the cracks would have had. He computed the primary porosity or interstitial pore space of the basalts to be between about 3 and 10 percent, whereas the crack porosity averged 18.5 percent of which 6 percent was unfilled with seconadry minerals.

Independent measurements of rock porosity and permeability should be made from field examples of altered basalts having a closer correspondence to repository conditions.

2.5.2. Mechanisms of Basalt Alteration

2.5.2.1. Introduction

Quantification of basalt alteration mechanisms is necessary if we are to determine the amount of rock alteration in a repository. In the following section, I will review the available information which allows for preliminary estimates of reaction rates and the planning of further experiments. The emphasis is initially placed on an examination of the mechanisms governing glass alteration, because the glass mesostasis of a basalt alters before the finely crystalline or the phenocryst minerals, and because more information is available in the literature.

Silicate glasses, when exposed to the aqueous phase, are subject to a number of chemical processes:

(1) Surface adsorption and exchange

(2) Diffusion of ions in and out of the silicate lattice

(3) Reactions leading to the devitrification of the glass lattice.

(4) Aqueous and surface diffusion of reactants and products to the surface through pores and along grain boundaries.

(5) Surface dissolution.

(6) Precipitation.

Of these, the last four are of greater importance in predicting alteration rates. I start with a discussion of the solid state diffusion processes causing hydrolysis and devitrification. Next, I discuss surface dissolution. Finally, I briefly review mixed reactions involving aqueous, grain boundary and solid state diffusion, and first order surface reactions. This last situation applies more generally to crystalline basalts than to glasses.

2.5.2.2. Alteration of Basalt Glasses by Solid State Diffusion

Although there is an extensive literature on experimental obsidian hydration, similar data on basalt glass alteration is limited to the low temperature studies of Furnes (1975) and Crovisier et al., (1983). Higher temperature leaching studies on pulverized basalt containing a glass mesostasis could be interpreted by inspection of the variation of dissolved components as a function of time, e.g. the data of Grandstaff (cited in Apted and Myers, 1982). The material used by Grandstaff was carefully sized Umtanum basalt, which is reported to contain a glass mesostasis, (Noonan et al., 1981). Therefore the approximate time the grains become completely hydrated (and devitrified) might be identified by examination for discontinuities in the solute leaching curves with time.

Hydration takes place initially by the diffusion of the hydronium ion into the glass from the aqueous phase. The diffusion process generally obeys Fick's second law. Empirical correlations of alteration thickness as a function of time can be obtained by setting the appropriate boundary conditions and solving for the average thickness travelled by the diffusing species. The resulting expression, known as the parabolic rate law, is usually simplified to:-

$$x^2 = kt \qquad (1)$$

where

x = the thickness of the hydrated layer, (m).
k = the hydration rate constant, ($m^2.s^{-1}$).
t = time, (s).

The hydration rate is temperature dependent, and follows the Arrhenius rate equation:-

$$k = Ae^{E/RT} \qquad (2)$$

where

A = a constant, ($m^2.s^{-1}$).
E = the activation energy, (Joule.$mole^{-1}$).
R = the universal gas constant, (Joule.K^{-1}.$mole^{-1}$).
T = the absolute temperature, (K).

Equations (1) and (2) may be combined and rearranged to give:-

$$\ln(x^2/t) = \ln A - \frac{E}{R}.\frac{1}{T} \qquad (3)$$

By plotting experimental values of $\ln(x^2/t)$ versus $1/T$, a graph is obtained permitting correlation of data from different sources and interpolation of high temperature laboratory with lower temperature field observations. It may also allow estimation of the apparent activation energy of the diffusion process. Although it is not clear what is involved, devitrifiation subsequent to hydration also appears to obey a parabolic rate law in obsidian, possibly because further diffusion of reactants and products through the hydrated layer controls devitrification.

In Fig. 2.4, the experimental data from several sources for hydration and devitrification of various silicate glasses is plotted including those from Michels et al., (1983) on obsidian, and Crovisier et al., (1983) and Furnes, (1975) on basaltic glasses together with data reported in Lofgren, (1968), and White and Claassen (1980). The positions of the data points for basalt glass hydration and devitrification derived from Grandstaff, (Apted and Myers, 1982) and the interpolated slope correlates reasonably well with the corresponding data for borosilicate glass from McCarthy et al., (1978b).

Fig. 2.4 includes the best fit curves for obsidian hydration, obsidian devitrification, and sodium diffusion in glass. Noteworthy is the similarity of the slopes of the lines for all three processes, even though the rates at a given temperature may range through as many as four orders

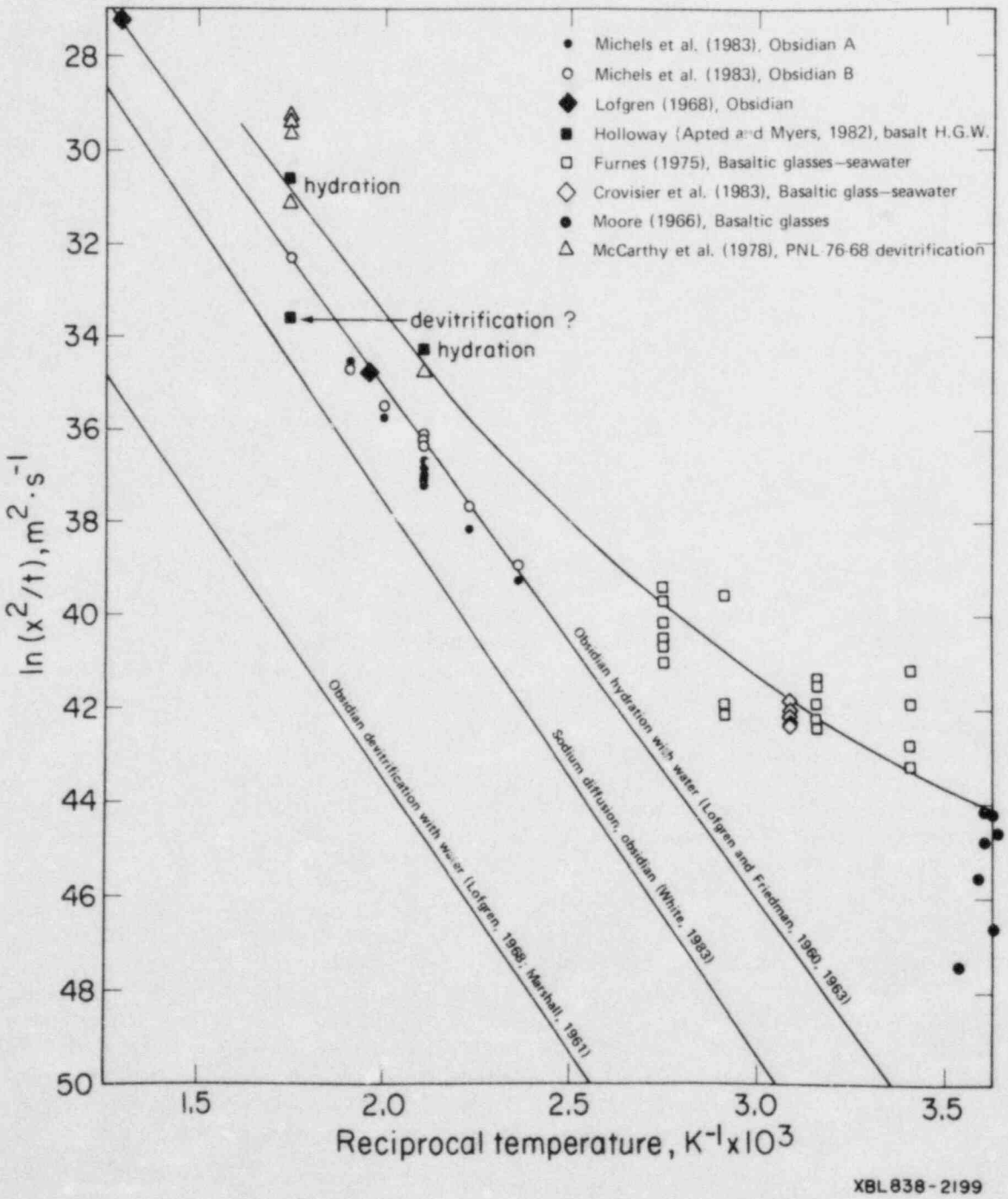

Figure 2.4. Diffusion controlled alteration of various natural glasses.

of magnitude.

Fig. 2.4 also includes a smoothed best fit curve to all data relating to basalt glass hydration and devitrification. Unlike obsidian glass, it appears that deyhydration and devitrification occur almost simultaneously, so that it is difficult to discriminate between the two mechanisms with the available data. Data fitted include that taken from field observations, as discussed below. The deviation of the basalt devitrification slope with falling temperature could be attributed to mixed diffusion through both aqueous and solid phases due to disruption of the outer layers of the altered glass, but this requires further study. The interpretations are quite speculative, since the available data are both insufficient and incomplete. Yet they provide a basis for designing more laboratory experiments to obtain better data.

Naturally occurring vitreous forms of basalt most commonly result from submarine quenching of pillow lavas when a glassy rind known as sideromelane is produced. Water quenched lava may also shatter to produce a granulated tuff like material called hyaloclastite. Subsequent alteration of these vitreous forms by water leads to the formation of an amorphous or partially crystalline material known as palagonite. This process has been studied by sevearal investigators, (Ailin-Pyzik and Sommer, 1981; Furnes, 1974; 1980; Hay and Iijima, 1968a,b; Hekinian and Hoffert, 1975; and Noack, 1981). An excellent summary is provided by Honnorez, (1981).

It is difficult to correlate basalt alteration rates in the laboratory with those in the field, because there is no accurate way of estimating the duration of exposure. A study by Moore (1966) on the palagonization of basalt in seawater does provide us with some help. Moore studied the palagonite rims of submarine pillow lavas dredged from the sea near Hawaii. Some of the rims were coated with a manganese oxide layer that is believed to accumulate at a roughly constant rate through precipitation from sea water. This rate is estimated to be about 3 mm per million years, (Bender et al., 1966). Values of $\ln(x^2/t)$ were calculated from Moore's data and plotted on Fig. 2.4. The correlation with laboratory data is improved when the added thickness of the manganes dioxide layer is included.

Moore also cites in the same paper a single measurement of the average thickness of a palagonite rim produced by lakewater on an A.D. 894 basalt lava flow from Mt Fujii, Japan. The estimated $\ln(x^2/t)$ is much less than for lavas exposed to seawater for a corresponding length of time, which Moore attributes to the more corrosive effect of seawater.

The basalt hydration/devitrification curve in Fig. 2.4 can be checked against field observations of basalt alteration in the Columbia River basin. Measured ambient temperatures in the basalt flows at the Hanford Reservation, Washington, range from 10°C near the surface to 60°C at a depth of 4,000 feet. By interpolation, we can calculate the expected maximum thicknesses of alteration rims surrounding fractures as a function of the age and depth of the buried basalt as shown in Table 2.1. These compare well with observed alteration if it is assumed that the flows have been saturated with water since their formation.

Table 2.1

CALCULATED THICKNESS OF ALTERATION ZONES ADJACENT TO WATER SATURATED FRACTURES IN PASCO BASIN BASALTS

T, °C	$\ln(x^2/t)$	Alteration Zone Thickness, mm.		
		$t = 10^6$ yr	$t = 10^7$ yr	$t = 10^8$ yr
25	-43.12	2.43	7.69	24.3
45	-42.13	3.99	12.6	39.9
65	-41.03	6.92	21.9	69.2

Note:

The maximum observed alteration thicknesses in basalts from the Pasco Basin is 5 mm. Ages of these basalts range fromm 16.5 my for Lower Grande Ronde to < 12 my in the Saddle Mountain basalts, (Myers and Price, 1979). Present ambient temperatures range from about 25°C in the Mabton Interbed to 58°C in the Umtanum Flow, (Rockwell Hanford Operations, 1982).

2.5.2.3. Surface Dissolution Rates

Zero order surface dissolution rates of the rock forming components as a function of temperature are needed in the proper design of autoclave dissolution experiments. They are difficult to estimate from available experimental data without correction for the simultaneous precipitation reactions. Best estimates are probably obtained by measuring the initial rate of silica dissolution. Silica, as the principal structural component of the glass or cryptocrystalline mesostasis, probably reflects the actual dissolution rate of the structure more accurately than do interstitial cations.

The rate of surface reaction can be written thus:-

$$\Delta C_i = k'_i S X_i \Delta t \qquad (4)$$

where:-

C_i : the concentration of component i, ($g.mole.m^{-3}$)

k'_i = the zero order surface dissolution constant, ($g\ moles.m^{-2}.s^{-1}$)

S_2 = the surface area per unit volume of solution, ($m^2.m^{-3}$)

X_i = mole fraction of component, i, (-)

The rate constant is related to temperature by the familiar Arrhenius equation:-

$$k_i = Ae^{E/RT} \tag{5}$$

and

$$\log k_i = \log A + \frac{E}{2.303R} \cdot \frac{1}{T} \tag{6}$$

The logarithms of the zero order dissolution rate constants, based on total weight loss, silica dissolution, and sodium dissolution from rhyolitic glass and from basaltic glass, basalt and diabase dissolution were determined from data in a number of published sources and plotted against $1/T$ (K^{-1}) as illustrated in Figs. 2.5a and b. The somewhat surprising result to emerge is that silica dissolution rates are about four orders of magnitude slower for basalts than for rhyolites at temperatures above 150°C. A possible explanation may be the effect of competing reactions precipitating dissolved silica in the case of basalt, due to the presence of higher concentrations of alkali and alkali earth metals in the aqueous phase. Another contributing factor may be the catalysing effect of higher ionic strength solutions in the precipitation of secondary phases.

Also plotted on Figs. 2.5a and b is the average zero order dissolution rate for silicate minerals from a number of different sources as determined by Wood and Walther, (1983). Their calculated rate correlates well with dissolution data for basaltic materials, but not for rhyolitic glass. Further study will be required to explain the difference.

2.5.2.4. Mixed Reactions

Alteration of basalt proceeds not only by diffusion of ions into and out of the glass mesostasis and its devitrification product, but by diffusion of ionic species into the rock interior through the aqueous phase saturating microfractures and pores and by surface diffusion along intergranular boundaries. Further reactions then proceed on the internal surfaces with primary minerals and glass, if present.

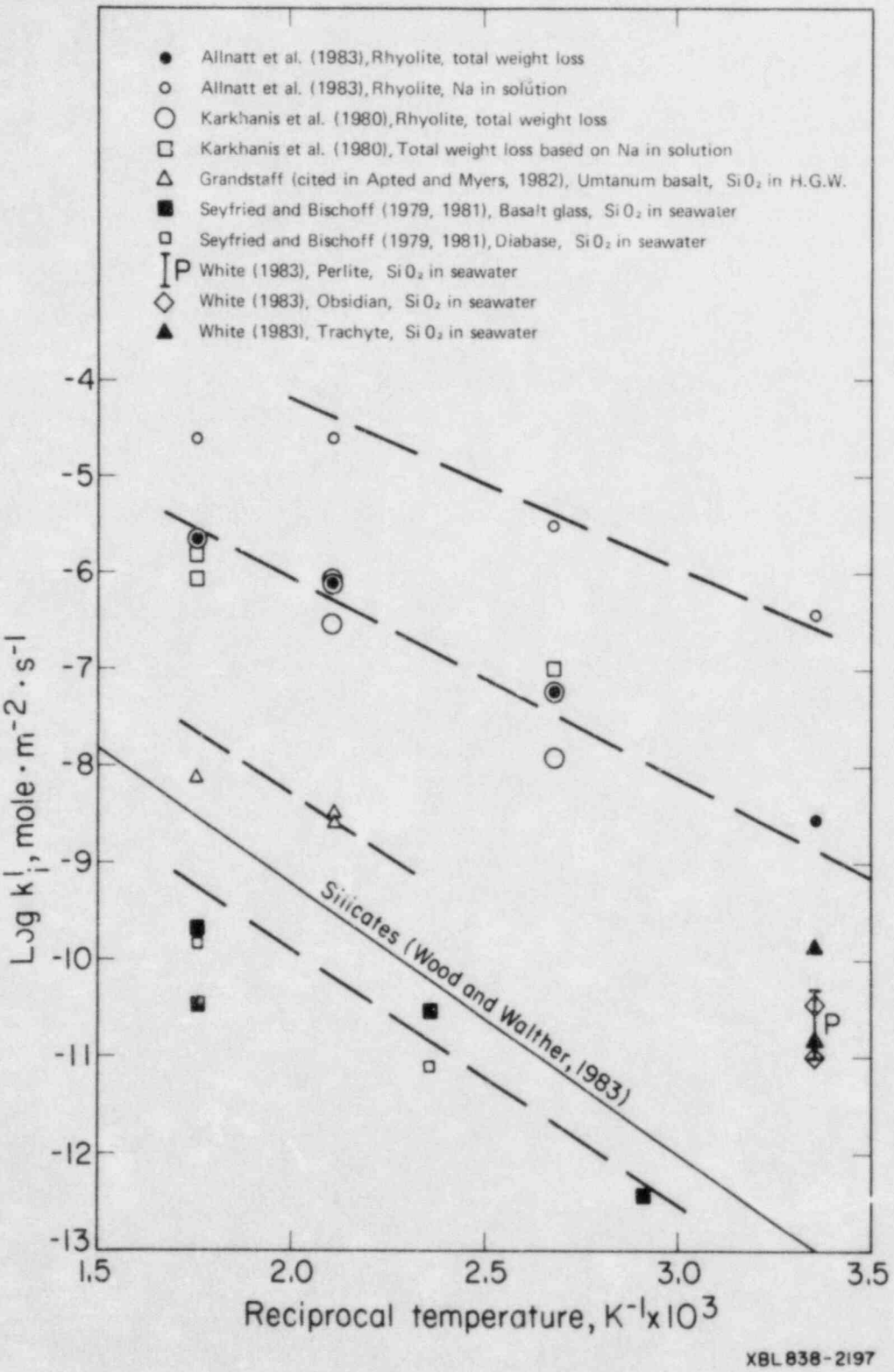

Figure 2.5a. Zero order surface dissolution constant vs reciprocal of absolute temperature for various rocks in aqueous solution.

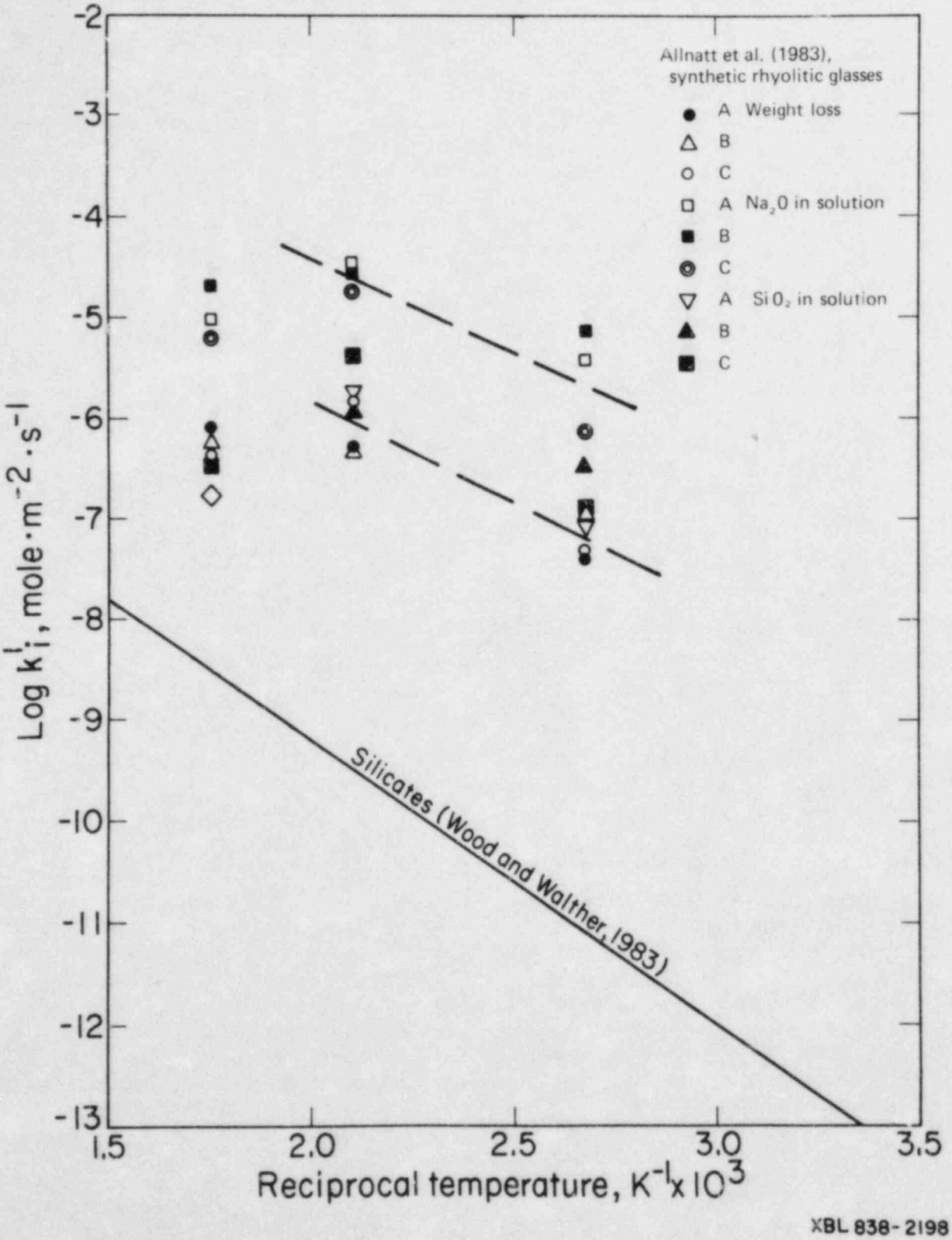

Figure 2.5b. Zero order surface dissolution constant vs reciprocal of absolute temperature for various synthetic rhyolitic glasses in aqueous solution.

Differential equations describing such processes can be quite complex, and would be difficult to formulate, particularly with present uncertainties regarding the chemical processes taking place. However, simplified expressions leading to analytical solutions can be used to obtain approximate representations of the expected alteration behaviour. One such form, in which only first order surface chemical reactions take place, and diffusion is assumed to be through the aqueous pores, can be written thus:-

$$\frac{\delta C_i}{\delta t} = \frac{D_i \delta^2 C_i}{\tau \delta x^2} - \alpha C_i \qquad (7)$$

where

C_i = the concentration of the species, i, in the aqueous phase. During smectitization of glass and olivine, i would be the hydronium ion, $(H_3O)^+$, (moles.m^{-3}solution)

D_i = the diffusion coefficient of the aqueous species, i, ($m^2.s^{-1}$).

x = the depth of penetration into the rock, (m).

α = the first order heterogenous rate constant of the reacting species, C_i, with the rock, (s^{-1}).

τ = the tortuosity coefficient of the pores, (-).

If steady state conditions are assumed, a reaction zone thickness can be calculated. Unfortunately, the information available regarding the first order rate constant for surface attack of the glass by the hydroxonium ion is unknown over the temperature range of interest.

Preliminary calculations assuming a first order precipitation reaction rate equivalent to that for quartz precipitation, for which data is available (Apps et al., 1975), show that the reaction zone thicknesses expected in altering crystalline basalts are in close accord with those observed submerged in seawater under preburial conditions. Such reaction zones are a few centimeters thick, (Bohlke et al., 1980; Honnorez, 1981). At higher temperatures, the reaction zone thickness is calculated to become rapidly thinner, until at 350°C, it will only be between 1 and 10μm thick. Estimates of the steady state rate at which the reaction front advances through the rock are also in reasonable accord with field estimates of the time that the basalt has been exposed to seawater. Above 150°C, the rate of alteration becomes so fast, that by 350°C, pervasive alteration would be complete in most normally fractured basalt within a few years.

These calculations explain why hydrothermal alteration in the field is pervasive, and sometimes complete when ambient temperatures exceed 150°C. Field data could not therefore yield estimates of alteration rates. This emphasizes the necessity of performing laboratory experiments, both to clarify the mechanisms involved, and quantify the rates of alteration, so that host rock alteration in a repository might be predicted.

2.6. Conclusions

The following conclusions are drawn from the findings of this paper:

(1) Because the water/rock ratio in a basalt repository will be low, the system will be "rock dominated", and the groundwater composition will be primarily controlled by the secondary mineral assemblages.

(2) The secondary mineral assemblages of hydrothermally altered basalts as a function of temperature are remarkably similar in a wide range of reported occurrences. In many, the water/rock ratio is similar to that expected in a basalt repository in the Pasco Basin. Therefore rock dominated hydrothermal alteration in basalts is an excellent natural analogue of alteration expected in a basalt host rock repository, and the secondary mineralogy can be predicted with reasonable certainty.

(3) Secondary mineral assemblages arising from hydrothermal alteration in basalts are in part metastable.

(4) Laboratory experiments simulating hydrothermal alteration of basalts produce dominantly metastable mineral assemblages, somewhat similar to those observed in the field at higher temperatures.

(5) The differences in chemical potentials of the mineral forming components between thermodynamically stable assemblages and those metastable assemblages found in the field or synthesized in the laboratory, are relatively small, and not expected to cause significant differences in groundwater composition. Therefore laboratory experiments will fairly replicate the repository groundwater compositions for the purpose of measuring radioelement solubilities.

(6) Groundwater chemical potentials in hydrothermally altered basalts show smooth trends as a function of temperature. The groundwater composition can be defined in terms of temperature and total chloride concentration. This implies that repository groundwater compositions as well as Eh and pH can be predicted, and hence also radionuclide concentrations if the thermodynamic properties of aqueous species and solid phases

of the radioelement are known. With few exceptions, thermodynamic data are inadequate. Therefore direct measurement of radioelement solubilities under simulated repository conditions must be carried out.

(7) The stability of canister corrosion products can be predicted, given the repository pH and Eh. Specific corrosion rates can be determined only by testing candidate materials under repository conditions.

(8) Field evidence shows that many elements are dispersed to greater or lesser extent during hydrothermal alteration. Some of the secondary minerals will act as hosts for radioelements, e.g. zeolites may incorporate cesium, and secondary allanite or epidote will probably incorporate rare earths and the actinides. Iodide appears to be less mobile than either chloride or fluoride, but no explanation is presently available for this behaviour.

(9) Direct experiments, field interpretation of secondary mineralogy and thermochemical calculations should serve to provide the needed information to predict thermodynamic and kinetic controls to radionuclide migration.

(10) Porosity and permeability changes during hydrothermal alteration in the field have been reported, but not quantified. Field and laboratory measurements of changes in these rock properties will be required.

(11) Preliminary estimates of basalt glass hydration and devitrification indicate that it is between three and several hundred times faster than obsidian hydration depending on temperature. These estimates appear to correlate well with field observations of basalt alteration in the Pasco basin of Washington.

(12) Measured surface dissolution rates for silica from basalt rocks correlate well with the zero order dissolution rates of silicate minerals. However, they are at least two orders of magnitude slower than rhyolite glass dissolution rates. Further study will be required to explain the difference.

(13) Preliminary calculations of steady state crystalline basalt alteration rates involving aqueous diffusion into pores, followed by surface chemical reaction suggest that the reaction zone thickness will be centimeters thick at 25°C, but will become extremely thin above 150°C. However, the rate of alteration would become so fast that alteration would be pervasive in normally fractured basalt within a few years. Therefore rock alteration rates above 150°C cannot be estimated from field observations. This highlights the necessity of performing laboratory experiments to quantify basalt alteration rates to predict similar

processes in a waste repository. Information on first order precipitation reactions involving the formation of secondary minerals is largely unknown and requires interpretaion of literature data and further experimentation.

2.7. Recommendations

The principal recommendations emerging from this paper are as follows:-

(1) Conduct experiments to identify and quantify the mechanisms of basalt hydrothermal alteration.

(2) Determine the kinetics of mineral precipitation.

(3) Measure radioelement solubilities as a function of temperature in solutions equilibrated with basalt.

(4) Conduct corrosion tests on candidate canister materials at elevated temperatures in solutions equilibrated with basalt, and in the presence of a suitable radiation field.

(5) Extend the existing capability of computing groundwater chemical potentials at elevated temperatures to include more reliable aluminum speciation, and where possible, thermodynamic data on radioelement species.

(6) Conduct porosity and permeability measurements on altered and unaltered basalts from both the field and laboratory experiments.

2.8. Planned Research

The information obtained in this paper can be applied to the design of experiments to measure rock alteration rates at elevated temperatures and predict host rock behaviour to radionuclide migration in the near field. Previous experiments to study the hydrothermal alteration of rocks and natural glasses often entailed leaching of crushed, screened and sized rock in stationary or rocking autoclaves. The disadvantages of such experiments when considered in the context of present goals may be summarized as follows:-

(1) Quantitative interpretation of reaction rates is not possible particularly when different minerals are reacting at differing rates.

(2) Spatial relations between secondary phases in alteration zones and the unaltered rock cannot be obtained.

(3) The profiling of alteration zones by electron microprobe is difficult, if not impossible.

(4) Examination of surface structure or chemistry by auger electron spectroscopy, XPS, or SIMS is difficult.

Therefore surface characterization of radionuclide adsorption is difficult, if not impossible.

(5) It is not possible to measure changes in the physical properties of the rock resulting from alteration such as porosity and permeability. Specific surface area changes are also difficult to evaluate, because physical comminution or heterogeneous nucleation may have taken place during agitation of pulverized material.

To overcome these difficulties, a different approach must be taken.

Experiments have been designed to meet the following needs:

(1) Data must be obtained to predict alteration rates in fractured basalt between 25 and 250°C and over time spans between 1 and 10,000 years. Rate controlling reactions, and secondary mineral formation in relation to alteration of the basalt will be identified.

(2) Radionuclide adsorption and retardation under the conditions cited above must be predictable.

(3) The data must be amenable for incorporation in radionuclide transport models replicating the waste repository environment.

(4) The data must be reconcilable with field observations of natural processes in order to bridge the time gap between plausible experimental schedules and the repository containment period.

The most appropriate means of obtaining information on the kinetics of rock-water interactions is through the leaching of rock fragments with controlled geometry. The depth of penetration of alteration in a rock during a laboratory experiment is small, because of the relatively short exposure time. The rock sample configuration should therefore be one that maximizes surface area in relation to volume so that the volume of the affected rock in relation to the autoclave capacity is optimized. The sample should also have a flat surface of at least one square centimeter to permit surface characterization studies. For these and other less important reasons, a disc, wafer or coupon configuration is preferable to others.

The experimental configuration chosen permits the simultaneous leaching of up to twelve rock wafers, two inches in diameter and half a centimeter thick, as shown in Fig. 2.6. The choice of size and number of wafers is based on the requirements for porosity and permeability analyses, surface chemical and mineralogical analyses, rock mass to solution volume ratio, and solution sampling strategy. The last item also determined the minimum autoclave capacity of 600 ml.

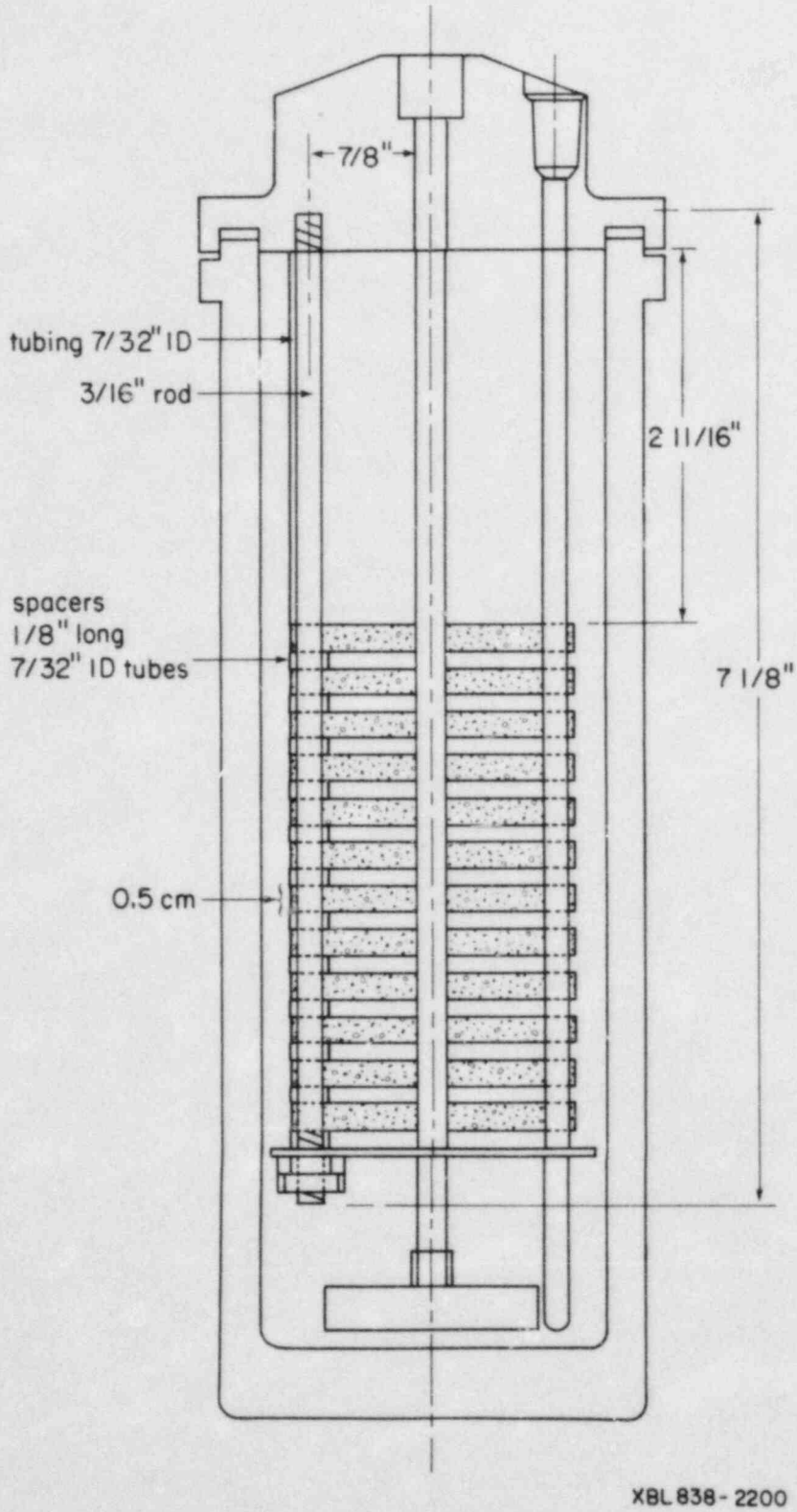

Figure 2.6 Configuration of rock wafers in a 600 ml autoclave.

The preferred autoclave material is titanium, because for all practical purposes, it is chemically inert under the operating conditions of the experiment, and is unlikely to interfere with the chemical composition of the solution. However, titanium does not possess the strength for practical use above 2,000 psi and 250°C, so for operation above this temperature and pressure, Hastelloy-C 276 was selected instead.

Experiments will be conducted between 150°C and 350°C. This range differs from that expected in a repository, which in basalt will vary from ambient rock temperature to about 250°C. However, data can be acquired more rapidly at higher temperatures, provided caution is excercised, because different chemical reactions may predominate outside the region of interest, even though field evidence does not suggest this. It is also hoped that the experimental results may be extrapolated confidently to the experimentally intractable region below 150°C. Experiments will be conducted in the two phase region, along the saturation curve of the aqueous phase.

REFERENCES

Ailin-Pyzik, I. B., and Sommer, S. E., 1981. Alteration of DSDP Basaltic Glasses, Microscale Chemical Effects of Low Temperature. Journal of Geophysical Research 86, p. 9503-9510.

Allnatt, A. R., Bancroft, G. M., Fyfe, W. S., Jacobs, P. W. M., Karkhanis, S. N., Melling, P. J., Nishijima, A., Vempati, C. S., and Tait, J., 1983. Leaching Behaviour and Electrical Conductivity of Natural Rhyolite and Modified Synthetic Rhyolite, Chemical Geology 38, p. 329-335.

Apps, J. A., Madsen, E. L., and Hinkins, R. L., 1975. The Kinetics of Quartz Dissolution and Precipitation, Energy and Environment Division Annual Report, 1975, LBL-5299, p. 12-15.

Apted, M. J., Myers, J., 1982. Comparison of the Hydrothermal Stability of Simulated Spent Fuel and Borosilicate Glass in a Basaltic Environment, RHO-BW-ST-38 , 78 p.

Arnorsson, S., Gunnlaugsson, E., and Svavarsson, H., 1983a. The Chemistry of Geothermal waters in Iceland. II. Mineral Equilibria and Independent Variables Controlling Water Compositions, Geochimica et Cosmochimica Acta 47, p. 547-566.

Arnorsson, S., Gunnlaugsson, E., and Svavarsson, H., 1983b. The Chemistry of Geothermal Waters in Iceland. III. Chemical Geothermometry in Geothermal Investigations, Geochimica et Cosmochimica Acta 47, p. 567-577.

Bender, M. L., Teh-Lung Ku, and Broecker, W. S., 1966, Manganese Nodules-Their Evolution, Science 151, p. 325-328.

Benson, L. V., and Teague, L. S., 1982, Diagenesis of Basalts from the Pasco basin. Washington-I. Distribution and Composition of Secondary Mineral Phases, Journal of Sedimentary Petrology 52, p. 595-613.

Bischoff, J. L., and Dickson, F. W., 1975, Seawater-Basalt Interaction at 200°C and 500 Bars: Implications for Origin of Sea-floor Heavy-metal Deposits and Regulation of Seawater Chemistry, Earth and Planetary Science Letters 25, p. 385-397.

Bohlke, J. K., Honnorez, J., and Honnorez-Guerstein, B. M.,

1980, Alteration of Basalts from Site 396B, DSDP: Petrographic and Mineralogic Studies, /f2Contributions to Mineralogy and Petrology 73, p. 341-364.

Bonatti, E., 1965 Palagonite, Hyaloclastites and Alteration of Volcanic Glass in the Ocean, Bulletin Volcanologique 28, p. 257-269. Bowman, H., Asaro, F., and Carmichael, I., 1975. Evidence in Support of a Homogeneous Source for Alkalic Basalts, Energy and Environment Annual Report, 1975, LBL-5299, p. 28-29.

Crovisier, J. L., Thomassin, J. H., Juteau, T., Eberhart, J. P., Touray, J. C., and Baillif, P., 1983. Experimental Seawater- Basaltic Glass interaction at 50°C: Study of Early Developed Phases by Electron Microscopy and X-ray Photoelectron Spectometry, Geochimica et Cosmochimica Acta , 47, p. 377-387.

Dickson, F. W., Potter, J., Rytuba, J., and Radtke, A. S., 1978. Reaction of Rhyolite with H_2O and NaCl-H_2O at 300°C and 500 Bars. (Abs). EOS , 59, p. 1221.

Floyd, P. A., and Fuge, R., 1982. Primary and Secondary Alkali and Halogen Element Distribution in Iceland Research Drilling Project Basalts from Eastern Iceland, Journal of Geophysical Research 87, No B8, p.6477-6488.

Furnes, H., 1975. Experimental Palagonitization of Basaltic Glasses of Varied Composition, Contributions Mineralogy and Petrolology 50, p. 105-113.

Furnes, H., 1974. Volume Relations between Palagonite and Authigenic Minerals in Hyaloclastites, and its Bearing on the Rate of Palagonitization, Bulletin Volcanologique 38, p. 173-186.

Furnes, H., 1980. Chemical Changes During Palagonitization of an Alkaline Olivine Basaltic Hyaloclastite, Santa Maria, Azores, Neues Jahrbach fur Mineralogische Abhandlungen 138, p. 14-30.

Gibson, I. L., Kinsman, J. J., and Walker, G. P. L., 1966. Geology of the Faskrudsfjordur Area, Eastern Iceland, Visindafelag Isl. Greinar 2, p.1-52.

Gunnlaugsson, E., and Arnorsson, S., 1982. The Chemistry of Iron in Geothermal Systems in Iceland, Journal of Volcanology and Geothermal Research 14, p.281-299.

Hajash, A., 1975. Hydrothermal Processes along Mid Ocean Ridges: An Experimental Investigation, Contributions of Mineralogy and Petrology 53, p. 205-226.

Hajash, A., and Archer, P., 1980. Experimental Seawater/Basalt Interactions: Effects of Cooling, Contributions to Mineralogy and Petrology 75, p.1-13.

Hajash, A., and Chandler, G W., 1981. An Experimental Investigation of High Temperature Interactions between Seawater and Rhyolite, Andesite, Basalt and Peridotite, Contributions to Mineralogy and Petrology 78, p.240-254.

Hay, R. L., and Iijima, A., 1968a. Nature and Origin of Palagonite Tuffs of the Honolulu Group on Oahu, Hawaii, Geological Society of America Memoire 116, p. 331-376.

Hay, R. L., and Iijima, A., 1968b. Petrology of Palagonite Tuffs of Koko Craters, Oahu, Hawaii, Contributions to Mineralogy and Petrology 17, p. 141-154.

Hekinian, R., and Hoffert, M., 1975. Rate of Palagonitization and Manganese Coating on Basaltic Rocks from the Rift Valley in the Atlantic Ocean near 36 50 N, Marine Geology 19, p. 91-109.

Honnorez, J., 1981, The Aging of the Oceanic Crust at Low Temperature, The Sea 7, (C. Emiliani, Ed) p. 525-587.

Humphris, S. E., and Thompson, G., 1978. Hydrothermal Alteration of Oceanic Basalts by Seawater, Geochimica et Cosmochimica Acta 42, p. 107-125.

Johnson, D. M., 1980. Crack Distribution in the Upper Oceanic Crust and its Effects upon Seismic Velocity, Seismic Structure, Formation Permeability, and Fluid Circulation. Legs 51, 52, 53, Part 2 of the Cruises of the Drilling Vessel Glomar Challenger, San Juan, Puerto Rico to San Juan, Puerto Rico, November 1976-April 1977. Deep Sea Drilling Project, Initial Report 53:2, p.1479-1490.

Karkhanis, S. N., Bancroft, G. M., Fyfe, W. S., and Brown, J. D., 1980. Leaching Behavior of Rhyolite Glass, Nature 284 p. 435-437.

Keith, T. E. C., and Barger, K. E., 1982. Hydrothermal Alteration in Core from Drill Hole Newberry 2, Oregon, Transactions of the American Geophysical Union (EOS) (abstract) 63, no. 45, p. 1128.

Komarneni, S., Scheetz, B. E., McCarthy, G. J., and Coons, W. E., 1980. Hydrothermal Interactions of Cesium and Strontium Phases from Unreprocessed Fuel with Basalt Phases and Basalts, Rockwell Hanford Operations,

Rockwell International report RHO-BWI-C-70,

Kristmannsdottir, H., 1979. Alteration of Basaltic Rocks by Hydro- thermal Activity at 100-300°C, International Clay Conference 1978 (Developments in Sedimentology) 27 (M. M. Mortland and V. C. Farmer, Eds) Elsevier Scientific Publishing Co., Amsterdam, Oxford and New York, p. 359-367.

Kristmannsdottir, H., 1982. Alteration in the IRDP Drill Hole Compared with Other Drill Holes in Iceland, Journal of Geophysical Research 87, No B8, p. 6525-6531.

Kristmannsdottir, H., and Tomasson, J., 1978. Zeolite Zones in Geothermal areas in Iceland, Natural Zeolites, Occurrence, Properties, Use (L. B. Sand and F. A. Mumpton, Eds.), p. 277-284 Pergamon, New York.

Lofgren, G. E., 1968. Experimental Devitrification of Rhyolite Glass, PhD Dissertation, Stanford University, 99 p.

Marshall, R. R., 1961. Devitrification of Natural Glass, Geological Society of America Bulletin 72, p. 1493-1520.

McCarthy, G. J., Scheetz, B. E., Komarneni, S., Barnes, M., Smith, C. A., Lewis, J. F., and Smith, D. K., 1978a. Simulated High-Level Waste-Basalt Interaction Experiments. First Interim Progress Report, Rockwell Hanford Operations, Rockwell International report RHO-BWI-C-12, 68 p.

McCarthy, G. J., Scheetz, B. E., Komarneni, S., Barnes,M., Smith, C. A., Smith, D. K., and Lewis, J. F., 1978b. Simulated High-Level Waste-Basalt Interaction Experiments. Second Interim Progress Report. Rockwell Hanford Operations, Rockwell International report RHO-BWI-C-16, 21 p.

McCarthy, J. G., Scheetz, B. E., Komarneni, S., Smith, D. K., 1978c. Reaction of Water with a Simulated High-Level Nuclear Waste Glass at 300°C and 300 Bars, Rockwell Hanford Operations, Rockwell International report RHO-BWI-C-35, 64 p.

Mehegan, J. M., Robinson, P. T., and Delaney, J. R., 1982. Secondary Mineralization and Hydrothermal Alteration in the Reydarfjordur Drill Core, Eastern Iceland, Journal of Geophysical Research 87, No B8, p. 6511-6524.

Michels, J. W., Tsong, I. S. T., Nelson, C. M., 1983. Obsidian Dating and East African Archeology, Science 219,

p. 361-366.

Moody, J. B., Meyer, D., and Jenkins, J. E., 1983. Experimental Characterization of the Greenschist/Amphibolite Boundary in Mafic Systems, Americal Journal of Science 283, p.48-92.

Moore, J. G., 1966. Rate of Palagonitization of Submarine Basalt Adjacent to Hawaii, U.S. Geological Survey Professional Paper 550-D, p. D163-D121.

Mottl, M. J., and Holland, H. D., 1978. Chemical Exchange during Hydrothermal Alteration of Basalt by Seawater-I. Experimental Results for Major and Minor Components of Seawater, Geochimica et Cosmochimica Acta 42, p. 1103-1115.

Mottl, M. J., Holland, H. D., and Corr, R. F., 1979. Chemical Exchange during Hydrothermal Alteration of Basalt by Seawater-II. Experimental Results for Fe, Mn, and Sulfur Species, Geochimica et Cosmochimica acta 43, p. 869-884.

Mottl, M. J., and Seyfried, W. E., 1980. Sub-Seafloor Hydrothermal Systems Rock-Vs Seawater-Dominated, Benchmark Papers in Geology 56, (P. A. Rona and R. P. Lowell, Eds.) No 4, p. 66-82. Dowden, Hutchinson and Ross, Inc., Stroudsburg, Pennsylvania.

Myers, C. W., and Price, S. M., Principal Authors, 1979. Geologic Studies of the Columbia Plateau, A Status Report, Rockwell Hanford Operations, Rockwell International report, RHO-BWI-ST-4, 365 p. plus appendices.

Noonan, A. F., Fredriksson, K., and Nelen, J., 1981. Phase Chemistry of the Umtanum Basalt, A Reference Repository Host in the Columbia Plateau, Proceedings of the Third International Symposium on the Scientific Basis for Nuclear Waste Management, (C. B. Moore, Ed.), Plenum Press, p.51-58.

Noack, P. Y., 1981. La Palagonite: Caracteristiques, Facteurs d'Evolution et Mode de Formation, Bulletin Mineralogique 104, p. 36-46.

Palmason, G., Arnorsson, S., Fridleifsson, I. B., Kristmannsdottir, H., Saemundsson, K., Stefansson, V., Steingrimsson, B., and Tomasson, J., 1979. in Deep Drilling of the Atlantic Ocean: Ocean Crust p. 43-65, The American Geophysical Union, Washington, D.C.

Rockwell Hanford Operations, 1982. , Geochemistry, Section 6; Basalt Waste Isolation Project Site

Characterization Report, Rockwell Hanford Operations, Rockwell International report.

Seyfried, W., and Bischoff, J. L., 1977. Hydrothermal Transport of Heavy Metals by Seawater: The Role of Seawater/Basalt Ratio, Earth and Planetary Science Letters 34, p. 71-77.

Seyfried, W. E., and Bischoff, J. L., 1979. Low Temperature Basalt Alteration by Seawater: An Experimental Study at 70°C and 150°C, Geochimica et Cosmochimica Acta 43, p. 1937-1947.

Seyfried, W. E., and Bischoff, J. L., 1981. Experimental Seawater-Basalt Interaction at 300°C , 500 bars, Chemical Exchange, Secondary Mineral Formation and Implications for the Transport of Heavy Metals, Geochimica et Cosmochimica Acta 45, p. 135-147.

Seyfried, W. E., Mottl, M. J., Bischoff, J. L., 1978. Seawater/ Basalt Ratio Effects on the Chemistry and Mineralogy of Spilites from the Ocean Floor, Nature 275, p. 211-213.

Sigvaldason, G. E., 1962. Epidote and Related Minerals in Two Deep Geothermal Drill Holes, Reykjavik and Hveragerdi, Iceland, U.S. Geological Survey Professional Paper 450-E p. E77-E84.

Smith, M. J., Principal Author, 1980. Engineered Barrier Development for a Nuclear Waste Repository in Basalt: An Integration of Current Knowledge, Rockwell Hanford Operations, Rockwell International report RHO-BWI-ST-7, 617 p.

Staudigel, H., and Hart, S. R., 1983. Alteration of Basaltic Glass: Mechanisms and Significance for the Oceanic Crust- Seawater Budget, Geochimica et Cosmochimica Acta 47, p. 337-350.

Thomassin, J. H., Touray, J. C., 1979. Etude des Premiers Stades de L' Interaction Eau-Verre Basaltique: Donnees de la Spectrometrie de Photoelectrons (XPS) et de la Microscopie Electronique a Balayage, Bulletin Mineralogique 102, p. 504-599.

Tomasson, J., Kristmannsdottir, H., 1972. High Temperature Alteration Minerals and Thermal Brines, Reykjanes, Iceland Contributions to Mineralogy and Petrology 36, p. 123-134.

Viereck, L. G., Griffin, B. J., Schmincke, H.-U. and Pritchard, R. G., 1982. Volcaniclastic Rocks of the

Reydarfjordur Drill Hole, Eastern Iceland 2. Alteration, Journal of Geophysical Research No B8, p. 6459-6476.

Walker, G. P. L., 1959. The Amygdale Minerals in the Tertiary Lavas of Ireland. II. The Distribution of Gmelinite, Mineralogical Magazine 32, p. 202-217.

Walker, G. P. L., 1960a. Zeolite Zones and Dike Distribution in Relation to the Structure of the Basalts of Eastern Iceland, Journal of Geology 68, p. 515-528.

Walker, G. P. L., 1960b. The Amygdale Minerals in the Tertiary Lavas of Ireland. III. Regional Distribution, Mineralogical Magazine 32, No. 250, p. 503-527.

White, A. F., 1979. Dissolution Kinetics of Silicate Rocks-Application to Solute Modeling, in Chemical Modeling in Aqueous Systems, Speciation, Sorption, Solubility, and Kinetics, ACS Symposium Series 93, (E. A. Jenne, Ed.) American Chemical Society, Washington D.C., p. 447-473.

White, A. F., 1983. Surface Chemistry and Dissolution Kinetics of Glassy Rocks at 25°C, Geochimica et Cosmochimica Acta 47, p. 805-815.

White, A. F., and Claassen, H. C., 1980. Kinetic Model for the Short-Term Dissolution of a Rhyolitic Glass, Chemical Geology 28, p. 91-109.

Wolery, T. J., and Sleep, N. H., 1976. Hydrothermal Circulation and Geochemical Flux at Mid-Ocean Ridges, Journal of Geology 84, p. 249-275.

Wood. B. J. and Walther, J. V., 1983. Rates of Hydrothermal Reactions, Science 222, p. 413-415.

Wood, D. A., Gibson, I. L., Thompson, R. N., 1976. Elemental Mobility during Zeolite Facies Metamorphism of the Tertiary Basalts of Eastern Iceland, Contributions to Mineralogy and Petrolology 55, p. 241-254.

2.2 NEAR FIELD CHEMICAL SPECIATION:

THE REACTION OF URANIUM AND THORIUM WITH HANFORD BASALT AT ELEVATED pH

Dale L. Perry
Earth Sciences Division
Lawrence Berkeley Laboratory
Berkeley, CA 94720

ABSTRACT

The hydrolysis of radionuclides such as thorium and uranium and their subsequent chemisorption on Hanford basalt have been studied using a variety of techniques, including x-ray photoelectron and infrared spectroscopy. Data obtained to date indicate mixed complexes of uranium and thorium to be on the basalt surface, the complexes being radionuclide oxides, hydrated oxides ("hydroxides"), and carbonates. These findings are discussed with respect to their importance for input for models describing speciation and dissolution processes involving nuclear waste repository materials such as Hanford basalt.

2.2.1 INTRODUCTION

2.2.1.1. Background and Objectives

One of the most important areas of research that is useful in determining the suitability of a nuclear waste repository site and its performance in retaining the waste is that of determining the chemical species involved in the interaction of the nuclear waste with the geologic material of the repository and subsequent interaction and migration by means of groundwater. Various different radionuclide species will exhibit different chemistries and solubilities; these differences may result in variable chemical forms (such as colloids) by which the radionuclides migrate. Furthermore, the solubilities of the radionuclide species will affect their concentrations in the groundwater and also the amounts of the radionuclides that will chemisorb/precipitate onto the surrounding geologic media. These geochemical conditions, along with others such as native groundwater chemistry, must be addressed and evaluated if there is to be a really thorough understanding of the effects they have on the movement of radionuclides in the ground.

2.2.1.2 Issues Addressed by This Research

Research at Lawrence Berkeley Laboratory has attempted to answer a wide number of questions that relate to understanding the phenomena related to mechanisms that control the near field speciation, reaction rates, and the stability of the species that are generated. Specifically, issues such as the following have been addressed: What are the initial species of radionuclides that are released from proposed waste forms and the species that are generated under repository conditions? What chemical species result from the interaction of radionuclides such as uranium with Hanford basalt and Nevada Test Site tuff? What control will the near field species have on the far field source term? How are radionuclide adsorption and precipitation affected by geochemical conditions that are similar to those of a repository? the far field source term? How are radionuclide adsorption and precipitation affected by geochemical conditions that are similar to those of a repository?

2.2.1.3 Scope of Research

Studying the various chemical species resulting from the interaction of radionuclides with Hanford basalt and groundwaters has been done by using a wide variety of techniques to obtain data on both the bulk chemical precipitates from the reactions and the resulting species that have been chemisorbed. These data, along with the data derived from other experimental approaches and data taken in conjunction with other materials found in a repository backfill, can be used to assess the retention performance characteristics of a basalt repository material such as that found at the Hanford site. A knowledge of these species that actually exist in the solid phase will be important for determining what dissolution mechanisms (what species are undergoing dissolution, etc.) are operable in the migration of uranium, thorium, and other radionuclides. Spectroscopic techniques such as x-ray photoelectron (1) and Auger spectroscopy (2) will be extremely valuable in assessing the migration of radionuclides through both the near and far field in a repository, since much information can be obtained about the types of radionuclide species present, the amounts of the radionuclides, and segregation of ele-ments on the surface. When coupled with other techniques such as transmission infrared and energy dispersive x-ray spectroscopy which give chemical information that is related more to the bulk, these surface approaches give an extremely comprehensive picture of the chemistry of the radionuclide being studied and its interaction with repository materials.

2.2.2 METHODS

Vacuum surface studies in this investigation were conducted using x-ray photoelectron spectroscopy (1). Additional species studies aimed at verifying functional groups that were present in the hydrated uranium and thorium oxides and hydroxides were performed with conventional dispersive infrared spectroscopy in which samples were prepared as both Nujol mulls and KBr pellets (~1% sample in the KBr matrix). Elemental analyses were performed by standard analytical techniques by the analytical laboratories of the Department of Chemistry, University of California, Berkeley.

2.2.2.1 Thorium (IV)/Basalt Interaction

In a typical experiment, thorium(IV) was reacted with Hanford basalt at pH values of 10-12; the surface of the basalt and accompanying precipitates were then studied by x-ray photoelectron, infrared, and other techniques. Fig. 1 shows a survey (0-1000 eV) x-ray photoelectron spectrum of thorium that has been chemisorbed onto (and subsequently reacted with) Hanford basalt. The different photoelectron lines such as the Th 4f, Ca 2p, and Si 2p reflect both the thorium species and mineralogical composition of the rock surface.

Several features of the basalt surface chemistry were observed after a detailed study of the lines of several of the elements. Fig. 2 shows high resolution oxygen 1s spectra of the same sample, the binding energy (averaged, charge referenced against the carbon 1s = 284.6 eV line) being 531.4 eV for the original "as reacted" surface. This is a normal value for the OH^- (and CO_3^{2-}) species (3) on a surface and is not unexpected for a basalt surface at high pH. Additionally, one also observed asymmetry on both the high and low binding energy sides of the peak, possibly indicating more than one oxygen species. Indeed, when the peak is deconvoluted, peaks are also observed that are indicative of surface water and lattice oxides that are inherent to the rock.

Fig. 3, however, depicts the carbon 1s spectrum of the same Hanford basalt sample. The principal peak at 284.6 eV is due to the adventitious carbon peak that is used for the compensating of the surface charge in all of the x-ray photoelectron lines. The smaller peak, however, at 3.6 eV higher binding energy, is indicative of the CO_3^{2-} functional group and supports the inference of such a species from the oxygen 1s spectrum.

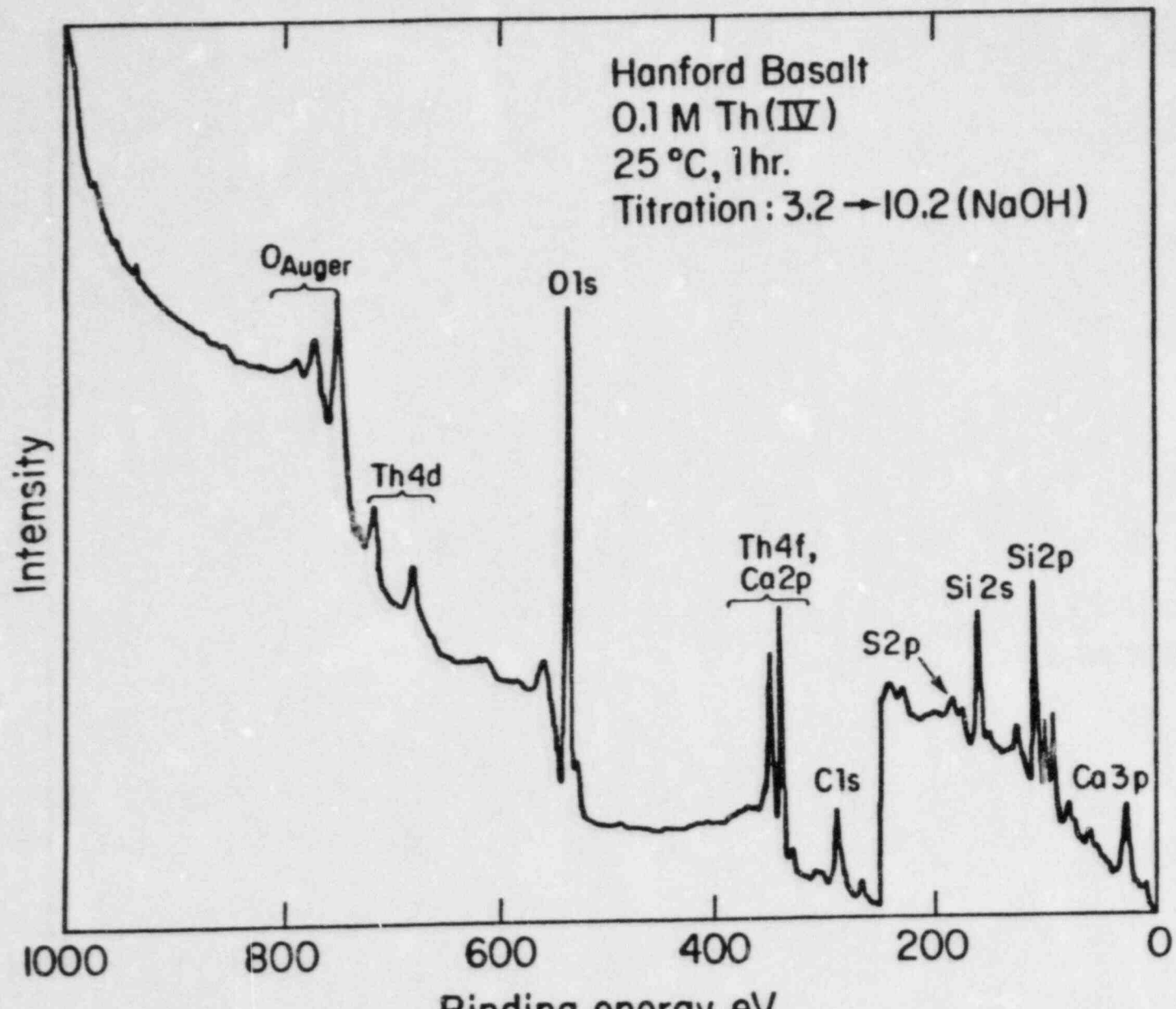

Figure 1. The X-ray photoelectron spectrum of TH(IV) on Hanford basalt.

XBL 837-2148

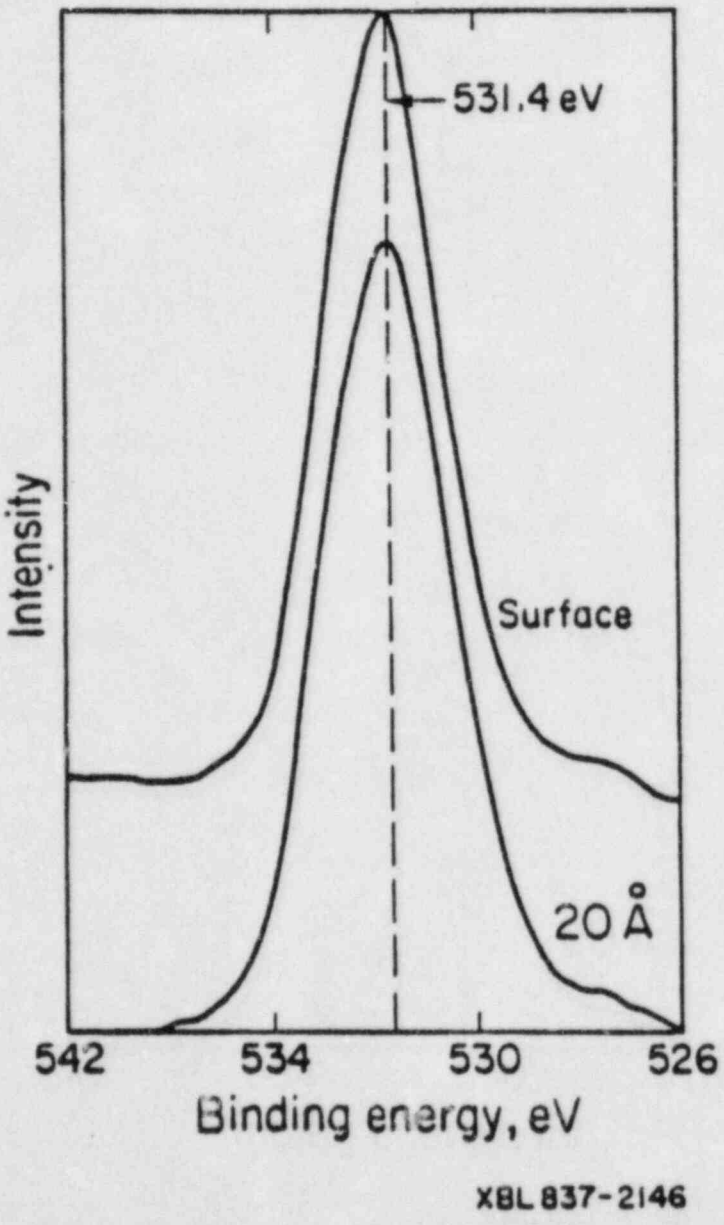

Figure 2. The oxygen 1s photoelectron spectrum of Th(IV) on Hanford basalt.

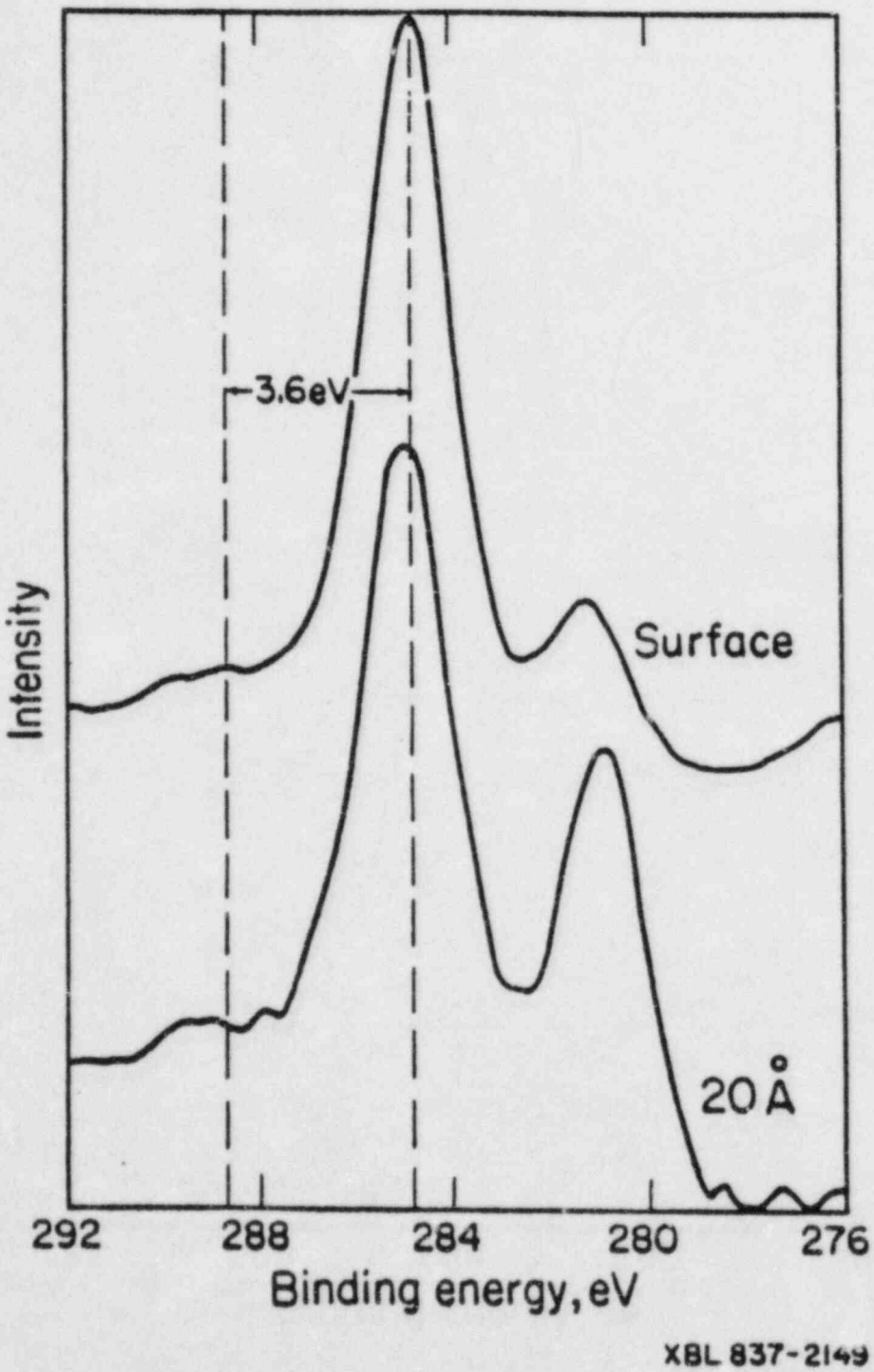

Figure 3. The carbon 1s photoelectron spectrum of Th(IV) on Hanford basalt.

On ion sputtering away ~20Å (relative to a Ta_2O_5 standard) of the basalt surface, the concentration of thorium remained unchanged at 2-4% (atomic concentration) of the surface being examined, thus indicating that the thorium species was not merely lightly chemisorbed but had instead penetrated into the rock bulk. Indeed, the thorium and carbon spectra in Fig. 2 and 3 showed virtually no change between the surface layer and the layer remaining after 20Å had been removed. Variable take-off angle x-ray photoelectron spectra (4) taken of this sample surface also indicated significant penetration into the sample bulk. These data are consistent with a process involving the chemisorption of CO_2 onto (and subsequent reaction with) a hydrated thorium oxide ($ThO_2 \cdot xH_2O$, or "$Th(OH)_4$"), thus forming a mixed oxide/hydroxide-carbonate. This reaction phenomenon has been reported previously for plutonium (5) in the research literature.

Data such as these are extremely important, since a thorough knowledge of the radionuclide species is important in dissolution experiments of actinide and radionuclide species that have been experimentally shown to actually be formed on basalt. Modeling of precipitation/dissolution processes using only a single species such as ThO_2, for example, would not be correct. In the course of this research, we have also shown that the chemical characteristics of any thorium hydrolysis polymers generated at high pH values such as those found in groundwater will change rather dramatically with respect to their thermal and chemical history (6).

2.2.2.2 Uranium(VI)/Basalt Interaction

In the study of the uranium(VI)/Hanford basalt reaction, the experimental conditions were the same. As with the thorium(IV)/basalt system, both the bulk precipitate resulting from the high pH (10-12) hydrolysis of the uranium and the Hanford basalt surface were studied using surface and bulk-oriented spectroscopic approaches. The compositions of the surface of the Hanford basalt and the accompanying precipitates were identical in terms of species present with the exception of the concentration of rock-inherent metal ions such as aluminum and silicon sometimes varying in both the precipitate and on the basalt surface. Accordingly, the major research was aimed at a rigorous study of the hydrolysis products of uranium(VI) produced in high pH aqueous solutions under repository conditions.

All of the experiments were conducted using the dioxouranium(VI), or uranyl, ion, the most air-stable form

of uranium(VI) found in natural systems. Because of the rather large number of compounds and compound mixtures produced by varying the preparative procedure, two standard sets of hydrolysis products were prepared and used for all measurements for the present study. First, two different concentrations of the uranyl ion solution being hydrolyzed were used in order to determine if there was any initial uranyl ion solution concentration dependence on the final product. Second, variable counterions such as chloride, nitrate, and acetate were used in preparing the uranyl solutions at the two different concentrations so as to check for an anion dependency. The same hydrolysis precipitate for a given synthetic route was used to perform all analyses and spectroscopic studies in order that data for a particular preparation were comparable to those data for other different synthetic routes. For purposes of this study, the basalt was not used, since species from the rock material complicated the x-ray diffraction patterns and spectra of the samples containing the uranium(VI) species.

As expected, the complexes that resulted from the hydrolysis of the parent uranyl salts were of variable composition with respect to uranium oxide, uranyl hydroxides, cations such as sodium and ammonium, and water. Elemental analyses showed the precipitates to contain variable amounts of sodium or ammonium cations, while the thermolysis of the solids (monitored by mass spectrometry) also showed a variable water content for each of the samples. The elemental analyses were consistent with varying amounts of products of the type $UO_2(OH)_2 \cdot xH_2O$ and $UO_3 \cdot xH_2O$ for the base-effected hydrolysis products, with small amounts of sodium and ammonium ions being occluded in the lattice. X-ray photoelectron data (discussed below) also supported formulas of these types. When the initial precipitates were examined by energy dispersive x-ray spectroscopy and elementally mapped, some segregation of the sodium ion was observed; accordingly, all samples were ground using an agate mortar and pestle before spectroscopic measurements were made in order to assure a homogeneous bulk sample.

The analytical data for the NH_4OH-effected hydrolysis products were consistent with the previously reported complex of stoichiometry $3UO_3 \cdot 5H_2O$; again, however, this principal product was also found to be a mixture of forms of $UO_2(OH)_2$ contaminated with the ammonium cation, and the amount of water again varied from sample to sample.

All attempts to prepare one synthetically pure sample of uranyl hydroxide product which was contaminant-free were

unsuccessful. All NaOH--hydrolysis compounds contained approximately 3-5% sodium, regardless of the rate at which NaOH was added to the solution of the parent salt, the concentration of the parent salt, or the anionic counterion. The only exception of this was the hydrolysis of $UO_2Cl_2 \cdot 3H_2O$, in which the final hydrolysis product also always contained traces (1% or less) of the chloride ion. An examination of infrared spectra, wet chemical analyses, and other analytical and spectroscopic data failed to show any acetate or nitrate species after hydrolysis. The most consistently reproducible analytical results were obtained for the NH_4OH- effected compound; the hydrogen and nitrogen analyses, for example, were virtually identical for all three samples studied here. Also, the x-ray photoelectron spectral data discussed below would be consistent with minor amounts of other hydrolysis products being present as contaminants. Previous reports have noted that small changes in the structures of some of the hydrolysis products studied here can occur without being detected in the x-ray diffraction patterns. These changes would result in minor products that could not be easily detected.

In agreement with the results reported by previous investigators the initial precipitates consisted of the β - and γ-forms of $UO_2(OH)_2$ (Fig. 4 and 5) and $UO_3 \cdot 2H_2O$. Infrared and x-ray powder diffraction data were in excellent agreement with those previously reported for these compounds.

The x-ray photoelectron data for the hydrolysis products (Tables I and II) support the presence of uranium species of the uranyl oxide and hydroxide type. Samples A-F were prepared by hydrolysis of uranium(VI) with 1.0 M NaOH, while samples G-I were prepared by hydrolysis of uranium(VI) with 1.0 M NH_4OH; multiple samples were prepared in order to check for consistency in the hydrolysis products. The oxygen 1s averaged binding energies vary from 530.8 to 531.9 eV; they can be further deconvoluted in some cases (Table II) into the oxide and hydroxide component lines. This range of values encompasses the set of binding energies which are usually observed in the 531.0 - 531.6 eV range and assigned to the carbonate functional group. The actual O 1s binding energy for a typical uranyl carbonate such as $K_4UO_2(CO_3)_3$ is 530.6 eV, which also coincides with the "oxide" component of the doublets tabulated in Table II. Because of the basicity of the uranium hydrolysis products studied here, chemisorption of carbon dioxide from the atmosphere by the samples and subsequent complexation as a uranyl carbonate cannot be precluded. As mentioned above, other researchers have observed the absorption of CO_2 by other basic actinide complex surfaces such as plutonium(IV)

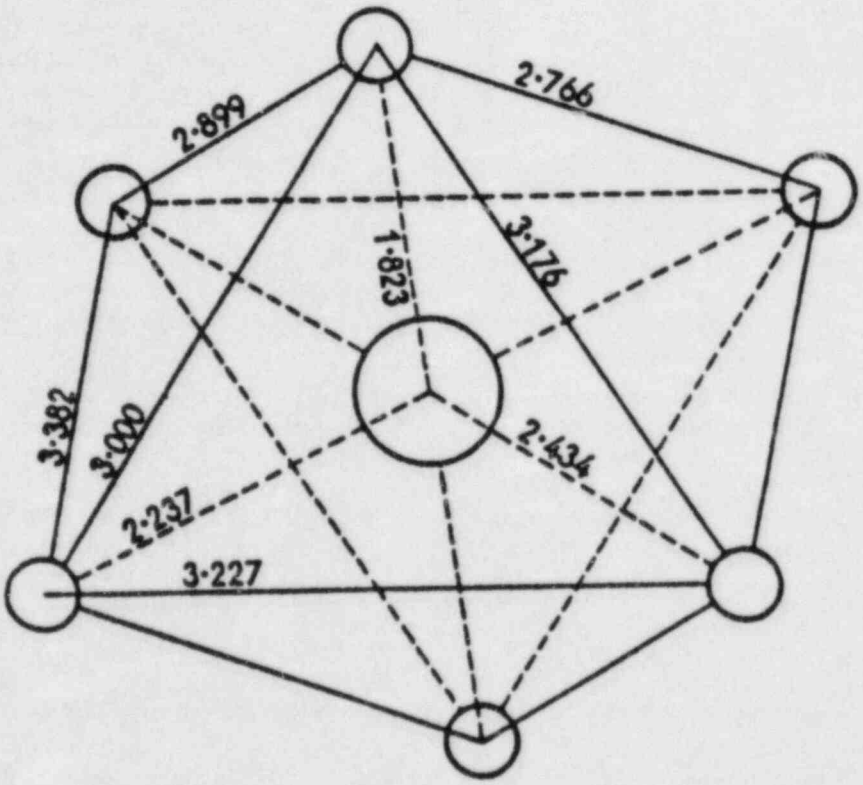

Figure 4. Interatomic distances (Å) in an isolated octahedron of β-$UO_2(OH)_2$. [Taken from R. B. Roof, D. T. Cromer, and A. C. Larson, Acta Cryst., 17, 701(1964).]

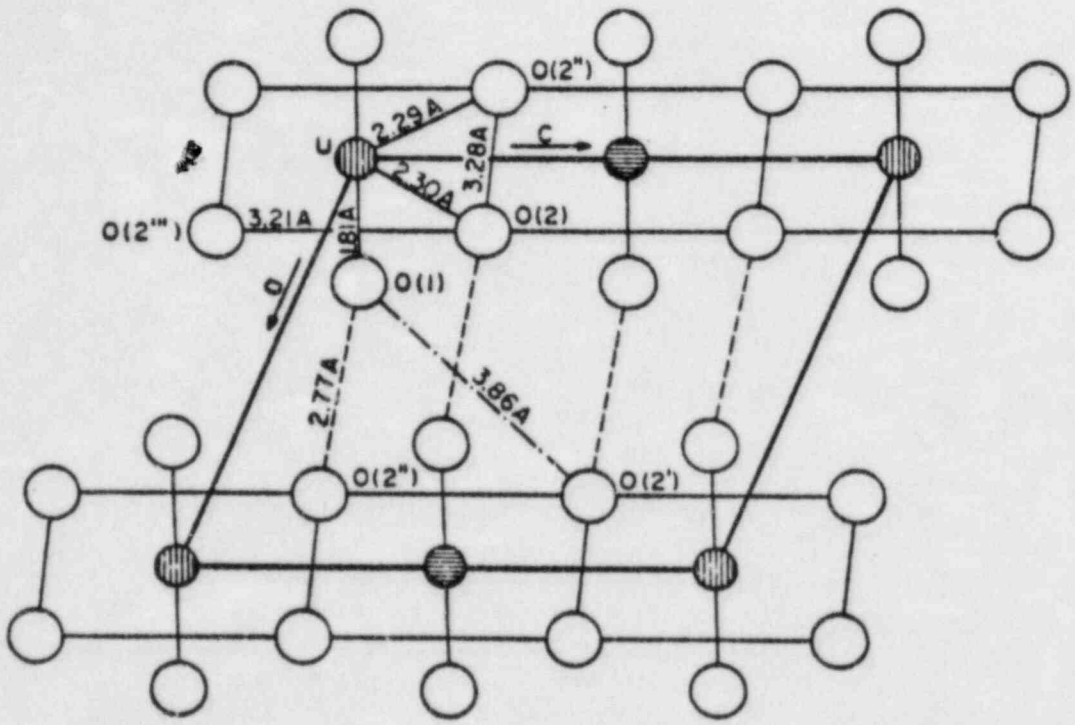

Figure 5. Interatomic distances (Å) in the structure of γ-$UO_2(OH)_2$ shown for several octahedra. [Taken from S. Siegel, H. R. Hoekstra, and E. Gebert, Acta Cryst., B28, 3469(1972).]

Table I. Binding Energies[a,b] of Uranyl Salts and Their Hydrolysis Products.

Sample	O 1s	U $4f_{7/2}$	U $4f_{5/2}$
$UO_2Cl_2 \cdot 3H_2O$	531.9 (2.3)[c]	382.3 (2.4)[c]	393.0 (2.4)[c]
$UO_2(NO_3)_2 \cdot 6H_2O$	532.1 (2.8)	382.1 (3.9)	392.8 (3.9)
$UO_2(CH_3COO)_2 \cdot 2H_2O$	531.9 (2.4)	382.5 (3.2)	393.3 (3.3)
A	530.8 (2.8)	381.5 (2.9)	392.3 (2.6)
B	530.8 (2.6)	381.5 (2.9)	392.4 (2.5)
C	531.1 (3.0)	381.8 (2.7)	392.6 (2.7)
D	531.1 (3.0)	381.8 (2.6)	392.5 (2.5)
E	531.0 (2.9)	381.8 (2.8)	392.4 (2.6)
F	530.9 (3.1)	381.6 (2.5)	392.4 (2.4)
G	530.8 (2.9)	381.7 (2.6)	392.2 (2.6)
H	531.2 (3.0)	381.8 (2.7)	392.0 (2.6)
I	531.9 (3.0)	381.8 (2.7)	392.4 (2.6)

[a]Electron volts, eV.

[b]Calibrated against the adventitious carbon line taken as C 1s = 284.6 eV.

[c]Numbers in parentheses represent the full width at half maximum (FWHM) of the photoelectron line, in eV.

Table II. Binding Energies[a,b] of the Deconvoluted Oxygen 1s Photoelectron Lines of NaOH-Promoted Uranyl Hydrolysis Products.

Sample	O 1s (I)[c]	O 1s(II)[d]	Width[e]	Area Ratio (I/II)
A	(f)	(f)	(f)	(f)
B	530.4	531.1	2.3	1:2.2
C.	530.1	531.5	2.1	1:1.7
D	530.2	531.4	2.3	1:2
E	530.2	531.5	2.3	1:1.4
F	530.2	531.3	2.7	1:1.7

[a]Electron volts, eV.

[b]Calibrated against the adventitious carbon line taken as C 1s = 284.6 eV.

[c]Lattice "oxide" value; please see text.

[d]Lattice "hydroxide" value; please see text.

[e]Full width at half maximum, FWHM, eV.

[f]Could not be fitted as two peaks.

polymers formed by the NaOH effected hydrolysis of plutonium(IV) salts in aqueous solutions (5); this in effect forms Pu(IV) carbonate complexes as surface layer complexes with oxide/hydroxide, and the same reaction occurs here to some extent.

Indeed, there is tentative evidence in this study to support such a phonomenon with the present series of hydrolysis products. First, the elemental analyses always indicate a certain amount of bulk carbon to be present in the samples, the carbon content increasing slightly upon standing in the open air for several weeks. Second, small infrared bands or inflections at 890 and 1350 cm^{-1} that appear in the spectra of the Pu(IV) polymers (5) also appear in the infrared spectra of the uranyl hydroxide samples studied here. A reaction of this type should not be unexpected for the basic uranium hydrolysis products studied here, especially in light of their similarity to the Pu(IV) polymers. Also, many metal hydroxides such as $Pb(OH)_2$ also exhibit carbonate layers in their x-ray photoelectron spectra (7).

2.2.3. OTHER RESEARCH IN PROGRESS AND PLANNED RESEARCH

Several other areas of research related to chemical species in waste repository environments are currently ongoing at Lawrence Berkeley Laboratory. Research has been conducted on the identification of lead oxides (7) by using x-ray photoelectron and Auger spectroscopy. Studies are also being conducted on hydrolysis products of uranium (8) such as $[(UO_2)_2(OH)_2]^{2+}$ that are formed at high pH under nuclear waste repository conditions, europium (a component of PNL 76-68 borosilicate glass) oxides and carbonates and their interaction with water (9), and uranium/EDTA complexes (10) which have been implicated in the migration of uranium and other radionuclides from nuclear waste burial sites (11). Research is also being conducted on radionuclide interaction with clays and silicate glasses in order to understand the solubility of the waste package containing the radionuclides and subsequent reactions with backfill material.

In almost any scenario involving the migration of radionuclides from a repository site, the dissolution of the radionuclide species in groundwater as an initial step in the process before migration occurs. Possibly just as important, however, is the interaction of these aqueous radionuclide solutions with other canisters that have not yet been breached. Metals ions that are leached from the canister material will contribute new chemical

species to the solution, thus changing the chemistry of the aqueous migrating solutions. The chemical interaction of radionuclides and metal ions with the canister material also can be extended to include the interaction of ions in the groundwater that will attack the canister at high temperatures before canisters might be breached. These studies will lead to new insight into mechanisms and kinetics of canister corrosion and degradation under repository conditions.

Research at Lawrence Berkeley Laboratory had addressed the problem of radionuclide/canister interaction using surface techniques such as Auger and X-ray photoelectron spectroscopy. Preliminary evidence has shown that potential canister materials such as 304L stainless steel are degraded as a function of time, temperature, anion form, etc. when reacted with uranium. Surface phenomena of the reacted stainless steel have been studied as well as precipitated uranium crusts that form on the surface. The different chemistries of both the surface and the resulting uranium complexes have been compared as a function of different experimental parameters such as those listed above.

An equally important area of ongoing research at Lawrence Berkeley Laboratory is the study of oxidation-reduction analogues of actinides. Research here has shown that the thermally-induced oxidation/ decarboxylation of cerium (III) carbonates does not produce only a cerium (IV) oxide; instead, a mixed cerium (III,IV) complex of oxide and carbonate species is produced. This has quite significant effects on attempts at modeling radionuclide dissolution/ migration, since both mixed oxidation state and anionic forms will be involved in the dissolution process.

2.2.4. RECOMMENDATIONS

Further studies will have to be conducted in the area of radionuclide interaction with Hanford basalt and Nevada Test Site tuff. First, better identification and documentation of the chemical species produced on the rock surfaces will have to be made. While it is extremely significant that a mixed hydroxide/carbonate complex is present on the surface of Hanford basalt reacted with thorium, uranium, and other radionuclides, virtually no data currently exist in the literature on the chemisties of these species. Data in the x-ray photoelectron and other spectroscopic literature refer only to them as "hydroxide/carbonate complexes"; there are no data at present to routinely determine exactly which complex is present. Also, dissolution mechanism

studies are difficult to conduct on radionuclide species without knowing what one is actually dissolving. Mere guesses will only result in models that are incorrect.

Second, a better understanding of the actual solubility of these species is needed. This can be obtained by studying the dissolution of the species from the basalt or tuff under different geochemical conditions by monitoring the changes in the concentration of a radionuclide on a rock surface, in the rock bulk, and in the solution with which the rock material is reacting. This can be accomplished by using surface techniques as well as more conventional solution analytical techniques such as atomic absorption spectroscopy to monitor the radionuclide solutions.

Third, the absolute rates of migration into and out of the rock bulk must be experimentally determined. Again, by careful monitoring of the rock and solution involved in the interaction, this can be determined quite accurately by numerous spectroscopic techniques that can be applied to surface and solution quantitative analyses.

Fourth, the chemistry of these systems, their reactions under reducing environments (as might be found in conjunction with pyrite, for example), and how the subsequent reaction products migrate will also have to be studied. Chemical environments in which redox reactions are possible will almost certainly result in different radionuclide species (such as mixed oxidation species if higher oxidation state radionuclides are involved) being formed and thus different migration rates. These problems and approaches are all currently being addressed at Lawrence Berkeley Laboratory in order to better understand radionuclide migration processes in Hanford basalt and Nevada Test Site tuff.

ACKNOWLEDGMENTS

The author wishes to thank Ken Bomben for performing the curve fitting of the x-ray photoelectron data, Helena Ruben for measuring the x-ray powder diffraction patterns, and Leon Tsao for preparation of the uranium and thorium/Hanford basalt samples.

2.2.6. REFERENCES

1. Siegbahn, K., "Atomic and Solid State Structure Studied by Means of Electron Spectroscopy", Almquist and Wiksells, Upsala, 1967.

2. Alford, N. A., A. Barrie, I. W. Drummon, and Q. C. Herd, "Auger Electron Spectroscopy (AES). An Appraisal", Surface and Interface Analysis, vol. 1, pp. 36-44, 1979.

3. Perry, D. L., D. W. Bonnell, G. D. Parks, and J. L. Margrave, "Spectroscopic Studies of High Temperature Materials. I. The Use of X-Ray Photoelectron Spectroscopy (XPS) to Study the Surface Chemistry of Copper, Cobalt, and Nickel Ferrites", High Temperature Science, vol. 9, pp. 85-98, 1977.

4. Ebel, M. F. and UJ. Wernisch, "Shading at Different Take-off Angles in X-Ray Photoelectron Spectroscopy", Surface and Interface Analysis, vol.3, pp. 191-193, 1981.

5. Toth, L. M. and H. A. Friedman, "The Infrared Spectrum of Pu(IV) Polymer", Journal of Inorganic and Nuclear Chemistry, vol. 40, pp. 807-810, 1978.

6. Perry, D. L., H. G. Brittain, and L. Tsao, "Luminescence of the Hydrolysis Products of Th(IV)", Journal of Luminescence, vol. 28, pp. 257-265, 1983.

7. Perry, D. L., L. Tsao, and J. A. Taylor, "An X-Ray Photoelectron Study of the Oxidation of Lead", Proceedings of the 30th National Symposium of the American Vacuum Society, Boston, 1983.

8. Perry, D.L., "Infrared and X-Ray Photoelectron Evidence for a Cation Stabilized Hydroxy-Bridged Uranyl Species, $[(UO_2)_2(OH)_2]^{2+}$", Inorganica Chimica Acta, vol. 65, pp. L209-211, 1982.

9. Perry, D.L. and H.B. Brittain, "Luminescence Studies of Europium Oxide Surface Species. Surface Oxide vs. Surface Hydroxides and Carbonates", Journal of Catalysis, vol. 77, pp. 94-103, 1982.

10. Perry, D.L., "Solid State Spectroscopic Studies of the Uranyl-EDTA System", 179th National Meeting of the American Chemical Society, Houston, 1980.

11. Means, J.L., D.A. Crerar, and J.O. Duguid, "Migration of Radioactive Wastes: Radionuclide Mobilization by Complexing Agents", Science, vol. 200, pp. 1477-1481, 1978.

2.3 THERMODYNAMIC PROPERTIES OF CHEMICAL SPECIES OF WASTE RADIONUCLIDES

R.J. Silva and H. Nitsche

Earth Sciences Division
Lawrence Berkeley Laboratory

ABSTRACT

An experimental program has been initiated at LBL to identify and investigate key thermodynamic properties of chemical species of waste radionuclides that are important to the control of solution concentrations and migration rates in an underground repository setting. Precipitation of stable solid phases will retard the migration of radionuclides relative to the average velocity of groundwater; on the other hand, formation of aqueous complexes will tend to reduce this retardation effect. Thus, it is important in the assessment and predication of amounts and rates of release of waste radionuclides from an underground facility as required for licensing by 10CFR60 that all major compounds and solution complexes be included and reliable thermodynamic data on solubilities and complexation be used in modelling calculations.

The object of the program is to identify gaps or conflicts in thermodynamic data on the solubilities of compounds and on the formation of solution complexes of waste radionuclides needed for the reliable prediction of solution concentrations. It involves laboratory measurements necessary to (1) generate specific new data, where none exists, in order to demonstrate the importance of a particular solution species, compound or solution parameter (e.g. temperature, Eh, etc.) and to (2) resolve conflicts in existing thermodynamic data on important species or compounds.

The measurement of the solubility of $AmOHCO_3$ in 0.1 M $NaClO_4$ at 25°C and 1 atmosphere pressure has been completed. From the experimental data, an average solubility product quotient, Q_{sp}, was evaluated for the reaction,

$$AmOHCO_3\ (S) + 2H^+ = Am^{3+} + HCO_3^- + H_2O$$

The logarithm of Q_{sp} was calculated to be 2.74 $\pm$.17.

Speciation calculations, using this new data plus reported data on the solubility of $Am(OH)_3$ and the hydrolysis and carbonate complexation of Am^{3+}, indicate that the presence of carbonate can have a substantial effect on the nature of compounds and solution species formed by americium in ground waters. Since actinides in a given oxidation state tend to exhibit similar chemical properties, this reslt should apply to other actinides in the trivalent state. Thus, the effect of carbonate on the solubilities and complexation of trivalent actinides should be included in any predictive modelling studies required for licensing.

2.3.1 INTRODUCTION

In the event that the canister and waste form fail to contain radioactive waste materials, radionuclides will enter the local groundwater system. The radionuclides will react with various components of the groundwater, dissolved waste form materials, and the host rock to form insoluble compounds and solution complexes that can control concentrations and migration rates of the waste radionuclides. Since the time scale being considered is a 1000 years or longer, predictions based on realistic modelling studies provide the main avenue of assessment. Thus, reliable data on the nature and solubilities of compounds as well as the nature and formation constants of complexes of the waste radionuclides that form in natural systems are needed as a first step in the assessment and prediction of the amounts and rates of release of radionuclides from a proposed underground repository.

2.3.1.1 Issue Addressed By This Research

The primary issues concerning radionuclide containment in the near-field that are related to their chemical behavior are:

When, how, and at what rate are radionuclides released from the backfill? The near-field?

What are the important phenomena governing radionuclide migration in the near-field?

In addition to the primary issues, there are certain specific issues that are addressed in the program. They are:

What are the expected solubilities of released radionuclides versus time in the near-field?

What are the maximum concentrations of a given radionuclide expected in the back-fill and near-field over time and as a function of temperatures? How are these concentrations controlled?

How does speciation affect radionuclide solubilities?

How will the groundwater composition affect complexing and the solubilities of radionuclides?

2.3.1.2 Background

Computer models have been developed which predict the composition of radioactive waste in spent fuel and high-level reprocessed waste (Blomeke, 1974). Computer calculations show that the actinides, U-Cm, are major contributors to the radioactivity of the waste for storage times of 10^3 years or greater (Little, 1977; Barney, 1980). A number of inorganic components will be present in groundwaters which can form insoluble compounds and solution complexes with the actinides, e.g., hydroxide, carbonate, phosphate, fluoride, silicate and sulphate (Allard, 1982). While some thermodynamic data are reported in the literature on appropriate actinide compounds and solution complexes, there are serious gaps in the data bank and conflicts in reported values (Apps, et al., 1982). Since hydroxide and carbonate are common to all groundwaters, these anions are expected to play a dominant role in determining the speciation and solubilities of the important actinides (Allard, 1982; Moody, 1982). However, reliable thermodynamic data on the solubilities of trivalent actinide carbonate compounds and tetravalent actinide carbonate complexes are lacking.

Most of the available thermodynamic data on solubility product and complex formation constants come from measurements made at room temperature, however, elevated temperature may be present in a repository. Since solubilities and complexation are in general a function of temperature, measurements of the solubilities of critical actinide compounds and solution complexes as a function of temperature should be made in order to assess the relative importance of this parameter.

2.3.1.3 Objectives and Scope

The objective of this program is to identify gaps or conflicts in thermodynamic data on the solubilities of compounds and on the formation of solution complexes of the important waste radionuclides critical to the reliable prediction of the radionuclide solution concentrations in waste repository settings. It involves laboratory measurements necessary to (1) generate specific new data, where none exists, in order to demonstrate the importance of a particular species, compound or solution parameter (e.g., temperature) and to (2) resolve conflicts in existing thermodynamic data on important species or compounds. The information generated by this program will be such that it can be used by NRC to evaluate the adequancy of and provide guidance to DOE efforts.

2.3.2 THE EFFECT OF CARBONATE ON THE SOLUBILITY OF TRIVALENT AMERICIUM IN AQUEOUS SOLUTION

Data on trivalent lanthanide carbonates (Smith, 1976), good analogs for trivalent actinides, suggest that the carbonates of the latter should be quite insoluble. These compounds could be

2.3.2 THE EFFECT OF CARBONATE ON THE SOLUBILITY OF TRIVALENT AMERICIUM IN AQUEOUS SOLUTION (Continued)

important in the control of actinide solution concentrations but no data have been reported. The object of the work described here was to investigate the solubility of a trivalent actinide, americium, in an aqueous carbonate system.

2.3.2.1 Methods

2.3.2.1.1 Preparation and Characterization of Solid Phases

The preparation of rare earth carbonates via the formation and subsequent hydrolysis of the trichloroacetate complex in aqueous solution is a well established method for producing a pure, easily filterable and crystalline material (Salutsky, 1950; Head, 1963). The exact nature of the rare earth carbonate depends on the atomic number of the rare earth and is quite sensitive to the preparative conditions, e.g. temperature, CO_2 pressure and the washing procedure. The octahydrate, $R_2(CO_3)_3.8H_2O$, is usually formed by the first numbers of the rare-earth series, e.g., La, while the dihydrate, $R_2(CO_3)_3.2H_2O$, is usually formed by the middle and end members of the series, e.g., Nd-Yb. (Head, 1964). Charles has also reported that, even using the same procedures and conditions, some rare earths form the dihydrate, e.g., Nd, while others form the basic carbonate, $ROHCO_3$, e.g. Pr (Charles, 1965). The compounds are, however, usually pure. Because of these complications, it seemed prudent to first test the preparative method and the stability of the resulting solid phase with neodymium, a good analog element for americium.

Approximately 10 mg of neodymium carbonate was prepared by the trichloroacetate method. The d-spacings and relative intensities derived from an x-ray powder diffraction pattern of the material are given in Table 1 under Nd solid phase I. Head and Holley have investigated the preparation and thermal decomposition of the rare earth dihydrates (Head, 1963; Head, 1964). These elements were stated to form dihydrates that were isostructural and that had similar X-ray powder diffraction patterns. Unfortunately, these patterns were not published. However, an original x-ray film containing the powder diffraction pattern of the $Nd_2(CO_3)_3 \cdot 2H_2O$ (assigned from the results of chemical analysis) was recently obtained from C.E. Holley of LANL and analyzed. The d-spacings and relative intensities are given in Table 1. Our material appeared to be pure, microcrystalline $Nd_2(CO_3)_3.2H_2O$.

The $Nd_2(CO_3)_3.2H_2O$ solid was then placed in a polypropylene cell containing an aqueous solution composed of 0.1 M $NaClO_4$ and 2×10^{-4} M HCO_3^- at a pH of 6.12. After a contact time of 3 weeks, an x-ray powder diffraction pattern was again obtained on the solid. The resulting powder pattern is given in Table 1 under Nd solid phase II. The pattern was distinctly different from that of the Nd solid solid phase I but

Table 1. Comparison of X-ray Powder Diffraction Patterns of Nd Solid Phases and Reported Patterns.

Nd Solid Phase(I)		$Nd_2(CO_3)_3.2H_2O$[a]		Nd Solid Phase(II)		$NdOHCO_3$[b]	
d(Å)	I[c]	d(Å)	I[c]	d(Å)	I[c]	d(Å)	I[d]
7.69	m	7.56	m	5.50	w	5.50	30
5.80	s	5.68	s	4.28	s	4.28	100
4.73	s	4.67	s			4.24	15
3.99	s	3.93	s	3.67	m	3.68	35
3.88	w	3.83	w			3.65	25
3.66	m	3.62	m	3.31	w	3.32	35
3.13	w	3.09	s			2.94	25
3.05	s	3.02	s	2.92	m	2.91	50
		3.98	w	2.63	w	2.63	30
		2.87	w	2.48	w	2.48	25
2.77	w	2.75	w	2.40	w	2.40	10
2.61	m	2.58	s	2.32	w	2.32	40
		2.25	w			2.31	18
		2.17	w	2.05	m	2.05	40
		2.08				2.03	13
2.03	m	2.02	m	1.99	m	1.98	40
1.99	w	1.98	w	1.93	w	1.93	25
1.88	m	1.87	m	1.88	w	1.88	10
1.84	m	1.83	m	1.83	w	1.83	19
1.79	m	1.78	m				
1.75	m	1.74	w				
1.57	w	1.56	m				

(a) Holley, 1983.
(b) Dexpert, 1974.
(c) Relative intensities visually estimated. S = Strong; m = medium; w = weak.
(d) Relative intensities by diffractometer.

2.3.2.1.1 Preparation and Characterization of Solid Phases (Continued)

nearly identical to the powder pattern reported for $NdOHCO_3$-Type A (Dexpert, 1974). There was no longer any evidence in the pattern for $Nd_2(CO_3)_3.2H_2O$. The starting material had converted to the basic carbonate during the 3 week contact time. Apparently, the basic carbonate is more stable than the normal dihydrate under our solution conditions.

An attempt was made to prepare $Am_2(CO_3)_3.2H_2O$ by the same procedure as was used to prepare the $Nd_2(CO_3)_3.2H_2O$. However, the X-ray powder diffraction pattern of the resulting Am compound was very similar to that of the $NdOHCO_3$ and not $Nd_2(CO_3)_3.2H_2O$. The preparation of the solid was repeated with the Am and the X-ray diffraction analysis of the solid gave a pattern again similar to the Nd basic carbonate. The d-spacings and relative intensities obtained from the pattern are given in Table 2 under Am solid phase I. Since the results with Nd suggested that the basic carbonate is more stable than the dihydrate in our aqueous carbonate system, no further attempts were made to produce the normal carbonate dihydrate of Am. It seemed more appropriate to measure the solubility of the basic carbonate of americium.

2.3.2.1.2 Solubility Measurements

The solubility studies with trivalent americium were conducted in two parts. The first involved following to steady state the concentration of Am in a solution initially free of the element, i.e. undersaturation with respect to precipitation, but which had been placed in contact with the solid phase $AmOHCO_3$. The second involved following to steady state the concentration of Am in a solution initially supersaturated in Am with respect to the precipitation of a solid phase but no solid initially present. Much of the equipment and techniques used in these measurements have been described elsewhere (Silva and Yee, 1982).

In order to obtain a reliable value for the solubility product quotient for the reaction,

$$AmOHCO_3(s) + 2H^+ = Am^{3+} + H_2O + HCO_3^-,$$

the pH range available for measuring the solubility was somewhat limited. It was necessary to keep the pH to less than about 6.5 to avoid significant hydrolysis of the Am^{3+} ion but greater than about 5 to avoid possible dissolution of all of the available starting solid (8 mgs). In addition, the CO_3^{2-} concentration was set sufficiently low so as to avoid significant carbonate complexation of the Am^{3+} ion, i.e., $\sim 10^{-8}$M. A pH of 6.12 was selected as it is within a reasonably well buffered region where the concentrations of H_2CO_3 and HCO_3^- are equal. A computer controlled pH-stat was used to maintain a pH near this value. The bicarbonate,

Table 2. Comparison of X-ray Powder Diffraction Patterns of Am Solid Phases

Am Solid Phase(I)		Am Solid Phase(II)		Am Solid Phase(III)	
d(Å)	I[a]	d(Å)	I[a]	d(Å)	I[a]
5.51	w	5.50	w	5.51	w
4.28	s	4.28	s	4.28	s
3.68	m	3.67	m	3.67	m
3.32	w	3.31	m	3.33	w
		2.94	w		
2.92	m	2.92	m	2.91	m
2.63	w	2.64	w	2.64	w
2.48	w	2.48	w	2.48	w
2.40	w	2.40	w	2.41	w
2.33	m	2.34	m	2.33	m
		2.32	w		
		2.13	w	2.13	w
2.05	w	2.05	m	2.05	m
1.98	w	1.99	w	1.99	w
1.93	w	1.93	w	1.92	w
		1.89	w		
		1.84	w		

(a) Intensities visually estimated. s = strong; m = medium; w = weak.

2.3.2.1.2 Solubility Measurements (Continued)

and thus carbonate, ion concentration was fixed by maintaining a gas mixture of 0.792 + .010% CO_2 and 99.3% Ar over the aqeuous phase. The equilibrium concentrations of bicarbonate and carbonate ions in the aqueous phase under these conditions were calculated to be 2.05×10^{-4} M and 2.25×10^{-8} M, respectively, using the carbonate equilibrium quotients for 0.1 M ionic strength given in Table 5. To fix the ionic strength, an aqueous solution of 0.1 M $NaClO_4$ was used as supporting electrolyte. Two titrations of 50 mls of the aqueous phase at starting pH values of 6.14 with 0.100 M HCl to the end point of the HCO_3^- to H_2CO_3 conversion were made prior to the initiation of the solubility experiments. From the results, the bicarbonate ion concentration was calculated to be $2.67 \pm .16 \times 10^{-4}$ M. The bicarbonate ion concentration was calculated to be $2.15 \pm .17 \times 10^{-4}$ M from the CO_2 partial pressure in the gas mixture.

2.3.2.1.3 Solubility Measurements from Unsaturation

Approximately 8 mgs of the crystalline $AmOHCO_3$ were placed in the polypropylene cell with 50 mls of the aqueous phase at 25±1°C and 1 atmospherepressure. The cell was rotated continuously at 150 rpm with an orbit shaker. The solution concentration of the Am was then followed to steady state. Two 1 ml aliquots of the aqeuous phase were taken after 1, 3, 7, 14, 21, and 30 days equilibration time. After centrifugation at 15,000 RPM for 15 minutes, measured portions of the aliquots were taken and acidified in counting vials. The Am concentrations were determined from the results of liquid scintillation counting of these portions. For our centrifuge system, it was estimated that particles of about 0.1 μm diameter and larger should be removed from solution (Svedberg, 1940). The pH meter and electrode were recalibrated with buffers after each sampling period. The beta-emitting daughter, ^{239}Np, was found not to be in nuclear decay equilibrium with the ^{243}Am in solution at the times of sampling. Because the ^{239}Np adds to the measured total count rates of the aliquots, the samples required counting periodically for 3-4 weeks to allow secular equilibrium to be established so the appropriate counting corrections for the Np could be made.

At the end of the 30 day period, two additonal 5 ml aliquots of the aqueous phase were taken. After centrifugation, the aliquots were split into two fractions. On fraction, 2 mls, was passed through a 0.2 μm acrodisc filter while the other fraction, 3 mls, was passed through a 0.015 μm Nuclepore filter. The first one-half of the fraction through the filters were discarded and a measured portion of the remaining filtrate analyzed for Am by liquid scintillation counting.

Also, at the end of the 30 day period, the solid phase remaining in the cell was subjected to X-ray diffraction analysis. The results obtained from the powder are given in the Table 2 under $AmOHCO_3$(II). The powder pattern was identical to that of the starting material, $AmOHCO_3$(I). There was no change in the solid phase during these dissolution measurements.

2.3.2.1.4 Solubility Measurements from Supersaturation

At the conclusion of the first part of the studies described above, the aqueous phase in the cell was made 0.1M in $HClO_4$, by the addition of the acid to dissolve the remaining solid $AmOHCO_3$. The concentration of Am was determined as before. The results indicated that the solid phase had dissolved and that all of the Am initially present in the cell was in solution. The volume of the aqueous phase was adjusted to 50 mls by the addition of water and solutions of $NaHCO_3$ and NaOH in such a manner as to again produce an aqueous phase 0.1M in $NaClO_4$, 2×10^{-4}M in HCO_3^- and at a pH of 6.12. The remainder of the experiment proceeded as in the first part of these studies.

Aliquots of the aqueous phase were taken after 1, 3, 7, 14, 22, 31, 37, 44 and 51 days equilibration time in order to follow the Am solution concentration to steady state. At the 51 day period, in addition to separation of phases by centrifugation, aliquots were filtered as before. At this time, the solid phase that had precipitated was subjected to X-ray diffraction analyses. The information obtained from the powder pattern is given in Table 2 under $AmOHCO_3$(III). The powder pattern was identical to that of $AmOHCO_3$(I) and $AmOHCO_3$(II).

2.3.3 RESULTS

2.3.3.1 Solubility from Undersaturation

The results of the measurements of the solubility of the crystalline $AmOHCO_3$ are given in Table 3. The pH values given are the average values observed during each equilibration period. The errors in the pH values were estimated from the inherent reproducibility of measurements with the pH meter and electrodes, both on the dissolver solution and buffers, and the root mean square deviations of pH values (measured every two hours) from the averages. No corrections were made for liquid junction potential differences.

The values and errors assigned to the Am solution concentrations are the average and deviations from the average of the two aliquots taken at each sampling period.

The values of the bicarbonate concentrations were calculated from the partial pressure of CO_2 over the aqueous phase, i.e., $0.00792 \pm .0004$ atmospheres and the average pH value during the period using the carbonate equilibrium quotients given in table 5. The hydrogen ion activities obtained

2.3.3.1 Solubility from Undersaturation (Continued)

from the pH values were converted to concentrations using an activity coefficient of 0.78. The source of this value will be discussed later in this report.

Since the Am solution concentrations did not vary appreciably after the 7 day equilibration time, it was assumed that steady state had been achieved in the dissolution reaction. Some variation in the Am concentrations between equilibration times is due to differences in the pH.

The Am concentrations of the solutions passed through the two different pore size filters at the 30 day period agree to within experimental error. However, these values are only about 65% of the Am concentration of the centrifuged samples. Whether this difference was due to insufficient separation of solid and aqueous phases by our centrifugation system or due to loss of Am via adsorption of soluble species by the filters was not determined. Since the source of this discrepancy was not known, the three values were given equal weight in subsequent data analysis and the separation of solid and aqueous phases was considered to be adequate.

2.3.3.2 Solubility from Supersaturation

The results of the measurements of the solution concentrations of Am as a function of equilibrium time during the precipitation of $AmOHCO_3$ are given in Table 4. The values for the average pH, the Am concentrations and bicarbonate concentrations and their associated errors were obtained as described in the previous section.

As can be seen in Table 4, the Am concentrations decreased during the first month of the measurements but then remained relatively constant for the following 20 days. Therefore, it was assumed that steady state had been achieved.

As in the dissolution experiments, the Am concentrations measured for the filtered samples at the 51 day equilibration time agreed reasonably well but were only about 60 percent of the value measured for the centrifuged samples. The three values were given equal weight in subsequent data analysis. The separation of solid and aqueous phases was assumed to be adequate.

2.3.3.3 Evaluation of Solubility Product Quotients

Solubility product quotients, Q_{sp}, were calculated from the data given in Tables 3 and 4 for the following reaction,

$$AmOHCO_3(s) + 2H^+ = Am^{3+} + HCO_3^- + H_2O$$

Table 3. Results of Solubility Measurements by Dissolution of $AmOHCO_3$.

Equil. Time (days)	pH	Conc. Am (moles/l)	Conc. HCO_3 (moles/l)	Sol. Prod. Quot., Q_{sp}	log Q_{sp}
1	6.13±.03	$2.86\pm.25\times10^{-5}$	$2.09\pm.18\times10^{-4}$	$6.32\pm.10\times10^{3}$	3.80±.06
3	6.13±.03	$1.19\pm.04\times10^{-5}$	$2.09\pm.18\times10^{-4}$	$2.63\pm.36\times10^{3}$	3.42±.06
7	6.15±.03	$2.17\pm.54\times10^{-6}$	$2.19\pm.19\times10^{-4}$	$5.51\pm1.56\times0^{2}$	2.74±.11
14	6.13±.03	$2.39\pm.21\times10^{-6}$	$2.09\pm.18\times10^{-4}$	$5.28\pm.85\times10^{2}$	2.72±.06
21	6.14±.03	$2.02\pm.04\times10^{-6}$	$2.14\pm.19\times10^{-4}$	$4.79\pm.65\times10^{2}$	2.68±.06
30	6.14±.03	$2.29\pm.03\times10^{-6}$(a)	$2.14\pm.19\times10^{-4}$	$5.43\pm.73\times10^{2}$	2.73±.06
		$1.54\pm.13\times10^{-6}$(b)		$3.65\pm.58\times10^{2}$	2.56±.06
		$1.40\pm.13\times10^{-6}$(c)		$3.32\pm.55\times10^{2}$	2.52±.07

(a) Centrifugation; (b) centrifugation plus 0.2 μm filtration; (c) centrifugation plus 0.015 μm filtration.

Table 4. Results of Solubility Measurements by Precipitation of $AmOHCO_3$.

Equil. Time (days)	pH	Conc. Am (moles/l)	Conc. HCO_3 (moles/l)	Sol. Prod. Quot., Q_{sp}	log Q_{sp}
0	.009	$6.61\pm.21\times10^{-4}$	-	-	
1	6.09±.03	$3.66\pm.13\times10^{-4}$	$1.91\pm.17\times10^{-4}$	$6.14\pm.82\times10^{4}$	4.79±.06
3	6.11±.03	$3.15\pm.05\times10^{-4}$	$2.00\pm.18\times10^{-4}$	$6.07\pm.82\times10^{4}$	4.78±.06
7	6.12±.03	$3.56\pm.13\times10^{-4}$	$2.05\pm.18\times10^{-4}$	$7.35\pm1.02\times10^{4}$	4.87±.06
14	6.10±.03	$7.86\pm1.67\times10^{-5}$	$1.95\pm.17\times10^{-4}$	$1.41\pm.35\times10^{4}$	4.15±.10
22	6.13±.03	$7.67\pm.72\times10^{-6}$	$2.09\pm.18\times10^{-4}$	$1.70\pm.28\times10^{3}$	3.23±.07
31	6.14±.03	$3.21\pm.14\times10^{-6}$	$2.14\pm.19\times10^{-4}$	$7.60\pm1.07\times10^{2}$	2.88±.06
37	6.13±.03	$4.42\pm.17\times10^{-6}$	$2.09\pm.18\times10^{-4}$	$9.77\pm1.36\times10^{2}$	2.99±.06
44	6.13±.03	$4.71\pm.30\times10^{-6}$	$2.09\pm.8\times10^{-4}$	$1.04\pm.15\times10^{3}$	3.02±.06
51	6.11±.03	$4.88\pm.11\times10^{-6}$(a)	$2.00\pm18\times10^{-4}$	$9.40\pm13\times10^{2}$	2.97 ±06
		$3.65\pm.06\times10^{-6}$(b)		$7.03\pm.95\times10^{2}$	2.85±.06
		$3.20\pm.32\times10^{-6}$(c)		$6.16\pm1.03\times10^{2}$	2.79±.07

(a) Centrifugation; (b) centrifugation plus 0.2 μm filtration; (c) centrifugation plus 0.015 μm filtration.

Table 5. Thermodynamic Quotients Used in MINEQL Calculations for 25°C and 0.1 M Ionic Strength.

Reaction	log Q	Ref
$Am^{3+} + H_2O = AmOH^{2+} + H^+$	-7.7	Edelstein, 1982
$Am^{3+} + 2H_2O = Am(OH)_2^+ + 2H^+$	-16.6	Silva, 1982
$Am^{3+} + 3H_2O = Am(OH)_3^o + 3H^+$	-24.8	Silva, 1982
$Am^{3+} + 4H_2O = Am(OH)_4^- + 4H^+$	<35	Silva, 1982
$Am^{3+} + CO_3^{2-} = AmCO_3^+$	6.11	Lundquist, 1982
$Am^{3+} + 2CO_3^{2-} = Am(CO_3)_2^-$	10.1	Lundquist, 1982
$Am(OH)_3(s) + 3H^+ = Am^{3+} + 3H_2O$	16.5	Silva, 1982
$AmOHCO_3(s) + 2H^+ = Am^{3+} + HCO_3^- + H_2O$	2.74	this work
$CO_2(g) + H_2O = H_2CO_3$	-1.48	Harned, 1943
$H_2CO_3 = H^+ + HCO_3^-$	-6.12	Phillips, 1982
$HCO_3^- = H^+ + CO_3^{2-}$	-9.97	Phillips, 1982

2.3.3.3 Evaluation of Solubility Product Quotients (Continued)

The quotient is defined as,

$$Q_{sp} = \frac{m_{Am} \cdot m_{HCO_3}}{m_H^2}, \qquad (1)$$

where m refers to the molar concentrations. The concentration of hydrogen ion was taken to be,

$$m_H = \frac{a_H}{\gamma_H},$$

where a_H is the activity of H^+, derived from the measured pH, and γ_H is the activity coefficient estimated to be 0.78 for our solution conditions. The mean activity coefficients for 0.1 M HCl and 0.1 M $HClO_4$ are nearly the same, i.e. 0.80 (Robinson, 1959). The mean activity coefficient of HCl in 0.1M NaCl is 0.78 (Harned, 1958). Assuming a similar trend, the mean activity coefficient of $HClO_4$ in 0.1 M $NaClO_4$ was estimated to be 0.78.

The Am^{3+} ion can undergo some hydrolyses and carbonate complexation under our solution conditions. Therefore, it is necessary to estimate the degree of these reactions and correct the total Am solution concentrations given in tables 3 and 4 for hydrolysis and carbonate complexation to obtain values for the concentration of the free 3+ ion.

The first hydrolysis constant for Am^{3+} has not been measured, however, this quotient has been reported for Cm^{3+} at an ionic strength of 0.1 M (Edelstein, 1982). Since Am and Cm are adjacent actinides of nearly the same ionic radius, the value for Cm^{3+} should be a good approximation for Am^{3+}. The value for the hydrolysis quotient is given in table 5. From this quotient, the $AmOH^{2+}/Am^{3+}$ concentration ratio for a pH of 6.12 was calculated to be 0.021.

Data on the first and second formation constants, β_1, and β_2, for the carbonate complexes of Am^{3+} have been obtained from studies carried out in 1 M $NaClO_4$ (Lundquist, 1982). The reaction and β_1 for 1 M $NaClO_4$ are:

$$Am^{3+} + CO_3^{2-} = AmCO_3^+; \quad \beta_1 = \frac{m_{AmCO_3}}{m_{Am}\, m_{CO_3}} = 6.46 \times 10^5$$

2.3.3.3 Evaluation of Solubility Product Quotients (Continued)

Unfortunately there are no data on mean activity coefficients of appropriate Am salts in mixed electrolyte systems which could be used to correct the quotients obtained in 1 M $NaClO_4$ to 0.1 M $NaClO_4$. As the next best approximation, it was decided to use mean acitivity coefficients of $LaCl_3$-HCl mixtures that have been measured experimentally (Khoo, 1981). For dilute solutions of $LaCl_3$ in 1 M and 0.1 M HCl, mean activity coefficients of 0.34 and 0.46, respectively, were reported. The mean activity coefficient for appropriate carbonate species in a mixed electrolyte were estimated using Pitzer's equations (Pitzer, 1973). Ion interaction parameters used in the calculations for carbonate species (Pitzer and Mayorga, 1973) and $NaClO_4$ (Peiper and Pitzer, 1981) are reported in the literature. Single ion activity coefficients of 0.33 for CO_3^{2-} and 0.63 for Na^+ in 1 M $NaClO_4$ and 0.59 for CO_3^{2-} and 0.77 for Na^+ in 0.1 M $NaClO_4$ were calculated. The single ion activity coefficient for $AmCO_3^+$ was taken to be equal to that of Na^+. The value of β_1 in .1M $NaClO_4$ is related to that in 1 M $NaClO_4$ by the relationship,

$$\beta_1(.1\underline{M})\left(\frac{\gamma_{AmCO_3}}{\gamma_{Am}\gamma_{CO_3}}\right)_{.1\underline{M}} = \beta_1(1\underline{M})\left(\frac{\gamma_{AmCO_3}}{\gamma_{Am}\gamma_{CO_3}}\right)_{1\underline{M}}$$

The resulting estimate for $\beta_1(.1\underline{M})$ was 1.28×10^6. Using this quotient, a value for the $AmCO_3^+/Am^{3+}$ concentration ratio of 0.027 was calculated. Combining this ratio with that estimated for $AmOH^{2+}/Am^{3+}$, i.e. 0.021, it was estimated that 95% of the total Am in solution was as the free Am^{3+}. The total Am concentrations given in tables 3 and 4 were reduced by this percentage before the calculations of the Q_{sp}'s. The solubility product quotients calculated using equation (1) are given in tables 3 and 4 along with their logarithmic values.

2.3.3.4 Discussion

In order to test the effect of the presence of carbonate on the solubility of Am^{3+}, a series of speciation calculations were performed for several pH values and carbonate concentrations. Only the solid phases $Am(OH)_3$ and $AmOHCO_3$ were considered and only hydrolysis and carbonate complexing of Am^{3+} were considered. The reactions and constants used in the calculations are given in table 5. A mean value and least squares error of 2.74 ±.17 for the logarithm of the solubility product quotient for $AmOHCO_3$ was calculated from the six

2.3.3.4 Discussion (Continued)

values obtained at the final sampling times from both the dissolution and precipitation experiments, i.e. the centrifuged, centrifuged plus 0.2 μm filtered and centrifuged plus 0.015 μm filtered samples.

Since this analysis involves the solution of a number of coupled equations simultaneously, the calculation of the concentration of solution species and solubilities from the thermodynamic data were made using a computer program called MINEQL (Westall, 1976). MINEQL is a computer code designed to accept a list of components of a solution and their total analytical concentrations, solve the appropriate set of mass balance and equilibrium constant expressions, and produce a list of the identities and concentrations of all species formed by interactions among the components and between them and/or water. Data processing involves reading the input solution composition, identifying the complexes expected, fetching the required stability constants, and deriving the appropriate mass balance expressions. The resulting set of stability and mass balance expressions is solved by the Newton Raphson method, using the correctness of the mass balances as the criterion of successful solution.

Figure 1 shows a plot of the logarithm of the calculated concentrations of the various Am solution species (dashed curves) and the sum of the concentrations, i.e., the solubility line (solid curve). The solid curve is labelled with the stable solid phase. This calculation represents the basis line for the absence of CO_2. Figure 2 shows a similar plot for a partial CO_2 pressure of $10^{-3.5}$ atmos. (Normal concentration in air). Figures 3 and 4 show plots for constant total carbonate concentrations of 2×10^{-3} M, and 2×10^{-4} M, respectively, concentrations within the range of most groundwaters.

2.3.4 CONCLUSIONS

The results of the measurements and MINEQL calculations lead to the following conclusions:

(1) The presence of carbonate, at normal groundwater concentrations, can have a substantial effect on the nature (and solubility) of Am compounds as well as solution species.

(2) The solid phase $AmOHCO_3$ is predicted to be more stable than $Am(OH)_3$ over the pH range 6 to 9.5. Factors of 10 to 10^4 lower solubilities (depending on the pH and carbonate concentration) compared to $Am(OH)_3$ could be expected.

(3) The carbonate complexes of Am, $AmCO_3^+$ and $Am(CO_3)_2^-$, are predicted to be major solution species for pH values of about 7 and higher.

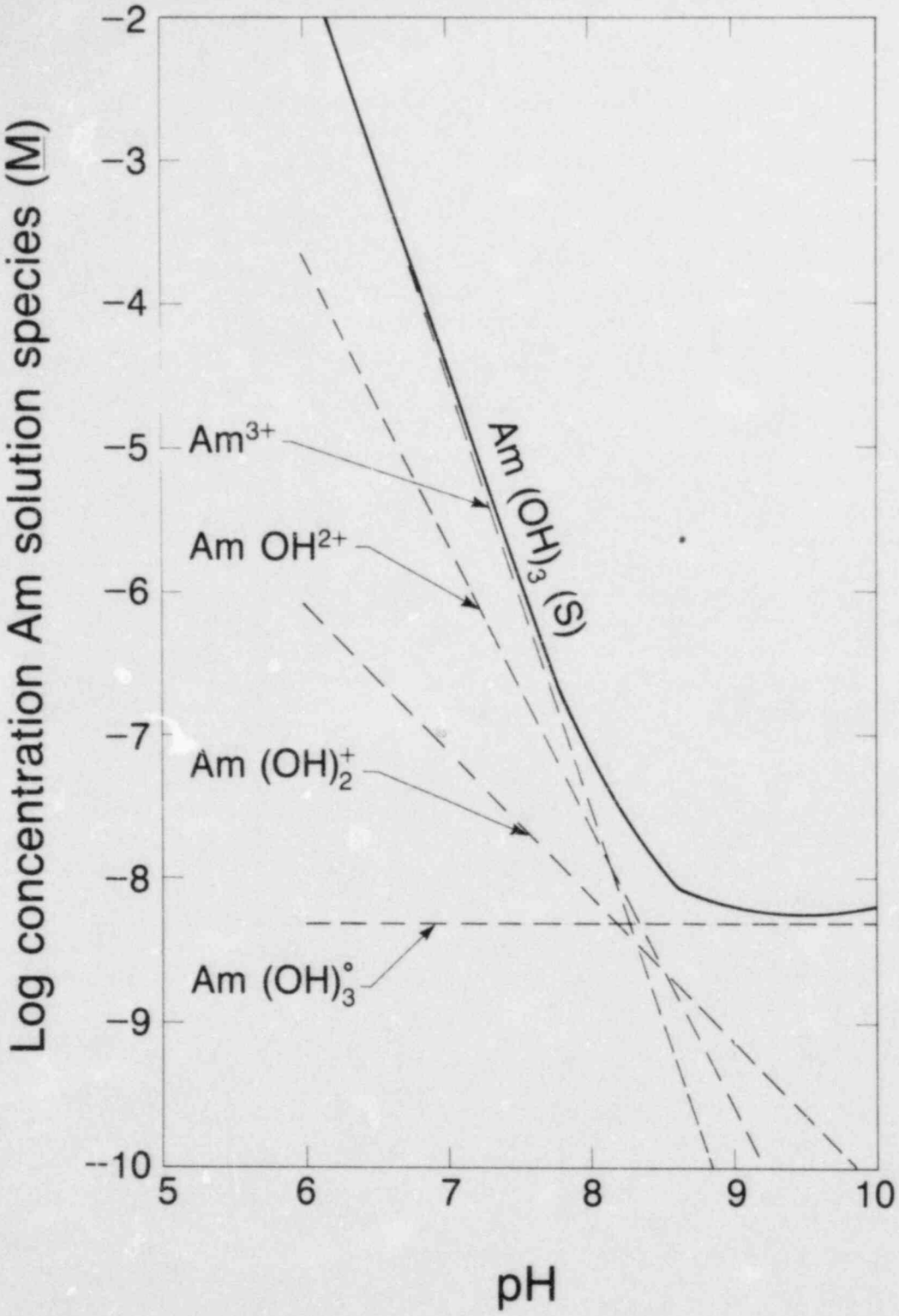

Figure 1. Calculated concentrations of Am solution species (dashed curves-labelled with species) and their sum (solid-curve-labelled with the controlling solid phase) as a function of pH for 0.1M ionic strength and a CO_2 partial pressure of zero atoms.

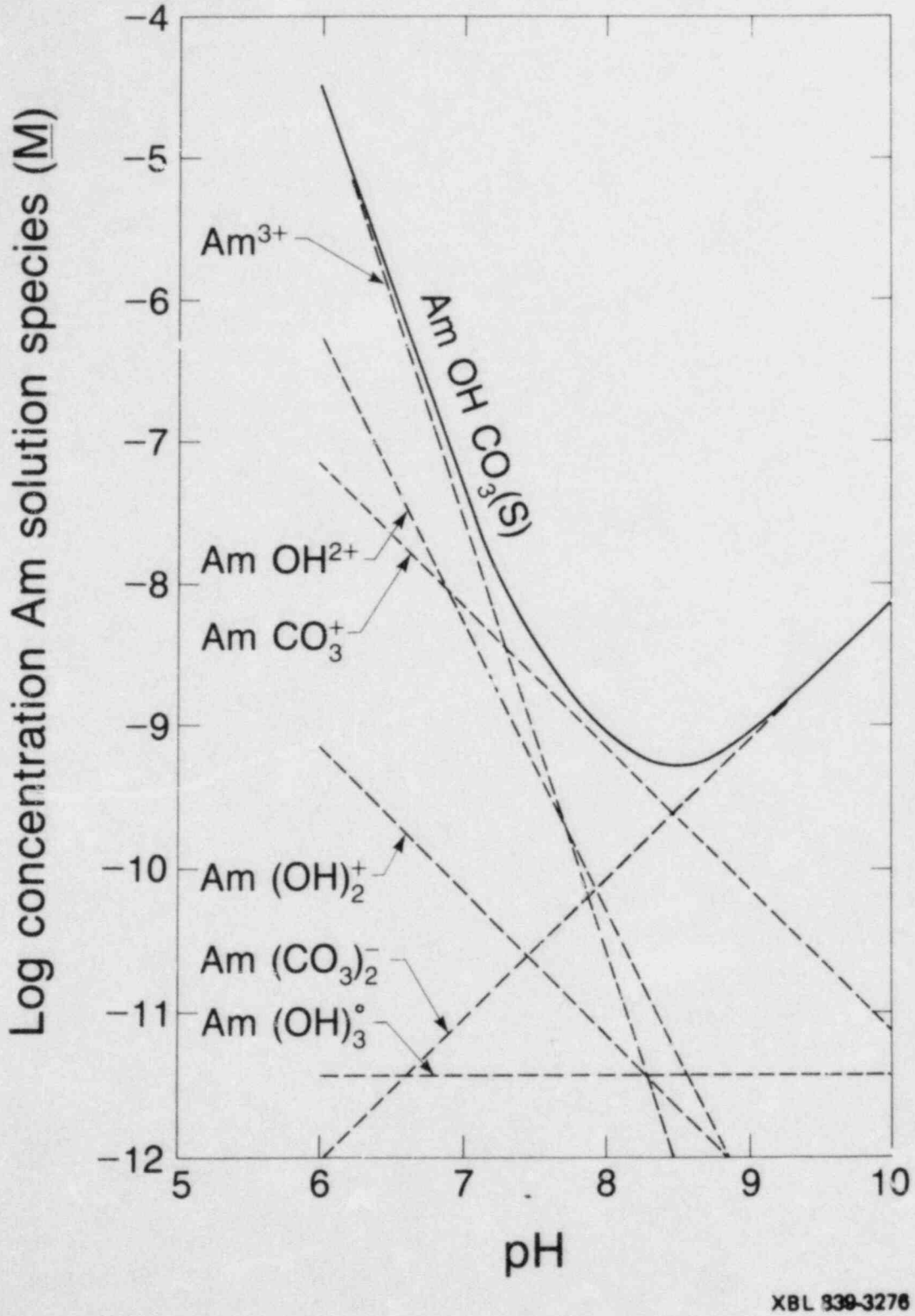

Figure 2. Calculated concentrations of Am solution species and their sum as a function of pH for 0.1M ionic strength and a CO_2 partial pressure of $10^{-3.5}$ atms.

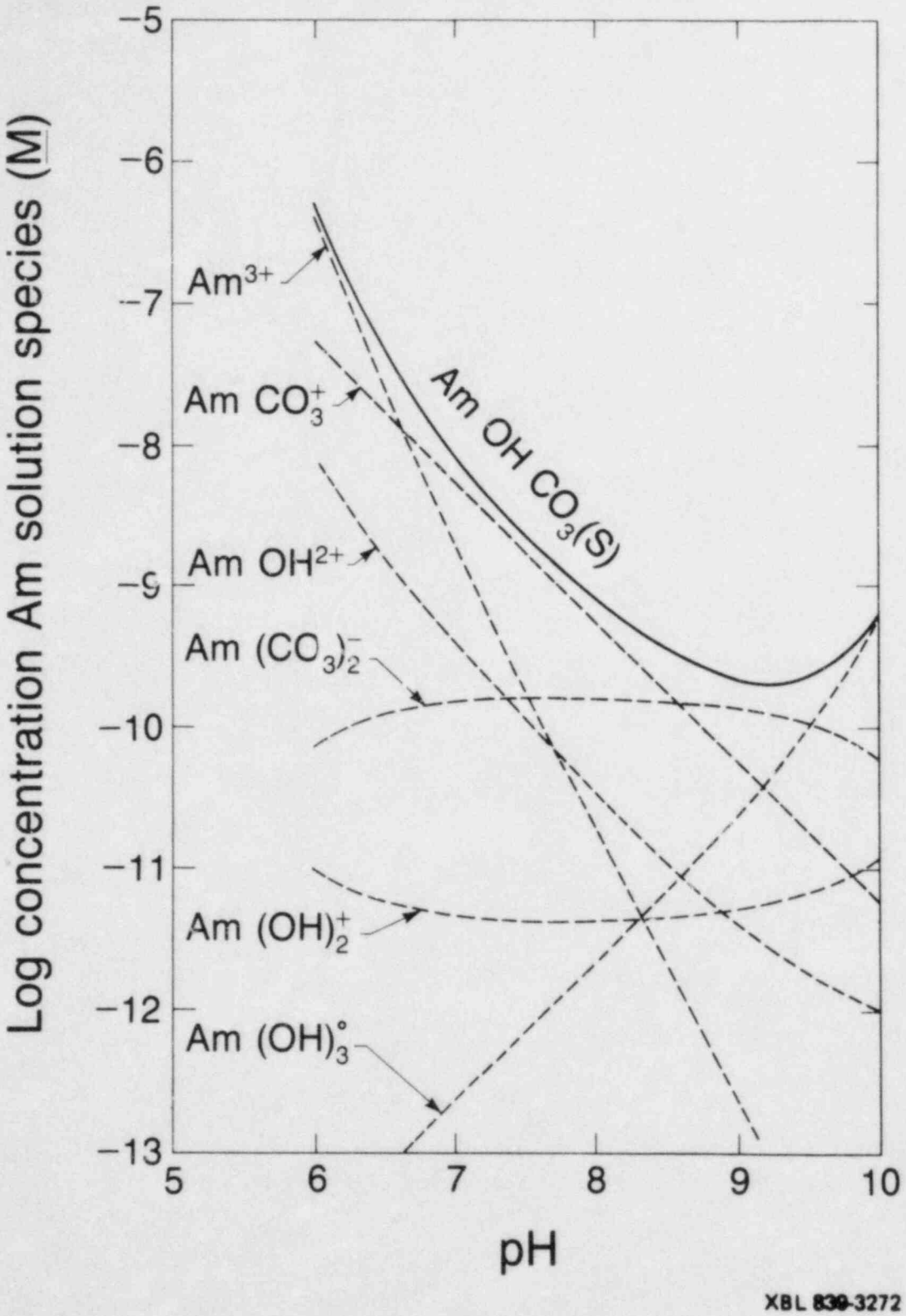

Figure 3. Calculated concentrations of Am solution species and their sum as a function of pH for 0.1M ionic strength and a total carbonate concentration (all species) of 2×10^{-3}M.

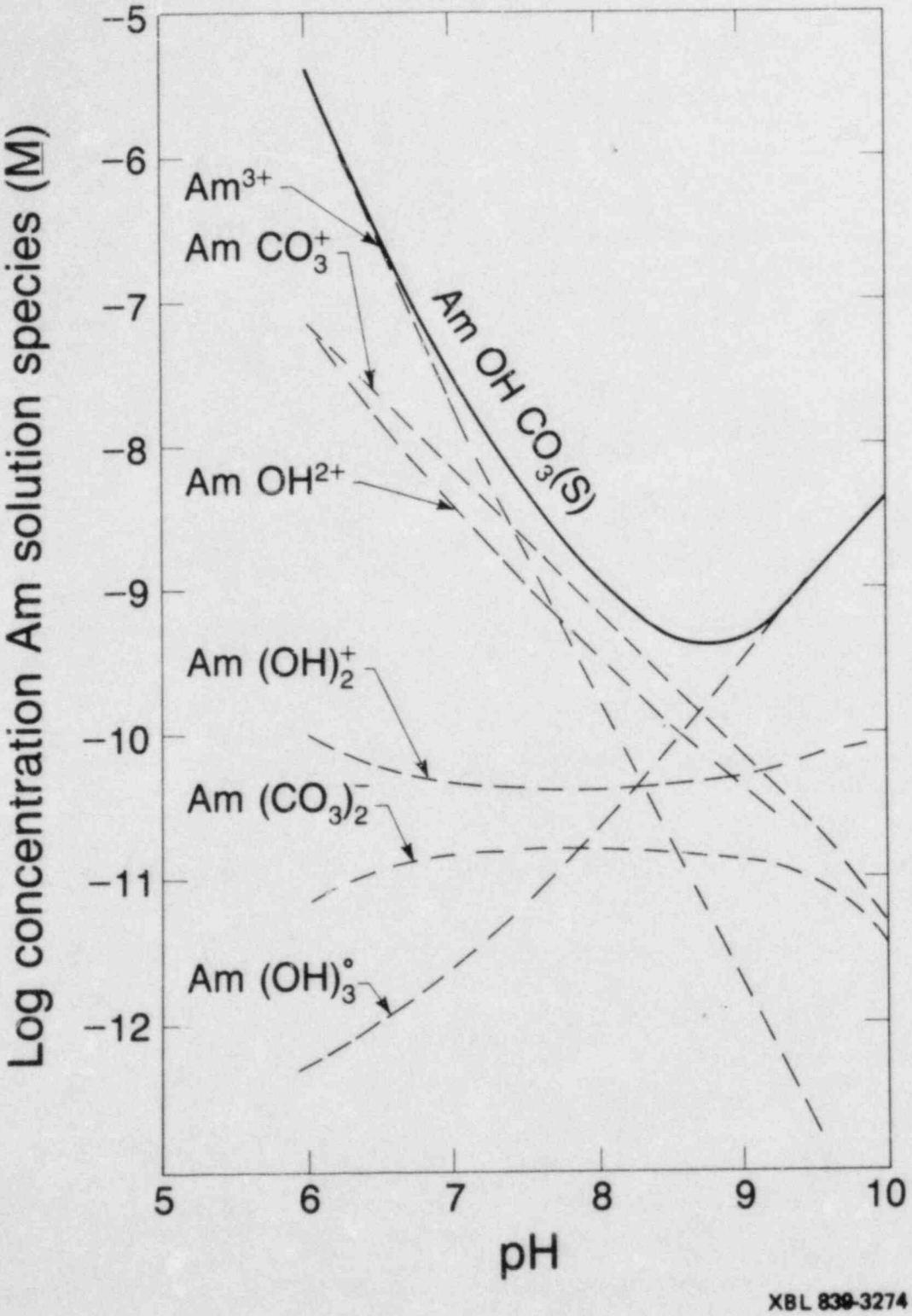

Figure 4. Calculated concentrations of Am solution species and their sums as a function of pH for 0.1M ionic strength and a total carbonate concentration (all species) of 2×10^{-4}M.

2.3.5 RECOMMENDATIONS

(1) The predictions based on MINEQL calculations should be checked by experimental measurements. It is possible that other solution complexes of unknown character have been omitted that could increase the solubility of Am, e.g., hydroxycarbonate complexes. Other more stable solid phases, perhaps the normal carbonate, may be important for CO_3^{2-} concentrations higher than those present in these measurements, e.g., at pH values of 8-10 under atmospheric CO_2, and could further decrease the solubility of Am.

(2) Since the trivalent state of plutonium is an important species under reducing conditions, experiments should be conducted to determine if the hydroxycarbonate is a significant solid phase for Pu^{+3} and should be included in modelling calculations.

(3) The formation of carbonate compounds and solution complexes should be considered in any modelling calculations used to predict the chemical behavior of actinides when the trivalent state is involved.

2.3.6 PLANNED RESEARCH

Other areas of study that are related to the issues listed in the introduction and are presently under investigation are:

(1) Measurement of solubility of americium phosphate in aqueous solutions.

(2) Carbonate complexation of Pu (IV) in aqueous solution.

(3) The effect of temperature change on the solubilities of actinide oxides, hydroxides and/or carbonates.

2.3.7 ACKNOWLEDGEMENTS

The authors wish to thank C.E. Holley, Jr. of the Los Alamos National Laboratory for making available to them the X-ray film of the powder diffraction pattern of $Nd_2(CO_3)_3 \cdot 2H_2O$. The help of A. Zalkin of the Lawrence Berkeley Laboratory in the interpretation of the powder patterns is gratefully acknowledged. Thanks are due J. J. Bucher for helpful advise on estimating activity coefficients.

2.3.8 REFERENCES

Allard, B., 1982. "Solubilities of Actinides in Neutral and Basic Solution". Actinides in Perspective, N. Edelstein, ed., Pergamon Press, N.Y., pp. 553-580.

2.3.8 REFERENCES (Continued)

Apps, J. A., C. L. Carnahan, P. C. Lichtner, M. C. Michel, D. Perry, R. J. Silva, O. Weres and A. F. White, 1982. Status of Geochemical Problems Relating to the Burial of High-Level Radioactive Waste, 1982. NUREG/ CR-3062. U.S. Nuclear Regulatory Commission, Washington, D.C., pp. 106-119.

Barney, G. S., and B. J. Wood, 1980. Identification of Key Radionuclides in a Nuclear Waste Repository in Basalt. RHO-BWI-ST-9. Rockwell International, Rockwell Hanford Operations Energy Systems Group, Richland, Washington 99352.

Blomeke, J. O., C. W. Kee, and J. P. Nichols, 1974. Projections of Radioactive Wastes to be Generated by the U. S. Nuclear Power Industry. ORNL-TM-3965. Oak Ridge National Laboratory, Oak Ridge, Tennessee 37830.

Charles, R. G. , 1965. "Rare-earth Carbonates Prepared by Homogeneous Precipitation," J. Inorg. Nucl. Chem., 27, pp. 1489-1493.

Dexpert, H. and P. Caro, 1974. "Determination de la Structure Crystalline de la Variete a des Hydroxycarbonates de Terres Rares $LnOHCO_3$", Mat. Res. Bull., 9, pp. 1577-1586.

Edelstein, N. J. Bucher, R. Silva, and H. Nitsche, 1982. Thermodynamic Properties of Chemical Species in Nuclear Waste: Topical Report. ONWI/LBL-14325, Officed of Nuclear Waste Isolation, Battelle Memorial Institute, Columbus, Ohio, p. 50.

Harned, H. S. and R. Davis, Jr., 1943 "The Ionization Constant of Carbonic Acid in Water and the Solubility of Carbon Dioxide in Water and Aqueous Salt Solutions from 0 to 50°." J.A.C.S., 65, pp. 2030-2037.

Harned, H. S. and B. B. Owen, 1958. The Physical Chemistry of Electrolyte Solutions. Table 14-2-1A, Reinhold, N. Y., p. 748.

Head, E. L., and C. E. Holley, Jr., 1963. The Preparation and Thermal Decomposition of Some Rare Earth Carbonates. Rare Earth Research III, Gordon and Breach, New York, pp. 51-63.

Head, E. L. and C. E. Holley, Jr., 1964. "The Preparation and Thermal Decomposition of the Carbonate of Tb, Dy, Ho, Er, Tm, Yb, Lu, Y, and Sc." Rare Earth Research IV, Gordon and Breach, N. Y., pp. 707-718.

2.3.8 REFERENCES (Continued)

Khoo, K. H., T.K. Lim and C. Y. Chan, 1981. "Activity Coefficients in Aqueous Mixtures of Hydrochloric Acid and Lanthanum Chloride at 25°C." J. Sol. Chem., 10, pp. 683-691.

Holley, C.E. Jr., 1983. Private Communication.

Little, A. D., 1977. Technical Support of Standards for High-Level Radioactive Waste Management, vol. A, Source term characterization. EPA Report 520/4-79-007A. United States Environmental Protection Agency, Office of Nuclear Waste Isolation, Washington, D. C. 20460.

Lundquist, R., 1982. Hydrophilic Complexes of the Actinides. I. Carbonates of Trivalent Americium and Europium, Acta Chem. Scand., A36, p. 741-750.

Moody, J. B., 1982. Radionuclide Migration/Retardation: Research and Development Technology Status Report, ONWI-321, Office of Nuclear Waste Isolation, Battelle Memorial Institute, Columbus, Ohio.

Peiper, J. L. and K. S. Pitzer, 1982. "Thermodynamics of Aqueous Carbonate Solutions Including Mixtures of Sodium Carbonate, Bicarbonate and Chloride", J. Chem. Thermodynamics, 14, pp. 613-638.

Pitzer, K. S., 1973. "Thermodynamics of Electrolytes. I. Theoretical Basis and General Equations." J. Phys. Chem., 77 (No. 2), pp. 268-277.

Pitzer, K. S., and G. Mayorga. 1973. "Thermodynamics of Electrolytes. II. Activity and Osmotic Coefficients for Strong Electrolytes With One or Both Ions Univalent," J. Phys. Chem., 77 (No. 19), pp. 2300-2308.

Phillips, S. L., 1982. Hydrolysis and Formation Constants at 25°C. Lawrence Berkeley Laboratory report LBL-14313, Berkeley, California, p. 50.

Robinson, R. A. and R. H. Stokes, 1959. Electrolyte Solutions, Appendix 8.10, Butterworth, London, pp. 491-492.

Salutsky, M. L., and L. L. Quill, 1950. "The Rare Earth Metals and their Compounds. XII. Carbonates of Lanthanum, Neodymium and Samarium", J. Amer. Chem. Soc., 72, p. 3306-3307.

Silva, R. J., 1982. The Solubilities of Crystalline Neodymium and Americium Trihydroxides. A topical report. ONWI/LBL-15055, Lawrence Berkeley Laboratory, Berkeley, CA.

Silva, R. J., and A. W. Yee, 1982. Geochemical Assessment of Nuclear Waste Isolation, "Testing of Methods for the Separation of Solid and Aqueous Phases - a Topical Report,," NUREG/LBL-14696, Lawrence Berkeley Laboratory, Berkeley, CA.

Smith, R. M., and A. E. Martell, 1976. Critical Stability Constants, Vol.4, Inorganic Complexes, Plenum Press, New York, p. 37.

Svedberg, T., and K. O. Pedesson, 1940. The Ultracentrifuge, Part I, Chap A. Oxford Clarendon Press, Oxford, England, pp. 5-15.

Westall, J. C., J. C. Zachary, and F. M. M. Morel, 1976. MINEQL, A Computer Program for the Calculation of Chemical Equilibrium Composition of Aqueous Systems, Techn. Note 18, Dept. Civil Eng., Massachusetts Institute of Technology, Cambridge, MA.

2.4 THE UNCERTAINTIES IN THE THERMODYNAMICS OF BASALT-OXYGEN AND BASALT-WATER REACTIONS

D. G. Schweitzer and M. S. Davis
Brookhaven National Laboratory
Upton, New York, 11973

ABSTRACT

One of the most important factors affecting the ability to isolate high level radioactive waste in a geologic repository, is the environment around the waste packages. Corrosion of metallic containers, release of radionuclides from the waste form and their transport through the environment are all affected by the chemical and physical properties of the surrounding media and the groundwater. Uncertainties in these properties need to be evaluated in order to predict the time of containment and the migration of radionuclides to the accessible environment.

Recently, BWIP (Basalt Waste Isolation Project) calculations on the basalt-water and basalt-oxygen equilibria have been used to claim that the environment of a high level waste repository in basalt is reducing in character. Based on these equilibria it has been assumed that the oxygen fugacity will be so low that corrosion will be inhibited and the hydrogen overpressure will be so high that radiolysis may be inhibited.

In this paper we have repeated the BWIP calculations using thermodynamic data from two sources, the JANAF Thermochemical Tables (1971) and Kubaschewski (1974). An estimate of the uncertainties in the thermochemical data is included. Our analysis indicates that the uncertainties in the basic thermodynamic data lead to about 30 orders of magnitude in uncertainty in the oxygen fugacity for the magnetite-hematite reaction (10^{-86} to 10^{-57} atm) and about 15 orders of magnitude uncertainty in the hydrogen equilibrium pressure (10^{-12} to 10^{+3} atm).

Using the range of oxygen fugacities assumed in the Site Characterization Report (SCR, 1983) we calculate equilibrium hydrogen pressures of 10^{-9} to 10^{-6} atm rather than the 2 to 10 atm given.

We also analyzed the assumptions made with respect to basalt-water reactions in the SCR. A vast volume of literature exists on reactions involving magnetite and hematite in water at temperatures pertinent to basalt repositories (50° to 350°C). These data show that Fe_3O_4 and Fe_2O_3 can coexist in water with oxygen fugacities from about 10^{-4} to 1 rather than the calculated oxygen fugacities of $\sim 10^{-60}$ to 10^{-30} given in the SCR.

Based on our calculations there appears to be neither theoretical nor factual evidence to support the optimistic assumptions on corrosion and radiolysis made in the BWIP Site Characterization Report.

2.4.1 Introduction

The interaction of a high level waste (HLW) package with the repository environment will determine the lifetime of the package. The way in which released nuclides interact with the host rock will determine the rate at which they are transported to the accessible environment. The physical and chemical properties of the environment and the way in which these are altered by the waste package need to be characterized so that reliable predictions of containment times, release rates and transport of radionuclides can be made. The uncertainties in the measured or calculated properties need to be defined so that the validity of and the uncertainties in the long term predictions of waste package/repository performance can be assessed.

The objective of the work reported here is to demonstrate that the uncertainties in the data base used to predict the environment around a high level waste package in a basalt repository result in a need to develop new experiments which realistically approximate the expected conditions in the repository.

2.4.2 Issues

The dominant issue to be addressed is a definition of the environment experienced by a HLW package in basalt, how this environment changes as a result of the waste package and ultimately how the environment affects the predicted lifetime and releases from a waste package. Specific concerns inherent include:

1. Changes induced and uncertainties in the groundwater properties caused by radiation, heat, weathering of basalt surfaces, and the presence of barrier materials.

2. Uncertainties in container lifetime as a results of changes and uncertainties in the repository water characteristics.

3. Solubilities of radionuclides under anticipated conditions and the uncertainties in these limits resulting from changes in the repository water chemistry (pH, redox characteristics, ionic composition).

4. Formation of and transport of colloids as a function of anticipated conditions and uncertainties in those conditions.

2.4.3 Methods

In this paper published thermochemical data have been used to calculate the equilibrium oxygen fugacity for the magnetite-hematite reaction and for the reaction of magnetite with water at temperatures representative of those anticipated in a basalt repository. These calculations included an estimate of the uncertainties in the thermochemical data and an evaluation of the impact of those uncertainties in predicting the environment of a waste package in basalt. In addition, literature on the behavior of magnetite and hematite in water at temperatures between 50°C and 350°C has been reviewed to determine the actual range of conditions under which hematite or magnetite are present and under which conditions they can coexist.

The two sources of published thermochemical data used in this analysis are the JANAF Tables (1971) and the Fourth Edition of "Metallurgical Thermochemistry" (Kubaschewski, 1974).

Kubachewski (1979) has given "probable limits of accuracy" where possible. It is noted that while these limits are not necessarily those given by the original authors, the limits quoted are felt to insure that newer determinations of a property will not fall outside the range given. In addition, Kubachewski notes that values of a property obtained by an "approximate method and not checked by other means may sometimes be subject to a very large and quite unknown error." In those cases where thermochemical values have to be estimated, Kubaschewski notes that some properties, such as entropies and heats of fusion, are easier to estimate than, for example, the heats of formation which are "the most important for free energy calculations."

2.4.4 Results

Uncertainty Analyses

In order to determine if a basalt HLW repository environment is favorable with respect to corrosion and radiolysis, relationships between Eh, pH and oxygen fugacity have been proposed (SCR, 1983). Although the NRC (NUREG-0960) has pointed out many problems in relating Eh, pH and oxygen fugacity through explicit formalisms, the effects of intrinsic uncertainties in the basic thermodynamic data have not been analyzed with respect to the validity of the conclusions drawn from these data.

In this section we deal with the effects of uncertainties associated with data used for the basic BWIP assumption made for a basalt environment, viz., that if equilibrium occurs, the oxygen fugacity is controlled by the reaction

$$4Fe_3O_4 + O_2 \rightleftharpoons 6Fe_2O_3.$$

For a buffered system the equilibrium constant, K, is:

$$K = \frac{(a_{Fe_2O_3})^6}{(a_{Fe_3O_4})^4 (f_{O_2})}$$

where for excess solids the activities of Fe_2O_3 ($a_{Fe_2O_3}$) and Fe_3O_4 ($a_{Fe_3O_4}$) are defined as unity so that

$$K = \frac{1}{f_{O_2}} = \frac{1}{p_{O_2}}$$

(p_{O_2} is the oxygen fugacity in atmospheres).

In general, the equilibrium constant is obtained from free energy measurements through the relationship $\Delta G^o_T = - RT \ln K$ (where T is in ^oK).

The free energy change for the reaction at a given temperature (ΔG^o_T) can be obtained from direct measurements of the reaction itself if they are available, or from tables of the free energy of formation of the respective oxides from their elements by simple combinations such as

$$4Fe_3O_4 \quad \rightleftharpoons \quad 12Fe + 8O_2 \qquad \Delta G_{300} = + 972{,}120$$

$$12Fe + 9O_2 \quad \rightleftharpoons \quad 6Fe_2O_3 \qquad \Delta G_{300} = -1{,}065{,}588$$

$$4Fe_3O_4 + O_2 \quad \rightleftharpoons \quad 6Fe_2O_3 \qquad \Delta G_{300} = -93{,}468.$$

The values used in these equations are from the JANAF Tables (1971).

Although the free energies are generally given to six or seven significant figures for calculational convenience, the free energies of formation of iron oxides from their elements are generally not known to better than about ±5% at temperatures from 300°K to about 600°K (see pages 423-424 of "Metallurgical Thermochemistry," 4th Edition) (Kubaschewski, 1974).

Consider the reaction

$$4Fe_3O_4 + O_2 \quad \rightleftharpoons \quad 6Fe_2O_3 \qquad \Delta G_r \pm U_r$$

in which ΔG_r is the free energy and U_r is the uncertainty in the value. If U_r is not available from measurements of the reaction as written, it could be estimated from uncertainties in the free energy of formation reactions:

$$4Fe_3O_4 \quad \langle\!=\!\!=\!\rangle \quad 12Fe + 8O_2 \qquad \Delta G_1 \pm U_1$$

$$12Fe + 9O_2 \quad \langle\!=\!\!=\!\rangle \quad 6Fe_2O_3 \qquad \Delta G_2 \pm U_2$$

where $\Delta G_r = \Delta G_1 + \Delta G_2$. For random errors

$$U_r = (U_1^2 + U_2^2)^{1/2}.$$

However, the uncertainty for the reaction

$$4Fe_3O_4 + O_2 \quad \langle\!=\!\!=\!\rangle \quad 6Fe_2O_3$$

over the temperature range from 298°K to 1460°K is given by Kubaschewski (1974) as ± 16,000 cal. For this value of the uncertainty, the free energy values from the JANAF Tables yield equilibrium oxygen fugacities for the magnetite-hematite reaction at 300°K from between 9×10^{-81} to 2×10^{-57} where the values for ΔG_r from Kubaschewski (1974) yield f_{O_2} values between 5×10^{-86} and 2×10^{-61} giving a spread of about 30 orders of magnitude between the two sets of data and about 25 orders of magnitude uncertainty within each data set.

In practice, the equilibrium O_2 fugacity for the magnetite-hematite reaction determines the condition for which both oxides can coexist with each other and with water if equilibrium with water is also assumed. Since the magnetite-hematite reaction is assumed to control the oxygen fugacity, the hydrogen pressure in equilibrium with water at this oxygen fugacity is determined from

$$2H_2O \quad \langle\!=\!\!=\!\rangle \quad 2H_2 + O_2 \qquad \Delta G_{300} = + 109{,}234 \pm 600$$

or

$$K = \frac{(pH_2)^2(pO_2)}{(pH_2O)^2} \qquad 1 \times 10^{-80}$$

(with an uncertainty spread in K of between 4×10^{-80} to 5×10^{-81} atm).

For the assumption that the oxygen fugacity is governed by the magnetite-hematite equilibrium, substitution in the water equilibrium equation yields H_2/H_2O ratios from 10^{-12} to 2 for JANAF Table data at 300°K and 10^{-10} to 10^{+3} for Kubaschewski's data at 300°K. Under these conditions (or any other condition where the activity of $H_2O = 1$) the above values are simply the values of the hydrogen pressure in atmosphere that would occur if:

a) the magnetite-hematite reaction controlled the oxygen fugacity
b) magnetite and hematite were in equilibrium with each other, O_2 and H_2O and
c) if H_2O were in equilibrium with gaseous H_2 and O_2.

There are several points related to basalt reactions that are worth noting about H_2, O_2, H_2O equilibria at low temperatures. For water to be in equilibrium with both gaseous O_2 and H_2 near ambient temperatures, the H_2 content of air would have to be $\sim 10^{-40}$ atmospheres. In actual fact, the hydrogen pressures in air over water range from 10^{-7} to 10^{-6} atmospheres throughout most of the world. Equilibria involving dissociation of water into H_2 and O_2 or recombination of H_2 and C_2 to yield water do not appear to be achieved at these low temperatures and pressures. On the other hand, O_2 and H_2 gases dissolved in H_2O can reach equilibrium with their corresponding gas phases at these temperatures. For example, the solubility of O_2 in H_2O at $\sim 300^oK$ in equilibrium with air ($f_{O_2} = 0.2$) is about 10 ppm by weight. At equilibrium, the activity of O_2 in each phase is equal so that 10 ppm dissolved O_2 in water has an oxygen activity of ~ 0.2. In considering the following two reactions:

$$2Fe_3O_4 + H_2O \rightleftharpoons 3Fe_2O_3 + H_2$$

$$4Fe_3O_4 + O_{2(H_2O)} \rightleftharpoons 6Fe_2O_3$$

[where $O_{2(H_2O)}$ denotes O_2 gas dissolved in H_2O] the latter reaction should predominate.

Since one part per billion of dissolved O_2 has an O_2 activity of $\sim 10^{-5}$, this reaction is highly favored over the reaction of magnetite with water to form hematite and hydrogen.

The uncertainty in the equilibrium values for the direct reaction of magnetite with H_2O is not available. It can be estimated from the following combinations of reactions:

$$2Fe_3O_4 + 1/2\ O_2 \rightleftharpoons 3Fe_2O_3 \qquad \Delta G_1 \pm U_1\ (300^oK)$$

$$H_2O \rightleftharpoons H_2 + 1/2\ O_2 \qquad \Delta G_2 \pm U_2\ (300^oK)$$

$$2Fe_3O_4 + H_2O \rightleftharpoons 3Fe_2O_3 + H_2 \qquad \Delta G_3 \pm U_3\ (300^oK)$$

where $\Delta G_3 = \Delta G_1 + \Delta G_2$ and $U_3 = (U_1^2 + U_2^2)^{1/2}$.

From Kubaschewski $\Delta G_1 = -49{,}534$ and $U_1 = \pm 8{,}000$; $\Delta G_2 = +54{,}583$ and $U_2 = \pm 300$ so that $\Delta G_3 = +5{,}050 \pm 8{,}000$.

Similar treatment of the data from the JANAF Tables would yield $\Delta G_3 = +7{,}883 \pm 8{,}000$.

The ΔG for the pure water reaction ranges from about +16,000 to -3,000. The uncertainties in the reaction

$$2Fe_3O_4 + H_2O \rightleftharpoons 3Fe_2O_3 + H_2$$

are so large that it is not known whether magnetite should react with water to form hematite spontaneously or hematite should react with H_2 to form magnetite. The uncertainty in this reaction implies that at one extreme, equilibrium might be achieved when the dissolved hydrogen concentration is about one part in 10^{18} by weight ($f_{H_2} \sim 10^{-12}$) or at the other extreme, equilibrium is achieved when the hydrogen overpressure is about 100 atmospheres. In practice, there are a great deal of data that show that magnetite does not, in fact, react measurably with deoxygenated water from ambient temperatures to about 250°C. (See, for example, Berry, W. E., 1979 and MacDonald, D. D., 1983.)

For gas or vapor phase reaction the relative stabilities of the two iron oxides would be determined by the value of the H_2 to H_2O ratio. Data reported by Rau (1972) indicates that equilibrium between Fe_2O_3 and Fe_3O_4 in H_2 and H_2O vapor occurs at 500°C when the hydrogen-to-water ratio is approximately 10^{-4}. Rau estimates that the oxygen partial pressure at this temperature is of the order of 10^{-20} atmospheres.

The uncertainties in the free energy of the reaction of magnetite with oxygen dissolved in water are also sufficiently great to cause wide ranges of uncertainty in the equilibrium $O_{2(H_2O)}$ value in

$$4Fe_3O_4 + O_{2(H_2O)} \rightleftharpoons 6Fe_2O_3.$$

However, in this case the ΔG for the reaction as written is negative throughout the whole uncertainty range. In principle, if kinetics do not prevent reaction, there is some reasonably low value of $O_{2(H_2O)}$ above which Fe_3O_4 should be converted to Fe_2O_3 in this temperature range.

The above arguments show that even for very small quantities of dissolved O_2 in H_2O, under those conditions where magnetite is converted to hematite in liquid H_2O, it will likely convert without the generation of H_2.

Summary of Experimental Evidence: Kinetic Effects and Thermodynamic Uncertainties

It has been known for some time that the corrosion product formed on boiler steels at low dissolved oxygen (ppb) is magnetite whereas at higher oxygen concentrations, both magnetite and hematite are formed. Similar behavior is observed in water cooled reactors. In PWR's that have relatively high hydrogen levels the corrosion products are mainly Fe_3O_4. In BWR's the corrosion products are largely Fe_2O_3 with some Fe_3O_4 (Brutschy, 1962). Oxide films formed on iron-base alloys in high temperature water consist of either one or two layers depending on conditions. One layer is formed when the hydrogen formed from the reactions

$$Fe + 2H_2O \rightleftharpoons Fe(OH)_2 + H_2$$

$$3Fe(OH)_2 \rightleftharpoons Fe_3O_4 + H_2 + H_2O$$

diffuses through the metal away from the oxide. The two-layer Fe_3O_4 film appears to form when the H_2 diffuses through the oxide and remains in the aqueous phase.

There are many publications (Strauss, M. B., 1960; Bloom, M. C., 1960; Coriou, H., 1967; Kirsch, H., 1965; Brush, E. G., 1972; Wilde, B. E., 1968) showing the formation of both magnetite and hematite on steel in water containing oxygen at temperatures (50°-300°C) where according to equilibrium thermodynamic data only Fe_2O_3 should be stable. Two types of measurements under which magnetite-hematite layers are formed give strong circumstantial evidence that kinetics do not appear to be the cause of the differences between observation and thermodynamic predictions. Under certain conditions single layer Fe_2O_3 films can be formed. Ruther and Hart (1968) found that if the water contained more than 130 ppm of O_2 only Fe_2O_3 formed on carbon steel. At lower oxygen concentrations Fe_3O_4 and Fe_2O_3 are formed. In water containing 0.03 ppm O_2 at 125°C and 288°C, X-ray diffraction analyses show that the film is magnetite.

Sawachka and Pearl (1970) showed that corrosion rates of carbon steels decrease with increasing oxygen in the water over the range 2 to 200 ppb oxygen and 40°C to 200°C. Maxima in the corrosion rates occur with temperature and with O_2 concentration presumably because of differences in the protective properties of the oxide films formed.

In addition to data showing that the magnetite-hematite reaction depends on relatively small O_2 changes in a given temperature range, it is also known that for water containing 8 ppm O_2, only Fe_3O_4 forms at 50°C and 100°C. However, the film formed in water with 8 ppm O_2 at 175°C and 288°C

has an inner layer of Fe_3O_4 and an outer layer of Fe_2O_3. Furthermore, the nature of the films is pH dependent. Rae and Yatabe (1967) found that the corrosion rates of carbon steel in pH 10 water at 150 to 200°C were about the same as the rates at 260 to 315°C.

Since magnetite and hematite can both be formed, it is unlikely that the discrepancies between thermodynamic data for the Fe-H_2O system at elevated temperatures (Macdonald, D. D., 1972) and observations at low (50°-100°C) and moderate (175°-300°C) temperatures are attributable solely to kinetic effects.

2.4.5 Conclusions

Uncertainty analyses of thermochemical data on magnetite-hematite equilibria with water and with oxygen do not support the assumptions that these reactions will produce an environment with extremely low oxygen fugacities and hydrogen overpressures that may inhibit radiolysis. An analysis of existing literature from corrosion in water cooled reactors and corrosion on boiler steels also contradicts assumptions that magnetite will react with water to produce appreciable amounts of H_2 and develop very low oxygen fugacities.

In using tabulated thermochemical data, it should be recognized that standard tables of thermodynamic data are for the most part developed through an extrapolation of experimentally determined properties at temperatures often well in excess of those anticipated for the system of interest. Therefore, there is uncertainty not only in the validity of using higher temperature data to extrapolate to lower temperature regions, but also in the methods used to extrapolate the data. For example, the values of thermodynamic properties listed in the NBS Tables of Thermodynamic Properties (1982) are chosen to provide internal consistency in the tables. When several different measurements of a property have been made, a choice is made in determining the best value to be used. Once a choice is made the value is fixed. If newer measurements become available they cannot be incorporated into the NBS tables without carefully analyzing the effect of the new data on properties of related substances. The accuracy of the NBS Tables are, in general, considered to be within 8 to 80 units of the last unit while Kubachewski (1979) has given "probable limits of accuracy" where possible. It is noted that while these limits are not necessarily those given by the original authors, the limits quoted are felt to insure that newer determinations of a property will not fall outside the range given. In addition, Kubachewski notes that values of a property obtained by an "approximate method and not checked by other means may sometimes be subject to a very large and quite unknown error." In those cases where thermochemical values have to be estimated, Kubaschewski notes that some properties, such as entropies and heats of fusion, are easier to estimate than,

for example, the heats of formation which are "the most important for free energy calculations."

Therefore, while these types of compilations provide a data base for the calculation of thermodynamic properties they are arranged to maintain an internal consistency and do not necessarily reflect the most recent data available. The values compiled do have uncertainties both in the values determined from experimental data and the values obtained by a method of approximation. For those properties that must be estimated, the values may be subject to very large error.

When an uncertainty analysis of the thermochemical data is applied to the hematite-magnetite equilibrium with O_2 and H_2O the results indicate that the intrinsic uncertainties and the lack of understanding of magnetite-hematite reactions with H_2O and O_2 preclude any realistic predictions that could be used to estimate the corrosion or radiolysis reactions that a waste package would be subject to in a basalt repository.

In view of the sensitivity of magnetite-hematite reactions to small quantities of dissolved hydrogen and oxygen, it is likely that radiolysis of groundwater will be a major factor in determining the behavior of waste packages in basalt environments.

The uncertainties in both theory and data indicate that the NRC will require new experiments that realistically approximate the expected conditions in order to evaluate the performance of waste packages in a basalt repository.

2.4.6 Recommendations

The uncertainties and complexities of predicting the redox properties in the near field and the far field are so great that the NRC should not undertake any program to determine generic properties. If the DOE uses redox properties of either the near field or the far field as part of a demonstration of compliance with NRC or EPA criteria (e.g. solubility limits of radionuclides for controlled release) then realistic engineering tests should be designed and performed to address specific issues. These should be done under anticipated conditions that include the effects of temperature and radiation.

2.4.7 Acknowledgments

This work is an extension of work sponsored by the NRC Office of Nuclear Material Safety an Safegurards.

The authors gratefully acknowledge Ms. Grace Searles for her careful preparation and editing of this manuscript.

2.4.8 References

Berry, W. E. and R. B. Diegle, "Survey of Corrosion Product Generation, Transport and Deposition in Light Water Reactors," EPRI NP-522, March 1979.

Bloom, M. C., 21st Annual Water Conference, Pittsburgh, 1960.

Brush, E. G. and W. L. Pearl, Corrosion 28, 129, 1972.

Brutschy, F. J., R. S. Gilbert and R. N. Osborne, "The Behavior of Corrosion Products in Boiling Water Reactors," International Atomic Energy Agency Conference on the Corrosion of Reactor Materials, Salzburg, Austria, June 1962.

Coriou, H., L. Grall, M. Pelras and A. Perez, Corrosion et Anticorrosion 23, 57, 1967.

DOE/RL-823, Vol. 1, "Site Characterization Report for the Basalt Waste Isolation Project," Department of Energy, November 1982.

JANAF Thermochemical Tables, Second Edition, NSRDS-NBS 37, June 1971.

Kirsch, H., Achiv fur Eisenhüttenwesen 36, 603, 1965.

Kubaschewski, O. and C. B. Alcock, Metallurgical Thermochemistry, Fifth Edition, Pergamon Press, 1979.

Macdonald, D. D., G. R. Sheirman and P. Butler, "The Thermodynamics of Metal-Water Systems at Elevated Temperatures. II. The Iron-Water System, AECL-4137, Atomic Energy of Canada, Ltd., 1972.

Macdonald, D. D., S. Smialowska and S. Pednekar, "The General and Localized Corrosion of Carbon and Low Alloy Steels in Oxygenated High Temperature Water," EPRI NP-2853, February 1983.

Potter, E. C. and G. M. W. Mann, "Oxidation of Mild Steel in High Temperature Aqueous Systems," Proc. First International Congress Metallic Corrosion, Buttersworth, London, 1962, pp. 417-423.

Rae, H. K. and E. Yatabe, "Formation and Release of Corrosion Products by Carbon Steel in Water at pH 10, 150 and 205°C," Proc. Tripartite Conference on Transport of Materials in Pressurized-Water Nuclear Systems, AECL-1265, Atomic Energy of Canada Limited, June 1967.

Rau, H., "Thermocynamics of the Reduction of Iron Oxide Powders With Hydrogen," J. Chem. Thermodynamics 4, 57, 1972.

Ruther, W. E. and R. U. Hart, Corrosion 19, 127, 1968.

Sawachka, S. G. and W. L. Pearl, "Corrosion Product Chemistry of a Boiling Water Reactor," Proc. 31st International Water Conference, Pittsburgh, Pennsylvania, 1970, pp. 67-70.

Strauss, M. B. and M. C. Bloom, J. Electrochem. 107, 2, 1960.

Wagman, D. D., and others, The NBS Tables of Chemical Thermodynamic Properties," J. of Phys. and Chem. Reference Data 11, Supplement No. 2, 1982.

Wilde, B. E., Corrosion 24, 338, 1968.

2.5 VALENCE EFFECTS OF SORPTION
Laboratory Control of Valence State

R. E. Meyer
W. D. Arnold
F. I. Case

Oak Ridge National Laboratory
Oak Ridge, TN 37831

ABSTRACT

Estimation of the rates of migration of nuclides from nuclear waste repositories requires knowledge of the interaction of these nuclides with the components of the geological formations in the path of the migration. These interactions will be dependent upon the valence state and speciation of the nuclide. If the valence state is not known, then there can be little confidence in use of the data for safety analysis.

Experiments designed to measure interaction of multi-valent nuclides and minerals must therefore include some form of valence state control. One of the more common methods is use of chemical reagents, including redox couples, which can hold the potential to relatively specific potentials. The disadvantage of added chemical reagents is that they may alter the characteristics of the sorption reactions by interaction with the sorbent. Electrochemical methods can also be used, and they have the advantage that they do not add reagents to the solution.

An electrochemical method of valence state control was developed which makes use of a porous electrode in a flow system containing a column of the adsorbent. By use of this method and solvent extraction analyses of the valence states, a number of reactions of interest to HLW repositories were investigated. These include the reduction of Np(V) and Tc(VII) by crushed basalt and other minerals. For the reduction of Np(V) by basalt, the experiments indicate that sorption on basalt increases with pH and that

most of the Np is reduced to Np(IV). The adsorbed Np(IV) is very difficult to remove from the basalt. For the experiments with Tc(VII), the results are considerably more complicated.

The results of these experiments are used to assess some of the techniques and methods currently used in safety analyses of proposed HLW repositories. Perhaps the most important consideration is that predictive modeling of valence change reactions, such as the reduction of Np(V) and Tc(VII), must be used with considerable caution, and the occurrence of such reactions should be verified as best as possible with experiments using valence state control and analyses.

2.5.1 INTRODUCTION

Sorption of nuclides on host mineral formations around high level waste repositories is one of the major mechanisms by which they may be retarded in the event that a breach of the repository occurs and the nuclides are mobilized by groundwater flowing through the repository. For a given nuclide, there will usually be substantial differences in the extent to which it is adsorbed depending upon its chemical speciation. The speciation will depend upon the valence state of the nuclide and the chemical composition of the groundwater-mineral system. The research described in this report deals with techniques for laboratory control and experimental detection of valence state reactions. The results of this research are then used for assessment of the redox geochemistry of processes affecting migration of nuclides.

2.5.1.1 Issues Addressed by this Research

The primary issues addressed by this work are: 1. The identification of the important phenomena that govern radionuclide migration in the near and far field. 2. The determination of the conditions that will affect these phenomena.

From these primary issues the following key technical issues may be listed:

1. What are the effects of valence state change of a nuclide on sorption and other removal processes?
2. How best can redox reactions be identified and studied in the laboratory?
3. What are the variables that affect redox reactions?
4. Can the kinetics of redox reactions (and other reactions) be assumed to be rapid enough to assure redox equilibrium during radionuclide transport?
5. Could backfill materials be used to cause valence change reactions that favor retardation? If so, what types of backfill materials might be used?
6. Can the redox properties of both far and near field systems be described adequately by a single parameter, Eh, and if so will determination of this parameter be sufficient for prediction of redox reactions that affect the migration of nuclides?

2.5.1.2 Background and Objectives

For some nuclides present in nuclear waste, the formation of lower valence states could significantly increase the sorption of the nuclide and consequently its retention in the host rock. For example, if Tc-99 is to be retarded significantly, it is necessary that it be present in a lower valence state (VANDERGRAAF 1983, FRANCIS 1980, BONDIETTI 1979, ALLARD 1979, STRICKERT 1980). In the oxidized (VII) state, it exists as the anion TcO_4^-, which is poorly adsorbed under the conditions of proposed repositories (PALMER 1981). For Np, the normal stable oxidized state is Np(V) and it exists as NpO_2^+ in aqueous solutions at normal environmental pH values (BURNEY 1974). If it is reduced to Np(IV), it can form the very insoluble oxide, NpO_2. Similar considerations apply to plutonium and uranium which can exist in several valence states and form highly insoluble oxides (SALTER 1982, SERNE 1982). Thus, it is extremely important when studying these reactions in the laboratory that the valence state be known before and after sorption.

It is possible that valence change reactions of technetium, neptunium, and other multi-valent elements could be caused by species in the groundwater such as dissolved oxygen or ferrous ions. It is also possible that the nuclides may first be adsorbed on the mineral surfaces and then reduced or oxidized by components of the minerals. In both cases, the products could be either more or less strongly adsorbed than the original species. If the valence change reaction proceeds by a heterogeneous reaction on the mineral's surface, then conditions of the groundwater are not very important, and attempts to determine the redox properties of the groundwater will not be pertinent; the important factor will be the redox properties of the minerals. Thus, it is important that the path of valence change and sorption reactions be known before they can be studied intelligently.

The primary objective of our program, "Valence Effects on Sorption", is investigation of redox and sorption processes that are critical to the prediction of migration of nuclides from the various repository sites that have been proposed. These investigations include study of laboratory techniques for valence state analysis and control and application of these techniques to the study of pertinent redox and sorption reactions. In particular, this project emphasizes use of electrochemical flow cells for valence control and solution conditioning. These techniques have not been used before for this purpose, and they allow control of valence state without the uncertainties introduced by the addition of redox buffers to the solutions. The results of these investigations are to be used to assess the predictions given in the Site Characterizaton Reports for the proposed repositories relative to retardation of nuclides, especially when redox mechanisms are involved.

2.5.1.3 Scope of Research

The approach used in this project is to try to identify experimentally in the laboratory the paths of pertinent sorption and redox reactions that occur in a simulated host-rock groundwater system, and, by making use of techniques of valence control and analysis, study the reaction and its dependence on the pertinent variables. Once the reaction path is

identified, then it will be possible to study its behavior as a function of the experimental conditions.

Electrochemical techniques are utilized in this project to adjust the valence state of nuclides to desired valence states, thus allowing study of sorption or other properties of that particular valence state. For example, it is possible to hold the oxidation state of a nuclide in an oxidized valence state, and then pass the solution containing the nuclide through a column of an adsorbent. In this way, the sorption properties of a species in that particular valence state can be investigated. If the adsorbent is expected to have redox properties, then it is possible to test for the presence of another valence state on the adsorbent by leaching it and testing the resultant leachate for the presence of different valence states. These operations must be done very quickly in a controlled atmosphere box in order to prevent any further valence change during the leaching and valence state analyses. In this way the reaction paths can be identified for various nuclide-mineral combinations, and evidence can be gathered relative to whether redox reactions occur on the surface (heterogeneous reaction) or in the solution (homogeneous reaction). Because we usually deal with very small concentrations of nuclides, it is not possible to determine speciation of nuclides in solution or adsorbed nuclides with conventional spectroscopic methods, and we must rely on accumulation of indirect chemical evidence for the identification of species.

2.5.2 EXPERIMENTAL TECHNIQUES

2.5.2.1 General Methods

We have concentrated so far upon reactions of Np(V) and Tc(VII) in this program. Our first task was to survey sorption of these nuclides on a variety of minerals in both air-saturated and anoxic conditions by means of standard test tube experiments. The goal was to look for differences in behavior which might be indicative of redox reactions. For minerals where there was evidence that redox reactions were important, the reactions were and are being studied by valence control and analysis techniques.

Length limitations do not permit a detailed description of these techniques. They are described in detail elsewhere (MEYER 1983, MEYER 1984).

2.5.2.2 Anoxic conditions

For studying redox reactions under anoxic conditions, a high quality controlled atmosphere box is necessary. We use boxes manufactured by Vacuum Atmospheres Company, Hawthorne, CA. The real problem in using any box of this type is to determine the level of dissolved oxygen in the experimental solutions. We have tried several membrane-type oxygen sensors, but we have found them to drift and to be unreliable for this use because they must always be calibrated immediately before use. We therefore use an alternative system (MEYER 1972) which is based on the coulometric principle of reduction. If a solution which contains dissolved oxygen flows though a reducing electrochemical cell at a known flow rate and if electrochemical conditions are such that the oxygen is reduced with 100% efficiency, then the dissolved oxygen content will be directly proportional to the reduction current and the flow rate though the cell. Essentially 100 percent reduction efficiency can be achieved through use of a porous flow-through electrode. We are now monitoring the oxygen content of test solutions which are continuously equilibrated with the atmosphere in the box, and we find dissolved oxygen levels of from 5 to 30 parts per billion. This is higher than we would like but seems to be the best achievable with this type of system. We also continuously monitor the oxygen content of the argon in the box with a gas-phase oxygen meter. Generally we find from 0.2 to 0.6 ppm oxygen in the gas.

2.5.2.3 Valence Analyses

Valence state analysis is an essential part of our procedures, and we use solvent extraction to check for the presence of a particular valence state. We use thenoyltrifluoroacetone (TTA), 0.5M in xylene to check for the presence of Np(IV), which is extracted from 1M HCl with very high distribution coefficients. The presence of Np(VI) is determined by solvent extraction with tri-n-octylamine (TOA), 10% by volume in xylene, from 4M HCl. To test

for the presence of Tc(VII), we use tetraphenyl arsonium chloride, 0.05 M in chloroform. We know of no method for testing for the presence of other valence states of Tc.

The valence state of adsorbed species may be inferred from use of these solvent extraction procedures on acid leachates of the minerals after sorption experiments. These leach experiments, generally done with 1M HCl, must be done quickly in a controlled atmosphere box under oxygen-free conditions in order to minimize change of valence of the adsorbed species. These experiments rely on the assumption that the valence state does not change upon leaching with HCl.

2.5.2.4 Electrochemical Apparatus

The valence state of an element can, in favorable situations, be controlled by electrochemical means. Briefly, our apparatus for doing this consists of a silver or platinum porous electrode, through which solution which contains the nuclide is pumped. In one configuration, the solution then passes through a column of an adsorbent. The potential of the electrode is set to a value which adjusts the nuclide to the appropriate valence state. The apparatus has been described in detail (MEYER 1983, MEYER 1984). We have used it to produce Np(IV) and to maintain Np(V) in the (V) valence state. Similar experiments were performed with Tc.

This apparatus can also be used for other purposes. It can, for example, be used to remove the last traces of oxygen from solutions and thus produce solutions which have essentially no dissolved oxygen. It is also useful for adjusting the pH and producing carbonate-free basic solutions. It is very difficult to produce carbonate-free solutions with standard basic laboratory reagents because they invariably contain some carbonate.

2.5.3 EXPERIMENTAL RESULTS

We present here examples of several types of experiments, and then summarize the results of our experiments to date.

In Figure 1, we show the result of test tube batch experiments for Np(V) sorption on eighteen different minerals. Sorption of Np(V) on each mineral was determined both under oxic and anoxic conditions. At first sight, the graph looks like a scatter plot, but closer examination allows the following conclusions. In each case, the nuclide was Np at trace concentration which we had adjusted to 100% Np(V). In Figure 1, the open squares represent oxic experiments, and the closed squares are anoxic. For many minerals, very high distribution coefficients were obtained for oxic conditions. This demonstrates that it is not necessary to produce anoxic conditions in the solution to cause Np to be retained by some minerals. In fact, at pH 8 to 10, the range of interest, values of Rs were always at least 10 to 100 liters/kg. From these experiments alone, one cannot tell whether Np(V) was reduced. That knowledge requires further experimentation. Individual graphs for each mineral shown in Figure 1 are given in MEYER (1983).

In Table 1, we show results of an experiment with Np(V) sorption on basalt in which we adjusted our electrochemical apparatus so that Np remained in the (V) state. This is confirmed by the numbers in the fourth row of Table 1 which show 100, 99.7, 98.5, and 100 for the percent of Np(V) in solution. The Np on the basalt was primarily Np(IV), and these results indicate that basalt was reducing the Np(V). In Figure 2, we show a summary of our experiments to date with basalt at trace level Np. The basalt samples marked U were from the Umtanum flow and were selected to be as uniform as possible and free of alteration zones. They were ground without any contact with steel or iron. It is interesting that the primary variable affecting sorption of Np(V) appeared to be pH and that little if any significant difference was observed between oxic and anoxic experiments. From these observations, we tentatively conclude that NpO_2^+ is first adsorbed on the basalt as NpO_2^+, with the amount adsorbed dependent primarily on pH. The reduction reaction then occurs on the surface, probably by ferrous ion within the basalt. The basalt marked W in Figure 2 was obtained from the WISAP program (SERNE 1982) and was contaminated with metallic iron. High values of Rs were observed because of this iron contamination.

TABLE 1
Column Experiments, Np on Basalt

Sorption of Np(V) on crushed basalt. Recirculating column experiments with porous electrode set to indicated potential

	Anoxic	Anoxic(dupl)	Oxic*	Oxic*
Rs, L/kg	27.3	21.3	78.7	52.3
Eh, V vs H	+0.298	+0.282	+0.266	+0.287
pH	6.6	6.78	7.71	7.54
% Np(V) in solution	100	99.7	98.5	100
% Np(IV) on basalt	89	94.6	95.5	94.7

*The first oxic test was a desorption experiment in which basalt with adsorbed Np from an anoxic experiment was taken out into the atmosphere and the solution saturated with oxygen. The second oxic experiment was a sorption experiment in air.

For Tc, the results are somewhat different. We have found little or no sorption of technetium under oxic and anoxic conditions on a great variety of minerals. A typical result is that shown for clinoptilolite in Figure 3. There appears to be no significant difference between oxic and anoxic conditions, and there is a general decrease of Rs with pH. Low values of Rs are observed in the pH range of natural systems. In other investigations under oxic conditions, we have found some sorption of Tc(VII) at low pH but very low values of Rs at higher pH for most natural adsorbers (PALMER 1981).

We have also investigated Tc(VII) sorption under anoxic conditions in a column apparatus on alumina and basalt. We used alumina because it is a good non-reducing sorbent and serves as a basis for comparison with a

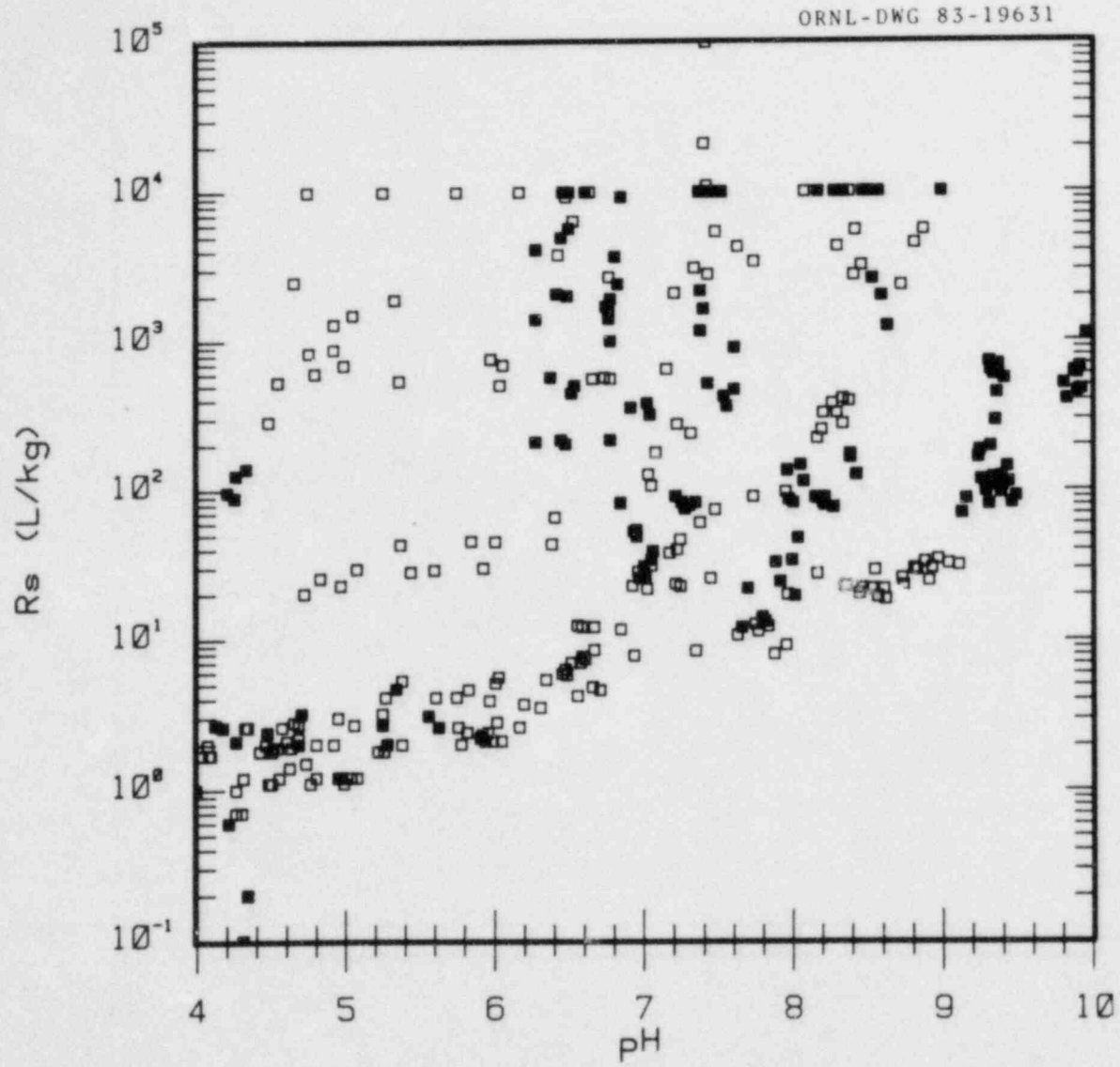

Fig. 1 Sorption ratios for Np(V) on 18 different minerals (listed in text). Trace Np(V). 0.1 M NaCl. Open symbols oxic. Closed symbols anoxic. Test tube batch.

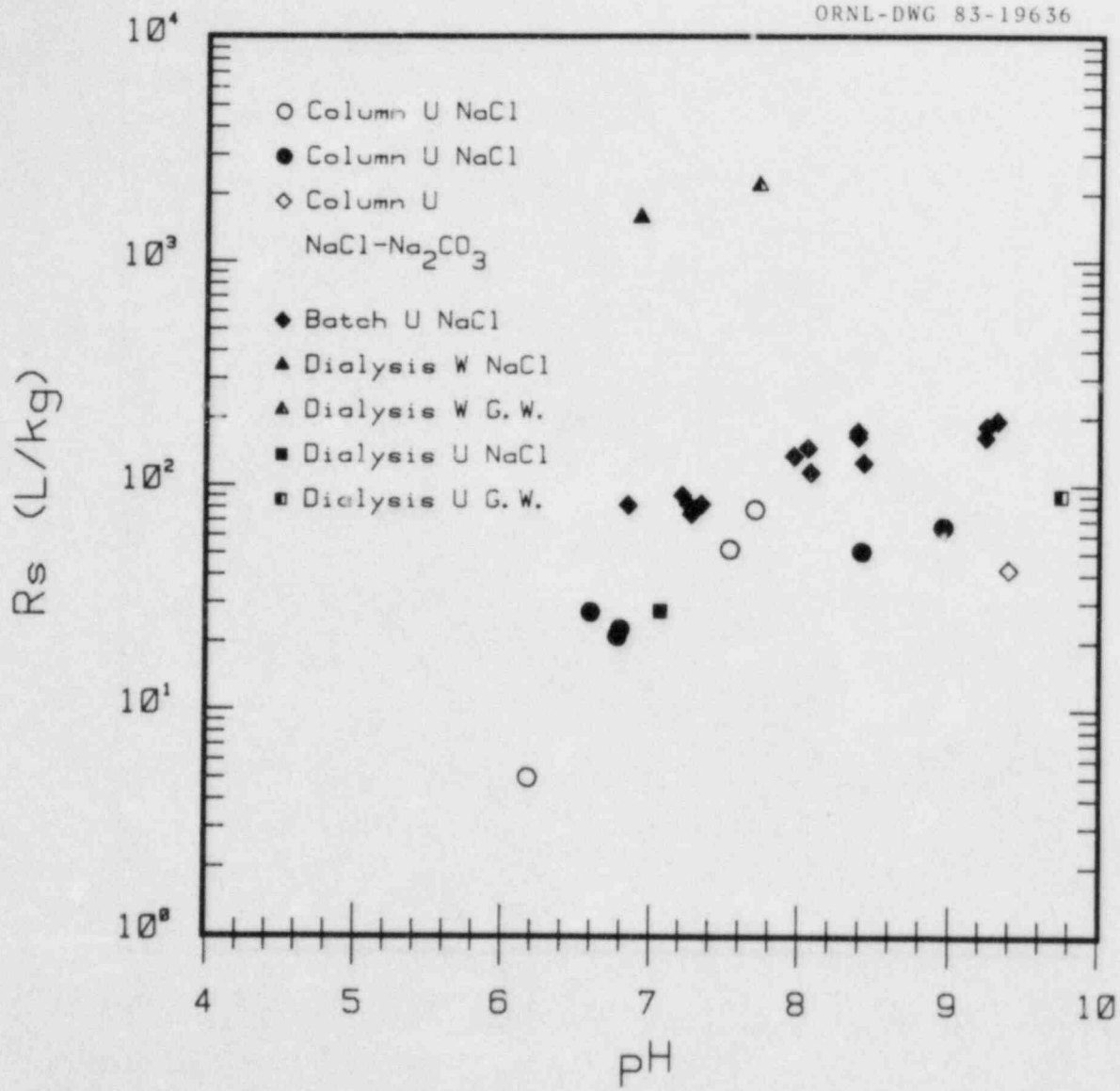

Fig. 2 Sorption of Np(V) on basalt as a function of pH from 0.1M NaCl or simulated ground water. Trace Np. U = Umtanum. W = WISAP. Open symbols oxic. Others anoxic.

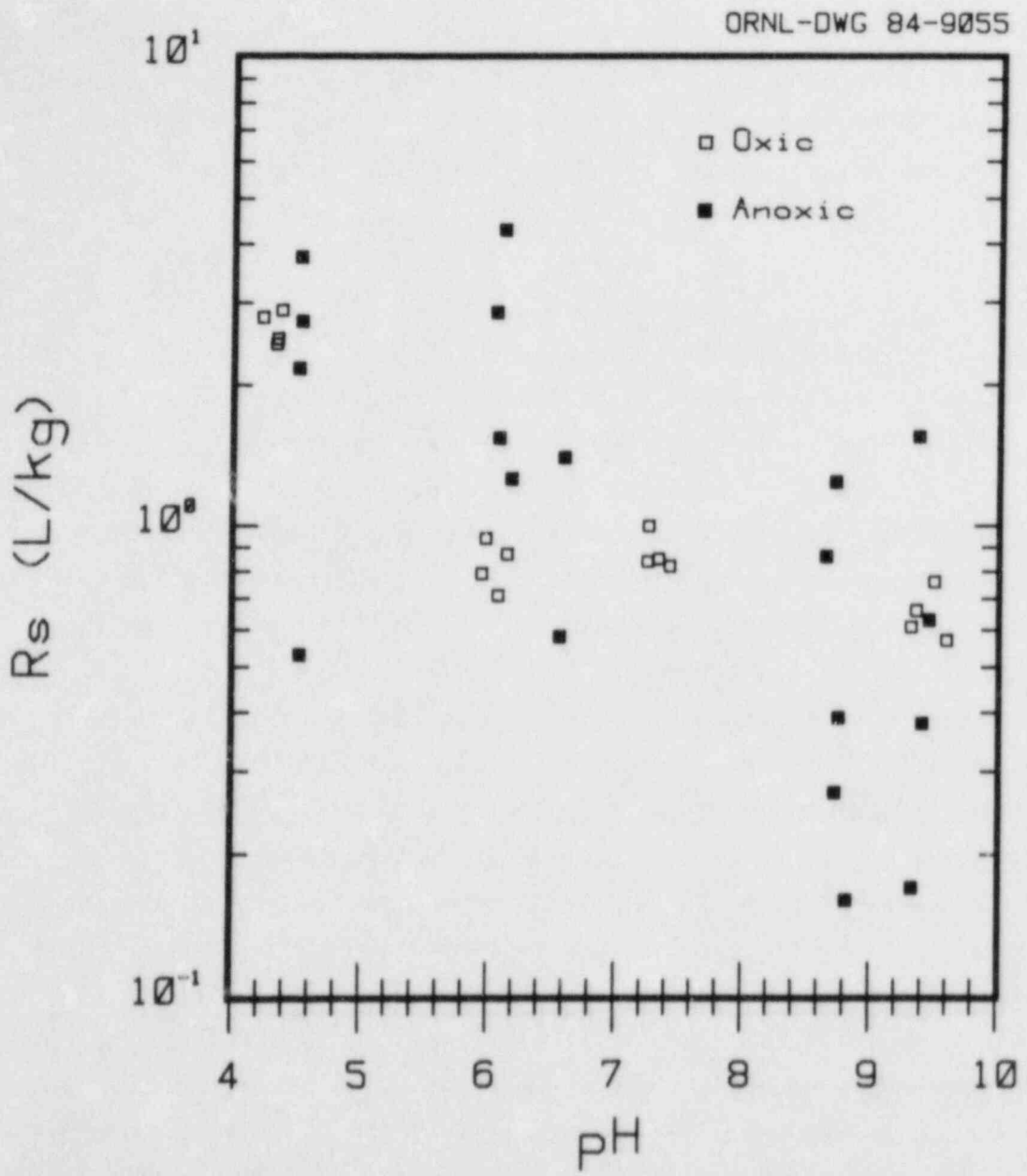

Fig. 3 Sorption of Tc-95m on clinoptilolite from 0.1M NaCl. Comparison of aerated and de-aerated solutions.

material like basalt which has been reported to be reducing to Tc(VII) (SALTER 1982). The experiments with alumina showed that Tc(VII) that was reduced electrochemically was strongly adsorbed on alumina and other parts of the apparatus. For basalt, we consistently observed very slow decreases in concentration of Tc in the solution. If metallic iron was present in the basalt, then reduction of Tc(VII) occurred very rapidly. It is therefore extremely important to make sure that the basalt is not contaminated with iron or other reducing materials during sample preparation.

2.5.4 CONCLUSIONS

We have shown that reaction paths for Np(V) and Tc(VII) can, with appropriate techniques, be followed to a considerable extent with respect to redox and sorption reactions on minerals. The techniques are not difficult, but they do require, especially for Tc, use of a high-quality controlled atmosphere box. Our experiments with Np(V) showed that adsorption of NpO_2^+ increased with pH for almost all of the materials which we tested. When Np(IV) was formed electrochemically within the solution, it was adsorbed on most of the surfaces in the apparatus and essentially no Np(IV) was detected in the solution. Tests with basalt under both anoxic and oxic conditions demonstrated that the Np(V) adsorbed on basalt was reduced to Np(IV) and was very difficult to remove. However, there was always some Np(V) on the surface, from 5 to 10% of the total adsorbed Np. These results suggest that NpO_2^+ is first adsorbed on the basalt, and then it is reduced on the surface, presumably by components of the basalt. This reduction is independent of redox conditions in the solution. On the other hand, the reduction of Tc(VII) was extremely sensitive to dissolved oxygen, and tests under anoxic conditions with ground basalt showed very slow rates of reduction. Only when metallic iron was present did we find rapid reduction of Tc(VII). The reduction of Tc(VII) on mineral surfaces seemed to be very sensitive to surface conditions. This is confirmed by our work and the work of others (VANDERGRAAF 1983, FRANCIS 1980, BONDIETTI 1979, ALLARD 1979, STRICKERT 1980, PALMER 1981).

2.5.5 RECOMMENDATIONS

In view of the above experimental results, it is possible to judge some of the methods proposed to study and predict redox reactions in host rock groundwater systems. Our results suggest that reduction of Np(V) and Tc(VII) may occur as a surface reaction, and not within the groundwater. Further, we have shown that if Np(IV) is formed in solution, it will adsorb on just about any surface available. The same is true of Tc. Therefore, if we add a redox buffer that will reduce Tc(VII) or Np(V) in the solution, the reduced Np or Tc will adsorb on just about any surface. But adding a redox buffer may not simulate the actual conditions in the host rock groundwater system, especially if the reduction occurs on the surface of the mineral rather than in the solution. In fact if the buffer happens to reduce Tc(VII) or Np(V) rapidly, the use of the buffer might give very misleading results, for it is likely that the reduced products of Np and Tc will adsorb (or precipitate) rapidly on any surface available. If only the surface of a particular mineral can reduce the Tc, then the use of the buffer will not in any way be representative of the actual process in the host rock. If, on the other hand, reduction of Np(V) and Tc(VII) does occur in the groundwater, then use of a redox buffer could be useful in determining the extent of sorption of reduced forms of the nuclide, provided that the redox buffer does not interfere with the adsorption process. This latter condition is difficult to demonstrate. Thus, we would certainly recommend against use of redox buffers unless the reaction path for the process under study and the effects of the buffer on the adsorbent were clearly understood.

Similar considerations apply to the use of 'Eh' probes, inert electrodes that are inserted into the groundwater in attempts to measure a system 'Eh'. In a thoroughly deoxygenated solution with very little Fe^{2+} or Fe^{3+} in the solution, there is little that can poise the potential of the electrode. If the reaction is a surface reaction, then the potential of the 'Eh' probe will have little relation to the ability of the surface to reduce. Furthermore, it is difficult even to define what is meant by the effective 'Eh' of a host-rock-groundwater system unless the reactions that control the redox properties are known and their kinetics well understood.

Also, unless these reactions are in complete thermodynamic equilibrium with the indicator electrodes and all redox couples in the system, there can be little confidence in measurement of potentials on indicator electrodes. These considerations have been described in detail elsewhere (MEYER 1983, MEYER 1984).

The electrochemical method of valence state control has the advantage that its use does not introduce chemical species into the solution which might affect the sorption process. Also, one can easily set the potential to any value within the range of stability of water. It must be emphasized however that only the species in the solution can be adjusted with this method. The solid phases are unaffected. Thus its primary use, as with redox buffers, is to investigate the sorption of various valence states on solid materials.

Our experiments have shown so far that Tc(VII) is reduced very slowly by crushed basalt. Basalt repositories are predicted to be reducing to Tc(VII) from thermodynamic considerations, but there are uncertainties relative to these predictions (NUREG-0960, 1983). It is possible that the kinetics of the reaction may be unfavorable, or in the actual flow paths of the groundwater, the repository is not as reducing as is predicted. In that case, it might be beneficial to add backfill material. From the work that we have done, a mixture of hydrous oxides and metallic iron should be extremely effective in removing both Np and Tc. Although we have not yet carried out work with uranium and plutonium, we suspect that this mixture might also be effective with these materials.

2.5.6 PLANNED RESEARCH

We have introduced electrochemical techniques to study effects of valence change on sorption and to follow the reaction path for valence change reactions that have been identified as important in safety analyses for given sites, and these techniques were used to identify possible reaction paths for neptunium sorption on basalt. In order to test further the applicability of these techniques, we plan work with other systems, particularly for technetium reactions, which tend to be difficult to reproduce, and

possibly with uranium and plutonium reactions. In particular, we need to investigate these methods for materials that will be in the flowpath of groundwaters from basalt, tuff, and other possible host rock systems.

One of the troublesome aspects of predicting migration of nuclides is the possibility of large changes of sorption due to the formation of negatively charged complexes such as the carbonate complexes of uranium. Our apparatus allows us to prepare essentially carbonate-free and oxygen-free solutions at high pH. This is difficult to do by ordinary techniques because most alkaline chemical reagents easily adsorb carbon dioxide from the atmosphere. We plan to prepare such solutions and investigate effects of valence change and carbonate complexation on sorption reactions.

ACKNOWLEDGEMENTS

We would like to thank J. S. Johnson and G. D. O'Kelley of the Chemistry Division of ORNL for helpful discussions and advice. For advice in geology, we thank the geologists and geochemists in the Chemistry Division, M. T. Naney, D. R. Cole, J. G. Blencoe, and S. E. Drummond.

REFERENCES

ALLARD 1979. B. Allard, H. Kigatsi, and B. Torstenfelt, *Radiochem. Radioanal. Letters* 37, 223 (1979).

BONDIETTI 1979. E. A. Bondietti and C. W. Francis, *Science* 203, 1337 (1979).

BURNEY 1974. G. A. Burney and R. M. Harbour, *Radiochemistry of Neptunium*, NAS-NS-3060, 1974.

FRANCIS 1980. C. W. Francis and E. A. Bondietti, "Sorption-Desorption of Long-Lived Radionuclide Species on Geologic Media," *Task 4 Third Contractor Information Meeting, Waste Isolation Safety Assessment Program*, Vol. II, PNL-SA-8571, p. 81, 1980.

MEYER 1972. R. E. Meyer, F. A. Posey, and P. M. Lantz, *Desalination* 11, 329 (1972).

MEYER 1983. R. E. Meyer, W. D. Arnold, F. Case, S. Y. Shiao, and D. A. Palmer, *Valence Effects on Adsorption — A Preliminary Assessment of the Effects of Valence State Control on Sorption Measurement*, NUREG/CR-2863 ORNL-5905, 1983.

MEYER 1984. R. E. Meyer, W. D. Arnold, and F. I. Case, *Valence Effects on the Sorption of Nuclides on Rocks and Minerals*," NUREG/CR-3389 ORNL-5978, 1984.

NUREG-0960 1983. *Draft Site Characterization Analysis of the Site Characterization Report for the Basalt Waste Isolation Project*, NUREG-0960, p. 5-6, 1983.

PALMER 1981. D. A. Palmer and R. E. Meyer, *J. Inorg. Nucl. Chem.* 43, 2979 (1981).

SALTER 1982. P. F. Salter and G. K. Jacobs, "Evaluation of Radionuclide Transport: Effect of Radionuclide and Solubility," Scientific Basis for Nuclear Waste Management Symposium V, W. Lutze, ed., North Holland, Amsterdam, 1982.

SERNE 1982. R. J. Serne and J. F. Relyea, *The Status of Radionuclide Sorption — Desorption Studies Performed by the WRIT Program*, PNL-3997, 1982.

STRICKERT 1980. R. Strickert, A. M. Friedman, and S. Fried, *Nuclear Technology* 49, 253 (1980).

VANDERGRAAF 1983. T. T. Vandergraaf, K. V. Ticknor, and I. M. George, "Reactions between Technetium in Solution and Iron-Containing Minerals under Oxic and Anoxic Conditions," presented at the International Symposium on Geochemical Behavior of Disposed Radioactive Waste, 185th National Meeting of the American Chemical Society, Seattle, WA March 20-25, 1983, to be published in an ACS Monograph.

2.6. SURFACE OXIDIZATION-REDUCTION REACTIONS IN COLUMBIA PLATEAU BASALTS

Art F. White and Andy Yee

Lawrence Berkeley Laboratory
University of California
Berkeley, CA 94720

2.6.1. ABSTRACT

Results are presented which define principal oxidation-reduction reactions expected between ground water and iron in the Umtanium and Cohassett basalt flows of south central Washington. Data include kinetics of aqueous iron speciation, rates of O_2 uptake and nature of oxyhydroxide precipitates. Such data are important in predicting behavior of radionuclides in basalt aquifers including determination of valence states, speciation, solubility, sorption, and coprecipitation on iron oxyhydroxide substrates and colloids.

Analyses of the basalt by XPS indicates that ferrous iron is oxidized to ferric iron on the surface and that the total iron decreases as a function of pH during experimental weathering. Iron oxyhydroxide phases did not form surface coating on basalt surfaces but rather nucleated as separate phases in solution. No significant increases in Cs or Sr sorption were observed with increased weathering of the basalt. Concurrent increases in Fe(II) and decreases in Fe(III) in slightly to moderately acid solutions indicated continued oxidization of ferrous iron in the basalt by the reaction:

$$\underset{\text{Basalt}}{(\text{Fe(II)}\cdot 1/z\ M^z)} + \underset{\text{solution}}{\text{Fe(III)}} \rightarrow \underset{\text{Basalt}}{\text{Fe(III)}} + \underset{\text{solution}}{\text{Fe(II)}} + \underset{\text{solution}}{1/z\ M^z}$$

which involves a net transfer of an electron and cation, M, into solution from the basalt phase.

At neutral to basic pH, Fe(II) was strongly sorbed onto the basalt surface ($K_d = 6.5 \times 10^{-3}$ l$\cdot$ m^2) resulting in low dissolved concentrations even under anoxic conditions. The rate of O_2 uptake increased with decreasing pH. Diffusion rates ($\sim 10^{-14}$ cm$^2 \cdot$ s^{-1}), calculated using a one dimensional analytical model, indicate grain boundary diffusion. Comparisons of Eh values calculated by Pt electrode, dissolved O_2 and Fe(II)/Fe(III) measurements showed considerable divergence, with the ferric-ferrous couple being the preferred method of estimating Eh.

2.6.1. INTRODUCTION

Oxidization-reduction (redox) reactions involving ground water, both under hydrothermal near field and ambient far field conditions, and electro-chemically active iron in a basalt mineral assemblage will have a major impact on the extent of radionuclide migration and therefore the long term performance of a nuclear repository. Concentration levels and rates of transport of radionuclides are dependent on solubility and complexation which in turn are functions of the elemental valency state and redox state. In addition, radionuclide concentrations will be modified by coprecipitation and sorption which will involve aquifer substrates such as Fe and Mn oxyhydroxides, the stability of which are also Eh dependent.

a) Issues Addressed by Research

An experimental program was undertaken to define redox controls of geochemical reactions between basalt and simulated ground water. The goal is to define both chemical mechanisms and quanitative rates which can be incorporated into a coupled chemical hydrologic model mandated by 10CFR 60.

Issues addressed by the research are:

1) What are the principal redox reactions in a basalt aquifer?

2) What would be the effects of O_2 introduced into ground water from the repository and what are the rates of consumption?

3) What are the kinetics of iron oxyhydroxide formation in a basalt aquifer and how does this affect radionuclude sorption, coprecipitation and colloid transport?

4) Is determination of iron speciation in ground water an effective method of estimating Eh?

b) Background

High concentrations of electroactive iron at low pH, such as in mine drainages, have been shown to strongly control the Eh of geochemical systems (Norstrom et al, 1979). The effects of Fe(II)/Fe(III) concentrations on Eh in neutral to alkaline pH ground waters of the Columbia Plateau basalts and on radionuclide valency states and solubilities have not been adequately assessed. In addition, such ground waters have generally been considered devoid of dissolved O_2, which

can strongly buffer Eh, because of oxidization of iron-containing minerals. However recent data (Winograd and Robertson, 1982), showing appreciable dissolved O_2 in several old ground water systems, suggest that iron oxidization in aquifers may be slower than expected. The residence times of extraneous oxygen, introduced by repository development, and associated effects on aquifer Eh conditions must be assessed.

Finally, radionuclides have been found to be strongly sorbed and coprecipitated with iron oxyhydroxides (Hildebrande and Blume 1974). The nucleation mechanisms and morphologies of such oxhydroxides, formed by interaction with the aquifer, will influence sorption capacities. Kinetics of formation will also determine whether or not such phases will form mobile colloids or immobile substrates. Siever and Woodford, (1979) for example, proposed that iron silicates such as basalt become armored with oxhydroxide substrates processing very high surface areas and exchange capacities.

c) Scope of Research

The research presented in this paper is confined to a experimental study of oxidation-reduction kinetics in basalt/water reactions. Research at present has only been conducted at 25°C which would be representative of far field conditions at relatively shallow depth. Additional higher temperature experiments are planned. Maximum reaction times for water/ basalt reactions were limited to 8 months.

2.6.3. METHODS

The Grande Ronde Basalt (6-16 myp) comprises approximately 70% of the total basalt accumulation of the Pasco Basin, south central Washington U.S.A. (Meyers and Price, 1979). Fresh samples of the Umtanum and Cohassett flow units were obtained from drill core and outcrop material respectively.

The bulk chemistries of the Grande Ronde samples are presented in Table 1. Although total iron is very similar, ferric iron is higher in the Umtanum basalt possibly due to greater high temperature oxidization of iron oxides (Haggerty, 1976).

The bulk mineralogy (Noonan, 1980) are summarized in Tables 1 and 2. Dominant iron silicates include clinopyroxenes, augite and pigeonite with relatively rare olivine. Titaniferous magnetite is the dominant iron oxide, occurring as dendritic or coarsely crystalline grains. An interstitial glassy ground mass or mesotasis is abundant.

TABLE 1

Chemical analyses of Columbia Plateau basalt (wt. percent)

	Cohassett Bluffs flow of the Grande Ronde Formation	Umtanum flow of the Grande Ronde Formation
SiO_2	53.41	54.90
TiO_2	1.79	2.17
Al_2O_3	15.00	14.34
Fe_2O_3	4.36	4.81
FeO	9.42	8.71
MnO	0.20	0.22
MgO	4.99	3.48
CaO	8.86	7.30
Na_2O	2.82	2.66
K_2O	1.00	1.48
P_2O_5	0.27	0.35
	102.12	100.42

TABLE 2

Primary Minerology and Iron Content of Umtanum Basalt (after Noonan, 1980)

	Wt. % of Basalt	Wt % iron in plase
Plagioclose	25-50	.07-.09
Augite	20-45	15-18
Pigeonite	0-10	21-22
Olivine	0-3	33-53
Magnetite	0-7	68-72
Mesostosis	15-70	1-11

Experimental conditions of individual basalt/water reactions are reported in Table 3. Solutions were buffered using different ratios of $NaHCO_3$, HCl and dissolved CO_2.

Flasks containing basalt were periodically opened and dissolved oxygen (D.O.) was measured using an Orion electrode (± 0.05 ppm). Experiments using O_2 free solutions indicated that the minimum measureable D.O. value was ~ 0.20 ppm due to O_2 contamination during introduction of the electrode into the flask. The Eh of the solution was subsequently measured using an Orion Pt electrode calibrated against a Zobell solution. An aqueous sample was immediately extracted by a gas tight syringe, filtered (0.2 μm), acidified and analyzed for Fe(II) and total iron. Other major dissolved components, including Na, K, Ca, Mg, Si and Al, were analyzed later.

Aqueous iron was determined spectrophotometrically using a ferrozine chromagen (Gibbs, 1979) with a lower limit of detection of 10 $\mu g.l^{-1}$. Because ferrozine reacts only with the ferrous ion, the Fe(II)/Fe(III) ratio in solution was conveniently determined by reducing a sample split with hydroxylamine, measuring total iron, and calculating Fe(III) by the difference relative to Fe(II).

Ferrous-ferric iron in the bulk basalt samples (Table 1) was also determined from Fe(II) and total iron. Ferrous iron was analyzed by dissolving the basalt in a HF solution containing V(V) which oxidized Fe(II) as it dissolved into solution (Wilson, 1955). Fe(II) was determined by titration of excess V(V). Total iron was determined in the HF solution by atomic absorption spectrometry.

The iron concentration and oxidization states on the composite surfaces (< 20 Å thickness) of basalt mineral grains were determined using X-ray photoelectron spectroscopy (XPS). The theory, instrumentation and application of XPS to geological studies have been reviewed by Bancroft et al. (1979) and applied to iron silicates by Berner and Schott (1982).

2.6.4. RESULTS

Iron Release from Basalt

Release of chemical species into solution during experimental dissolution of basalt was found to be highly incongruent as shown for Umtanum basalt in Figure 1. Relatively rapid

TABLE 3

Summary of selected experimental parameters

Experiment No.		Initial sol. composition	basalt ($gm.\ell^{-1}$)	Intial O_2 (ppm)	Intial pH	Final O_2 (ppm)	Final pH	Total time (s)
Closed system	1	D.I. H_2O	80	<0.20	9.63	0.80	9.15	6.8×10^6
	2	D.I .H_2O	80	9.23	5.46	0.17	5.62	6.3×10^6
	3	D.I. H_2O	80	<0.20	4.94	<0.20	5.58	7.8×10^6
	4	D.I. H_2O	80	9.34	2.62	0.95	3.80	2.3×10^6
	5	10 ppm Fe(II)	16	9.48	6.50	7.86	6.48	3.4×10^5
	6	70 ppm Fe(II)	16	9.48	6.50	2.20	6.35	3.4×10^5
Open system	7	2 ppm Fe(III)	2.6	~ 9	3.46	~ 9	3.52	9.3×10^4
	8	2 ppm Fe(III)	13.3	~ 9	3.42	~ 9	3.46	9.3×10^4
	9	2 ppm Fe(III)	2.6	~ 9	4.48	~ 9	4.53	9.3×10^4
	10	2 ppm Fe(III)	13.3	~ 9	4.02	~ 9	4.57	9.3×10^4

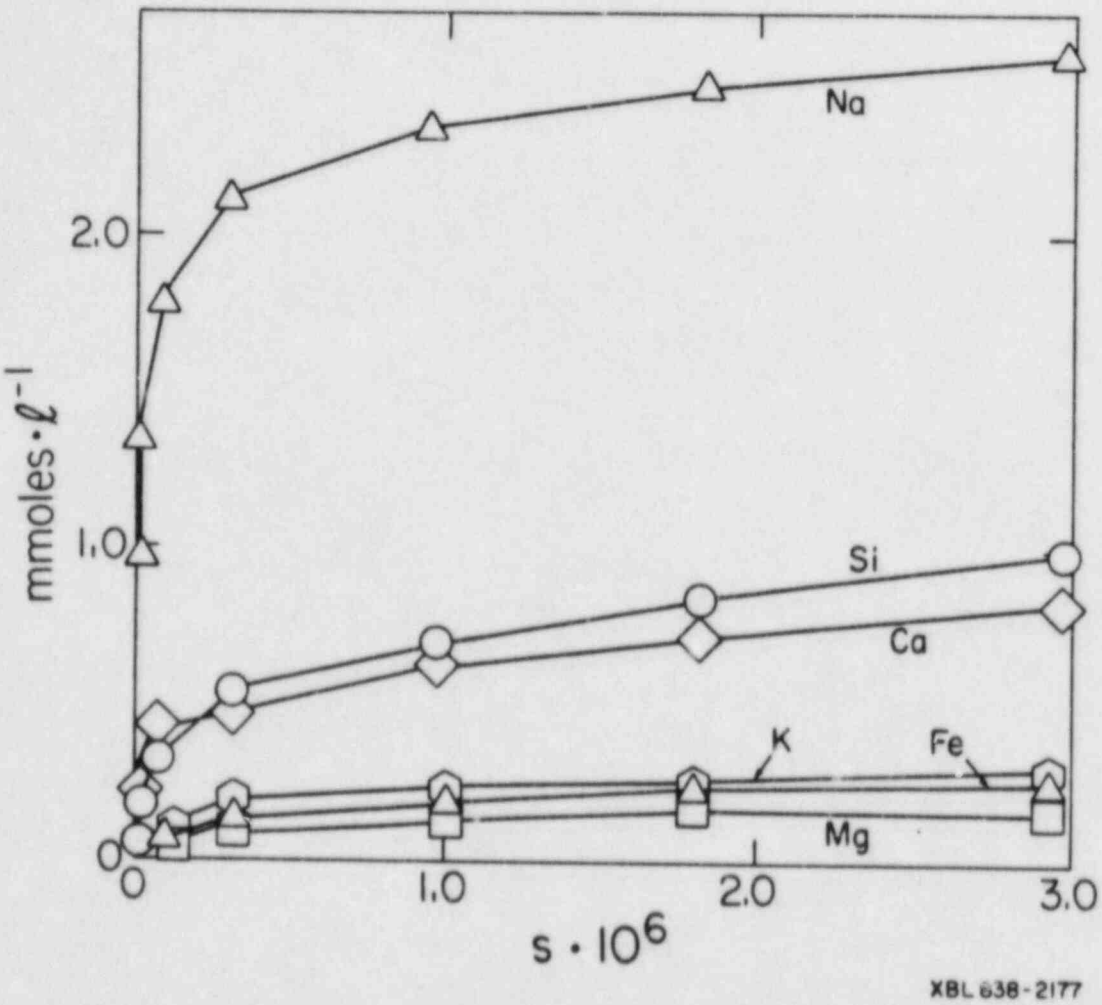

Fig. 1. Release of major chemical species during weathering of Umtanum basalt over 75 days at an average pH of 5.5

release of Na and Si, common for glassy rocks (White et al. 1980), suggests preferential dissolution of the alkali-silica rich mesotasis. Dissolution rates become linear at longer reaction times.

As indicated by dissolution data in Figure 2, aqueous iron concentrations are strongly pH dependent. At moderately acidic pH, the dominant Fe(II) species increase initially with time and then level off in a pattern similar to that reported for basalt by Siever and Woodford (1979). Dissolution data for iron does not appear to fit any simple linear or parabolic rate law. Figure 2 shows that the rate of Fe(II) release is only slightly faster at low PO_2 than at high PO_2. No detectable Fe(II) was found in solutions below pH 7.0. Fe(III) concentrations, low over the entire pH range, initially increased in solution and then decreased below detection limits at longer times. As shown in Figure 2, detection limits are higher at lower pH since Fe(III) is calculated from the difference between relatively large but similar concentrations of both total iron and Fe(II). Calculation of saturation states using the WATEQF speciation code (Plummer et al. 1976) indicates that above a pH of 5.5 Fe(III) concentrations are generally supersaturated with respect to amorphous iron hydroxide $Fe(OH)_3$ (log IAP/K, 0-2). Declines in aqueous concentrations in this pH range may be due to onset of such oxyhydroxide precipitation.

In undersaturated solutions at low pH, Fe (III) concentrations are also generally below detection limits (Figure 2). As indicated in Table 1, appreciable Fe(III) is contained in the basalt phase assemblage as well as on the surface. The absence of Fe(III) in solution at low pH implies either that the dissolution of Fe from basalt is highly incongruent, i.e. Fe(II) is released and Fe(III) is retained in the mineral assemblage or that Fe(III) is being either reduced or removed from solution by some other process.

Surface Chemistry

Surface compositions and iron oxidation states were characterized by X-ray photoelection spectroscopy (XPS). Typical spectra for iron $2p_{1/2}$ and $2p_{3/4}$ peaks are shown in Figure 3 for fresh and reacted Umtanum basalt. As indicated, progressive decreases in peak intensities occur with decreasing pH of reaction.

The electron binding energies of the spectral peaks can be used to estimate the surface oxidization state of iron provided that corrections are made for surface charging. Table 4 lists measured binding energies and corrected energies based on charging shifts of the adventitious carbon

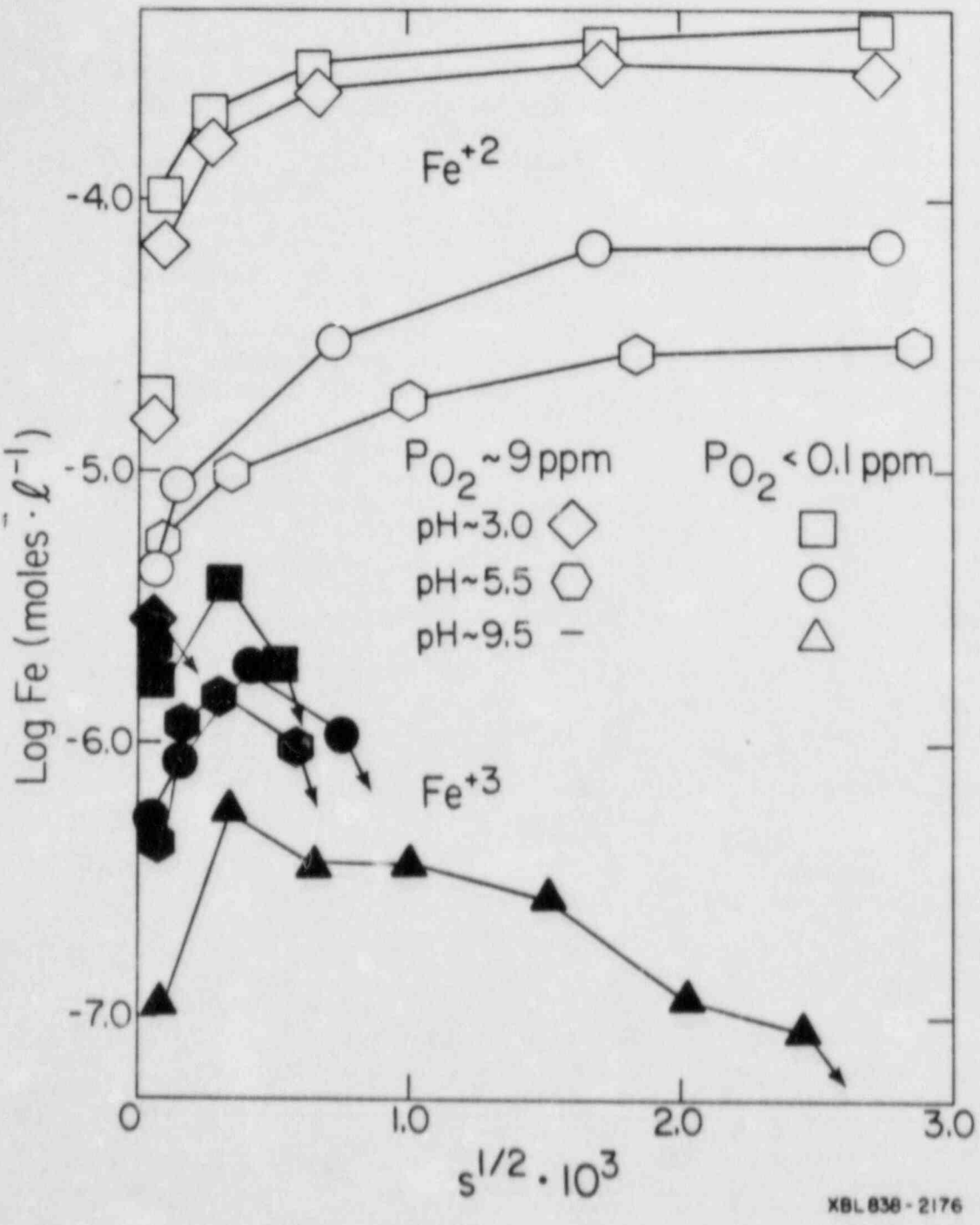

Fig. 2. Fe(II) and Fe(III) concentrations in solutions during weathering of Umtanum basalt. Open and solid points are Fe(II) and Fe(III) respectively.

TABLE 4

Measured and corrected XPS peak positions for iron (ev).

Experiment	$C_{1s(measured)} - C_{1s(284.6)}$	Measured $Fe_{2p\ 3/2}$	Corrected $Fe_{2p\ 3/2}$
blank	2.60	714.9	712.3
1	2.60	714.7	712.1
2	2.80	714.1	711.3
3	2.70	714.5	711.8
4	2.50	714.7	712.2
5	2.60	714.5	711.9
6	2.60	714.0	711.4

energies based on charging shifts of the adventitious carbon 1_s peak from a standard state of 284.6 eV (Wagner et al., 1979). The average shift of 2.6 eV in the $2p_{3/2}$ iron peak, due to charging, is shown in Figure 3. Corrected binding energies for the $2p_{3/2}$ peak correspond closely to Fe(III) reported in Fe_2O_3 (712.0 to 712.2 eV; Allen et al., 1974; McIntyre and Zetaruk, 1977), but are higher than Fe(II) in FeO(709.3 eV). The binding energy separation of 13.5 eV (Figure 3) also agrees with that reported by Wagner et al. (1979).

As suggested by the decreases in spectral intensities in Figure 3, decreasing reaction pH produces a quanitative drop in surface iron concentrations in Figure 4. At a pH of 3.5, half of the total iron has been removed from the basalt surface. Iron decreases, particularly at high pH, indicate that iron oxyhyroxide coatings do not form on experimentally weathered basalt as postulated by Siever and Woodford (1979).

The effect of oxyhyroxide precipitation from solution on the surface chemistry of basalt was investigated by the addition of Fe(II) to solutions at neutral pH. As indicated in Figure 4, resulting oxyhyroxide precipitation from a 70 ppm Fe(II) solution doubled the surface iron concentration while precipitation from a 10 ppm Fe(II) solution failed to increase the surface concentration to a level initially present on the unreacted basalt. The initial Fe(II) solutions were also tagged with 1×10^{-4}M $CsCl_2$ and $SrCl_2$ to determine if co-precipitation or sorption occurred in oxyhyroxide phases

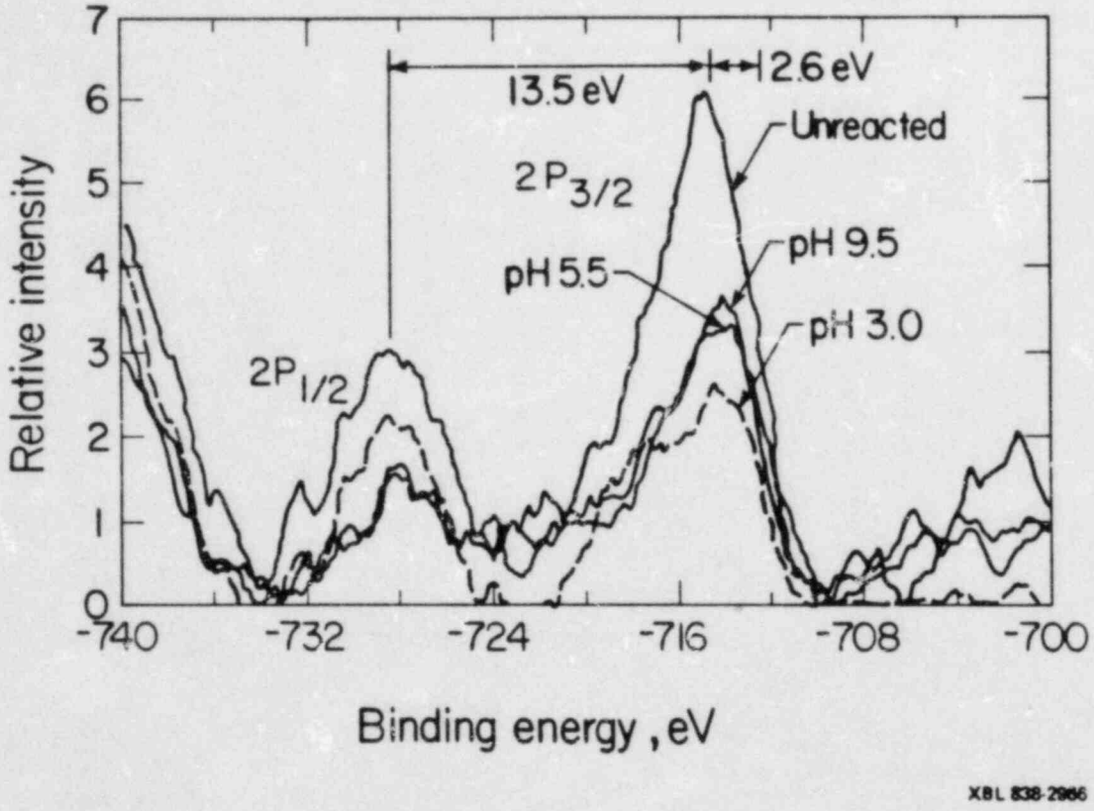

Fig. 3. XPS spectra for $2P_{1/2}$ and $2\ P_{3/2}$ iron peaks showing decrease in intensity with decrease in reaction pH. An average 2.6 ev shift is due to surface charging.

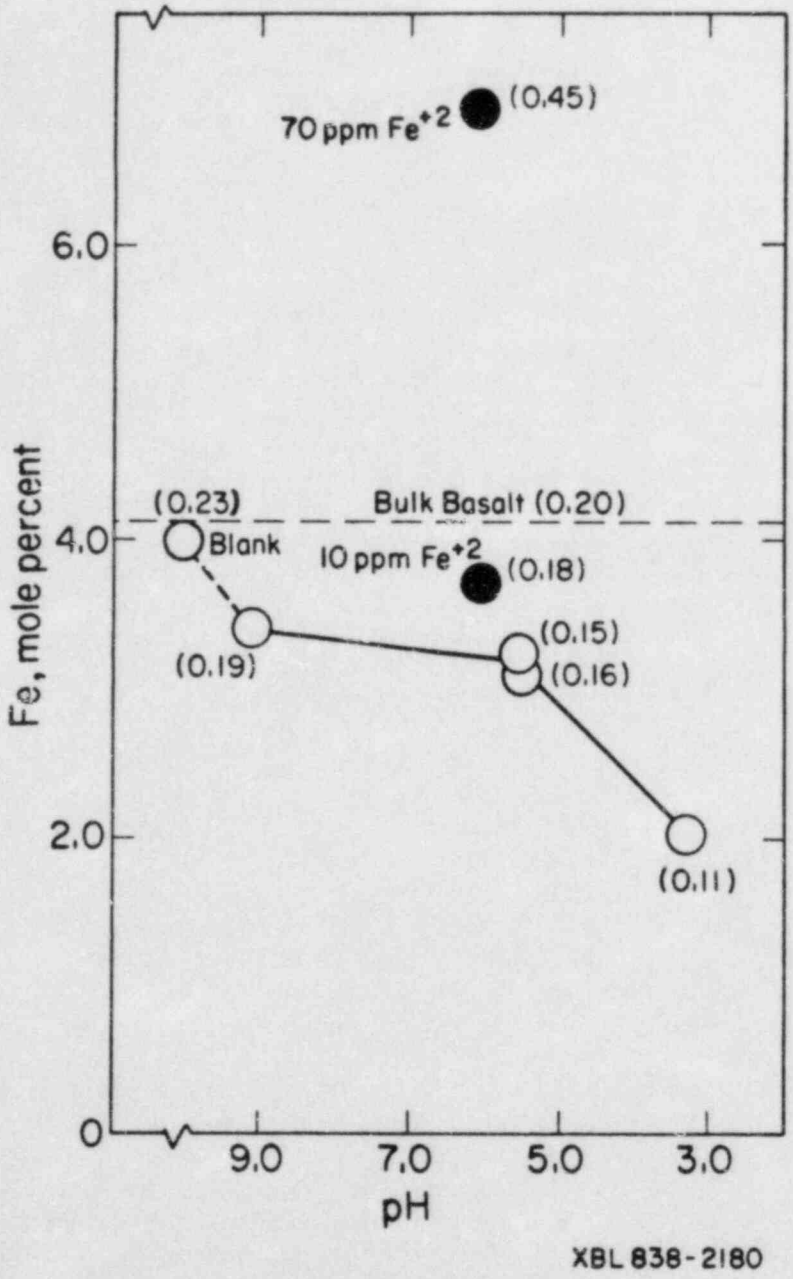

Fig.4. Atomic percentages of Fe on the basalt surface as a function of pH. Closed circles are compositions resulting from addition of aqueous Fe(II). Numbers in parentheses are Fe/Si ratios.

on the basalt surface. In all cases, the $3d_{5/2}$ peaks for Cs and Sr were found to be below XPS sensitivity levels. The above results suggest that iron oxyhydroxides form by homogeneous nucleation in solution rather than as surface coatings on iron silicate grains, a conclusion supported by visual inspection of suspended oxyhyroxide phases in solution.

Oxidation - reduction in solution

As previously indicated, at low pH Fe(III) is absent in solutions reacting with a basalt phase assemblage with signifiant ferric iron. To determine the fate of Fe(III), initial solutions containing 2 ppm ferric iron were prepared (experiment 7-10 Table 3). As shown in Figure 5, Fe(III) is stable in blank solutions at pH 3.5 and 4.5, indicating no reduction to Fe(II) nor precipitation as an oxyhydroxide. However addition of Cohassett basalt decreased Fe(III) in solution at a rate proportional to pH and the basalt surface area. During the same time interval, Fe(II) showed significant increases. At pH 3.5, the final Fe(II) concentration greatly exceeded the initial Fe(III) concentration, indicating an iron contribution from basalt dissolution (Figure 2). At pH 4.5 the total iron in solution remained nearly constant over time.

One obvious explanation for the Fe(III) decrease and Fe(II) increase is that ferric iron is being reduced to ferrous iron in solution in the presence of basalt. In order to uniquely define the mechanism, aqueous $^{59}Fe(III)$ was used as a radioactive tracer. If Fe(III) was totally reduced to Fe(II) in from basalt dissolution (figure 2). At pH 4.5 the total iron in solution remained nearly constant over time.

One obvious explanation for the Fe(III) decrease and Fe(II) increase is that ferric iron is being reduced to ferrous iron in solution in the presence of basalt. However the possibility exists that corresponding changes are simply coincidental i.e. all of the Fe(II) is contributed from the basalt and Fe (III) is being loss by an independent mechanism such as basalt-induced precipitation or sorption. In order to uniquely define the mechanism, aqueous ^{59}Fe (III) was used as a radioactive tracer. If Fe(III) was totally reduced to Fe(II) in solution, the count rate should remain constant with time. If the original Fe(III) was incorporated into a solid phase the count rate should approach zero in solution. As shown in figure 5c, ^{59}Fe concentrations do decrease with time with increasing pH and basalt surface

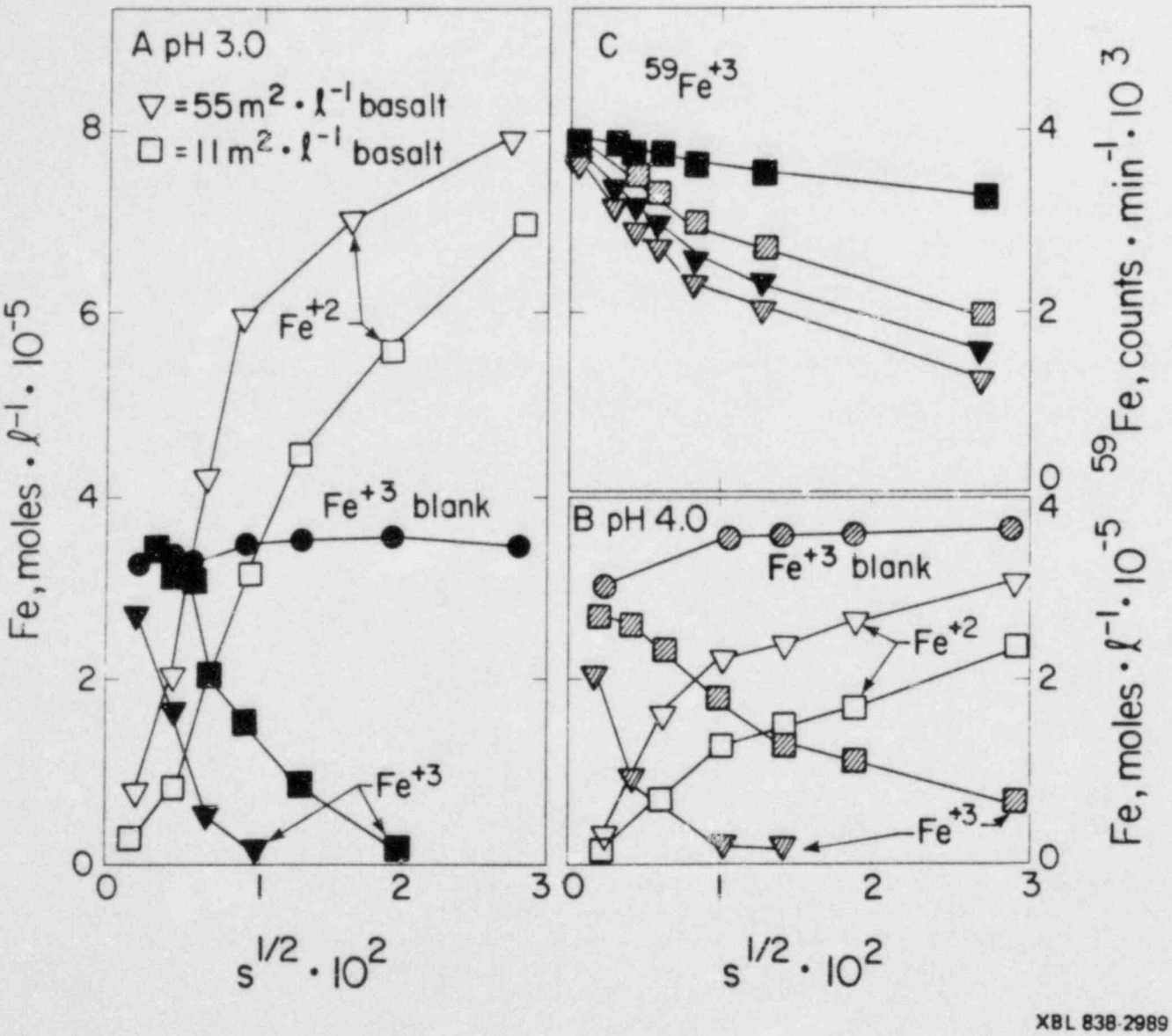

Fig. 5. Trends in Fe speciation with time in solutions initially containing 2 ppm Fe SO_4 and varying amounts of Sentinel Bluffs basalt. Open points are Fe (II) concentrations and solid and hatched points are Fe(III) concentrations at pH.3 (a) and OH 4.5 (b) respectively. $^{59}Fe(II)$ is plotted as counts per min. (c).

areas. However the ^{59}Fe decrease is less and the rates much slower than that of Fe(III), indicating that direct reduction of iron must occur in solution.

At pHs greater than 6.0, Fe(II) is rapidly depleted in solution, as indicated by the lack of measurable Fe(II) in the basalt dissolution studies (figure 2). Iron concentrations in this pH range are controlled by the precipitation of oxyhydroxides;

$$Fe^{+2} + 1/4O_2 + 2O\bar{H} + 1/2H_2O \rightarrow Fe(OH)_{3\,\text{amorphous hydroxide}} \quad (2)$$

$$Fe^{+2} + 1/4O_2 + 2O\bar{H} \rightarrow 1/2\ H_2O + Fe(OH)_{\text{goethite}}. \quad (3)$$

A number of studies (Stumm and Lee, 1961; Pankow and Morgan, 1981; and Davison and Seed, 1983) have shown that Fe(II) oxidation kinetics obey the rate law;

$$\frac{d[Fe(II)]}{dt} = k\,[Fe(II)]pO_2\,(OH^-)^2 \quad (4)$$

where [FeII] is the measured concentration, (mol. l^{-1}), PO_2 is the partial pressure (atm.) and OH^- is the activity. When pH and O_2 are constant, equation 2 reduces to;

$$\frac{d\,[Fe(II)]}{dt} = k_1\,[Fe(II)] \quad (5)$$

where $$k_1 = k\,(OH^-)^2 pO_2 \quad (6)$$

Experiments were conducted at a buffered pH of 6.5 and at atmospheric O_2 to determine the effects of basalt interaction on oxidation kinetics of Fe(II) at near neutral pH. As shown by the example in figure 6. Fe(II) oxidation rates in blank solutions display a linear relationship between log [Fe(II)] and time as predicted by equation 3. The slope of the line, which coresponds to $k_1/2.3$ results in rate constant (k) of 1.64×10^{14} mol.$^{-2}$ atm^{-1} min^{-1} which falls within the range of rate constants summarized by Davison and Seed (1983).

The addition of basalt to solutions at near neutral pH has the effect of greatly accelerating the Fe(II) decrease (figure 6). The rates become non-linear with respect to equation 3 and proportional to the total surface area of the basalt present suggesting uptake by the solid.

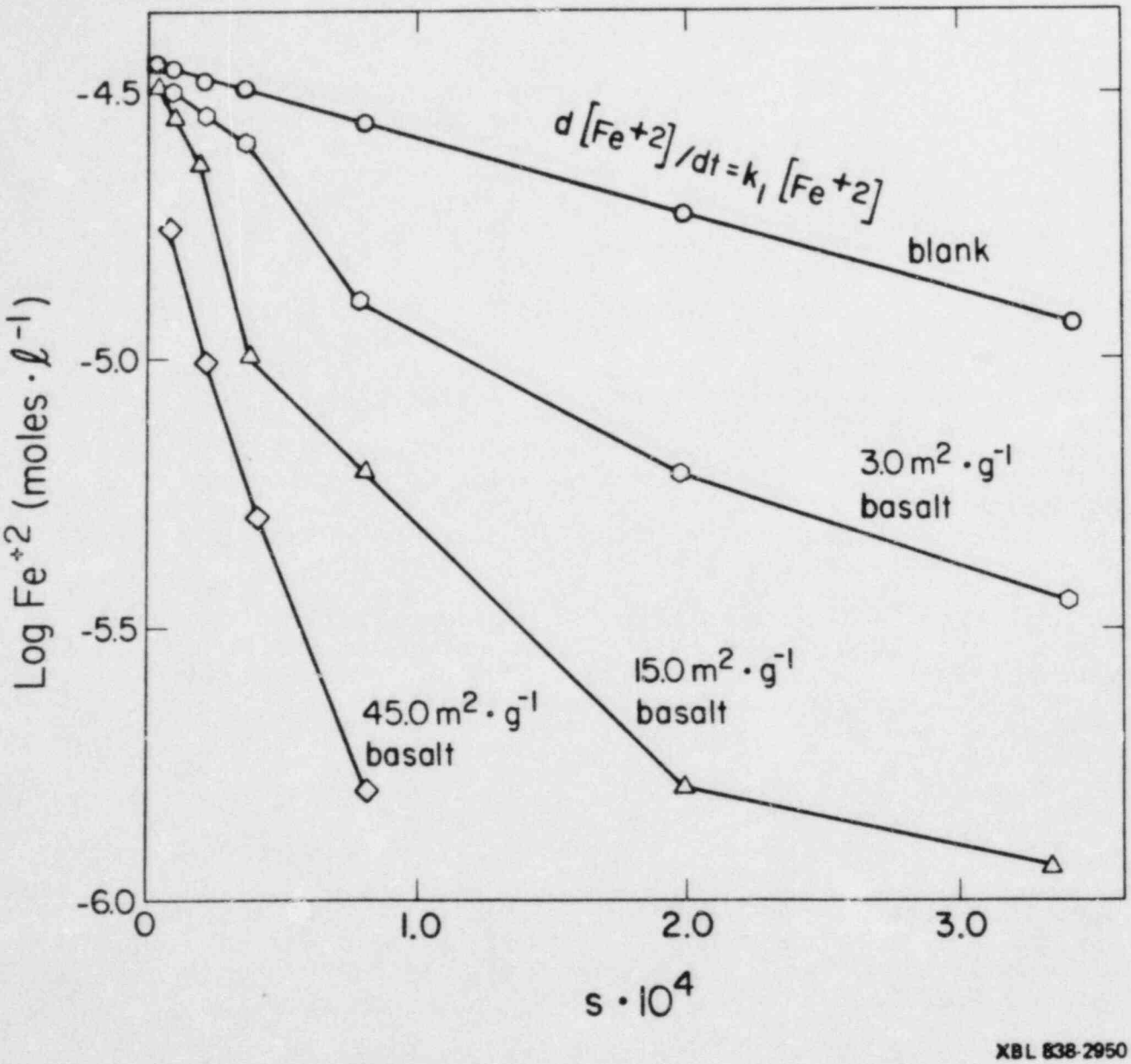

Fig. 6. Oxidization rate of Fe(II) in solution with varying amounts of basalt. Upper-most data show fit of blank solution data to first order rate law (eq.5).

Uptake of dissolved oxygen

To test the effect of oxyhydroxide precipitation in controlling both dissolved Fe(II) and O_2 concentrations at neutral pH, solutions were saturated at a given PO_2, Fe(II) added, and PO_2 measured after the system achieved equilibrium. As indicated in figure 7, the 4 to 1 ratio between total Fe(II) consumed (moles. l^{-1}) and the final dissolved O_2 content (moles. l^{-1}) reproduces the stiochiometry of reactions 2 and 3. Addition of basalt to the solutions decrease the initial Fe(II)- final PO_2 ratios to less than 4 to 1. This decreased slope, which is proportional to the basalt surface area, implies a loss of Fe(II) from solution not associated with the formation of iron hydroxide or goethite.

Rates of O_2 uptake were also monitored in the long term closed system experiments (1-4, table 3) in which iron chemistry was controlled solely by basalt reaction. Examples of O_2 uptake are shown in figure 8. The generally parabolic decrease in oxygen with time suggests a diffusion controlled reaction. Rates can be modeled assuming diffusion into basalt from a well-stirred solution of finite extent. Due to generally slow solid state diffusion rates at ambient temperature, the basalt can be represented as a infinite one-dimensional slab.

An analytical solution to Ficks second law of diffusion with appropriate boundry conditions is presented by Carslaw and Jaeger (1959) for analogous heat diffusion. The measured O_2 concentration, C, is related to the initial O_2 concentration, C_o, by the relationship;

$$C = C_o e^{\frac{Dt}{l}} \operatorname{erfe} \frac{DT}{l}$$

where D is the oxygen diffusion coefficient and t is time in seconds. The solution length, l, (cm) is the one dimensional representation of solution volume (cm^3) divided by basalt surface area (cm^2).

The dotted lines in figure 8 are solutions to equation (7) fitted to the experimental data. As indicated, oxygen diffusion appears pH dependent. The relative magnitudes of the diffusion coefficients, 10^{-14} cm^2 s^{-1}, suggest more rapid grain boundry diffusion rather than slower O_2 diffusion within silicate structures of the basalt mineral assembage.

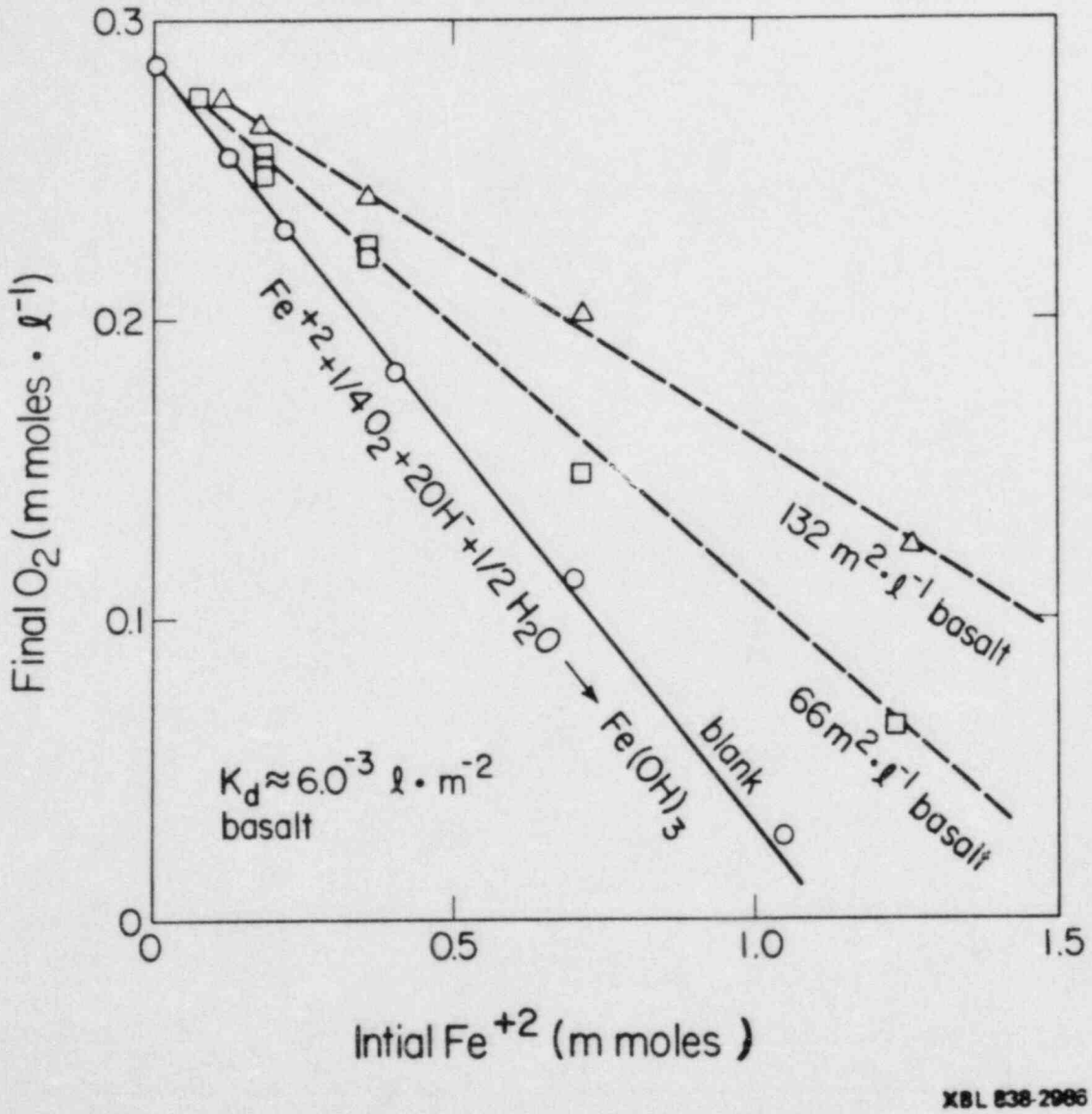

Fig. 7. Relationship between initial Fe(II) and final dissolved oxygen concentrations after equilibrium with oxyhydroxide. Lower line shows stiochiometric relationship for blank solution while progressive deviations with increasing basalt content indicated Fe sorption as described by eq. 10.

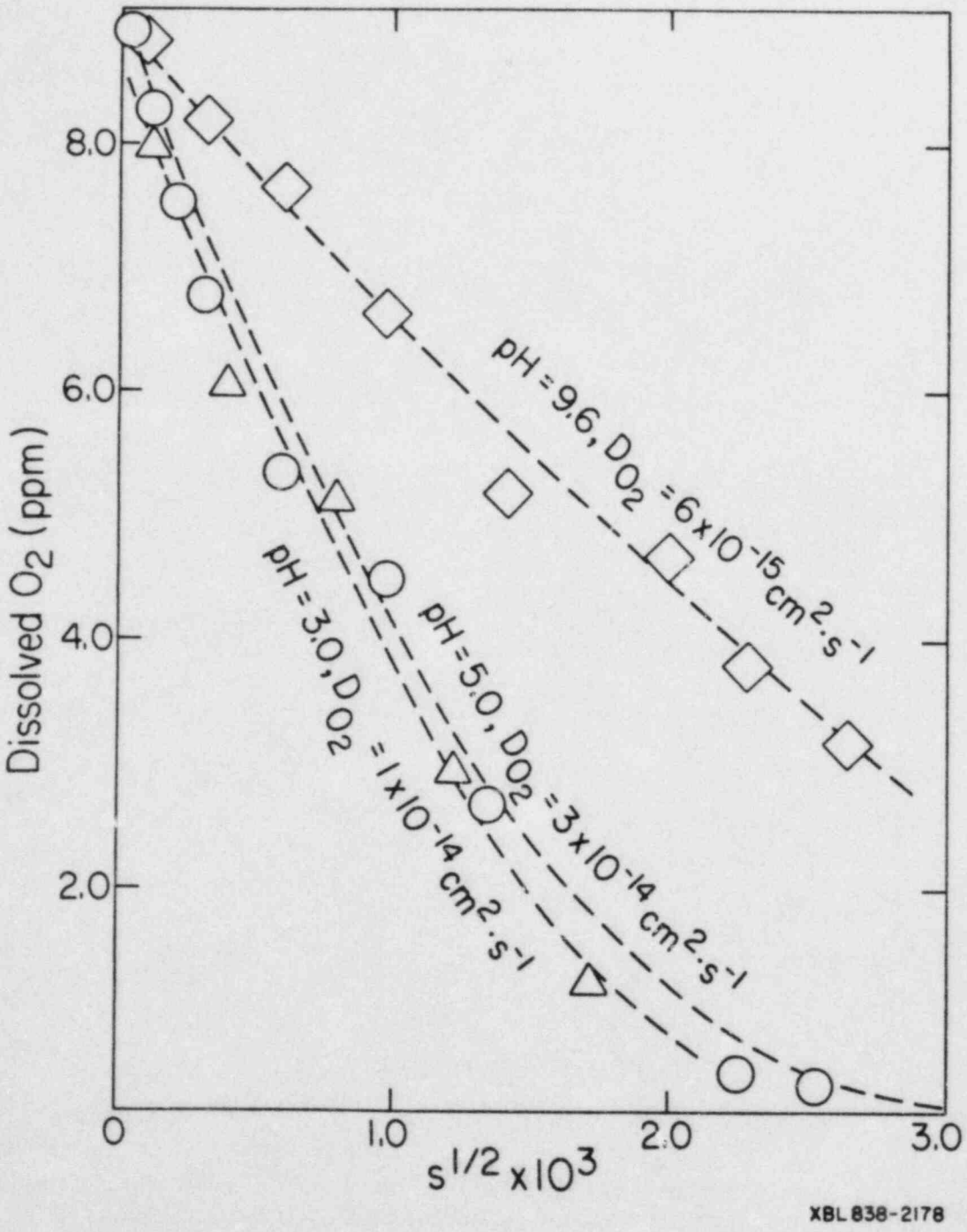

Fig. 8 Oxygen loss in solution during basalt/water interaction at differing pHs. Dashed lines are fits to diffusion model assuming the indicated diffusion coefficients.

Although there was no attempt in this study to assess the overall oxidization-reduction kinetics of basalt relative to individual mineral phases, it is interesting to compare O_2 uptake rates between basalt and individual mineral phases being measured in inconcurrent studies. Such data are plotted in figure 9. As indicated rates of O_2 uptake for basalt are much faster than for silicate phases. Of particular interest is the relatively slow rate for O_2 uptake in augite, which as shown in table 2, is the dominant iron silicate phase in basalt. These results suggest that magnetite is probably the dominant sink for O_2.

Comparison of Eh values

The data provides an opportunity to compare experimentally controlled and measured Eh values using several different techniques. The measureable reactions are;

$$2\ Hg_{\ell} + 2\ Cl^{-} \rightarrow Hg_2Cl_2 + 2\ e^{-} \qquad (11)$$

$$Fe^{+2} \rightarrow Fe^{+3} + e^{-} \qquad (12)$$

and $$H_2O \rightarrow 1/2O_2 + 2H^{+} + 2e^{-}. \qquad (13)$$

Equation (11) is the calomel-platinum electrode couple which directly measures the EMF of the solution; equation 12 is the ferrous-ferric couple measured in solution; and equation 13 is the oxidization potential of water. The computer speculation code WATEQ 2 (Ball et al 1981) has the necessary options of evaluating Eh based on the above equations.

Figure 10 shows the results plotted on the Eh-pH stability field for various aqueous and solid iron phases. The stability field for $Fe(OH)_3$ is plotted for variable Fe(II) concentrations (eq.2). Also shown are the upper and lower stability limits of water. Each experimental measurement at a given pH has three Eh values based on equations 11-13. Eh based on oxygen measurements closely follow the slope of the O_2-H_2O stability boundry. As discussed by Baas Becking et al (1960,) measured Eh values of natural systems nearly always fall well below but parallel to this stability line. Sato (1960) defined a lower boundry, based on a rate controlling H_2O_2-O_2 reaction as

$$Eh = 1.04 - 0.059\ pH. \qquad (14)$$

Eh values based on the ferrous-ferric iron couple (eq. 12) are univarient with respect to pH and lie along the metastable Fe(II)/Fe(III) boundry.

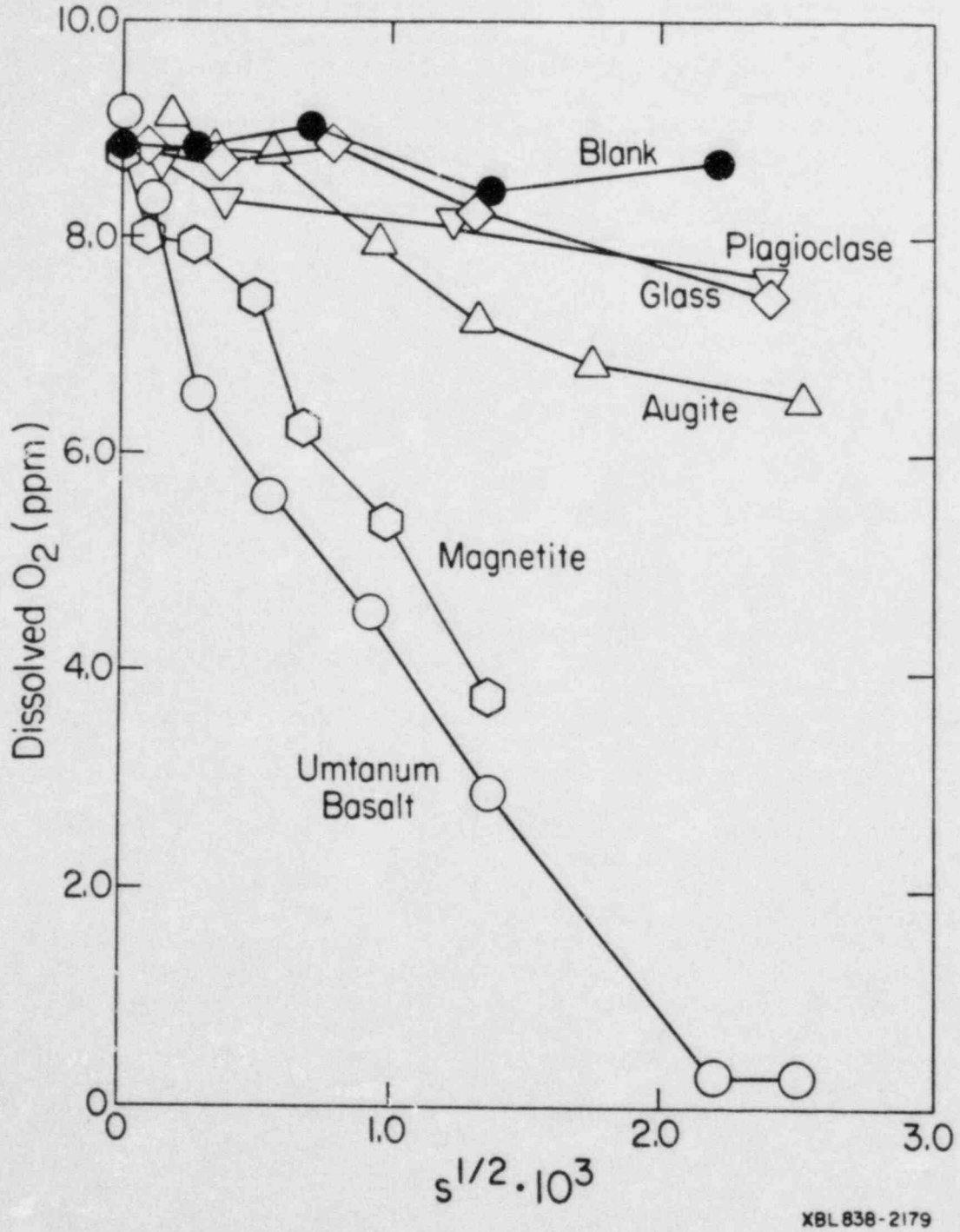

Fig. 9. Comparison of O_2 losses in solution for basalt and a number of individual silicate phases common to basalt.

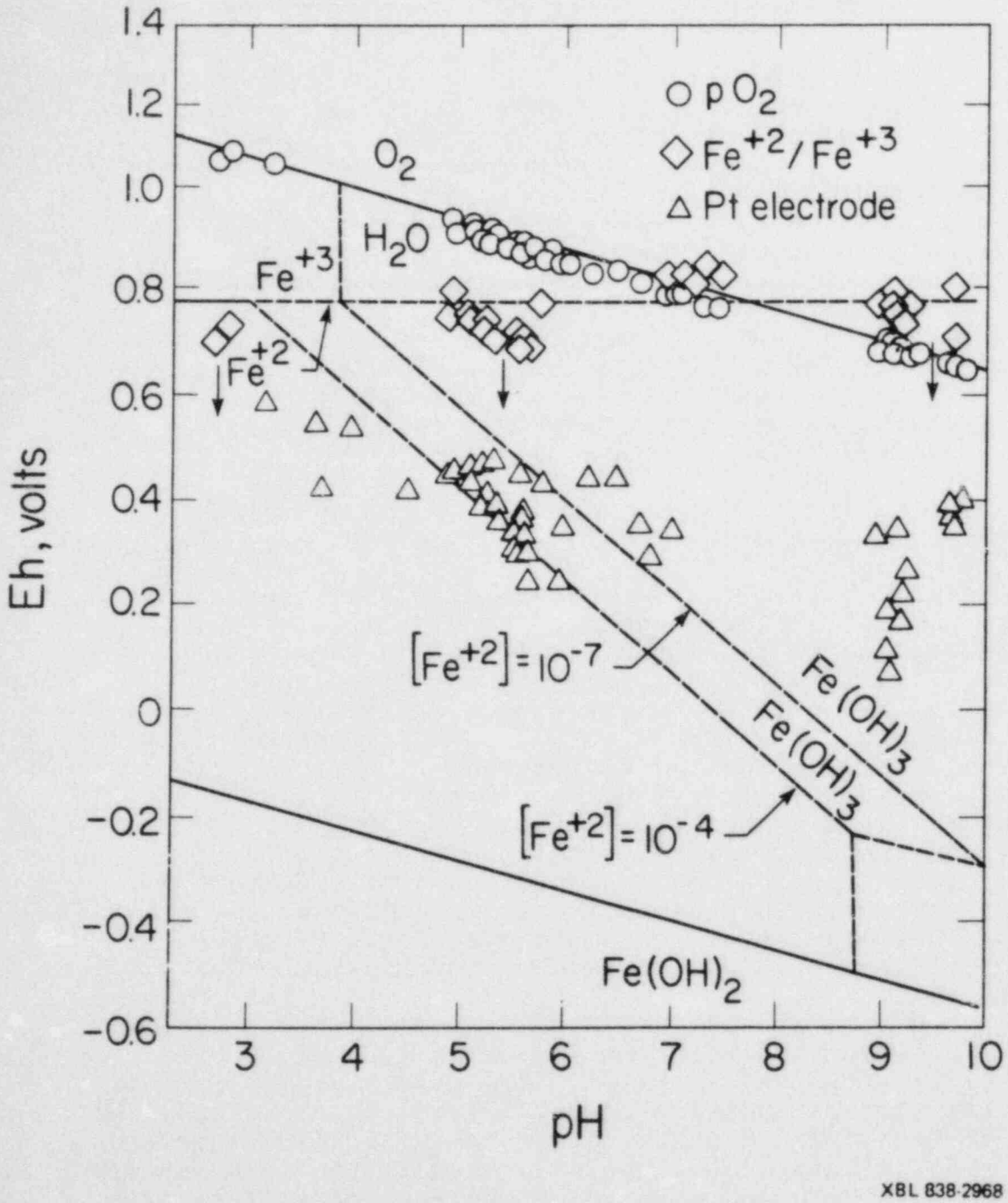

Fig. 10. Relationship between pH and Eh determined by electrode, dissolved oxygen and Fe(II)/FE(III). Also shown ar stability fields for dissolved iron and amorphous $Fe(OH)_3$.

The downward pointing arrows for Fe-determined Eh indicate solutions in which only Fe(II) species were measured. At neutral to alkaline pHs, found in basalt groundwater, an empirical correlation exists between Eh calculated from D.O. and Fe(II)/Fe(III).

Eh measurements by electrode generally result in much lower values than either of the other techniques even in high O_2 solutions. As indicated by Natarajon and Dwasaki (1976) a concentration of iron in excess of 10^{-2} m is required to observe exclusively the potential of the ferric-ferrous iron couple. Such concentrations are much higher than obtained in the experimental systems. Measured Eh values suggest mixed potentials, at least partially controlled by surface PtO coatings on the electrode. Based on the above analysis, direct measurement of the Fe(II))/ Fe(III) couple is the best estimate of Eh. The only difficulty is determination of very low iron concentrations at neutral to alkaline ph.

2.6.5. CONCLUSIONS

The preceeding results indicate significant interaction between the basalt mineral assembage and dissolved Fe(II), Fe(III), and O_2 during simulated basalt/ground water interaction. The loss of iron from the basalt surface with decreasing pH corresponds, as expected, to an increase in the aqueous solution. In no case does an increase in surface iron occur, indicating the absence of a oxyhydroxide coating as proposed by Siever and Woodford (1979). No significant increase in sorption capacity Cs or Sr was indicated. As indicated by XPS binding energies, reduced iron contained within the basalt is oxidized on the surface of even the unreacted samples stored under atmospheric conditions. Oxidization of iron on the surfaces of amphiboles and pyroxenes has also been demonstrated by Berner and Schott (1982).

In acidic solutions with pHs less than 5.5 and undersaturated with oxyhydroxide phases, iron exists predominantly in the Fe(II) state. Addition of Fe(III) species results in reduction to Fe(II) in solution. Presumably Fe(III) dissolved from the oxidized basalt surface is reduced in the same manner. This relationship, coupled with an apparent absence of other oxidizable species in solution, suggests that an oxidation-reduction couple exists between Fe(II) and Fe(III) on the basalt surface and in solution. Such a couple can be written in the form,

$$\underset{\text{basalt}}{(Fe(II)\cdot 1/2\ M^z)} + \underset{\text{solution}}{Fe(III)} \rightarrow \underset{\text{basalt}}{Fe(III)} + \underset{\text{solution}}{1/2M^z} + Fe(II) \qquad (8)$$

where the reduction of iron in solution is charged balanced by the dissolution of a cation of charge z from the basalt. As shown by the data in figure 1, any number of cations re eased into solution during experimental weathering can fulfill this requirement. The driving chemical forces behind equation 8 is apparently the continued oxidiation of Fe(II) beneath the already oxidized surface of the basalt and the acceptance of electrons from solution.

At neutral to basic pH, reduction of iron in solution by reaction 8 is countered by the oxidization of iron during precipitation of ferric oxyhydroxides (eq. 2 and 3). Based on the absence of Fe(II) in solution of pHs greater than 5.5, the net free energy of the opposing oxidization-reduction reactions must favor oxyhydroxide precipitation over surface oxidization.

In blank solutions, kinetic rate data for Fe(II) oxidization (eq. 5), as well closed system oxygen uptake (eqs. 2 and 3), indicate control by oxyhydroxide precipitation. However in the presence of basalt, the rate of Fe(II) loss is accelerated and the Fe(II)-O_2 stiochiometery becomes less than that predicted by precipitation. Such deviations, coupled with observed losses of ^{59}Fe at low pH, suggest that aqueous iron is being sorbed into the basalt surface. Such sorption can be separated from concurrent oxyhydroxide precipitation at neutral to basic pH based on deviations in final O_2 concentrations from those predicted by eq. 2 and 3. Simple sorption equilibrium can be assumed between the basalt surface and the aqueous solution,

$$[Fe(II)]_{solid} = k_d [Fe(II)]_{solution} \quad (9)$$

The stoichiometry of equation 2 for example can be rewritten as,

$$[Fe(II)\ [1-k_dS] + 1/4O_2 + 2OH^- + 1/2\ H_2O \rightarrow Fe(OH)_{3amorphous} \quad (10)$$

where S is the basalt surface area ($m^2\ l^{-1}$). The dashed lines in figure 7 show the fits to the experimental data using a k_d of $4.0 \times 10^{-3} l \cdot m^2$.

Rate data indicate that oxygen uptake increases in basalt with decreasing study are very rapid. However, the diffusion control indicates decreasing rates with time. For naturally weathered aquifer substrates, O_2 uptake may be very slow. Current O_2 data in basalt is very meager and is suspect due to atmosheric contamination during pumping. Air tight packer tests are required. A insitu test involving the injection of O_2 into a aquifer and uptake monitoring would produce best estimate of rates.

3) The Fe^{+2}/Fe^{3} distributions in secondary minerals formed during ground water alteration of basalt would also be useful in estimating oxidation reduction controls. Aeral distributions and distributions as a function of depth may also delineate present and past redox conditions.

4) Methods of estimating insitu Eh needs further development. As indicated in this study comparative Eh measurements under tightly controlled conditions involving purified gases in glove boxes resulted in very poor agreement. Such measurements made down hole or using pumped wells are much more difficult. Proposed downhole Pt probes do not appear to be very effective technique-based on experimental studies. The use of sealed down hole samples coupled with determination of several redox couples in solution, such as Fe^{+2}/Fe^{+3}, As^{+3}/As^{+3}, and $S^{=}/SO_4^{=}$ and CO_2/CH_4, would be a most accurate technique.

5) At present, methods of calculating redox conditions in natural systems is somewhat limited. The WATEQ 2, 3 and 4 codes developed by the U.S.G.S. contain the greatest number of redox options allowing calculations involving various redox couples, PO_2 and Pt electrode measurements. Portions of these code were modified and rewritten into FORTRAN IV in this study and a radionuclide data base is being incorporated into the code at PNL.

Such codes do not incorporate kinetic rate data of the type defined for Fe redox in this study. Such data would be critical in defining redox conditions in a dynamic coupled chemical-hydrologic transport model required for repository site accessment. Some parameters such as O_2 diffusion can be readily incorporated into the finite element methods used in such models.

2.6.7. PLANNED RESEARCH

Additional experimental basalt studies will be conducted at elevated temperatures to simulate ambient deep ground water temperatures. These experiments will be limited to 100°C and techniques and experimental methods employed in this study will be applicable. More detailed experiments on oxygen diffusion mechanisms are underway using ^{18}O gas. Diffusion profiles will be determined in basalt minerals using Ar sputtering coupled with secondary ion mass spectroscopy.

The previous results suggests that the iron oxide mineralogy is controlling the overall iron and oxygen kinetics. A more detailed study of magnetite reaction kinetics may result in a method of estimating aquifer

redox conditions both for naturally weathered basalt as well as for other proposed host rocks such as tuff and granite. Measurements of O_2 diffusion rates as functions of iron oxide mineralcgy and content are planned.

2.6.8. ACKNOWLEDGMENTS

The authors would like to thank Dale Perry and Joan Delany of LBL, Jim Ball of the U.S.G.S and Robert Berner of Yale University for helpful suggestions and comments. This work was funded by the U.S. Nuclear Regulatory Commission.

2.6.9. REFERENCES

Allen, G.C., Curtis, M.T., Hooper, A.J. and Tucker, P.M., 1974 Photoelectron binding energies for iron oxides. Chem. Soc. Dalton 1526

Bancroft, G.M., Brown, J.R., and Fyfe, W.S., 1979. Advances and applications of X-ray photoelectron spectroscopy (ESCA) in mineralogy and geochemistry. Chemical Geol., 25: 227-235.

Berner, R.A. and Schott, J., 1982. Mechanisms of pyroxene and amphibole weathering II. Observations of soil grains. Amer. J. Science, 282: 1214-1231.

Canslaw, H.S. and Jaeger, J.C., 1959. Conduction of Heat in Solids. Oxford Press, London 507 p.

Davidson, W. and See, G., 1983. The kinetics of the oxidation of ferrous iron in synthetic and natural waters. Geochem. Cosmochem, Acta, 47: 67-79.

Gibbs, M.M., 1979. A simple method for the rapid determination of iron in natural waters. Water Research, 13: 295-297.

Haggerty, S.E., 1976, Oxidation of opaque oxides in basalt. in Oxide Minerals Short. Course Notes, Minerals Soc. Amer. Hgl-Hg 100.

Hilderbrande, E.E., and Blume, W.E., 1974. Lead fixation by iron oxides. Naturwessen-schaftger 61, 169-170.

McIntyre, N.S. and Zetaruk, D.G., 1977. Structure and binding energies of iron oxides. Anal. Chem. 49: 1521.

Meyers, C.M. and Price, S.M. 1979. Geologic studies of the Columbia Plateau: A status report. Rockwell Hanford Operations, Richland; Wash: RHO-BWI-ST-4.

REFERENCES (Continued)

Nordstrom, D.K., Jenne, E.A., and Ball, J.W., 1979. Redox equilibria of iron in acid mine waters. Amer. Chem. Soc. Symp. Series 93: 51-77.

Noonan, A.F., 1980. Phase chemistry of the Umtanum basalt: A reference repository host in the Columbia Plateau. RHO-BWI-SA-77, Rockwell. Hanford Operations, Richland, Washington.

Pankow, J.F. and Morgan, J.J., 1981. Kinetics for the aquatic environment. Enviro. Sci. Tech. 15: 1155 - 1164.

Plummer, L.B., Jones, B.F. and Truesdell, A.H., 1976. WATEQF- a. FORTRAN IV version of WATEQ, a computer program for calculating chemical equilibrium of natural waters. U.S. Geol. Water Res. Invest. No. 76-13, 61 p.

Siever, R., and Woodford, N., 1979. Dissolution kinetics and weathering of mafic minerals. Geochem. Cosmo. Chem. Acta, 43:717-724.

Stumm, W. and Lee, G.F., 1961, Oxygenation of ferrous iron. Ind. Eng. Chem. 53: 143-146

Wagner, C.D., Riggs, W.M., Davis, L.E., Mouldew, S.F., and Muilenberg, G.E., 1979. Handbook of X ray Photoelectron Spectroscopy, Perken-Elmer Corp. Eden Praire, Minn. 190 p.

White, A.F., Claassen, H.C. and Benson, L.V., 1980. The effect of dissolution of volcanic glass in the water chemistry in a tuffaceous aquifier, Rainier Mesa, Nev. U.S. Geol. Survey. Water Supply Paper 1535 Q 34p.

Winograd, I.J. and Robertson, F.N., 1982. Deep oxygenated ground water: anomaly or common occurrence. Science, 216: 1227-1229.

Wilson, A.D., 1955. Determination of ferrous iron in silicate minerals by a volumetric method. Bull. Geol. Soc. Great Britain; 9:56.

2.7 EVALUATION OF DOE RADIONUCLIDE SOLUBILITY DATA AND SELECTED RETARDATION PARAMETERS: DESCRIPTION OF CALCULATIONAL AND EXPERIMENTAL ACTIVITIES*

A. D. Kelmers,† R. J. Clark,** N. H. Cutshall,††
J. S. Johnson,‡ and J. H. Kessler†

ABSTRACT

An experimentally oriented program has been initiated to support the NRC analysis and licensing activities related to high-level nuclear waste repositories. The program will allow the NRC to independently evaluate key geochemical values used in the site performance assessments submitted by the DOE candidate repository site projects. Key radionuclide retardation factor values, particularly radionuclide solubility and sorption values under site-specific geochemical conditions, are being investigated. The initial efforts are being directed toward basalt/groundwater systems relevant to the Basalt Waste Isolation Project (BWIP) candidate site in the Pasco Basin. Future work will consider tuff and salt/groundwater systems that are relevant to other candidate sites. Initial experimental results with technetium have been in agreement with the BWIP values for basalt/groundwater systems under oxic redox conditions: high solubility and no sorption. Under reducing conditions, however, the experimental work yielded results different from the technetium values recommended by BWIP. In the presence of hydrazine to establish reducing conditions, an apparent solubility limit for technetium of about 5×10^{-7} mol/L was encountered; BWIP recommended calculated values of 1×10^{-12} to 1×10^{-14} mol/L. Experimental evidence concerning sorption of reduced technetium species is incomplete at this time. Equilibrium speciation and saturation indices were calculated for well-water data sets from BWIP using the computer code PHREEQE. Oversaturation was indicated for hematite and quartz in all data sets. Near-surface water samples were undersaturated with calcite, but most deep-water samples were oversaturated with calcite and other carbonate minerals.

---

* Supported by the NRC Office of Nuclear Materials Safety and Safeguards.
† Chemical Technology Division, Oak Ridge National Laboratory, Oak Ridge, Tennessee.
**Department of Chemistry, Florida State University, Tallahassee, Florida.
††Environmental Sciences Division, Oak Ridge National Laboratory, Oak Ridge, Tennessee.
‡ Chemistry Division, Oak Ridge National Laboratory, Oak Ridge, Tennessee.

2.7.1 INTRODUCTION

Oak Ridge National Laboratory (ORNL) is supporting the NRC staff analysis of DOE high-level waste repository candidate site geochemical data by a laboratory-oriented effort to evaluate key radionuclide retardation information. The activity is focused on radionuclide solubility values and on other retardation parameters (primarily radionuclide sorption), as well as various experimental strategies, laboratory techniques, and calculational methodology. The results of this activity will help the NRC staff to independently review and analyze key data values employed in DOE site performance assessment analyses and the methods used to develop these values, and will help the NRC define uncertainties in the data. The results will also aid in identifying areas requiring additional attention by the DOE site programs and/or by NRC/Research activities.

The work emphasis is paralleling the DOE candidate site development activities. Attention is first being directed toward values that quantify the behavior of radionuclides in basalt/groundwater systems relevant to the BWIP candidate site in the Pasco Basin. In the future, the work will include tuff/groundwater systems relevant to the Nevada Nuclear Waste Isolation Investigations (NNWSI) candidate site at Yucca Mountain and salt/groundwater systems relevant to the Office of Nuclear Waste Isolation (ONWI) bedded and/or domal salt candidate sites. The effort this year has encompassed both experimental measurements and investigation of calculational methodology. The experimental efforts have been limited to two key radionuclides: technetium and neptunium. They are potentially significant contributors to radioactivity releases to the accessible environment in groundwater-ingress — groundwater-migration events after waste emplacement, since these nuclides may exhibit poor retardation behavior in some geologic systems. The calculational efforts have been evaluating methods of calculating groundwater composition and correlating the composition with the host rock minerals.

The key issues being addressed by this work encompass the following:

Level 1 - General

- Are the geochemical values developed by DOE and used in the DOE site performance assessment to show favorable predicted radionuclide release behavior both conservative and defensible, and are the values precise and accurate enough for the NRC site analysis needs? (The assumption is that values which DOE asserts support unfavorable site-release behavior predictions need not be analyzed by the NRC.)

Level 2 - Intermediate

- Is the limiting solubility of radionuclides in the engineered barrier facility and/or the far-field asserted to be a significant favorable retardation parameter in the DOE site performance assessment?

- Is radionuclide sorption in the engineered barrier facility and/or in the far-field asserted to be a significant favorable retardation parameter in the DOE site performance assessment?

Level 3 - Specific

- If radionuclide limiting solubility is an important favorable retardation parameter, were the limiting solubility values calculated or experimentally measured?

- If the limiting solubility values were calculated, are the calculational methodology and thermodynamic data base adequate for each key radionuclide and for all the groundwater compositions and rock components encountered along the release pathway(s)?

- If the limiting solubility values were experimentally measured, are they saturated solution concentrations? Were the experimental methods and test parameters suitable and sufficient? Were both in situ groundwater and groundwater compositions altered by interaction with the waste package and engineered barrier facility components used? Was the saturated solution concentration obtained by convergence from both over- and undersaturation, and were all key radionuclides measured?

- If radionuclide sorption is an important favorable retardation parameter, were the experimental methods suitable and sufficient? Did the test parameters encompass the geochemical parameters expected in the repository? Were all the host rock phases considered? Were in situ and altered groundwater compositions employed, and were all key radionuclides measured?

2.7.2 TECHNETIUM

2.7.2.1 BWIP Solubility and Sorption Values

Technetium has been identified as one of the key radionuclides in a nuclear waste repository in basalt, i.e., one of the radionuclides which appear to pose the greatest potential hazard to man (BARNEY 1980). Table 1 summarizes the published BWIP data for technetium solubility in Grande Ronde groundwater and sorption on basalt, secondary minerals, or interbed materials from Grande Ronde groundwater.

For oxidizing conditions, the BWIP reports provide no estimate of the solubility limit of technetium, and they recommend a sorption distribution coefficient of 0 mL/g (no sorption) for basalt, secondary minerals, or interbed materials. Other references (PAQUETTE 1980) state that the solubility of the pertechnetate anion, TcO_4^-, the form of Tc(VII) expected under BWIP oxidizing conditions, is as high as 11 mol/L for sodium pertechnetate. Palmer (1981) has reported the sorption of pertechnetate under oxic conditions on basalt, giving a mean distribution coefficient of 4.7 ± 8.9 mL/g. The adsorption of pertechnetate on basalt was explored in column experiments (FRANCIS 1979) that suggested the apparent sorption was actually due to reduction to an insoluble form of technetium.

Table 1. Summary of BWIP solubility and sorption values for technetium

	Redox condition		
	Oxidizing	Reducing	Reference
Solubility, mol/L	---[a]	1×10^{-12}	SALTER 1981a
	---[a]	$>10^{-14}$	EARLY 1982
Sorption, mL/g			
Basalt	0	29	SCR 1982
	0 to 7	29	SALTER 1981c
Secondary minerals	0	50	SCR 1982
	0	---[a]	SALTER 1981b
Interbed	0	70	SCR 1982
	2 to 3	46 to 104	BARNEY 1982

[a]No value given.

Under the reducing conditions expected in the BWIP basalt in the far-field, Tc(VII) dissolved in groundwater is expected to be reduced to Tc(IV), and the stable technetium solid, TcO_2, is expected to crystallize (SALTER 1981a). The available thermodynamic data for Tc(IV) is reported to be limited and suitable only for estimating a limiting solubility of $>1 \times 10^{-14}$ mol/L (EARLY 1982). Other references (PAQUETTE 1980) state that Tc(IV) may be present as $TcO_2 \cdot 2H_2O$, which has a reported solubility of 5×10^{-5} mol/L (LEFORT 1963). Paquette (1980) states that this measured solubility may be too high. Moderately high technetium sorption distribution coefficients of 29 to 70 mL/g are reported (Table 1) for basalt, secondary minerals, or interbed materials under reducing conditions. However, since Barney (1982) states that technetium precipitates at concentrations $>1 \times 10^{-7}$ mol/L under reducing conditions, some of the BWIP distribution coefficient measurements may actually involve technetium precipitation in the sorption test.

Although not explicitly stated in the Site Characterization Report for the Basalt Waste Isolation Project, no technetium retardation due to limited solubility or sorption on repository minerals is expected under oxidizing conditions. Under reducing conditions, technetium retardation in the BWIP far-field is apparently expected to result primarily from the low calculated limiting solubility of reduced technetium under the anticipated site far-field redox potential (EARLY 1982). Additional retardation of reduced technetium by sorption on basalt, secondary minerals, and interbed materials also is apparently expected. Thus, information on both the solubility and sorption values for reduced technetium is important for the NRC BWIP-analysis activities.

2.7.2.2 Experimental Methods

Batch contacts to measure sorption distribution coefficients and establish the apparent solubility limit of technetium were carried out under the following test parameters:

Solids - Sentinel Gap outcrop basalt was crushed in an agate mortar to 20–70, 70–235, and <235-mesh particle size samples. Some samples were ultrasonically washed to remove adhering fine particles. Most of the samples were crushed in air, but a few were crushed and maintained under an argon atmosphere. Clinoptilolite from Hector, California, or Buckhorn, New Mexico, was used as received; the particle size was 40–150 μm.

Groundwater - Synthetic basalt groundwaters GR-1 and GR-2 were prepared as described by Salter (1981b). The solutions were traced with ^{95m}Tc (as $NaTcO_4$) and with ^{99}Tc (as NH_4TcO_4) at technetium concentrations of 1×10^{-12} to 1×10^{-5} mol/L. In some tests, the traced groundwater was deaerated by successive freeze-thaw cycles to the 10-ppb oxygen range, while in other tests reducing conditions were simulated by the addition of 0.07 mol/L hydrazine hydrate.

Groundwater/Solids Ratio - Most batch contacts were carried out at a groundwater/basalt ratio of 10 mL/g. In some tests, no solids were present; in others, the effect of varying the liquid/solid ratio was explored.

Contact - The batch contacts were carried out in glass bottles that were sealed with a plastic screw cap with a PVC cap liner. The contact times varied. Some tests were at laboratory ambient temperature (23°C), but most were conducted at 60°C in an air environment.

Liquid/Solids Separation - After completion of the contact, the solids and liquid were separated by centrifugation at 3000 relative centrifugal force (rcf) for 30 min. Samples contacted at 60°C were centrifuged at ambient temperature. An aliquot of the clear supernate was withdrawn for technetium analysis. In some cases, the radioactive material adhering to the tube and cap liner was also counted.

Technetium Analysis - The ^{95m}Tc gamma peak at 0.204 meV was counted in a Packard Auto-Gamma Scintillation Spectrometer.

2.7.2.3 Results

Oxidizing Conditions

A number of batch contact tests were carried out with both Sentinel Gap basalt and clinoptilolite, a secondary mineral observed in some BWIP samples (SCR 1982). The tests were conducted at room temperature and at 60°C for technetium concentrations ranging from 1×10^{-12} to 1×10^{-6} mol/L in groundwaters GR-1 and GR-2. Most tests were continued for 3 days, but some ran as long as 90 days.

No sorption was observed on basalt or clinoptilolite. In all tests, the concentration of technetium in the solution recovered after contact was within ±10% of the initial concentration.

Reducing Conditions

Two different experimental approaches were used in an attempt to achieve reducing, or at least nonoxidizing, conditions for the batch contact tests that would be relevant to the expected BWIP far-field conditions. For these

tests, hydrazine was added to the synthetic groundwaters GR-1 and GR-2, as was done in the BWIP experiments (BARNEY 1982; SALTER 1981b; and SALTER 1981c). A hydrazine concentration of 0.07 mol/L was selected since this is in the range used by BWIP. The second experimental approach involved putting some synthetic groundwater solutions through a series of successive freeze-thaw cycles to deaerate them and crushing and grinding the basalt chunks in an inert-atmosphere box. The contact samples were also prepared and sealed in the box.

The experimental results (Table 2) with basalt in the presence of hydrazine were quite different from those under oxic conditions. The tests were carried out for 18 or 24 days at 60°C. Parallel blanks containing no basalt were run.

Table 2. Technetium removal from hydrazine-containing solutions in the presence and absence of basalt

Liquid	Solid	Initial Tc (mol/L)	Final Tc (mol/L)
GR-1	Basalt	1×10^{-10}	8.3×10^{-11}
GR-2	None	1×10^{-10}	5.6×10^{-12}
GR-1	Basalt	1×10^{-8}	2.1×10^{-9}
GR-2	None	1×10^{-8}	5.3×10^{-10}
GR-1	Basalt	1×10^{-6}	3.6×10^{-7}
GR-1	Basalt	1×10^{-6}	1.2×10^{-7}
GR-1	None	1×10^{-6}	2.3×10^{-7}
GR-2	Basalt	1×10^{-6}	1.1×10^{-7}
GR-2	None	1×10^{-6}	2.3×10^{-7}
GR-2	None	1×10^{-6}	6.8×10^{-8}
GR-1	Basalt	2×10^{-6}	3.0×10^{-7}
GR-1	None	2×10^{-6}	3.3×10^{-7}
GR-2	Basalt	2×10^{-6}	3.4×10^{-7}
GR-2	None	2×10^{-6}	3.3×10^{-7}
GR-1	Basalt	5×10^{-6}	5.0×10^{-7}
GR-1	None	5×10^{-6}	4.1×10^{-7}
GR-2	Basalt	5×10^{-6}	6.2×10^{-7}
GR-2	None	5×10^{-6}	4.3×10^{-7}
GR-1	Basalt	1×10^{-5}	8.2×10^{-7}
GR-1	None	1×10^{-5}	4.8×10^{-7}
GR-2	Basalt	1×10^{-5}	6.2×10^{-7}
GR-2	None	1×10^{-5}	4.3×10^{-7}
GR-1	Basalt	5×10^{-5}	1.3×10^{-6}
GR-1	None	5×10^{-5}	5.5×10^{-7}
GR-2	Basalt	5×10^{-5}	8.5×10^{-7}
GR-2	None	5×10^{-5}	6.2×10^{-7}

All the tests at an initial technetium concentration of 1×10^{-6} mol/L or higher had nearly equivalent technetium concentrations in solution after separation, and the presence or absence of basalt seemed to have no solubility effect. These results indicate that a solubility limit had been reached and that the removal of technetium from the synthetic groundwaters was due to precipitation in the presence of hydrazine. If the values with and without basalt are combined, an apparent limiting concentration of $\sim 5 \times 10^{-7}$ mol/L is obtained. The few batch contacts conducted at initial concentrations of $< 1 \times 10^{-6}$ mol/L gave results suggestive of moderate sorption effects. However, the sorption appeared not to be dependent upon the presence of basalt and occurred in the absence of basalt on the glass bottle and PVC cap liner. Additional tests are underway to attempt to determine whether sorption of reduced technetium ions of unknown speciation is occurring.

Interpretation of the solubility results from the tests at initial technetium concentrations of $> 1 \times 10^{-6}$ mol/L is complicated by two factors. First, appreciable sorption or adhesion of technetium was detected on the glass sample tubes and the PVC cap liner, regardless of the presence or absence of basalt. When the technetium in the solution, in the solid, on the tube, and on the cap liner was counted, ~90% of the technetium initially added was accounted for. Second, the GR-1 and GR-2 synthetic groundwaters were not stable at 60°C with added hydrazine, and a significant volume of precipitate formed, which could be scavenging or carrying technetium. The composition of the precipitate is under investigation. Thus, at the present time, caution is suggested in accepting the apparent solubility limit of $\sim 5 \times 10^{-7}$ mol Tc/L as representing solution saturation in contact with TcO_2 or $TcO_2 \cdot xH_2O$ solids. Additional experiments are underway.

Some preliminary results were obtained (Table 3) on technetium removal from solution during experiments in which basalt was first ground in an inert atmosphere and then contacted with solutions that had been deaerated by freeze-thaw cycling and sealed in a vacuum system.

Table 3. Technetium removal from solution by basalt[a]

Basalt pretreatment	Initial Tc (mol/L)	Tc removed (%)
Ground in air	Tracer	0
Exposed to air for 2 h	1×10^{-8}	10
Ground in inert atmosphere	1×10^{-8}	30

[a]Solutions deoxygenated by freeze-thaw cycles.

These preliminary results suggest that freshly exposed basalt surfaces which have not been allowed to contact air are capable of removing some technetium from solution, possibly by reduction and sorption of unknown technetium species. This effect is diminished by the exposure of the basalt to air. Additional tests are underway to explore this apparent native basalt reducing capability.

2.7.2.4 Discussion and Conclusions

Oxidizing Conditions

Oxidizing groundwater conditions will likely exist in the BWIP repository engineered barrier facility and the disturbed zone both before repository closure and for some time after closure. Oxidizing conditions could also exist in migrating groundwater for some distance into the far-field, depending on the rate of reduction and the reducing capacity of the BWIP host rock assemblage. Therefore, knowledge of technetium behavior under oxidizing conditions is important for performance assessment activities.

The ORNL work to date has been similar to the BWIP assertions or recommended values for technetium behavior under oxidizing conditions. No sorption was observed on basalt or clinoptilolite (a typical secondary mineral), and no

solubility limit was encountered in any test. Thus, it appears that if technetium can exist as pertechnetate in groundwater at the BWIP site, it would be expected to migrate at the groundwater migration velocity.

Reducing Conditions

The unaltered or unexposed basalt is expected to reduce technetium in the far-field to Tc(IV) (EARLY 1982). A very low calculated limiting solubility of $>1 \times 10^{-14}$ (EARLY 1982) or 1×10^{-12} (SALTER 1981a) is given in BWIP reports and, although not explicitly stated in the Site Characterization Report (SCR 1982), it appears that BWIP may be anticipating substantial retardation of technetium in the far-field due to the low calculated limiting solubility values. Further retardation also seems to be expected by BWIP due to the moderate sorption distribution coefficients reported. Therefore, evaluation of these solubility and sorption values is important for the NRC performance assessment analysis.

The ORNL work to date has not been in agreement with either the BWIP recommended Tc(IV) solubility or the sorption values. An apparent saturated solution concentration value of $\sim 5 \times 10^{-7}$ mol/L for reduced technetium has been measured both in the presence and in the absence of basalt under the reducing conditions established by 0.07 mol/L hydrazine in the synthetic groundwater. This value is closer to the measured value of 5×10^{-5} mol/L for $TcO_2 \cdot 2H_2O$ (LEFORT 1963) than to the BWIP calculated values. It is also near the value of 1×10^{-7} mol/L suggested by Barney (1982). At the present time, it seems that the BWIP calculated solubilities may be unrealistically low. Additional solubility tests are planned, utilizing a controlled-atmosphere box for isolation from air rather than artificially establishing reducing conditions through the introduction of hydrazine. The effects of groundwater composition and experimental procedures are also being investigated.

The ORNL work to date suggests than some sorption of unknown reduced technetium species might be occurring either in the presence or absence of basalt. Additional tests are underway to quantify this sorption. The tests do not, however, agree or disagree with the BWIP sorption distribution coeffi-

cient values. If the obvious precipitation occurring in the tests is ignored and sorption distribution coefficients are calculated as was done in the BWIP work, similar distribution coefficient values can be obtained. This agreement may be largely fortuitous, however, since valid distribution coefficient values cannot be measured in the presence of precipitated radionuclide solids.

The results with deaerated solutions in contact with basalt crushed in an inert atmosphere indicate that fresh surfaces of the native basalt can remove Tc(VII) from solution, possibly by reduction. However, this capability seems to be rapidly lost on contact with air. This observation is not inconsistent with the BWIP assertion that reducing conditions will be established in the repository far-field. However, reaction kinetics involving Tc(VII) in solution and active species in the basalt [such as Fe(II)] could be unfavorable for reduction.

2.7.3 NEPTUNIUM

2.7.3.1 BWIP Solubility and Sorption Values

Neptunium has also been identified as a key radionuclide in a basalt repository (BARNEY 1980). The published BWIP information on neptunium solubility in Grande Ronde groundwater and sorption on basalt, secondary minerals, and interbed materials from Grande Ronde groundwater is summarized in Table 4. Although not explicitly stated in the Site Characterization Report (SCR 1982), neptunium retardation in the BWIP disturbed zone and/or far-field is expected to result from a combination of low solubility in the groundwater under the anticipated reducing conditions and moderate sorption on basalt, secondary minerals, and interbed materials under oxidizing or reducing conditions. Thus, evaluation of information on both sorption and solubility of neptunium is important for the BWIP analysis activities.

Table 4. Summary of BWIP sorption and solubility values for neptunium

	Redox condition		
	Oxidizing	Reducing	Reference
Solubility, mol/L	---[a]	1.1×10^{-10}	EARLY 1982
	---[a]	1.0×10^{-15}	SALTER 1981a
Sorption, mL/g			
Basalt	10	200	SCR 1982
	15	200	SALTER 1981c
Secondary minerals	50	200	SCR 1982
	37 to 54	---[a]	SALTER 1981a
Interbed	20	50	SCR 1982
	14 to 26	34 to 600	BARNEY 1982

[a]No value given.

2.7.3.2 Laboratory Progress

Controlled-atmosphere glove boxes are being installed in an alpha-containment laboratory to carry out anoxic solubility and sorption tests with appreciable quantities of neptunium. The glove boxes were transferred from a decommissioned plutonium production line, and substantial decontamination and modification have been required to adapt them to this experimental program. The boxes have been received and decontaminated, are presently being modified, and will be ready for use soon. In the meantime, solutions and samples are being prepared for neptunium sorption/solubility experiments under relevant oxic conditions. The batch contact tests have recently been initiated, and results are not yet available.

2.7.4 GEOCHEMICAL MODEL CALCULATIONS

Geochemical data may be used to infer directions and rates of flow as well as compositional trends for groundwater near a waste repository site. Often, however, the constituents of groundwater interact so that treatment of a single parameter may also be affected by reactions among the constituents. Chemical modeling provides a framework within which multiple components may be considered simultaneously in assessing the reactions that occur. Several chemical codes have been developed recently to determine the state that would be attained by a given set of constituents at equilibrium, and to simulate the possible courses of reactions toward ultimate equilibrium (JENNE 1979). Advantages and disadvantages of these codes, as well as precautions in their literal application, have been discussed elsewhere and will not be repeated here. It is recognized, however, that the application of chemical equilibrium codes may generate results that do not necessarily represent the system of interest if: (1) that system is not at equilibrium, (2) the basic thermodynamic data are incorrect, (3) the model does not include relevant chemical species, or (4) the input data are inaccurate. Recognizing these limitations, it is nevertheless often useful to make such calculations to estimate the direction in which equilibrium lies and the degree of departure from equilibrium for a given solution.

Compositional data for Hanford area groundwaters were entered as starting values in the computer code PHREEQE (PARKHURST 1980), and equilibrium speciation and saturation indices were calculated. The standard data base was used for these preliminary runs of the code. Data from groundwater samples collected from depth intervals in each of four deep wells (DC15, DC6, DB15, and DC14) were used. Apparent oversaturation with respect to several common minerals was found; for example, most samples were calculated to be oversaturated with quartz and hematite, and many are oversaturated with chalcedony, goethite, calcite, and fluorite. The iron minerals and amorphous ferric hydroxide are generally found to be oversaturated; this is believed to reflect artifacts in the input compositional data. Iron concentrations are normally low in groundwaters, and the analysis may actually be determining colloidal ferric oxyhydroxide species rather than ionic species, as

assumed by the model. Apparent oversaturation with quartz and chalcedony is believed to reflect the dissolution of the glass phase from the basalt and the lack of an effective reaction pathway to remove the solubilized silica from solution. The silica oversaturation may result from the relatively high dissolution rates for volcanic glass, compared with the slow rates of formation of silica minerals such as quartz.

Trends of the saturation indices with depth (and hence with increasing temperature and pressure) are evident but not always consistent. For example, quartz oversaturation appears to increase slightly with depth in well DC15 but decreases slightly in wells DC6 and DB15. In well DC14, which lies to the north of the other wells examined, there is a dramatic decline in the quartz saturation index with depth. On the other hand, calcite and fluorite saturation indices consistently increase with increasing depth, usually indicating undersaturation near the top of the well and oversaturation at depth. For wells DC15 and DC14, the computations were run for an isothermal profile at 25°C, as well as at the formation temperature. While the carbonate mineral saturation was reduced by adjusting to an isothermal profile, it was not altogether removed. Consequently, the depth trend in saturation indices for calcite and other minerals appears to represent some real changes that are occurring in groundwater composition.

A similar computational analysis of groundwater samples from aquifers of the Columbia Plateau basalts was reported by BWIP (DEUTSCH 1982) using the code WATEQ2. In that analysis, calcite was found to be at equilibrium with the groundwaters, and most of the samples were at equilibrium with amorphous silica (glass). Computations indicated amorphic ferric hydroxide oversaturation, and the groundwaters were either over- or undersaturated with respect to various clays and secondary minerals. The results were interpreted as suggesting that the process of dissolution of basaltic glass and deposition of secondary minerals is still continuing, despite the long history of basalt contact with groundwater.

2.7.5 ACKNOWLEDGMENTS

The authors wish to acknowledge the excellent technical assistance of C. G. Westmoreland and G. C. Young, and the editorial assistance of L. H. Bell.

2.7.6 REFERENCES

BARNEY 1980. G. S. Barney and B. J. Wood, *Identification of Key Radionuclides in a Waste Repository in Basalt*, RHO-BWI-ST-9, Rockwell Hanford Operations, Richland, Wash., May 1980.

BARNEY 1982. G. S. Barney, *Radionuclide Sorption of Columbia River Basalt Interbed Materials*, RHO-BW-SA-198 P, May 1982.

DEUTSCH 1982. W. J. Deutsch, E. A. Jenne, and K. M. Krupka, *Computed Solid Phases Limiting the Concentrations of Dissolved Constituents in Basalt Aquifers of the Columbia Plateau in Eastern Washington*, PNL-4089, Battelle Pacific Northwest Laboratories, Richland, Wash., August 1982.

EARLY 1982. T. O. Early, D. R. Drewes, G. K. Jacobs, and R. C. Routson, *Geochemical Controls on Radionuclide Releases from a Nuclear Waste Repository in Basalt: Estimated Solubilities for Selected Elements*, RHO-BW-ST-39 P, Rockwell Hanford Operations, Richland, Wash., September 1982.

FRANCIS 1980. C. W. Francis and E. A. Bondiette, "Sorption-Desorption of Long-Lived Radionuclide Species on Geologic Media," in *Task 4, Third Contractor Information Meeting*, editor J. F. Relyea, PNL-SA-8571, Battelle Pacific Northwest Laboratories, Richland, Wash., 1980.

JENNE 1979. E. A. Jenne, "Chemical Modeling in Aqueous Systems," American Chemical Society Symposium Series 93, 1979.

LEFORT 1963. M. Lefort, "Oxydo-reduction du Couple TcO_2-TcO_4 en Solutions Diluees sous l/Effect du Rayonnement Gamma," *Bull. Soc. Chim. Fr.*, p. 882, 1963.

PALMER 1981. D. A. Palmer and R. E. Meyer, "Adsorption of Technetium on Selected Inorganic Ion-Exchange Materials and on a Range of Naturally Occurring Minerals Under Oxic Conditions," J. Inorg. Nucl. Chem. 43, 2979, 1981.

PAQUETTE 1980. J. Paquette, J. A. K. Reid, and E. L. J. Rosinger, *Review of Technetium Behavior in Relation to Nuclear Waste Disposal*, Atomic Energy of Canada Technical Report TR-25, November 1980.

PARKHURST 1980. D. L. Parkhurst, D. C. Thorstenson, and L. N. Plummer, *PHREEQE — A Computer Program for Geochemical Calculations*, U.S. Geological Survey, Water Resources Investigations Report 80-96, 1980.

SALTER 1981a. P. F. Salter and G. K. Jacobs, *Evaluation of Radionuclide Transport: Effect of Radionuclide Sorption and Solubility*, RHO-BW-SA-192 A, Rockwell Hanford Operations, Richland, Wash., 1981.

SALTER 1981b. P. F. Salter, L. L. Ames, and J. E. McGarrah, *Sorption of Selected Radionuclides on Secondary Minerals Associated with the Columbia River Basalts*, RHO-BWI-LD-43, Rockwell Hanford Operations, Richland, Wash., April 1981.

SALTER 1981c. P. F. Salter, L. L. Ames, and J. E. McGarrah, *The Sorption Behavior of Selected Radionuclides on Columbia River Basalts*, RHO-BWI-LD-48, Rockwell Hanford Operations, Richland, Wash., August 1981.

SCR 1982. *Site Characterization Report for the Basalt Waste Isolation Project*, DOE/RL 82-3, U.S. Department of Energy, Nevada Operations Office, Las Vegas, November 1982.

3.0 BACKFILL RESEARCH

Overpack and backfill materials have been proposed as a major component of the multibarrier system. Backfill systems are more amenable to performance assessment than waste package and geologic barriers because: (1) they are simpler systems in terms of number of components; (2) they are found in natural systems which have been subjected to repository conditions for thousands to millions of years and therefore provide a basis for long term predictability; and (3) the relatively small volumes of backfill materials specified in repository designs can be tested by laboratory and field tests at emplacement scales. The important attributes of the material (or combination of materials) selected is that it be relatively inexpensive, readily available, relatively impermeable, thermally conductive and stable, capable of providing mechanical strength after closure, highly sorptive to toxic ions, chemically compatible with the geologic environment and the waste package, reduce canister corrosion, and if possible serve as a fissure sealant (LeBell, 1978; Soudek et al., 3.1). The testability, predictability, and potential effectiveness of backfill systems may significantly reduce uncertainties in performance assessments and therefore the NRC is sponsoring several efforts to provide a basis for safety assessments of backfill systems proposed by DOE. Preliminary research conducted by the NRC in this area confirms that a proper choice of overpack and backfill materials for most geologic environments can meet many of the above requirements and add confidence to confinement times of nuclear waste. (Soudek et al., 3.1; Couture and Seitz, 3.2; Peacor et al., 3.3). Laboratory tests conducted by NRC, DOE, and Sweden indicate that smectite, mixed-layer smectite/illite, or illite in combination with an additive for strength (e.g., crushed basalt or quartz sand) and scavengers added to remove mobile radionuclides (e.g., metallic iron) could meet the above requirements (Pusch, 1980; Wood, 1981; Pusch, 1983; Wood, 1983; Soudek et al., 3.1; Couture and Seitz, 3.2; Peacor et al., 3.3).

One of the fundamental difficulties in evaluating a waste barrier system or subsystem is to determine if the barrier can perform its function for long time periods (thousands of years or more). Laboratory and field tests can provide data and information that can be used to establish performance for the first several years. In addition, laboratory and field tests can be conducted for anticipated future conditions. Unfortunately, data from short term tests cannot be extrapolated, in most cases, over long time periods without introducing large uncertainties in results. New methods are now available for detecting very small changes in materials properties. Characterization using, for example, STEM/AEM techniques of both starting and product phases permits detection of small scale physical and chemical changes in backfill materials which are important for long term performance assessment. However, such characterization has been lacking in many experiments involving backfill materials. Because conclusions in many backfill experiments depend on characteristics of starting materials and small but significant phase changes, it is essential that a complete characterization of materials to be carried out, and that standard materials be used in all experiments (Peacor et al., 3.3). Fortunately, many of the materials currently being considered are found to exist for thousands to millions of years in natural systems under conditions which approximate

those anticipated in the repository. For a detailed summary of the performance of proposed backfill materials in natural systems see Peacor et al., 3.3.

An extensive list of the specific backfill issues that should be resolved prior to licensing are listed in Soudek et al., 3.1.

REFERENCES

Couture, R. A. and M. G. Seitz. 1984. "Physical Response of Backfill Materials to Mineralogical Changes in a Basalt Environment." In NRC Nuclear Waste Geochemistry '83, NUREG/CP-0052.

Peacor, D. R., E. J. Essene, J. H. Lee, and L. Kuo. 1984. "Characterization of Potential Backfill Materials for Buried Nuclear Wastes." In NRC Nuclear Waste Geochemistry '83, NUREG/CP-0052.

Pusch, R. 1980. "Permeability of Highly Compacted Bentonite," Svensk Kaerbraenslefoersoerjning AB, SKB-KBS-80-16, Stockholm.

Pusch, R. 1983. "Stability of Deep-Sited Smectite Minerals in Crystalline Rock--Chemical Aspects," Svensk Kaerbraenslefoersoerjning AB, SKBF-KBS-83-16, Stockholm.

Soudek, A., F. M. Jahnke, and C. J. Radke. 1984. "Ion-Exchange Equilibria and Diffusion in Engineered Backfill." In NRC Nuclear Waste Geochemistry '83, NUREG/CP-0052.

Wood, M. 1981, "Development and Testing of Waste Package Materials for a Nuclear Waste Repository Located in Basalt," Rockwell Hanford Operations, RHO-BWI-SA-145.

Wood, M. 1983, "Experimental Investigation of Sodium Bentonite Stability in Hanford Basalt," Rockwell Hanford Operations, RHO-BWI-SA-219P.

3.1 ION-EXCHANGE EQUILIBRIA AND DIFFUSION IN ENGINEERED BACKFILL

A. Soudek, F. M. Jahnke, and C. J. Radke

Chemical Engineering Department
University of California
Berkeley, CA 94720

Abstract

Engineered backfill can add confidence to confinement times of high-level nuclear waste stored in geologic media. This paper discusses the design and operation of a unique radial-flow diffusion cell to determine ion migration rates in backfill material under realistic repository conditions. New experimental results were reported for diffusion of CsCl in a background of NaCl into compacted bentonite and bentonite/quartz mixtures. Representation of the measured diffussion rates by the traditional, homogeneous porous-medium model significantly underestimates cesium penetration distances into the backfill. Surface diffusion is suggested as an additional mechanism by which cations transport in swollen montmorillonite; the surface diffusion coefficients for cesium is determined to be approximately 10^{-7} cm^2/s.

An electrostatic site-binding model is developed for ion-exchange equilibria on montmorillonite clay. The effects of pH, ionic strength, and specific adsorption are evaluated and compared favorably to new, experimental exchange isotherms measured on disaggregated clay. The electrostatic site-binding model permits a prediction of the influence of backfill compaction on K_d values. We find that for strongly adsorbing cations, compactions has little effect. However, anions exhibit significant Donnan exclusion with clay compaction.

3.1.1 Introduction

Ultimate isolation of high-level radioactive waste materials is a critical problem for the future of nuclear energy worldwide. Although many schemes have been proposed, including deep-space disposal, one promising method is underground storage in impermeable geologic formations [1]. This disposal technique involves burying spent nuclear fuel rods, several thousand meters below the surface, as shown in Figure 1. Once in place, the waste material should be protected by as many barriers as possible to prevent escape of harmful and long-lived radioactive elements [2]. Thus, the geologic environment must be carefully chosen for impermeability to water and for thermal stability; considerable effort is being directed towards choosing suitable sites [3-5]. Likewise, the cannister material should resist corrosion. Much study is currently underway on cannister design [6]. Finally, even if the first two barriers ultimately fail, it is possible to retard radioactive ion movement by ion exchange with secondary minerals located in the small fractures of the host formation. A large amount of research is currently exploring this third, far-field barrier [5,7,8].

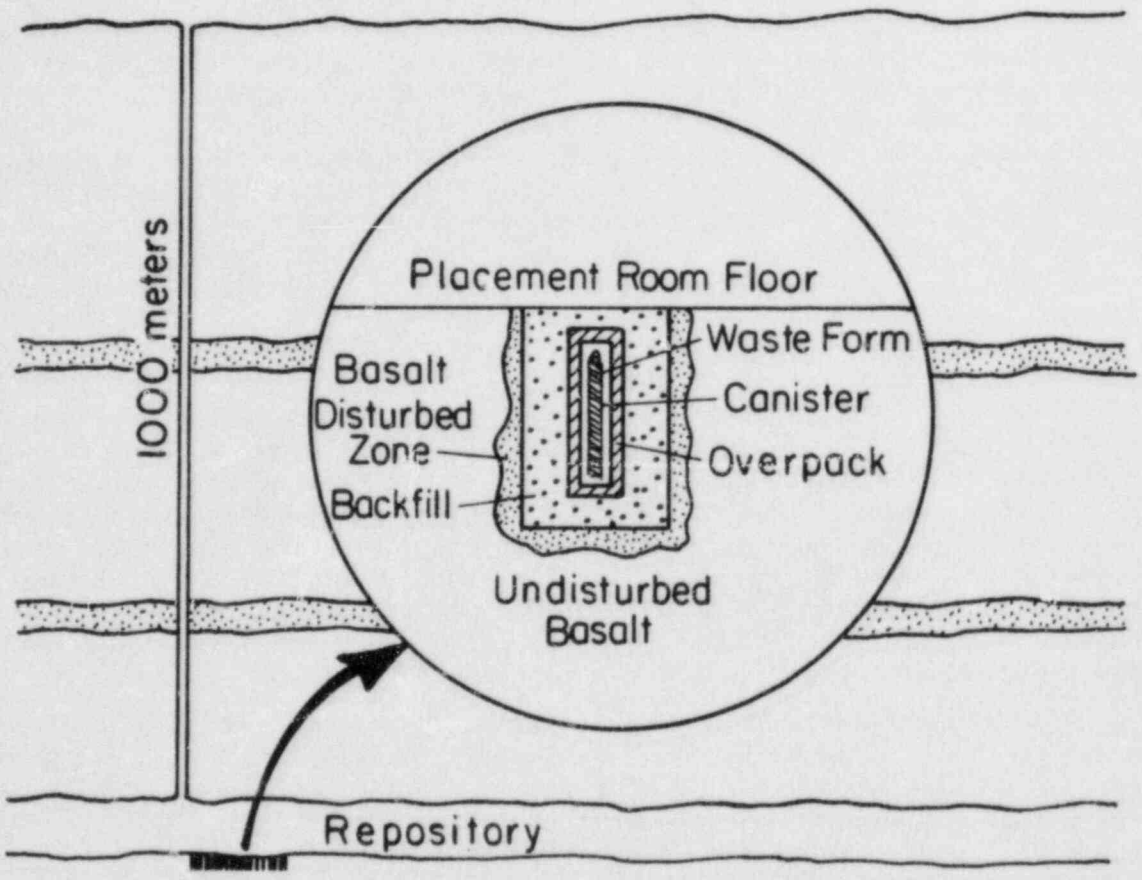

Figure 1. Schematic of the multiple barrier concept in a basaltic repository.

One possible additional barrier that has been given attention recently in the United States is that of a near-field backfill material (see Figure 1). Such an engineered barrier should be inexpensive, readily available, relatively impermeable, thermally conductive and stable, highly sorptive to toxic ions, compatible with the geologic environment and the waste package, and if possible, a fissure sealant [9]. One material that meets many of these qualifications is smectite or gelling clay. However, pure smectite gels are not strong mechanically, so a more likely barrier material would consist of crushed host rock or quartz sand and bentonite. Further, since montmorillonite is a cation exchanging clay, it may also be necessary to spice the backfill with anionic getters to retard any toxic radioanions.

The purpose of this project is to investigate experimentally, under realistic conditions, the migration rates of representative nuclides and their mixtures in proposed barrier materials and to formulate a quantitative model allowing the prediction of the effectiveness of such an engineered barrier. Specifically we address the primary issue of the reliability of engineered backfill to limit radionuclide release after cannister failure. Thus, the ultimate goal of this study is to provide reliable tools for evaluating a given backfill material and for designing the requisite amount and configuration of that backfill. We emphasize that our experimental program is general in that any backfill material can be evaluated for its ability to hinder radionuclide migration.

The first issue that arises in obtaining a physical description of ion migration in smectite gels residing next to a buried cannister is that of the major mode of ion transport. When nuclides are released from the waste cannister, they may migrate by convection and/or diffusion through the barrier gel to the host geologic environment. That diffusion is the dominant transport mechanism is demonstrated by the calculations of Neretnieks, which are reproduced here in Figure 2 [10]. This figure shows the time for an ion to travel 1 m from a cannister as a function of the bulk ground water velocity. K gives the dimensionless, ion-exchange slope at zero concentration. It is related to the more usual K_d value by $K = p_s K_d$ where p_s is the density of the solid clay particles in g/cm^3. At small velocities the migration time is independent of flow, indicating a diffusion mechanism. At large velocities the migration time decreases in proportion to the velocity, indicating pure convection. Figure 2 reveals that diffusion dominates when the water bulk velocity U is less than about 0.01 m/year. Estimates of expected bulk velocities fall around 0.001 m/year [10]. Figure 2 combined with the observations that clay permeabilities are low (i.e., 10^{-6} to $^{-9}$ μm^2, [11,12] and that typical hydraulic gradients are small [11] confirms that diffusion will be the only migration mode in bentonite backfills.

Based on this diffusion concept, the accepted procedure for designing backfill amount and configuration is to utilize the following transient diffusion equation [10] which we designate as the homogeneous, porous-medium model:

$$1 + \left(\frac{1-\varepsilon}{\varepsilon}\right) K \frac{\partial c}{\partial t} = D \frac{\partial 2c}{\partial x^2} , \qquad (1)$$

where c is the ion concentration in the void space, e is the gel porosity, D is the ion diffusion coefficient in the gel, t is time, and x is distance. Again, K is the dimensionless, exchange-isotherm slope at zero concentration.

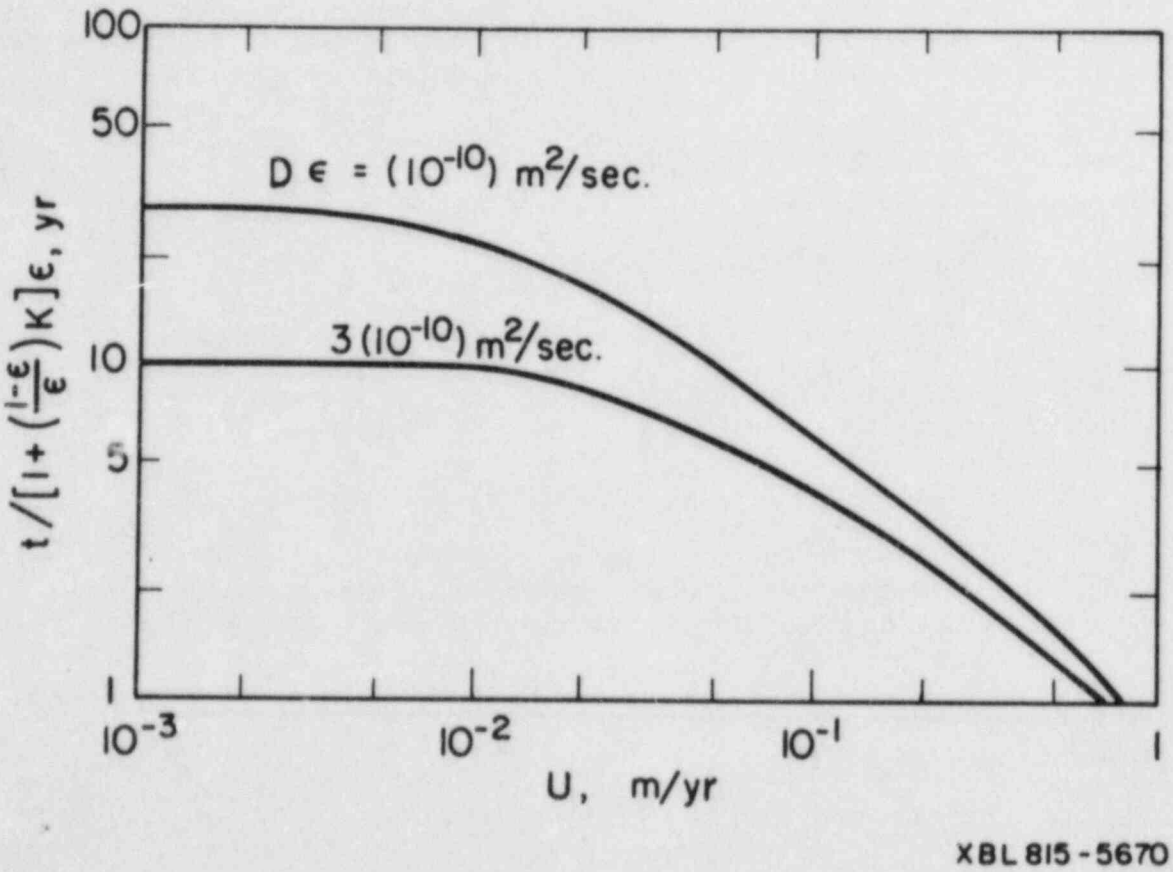

Figure 2

Ion migration time to travel 1 m in a sorptive porous medium as a function of bulk ground water velocity. D is the diffusion coefficient, ϵ is the medium porosity, and K is the ion-exchange slope at zero ion concentration.

Typically $K_d = K/p_s$ is measured on disaggregated backfill solids and Eqn. (1) is applied to establish migration times of specific radionuclides.

Eqn. (1) is quite restrictive. It assumes instantaneous exchange equilibria, a linear exchange isotherm and a constant diffusion coefficient. Both the isotherm and the diffusion coefficient are uninfluenced by multicomponent, compaction, and electrical effects. Most critically, the bentonite gel is viewed as a simple porous medium. That is, Eqn. (1) does not reflect the fact that montmorillonite gels are composed of highly asymmetric, highly charged platelets, the complicated interaction of which results in a gel structure, due to electric double layer, van der Waals, and specific forces. The detailed arrangement of individual particle within the montmorillonite gel has been studied widely [13-16], but is by no means fully understood. When Equ. (1) is written independently for each diffusing cation (and anion) there is a question of how electroneutrality is maintained. These reservations lead to the second major issue addressed by this research: the need to measure actual ion diffusion rates in compacted backfill so as to validate design calculations.

3.1.1.1 Issues Addressed by this Research

The primary issues concerning backfill performance are:

To what extent can backfill be relied upon, to:

Reduce the flow of water in the vicinity of the waste package?
Reduce canister corrosion?
Provide mechanical strength after repository closure?
Limit radionuclide release after breach of containment?

What are the potential backfill failure mechanisms which could result in:

a. acceleration in corrosion which exceed design limits
b. loss of mechanical strength specified by design limits
c. radionuclide releases which exceed specified design limits

Consideration of these primary issues leads to the identification of certain specific issues necessary for their resolution. The specific issues are the following:

1. How fast do radionuclides migrate in engineered barrier materials?

   i. What are the roles of Donnan ion exclusion, barrier composition and structure, irreversible or reversible adsorption, sorption kinetic uptake, solution speciation, co- and hydrolysis precipitation, multicomponent solution compositions, and lattice incorporation?

   ii. Are Kd (or isotherm) measurements on disaggregated backfill materials relevant?

2. Are anion getters needed in the backfill material?

i. Will getters influence host rock environment?

ii. Will getters influence waste package behavior?

3. Is thermal diffusion an important transport mechanism in backfill?

4. Can colloidal particles migrate through backfill material?

5. Will the backfill provide a strong, low-permeability, and swelling sealant against the waste package and against the disturbed host rock?

   i. Is diffusion the dominant transport mode as compared to advection?

   ii. Will the low hydraulic permeability of the backfill slow waste package dissolution rates?

6. How long does it take the backfill to be saturated with groundwater?

   i. Does backfill swell to minimize groundwater inhibition rates?

   ii. How can backfill be emplaced to maximize saturation time?

7. What are the short and long term geochemistry environments in the backfill (i.e., Eh, pH, T, solution in components)?

   i. How does the geochemistry influence the sealing and hydraulic behavior of backfill?

   ii. How does the geochemistry influence the retardation properties of the backfill?

   iii. What are the realistic (relevant) conditions and range of conditions under which the backfill properties should be studied?

8. Will groundwater hydraulic gradients displace the backfill away from the waste package?

9. What is the expected hydrothermal history of the backfill?

   i. What are the backfill thermal properties?

   ii. What is the expected wet-dry cycling behavior of the backfill?

   iii. How will wet-dry cycling and temperature history influence backfill properties (especially sealing and retardation)?

10. What are the chemical and physical interactions of backfill with the waste package and the disturbed host rock?

    i. Can backfill components and buffering adversely affect sorptive behavior of host rock?

    ii. Can backfill components alter dissolution/leaching rates of the waste package?

11. What are the expected chemical and physical alterations of the backfill?

    i. What are the roles of radiolysis, secondary minerals, clay dehydration, and temperature in altering backfill properties?

    ii. What are effects of cementation?

12. How should backfill be emplaced in the repository?

    i. What is the desired configuration of the waste canisters to take advantage of backfill properties?

    ii. Should backfill be used in the shafts and boreholes?

    iii. Should backfill be emplaced as bricks, granulated, or pelletized?

    iv. Should backfill be an integral part of the waste package?

13. What is the desired composition of the backfill to fulfill its roles?

    i. How much host crushed rock?

    ii. How much clay?

    iii. How much getter?

    iv. Is there a need for other specific components?

    v. What density is needed or achievable?

3.1.1.2 Previous Work

There are surprising few measurements of ion diffusion in compacted monmorillonite gels. Turk [17] and Nowak [18] found reasonable success in fitting their data to Eqn. (1), but Turk's systems were limited to moderate compactions (less than 30 w/o) at high ionic strengths (0.7 M background ionic strength), whereas Nowak studied much higher compactions (about 90 w/o clay), but his background ionic strengths were exceedingly high (about 4M). These results may not be valid if used directly to show the applicability of Eqn. (1) for an engineered barrier for two reasons. First, the structure of the montmorillonite gel is very sensitive to background ionic strength [15], and the ionic strength at which these experiments were conducted is significantly higher than that of 10^{-3} to 10^{-2} M found in typical basaltic (or granitic) groundwaters [19]. Secondly, K_d values are functions of background ionic strength [8].

Torstenfelt et al. [20,21], studying diffusion of radionuclides through a highly compacted montmorillonite at lower ionic strengths, recently found that Eqn. (1) cannot fit the migration behavior for any of the ions they consider. The cations Cs and Sr do not diffuse according to Eqn. (1). Also they migrate more rapidly than expected considering their sorption isotherms (i.e., using K_d values from the disaggregated clay). In fact, the ionic diffusion coefficients of Cs and Sr found by Torstenfelt et al. are even higer than those in bulk water. For the anion, TcO_4^-, Torstenfelt et al. report that it migrates

almost unhindered through the compacted montmorillonite. This result is unexpected since significant Donnan exclusion of anions might be anticipated in compacted montmorillonite gels [22].

The results cast further doubt on the homogeneous, porous-medium model which is perhaps not surprising, but, nevertheless, is discomforting. We feel that it is critically important to obtain reliable and well-defined measurements of ion diffusion in actual compacted barrier materials. Only then can physically correct models be established to permit reliable backfill design.

In this paper, we first discuss our measurements and theoretical modeling of equilibrium ion exchange on bentonite, including the role of compaction on K_d values. Next the design and operation of a prototype, radial-flow diffusion cell is outlined. Finally, new ion migration rates for cesium are presented and analyzed to suggest the importance of surface diffusion.

3.1.2 Ion-Exchange Equilibria

The role of ion exchange in retarding the migration of radionuclides in montmorillonite-based backfill is critical to the performance of such a barrier by fixing the value of $K = p_s K_d$ in Eqn. (1). Therefore, many workers have measured the sorption of various ions on montmorillonite and other materials in batch experiments [8,23]. Some report concentration-dependent K_d values [8]. However, the K_d value is properly defined as the slope of the adsorption isotherm in the limit of zero bulk concentration. Concentration-dependent K_d values actually correspond to chords along a nonlinear exchange isotherm at the given conditions of background ionic strength, pH, and Eh. When K_d is found to vary with concentration, it can no longer be used directly in Eqn. (1). Rather the slope of the isotherm should be employed with K replaced by $p_s\, dn/dc$, where n is the ion adsorption in moles per solid mass.

Exchange behavior on clays is complex, as attested by the recent review of the BWIP Site Characterization Report [24]. A striking example of these complications is that nine different laboratories were given identical rock samples and performed similar controlled uptake experiments, yet the resulting K_d values varied by a factor of over 100 [23]. Questions arise about irreversible adsorption [24,25], setting realistic Eh conditions [24], and multi-ion competition [24]. Finally, K_d values are almost always measured with dilute, disaggregated clay suspensions. How such values correspond to those expected in a compacted clay has not been addressed.

In this section we present, and compare to experiment, a new, electrostatic, ion-exchange model based on the concept of surface site-binding. A primary feature of the new theory is its ability to predict clay compaction effects.

3.1.2.1 Experimental Methods and Results

Cesium adsorption on bentonite was determined by standard batch techniques. Wyoming bentonite (Wards) was sieved to remove gritty impurities and the 200 to 400 mesh size fraction was saved for the experiments. To mimic expected backfill application no chemical pretreatment or dialysis was used.

0.2g of clay was added to 50 cm^3 of cesium chloride (Fisher, technical) solution at the desired pH (NaOH, Mallinckrodt, reagent) and background ionic strength (NaCl, Mallinckrodt, reagent) in shaker flasks. The flasks were blanketed with N_2, sealed, and agitated at 25°C until equilibrium was attained, which took approximately 2 days. After equilibration, the suspension was centrifuged and the supernatant filtered twice through 0.08-mm Nuclepore membranes to remove any small clay particles. Final cesium concentrations were measured with a Perkin-Elmer Atomic Adsorption Spectrophotometer. To control spurious ionization approximately 0.01 M KCl was added to all samples and standards. Accordingly, concentrations of cesium could be detected down to 10^{-6} M. No pH changes were observed during the adsorption experiments.

Figure 3 shows the exchange isotherm for cesium in mequiv/100g of solid at pH values of 7 and 9 and for two background ionic strengths of 10^{-2} M and 10^{-3} M in NaCl. Four decades of concentration and three decades of loading are displayed. Notice the absence of any pH dependence. For cesium concentrations less than about 10-4 M the isotherm is linear. Near 10-2 M in cesium the isotherm levels off to the accepted cation exchange capacity (CEC) of montmorillonite near 100 mequiv/100g [15,26]. Only at concentrations below 10^{-4} M will Eqn. (1) apply. Otherwise the isotherm slope must be utilized, as noted above.

Solid lines in Figure 3 correspond to the best-fit K_d values, which are 100 cm^3/g and 560 cm^3/g at 10^{-2} and 10^{-3} M NaCl, respectively. These values compare favorably with those reported in the literature [8,27]. Dashed lines in Figure 3 are predicted by the ion-exchange theory to be described.

3.1.2.2 Theory of Disaggregated Clay

The ion-exchange properties of montmorillonite originate from cation charge deficiencies within the tetrahedral and octahedral layers of the montmorillonite lattice [15,26,28]. To compensate for this positive charge deficiency, solution cations adsorb on the surface to maintain electroneutrality. Since the surface negative charge originates from a crystal defect, the faces of montmorillonite exhibit constant-charge behavior [29].

The edges of montmorillonite are crystalographically different. Here the lattice is fractured. Thus the edges would be expected to behave as inogenic surfaces due to broken Al-O and Si-O bonds [30]. However, the surface area of the faces is much greater than that of the edges, so that the adsorption behavior of a single montmorillonite platelet is governed mainly by the constant-charge faces [15,26,29].

To represent the specific interactions of solution cations with the negatively-charged montmorillonite surface we adopt site-binding equilibria. Let S^- denote a negative adsorption site. Then we write the following reactions:

$$S^- + Na^+ \overset{K_{Na}}{\rightleftharpoons} S^- - Na^+ \quad , \qquad (2)$$

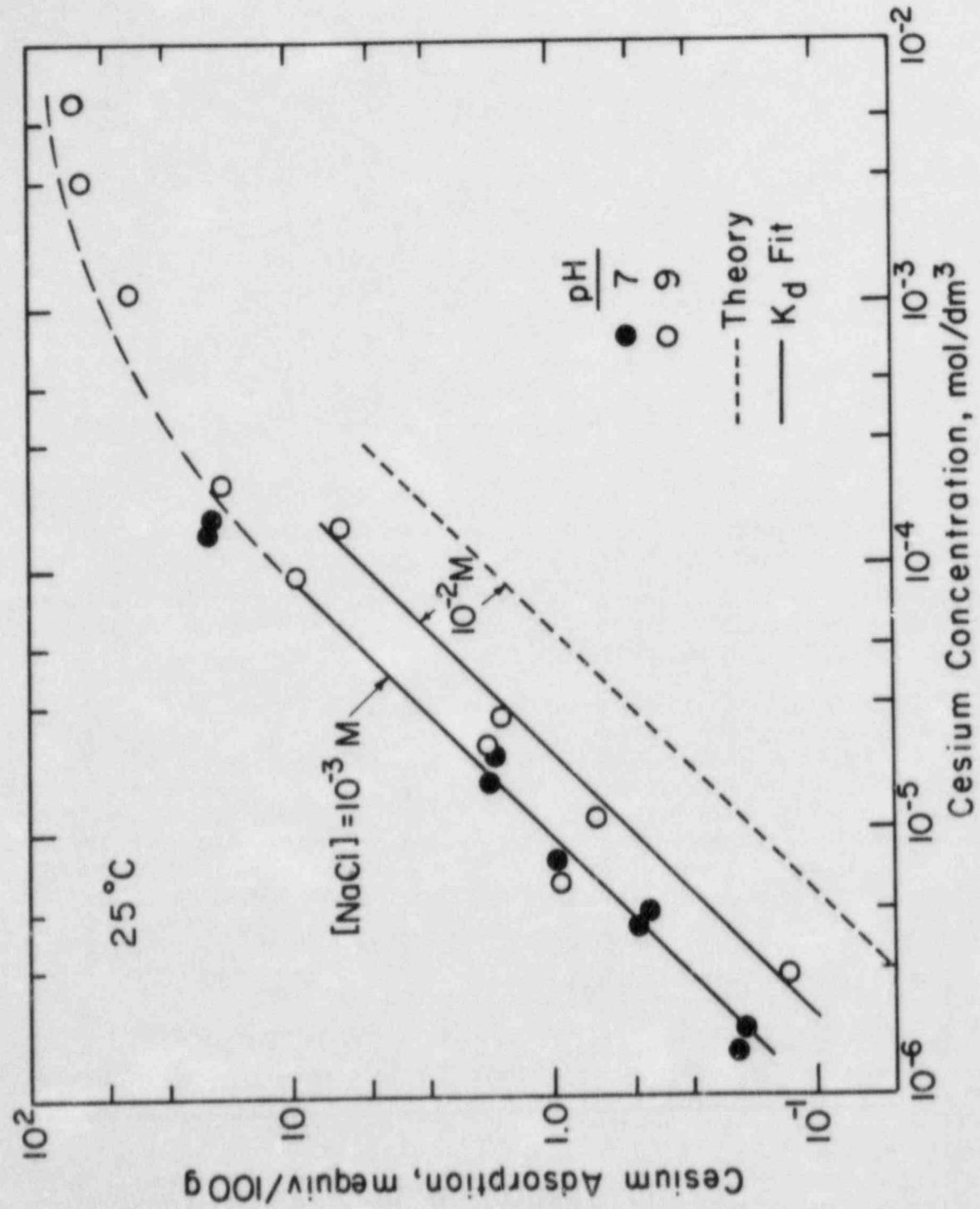

Figure 3

The Cs - Na ion-exchange isotherm on undialized bentonite at two background electrolyte concentrations of NaCl (10^{-2} and 10^{-3} M).

and

$$S^- + Cs^+ \overset{K_{Cs}}{\rightleftarrows} S^- - Sc^+ \qquad (3)$$

If Eqn. (3) is subtracted from Eqn. (2), then the standard mass-action expression for ion exchange emerges [22]. However, this is an oversimplified procedure because electrical effects are involved in the surface equilibria of Eqns. (2) and (3).

We adopt the treatment of Davis, James, and Leckie [31], and express the equilibrium constants of Eqn. (2) and (3) as

$$K_{Na} = \frac{(S^- - Na^+) \exp (F\phi_\beta/RT)}{(S^-)\ [Na^+]} \ , \qquad (4)$$

and

$$K_{Cs} = \frac{(S^- - Cs^+) \exp (F\phi_\beta/RT)}{(S^-)\ [Cs^+]} \ , \qquad (5)$$

where curved brackets () denote surface concentrations and square brackets [] denote bulk concentrations. ϕ_β is the electrostatic potential at the β-plane (to be defined) and F is Faraday's constant. Heuristically, the exponential factors in these expressions provide an electrical correction for the "local" cation concentrations adjacent to the surface.

To evaluate Eqns. (4) and (5) requires a detailed understanding of the electrostatics near the montmorillonite surface. Our picture, adapted from reference [31], is shown in Figure 4. Next to the negative clay surface partial dehydration and site-bindig occurs for specifically adsorbed cations. The centers of the site-bound cations fix the b or inner Helmholtz plane. Adjacent to the β-plane is the d-plane, which delineates the distance of closest approach of a fully hydrated cation. The classical Gouy-Chapman diffuse layer commences at the d-plane. Constant integral capacitances, C_1 and C_2, characterize the inner and outer regions. We set C_1 and C_2 equal to 150 and 20 μF/cm², respectively [31].

Let σ_o, σ_b, and σ_d denote in order the charge densities at the surface, at the β-plane, and in the diffuse double layer. Then electroneutrality demands that

$$\sigma_o + \sigma_\beta + \sigma_d = 0 \qquad (6)$$

The surface charge density is known from the CEC (i.e., 100 mequiv/100g) and the specific surface area of montmorillonite (i.e., 800 m²/g) [15,26] or $\sigma_o = 12\mu C/cm^2$. The inner layer charge is given by the amount of specifically adsorbed cations, $\sigma_\beta/F = (S^- - Na^+) + (S^- - Cs^+)$. Finally the diffuse-layer charge follows from the well-known results [15,29].

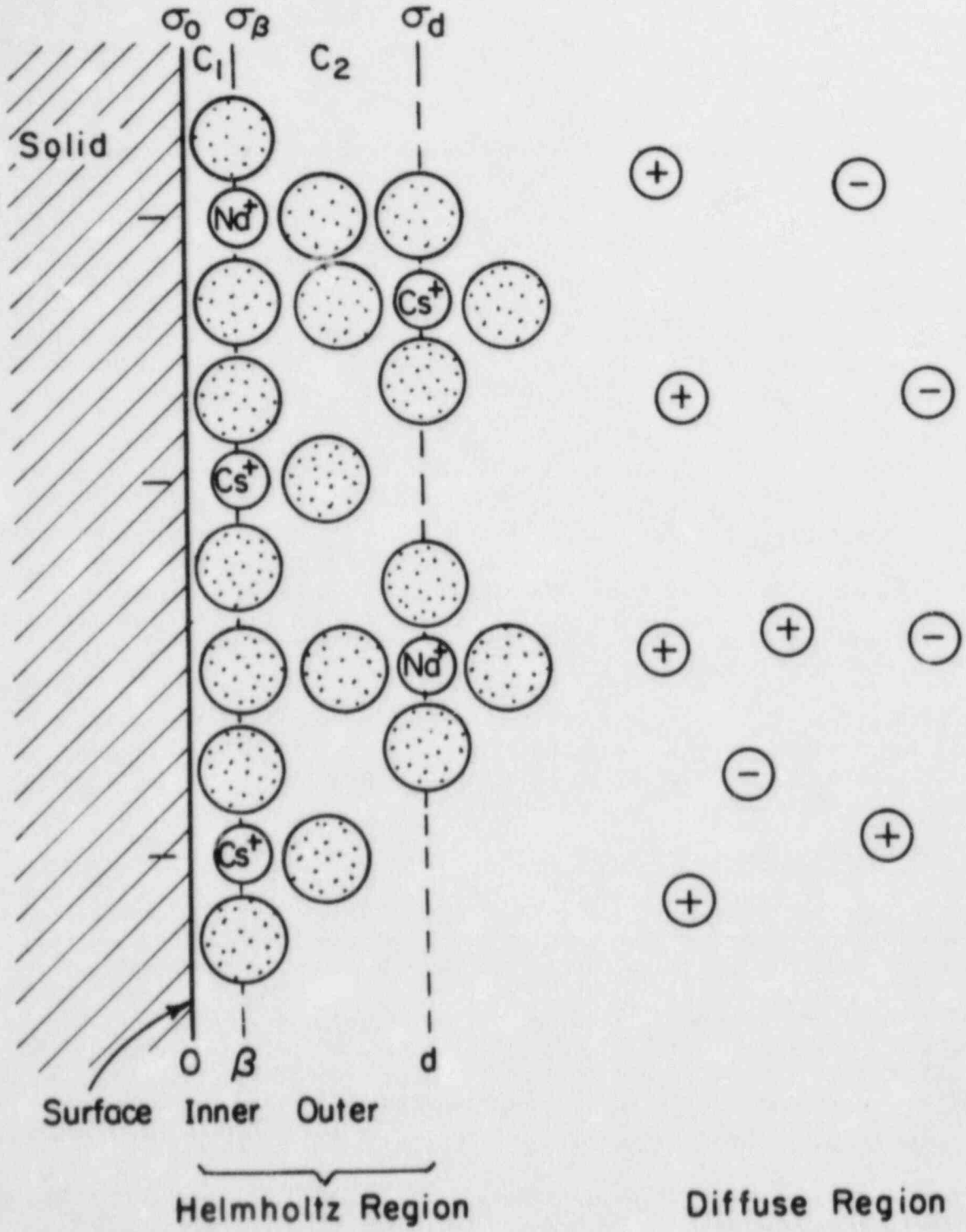

Figure 4. Schematic of the electrical structure for Cs-Na ion exchange at the montmorillonite/water interface. The symbols σ_o, σ_β, and σ_d denote the surface charge densities at the surface, at the inner Helmholtz plane and at the outer Helmholtz plane, respectively.

$$\sigma_o = - \sqrt{8\bar{\varepsilon}RT([Cs^+] + [Na^+])} \sinh (F\phi_d/2RT) \qquad (7)$$

where ε is the bulk permittivity of water. Solution of Eqn. (6) is trial-and-error in the electrostatic potentials ϕ_o, ϕ_b, and ϕ_d [31]. Once these are known the problem is fully specified.

Cation adsorption includes that specifically bound and that in the double layer:

$$\frac{n_{Cs}}{\Sigma} = (S^- - Cs) + 2\,[Cs^+]\,\lambda\,(\exp(-F\phi_d/2RT) - 1) \qquad (8)$$

where Σ is the specific surface area of montmorillonite, n is the ion adsorption in moles per solid mass, and λ is the Debye length. A similar expression holds for the ion uptake of sodium. From Eqn. (8) for cesium (and that for sodium) the exchange isotherm may be calculated.

Dashed lines in Figure 3 show the theoretical exchange isotherm for cesium. Two parameters are fit from the data at 10^{-3} M background NaCl. They are $K_{Na} = 100\ M^{-1}$ and $K_{Cs} = 130\ M^{-1}$ The model successfully fits the 10^{-3} M back ground electrolyte case over the entire range of cesium concentration from 10^{-6} to 10^{-2} M. However, prediction of the 10^{-2} M background electrolyte case is less appealing. A possible explanation is that the undialyzed clay likely contains impurity ions, such as calcium, so that not all exchange sites are available for cesium. This emphasizes the need to work with well-characterized systems for model development.

We stress that the electrostatic site-binding model can be extended to handle multicomponent adsorption, effects of pH, and irreversible adsorption. It is quite general. Extension of the ion-exchange model to compacted clay is discussed below.

3.1.2.3 Theory for Compacted Clay

Under compaction the montmorillonite clay particles come into close proximity. The electrical atmosphere enveloping each particle (see Figure 4) overlaps those of adjacent particles. This overlap influences ion adsorption.

To establish how important this compaction effect might be we approximate the gel as consisting of parallel, equally-spaced platelets and we apply the previous site-binding model. The only change that is required involves the diffuse layer charge, σ_d. During overlap Eqn. (7) is no longer valid. Rather σ_d must be obtained by solution to the Poisson-Boltzmann relation.

Let x be the distance variable measured from the d-plane, and let δ denote the value of x at the center line between two opposing platelets. The nonlinear Poisson-Boltzmann equation then reads for 1-1 electrolytes [29]:

$$\frac{d^2\phi}{dx^2} = \frac{RT}{F\lambda^2} \sinh \frac{F\phi}{RT} \quad , \; 0 \leq x \leq \delta \qquad (9)$$

with the boundary conditions that

$$\bar{\varepsilon} \frac{d\phi(0)}{dx} = \sigma_d \,, \tag{10}$$

and

$$\frac{d\phi(\delta)}{dx} = 0 \tag{11}$$

Eqn. (10) permits evaluation of σ_d for compacted clay which occurs when δ is shrunk. The rest of the site-binding model remains unchanged. Thus, Eqn. (6) is again solved by trial-and-error, only now for each trial Eqns. (9) - (11) must be calculated. We use a finite-difference scheme with Newton iteration. Once Eqn. (6) converges, cation adsorption between the clay platelets follows from a quadrature similar to Eqn. (8):

$$\frac{n_{Cs}}{\Sigma} = (S^- - C^+) + [Cs^+] \int_0^{\delta} (\exp(-F\phi/RT)-1)dx \tag{12}$$

Different values of δ correspond directly to varying degrees of compaction. For w very large the disaggregated exchange isotherm will result.

Figure 5 reports the calculated effect of compaction on cesium K_d values (i.e., $K_d = dn_{CS}/d[Cs^+]$ at $[Cs^+] = 0$) in 10^{-2} M background sodium chloride. In this figure h is defined as $(\delta + 3)\mathring{A}$ where the distance between the clay surface and the d-plane in Figure 4 is estimated to be $3\mathring{A}$. Thus 2h is the average, clay-particle separation distance in Angstroms. We discover that K_d for cesium changes only slightly even up to very high weight percent clay or equivalently down to very small separation distances. The reason for the insensitivity of K_d to compaction is that most all of the cesium is specifically adsorbed at the inner Helmholtz or β-plane and little is in the diffuse double layer. It is the diffuse region that most strongly responds to overlap; the inner region is not significantly affected. We conclude that for strongly adsorbing monovalent cations compaction will not be an important consideration in ion-exchange equilibria.

Although cation adsorption may not be strongly altered by compaction, the same is not true for the co-anions. As the positive electrical atmosphere between the platelets interpenetrates with compaction, more and more anions are expelled. The limit of complete expulsion corresponds to perfect Donnan exclusion, which is a common approximation made for cation exchange resins [22].

The proposed electrostatic site-binding model permits calculation of anion exclusion in compacted montmorillonite gels. Let $\langle[Cl^-]\rangle$ denote the average concentration of univalent anion between the overlapping platelets. When $\langle[Cl^-]\rangle = 0$, there is complete explusion of chloride from between the clay particles. Since anions in our model do not specifically adsorb, we write

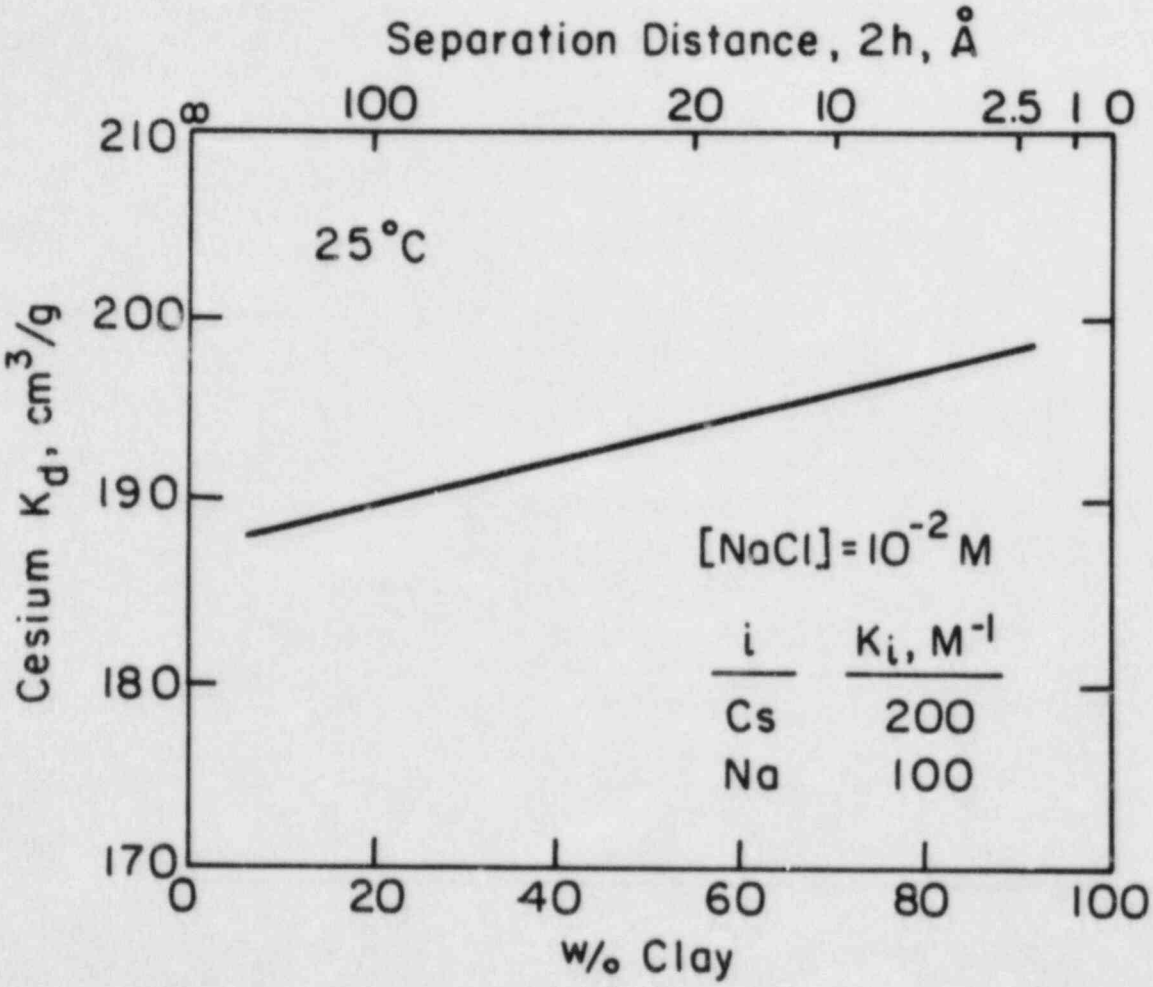

Figure 5. Calculated K_d values for Cs as a function of compaction. 2h is the average separation distance between the montmorillonite particles.

$$\frac{\langle [Cl^-] \rangle}{[Cl^-]} = \frac{1}{h} \int_0^{\delta} \exp(+F\phi/RT)dx \qquad (13)$$

Thus, along with cation adsorption, the role of compaction on anion expulsion may be calculated from the site-binding model.

Figure 6 reports the average chloride concentration between clay particles as a function of separation distance when CsCl = 10^{-3} M and NaCl = $9(10^{-3})$ M. Note the extremely strong rejection of the co-ion. At 50 w/o clay (~25Å plate separation) almost 90% of the anions are rejected. Complete Donnan exclusion of anions appears to be a reasonable approximation for compacted bentonite.

The results of Figure 6 seem to imply that migration of toxic radioanions through bentonite backfill should be difficult. However, Torstenfelt et al. report that anionic technecium passes through compacted bentonite as readily as through bulk water [20, 21]. Apparently, the clay particles in compacted bentonite do not arrange in parallel card stacks. The exact structuring of the particles is not known but is of critical importance to ion-diffusion rates, our next topic.

3.1.3 Ion Diffusion

Understanding and quantifying equilibrium ion exchange is the first part of the problem of ion migration in backfill. Ascertaining the validity of the homogenous, porous-medium diffusion model in Eqn. (1) is the second. For this we measure cation diffusion rates in compacted bentonite with a unique radial-flow diffusion cell.

3.1.3.1 Diffusion-Cell Design

Two general criteria should be met in designing a diffusion cell for backfill. First variable degrees of compaction should be allowed. Second, measurement of both the concentration response of an external solution, or ion depletion, and the concentration distribution within the backfill, or ion profiling, should be permitted.

The backfill material surrounding a nuclear waste canister will initially not experience significant compaction. However, if the site is enclosed, the barrier material may eventually experience forces as large as the difference between the lithostatic and hydrostatic heads. Therefore, to understand ion migration in backfills representative of those underground, the barrier material must be studied at various known degrees of compaction. This requires that the backfill be compressed against a solid support.

Ion depletion from an external bath in contact with the backfill gives an integral response to Eqn. (1), and is, therefore, not a precise gauge of migration behavior. Further, the ion-depletion technique demands that there be little or no external mass-transfer resistances, otherwise the diffusion resistance within the backfill is not measured. This is an especially important restriction for montmorillonite gels where large K_d values result in extremely small initial diffusion resistances. Conversely, ion profiling provides a differential response to Eqn. (1). However, ion profiling usually requires that the experiment be completely stopped for sampling.

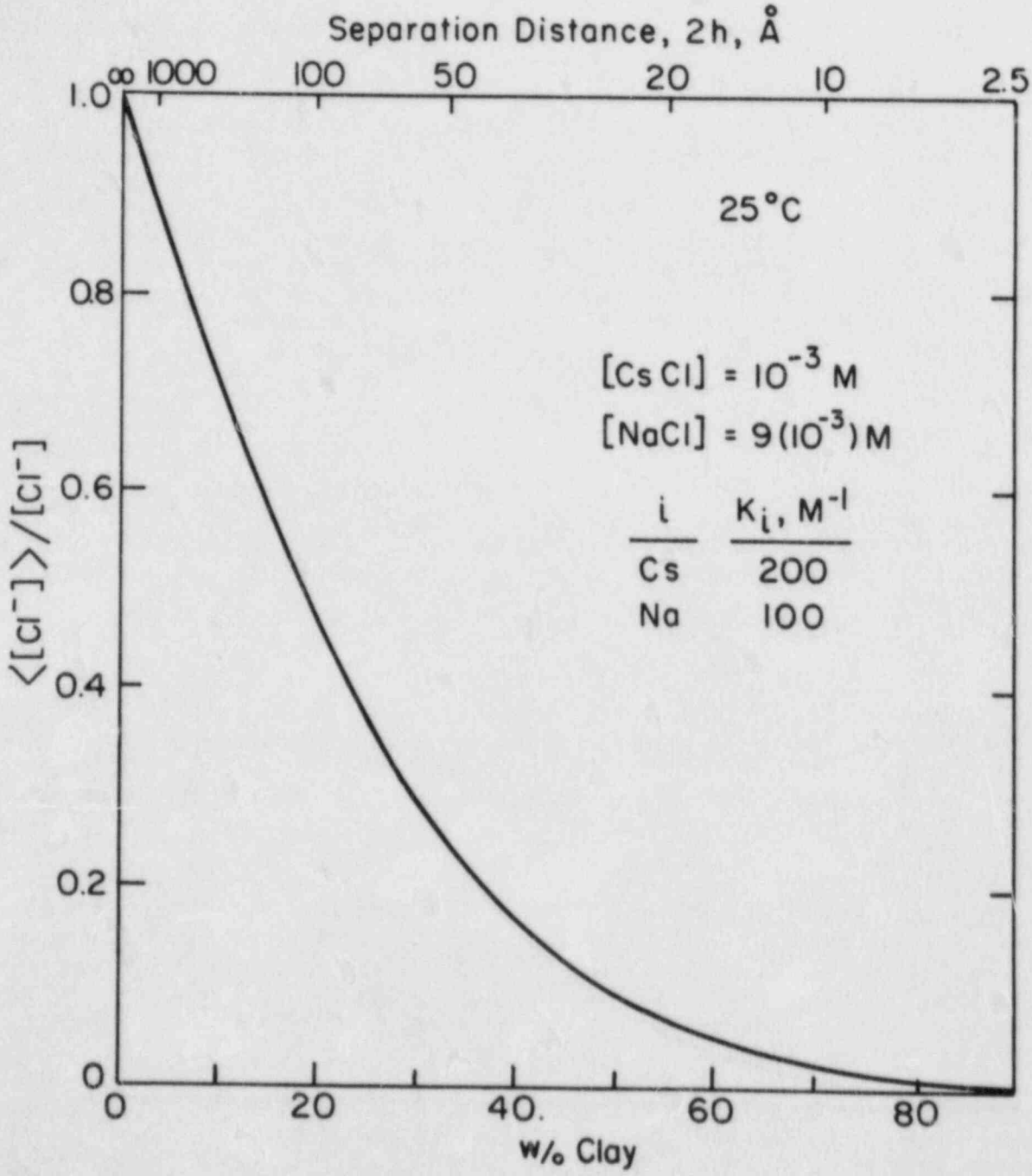

Figure 6. Calculated Donnan exclusion of univalent anions in a compacted montmorillonite gel. 2h is the average separation distance between the clay particles.

To obtain a more complete understanding of ion-migration rates in compacted backfill we employ both ion depletion and ion profiling. An extremely helpful advantage of using both techniques is that overall material balance can be checked.

Our diffusion-cell design is shown schematically in Figure 7 [32]. Backfill is confined between a drive piston and a Nuclepore membrane backed by a porous sintered metal disk. Each is sealed by Viton O-rings. The key feature of this cell is the radial flow of solution through the sintered metal support disk and out to a sample loop. This sample loop, which is not shown in Figure 7, consists simply of an FMI constant-displacement pump downstream to a magnetically-stirred solute chamber. The reason for convecting the external solution is to reduce mass-transfer resistance. Radial convection establishes an equally accessible surface through which ions transport uniformly to the backfill. As the concentration boundary-layer attempts to grow inward from the backfill perimeter, the increasing radial velocity provides a correction. This results in a boundary-layer thickness that is practically constant.

Extensive mass-transfer calculations, reported previously [33], demonstrate that a uniformly accessible surface (i.e., one with a constant mass-transfer, boundary-layer thickness) does emerge with the radial-flow design, and that there is negligible mass-transfer resistance in the sintered metal disk. Most of the external mass-transfer resistance is now confined to the thin (~ 10μm) Nuclepore membrane and is less than 1000 s/cm [33]. Such low resistances, usually less than 500 s/cm, have been confirmed by our ion-depletion results (i.e., the initial slope of the concentration fall in the sampling chamber measures any external mass-transfer resistances [34]).

The radial-flow configuration also allows the sintered metal disk to be supported throughout its entire length. A much greater compaction of the gel within the clay chamber is permitted. The maximum load the membrane can withstand is now a function of the strength of the support cap, which can be made as thick as desired.

In addition to assessing any external mass-transfer resistance we tested the radial-flow diffusion cell for uniform accessibility. If there is significant radial growth in the concentration boundary-layer, the flux of ions into the backfill will be greatest at the outside radial edge and least at the center line. This would invalidate any use of one-dimensional diffusion models, such as Eqn. (1), in the compacted gel.

To address the question of uniform accessibility we studied cesium radial profiles in an uncompacted agar gel [35]. Agar was chosen because it is readily sectioned and is relatively nonadsorbing so ions can transport rapidly through it. The experiments, described in reference [35], demonstrate that the radial-flow cell indeed leads to uniform accessibility.

3.1.3.2 Experiment

Wyoming bentonite, treated as described above, and unsieved Ottawa sand (quartz with 2 w/o kaolinite) are added in known quantities to an aqueous solution of the desired background ionic strength and pH. After stirring, the gel is homogenized in an ultrasonic bath for about eight hours, and then carefully placed in the diffusion cell so as to avoid trapping of any air bubbles. This technique leads to a backfill gel that is quite uniform in composition along

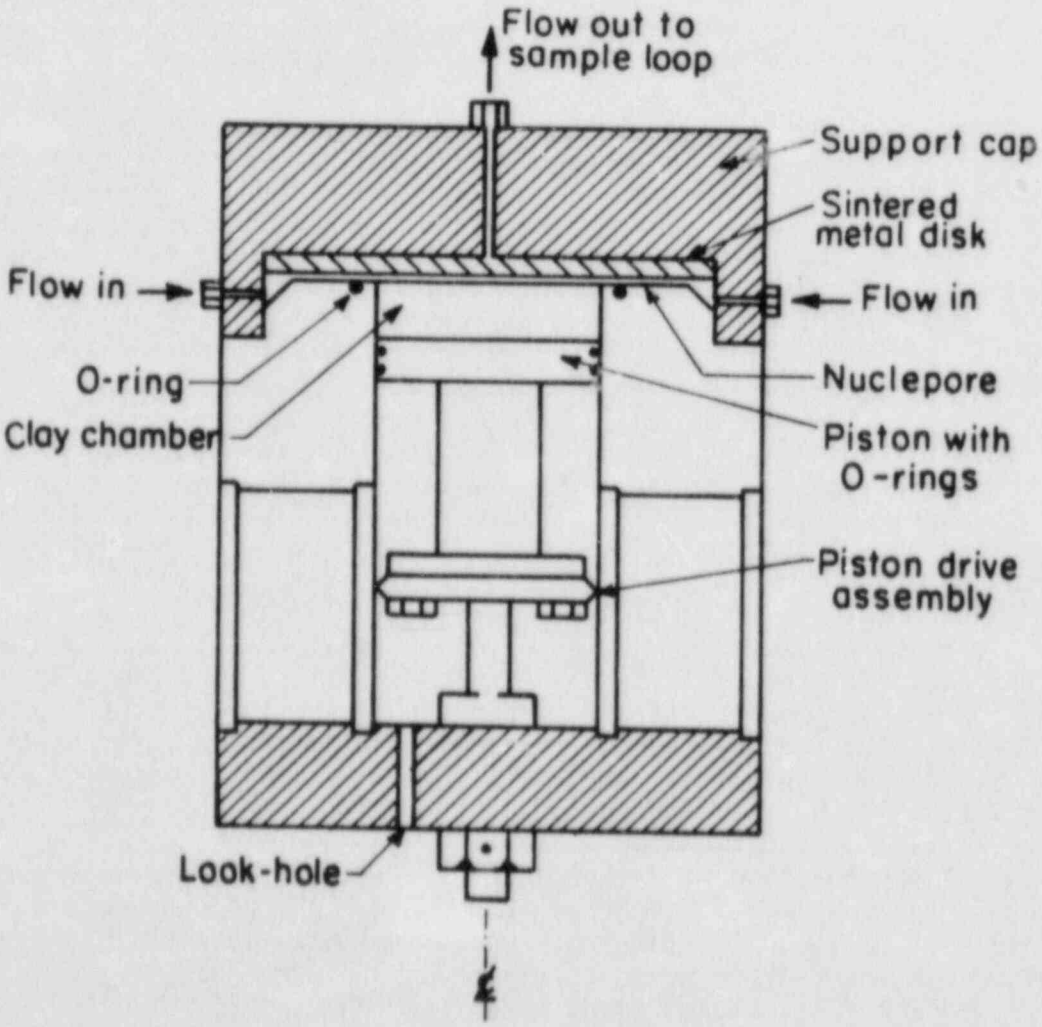

Figure 7. Schematic of the radial-flow diffusion cell. Not shown is the flow loop consisting of the pump and the solute sampling chamber.

its axis [36]. Next, the prewetted Nuclepore membrane (0.08-μm pore size) and sintered metal disk are placed on top of the gel, the entire apparatus assembled, and the drive piston tightened to the desired degree. Approximately 800 cm^3 of the corresponding aqueous solution is added to the wet-N_2-blanketed solute chamber and flow lines. The aqueous solution is then circulated to remove air bubbles before connection with the sintered metal disk. Finally, the solute chamber is spiked with a known amount of the ion under study and the diffusion experiment is started.

Intermittant samples are withdrawn from the solute chamber and are analyzed by AAS, as described above. This determines the ion-depletion history. At the completion of a run, the flow rate through the sintered metal disk is measured, as are the volumes of solution within the solute chamber and the flow lines. The cell is disassembled, and the gel is extruded and serially sectioned for determination of the profile of the diffusing ion.

Each gel segment is weighed and is immersed in 1M KCl for about two days to desorb the diffusing species. As shown in Figure 8, this procedure removes close to 100% of adsorbed cesium from montmorillonite for loadings above about 1 mequiv/100g. Below this number complete cesium desorption does not occur. At 0.1 mequiv/100g of loading about 90% is removed, or 10% is irreversibly adsorbed. Others have reported similar observations of irreversible adsorption on montmorillonite at small loadings [25].

With calibration curves like that in Figure 8, measurement of the desorbed ion concentrations (by AAS) gives a combined ion void concentration and adsorption profile in the clay gel. After the desorption treatment the clay is dried and the axial, weight-fraction profile is determined.

As a check on the internal consistency of the ion depletion and profile data from the diffusion cell we verify that the mass which leaves the solute chamber is equal to that accumulated in the gel. Agreement is always within several percent, about the estimated experimental error. An entire experiment with subsequent desorption and analysis lasts a little over a week.

3.1.3.3 Theoretical Interpretation

Validation of the homogenous, porous-medium model, Eqn. (1), or of any other proposed sorptive-diffusion model for compacted backfill, with data from the radial-flow diffusion cell requires a mathematical analysis coupling gel diffusion with ion depletion from the solute chamber. Unsteady species material balances must be written for the solute chamber and for the Nuclepore membrane in addition to Eqn. (1) for the gel.

Since the mass-transfer resistance within the sintered metal disk is negligible, diffusion through the Nuclepore membrane controls the ion flux out of the well-stirred solute tank. If V is the volume of that tank and c_1 is the transient ion concentration, then

$$V \frac{dc_1}{dt} = A \varepsilon_m D_m \frac{\partial c_m}{\partial x} \quad (t, -\delta_m) , \qquad (14)$$

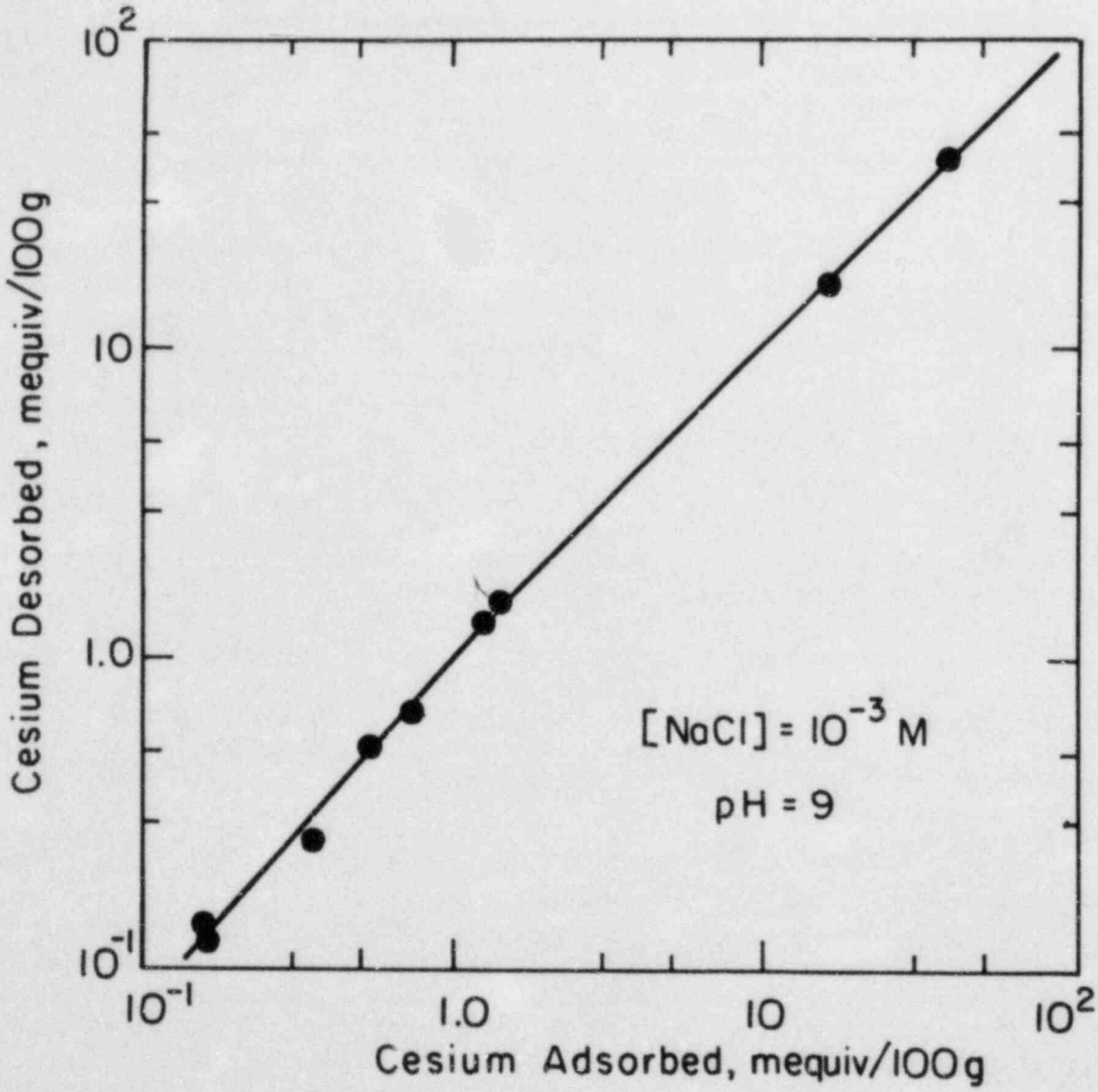

Figure 8. The amount of cesium desorbed from bentonite by 1 M KCl as a function of adsorption loading.

where A is the cross-sectional area of the clay chamber, and ε_m, D_m, and c_m are, respectively, the porosity, diffusivity, and the ion concentration in the membrane whose thickness is δ_m. x is the axial coordinate measured relative to the clay surface.

To an excellent approximation diffusion through membrane is at a pseudo-steady-state:

$$\frac{\partial^2 c_m}{\partial x^2} = 0 \tag{15}$$

Finally, Eqn. (1), or another appropriate model, is written for the gel.

Eqns. (1), (14), and (15) are coupled through several initial and boundary conditions. These are:

$$c_1(0) = c_1^o \ , \tag{16a}$$

$$c_m(t,-\delta_m) = c_1(t) \ , \tag{16b}$$

$$c(t,0) = c_m(t,0) \ , \tag{16c}$$

$$\varepsilon_m D_m \frac{\partial c_m}{\partial x} (t, 0) = \varepsilon D \frac{\partial c}{\partial x} (t,0) \tag{16d}$$

$$c(0,x) = 0 \ , \tag{16e}$$

and

$$c(t,\infty) = \frac{\partial c}{\partial x} (t,\infty) = 0 \tag{16f}$$

In Eqn. (16a) c_1^o is the initial ion concentration in the solute chamber. Care must be taken that enough backfill is placed in the diffusion cell so that during the time frame of an experiment the diffusing ion does not reach the drive piston. Otherwise the semi-infinite boundary condition, Eqn. (16f) does not apply.

Eqns. (1) and (14) through (16) are solved by numerical inversion of Laplace transforms according to the procedure of Stehfest [37]. The values of D and K in Eqn. (1) are evaluated from the experimental ion-depletion and profile data and examined for their physical significance.

An important advantage of having data from both ion-depletion transients and profiles is that the roles of D and K can be ascertained separately. For the transient ion-depletion curves only the product $D[1 + (1-\varepsilon)K/\varepsilon]$ enters the expressions. However, for the ion profiles the ratio $D/[1+ (1-\varepsilon)K/\varepsilon]$ also enters.

The combination of factors $\delta_m/(\varepsilon_m D_m)$ constitutes the external mass-transfer resistance. It is evaluated from the initial-time depletion data (as noted previously [34], and is small enough not to be of importance. All other quantities can be independently measured (e.g., V and A).

3.1.3.4 Results and Discussion

Figure 9 displays the depletion data for cesium with $c_i^o = 10^{-4}$ M diffusing in a 22 w/o bentonite gel saturated by a 10^{-2} M NaCl, pH = 10 background electrolyte. According to Figure 3, the cesium exchange isotherm is linear for the chosen initial concentration. A dashed line in Figure 9 represents the homogenous, porous-medium-model prediction (i.e., Eqn. (1)) using the bulk cesium chloride diffusion coefficient, $D \sim 10^{-5}$ cm^2/s, and the measured K_d value from Figure 3 of $K = \rho_s K_d = 1300$. Clearly, when applied in this manner, the homogenous, porous-medium model greatly underestimates the amount of cesium uptake into the gel.

Figure 10 shows the cesium profile in the 22 w/o gel corresponding to Figure 9 after 3 days of contact. The listed bar heights indicate to the total average cesium concentration in each serial section, including cesium in the pore fluid and that absorbed on the montmorillonite. Accordingly, the ordinate in Figure 9 reflects both contributions to the total concentration. Again, dashed lines correspond to the homogenous porous-medium-model prediction using measured values of D and K. Agreement between theory and data is poor.

Figures 11 and 12 give the corresponding cesium depletion and profile measurements in 10^{-2} M NaCl and pH = 10 electrolyte, but now for a 44 w/o backfill consisting of 75 w/o Ottawa sand and 25 w/o bentonite. Essentially the same behavior is observed as in Figures 9 and 10, indicating that quartz has little effect on cation migration rates. Again, the predictions of Eqn. (1), using the measured diffusion coefficient and ion exchange constant, are very poor, as demonstrated by the dashed lines.

Notice in Figures 10 and 12 that the measured cesium penetration into the gel is significantly larger than that predicted. Thus, the beneficial performance of a backfill may be severely overestimated if the homogeneous, porous-medium model is used for design calculations.

The small amount of irreversible cesium adsorption, seen in Figure 8 at low uptake, cannot explain the enhanced cesium transport rate in the gel. Likewise, any sorption kinetic effects must be discounted because they would inhibit migration rates.

As an alternative, we propose that the specifically bound cations in the inner Helmholtz plane have discernable mobility. There are now two parallel paths for ion diffusion in the gel: through pores between the clay particles and along the particle surfaces. Transport along surfaces is known as surface diffusion. It is a relatively common explanation for increased transport rates in liquid-filled, high-surface-area porous media [38,39,40].

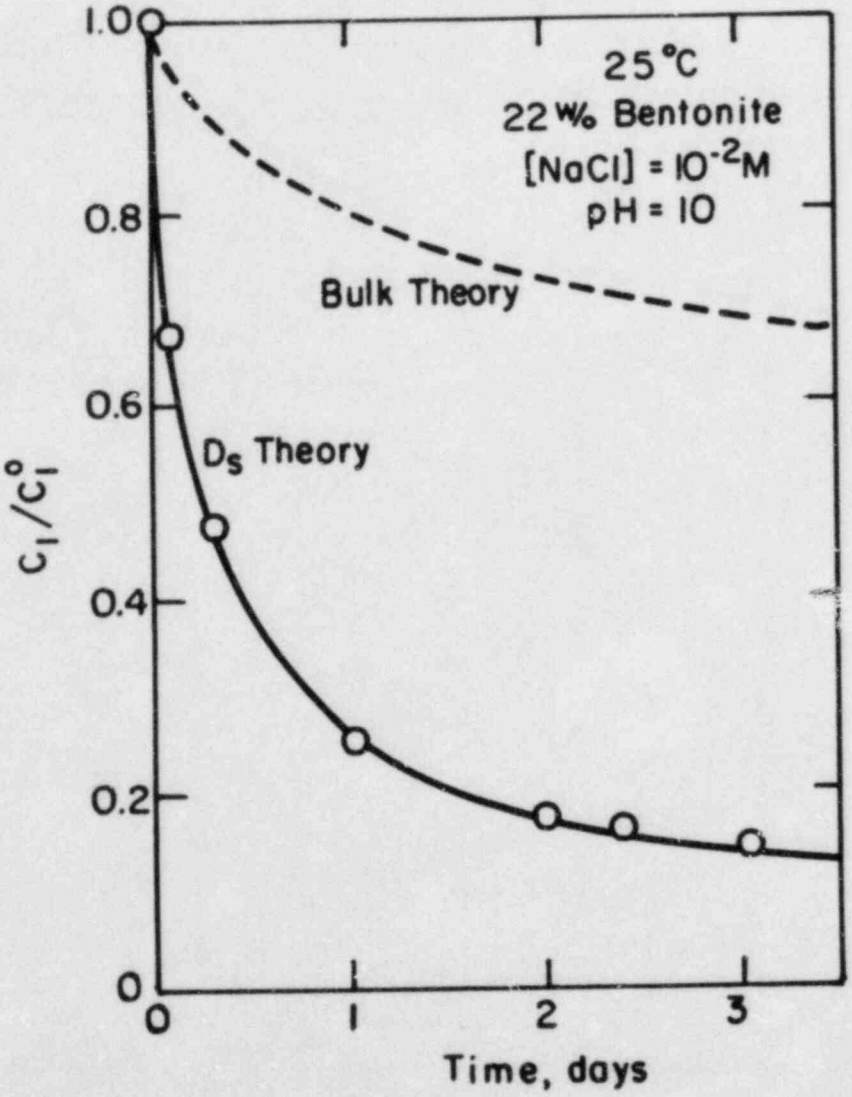

Figure 9. Cesium depletion from the solute chamber into a 22 w/o bentonite backfill. The initial cesion concentration in the chamber is $c_i^o = 10^{-4}$ M.

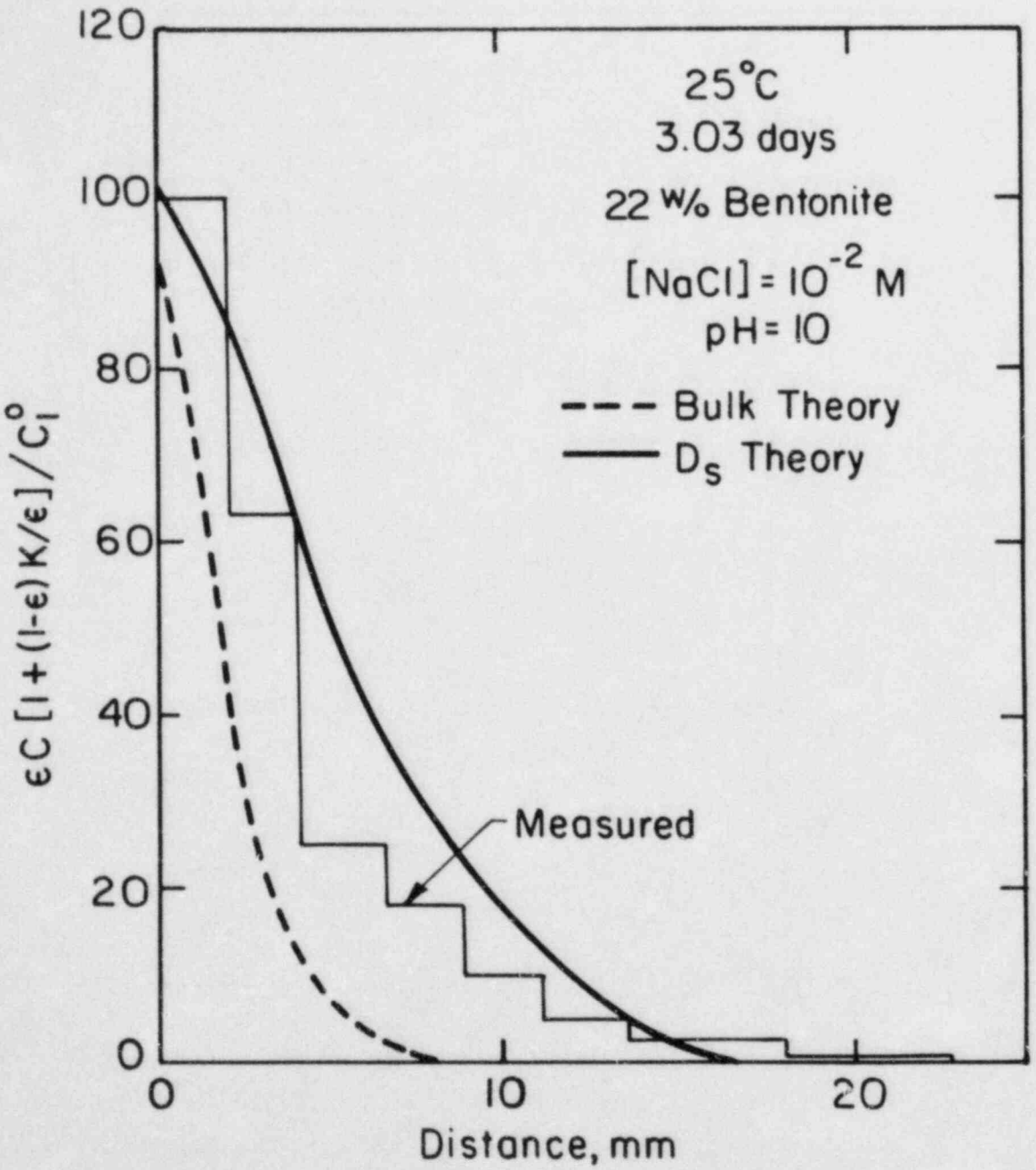

Figure 10. Cesium profile in a 22 w/o bentonite backfill after a 3-day contact time.

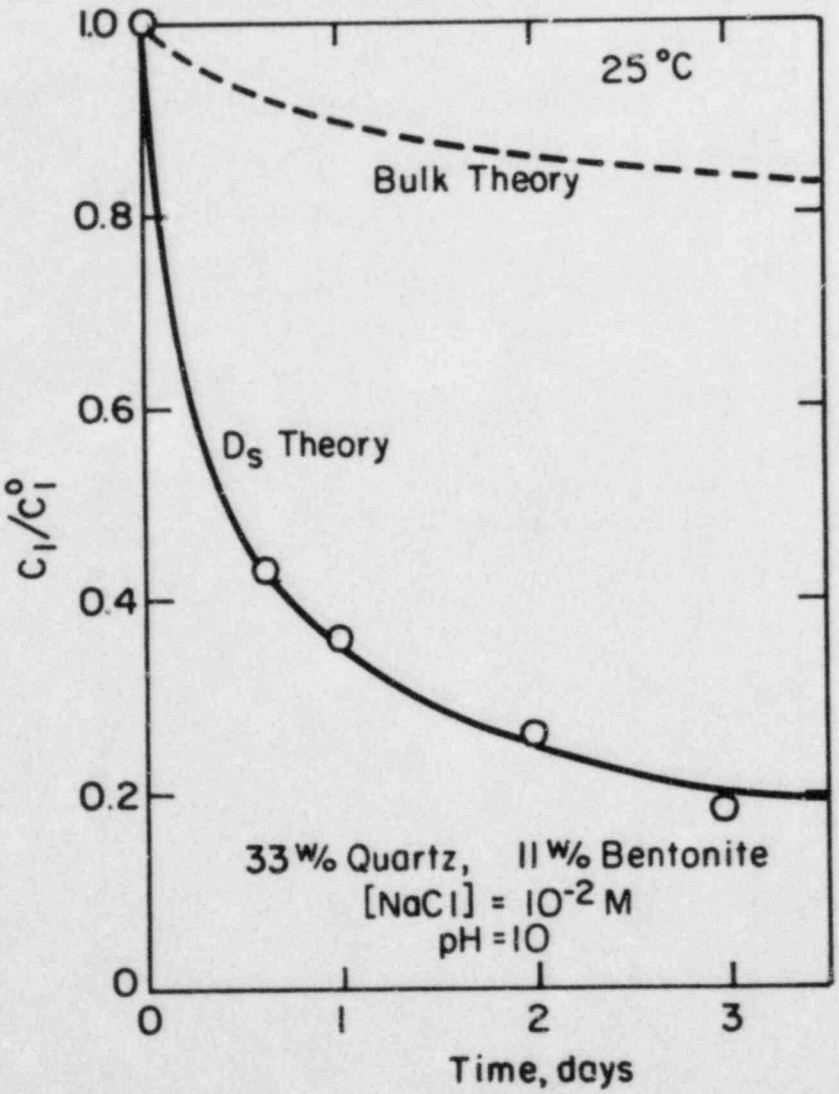

Figure 11. Cesium depletion from the solute chamber in a 33 w/o quartz and 11 w/o bentonite backfill. The initial cesium concentration in the chamber is $c_i^o = 10^{-4}$ M.

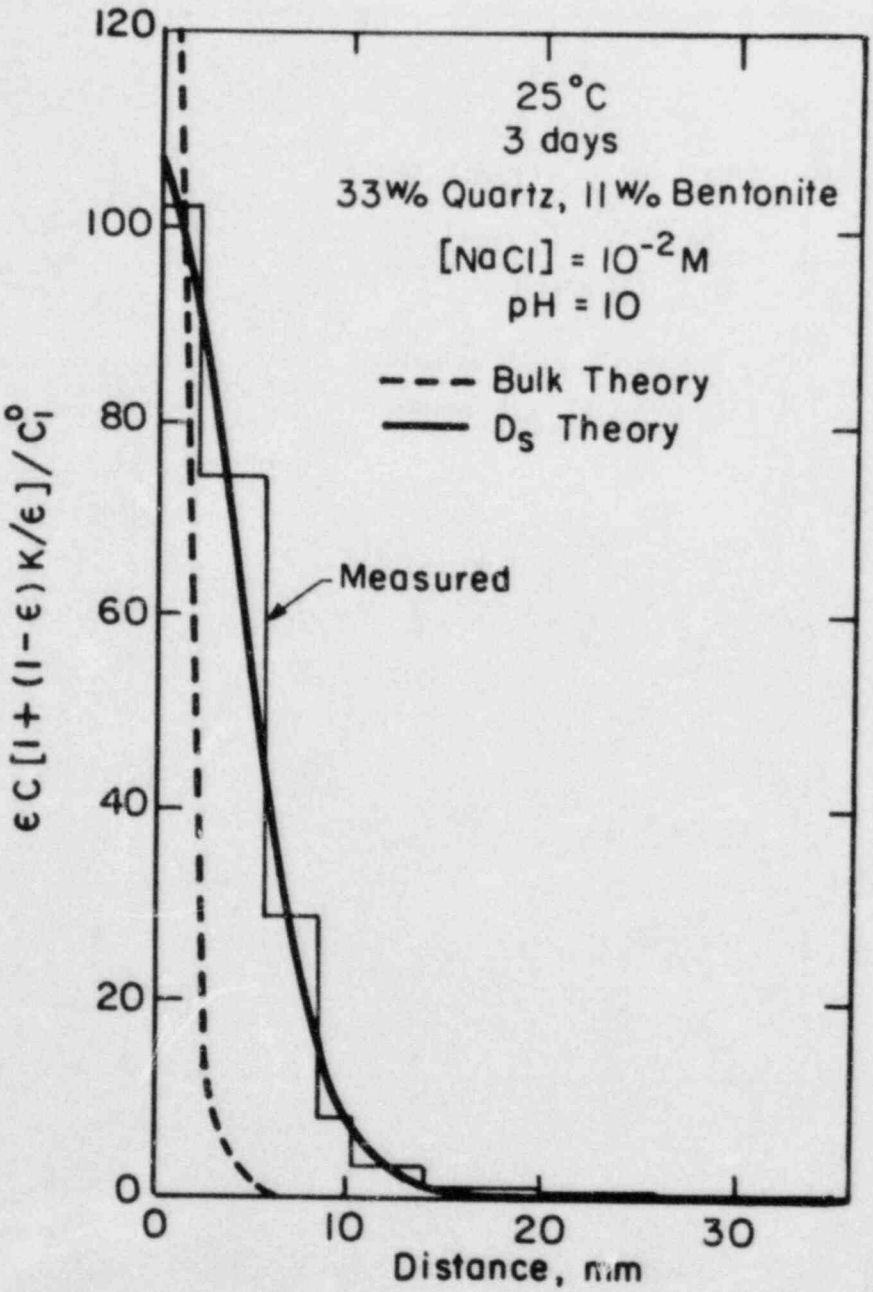

Figure 12. Cesium profile in a 33 w/o quartz and 11 w/o bentonite backfill after a 3-day contact time.

The accepted constitutive relation for surface transport is that ion flux is proportional to the negative gradient of adsorption; the constant of proportionality is the surface diffusion coefficient. If local equilibrium prevails and if the exchange isotherm is linear, then Eqn. (1) may readily be modified to account for surface transport [38,39,40]:

$$[1 + (\frac{1-\varepsilon}{\varepsilon})K] \frac{\partial c}{\partial t} = D [1 (\frac{1-\varepsilon}{\varepsilon})(\frac{D_s}{D})K] \frac{\partial 2c}{\partial x^2} , \qquad (17)$$

where D_s, which has units of cm^2/s, is the surface diffusion coefficient. When $D_s = 0$, or the specifically adsorbed ions are immobile, then Eqn. (17) reduces to Eqn. (1). Otherwise the effective diffusion coefficient, which controls transport in the gel, $D [1 + (\frac{1-\varepsilon}{\varepsilon})(\frac{D_s}{D})K]$, is enhanced.

Solid lines in Figures 9 through 12 give the best fit of the surface-diffusion model, using a value of 10^{-5} cm^2/s for D. The resulting parameters are displayed in Table 1. Although agreement between theory and experiment is much better, two parameters have been fit: D_s and K. Dashed lines in these figures are 'a priori' predictions with Eqn. (1).

Most distressing is the observation that K varies widely from the measured value of 1300. Also D_s and K are quite different for each experiment. Nevertheless, appeal to a surface-diffusion mechanism appears real. Otherwise, diffusion coefficients emerge which are greater than those in pure water. This effect was also noted by Torstenfelt et al. [20,21], although they did not attempt an explanation.

3.1.4 Conclusions

A unique, radial-flow diffusion cell has been designed to measure migration rates of radionuclides in compacted backfill under realistic conditions. The apparatus permits both ion-depletion and ion-profile determinations, and, therefore, can separate the effects of sorption retardation and effective diffusion coefficients. This is very important when validating proposed transport models.

Based on experiments performed to date, we find that the simple, homogeneous porous-medium model is inadequate for cesium chloride in a dilute background electrolyte of NaCl. Apparently, ions specifically adsorbed on the montmorillonite surface provide an additional diffusion flux through the gel.

A new electrostatic, site-binding model has been developed for ion exchange on montmorillonite. Applicaton of the theory is successful for cesium/sodium exchange over a wide range of loading and concentration. Extension of the site-binding theory to compacted clay gels shows little effect on K_d values for strongly adsorbing cations, but a dramatic Donnan exclusion of solution anions.

3.1.5 Nomenclature

A = cross-sectional area of diffusion cell, m^2.
c = diffusing ion concentration, mol/dm^3.
D = effective diffusion coefficient in backfill, m^2/s.
D_m = effective diffusion coefficient in membrane, m^2/s.
D_s = surface diffusion coefficient, m^2/s.
F = Faraday's constant, C/equiv.
h = half-thickness between clay platelets, m.
K_{Cs} = equilibrium constant in Eqn. (4), dm^3/mol.
K_{Na} = equilibrium constant in Eqn. (5), dm^3/mol.
K_d = diffusing-ion, zero-concentration slope of exchange isotherm, cm^3/g.
K = $p_s K_d$.
n = ion adsorption, mol/g.
R = ideal gas constant, J/(mol·K).
S^- = charged adsorption site on montmorillonite.
t = time, s.
T = temperature, K.
U = superficial velocity, m/s.
V = solute chamber volume, m^3.
x = distance, m.

Greek Symbols

δ = half distance from outer Helmholtz plate to midway between particles, m.
δ_m = membrane thickness, m.
ε = porosity.
$\bar{\varepsilon}$ = permittivity of water, C/(V·m).
λ = $\sqrt{\bar{\varepsilon}RT/[2F^2([Na^+] + [C_s^+])]}$, Debye length, m.
ρ_s = montmorillonite density, 2.5 g/cm^3.
σ = surface charge density, C/m^2.
Σ = specific surface area of montmorillonite, $800 m^2/g$.
ϕ = electrostatic potential, V.

Subscripts

d = outer Helmholtz plane and start of diffuse region.

m = membrane.

$_o$ = particle surface.

$_\partial$ = inner Helmholtz plane

$_l$ = solute chamber

Superscript

^{o} = initial.

3.1.6 References

1. Safe Handling and Storage of High-Level Radioactive Waste, a Condensed Version of the Proposals of the Swedish KBS-Project Stockholm, Sweden (1979).

2. Multibarrier Approach to Nuclear Waste, 1979, Chem. and Eng. News, p. 26, July 30.

3. Geologic Disposal of Nuclear Waste: Salt's Lead is Challenged, Science, 204 (4393), 1979, p. 603, May 11.

4. New Mexicans Debate Nuclear Waste Disposal, 1979, Chem. and Eng. News, p. 20, January 1.

5. Hunter, T. O., 1979, "Technical Issues of Nuclear Waste Isolation in WIPP." Sand 79-1117C.

6. Nuclear Waste Disposal: 1979, Alternatives to Solidification in Glass Proposed, 1979, Science, 204 (4390), p. 2389, April 20.

7. Landstgrom, O., Klockars, C. E., Holmberg, K. E., and Westerberg, S., 1978, "In-Situ Experiments on Nuclide Migration in Fractured Crystalling Rocks," OECD Nuclear Energy Agency, Sweden.

8. Silva, R. J., Benson, L. V., and Yee, A. W., 1979, "Theoretical and Experimental Evaluation of Waste Transport in Selected Rocks," LBL-9945, ONWI-45901AK, 1979.

9. LeBell, J. C., 1978, "Colloid Chemical Aspects of the Confined Bentonite Concept," KBS-97.

10. Neretnieks, I., 1977, "Retardation of Escaping Nuclides from a Final Depository," KBS-30.

11. Pusch, R., 1979, Highly Compacted Sodium Bentonite for Isolating Rock-Deposited Radioactive Waste Products," Nuclear Technology, 45, 153.

12. Michaels, A. S., and Lin, C. S., 1954, "Permeability of Kaolinite," Ind. and Eng. Chemistry, 46, 1239.

13. Norrish, K., 1954, "The Swelling of Montmorillonite," Disc. Faraday Soc. No. 18, 120.

14. Cebula, D. J., Thomas, R. K., Middleton, S., Ottewill, R. H., and White, J. W., 1979, "Neutron Diffraction from Clay-Water Systems," Clays and Clay Minerals, 27 39.

15. van Olphen, H., 1977, An Introduction to Clay Colloid Chemistry, Wiley-Interscience, New York.

16. Callaghan, I. C., and Ottewill, R. H., 1974, "Interparticle Forces in Montmorillonite Gels," Disc. Far. Soc., 57, p. 110.

17. Turk, J. T., 1976, "A Study of Diffusion in Clay-Water Systems by Chemical and Electrical Methods," Ph.D. Thesis, University of California, San Diego.

18. Nowak, E. J., 1983, "Diffusion of Radionuclides in Brine-Saturated Backfill Barrier Materials," Mat. Res. Soc. Symp. Proc., Vol. 15, p. 735, Elsevier.

19. Stumm, W., and Morgan, J. J., 1970, Aquatic Chemistry, Wiley-Interscience, New York.

20. Torstenfelt, B., Anderson, K., Kipatsi, H., Allard, B., and Olofsson, U., 1981, "Diffusion Measurements in Compacted Bentonite," Mat. Res. Soc. Symposium, Boston.

21. Torstenfelt, B., Kipatsi, H., Anderson, K., Allard, B., and Olofsson, U., 1982, "Transport of Actinides through a Bentonite Backfill," Mat. Res. Soc. Symposium, Berlin.

22. Helfferich, F., 1962, Ion Exchange, McGraw-Hill, New York.

23. Serne, R. J., Rai, D., and Relyea J. F., 1979, "Preliminary Results on Comparison of Adsorption-Desorption Methods and Statistical Techniques to Generate K_d Predictor Equations," U.S. DOE Report, PNL-SA-7352.

24. _____, 1983, "Site Characterization Analysis of the Site Characterization Report for BWIP," NUREG-0960, Vols. 1, 2, U.S. Nuclear Regulatory Commission, March.

25. Bladel, R. V., and Laudelat, H., 1967, "Apparent Irreversibility of Ion-Exchange Reactions in Clay Suspensions," Soil Sci. 104, 134.

26. Grim, R. E., 1968, Clay Minerology, 2nd ed., McGraw-Hill, New York.

27. Kenna, B. T., 1978, "Temperature and pH Effects on Sorption Properties of Subsea Clay," Sci. Basis for Nuclear Waste Management, ed. S.V. Topp, New York, p. 491.

28. Pommer, A. M., 1978, "Relation Between Dual Acidity and Structure of H-Montmorillonite," U.S. Geol. Survey Report, paper 386-C.

29. Kruyt, H. R., 1952, Colloid Science, Vol. 1, Irreversible Systems, Elsevier, New York.

30. Somasundaran, P., and Hanna, H. S , 1977, Physico-Chemical Aspects of Adsorption at Solid/Liquid Interfaces," in Improved Oil Recovery by Surfactant and Polymer Flooding, ed. D. O. Shah and R. S. Schechter, Academic Press, New York.

31. Davis, J. A., James, R. O., and Leckie, J. O., 1978, "Surface Ionization at the Oxide/Water Interface," J. Coll. and Int. Sci., 63(3), 480.

32. Radke, C. J., Apps, J. A., and Jahnke, F. M., 1981, "Geochemical Assessment of Nuclear Waste Isolation," NRC Fin B-3040, Quarterly Report, October 1 - December 31.

33. Jahnke, F. M., Apps, J. A., and Radke, C. J., 1982, "Geochemical Assessment of Nuclear Waste Isolation," NRC FIN 2 B-3040, Quarterly Report, January 31 - March 31.

34. Spahn, H., and Schlünder, E. V., 1975, "The Scale-Up of Activated Carbon Columns for Water Purification, Based on Results from Batch Tests," Chem. Eng. Sci., 30, 529.

35. Jahnke, F. M., Apps, J. A., and Radke, C. J., 1982, "Geochemical Assessment of Nuclear Waste Isolation," NRC FIN B-3040, Quarterly Report, October 1 - December 31.

36. Soudek, A., Jahnke, F. M., and Radke, C. J., 1983, "Geochemical Assessment of Nuclear Waste Isolation," NRC FIN B 3040, Quarterly Report, April 1 -June 30.

37. Stehfest, H., 1970, "Numerical Inversion of Laplace Transforms," Communications of ACM, 13(1), 47.

38. Neretnieks, I., 1976, "Analysis of Some Adsorption Experiments with Activated Carbon," Chem. Eng. Sci., 31, 1029.

39. Komiyama, H., and Smith, J. M., 1974, "Surface Diffusion in Liquid-Filled Pores," AIChE J., 20(6), 1110.

40. Komiyama, H., and Smith, J. M., 1974, "Intraparticle Mass Transport in Liquid-Filled Pores," AIChE J., 20(4), 728.

3.2 PHYSICAL RESPONSE OF BACKFILL MATERIALS TO MINERALOGICAL CHANGES IN A BASALT ENVIRONMENT*

Rex A. Couture and Martin G. Seitz

Argonne National Laboratory, Argonne, IL 60439

Abstract

Backfill materials surrounding waste canisters in a high-level nuclear waste repository are capable of ensuring very slow flow of groundwater past the canisters, and thereby increase the safety of the repository. However, in the design of a repository it will be necessary to allow for possible changes in the backfill. In this experimental program, changes in permeability, swelling behavior, and plastic behavior of the backfill at the temperatures, pressures, and radiation levels expected in a repository are investigated. The emphasis is on investigation of relevant phenomena and evaluation of experimental procedures for use in licensing procedures.

The permeability of a slightly compacted sand-clay mixture containing 25% bentonite, with a dry bulk density of 1.59 g/cm^3, was determined to be 0.9 x 10^{-18} m^2 in liquid water at 25°C. This is sufficiently low to demonstrate the potential effectiveness of proposed materials: for a pressure difference of 0.1 MPa across 30 cm of backfill, the projected flow rate at 200°C would be only 7 cm^3/yr per cm^2, provided that the bentonite retains its swelling properties. In practice, fractures in the host rock may form short circuits around the backfill, so an even lower flow rate is probable.

However, alteration by any of several mechanisms is expected to change the properties of the backfill. Crushed basalt plus bentonite is a leading candidate backfill for a basalt repository. Experiments show that basalt reacts with groundwater vapor or with liquid groundwater producing smectites, zeolites, silica, and other products that may be either beneficial or detrimental to the long-term performance of the backfill. Concentration of groundwater salts in the backfill by evaporation would cause immediate, but possibly reversible, reduction of the swelling ability of bentonite. Moreover, under some circumstances, gamma radiolysis of moist air in the backfill could produce up to 0.5 mole of nitric acid or ammonia per liter of pore space. The physical properties of

*Work supported by the U.S. Nuclear Regulatory Commission under Contract FIN A-2239.

altered materials may be sufficiently changed at conditions expected in the repository to substantially influence the long-term performance of backfill in a high-level waste repository.

3.2.1 Introduction

A mixture of expandable clay (e.g., bentonite) and crushed rock (e.g., basalt) has been proposed as water-retarding fill between the canister containing nuclear waste and the host rock of a repository. The use of this mixture, termed backfill in this work, seems essential for the performance of a high-level nuclear waste repository in basalt to meet licensing criteria. Also, a backfill may ensure an extra margin of safety for a tuff repository. The backfill would be one of multiple barriers required to compensate for uncertainties in predicting performance of the repository in a geologic setting.

Almost any swelling clay minerals will ensure slow flow through the repository. However, the backfill must withstand the severe environments expected in a repository and retain its essential properties. Proper repository design requires a knowledge of the response of the backfill to that environment. It is essential to explore the limitations of backfill so they can be circumvented or allowed for by design of the repository. If backfill retards flow at high temperatures, remains in place, and is stable in the repository environment, then it should function well in the repository for the time periods considered in licensing.

3.2.1.1 Issues Addressed by This Research

Within the area of concern, the unresolved general issues being addressed in this program are (1) what mineralogical changes will take place in the backfill and host rock and (2) whether the modified geologic materials have the properties of swelling behavior, permeability, and ability to seal fractures that are necessary to assure the safe disposal of nuclear waste.

The program is being performed in two parts, according to these two general issues. The first part is to identify mineralogical changes that occur in backfill at elevated temperatures (Peacor 1984). Conversion of montmorillonite in the backfill to illite, chlorite, paragonite, or mixed-layer illite-smectite under the conditions in the repository would cause a reduction in volume of the backfill or a reduction in the swelling pressure. If reduced volume leads to shrinkage cracks, the performance of the backfill may be seriously degraded.

Experiments have been run in the basalt-water and bentonite-water systems and are planned for the basalt-bentonite-water system (Peacor 1984). Because the reactions are fairly slow, state-of-the-art methods are being used to detect small changes in mineralogy that may be extensive over an extended period.

The second part of the program, described in this report, involves determination of changes in swelling pressure, permeability, and plastic behavior due to alteration. Also in this part of the program, the alteration of backfill materials by steam and by gamma radiation is investigated with regard to changes in physical properties of the backfill.

This paper is an attempt to define the important unknowns, and presents experimental data on (1) permeability of sand plus bentonite at 25°C and (2) alteration of basalt by groundwater vapor. Progress in this program and details of the experimental studies are reported elsewhere (Steindler 1983 a,b; 1984 a,b,c).

We anticipate that some of the methods and data from this work will also be applicable to the question of swelling behavior of secondary minerals in basalt, and may provide an answer to the question of whether swelling of clays can seal fractures opened by thermal or mechanical stresses.

Specific issues being addressed in the second part of this program are:

1. Can the long-term performance of backfill be accurately predicted from observations of materials treated hydrothermally in the laboratory?

2. Can processes leading to failure of backfill be identified in laboratory experiments or inferred from geologic settings?

3. How are laboratory measurements of permeability and swelling ability related to these properties as experienced in full-scale applications?

4. Will physical properties such as low permeability to water and plasticity be maintained under the elevated presures and temperatures of the repository?

5. Will growth of basalt alteration products cement the backfill or otherwise affect plastic behavior?

6. Will the ionizing radiation field expected in the proximity to waste canisters degrade the performance of backfill?

7. Is alteration in a vapor environment detrimental to the long-term performance of backfill?

3.2.1.2 Background and Objectives

Backfill Reactions

A mixture of basalt and bentonite has been chosen as the reference backfill material for a basalt repository. There are still questions as outlined below, that could cause the backfill to be less effective than freshly emplaced backfill.

The physical properties of bentonite are quite sensitive to change, depending on the composition of coexisting fluid. The key to its low permeability and ability to fill cavities is the expandability of montmorillonite, the major mineral component. However, the calcium, hydrogen, potassium, and cesium ion-exchange forms are not very expandable compared to the sodium form; partial conversion of the backfill to non-expandable forms may occur as a result of reaction with basalt. Furthermore, montmorillonite is not very expandable at high salt concentrations, and salt may be concentrated by evaporation of water from the heated regions of the repository. The expansion behavior also depends on pH, and hysteresis of expansion with wet-dry cycling has been observed (Norrish 1963).

Montmorillonite is probably unstable, although possibly not very reactive, under hydrothermal conditions in a basalt repository (Peacor 1984). Possible reaction products include illite, illite-smectite mixed-layer mineral, chlorite, albite, and paragonite. Several reviews (e.g., Soo 1983 a) have concluded from studies of natural sediments that bentonite is likely to be unstable and reactive in a repository at temperatures over approximately 100°C. However, there are few data on the reactivity of bentonite in a basalt repository environment. Wood (1983) has shown that bentonite does not alter rapidly in the presence of basalt in hydrothermal experiments, although the data suggest possible slight uptake of sodium and potassium from basalt by the bentonite, with possible alteration of the montmorillonite fraction of bentonite to less expandable phyllosilicates (Couture 1983). Data by Peacor (1984) support the slowness of reaction, and bentonite may well remain essentially unchanged in a basalt repository. However, the reaction may be limited by the rate of alteration of the basalt, and alteration of the bentonite may not be apparent in experiments until a large fraction of the basalt is altered.

Another possible problem is cementation. Observed hydrothermal reaction products of basalt include clinoptilolite, mordenite, illite or illite-smectite, and possibly silica minerals (Wood 1983). If crushed basalt is subjected

to a hydrothermal environment, it will be extensively transformed; it is possible that the backfill matrix will be cemented by secondary zeolites and silica. Formation of secondary minerals in the pores is expected to reduce permeability, but it may also cause embrittlement or reduce expandability of the bentonite. Pusch (1983) has presented evidence of poor expandability of bentonite due to natural cementation of smectite grains by silica and iron oxide. Also, we have found in the laboratory that dissolved substances can cement smectite grains on drying, so that the grains will no longer expand in water unless they are mechanically broken apart.

Other potential problems include physical removal of clay by water flow, formation of tubes or permeable zones by release of steam, and mass movement of the backfill in response to differential water pressures. The possibility of high local transient hydraulic pressures during resaturation of a repository needs to be considered. The permeability of the rock mass will not be uniform, as flow takes place mainly through fissures. The possibilities of the shifting of backfill and canisters and of the breaking of borehole seals in response to high differential water pressures needs to be carefully evaluated. This could cause partial loss of confinement of the backfill and increased permeability. In an extreme case, movement of backfill might conceivably cause settling of canisters.

Required and Attainable Permeabilities

Under ideal conditions, a swelling backfill can be highly effective at reducing flow. Measured permeabilities of candidate backfill materials are reported in Table 1 and are lower than that generally considered necessary to ensure integrity of the repository. The requirements for permeability are discussed in detail elsewhere (Anderson 1982; Steindler 1983 a) and summarized here. Only vertical flow of groundwater is considered.

On the basis of a limited number of measurements of hydraulic head (Gephart 1979; Steindler 1983 a), the maximum sustained vertical pressure difference across the backfill is assumed for this discussion to be 0.1 MPa.* This is based on the conservative assumption that the rock formation will not restrict flow of water through the repository, and allows for opening of fractures due to thermal and mechanical stresses

*However, catastrophic changes in hydrology have been postulated (Waste Isolation Systems Panel 1983) that could lead to larger pressure gradients.

Table 1. Permeability of clay and clay-sand mixtures

Material	Load (MPa)	Dry Bulk Density (g/cm^3)	Pressure Difference (MPa)	Permeability (m^2)
20% Na montmorillonite, 80% sand[a]	-	1.46	0.1 to 0.3	1×10^{-16} to 2×10^{-17}
25% Na montmorillonite, 75% sand[b]	-	2.10	3.4	7×10^{-19}
30% Na montmorillonite, 70% sand[c]	6.4	-	-	5×10^{-19}
30% Ca montmorillonite, 70% sand[c]	6.4	-	-	4×10^{-17}
30 kaolinite, 70% sand[c]	6.4	-	-	2×10^{-16}
Ca montmorillonite[c]	6.4	-	-	3×10^{-18}
Na and Ca bentonite[c]	0.1	-	-	1×10^{-16}
Na montmorillonite[d]	-	1.03	-	2×10^{-20}
Kaolinite	0.1	-	-	1×10^{-16}
	6.4	-	-	5×10^{-17}

[a]From Pusch (1979). Pusch reports a clay content of 17%, allowing for sand and silt in the bentonite.

[b]From Wheelwright (1981).

[c]From Grim (1962), p. 241.

[d]From Pusch (1980).

(Waste Isolation Systems Panel 1983). Convection will result in an additional pressure difference of less than this value (Steindler 1983 a). The pressure difference of 0.1 MPa across 30 cm of backfill with a permeability of 1×10^{-18} m^2 would give a flow rate of only 11 cm/yr of water* at 300°C, and

*That is, a column of water 11 cm high per year. The velocity of flow would be higher and would depend on the fracture volume of the rock formation.

7 cm/yr at 200°C. These flow calculations are based on the assumption that the flow rate varies inversely with the viscosity of water, but that the permeability is independent of temperature and water composition.

This calculation represents a worst case, because any fracture or fracture network that allows unrestricted flow of water to the backfill would probably also allow unrestricted flow around the backfill. Thus, a sustained pressure difference of 0.1 MPa is unlikely, and backfill with a permeability of 1×10^{-18} m^2 would be extremely effective at ensuring a low flow rate.

The same permeability has been suggested as the approximate value at which diffusion is as important a transport mechanism as flow (Anderson 1982). However, this estimate is based on an assumed pressure gradient that is much lower than that assumed here. It also includes uncertainties due to effects of temperature and other conditions.

The excellent impermeability of sodium montmorillonite results from its ability to swell in water to several times its dry volume. However, there are few data on its swelling behavior at high temperatures. Although differential thermal analysis has shown that some interlayer water is retained by sodium montmorillonite in a closed system at temperatures up to 403°C (Koster van Groos 1982), it was not determined whether, at these temperatures, montmorillonite is capable of the extreme swelling that occurs at room temperature. In addition, the combined effects of variable groundwater composition, high temperature, and alteration must be tested.

Most of the measurements in Table 1 were made at conditions far from those expected in a repository. For practical reasons, many of the measurements were made at very high pressure differences across short columns. The resulting high flow rates may lead to compaction* or redistribution of materials in the columns that would not occur at lower pressure differences and, therefore, may lead to erroneously low permeability measurements.

There are other possible experimental artifacts. Clogging of frits is an experimental phenomenon that could lead to large errors and must be evaluated. Some measurements have been made on columns that may have contained substantial amounts of air (e.g., Pusch 1979) and, as a result, may not have had representative permeabilities.

*If the pressure difference is a large fraction of the swelling pressure of the backfill, or exceeds it, compaction can result. Compaction due to flow is greatest at the outlet end of columns, resulting in inhomogeneity.

Objectives

The objectives of this research are to identify relevant processes and failure mechanisms of backfill and to establish uncertainties in the performance of backfill over the expected repository life of thousands of years considered in the licensing process. These objectives are being pursued primarily through an experimental program to identify the possible failure of backfill that would allow permeation by water and subsequent dispersal of radioelements.

Licensing decisions will be based on the contributions of the geologic setting and the backfill to the long-term isolation of nuclear waste. The methods and data from this research are also applicable to the clay minerals in the basalt host rock.

3.2.1.3 Scope of Research

The work is focused on materials that are suggested as backfill materials in programs of the Department of Energy. Results of this work are expected to be of direct use in evaluating licensing issues concerning the performance of proposed backfill.

The scope of the work includes investigation of relevant phenomena and evaluation of experimental procedures, but does not include the development of backfill or search for suitable materials. Moreover, issues such as cost, which do not relate to the safety of proposed backfill, are not addressed in this work.

3.2.2 History of Backfill Conditions

3.2.2.1 Sequence of Environmental Conditions

Assessing the performance of backfill for a commercial high-level nuclear waste repository is not a simple matter of determining the permeability, diffusion coefficients, thermal conductivity, etc., of the material at a single temperature and pressure. The history after emplacement will be complex, and there will be sequential changes in the environment. There are both physical and chemical (mineralogical) effects to be considered. The behavior of backfill materials has not been tested over the possible environmental range.

The processes to be considered include possible initial drying of the backfill before closure, alteration by steam, damage from radiation and radiolysis products, and alteration by liquid groundwater.

Depending on design, the maximum temperature could reach 300°C (Anderson 1982; Rockwell Hanford Operations 1982). During the high temperature period, there will be intense gamma radiation, probably on the order of 1 x 10^5 R/h at the canister surface.* Drying or distillation of groundwater may lead to concentration of salts.

The host rock may be dried out for several meters around the waste at the time the backfill is emplaced, depending on the length of time before emplacement, the effectiveness of cooling, and the permeability of the rock. Steam can be expected from a hydrous backfill mixture after emplacement. The steam may escape by the time of sealing; if so, the predominant gas in the repository will initially be relatively dry air.

3.2.2.2 Response to the Hydrothermal Environment

Time until Saturation with Liquid Groundwater

The time until saturation with liquid water is important because it determines, in part, (1) the maximum temperature attained in the hydrothermal system, (2) the duration of exposure to steam, (3) whether radiolysis will occur mainly in the vapor phase or the liquid phase, and (4) whether accumulation of dissolved salts is possible in or around the backfill. The time until saturation is difficult to predict because it depends mostly on the properties of the host rock. Rapid saturation will lead to a hydrothermal environment; slow saturation will lead to an environment of hot air plus water vapor during the thermal period. Hydrothermal alteration has received the most attention in the literature; however, we have shown that alteration of the backfill by vapor is also possible. Moreover, radiolysis products will be quite different in a vapor-dominated system than in a liquid-dominated system.

Unless the backfill is highly compacted, it will probably not delay the onset of saturation very much. The properties of the host rock, or possibly of the tunnel and shaft seals, will be much more important. If the rock is impermeable and tunnel and shaft seals are effective, as frequently assumed, saturation of the repository could take hundreds or thousands of years (Anderson 1982; Soo 1983 b; Wood 1981). However, if new fractures develop in the rock, or if existing fractures open in response to thermal stress or to mechanical stress

*The radiation intensity and temperature depend on design and remain to be determined (Anderson 1982; Rockwell Hanford Operations 1982). The radiation dose rate may be much lower if a shielded canister is used.

from excavation or tectonic activity (Waste Isolation Systems Panel 1983), saturation of the backfill could be rapid, requiring as little as a few months.*

The water pressure at a 1000-m depth is about 10 MPa, which is sufficient to rapidly saturate any clay barrier. Filling of fractures in the basalt by swelling of bentonite in the backfill and self-injection into cracks will do little to delay the onset of saturation. The highest degree of swelling of clay occurs only in the presence of liquid water, or possibly at relative humidities of very nearly 100%.† Unless the backfill is highly compacted, a high swelling pressure is likely only after most of the backfill is already wet.

Hydrothermal Alteration by Groundwater Vapor

The duration of exposure to groundwater vapor could be years. Recent experiments (Bates 1982) have demonstrated the corrosive power of steam on silicates. If substantial alteration of backfill by vapor occurs, the alteration products may be mineralogically or physically quite different from the hydrothermal alteration products. It is conceivable that vapor could cement the backfill before it expands, thereby preventing proper expansion. Natural cementation of bentonite is known to inhibit swelling in some instances (Pusch 1983). In view of the possible consequences, which include serious failure of the backfill, an investigation has been started on alteration of backfill materials by vapor.

Hydrothermal Alteration by Liquid Groundwater

Illite, mixed-layer illite/smectite, and paragonite are potential hydrothermal reaction products of bentonite. Some of the Grande Ronde basalts have high concentrations of

*In contrast, the regional hydrologic gradient and flow through the interbeds has been used to estimate a resaturation time of about 3000 yr (Anderson 1982). However, this calculation is apparently based on the assumption of a normal flow rate through the interbeds into the repository, and apparently does not take into account an increased flow rate due to filling of a void. Indeed, the filling of a repository is analogous to the filling of a well.

†Our experiments have shown that a macroscopically visible, high degree of swelling does not occur in steam at relative humidities of <97% at 260°C or lower (Steindler 1983 b), although differential thermal analysis in a pressurized system shows that smectites can retain some interlayer water at temperatures up to 403°C, about 40°C above the boiling point of water (Koster van Groos 1982).

potassium-rich glass (Table 2), which could cause partial conversion of smectite to illite provided the potassium is not taken up by alteration products.* Formation of illite or paragonite from montmorillonite would cause a reduction in volume of the backfill, or at least a reduction in the expected swelling pressure. If this causes development of shrinkage cracks, the performance of the backfill would likely be seriously degraded.

Table 2. Analyses of two immiscible glasses in Umtanum basalt[a]

Constituent	Matrix Glass (wt %)	Globule (wt %)
SiO_2	65.6	30.0
TiO_2	0.9	6.8
Al_2O_3	17.2	1.0
FeO[b]	3.1	43.1
MnO	N.D.[c]	0.4
MgO	Trace	1.0
CaO	3.7	11.0
Na_2O	4.4	N.D.
K_2O	5.1	Trace
P_2O_5	N.D.	5.7
SO_2	N.D.	1.0
Cl	N.D.	Trace

[a]From Peacor (1984).
[b]Total iron as FeO.
[c]Not detected.

*Illite has been observed as a hydrothermal alteration product of basalt at 300°C (Wood 1983). Conversion of smectite to illite was not detected during hydrothermal reaction of basalt-smectite mixtures (Wood 1983). However, partial conversion may be difficult to observe in a complex mixture. Furthermore, solution analyses from bentonite, basalt, and bentonite-basalt-groundwater systems suggest possible uptake of potassium and sodium from the basalt by the bentonite; paragonite was also observed as a possible product.

Crushed basalt in backfill, especially basalt that contains a glassy mesostasis, is highly susceptible to hydrothermal alteration. Formation of zeolites and silica is probable, with cementation a possible outcome. Cementation may be quite beneficial, adding strength to the backfill and reducing permeability; however, it may also cause brittleness and the loss of the ability of the backfill to heal cracks and to extrude and seal cracks. Formation of permanent cracks in the backfill could constitute a serious failure. Furthermore, alteration by steam of a granular backfill may prevent proper expansion and sealing. Pusch (1983) has shown that natural cementation of smectite grains can limit expandability. These possibilities are being examined in hydrothermal experiments at Argonne National Laboratory and the University of Michigan.

Alteration of backfill in a high thermal gradient has received little attention. A gradient of 100°C across 30 cm has been estimated for a repository (Altenhofen 1981), although the gradient will probably be lower in a wet system. Because the dissolved silica concentration in the backfill-water system depends greatly on temperature, it follows that there may be substantial mass transport in the backfill. Also, thermal diffusion (the Soret effect) has been shown to increase the effect of diffusional flux of most dissolved ions (Thornton 1983). Diffusion in a thermal gradient is not further discussed here, but one possible effect would be destabilization of montmorillonite in response to removal of silica.

3.2.2.3 Concentration of Groundwater Salts

During the saturation process, drying or distillation of groundwater may lead to substantial concentration of dissolved salts. Assume, for example, that groundwater flows toward the canisters through fractures adjacent to the backfill. If there is an escape pathway for steam (e.g., if borehole seals are imperfect) water will be distilled into cooler parts of the repository, leaving dissolved salts behind. The salts may eventually be washed into pore spaces in the backfill.

There are two potential problems due to salts in the backfill. The resulting increase in fluoride concentration may increase rates of hydrothermal alteration. In addition, bentonite is quite sensitive to dissolved salts and is much less expandable at high dissolved salt concentrations than at low concentrations. For example, assuming a dissolved sodium concentration of 0.015 M, and assuming a dry porosity of 35%, if a volume of groundwater equal to 5.8 times the volume of backfill is concentrated in the pore volume of the backfill, the resulting sodium concentration in the pore volume would be 0.25 M. We are not aware of any hydrothermal

data on the behavior of montmorillonite in such a system, but at room temperature this concentration would decrease the basal spacing from 115 Å to 19 Å (Brown 1961, p. 174). The increased permeability of bentonite in salt solutions is well known.

3.2.2.4 Radiolysis in the Gas Phase

During part of the repository history, the backfill and canister will likely be exposed to steam and air. Radiolysis of air efficiently produces oxides of nitrogen. In the presence of liquid water, nitric acid is formed; in the presence of water vapor and bases, nitrates are formed. At some time the oxygen may be entirely consumed by reaction with basalt. Nitric acid can also be produced from nitrogen and water in the absence of oxygen (Wright 1955). In this case, small amounts of ammonium ion and, presumably, hydrogen gas are also produced (Wright 1955). Ammonia may also be produced by reaction of nitric acid with basalt. The effects of nitric acid and ammonia on the backfill must be considered.

The possible production of nitric acid in a repository has been considered in detail (Steindler 1984 a). Experiments to determine the reactions of bentonite and basalt in a radiation field are nearly complete and show a yield of ∿2 atoms of oxidized nitrogen per 100 eV of adsorbed radiation at 200°C. Assuming an adequate supply of nitrogen and water vapor in a gas-filled repository, we have estimated the production of nitric acid to be 0.5 mole per liter of pore space, at a dose rate of 2×10^5 R/h, over the lifetime (∿30-yr half-life) of the gamma emitters. For backfill with 25% bentonite and 30% porosity, this is equivalent to about 40% of the cation exchange capacity. In a tightly sealed system, the maximum possible amount of acid generated would be about 0.05 mole per liter of pore space. However, we assume that gas will be free to diffuse into the backfill from adjacent rooms, through imperfect seals. We expect that, in the absence of liquid groundwater, NO_2 and NO will diffuse throughout the repository and possibly escape altogether. However, it is also possible that the gases will react with clay in the backfill. Montmorillonite has an extremely high surface area, and hydrolysis of NO_2 by interlayer water would acidify the clay. In a mixed vapor-liquid system, nitric acid would dissolve in liquid water. The alkalinity of ordinary nonflowing basaltic groundwater would be nearly two orders of magnitude too low to neutralize the estimated amount of acid. The presence of an appreciable amount of nitric acid may have a considerable effect on the hydrothermal alteration of backfill. The hydrogen-ion form of montmorillonite is known to be unstable at room temperature and not very expandable (Brown 1961). The effects of acid on the alteration of backfill materials at high temperature are untested.

Nitric acid is probably unstable in the presence of basalt; in the presence of water, part or all of it may be converted to ammonia. Alternatively, ammonia may form instead of nitric acid. Reaction with ferric iron in basalt to form ammonia would proceed according to the reaction,

$$8FeO + HNO_3 + 2H_2O = NH_4OH + 4Fe_2O_3$$

The NH_4^+ ion is also a potential problem because it behaves geochemically like K^+. Substitution of NH_4^+ for Na^+ in montmorillonite could lead to loss of expandability of the clay, by a process analogous to formation of illite.

3.2.3 Methods

In this section we describe laboratory methods for determining swelling behavior and permeability of backfill materials. The methods are being used to measure the properties of fresh materials over a wide range of possible repository conditions and to determine the properties of altered materials. The measurements are designed to be directly applicable to repository environments.

Figure 1 shows a simplified schematic of the equipment used for permeability measurements. Groundwater is pumped under pressure through a column of backfill, and the volume of water flowing from the column is determined by a graduated tube or capillary. A back-pressure regulator valve maintains pressure in the column, so that equipment can be used at high temperatures. Leak-free performance of the fittings is essential for reliable measurement, especially above 100°C. The static metal-to-metal seals are effective and less susceptible to leaks due to contamination by particles than are dynamic seals. They can also be inspected readily for evidence of leaks, even after use above 100°C. The equipment differs from most in that the flow rate into the column is measured and recorded continuously. Measuring the flow rate into and out of the column offers a means for independent testing for leaks. Hydration of long columns can also be studied without waiting for breakthrough of the water. By reversing flow through the column, it is possible to test for clogging of the outlet frit or clogging of the column itself due to flow. The equipment is very sensitive at low flow rates; by thermostating the system, flow rates as low as 0.1 μL/min have been measured at 25°C. This equipment was used for the measurements presented in this paper, except that the back-pressure regulator valve and the differential pressure transducer were eliminated for measurements at 25°C.

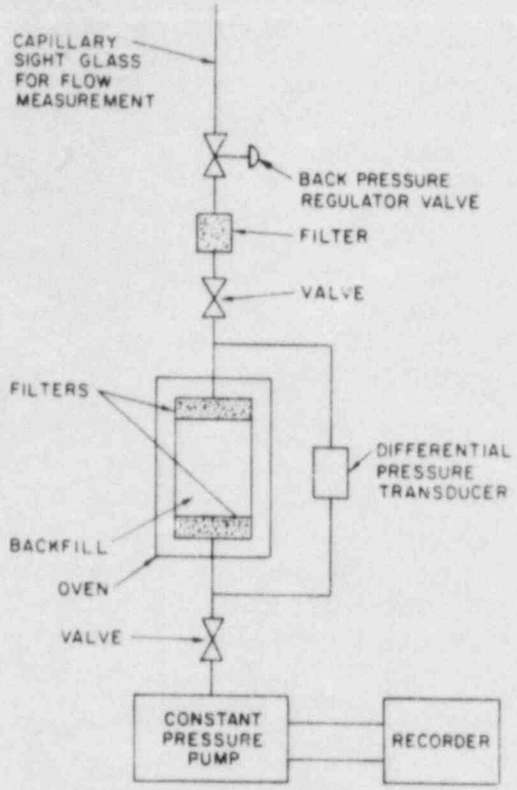

Fig. 1.

Diagram of the apparatus used to measure permeability of backfill materials. Flow rate and pressure are continuously recorded.

Soo (1983 b) has shown our proposed equipment for measuring swelling pressure at elevated temperatures. In addition, swelling behavior at room temperature is being determined by microscopic methods and by X-ray diffraction, which are very useful for studying small samples of hydrothermal run products and of naturally occurring alteration products.

3.2.4 Results

3.2.4.1 Permeability Measurements

The experiments reported here were designed to determine the permeability of backfill materials at realistic degrees of compaction and at flow rates and temperatures approaching those expected in a repository to determine the effect of flow (or pressure) on permeability, and to test some of the equipment to be used in later measurements.

Two columns, labeled A and B, were prepared with 25% bentonite (Envirogel, Wyo-Ben, Inc., 200 mesh) and 75% crushed, sieved sand packed in stainless steel tubes. Presumably, crushed basalt, with a wider range of grain sizes, plus bentonite will give lower permeabilities than measured here. The bentonite is a typical Wyoming bentonite, consisting mostly of montmorillonite (Peacor 1984), with a trace of illite or mica, and about 10% sand and silt. An analysis of

the montmorillonite, presented in Table 3, hows that it is a typical sodium montmorillonite. It is capable of swelling to many times its dry volume in water.

Column A was prepared using sand crushed to 80-140 mesh size (105-180 µm). The dimensions of the column were 1.89 cm in diameter x 7.00 cm long, and the dry bulk density was 1.59 g/cm^3. Column B was prepared using sand with 20-80 mesh size (180-840 µm). The dimensions were 1.89 cm in diameter x 6.85 cm long, and the dry bulk density was 1.72 g/cm^3. Fritted stainless steel discs with 2-µm nominal pore size were used, and the column was connected to a capillary tubing with commercial high-pressure, low-dead-volume fittings. The flow rate into the column was recorded continuously; the flow rate out of the column was measured with glass capillaries.

Table 3. Energy-dispersive X-ray analysis of montmorillonite from Envirogel 200 bentonite. The unpurified bentonite also contains 0.21% CO_2.

Constituent	Weight (%)
Na_2O	3.3
K_2O	0.13
CaO	0.70
MgO	4.0
Fe_2O_3[a]	3.2
Al_2O_3	20.5
SiO_2	68.1
Total[b]	100

Calculated formula:[c]

$Na_{0.38}Ca_{0.04}K_{0.01}Mg_{0.35}Al_{1.43}Fe(III)_{0.14}Si_{4.02}O_{10}(OH)_2 \cdot xH_2O$

[a]Oxidation state assumed.
[b]Adjusted to 100% for anhydrous compound.
[c]Calculated for 11 oxygens + 1 H_2O.

Figure 2 shows the hydraulic impedances of the two columns at 25°C during the saturation period, plotted as a function of total water in the columns. (The impedance is defined here as the hydraulic pressure divided by the flow rate, and is an inverse function of permeability.) The impedances of the columns increased as the columns filled, and it appears that the initial increase of each was linear.

An equivalent permeability can be calculated by dividing the column into a hypothetical dry portion and a water-saturated portion, and calculating the equivalent pressure gradient from the length of the water-saturated portion. At any point on the curves in Fig. 2, the permeability is proportional to the abcissa divided by the ordinate. On the assumption that the permeability does not decrease with time, the equivalent permeability establishes an upper limit for the permeability of the backfill material. The initial linear portions of the curves give equivalent permeabilities of 8×10^{-18} m^2 and 3×10^{-18} m^2 for columns A and B, respectively, which are, in fact, the highest permeabilities measured on those columns. These permeabilities are very low and are quite close to the value of 1×10^{-18} m^2 used in the flow calculations discussed in the introduction.

When water emerged from the outlet of column A, the flow rate was measured. The flow was then reversed and cycled through monotonically increasing rates followed by a reduced rate. The flow rates and permeabilities are shown in Fig. 3.

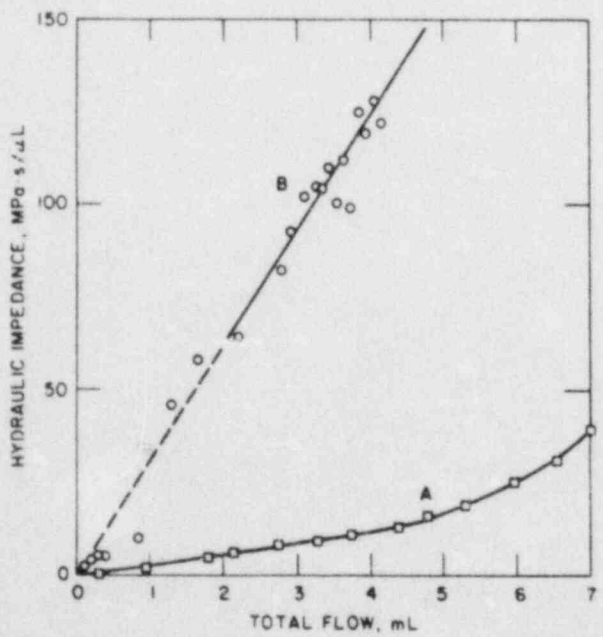

Fig. 2.

Hydraulic impedance at 25°C versus total flow into two colums containing 75% sand, 25% bentonite. Dry bulk densities: (A) 1.59 g/cm^3; (B) 1.72 g/cm^3.

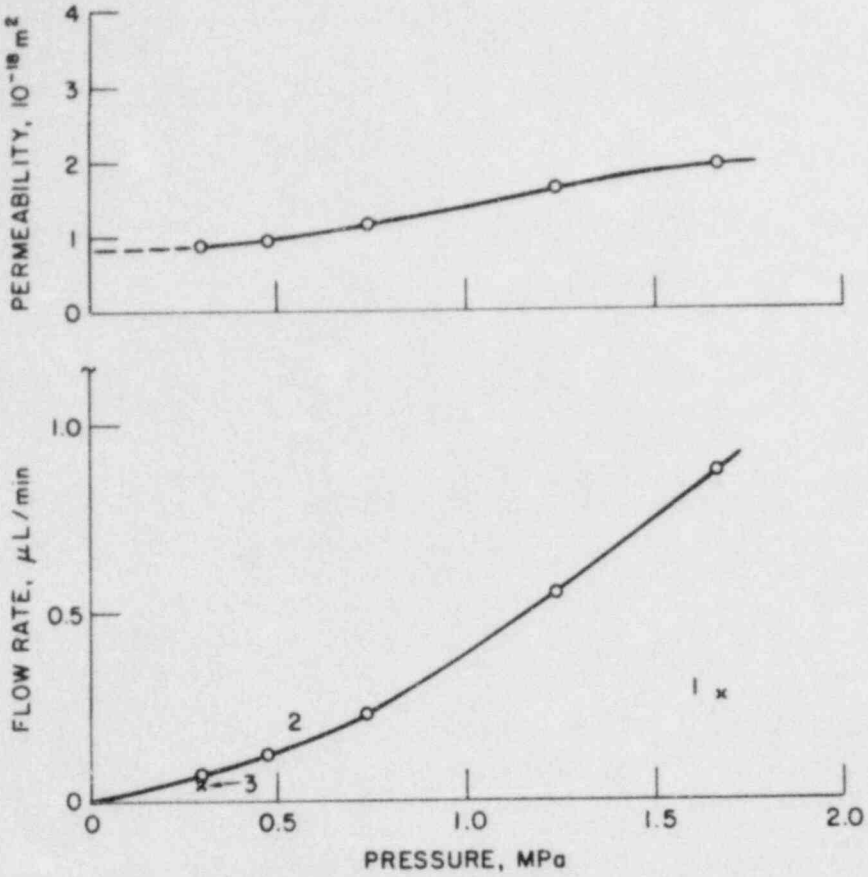

Fig. 3. Flow rate and permeability at 25°C of sand-bentonite column A with a dry bulk density of 1.59 g/cm^3. Experimental sequence: (1) initial flow direction; (2) reversed flow, low pressure followed by high pressure; (3) reversed flow, low pressure. Permeability is shown only for (2).

Reversing the flow caused a twofold increase in permeability. The difference may have been due to movement of clay particles within the column, resulting in partial clogging of the column or the frit. Inspection of the column just before the measurements were made rules out compaction as a cause. The permeability increased with pressure. At the lowest pressure (0.29 MPa) the permeability was only 0.89×10^{-18} m^2. Extrapolation to zero pressure suggests a permeability not much lower or higher than this value.

An increase in pressure from 0.29 to 1.66 MPa caused an irreversible decrease in permeability by about 1/4, as determined by subsequent measurements at 0.29 MPa. This shows that

flow had a small but significant effect on reducing permeability. The reduction of permeability by rapid flow was apparently somewhat greater during filling of the column than it was later.

3.2.4.2 Alteration of Basalt by Vapor

Basalt and bentonite were altered in water vapor in small, tubular autoclaves. The results are reported in detail elsewhere (Steindler 1984 b,c). Only the results for basalt are presented here. The basalt is a sample from the Umtanum formation, and consists mainly of plagioclase, augite, titanomagnetite (Fe/Ti atomic ratio = 3.06), and glass. There are two immiscible glasses, potassium-rich glass and iron-rich, yellow glass. The compositions are shown in Table 2. The potassium-rich glass is quite abundant; the rock contains 1.4% K_2O (Peacor 1984).

Small polished tablets of basalt were exposed to vapor and were kept away from the liquid. The relative humidity ranged between 58% and 100% at the experimental temperatures. Artificial basaltic groundwater and a 0.5 M Na_2SO_4 solution were used for the various experiments. The composition of the groundwater is shown in Table 4. The relative humidity

Table 4. Composition of groundwater used in vapor alteration experiments

Compound	Concentration (10^{-3} M)
NaCl	2.99
Na_2SO_4	1.12
$Na_2B_4O_6$	0.0331
NaF	1.95
Na_2CO_3	0.57
$NaHCO_3$	0.71
Na_2SiO_3	2.01
K_2SO_4	0.024
$CaSO_4$	0.032
$MgSO_4$	7.3×10^{-4}
HCl to pH 9.9	3.05

was controlled by adding limited amounts of water to the system or by reducing the activity of the groundwater with Na_2SO_4. Great care was taken to maintain uniform temperature inside the vessels.

The experimental conditions and results of experiments lasting about 10 days are summarized in Table 5. In some samples, the surface was extensively altered by reaction with vapor or with a thin film of water. The degree of alteration increased with increasing temperature and relative humidity.

Table 5. Summary of results of vapor alteration of basalt

200°C, 9 to 13 days
0.5 M Na_2SO_4 solution, ~97% relative humidity[a]
Slight tarnishing of some titanomagnetite
Very slight etching of plagioclase and growth of new phases
Groundwater solution, 100% relative humidity
Tarnishing of some titanomagnetite and augite grains
Glass was not detectably altered except by contact with liquid
$CaSO_4$ and NaCl formed on the hydrated surface
300°C, 10 days
Groundwater, 58% relative humidity[b]
Iron-rich glass was altered; goethite formed on the hydrated surface
Most titanomagnetite grains were tarnished; some, however, were not detectably altered
Augite was not altered
Plagioclase was etched
Groundwater, 79% relative humidity[b]
More extensive alteration than at 66% relative humidity
Augite very slightly etched and new phases formed
Groundwater, 100% relative humidity[b]
Smectite coats surface to depth of 3 μm
$CaSO_4$ and NaCl formed

[a]Estimated from Raoult's law.

[b]Calculated from amount of water, volume of vessel, and known density of saturated steam.

The effects of alteration by unsaturated vapor included zonal etching of plagioclase, alteration of the glass with formation of goethite [FeO(OH)], tarnishing of some of the titanomagnetite grains, and, in some samples, slight etching of augite. New crystalline phases formed on the surface. Because of the small size, no attempt was made to identify them, except for the goethite.

In saturated vapor, $CaSO_4$ and NaCl formed on the surface. At 300°C in saturated vapor, a layer of smectite about 3 μm thick formed on the surface.

Alteration of three samples over ten days with groundwater at relative humidities of 58%, 79%, and 100% clearly shows the effect of relative humidity. Figure 4 is a photomicrograph of the original unaltered basalt surface. Figures 5, 6, and 7 are photomicrographs of surfaces altered at the three relative humidities. As seen in Fig. 5, the glass was extensively altered at 58% relative humidity; the iron-rich glass appears to be replaced by goethite. The plagioclase was also etched, and most of, but not all, the titanomagnetite grains were tarnished. At 79% relative humidity (Fig. 6) the alteration was noticeably more complete; at 100% relative humidity (Fig. 7) the surface was covered to a depth of about 3 μm with a smectite-rich mixture of alteration products. Semiquantitative analyses of the smectite by scanning electron microscopy show about 2.5% K_2O, with the approximate atomic proportions,

$$K_{0.2}Na_{0.07}Ca_{0.07}Mg_{0.25}Fe(II)_{1.7}Al_{1.7}Si_{3.1}O_{11}$$

A strong X-ray diffraction peak at 1.54 Å suggests that the smectite is trioctahedral and, therefore, that the iron is in the ferrous state. The smectite swells very little in water compared to the swelling of sodium montmorillonite.

The results suggest that, under certain conditions, a basalt component of backfill may undergo extensive alteration by steam in a relatively short time. Alteration of the glass and plagioclase may be significant sources of potassium and calcium, which could adversely affect bentonite if they are not consumed by alteration products. Alteration of the iron-rich glass, which we have observed, may be an important mechanism for lowering the oxygen fugacity in a waste repository.

3.2.5 Conclusions and Discussion

The permeability of the two columns investigated, containing 75% sand and 25% bentonite, was very low. The column with a dry bulk density of 1.72 g/cm^3 initially had an effective permeability of 3×10^{-18} m^2, as defined by the

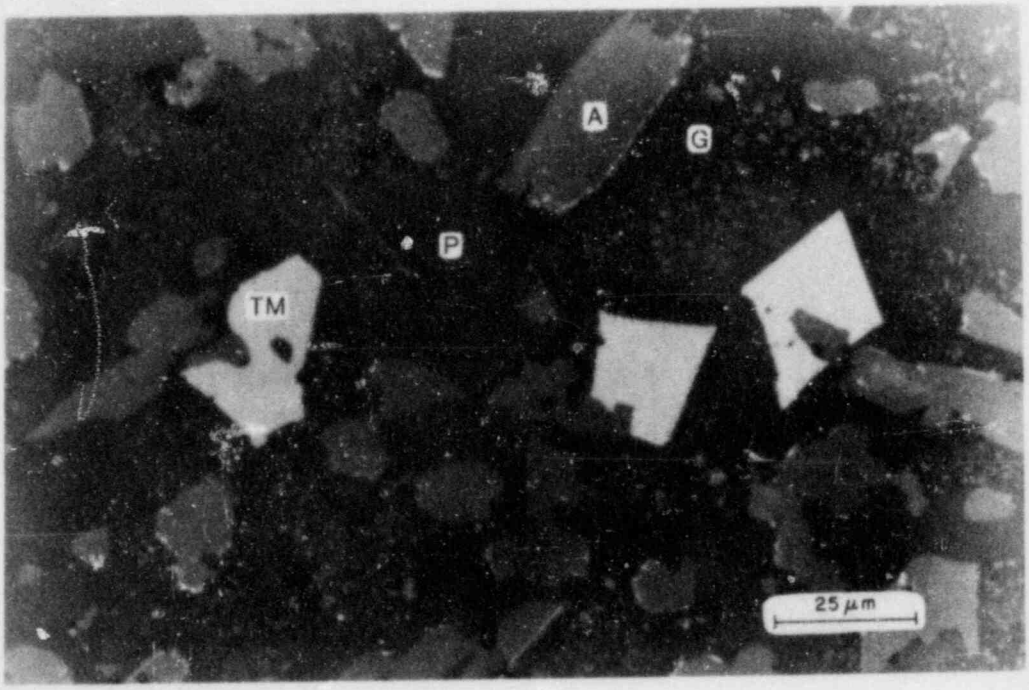

Fig. 4. Surface of unaltered basalt shown in reflected light. Labels mark glass (G), plagioclase (P), augite (A), and titanomagnetite (TM).

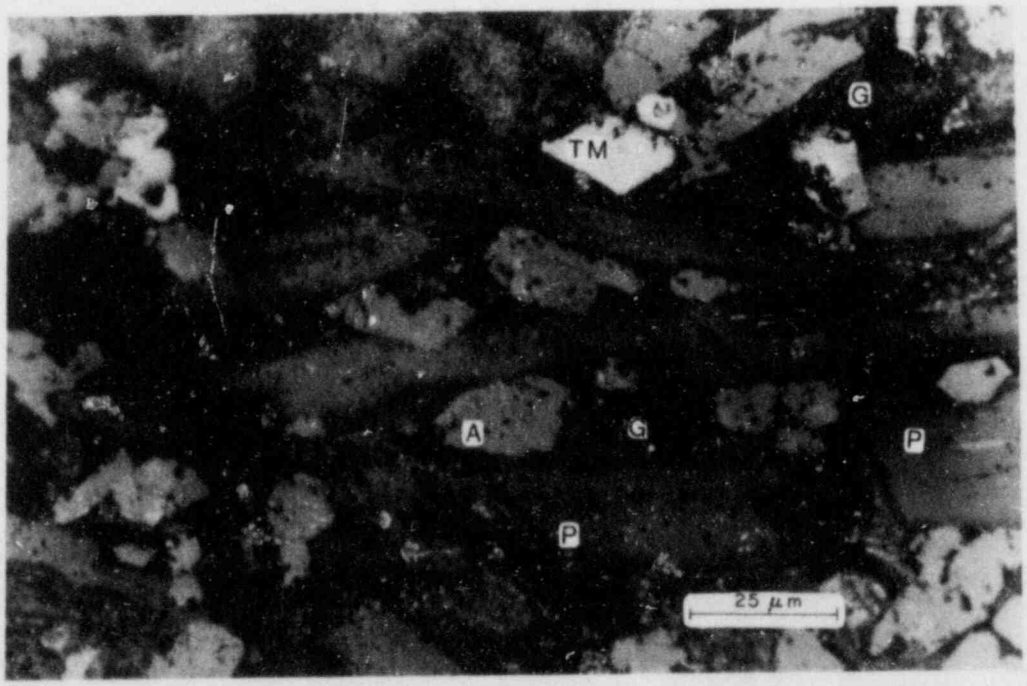

Fig. 5. Surface of basalt after alteration by groundwater vapor for 10 days at 300°C, 58% relative humidity. Marked are the alteration of glass (G), alteration of peripheral zone of plagioclase (P), unaltered augite (A), and titanomagnetite (TM). Most titanomagnetite grains are tarnished and show low-order interference colors. Reflected light.

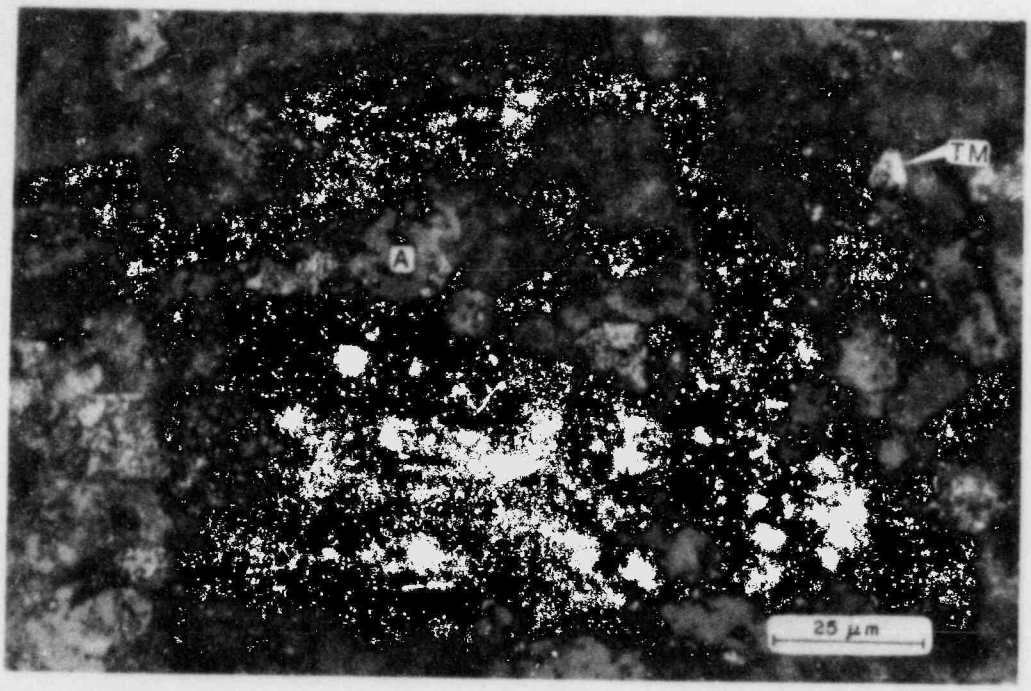

Fig. 6. Surface of basalt after alteration by groundwater vapor for 10 days at 300°C, 79% relative hulidity. More extensive etching of plagioclase (P) is shown; some grains of titanomagnetite (TM) still not detectably altered.

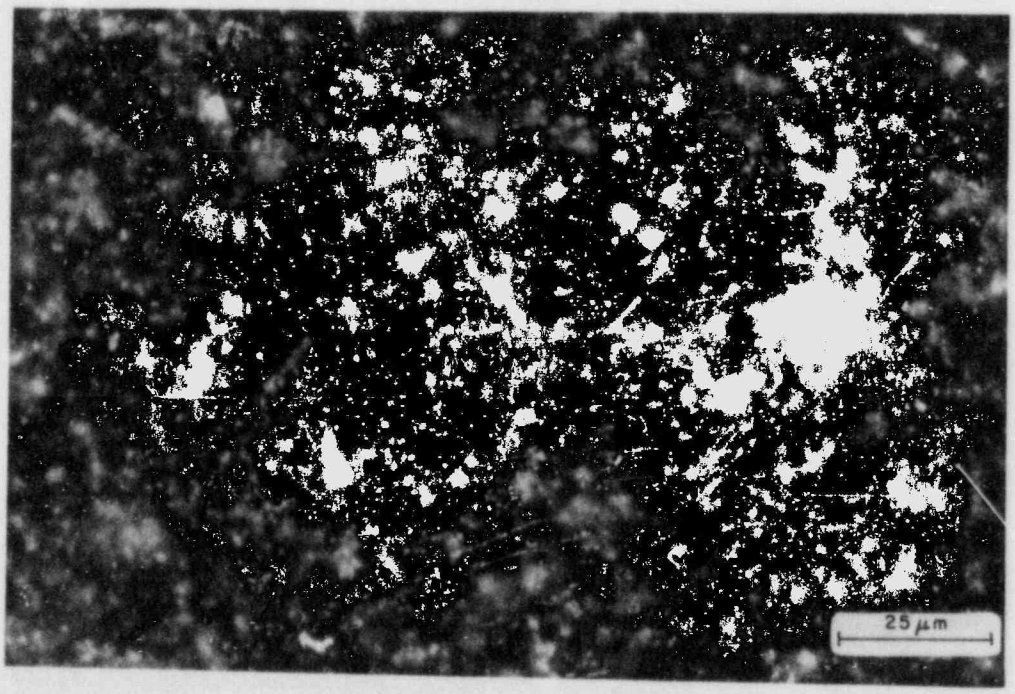

Fig. 7. Surface of basalt after alteration by groundwater vapor for 10 days at 300°C, 100% relative humidity. The surface is completely covered with a smectite clay.

flow rate of water into the dry column. The column was never completely saturated. We expect that the permeability would have decreased substantially at complete saturation.

The final permeability of 0.9×10^{-18} m^2 measured for the column with a dry bulk density of 1.59 g/cm^3 appears to be a representative value for that column. Surprisingly, it is much lower than the value of 2×10^{-17} m^2 obtained by Pusch (1979). The difference may be accounted for by the slightly lower clay content (about 17%) and lower density (1.53 g/cm^3) in Pusch's experiment compared to our experiment (22% and 1.59 g/cm^3, respectively). The effect of normal groundwater (compared to the pure water used for our experiment) will be tested in future experiments, but is not expected to be a major factor because the salt in normal basaltic groundwater ($[Na^+] \sim 0.015$ M) does not greatly affect the swelling of smectites (Brown 1961).

The possibility of leakage of water between the column of backfill and the column tubing is small, but cannot be ruled out. However, if leakage had occurred, the permeability of the backfill would have been lower than measured. Any minor leaks in the equipment would not affect the permeability measurements made at the column outlet. Any leaks in the high-pressure side of the system would mean that permeability measurements made on the basis of flow into the column would be erroneously high. Thus, undetected leaks would not invalidate the conclusion that the measured permeabilities are low.

The permeability depends on the pressure gradient and the history of the column. An increase in pressure gradient causes an immediate increase in permeability followed by a slow, irreversible decrease. The initial increase in permeability may be due to air in the column, hydrodynamic factors, or decreased swelling of clay against the inlet frit. The irreversible decrease is probably due to movement of particles within the column. The effects observed are minor over the range of pressures investigated. However, because there are at least two mechanisms with opposite effects, it follows that attempts to extrapolate measurements to lower pressures than those investigated experimentally should be done carefully. In some cases, extrapolation from very high to very low flow rates could give erroneously low values of permeability. Large extrapolations should be done only with knowledge of the phenomena. In this case, the minimum pressure gradient used in the measurements was 40 kPa/cm. This is about six times the maximum gradient expected across 15 cm of backfill (7 kPa/cm).

Data reported here also indicate that if groundwater vapor contacts crushed basalt at high temperatures in a repository, the basalt will be altered. In the experiments, plagioclase and glass were altered more rapidly than augite or

titanomagnetite. Potassium released from the glass and sodium and calcium released from the plagioclase are likely to be exchanged with exchangeable ions of the montmorillonite in the backfill, and may lead to alteration of the montmorillonite. The high potassium and iron content of the smectite that formed experimentally suggests that the smectite formed from the glass. The smectite has a much lower swelling capacity than sodium montmorillonite. Conversion of bentonite to such a smectite would probably increase the permeability of the backfill. However, we speculate that in a mixed basalt-bentonite system, at least part of the potassium will be consumed by newly formed smectite. Because the "dissolved" ionic concentrations will be much different in a vapor-dominated system than in a liquid-dominated system, there is no a priori basis to assume that the reaction products will be the same in both cases.

The effects of other alteration products on the backfill, such as iron oxides and zeolites (if formed), remain to be tested. It seems possible that alteration of the montmorillonite and cementation due to formation of zeolites and silica as alteration products may result in reduction in swelling ability and plasticity. However, formation of a smectite as the major phase during alteration at 300°C and 100% relative humidity is encouraging. Longer experiments will be necessary to study both the rates and products of alteration.

The alteration of iron-rich glass may have a major effect on the fugacity of oxygen in a repository. At 300°C, the glass is apparently altered by vapor much more rapidly than the titanomagnetite, and most of the goethite appears to be derived from the glass. At 200°C, the relative rates are not certain. It is likely that the glass will also have a major effect in a liquid-dominated system. Experimental or theoretical efforts to determine the rate of uptake of oxygen by the basalt should not ignore the glass and other iron-containing phases.

Radiolysis of air plus water vapor is expected to result in fixation of nitrogen, forming oxides or ammonia. Oxides of nitrogen are acidic, and would partition into the liquid phase, forming nitric acid. If there is a sufficient supply of nitrogen to the backfill, the amount of acid (or base) generated could be up to 0.5 mole per liter of pore space over the lifetime of the gamma emitters, or higher if the partial pressure of nitrogen is higher than 0.8 atmosphere. This is equivalent to about 40% of the ion exchange capacity of a backfill mixture containing 25% montmorillonite by weight and 30% pore space by volume. The course of events can probably not be predicted with certainty from available data. The possibilities include (1) diffusion of NH_3 and oxides of nitrogen away from the backfill and dissolution in groundwater

in relatively cool parts of the repository; (2) dissol tion of gaseous nitric acid or ammonia by interlayer water of montmorillonite (which has an extremely large specific surface area), resulting in alteration of the clay; and (3) dissolution of nitric acid or ammonia by liquid water in the backfill, resulting in alteration of the clay or basalt. Either nitric acid or ammonia may be highly detrimental to clay. The H^+ ion-exchanged form of montmorillonite is reportedly unstable at room temperature; ammonium ions behave mineralogically like potassium ions, and could lead to formation of an ammonium analog of illite.

3.2.6 Recommendations

We recommend specific laboratory tests, projections of laboratory test information to the repository environment, and possible features desired in repository design that would improve safety. These recommendations stem from the experimental results and analyses conducted in this program.

1. On the basis of presently available information, we recommend that backfill around the waste canister be included as part of the repository in basalt. The data show that fresh basalt-bentonite mixtures are capable of ensuring very low flow rates through a repository. The major products of alteration appear to be clays, on the basis of preliminary information. It is probable that almost any altered backfill, especially if clay-rich, will ensure a reasonably low flow rate through a repository, and may be preferable to no backfill at all.

2. Measurements of permeability and swelling behavior of backfill materials should be made as close as possible to, and over the complete range of, conditions anticipated in a repository.

3. Permeability measurements should include some method of evaluating the magnitude and effect of leaks, especially if dynamic seals, which can be contaminated with particles, are used.

4. Large extrapolations of permeability to low flow rates should be made carefully, and only with the understanding of the phenomena that lead to the measured permeability.

5. Nonswelling clay (or projected end products of alteration) may be used as an analog for determining the permeability of completely altered backfill clay.

6. Hydrothermal experiments should be done to evaluate the effects of nitric acid and ammonia on the stability of backfill materials.

7. Hydrothermal experiments on basalt and clay should be continued to evaluate the maximum possible extent of reaction in the repository. Specifically, it is important to determine if the alteration of clay in mixtures of clay and basalt is limited by the extent of the reaction of basalt.

8. Possible limits on expansion of clay due to cementation of smectite grains in the backfill should be evaluated in hydrothermal experiments.

9. Possible embrittlement of backfill due to formation of nonclay alteration products should be evaluated with hydrothermal experiments.

10. The effects of vapor alteration of backfill on plasticity and expandability should be evaluated.

11. The stability of backfill materials in a high thermal gradient should be evaluated.

12. Backfill should be designed to neutralize nitric acid without incurring significant damage (use of a fine grain size of powdered basalt might be one effective way to accomplish this).

13. Secondary clays in the host rock should be evaluated for the ability to expand in groundwater and accommodate widening of fractures.

14. Repository designs that permit accumulation of salts in backfill should be avoided if the backfill contains swelling clay.

15. Possible displacement of backfill due to transient pressure differences should be considered in the design of a repository.

3.2.7 Planned Research

Further work on mineralogical changes in the basalt-bentonite-groundwater and basalt-illite-groundwater systems is in progress. Determinations of plastic behavior and measurements of swelling behavior at high temperatures are planned. The use of backfill in a tuff repository is being studied.

3.2.8 Acknowledgments

We would like to thank Donald Alexander for many valuable discussions of the backfill problem, Martin Steindler for helpful discussions on radiation chemistry, Marcus Wood and Michael Smith for information on the progress of the Basalt Waste Isolation Project, Delbert Bowers for help with the permeability measurements and radiation experiments, Benjamin Tani for help with X-ray diffraction and electron microscopy, Paula McDaniel for help with analysis of clays, and Wyo-Ben, Inc. for bentonite samples. Neil Sturchio made several helpful suggestions on the manuscript. We also wish to thank Richard Keener for a thorough editing of the text and Lu Jensen and Roberta Riel for patient typing of several revisions of the manuscript.

3.2.9 References

Altenhofen, M. K., "Waste Package Heat-Transfer Analysis: Model Development and Temperature Estimates for Waste Packages in a Repository Located in Basalt," Rockwell Hanford Operations, RHO-BWI-ST-18, 1981.

Anderson, W. J., "Conceptual Design Requirements for Spent Fuel, High-Level Waste, and Transuranic Waste Packages," Rockwell Hanford Operations, RHO-BW-ST-25P, 1982.

Bates, J. K., L. J. Jardine, and M. J. Steindler, "Hydration Aging of Nuclear Waste Glass," Science 218:51-54, 1982.

Brown, G., "The X-Ray Identification and Crystal Structures of Clay Minerals," Mineralogical Society, London, 1961.

Couture, R. A., Argonne National Laboratory, letter to Donald Alexander, NRC, May 13, 1983.

Gephart, R. E., et al., "Hydrologic Studies within the Columbia Plateau, Washington: An Integration of Current Knowledge," Rockwell Hanford Operations, RHO-BWI-ST-5, 1979.

Grim, R. E., "Applied Clay Mineralogy," McGraw-Hill, New York, 1962.

Koster van Groos, A. F., and S. Guggenheim, "The Effect of Pressure on the Dehydration Reaction of Montmorillonite, SWy-1," Abstract, Circum-Pacific Clay Minerals Society, 19th Annual Meeting, Hawaii Institute of Geophysics, Hilo, August 1982.

Norrish, K., and J. A. Rausell-Colom, "Low-Angle X-Ray Diffraction Studies of the Swelling of Montmorillonite and Vermiculite," Proceddings Tenth National Conf. Clays and Clay Minerals, pp. 123-149, 1963.

Peacor, D. R., E. J. Essene, J. H. Lee, and L. C. Kuo, "Characterization of Potential Backfill Materials for Buried Nuclear Wastes," U.S. Nuclear Regulatory Commission, Status of NRC-Sponsored Research on Waste Management Geochemistry, this report, 1984.

Pusch, R., "Clay Particle Redistribution and Piping Phenomena in Bentonite/Quartz Buffer Material Due to High Hydraulic Gradients," Svensk Kaernbraenslefoersoerjning AB, SKBF-KBS-79-01, Stockholm, 1979.

Pusch, R., "Permeability of Highly Compacted Bentonite," Svensk Kaernbraenslefoersoerjning AB, SKB-KBS-80-16, Stockholm, 1980.

Pusch, R., "Stability of Deep-Sited Smectite Minerals in Crystalline Rock--Chemical Aspects," Svensk Kaernbraenslefoersoerjning AB, SKBF-KBS-83-16, Stockholm, 1983.

Rockwell Hanford Operations, "Site Characterization Report for the Basalt Waste Isolation Project," DOE/RL 82-3, 1982.

Soo, P. (ed.), "Review of DOE Waste Package Program," Brookhaven National Laboratory, NUREG/CR-2482, BNL-NUREG-51494, Vol. 3, 1983 a.

Soo, P. (ed.), "Review of Waste Package Verification Tests, Biannual Report," U. S. Nuclear Regulatory Commission, NUREG/CR-3091, BNL-NUREG-51630, 1983 b.

Steindler, M. J., et al., "Fuel Cycle Programs Quarterly Progress Report, July-September 1982," Section VII, Argonne National Laboratory, ANL-82-78, 1983 a.

Steindler, M. J., et al., "Fuel Cycle Programs Quarterly Progress Report, October-December 1982," Section IV, Argonne National Laboratory, ANL-83-19, 1983 b.

Steindler, M. J., "Fuel Cycle Programs Quarterly Progress Report, January-March 1983," Section II, Argonne National Laboratory, ANL-83-68, 1984 a.

Steindler, M. J., "Fuel Cycle Programs Quarterly Progress Report, April-June 1983," Section II, Argonne National Laboratory, ANL-83-78, 1984 b.

Steindler, M. J., "Fuel Cycle Programs Quarterly Progress Report, July-September 1983," Section II, Argonne National Laboratory, ANL-83-88, 1984 c.

Thornton, E. C., and W. E. Seyfried, Jr., "Thermodiffusional Transport in Pelagic Clay," Science 220:1156-1158, 1983.

Waste Isolation Systems Panel, "A Study of the Isolation System for Geologic Disposal of Radioactive Wastes," National Academy Press, Washington, 1983.

Wheelwright, F. J., et al., "Development of Backfill Material as an Engineered Barrier in the Waste Package System," Interim Topical Report, Pacific Northwest Laboratory, PNL-3873, 1981.

Wood, M., "Development and Testing of Waste Package Backfill Materials for a Nuclear Waste Repository Located in Basalt," Rockwell Hanford Operations, RHO-BWI-SA-145, 1981.

Wood, M., "Experimental Investigation of Sodium Bentonite Stability in Hanford Basalt," Rockwell Hanford Operations, RHO-BW-SA-219P, 1983.

Wright, J., J. K. Linacre, W. R. Marsh, and T. H. Bates, "Effect of Radiation on Heterogeneous Systems of Air or Nitrogen and Water," Peaceful Uses of Atomic Energy, Vol. 7, pp. 560-563, IAEA, Vienna, 1955.

3.3 ANALYSIS OF FACTORS AFFECTING THE STABILITY OF BACKFILL MATERIALS

Donald R. Peacor, Eric J. Essene,
Jung Hoo Lee, and Lung-Chuan Kuo

Department of Geological Sciences
The University of Michigan

ABSTRACT

Storage of high level nuclear waste in subsurface repositories involves a backfill material as a physical/chemical barrier between the solid waste canisters and host rock. Backfill materials may be subjected to reactions with groundwater at temperatures up to 300°C and pressures of several hundred bars. Chemical, structural, and textural changes due to hydrothermal reaction may degrade the backfill performance over the life of the repository. In order to evaluate the potential for such changes, we have: (1) carried out hydrothermal experiments on candidate backfill materials (smectite, illite, basalt) under conditions analogous to those at the repository, (2) performed a complete characterization of these materials before and after hydrothermal treatment using EMPA, XRD, SEM/EDS, and, especially, STEM/AEM techniques, and (3) recognizing that experimental time intervals are short and that conditions may only imperfectly mimic natural ones, we have reviewed and analyzed geologic systems which are analogous to the backfill systems. These serve as natural experimental systems with ages up to many tens of millions of years.

Basalt, smectite, and illite have been characterized in detail and are all found to be heterogeneous. The Umtanum basalt contains up to 25% of immiscible two-phase glasses and late opal and nontronite in fractures. These materials are especially subject to solution effects and the glass may provide K to groundwater. The kinetics of the smectite to illite and illite to muscovite transitions are primarily controlled by Al/Si diffusion which is sluggish, rather than by rapid alkali ion diffusion. Thus, even though smectite (bentonite), mixed-layer illite/smectite and illite are all metastable phases transitional to muscovite plus other phases, reactions occur so slowly that these phases are retained even within a geologic time scale for temperatures of approximately 150, 200 and 300°C, respectively. Temperature and rock/fluid ratio are the principal variables affecting reaction progress. A high ratio of Ca/K (perhaps supplied by solution of calcite) inhibits the transitions. If clay layers are compacted to form a continuous matrix, water may be prevented from penetrating the backfill and promoting the clay mineral transitions. Smectite-basalt mixtures with a high proportion of smectite and low porosity are an effective backfill material. Because illite retains some limited expandable qualities, but is subject to less severe change, it is superior to smectite.

Analysis of Factors Affecting the Stability of Backfill Materials

3.3.1 INTRODUCTION

The present concept of high level nuclear waste disposal involves the use of backfill material which isolates the canister that contains solid-form waste from the host rock. Potential backfill materials are natural geological materials such as smectite, illite, and basalt. The major functions of a backfill material are to minimize the migration of groundwater between the host rock and the canister system, to retard the migration of radionuclides in the groundwater, and to control Eh and pH of the groundwater in the repository. In light of these requirements, the performance of a backfill material is evaluated based on its mechanical strength, plasticity, permeability, swelling (crack-sealing) properties, heat conductivity and ion exchange capablity. Long-term stability of backfill is required to maintain its usefulness as a physical and chemical barrier. An ideal backfill material would be the one whose properties do not change or which, if changed, cause an improvement in high level waste isolation. The stability (or degradation) of any candidate backfill material must be determined experimentally under hydrothermal conditions because groundwater is available from the host rock, and because radioactive decay of the nuclear wastes causes a localized increase in temperature. A combination of XRD, SEM/EDS, and STEM/AEM analyses is essential to detect any appreciable reaction during hydrothermal treatment which might otherwise be overlooked in routine XRD and optical observations alone. The extension of these results to the long-term behavior of the backfill-host rock system requires knowledge of rates and mechanisms of reactions involved in these materials and on the nature of mineralogical/chemical evolution in natural geologic systems analogous to backfill-host rock system.

3.3.1.1 Issues Addressed by this Research

Our primary objectives in this research are concerned with the following questions:

1. What are the mineralogical changes in starting materials, if any, resulting from hydrothermal treatment? This requires complete characterization of both starting and product materials.
2. How do such changes influence backfill properties such as permeability?
3. What are the rates of change, if any, and how do these relate to the projected life of the repository?
4. What factors control changes in the backfill materials?
5. What measures can be taken to improve backfill performance, given observed degradation modes of these materials?

Each of these questions is directly addressed in the "CONCLUSIONS" section of this report.

3.3.1.2 Background

3.3.1.2.1 Smectite/Illite/Muscovite Transitions

Extensive studies have been devoted to an understanding of diagenesis (changes in mineralogy, texture, etc.) of argillaceous and clastic sediments. Comprehensive reviews are given, for example, by Singer and Muller (1983) and Kisch (1983); additional references are given by Larsen and Chilinger (1983). These studies are concerned, in part, with changes in the clay minerals smectite and illite in response to increasing temperature (to approximately 300°C), geologic time, solution chemistry, and physical factors such as permeability and porosity which in turn relate to rock/water ratios and fluid flow. As smectite and illite are prime candidates for backfill materials, and as the geologic parameters are equivalent to those of the repository, such geologic systems form natural analogues of the repository. Because times of many tens of millions of years are available for geological systems, they represent long-term experiments wherein the lack of reaction due to limited laboratory experiment durations is obviated.

The most important mineralogical process during diagenesis of sediments affected by increasing burial by overlying sediments (and/or tectonic effects) is the progressive conversion of detrital smectite into mixed-layer illite/smectite (I/S) (e.g., Weaver,1959; Burst, 1959, 1969; Powers, 1959, 1967; Carrigy and Mellon, 1964; Dunoyer de Segonzac, 1964, 1969; Dunoyer de Segonzac et al., 1966; Teodorovich et al., 1967; Artru and Gauthier, 1968; Steiner, 1968; Artru et al., 1969; Karpova, 1969; Muffler and White, 1969; Teodorovich and Konyukhov, 1970; Perry and Hower, 1970, 1972; Karpova and Timofeeva, 1971; Weaver and Beck, 1971; Eslinger and Savin, 1973; Hower et al., 1976; Boles and Franks, 1979) which eventually approaches 100% illite, and the successive transition of illite to muscovite (e.g., Velde and Hower, 1963; Karpova, 1966, 1967, 1969; Maxwell and Hower, 1967; Gavrilov and Aleksandrova, 1968; Logvinenko and Karpova, 1968; Artru et al., 1969; Dunoyer de Segonzac, 1969; Frey, 1969, 1970; Kossovskaya and Drits, 1970; Lewis, 1980).

Smectite includes a variety of expandable clay minerals, of which bentonite is a typical, specific example. The structure of bentonite (approximately Na_x $(Al,Mg)_2$ $(Si,Al)_4$ O_{10} $(OH)_2 \cdot nH_2O$; $x \approx 0.3$) consists of a unit of two tetrahedral layers (tetrahedral cation predominantly Si) sandwiched around a dioctahedral layer (octahedral cation predominantly Al). Such integral three-layer units alternate with layers of alkali cations plus H_2O. The alkali-cation layers may expand or contract as H_2O is added or subtracted in response to variable water pressure. Illite is derived from smectite principally by: (1) substitution of K in interlayer sites with concomitant loss of the Na and H_2O layer (so called "collapse" of the structure) (2) substitution of Al for Si. Thus illite has the approximate formula $K_{0.5}(Al,Mg)_2(Si_{3.5}Al_{0.5})O_{10}(OH)_2$. The transitions continue as illite transforms to muscovite ($KAl_2(Si_3Al)O_{10}(OH)_2$)

with the further substitution K+Al → □+Si. Concomitant changes include increasing order from a $1M_d$ to 2M structure (Yoder and Eugster, 1955; Velde and Hower, 1963; Karpova, 1966, 1967, 1969; Maxwell and Hower, 1967; Gavrilov and Aleksandrova, 1968; Logvinenko and Karpova, 1968; Artru et al., 1969; Dunoyer de Segonzac, 1969; Frey, 1969, 1970; Hosterman et al., 1970; Ludwig, 1973; Lewis, 1980) which is generally detected using X-ray diffraction, a further decrease in H_2O and a loss of so-called expandable layers. There is thus a continuous sequence of structures such that pure smectite has maximum expandability, mixed-layer I/S intermediate values and illite or muscovite is not expandable.

Weaver (1967) suggested that the K needed for the transitions is produced from breakdown of detrital K-feldspar and/or mica. This interpretation was supported by Hower et al. (1976) who observed a gradual disappearance of K-feldspar with increasing depth in Gulf Coast sediments. They suggested that K-feldspar may also be the source for Al. Weaver and Beck (1971) stressed the possible importance of the K supply from nearby shale formations during sandstone diagenesis. On the other hand, Boles and Franks (1979) proposed that the Al component of illite during the smectite-illite transition is entirely supplied from smectite layers and, therefore, some smectite must be consumed to form I/S. This implies that the smectite-illite transformation can proceed without Al from the pore solution. However, the supply of K (or other interlayer cations) is critical to the smectite-illite transition (or breakdown of smectite into a non-expandable phase), and these ions must be primarily supplied from pore solution because their amounts are lower in smectite than in illite (or other non-expandable phases).

The kinetics of the smectite-illite transformation have been studied experimentally in the temperature range of 150-400°C by Eberl and Hower (1976). They reported an activation energy of around 20 kcal/mole for the I/S transition, indicating the breaking of chemical bonds in tetrahedral/octahedral layers. It is important to note that this transition is more effective in K-saturated than in Na-saturated smectite. Eberl (1978) further showed that the inhibitory strength of monovalent ions for the smectite-I/S transition follows the order Li, Na, Cs, and K, and of divalent ions, Ca, Mg, Sr, and Ba, which is positively correlated to the magnitude of dehydration energy of these ions. This is because a higher negative charge in smectite layers is required to incorporate a cation with higher hydration energy into the interlayer site. Eberl and Hower (1977) showed that when reacted with water, Na-smectites typically break down into paragonite-bearing assemblages whereas K-smectite typically produces I/S. The inhibition of the smectite-I/S transition by Na, Ca, and Mg ions in the solution has also been demonstrated by Roberson and Lahann (1981).

Temperature ranges of the smectite-illite transition have been inferred from various field studies (Steiner, 1968; Burst, 1969; Muffler and White, 1969; Dunoyer de Segonzac, 1970; Perry and Hower, 1970, 1972; Eslinger and Savin, 1973; Foscolos and

Kodama, 1974; Hower et al., 1976; Boles and Franks, 1979). Most of these results indicate a temperature of about 100°C for the onset of I/S formation (e.g., Perry and Hower, 1970; Foscolos and Kodama, 1974). Lower temperatures have also been reported (e.g., 60°C, Hower et al., 1976; Boles and Franks, 1979). Complete conversion of smectite to illite is estimated to occur at temperatures as low as 200°C (from experiments: Khitarov and Pugin, 1966; Sabatier, quoted by Dunoyer de Segonzac, 1969; Hiltabrand et al., 1973). The range of temperature for the transformation of illite to muscovite is large (approximately 100-350°C). Oxygen isotope thermometry of coexisting quartz and illite from the Belt Series (Eslinger and Savin, 1973) indicates that 50% of the illite of the <0.5 μm size fraction would have been converted from the $1M_d$ to the 2M polytype at a temperature of about 290°C. Coal-ranks (detailed references in Kisch, 1974) and illite crystallinity (Weaver, 1961; Kubler, 1964, 1967; Weber, 1972a, 1972b; for detailed references see Kisch, 1983) are widely used as indicators of temperature, and thus degree of burial metamorphism (increasing depth, time, temperature) in a diagenetic sequence, and confirm this approximate temperature range.

Because the transitions occur at low temperatures, laboratory experiments which attempt to establish stability relations are inconclusive due to the slowness of reactions. It is not established that smectite or illite has a true stability field under geologic conditions. The detailed textural and chemical relations between them indicate that smectite and illite are metastable, with the state of transition being kinetically controlled. Thus availability of large fluid volumes, which promotes solution and crystallization, as well as increasing temperature or any other factor which influences reaction rate, promotes the transitions.

In summary, it appears that the smectite to illite conversion is complete at temperatures of approximately 200°C and that illite to muscovite conversion is complete at temperatures approaching 300°C. The reactions require a source of K and Al. The reacting clays are apparently metastable phases with reaction rates primarily controlled by temperature, the availability of fluids and concentrations of reacting cations in solution. However, under geological conditions which are analogous to the repository, smectite and illite may remain largely unaltered up to temperatures of 150 and 300°C, respectively. The relative significance of the factors affecting the reactions under the specific conditions of the repository remain to be determined, however.

3.3.1.2.2 Hydrothermal Alteration of Basalts

Hydrothermal reactions between basalt and seawater received extensive studies due mainly to their potential application to metallogenesis (e.g., Bischoff and Dickson, 1975; Bonatti, 1975; Humprhis and Thompson, 1978; Mottl and Holland, 1978; Hajash and Chandler, 1981; Seyfried and Bischoff, 1981; Crovisier et al., 1983). Seawater chemistries have been significantly modified

during reaction, and are marked by the increase in Ca, Si, K, Fe, Mn, Ba, Al due to leaching of the basalt, and decrease in Mg due to precipitation of Mg-bearing silicates. The pH of the resultant solution is primarily controlled by Mg-silicate formation. High water/rock ratios accelerate the basalt leaching due to decrease in pH value of the solution. The more acidic solution is also capable of retaining higher concentrations of heavy-metal ions which becomes a potential ore-forming fluid.

Solution chemistry, which is a function of temperature, controls the characteristics of alteration products. Smectite, anhydrite, and Ca-zeolites are predominant products of basalt-seawater interaction at low temperatures (200 to 300° C), which are gradually replaced by smectite-chlorite and Na-feldspars at higher temperatures. In experiments using solutions with simple chemistries, the chemical controls on speciation of alteration products is clearly demonstrated. For example, Kirov et al. (1979) found that analcime and mordenite are typically formed from basalt reacting with a Na-rich solution, whereas K-feldspar, clinoptilolite, and phillipsite appear in a K-rich solution. Keene et al. (1976) also observed that montmorillonite and phillipsite can be produced only when Na and K, respectively, are at sufficient concentrations in the solution reacted with a Hawaiian tholeiitic glass.

3.3.1.3 Objectives

Candidate backfill materials have been treated hydrothermally under repository pressure, temperature and chemical conditions to determine their stabilities. We have carried out an extensive, integrated characterization of both starting materials and the experimental products in order to determine changes, if any, in structure, texture or chemistry. Although methods such as X-ray diffraction, optical studies, electron microprobe analysis, and scanning electron microscopy are used, emphasis is given to the methods of scanning transmission and analytical electron microscopy (STEM/AEM), using techniques developed at The University of Michigan especially for the study of such systems. STEM/AEM may resolve small changes which cannot be detected by other methods. Such changes in experiments of several months duration may be of the greatest significance when extrapolated to thousands of years for the backfill.

Because the backfill materials are natural geologic materials, and because they will be subject to conditions of pressure, temperature and solution chemistry which are duplicated by natural geologic systems, the relative stabilities and properties of the analogous geologic systems must be reviewed. Because such systems have existed for many millions of years, they consist of critical natural experiments relating to long-term stabilities.

3.3.1.4 Scope of Research

Hydrothermal experiments involve three starting materials: basalt, smectite, and illite. Experimental conditions include: (1) A temperature range of 100-300°C, as these upper and lower limits represent the maximum and long-term temperatures expected in the repository (Apted and Myers, 1982). Temperatures above 300°C may be used to accelerate reaction rates. (2) A pressure near 300 bars, as this is the pressure equivalent to 1 km depth. (3) Solution chemistry corresponds to either distilled water or an artificial solution having cation concentrations and pH equal to those of the repository groundwater (Ferguson, 1982) (Table 1) (4) Rock/fluid (R/F) ratios of 0.02 to 2.5 as typical of natural hydrothermal fields (e.g., Savage and Chapman, 1982). (5) Durations of experiments typically are three months, but for low temperature runs where reactions proceed slowly, may be up to one year.

Initial experimental charges are of a single material so that characteristics of simple systems may first be determined, with charges consisting of mixtures used in later experiments. All starting and experimental products are characterized by thin-section optics, bulk chemical analysis, XRD, SEM/EDS, EMPA and STEM/AEM.

Geologic systems which include smectite and illite are emphasized as geological analogues as those are the phases of primary interest as a backfill material. Diagenesis through low grade metamorphism of such systems is reviewed emphasizing separate and still largely unpublished research of the authors on such systems.

3.3.2 METHODS

3.3.2.1 Hydrothermal Experiments

Hydrothermal experiments were carried out in Tem-Pres standard cold-seal pressure vessels heated in horizontal resistance furnaces with Eurotherm solid-state proportional temperature controllers. Prior to experiments, furnaces were accurately calibrated for temperature. This verified that temperature was effectively constant over the entire volume of a sample.

An experimental charge was prepared by packing approximately 0.03-0.07 g of powdered sample at one end of welded gold or silver tubing, adding approximately 0.02-0.1 cc of synthesized solution with composition similar to that of the groundwater at the repository (or distilled water in selected cases), and sealing the tubing with an arc welder. Typically, three charges were loaded at the bottom of the reaction chamber. Temperature and pressure were monitored using a chromel-alumel thermocouple with a potentiometer and pressure gauges calibrated by the manufacturer. Variations in temperatures and pressures never exceeded 2%. Charges were weighed before and after experiments in order to verify that capsules remained sealed for

Table 1. Chemical composition of groundwater in the Umtanum formation, Pasco Basin, Washington compared with sea water and river water compositions.

Species	1	2	3	4
Na^+	10540*	6.3	270	270
K^+	380	2.3	6	6
Ca^{2+}	400	15.0	2	2
Mg^{2+}	1270	4.1	0.3	-
H_4SiO_4	-	34.9	120	-
Cl^-	18980	7.8	190	190
F^-	1.3	-	32	32
SO_4^{2-}	2460	11.2	120	120
HCO_3^-	140	58.4	60	101
CO_3^{2-}	-	-	-	22

1: Average sea water (from Fergusson, 1982)
2: Average river water (from Fergusson, 1982)
3: Groundwater, Umtanum formation
4: Simulated groundwater used in the present experiment (pH buffered to 9.5 using carbonate/bicarbonate ions)
* All figures in ppm

the duration of the experiment.

3.3.2.2 XRD Analysis

Samples of both experimental products and starting materials were finely powdered and dispersed on glass slides. The XRD analyses were carried out using a Philips XRG 3100 generator operated at 35 kV and 15 ma using CuKα radiation. The samples were scanned from 2° to 50° 2θ at a rate of 1° 2θ/min. Samples containing clays were treated with standard expanding agents.

3.3.2.3 SEM/EDS Analysis

The analyses were conducted using a JEOL JSM-U3 instrument equipped with an energy dispersive X-ray detector operated at 15kV. Samples were spread on aluminum blocks and were coated with gold film. Mineral identification was determined using qualitative energy dispersive analyses when morphological data was not definitive.

3.3.2.4 STEM/AEM Analysis

Characterization by scanning transmission electron microscopy (STEM) was emphasized because it is capable of detecting changes in experimental charges which may remain entirely undetected by conventional methods. Subtle changes are to be expected in experiments occurring over time periods as short as several months and temperatures typical of the repository. STEM provides high resolution TEM images (up to 1.5 Å point-to-point resolution) while also yielding quantitative chemical analytical data (resolution of 300 Å in ideal cases) on the same areas. Structure, texture and chemistry (including gradients in chemistry) can be characterized, therefore, in single areas.

Lattice-fringe images of 7 Å resolution or less were routinely obtained in this study, especially for clay minerals. For resolutions greater than this defocus conditions must be calibrated in order to obtain valid structure images (Allpress et al., 1972; Anderson, 1978; Spence, 1981). As 001 spacings of clay minerals in this study are all equal to or greater than 7 Å, images could simply be obtained under optimum contrast conditions in order that they reflect true lattice periodicities.

Analytical data is obtained by measuring peak intensity ratios of energy dispersive spectra for particular elements from thin edges of the sample. This is called the "ratio method" (Cliff and Lorimer, 1972, 1975; Lorimer and Cliff, 1976) in contrast with the "absolute count method" as in EMPA. For silicate samples, peak ratios to Si are used. The concentration ratio of a particular element to Si can be measured from the peak intensity ratio by comparison with that of a standard with a well-known composition. The ZAF correction can be avoided because these analyses are conducted only on thin edges of

specimens (generally less than 0.5 micron in thickness) (Goldstein et al., 1977).

Quantitative data measurement using AEM invclves several problems inherent to the instrument: (1) the peak to background ratio is low since only a small volume of sample is excited; (2) peak resolution is poor (approximately 150 eV). The Mg, Al, and Si peaks partially overlap; (3) counts for light elements (especially for Na) are generally low, and elements lighter than Na are not detectable. Na and Mg contents, although detectable, are inherently inaccurate due to low counts; (4) spurious X-rays can be generated from areas other than those of the sample; (5) fluorescent X-rays can be excited from the bulk of the specimen by high energy white radiation (Bremstralung X-ray); (6) statistics are poor for the analysis mainly due to low peak/background ratios and (7) counts for alkali elements (especially K and Na) are variable due to diffusion induced by the electron beam.

Problems (1) and (6) can be alleviated by using the "ratio method" (Cliff and Lorimer, 1972; 1975) and by averaging a relatively large number of counts (Blake et al., 1983). Problem (4) was solved through a vigorous "clean-up" effort by Blake et al. (1980) and Allard and Blake (1982), involving substantial modification of the instrument. Problem (5), raised by Allard and Blake (1982), can be avoided by using crushed grain specimens. Problem (7), reported by Knipe (1979) and Lee and Peacor (1984b), can also be minimized by carefully calibrating the analytical conditions. Problems (2), (3), and (7), however, reduce precision of STEM analyses, although the accuracy of STEM analyses approachs that of EMPA in ideal cases (Isaacs et al., 1981).

Since powdered samples are mainly used in this study, two different sample preparation techniques were used for STEM/AEM studies. First, powder samples were settled on a flat surface, embedded in an epoxy, and cut perpendicular to the surface so that the layer stacking of clay minerals could be observed. Procedures for the preparation of ion-thinned samples (Blake and Peacor, 1981; Lee et al., 1984b) were then followed. Second, finely crushed samples were sparsely deposited with a C film on a Be grid. The first method (ion-thinned sample) was used for high resolution TEM observation of lattice fringes of clay minerals. The second method (crushed sample) was more frequently used because it requires less effort and uses smaller volumes of material.

The electron microscope used in this study is a JEOL JEM-100CX instrument which has been greatly modified for high-resolution analysis (Blake et al., 1980; Allard and Blake, 1982). The analytical procedure described by Isaacs et al. (1981) was used. Conditions of STEM analysis were carefully calibrated as discussed in Lee and Peacor (1984b).

3.3.2.5 Optical and Electron Microprobe (EMPA) Analysis

Standard petrographic microscope optical studies were carried out using polished thin sections of original geologic

materials. Luminoscope observations were also made of all sections. Following complete optical characterization those same polished sections were analyzed by electron microprobe techniques. Both qualitative energy dispersive and quantitative wavelength dispersive techniques were used. Conditions were effectively those of Isaacs et al. (1981). In the case of the basalt glass samples, thin sections used for EMPA were also submitted for ion milling, and analyzed by STEM.

3.3.2.6 Bulk Chemical Analysis

Following acquisition of bulk source materials, several kilograms of each were crushed and thoroughly mixed in order to obtain a source of homogeneous material for all further studies. Samples of each were submitted for chemical analysis by X-ray fluorescence analysis (XRF).

3.3.3 RESULTS

3.3.3.1 Characterization of Starting Materials

3.3.3.1.1 Smectite

Because XRD studies of several commercial bentonites showed that "Envirogel 200" was least subject to contamination by other phases and was highly ordered, we chose it as a representative smectite clay. Bulk chemical analysis is given in Table 2.

X-ray Diffraction - XRD patterns (see Fig. 11a) showed a sharp 001 peak with d=12.5 Å as typical of well ordered bentonite. The peak was slightly asymmetric toward higher d-values. Approximately 15% of the sample consisted of subequal amounts of calcite, quartz, and a 10 Å mica (illite as characterized by STEM/AEM data). Treatment with ethylene glycol resulted in expansion of 001 layers to 16.6 Å, as typical of bentonite.

In order to cause expansion of layers which is retained in the vacuum of the STEM, the smectite powder was expanded with 0.1 N laurylamine HCl solution following the technique introduced in Yoshida (1973). The expansion of smectite was monitored at each step until no significant changes in the X-ray diffraction pattern, occurred. The principal 001 peak splits into two separate peaks (Table 3), indicating a variable degree of structure expansion. As no further significant changes occurred with further treatments, it was concluded that the maximum expansion possible had occurred, and that the samples were suitable for TEM observations.

STEM/AEM Data - Qualitative AEM analysis showed that the bentonites are heterogeneous in composition. They fall into two categories, one of which is Al-rich, and one of which is Fe and Mg rich. Although Na is always the dominant large cation, there is also minor K and Ca (see Fig. 10a). Although K is generally higher than Ca, the proportions of K and Ca vary over a wide

Table 2. XRF analysis[+] of Wyoming bentonite and Fithian illite standard samples. (weight percent)

Oxide	Bentonite	Illite
SiO_2	59.8	54.8
TiO_2	0.20	0.91
Al_2O_3	17.7	18.6
Fe_2O_3[@]	3.79	7.63
MgO	2.11	1.69
MnO	0.02	0.01
CaO	1.71	0.61
Na_2O	2.24	0.49
K_2O	0.73	4.90
P_2O_5	0.08	0.25
LOI[&]	11.8	9.93
Total	100.2	99.8

[+]Analyzed by X-ray Assay Laboratories Ltd, Don Mills, Ontario.

[@]Total iron.

[&]Loss of ignition.

Table 3. Smectite d(001) expanded by 0.1 N laurylamine HCl treatment.

	PROCESS	d(001) (Å)
1.	initial 4-week treatment	24.2
2.	1st 1-day wash (water + alcohol)	23.3, 17.9
3.	2nd " (")	- 17.7
4.	3rd " (")	21.8, 16.1
5.	additional 1-week treatment	27.2
6.	1st 1-day wash (water + alcohol)	27.2, 17.0
7.	2nd " (")	22.6, 15.8
8.	3rd " (")	22.1, 15.1
9.	4th " (")	22.6-23.6, 14.9
10.	5th " (")	20.8, 15.0
11.	6th " (")	- 14.6
12.	7th " (")	20.8, 15.0

range.

Quartz appears in TEM images as sub-micron, subhedral crystals. The 10 Å phyllosilicate was shown to be illite by qualitative AEM analysis and through 10 Å lattice-fringe images. Calcite was not detected by STEM. Lastly, SEM images and qualitative EDS analytical data showed the presence of some zeolite grains, as well as rare grains of a phase appearing to be amorphous silica.

Figures 1 and 2 show typical untreated (unexpanded) smectite at different scales. The election diffraction patterns (insets) leading to these images have d(001)≈13.0 Å, in good agreement with the X-ray diffraction results. The patterns are generally streaked parallel to c*, however, indicating the presence of a range of spacings.

Figure 1 shows typical smectite layers. They are severely distorted and imperfect in a variety of ways. Figures 2a and 2b are both lattice-fringe images at high resolution. The lines shown are images of the layers of structure, several Angstroms in width, and are typical of all smectites that we have observed. Individual layer spacings can be seen to differ from one another. Detailed analyses shows that most are 13.0 Å in width on average, as consistent with a normal, hydrated smectite, but others have a width of 10 Å. This is presumeably due to collapse, with loss of water in the vacuum of the TEM of an original 13 Å layer. Imperfections in smectite structure such as undulating layers and variable layer spacings (Figs. 2a and 2b) are also commonly observed in natural smectite (Lee et al., 1984a).

Figures 3a and 3b show typical images of the expanded smectite (by laurylamine HCl). The electron diffraction patterns leading to these images show 001 layer spacings of 13 to 16 Å, as consistent with expanded layers as measured by X-ray diffraction. The same doubled 001 reflections are seen as in X-ray diffraction, and there is significant streaking parallel to c*, as indicative of stacking disorder.

Figures 3a and 3b are both high resolution lattice fringe images showing individual layers of structure. Most layers have widths of 14 to 16 Å, with very few approaching 10 Å, verifying the permanent expanding ability of laurylamine HCl. The layers show the same high degree of imperfection as shown in Figures 1 and 2.

SEM/EDS Data - Figure 4 illustrates the SEM image of a typical smectite grain and its EDS spectrum. Smectite occurs as stacked layers of thin, homogeneous units, which is consistent with STEM observations. Quartz (as well as calcite) occurs as granular aggregates or discrete grains. EDS spectrum shows that Na is the major interlayer cation, with subordinate K and Ca.

3.3.3.1.2 Illite

The illite is material obtained from the type locality at Fithian, Illinois, chosen in part because it is well studied material, the standard for illite. This is important because

Figure 1. A low magnification TEM image of an untreated Wyoming bentonite embedded in epoxy shows the form of smectite grains and their (001) structure layers oriented normal to the plane of the figure. The inset electron diffraction pattern shows an 001 layer stacking periodicity of 13.0 Å on average.

Figure 1

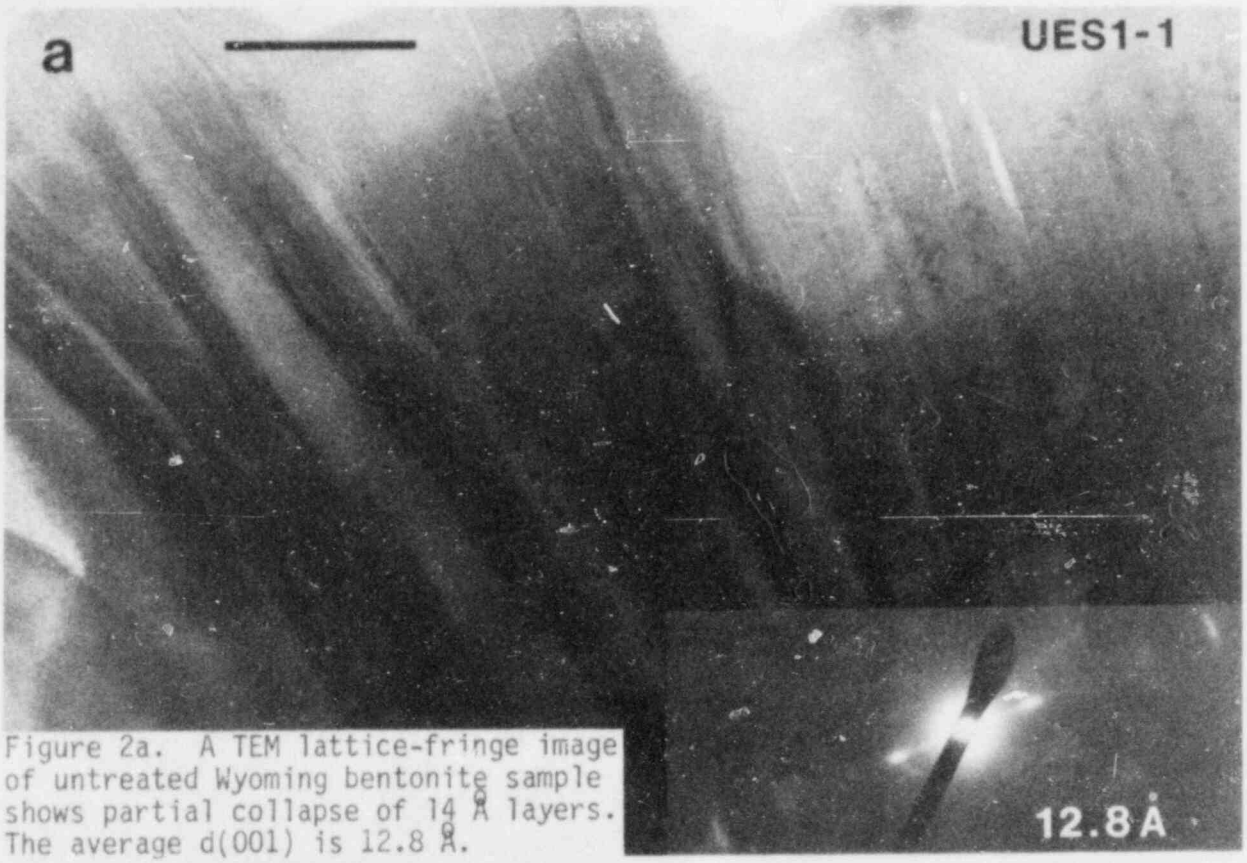

Figure 2a. A TEM lattice-fringe image of untreated Wyoming bentonite sample shows partial collapse of 14 Å layers. The average d(001) is 12.8 Å.

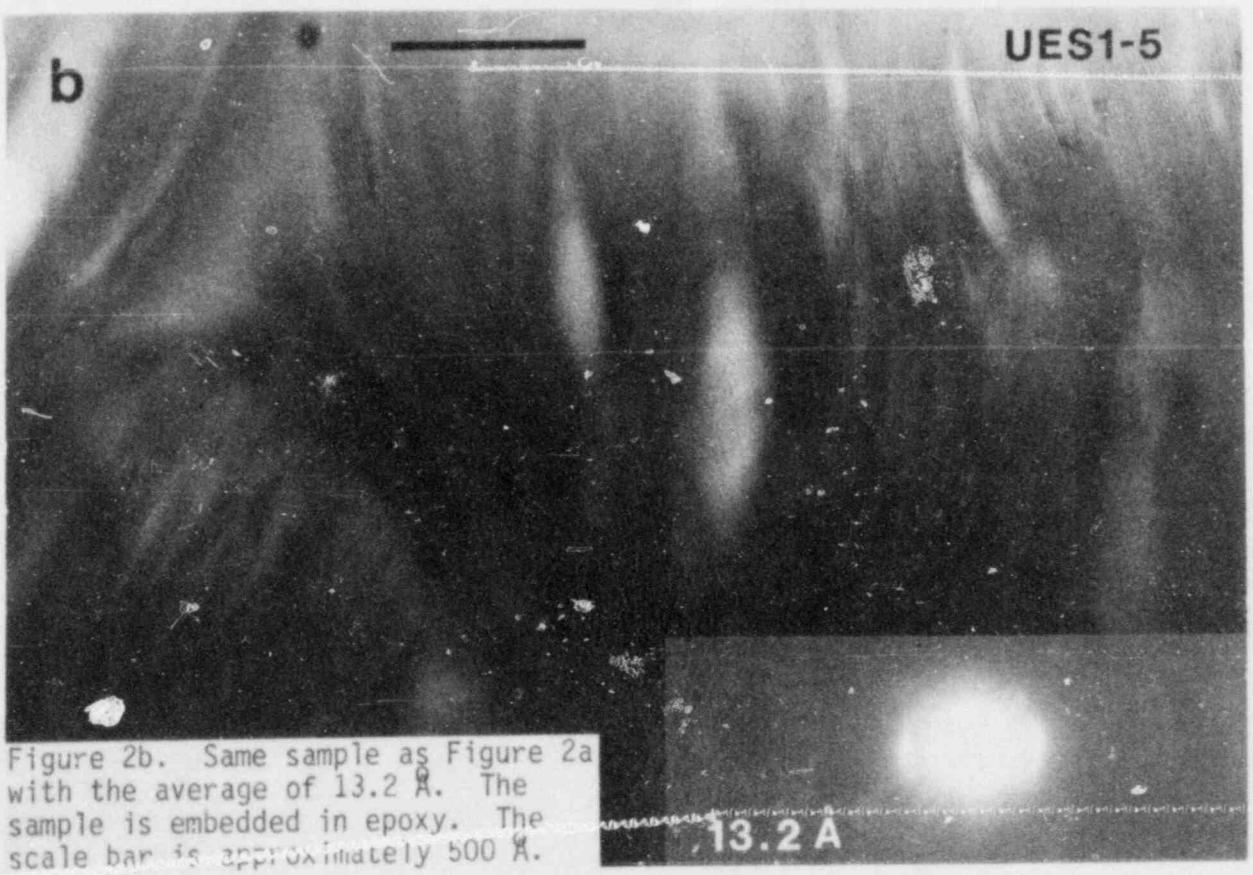

Figure 2b. Same sample as Figure 2a with the average of 13.2 Å. The sample is embedded in epoxy. The scale bar is approximately 500 Å.

Figure 2

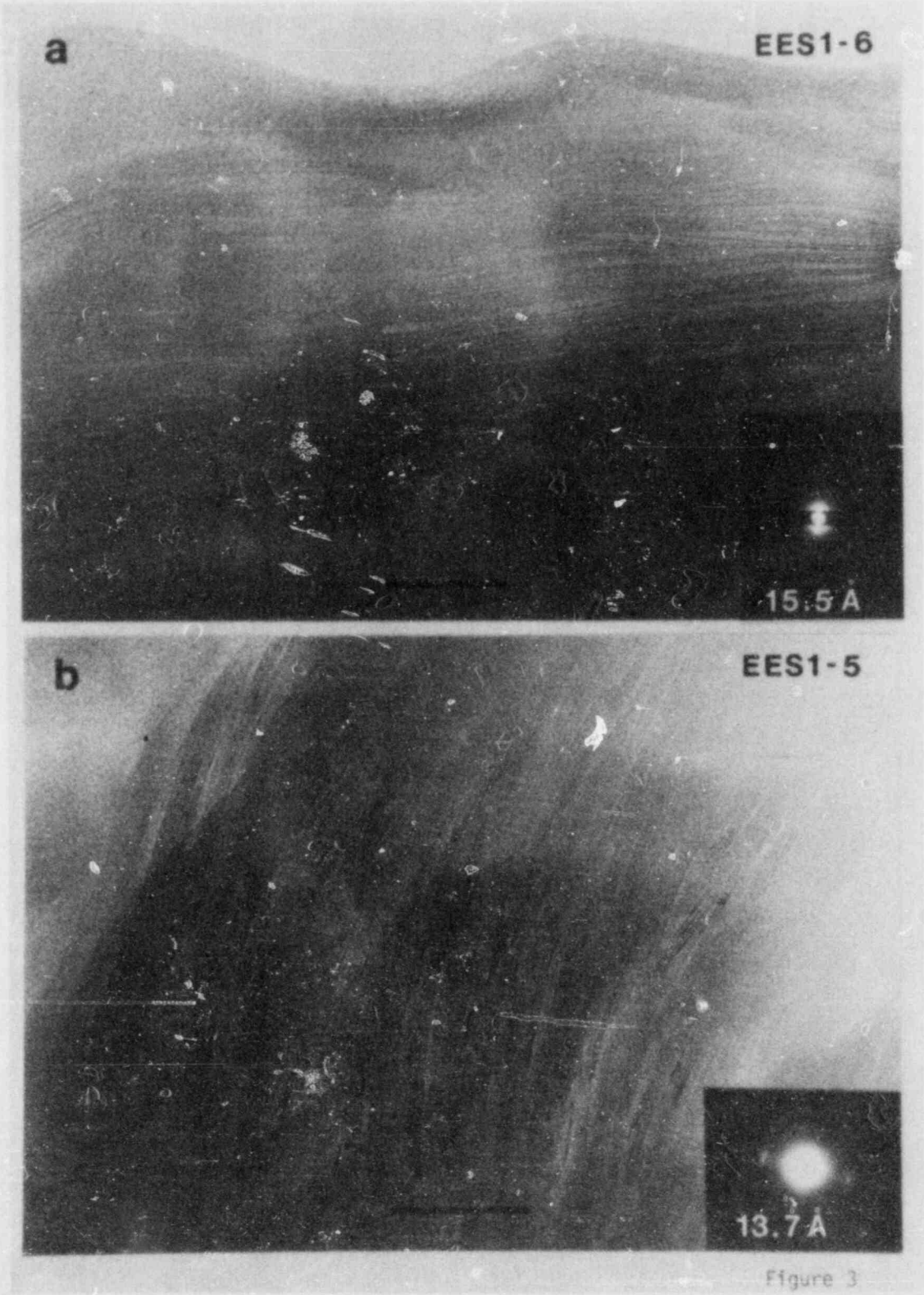

Figure 3

Figure 3. TEM lattice-fringe images of Wyoming bentonite expanded with 0.1 N laurylamine HCl indicating larger d values. The average d(001) of smectite layers are highly variable as shown in (a) 15.5 Å and (b) 13.7 Å. The sample is embedded in epoxy. The scale bar is approximately 500 Å.

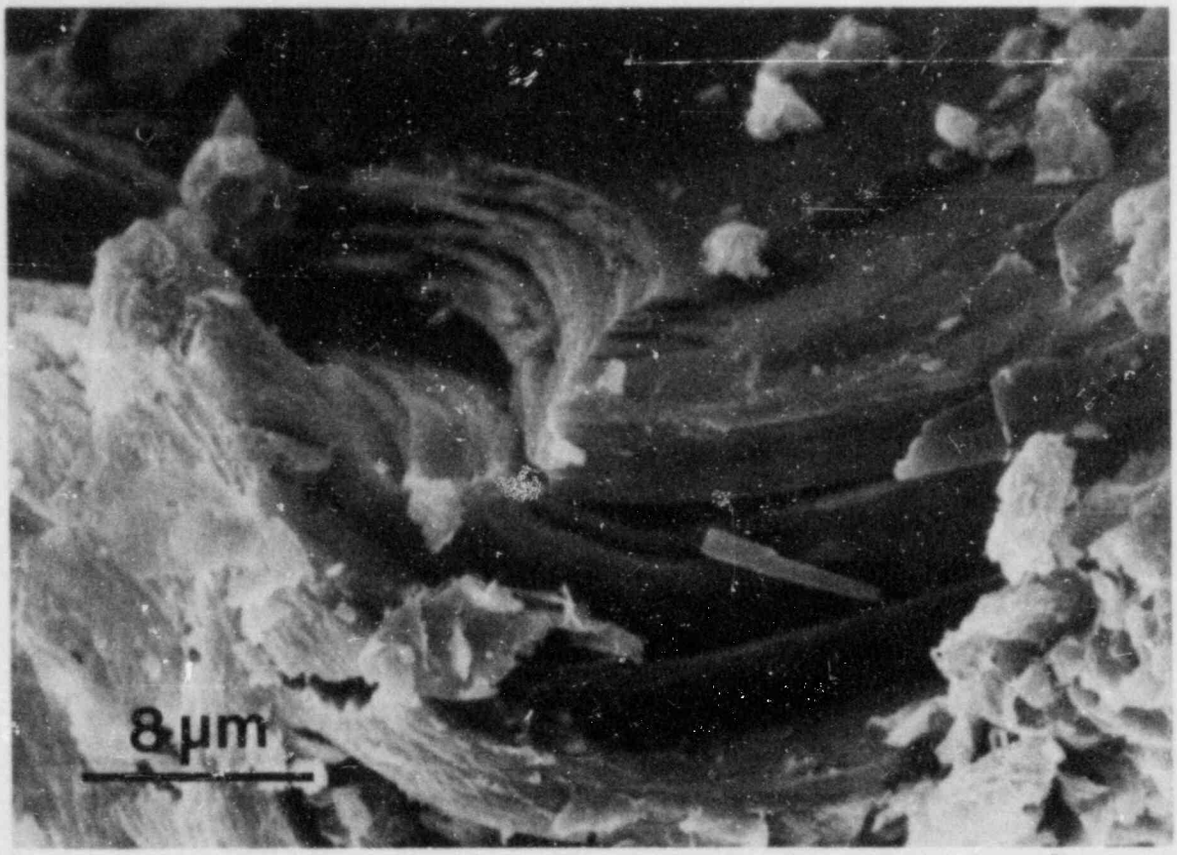

Figure 4a. A SEM image of bentonite. Smectite (grey) exhibits a platy habit and is composed of stacked layers of thin, homogeneous units. Several grains of granular quartz and calcite show light contrasts.

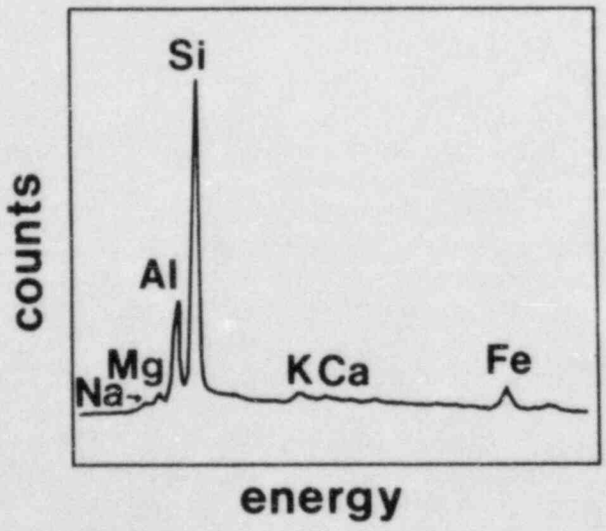

Figure 4b. An EDS spectrum of the smectite grain shown above (Fig. 4a) shows that Na as well as Ca and K are major interlayer cations.

illite has complex, variable properties and it is necessary to base reproducible results on such a standard, reproducible source.

The illite is even more heterogeneous than the smectite, but this is not unexpected as the samples are shale rock samples which typically contain several minerals. The heterogeneities fall into two categories.

(1) The illite is itself heterogeneous. X-ray diffraction shows that it is a mixed-layer illite-smectite, with approximately 20-30% expandable layers, so that structurally it exhibits a range of spacings from 10 to approximately 14 Å. Typical TEM images of Fithian illite samples (Figs. 5a and 5b) also demonstrate the presence of 14 Å smectite layers mixed in 10 Å illite layers (Fig. 5a). AEM analyses show two kinds of grains, although all have K as the dominant interlayer cation. One type has up to 20% Ca + Na relative to K. The other kind has approximately less than 5% Ca + Na. There is approximately twice as much of the Ca, Na-rich phase. Although there are two general categories, there is considerable variation in K, Ca and Na within each one.

(2) Additional phases are present. These include: a) Quartz (43%), which is a major component of the shale; b) Plagioclase feldspar (2%, variety albite with minor Ca, K) has been identified as a minor phase by both AEM and XRD; c) K-rich feldspar was identified in a single grain by AEM; d) Calcite was identified by XRD in Fithian illite samples obtained from a Clay Minerals Society standard sample (50% illite, 30% quartz, 14% calcite and 6% plagioclase feldspar), but has not been detected in our standard samples. The standard Fithian illite was treated with hydrogen-peroxide in order to remove organic material and was also submitted for X-ray fluorescence chemical analysis. The analytical values in Table 2 are in reasonable agreement with those predicted on the basis of the mineralogical analysis by X-ray diffraction.

3.3.3.1.3 Basalt

The core samples available to us (Umtanum Formation, 3078-3079 ft. level, well DC-6, Hanford Site, Washington) are dark gray, fine-grained, homogeneous basalts. XRF analysis and norm calculation (Table 4) show that it is a typical tholeiite. In thin section, Umtanum basalt displays hyalo-ophitic texture characterized by the presence of up to 30% of silicate mesostasis interstitial to plagioclase laths (typically less than 0.1 mm in width) as well as euhedral to subhedral augites (analysis in Table 4). Magnetite microphenocrysts are ubiquitous.

The core samples have several exposed fissure surfaces as well as ellipsoidal vesicles. The surfaces of these fissures are always coated with a layer of black, earthy, fine-grained clay material. The coating is usually decorated with yellowish-brown streaks manifesting the precipitation of Fe-bearing opaline material from Si-saturated solution. Large grains of opal, showing conchoidal fracture, are occasionally present. In

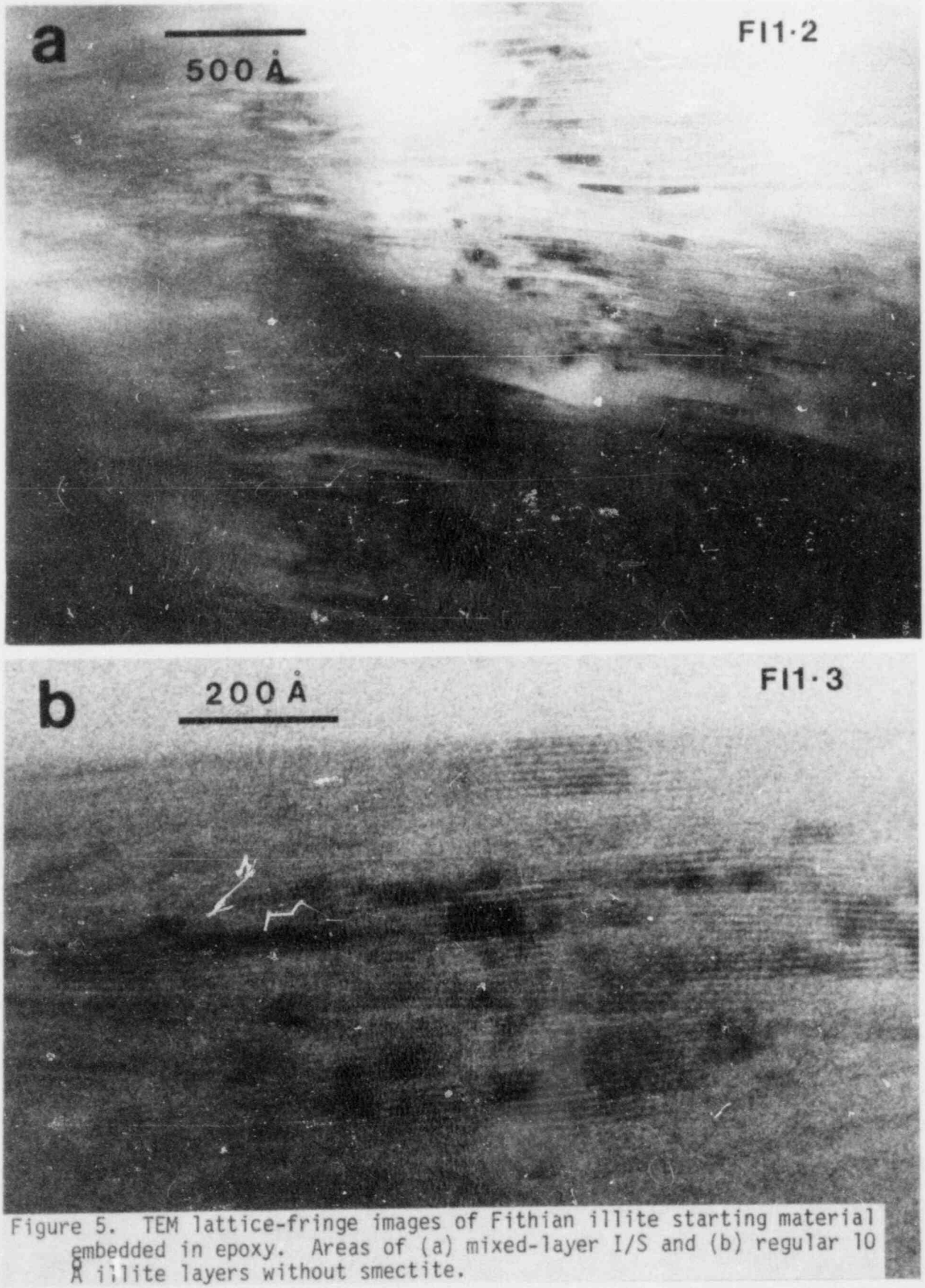

Figure 5. TEM lattice-fringe images of Fithian illite starting material embedded in epoxy. Areas of (a) mixed-layer I/S and (b) regular 10 Å illite layers without smectite.

Figure 5

Table 4. Bulk rock and augite analyses of the Umtanum Basalt

	Bulk rock*	augite**
SiO_2	53.1	50.67
TiO_2	2.10	0.92
Al_2O_3	12.8	2.85
Fe_2O_3@	3.6	-
FeO	11.0	16.85
CaO	7.11	13.01
MgO	3.65	15.66
MnO	0.22	nd#
Na_2O	3.15	nd
K_2O	1.39	nd
P_2O_5	0.33	nd
LOI	1.00	
total	99.5	99.96

*CIPW norm

Q	7.64
zr	0.02
or	8.21
ab	26.65
an	16.68
di	6.33
hd	7.46
en	6.15
fs	8.31
mt	5.21
il	3.98
ap	0.78

** Calculated formula:

$$(Ca_{0.53}Mg_{0.98}Fe_{0.53}Ti_{0.03}Al_{0.04})(Al_{0.09}Si_{1.91})O_6$$

which corresponds to $En_{45.5}Fs_{27.4}Wo_{27.1}$.

@ Fe_2O_3 calculated as $Fe_2O_3 = TiO_2 + 1.5$.

not determined

several cases, patches of white, thin layers of zeolites are sandwiched between black clay layers. Zeolites and quartz are dominant in vesicles.

Figure 6 shows SEM images of these fracture materials. The XRD analysis indicates that the black clay is nontronite, a Fe-rich smectite. The grains are homogeneous and compact (e.g., Fig. 6a). Opaline material occurs as linear arrays of spheroidal particles with relatively uniform size (about 0.1 mm in diameter), as contrasted with the blocky nontronite sandwiching them (Fig. 6b). Concentric fractures are characteristic. The EDS spectrum indicates that Fe is the major impurity in these grains, which is consistent with their yellowish-brown color. Epistilbite is found as aggregates of spherical crystals in an ellipsoidal amygdule (Fig. 6c). It is characterized by its spherical habit and its higher Ca/Si and Al/Si ratios than heulandite. Heulandite is found to be the major zeolite coexisting with the nontronite in the fractures. A typical heulandite crystal is presented in Figure 6d.

We have directed special attention to high resolution STEM/AEM characterization of the interstitial glass in the basalt because this glass is much more reactive than crystalline phases upon hydrothermal alteration, and its breakdown will modify the groundwater chemistry and consequently the nature of alteration products.

Figure 7a shows the TEM image of the glass and shows that it consists of two-phase, immiscible glasses. It consists of randomly distributed, dark glass globules (globular glass) in a transparent glass interstitial to plagioclase laths (matrix glass). The globular glasses show a bimodal size distribution: either 0.5-1.5 microns or less than 0.1 micron in diameter. Larger glass globules display various degrees of optical and chemical heterogeneity. Those labelled A (Fig. 7b) are compositionally homogeneous throughout the globule and show very smooth globular surfaces without appreciable variations in contrast. Those labelled B are extremely heterogeneous in composition and have irregular outlines with strong contrast changes within the globule. They contain domains of crystal-like phases which give rise to powder-like electron diffraction patterns. Those labelled C show lesser degrees of optical and chemical heterogeneities and surface irregularity than type B. The matrix glass typically shows higher contrast.

Energy dispersive spectra indicate that the globular glasses are characterized by high Si, Ca, and Fe contents with subordinate Mg, Al, P, S, Cl, K, Ti, and Mn (Fig. 8a). In one of the type B globular glasses a covariation of Ca and P was detected, indicating the possible presence of apatite as a crystalline phase. The bulk chemistry of type B glasses is very similar to that of type A globules. The matrix glass, on the other hand, consists mostly of Si with less Al and minor amounts of Na, Mg, K, Ca, Ti, and Fe (Fig. 8b). If the composition of the small globular glasses is similar to that of the larger ones, Fe, Ca, and Ti in the matrix glass may be partially contributed from these small globules.

Quantitative chemical analyses of the globular and matrix

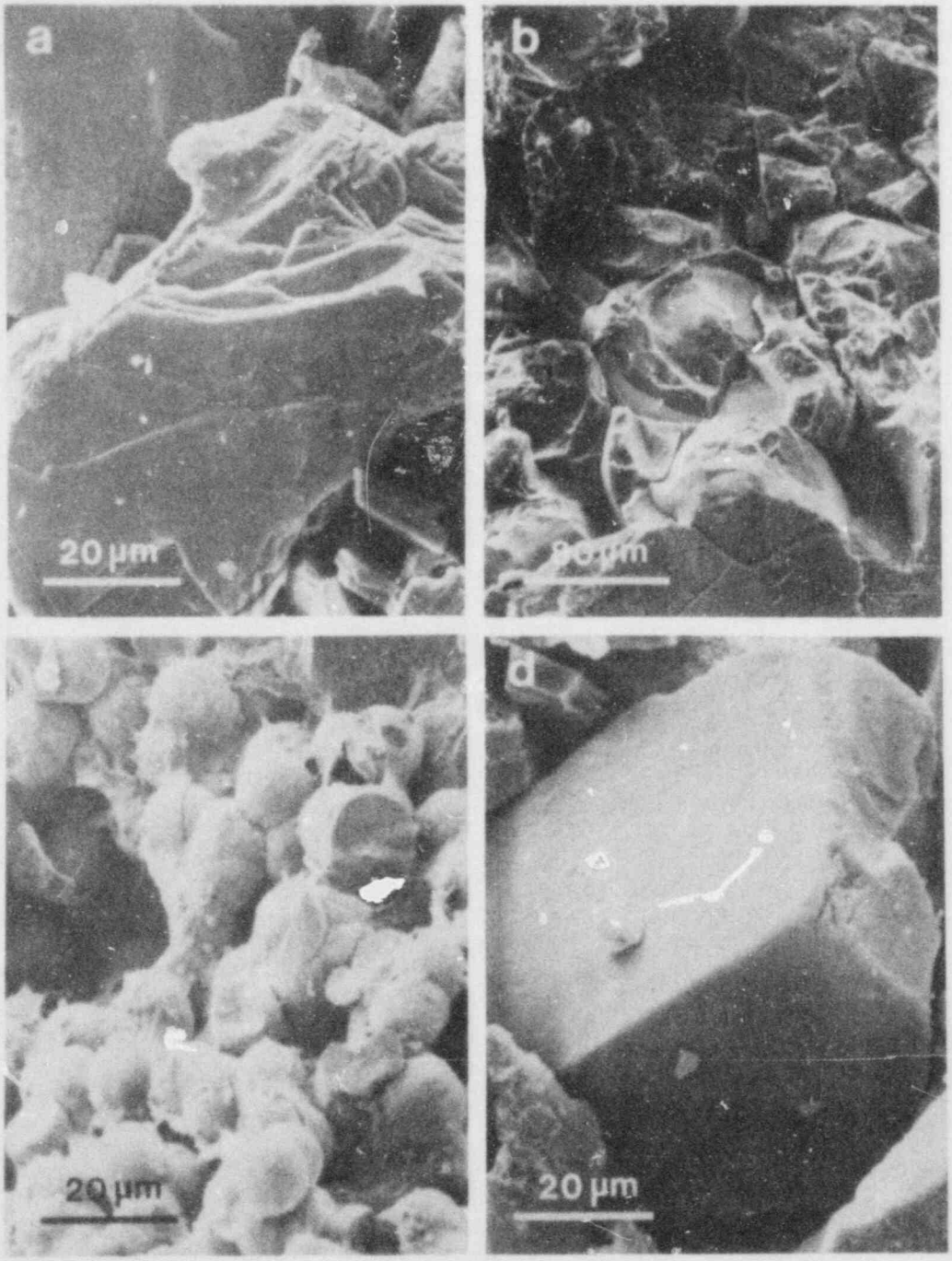

Figure 6. SEM images showing the morphology and occurrence of alteration assemblage in the fractures of the Umtanum basalt. (a) Platy, homogeneous nontronite. (b) Spheroidal aggregate of opaline material sandwiched between nontronite layers. Note the conchoidal fracture. (c) Aggregate of spherical epistilbite in an amygdule. (d) Heulandite crystal showing one perfect face (lower).

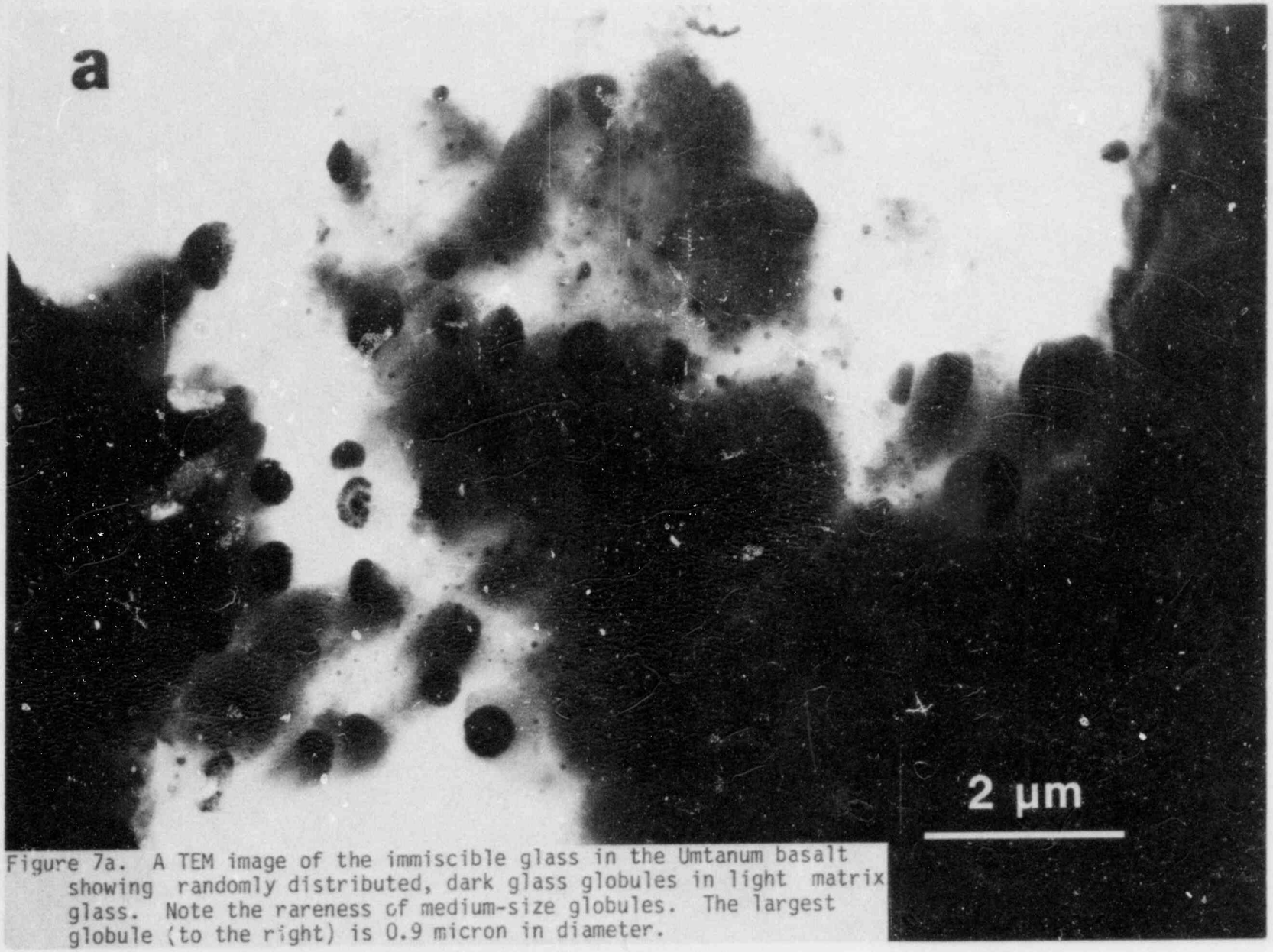

Figure 7a. A TEM image of the immiscible glass in the Umtanum basalt showing randomly distributed, dark glass globules in light matrix glass. Note the rareness of medium-size globules. The largest globule (to the right) is 0.9 micron in diameter.

Figure 7a

Figure 7b. An enlarged view of the immiscible glass showing the variations in chemistry and in optical homogeneity of globules; A, maximum homogeneity; B, maximum heterogeneity; and C, intermediate.

Figure 7b

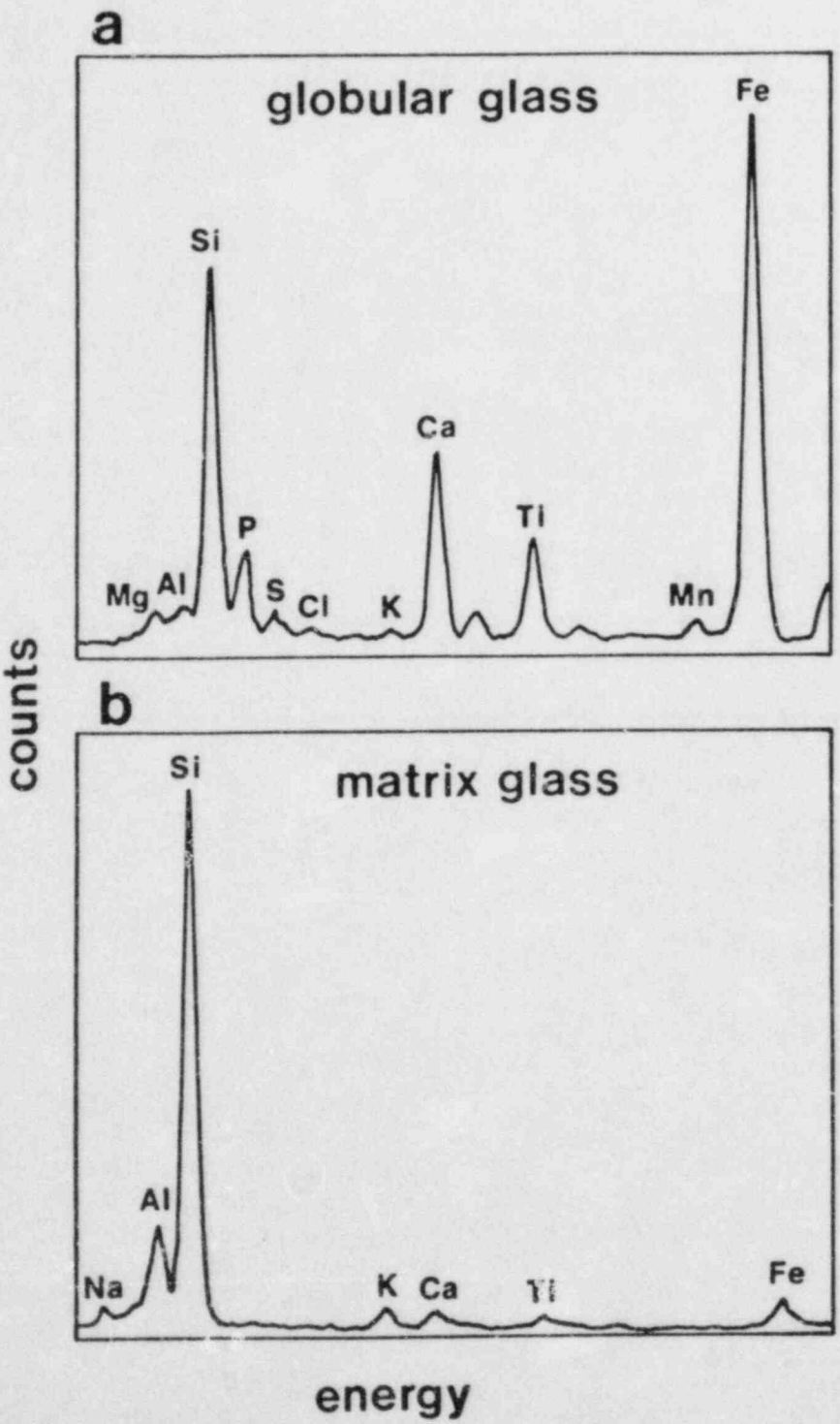

Figure 8. EDS spectra showing the chemistries of typical (a) globular, and (b) matrix glass. Note the enrichment of Si-Ca-Fe in the globules in contrast with the high Si-Al-K contents in the matrix glass.

glasses were performed using AEM techniques. The size of the electron beam was about 0.1 micron for point analyses and 0.5-2 microns for bulk analyses. Typically several point analyses were averaged to obtain composition of a homogeneous globular glass. Table 5 presents representative results. It can be seen that homogeneous (type A) globular glasses also show narrow compositional ranges (columns 1 and 2, Table 5), whereas heterogeneous ones display a more diverse composition range (columns 5 and 6, Table 5). The matrix glasses (columns 3, 4, Table 5) are typically rich in Si and Al, yielding high quartz and feldspar components in the CIPW norm, as contrasted with the high pyroxene, olivine, ilmenite, and apatite components for the globular glasses.

Both morphologic and chemical properties are consistent with the interpretation of subliquidus phase separation origin of these glasses. This is illustrated by a triangular plot (Fig. 9) in which the compositions of globular and matrix glasses are separated by a region of silicate liquid immiscibility (Roedder, 1978). Our compositions of matrix glasses are comparable with those of published data, but the globular glasses show lower Si and higher Fe, Ca, Ti, P, and Mg concentrations than the published values. We suggest that our results are more reliable because all the published data were obtained using EMPA techniques, where contamination from the surrounding matrix glass is likely because of the very similar sizes of globular glasses and electron beam.

3.3.3.2 Hydrothermal Experiments

Table 6 documents the mineralogical/chemical changes in the hydrothermally treated bentonite (smectite), illite, and basalt as compared with the starting materials. The findings on each run product are given as follows.

3.3.3.2.1 Smectite

300°C Runs - The XRD patterns of the hydrothermally treated bentonites show the same mineralogy as that of the untreated bentonite except for the disappearance of the calcite peaks. The d(001) value of the smectite in the run products (14.7 Å) is significantly larger than that of the untreated bentonite (12.9 Å), indicating a change in the character of the interlayer cation(s). The STEM/AEM analyses on the treated bentonites reveal a significant increase in Ca and decrease in K, while other elements do not show detectable changes (Fig. 10). The identical characteristics of all run products indicates that pressure is not an important factor in the hydrothermal reaction of the bentonite.

360°C Run - The product of this run shows essentially the same characteristics as those of the 300°C runs; i.e., the absence of calcite peaks and the increase in d(001) value of the smectite (Fig. 11b). We suggest that the extensive exchange of Ca for K occurred in the smectite interlayer due to the increase in Ca

Table 5. Representative AEM analyses of two immiscible glasses

	1	2	3	4	5	6
SiO_2	29.8	30.0	77.5	65.6	36.2	32.0
TiO_2	6.4	6.8	1.0	0.9	1.0[+]	8.9
Al_2O_3	0.8	1.0	14.4	17.2	2.1	1.6
FeO*	47.4	43.1	1.9	3.1	34.2	36.4
MnO	0.7	0.4	nd	nd	0.4	tr
MgO	0.8	1.0	tr	tr	2.7	tr
CaO	10.3	11.0	1.5	3.7	15.9	14.4
Na_2O	nd[@]	nd	1.2	4.4	nd	nd
K_2O	tr[&]	tr	2.4	5.1	0.3	1.0
P_2O_5	3.2	5.7	nd	nd	7.3	5.7
SO_2	0.6	1.0	nd	nd	nd	nd
Cl	tr	tr	nd	nd	tr	tr
CIPW norms (wt%) for $Fe^{3+}/Fe^{2+}=0.1$)						
Q	-	-	57.3	12.0	-	1.5
or	-	-	14.2	30.2	1.6	5.8
ab	-	-	10.2	37.2	-	-
an	2.1	2.8	7.4	12.1	5.0	1.7
C	-	-	7.2	-	-	-
di	0.8	0.6	-	-	2.9	-
hd	24.2	12.0	-	5.6	19.9	29.0
en	0.6	2.0	-	-	5.0	-
fs	18.6	44.3	1.8	1.2	39.3	25.8
fo	25.5	4.0	-	-	1.7	-
mt	7.5	6.9	-	-	5.5	6.1
il	12.0	12.9	1.9	1.7	1.8	16.8
ap	7.5	13.5	-	-	17.1	13.3
py	0.5	0.7	-	-	-	-

1, 2: homogeneous globular glasses; 3, 4: matrix glasses;
5, 6: heterogeneous globular glasses.
*Total iron as FeO
[+]Ti concentrated outside the area analysed within the globule
[@]nd: not detected
[&]tr: only trace amount present

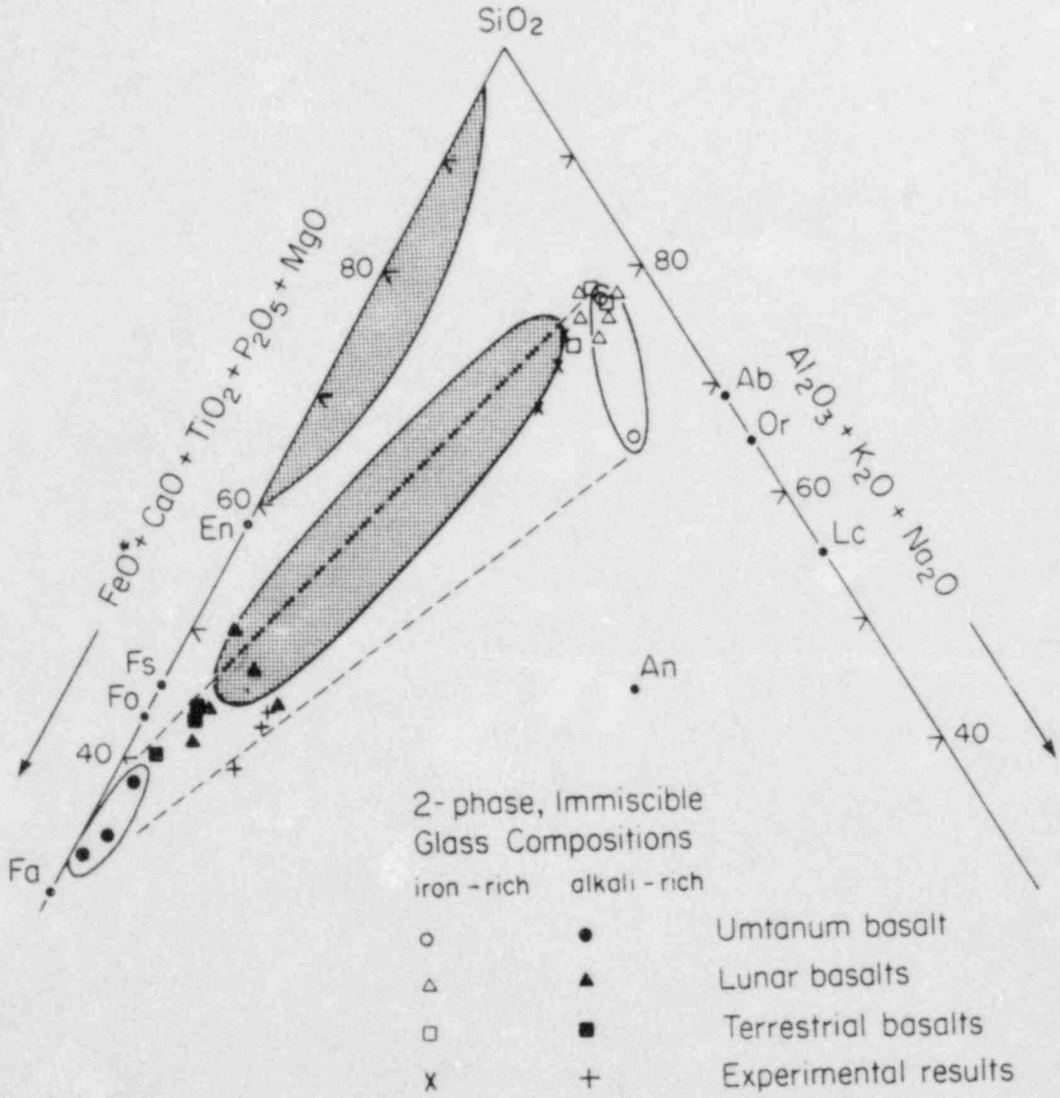

Figure 9. Triangular plot (in wt % oxides) of compositions of two immiscible glasses from Umtanum basalt in comparison to those of lunar and terrestrial basalts and to the experimentally determined immiscible gap (stippled area) in the simplified system, leucite-fayalite-silica.

Table 6. Conditions and results of hydrothermal experiments

Run #	T(^{o}C)	P(bars)	t(days)	R/F	Mineralogical changes
BN-C-32	300	350	91	2.25	disappearance of calcite Ca-K exchange in bentonite
BN-D-31	300	500	71	1.99	same as above
BN-A-35	300	800	70	1.86	same as above
BN685	360	300	96.5	0.36	same as above
BN454	460	300	92	0.45	disappearance of calcite formation of albite+quartz+ paragonite
IL-C-31	300	350	91	2.50	no detectable changes
IL-D-32	300	500	71	1.97	no detectable changes
IL-A-34	300	800	70	1.98	no detectable changes
IL680	360	300	96.5	0.42	appearance of kaolinite
IL455	460	300	92	0.52	appearance of kaolinite
BS-C-33	300	350	91	2.97	no detectable changes
BS-D-33	300	500	71	3.10	no detectable changes
BS-A-37	300	800	70	2.24	no detectable changes
BS681	360	300	96.5	0.54	appearance of smectite+ illite
BS450	460	300	92	0.47	appearance of smectite+ illite

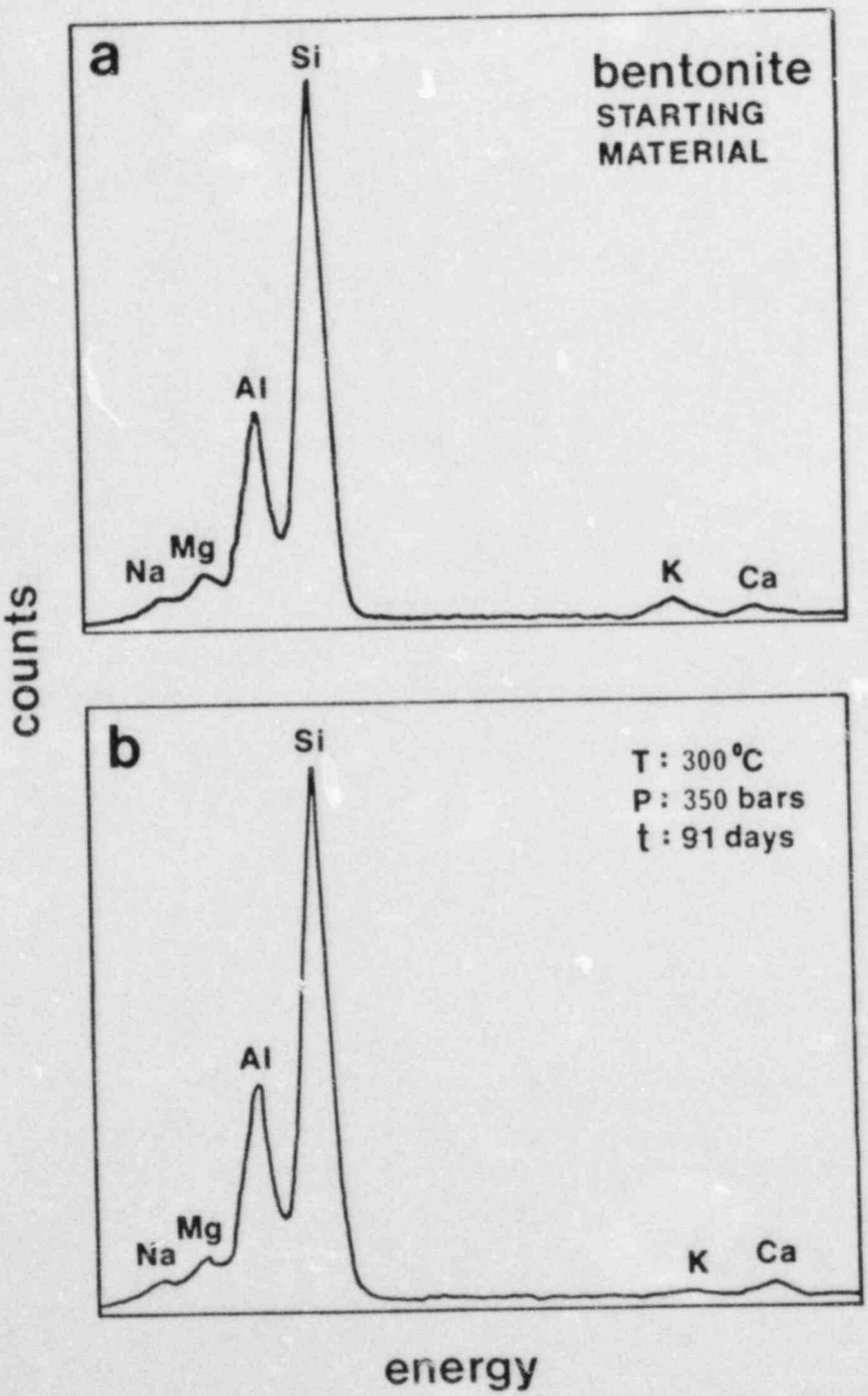

Figure 10. Energy dispersive X-ray spectra of bentonite for (a) starting material and (b) hydrothermally treated sample at 300°C and 350 bars for 91 days. The spectra show an increase in Ca and a decrease in K after the hydrothermal treatment.

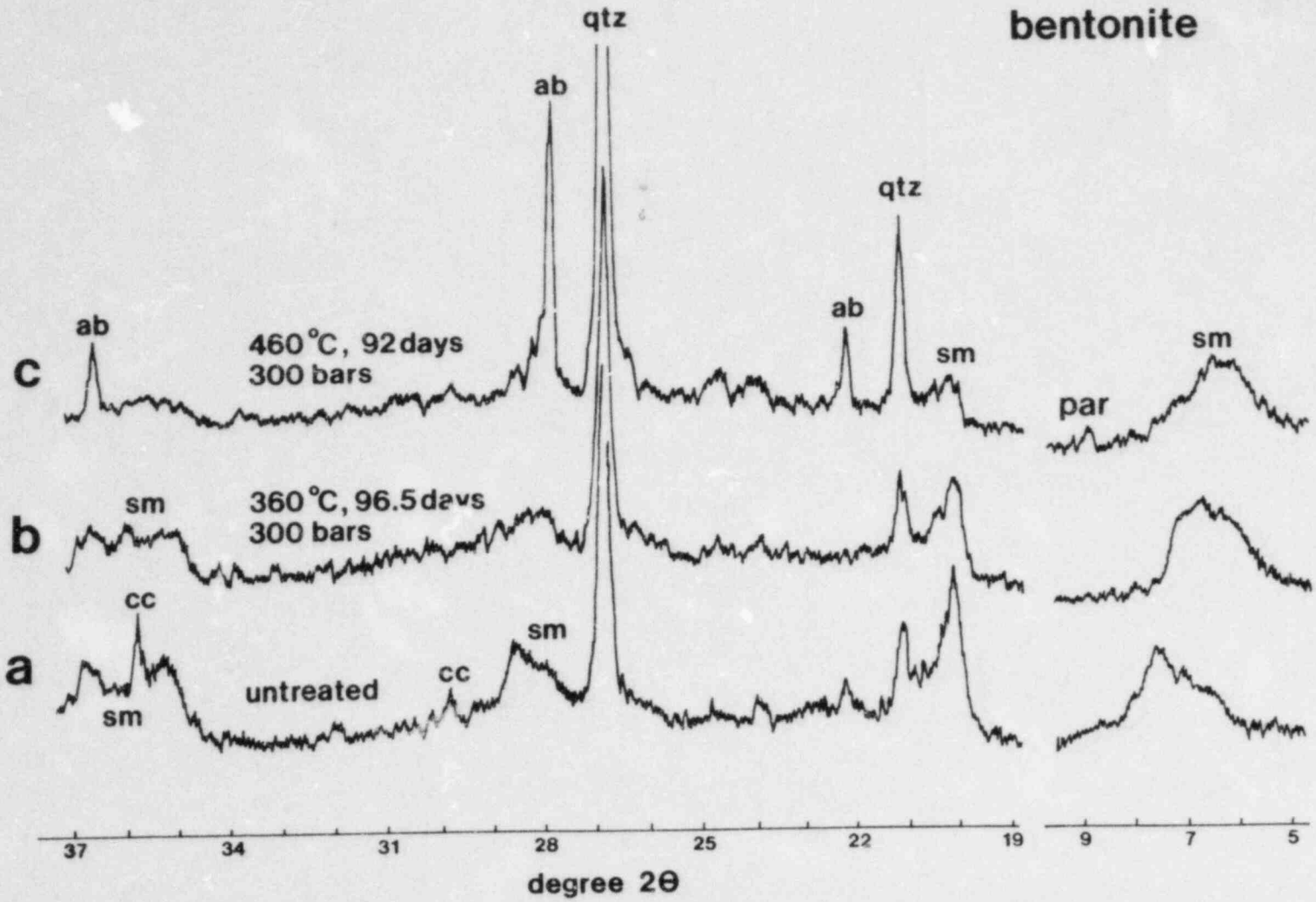

Figure 11. XRD patterns of bentonite; (a) starting material, and hydrothermally treated samples in two different run conditions; (b) 360°C, 300 bars, 96.5 days and (c) 460°C, 300 bars, 92 days.

concentration in the solution by calcite dissolution, whereas the structure of the smectite remained stable during the time period of the experiment.

460°C Run - The XRD pattern of this run product (Fig. 11c) shows the presence of strong albite peaks, an increase in the relative amount of quartz versus smectite, and the appearance of a 10 Å phyllosilicate. Because the original solution is rich in Na but poor in K, we suggest that this 10 Å phase is paragonite, a Na-rich mica, instead of illite.

Figure 12a shows the SEM images of the typical assemblage of the run product. Quartz occurs as recrystallized, euhedral aggregates masking the surface of the partially reacted smectite plate (Fig. 12b). Albite crystals are relatively coarse and are sparsely distributed. Paragonite (marked by the circles in Fig. 12a) is characterized by a platy morphology.

3.3.3.2.2 Illite

300°C Runs - All these products show identical XRD patterns which are essentially the same as that of the untreated illite. The patterns show the presence of quartz and feldspar as major impurities. The 001 peaks are broad and asymmetric to lower angles, indicating that the phyllosilicate crystals contain a significant fraction of interlayered smectite.

360 and 460°C Runs - Figure 13 shows the XRD patterns of these two runs with that of the starting material. The only noticeable difference is the appearance of a 7 Å phase in these run products. This phase may be septechlorite which is formed from smectite interlayered with illite, or kaolinite formed at the expense of feldspar. It appears that the relative amount of feldspar in the 460°C run is slightly smaller than that in the 360°C run and that in the starting material.

3.3.3.2.3 Basalt

300°C Run - There are no detectable differences between the treated basalts and the untreated basalt. The XRD patterns show dominant plagioclase (labradorite) as well as pyroxene and magnetite peaks.

360 and 460°C Runs - The only difference in XRD patterns between these two runs and that of the starting material is the appearance of a weak but definite 14 Å peak, indicating the production of smectite as an alteration product. This is confirmed by SEM observation in which feathery clay flakes are clearly observed (Fig. 14). Under TEM, however, both 10 Å (illite, Figs. 15a and 15b) and 14 Å (smectite, Fig. 15b) lattice fringe images were observed. The 10 Å phase, tentatively suggested as illite, occurs as discrete grains.

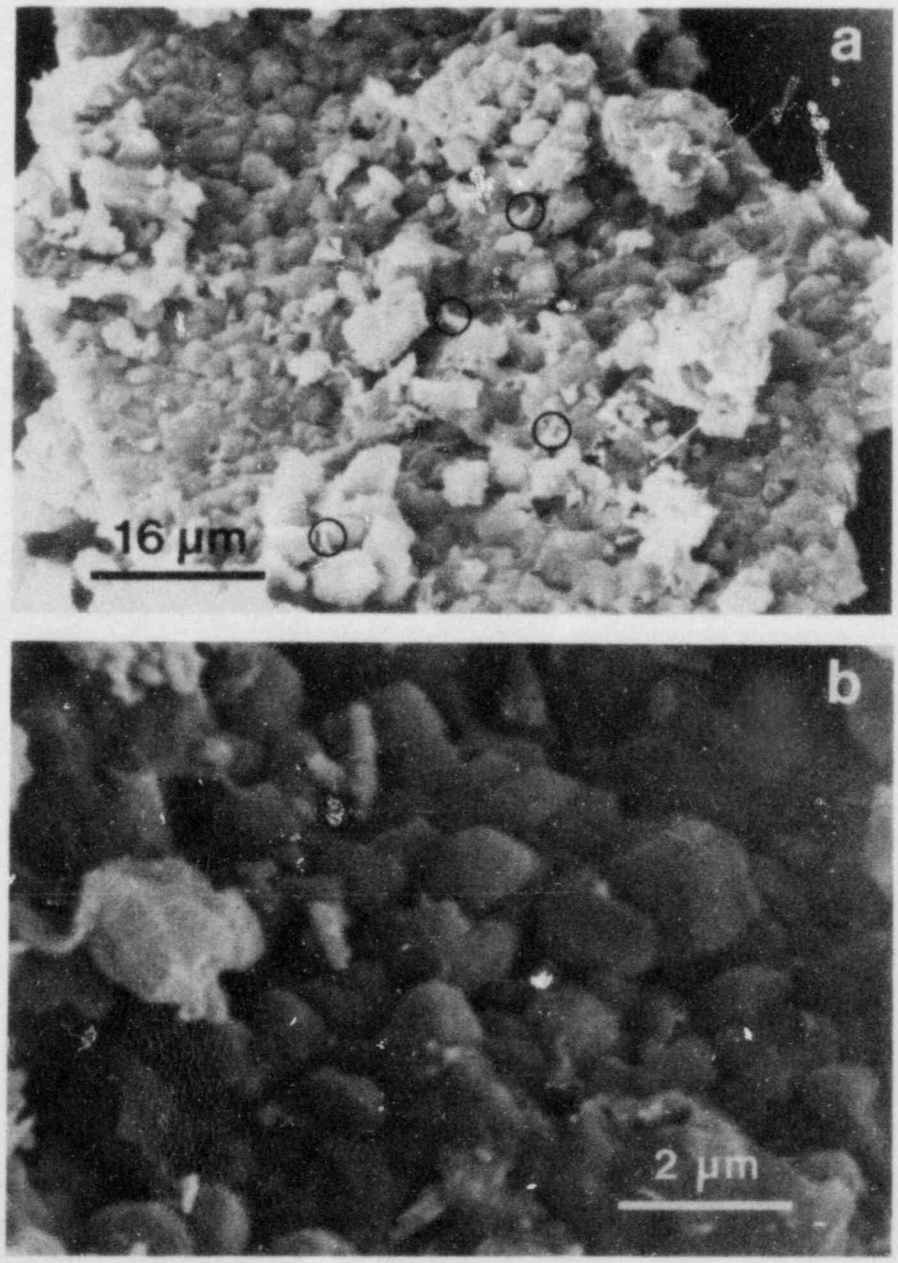

Figure 12. SEM photographs of run BN454 (bentonite, same sample as Fig. 11c). (a) Typical occurrence of quartz (grey), albite (white) and paragonite (marked by circles) on a smectite surface. (b) A detailed view of the same sample showing the morphology of crystallized aggregates of euhedral quartz.

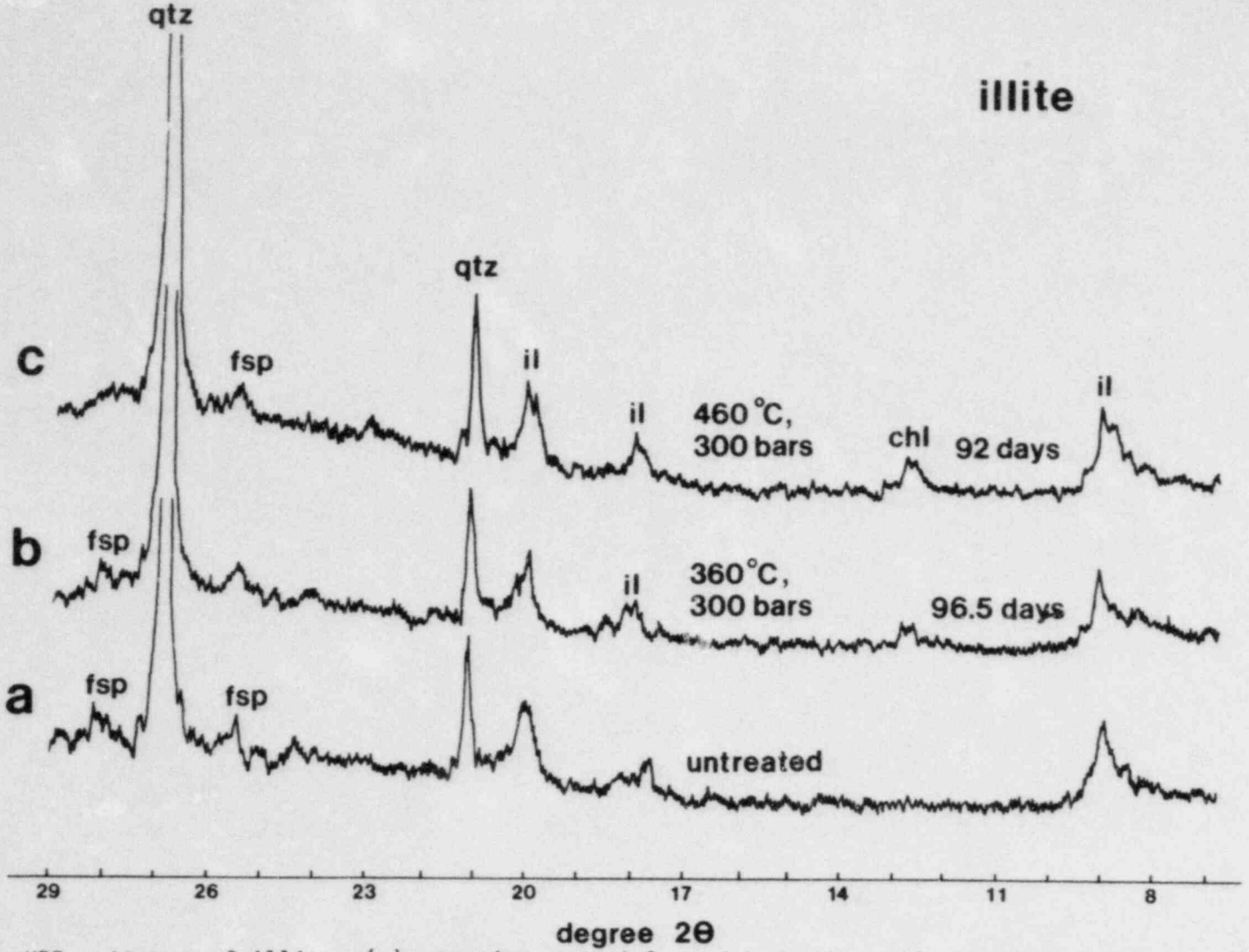

Figure 13. XRD patterns of illite: (a) starting material, and hydrothermally treated samples in two different run conditions; (b) 360°C, 300 bars, 96.5 days and (c) 460°C, 300 bars, 92 days.

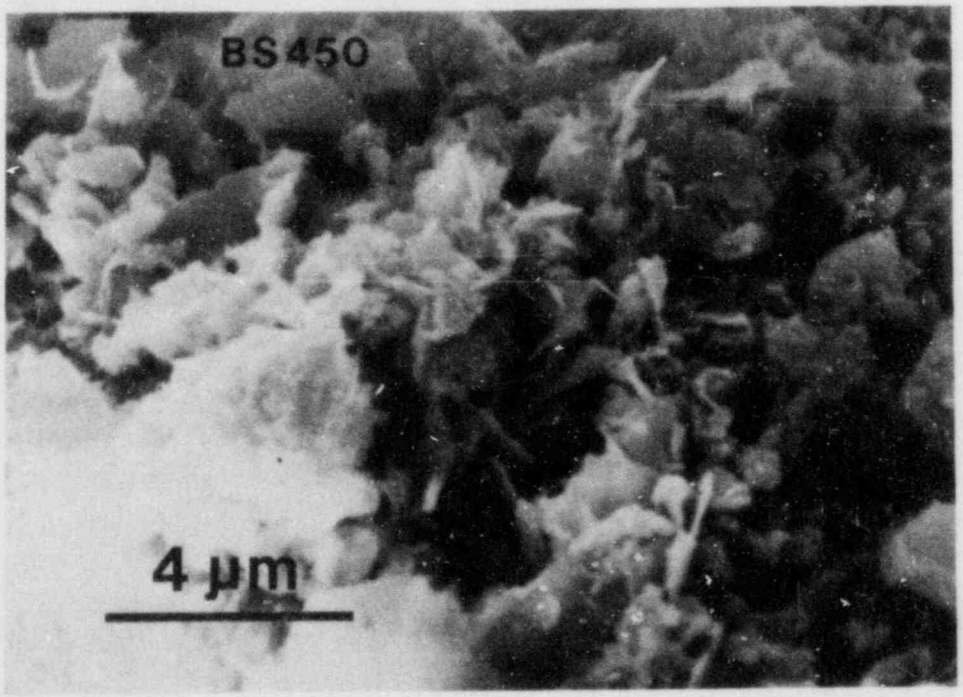

Figure 14. A SEM photograph of run BS450 (basalt, same sample as Fig. 13c) showing occurrences of clay minerals (flaky "feathers" at lower center).

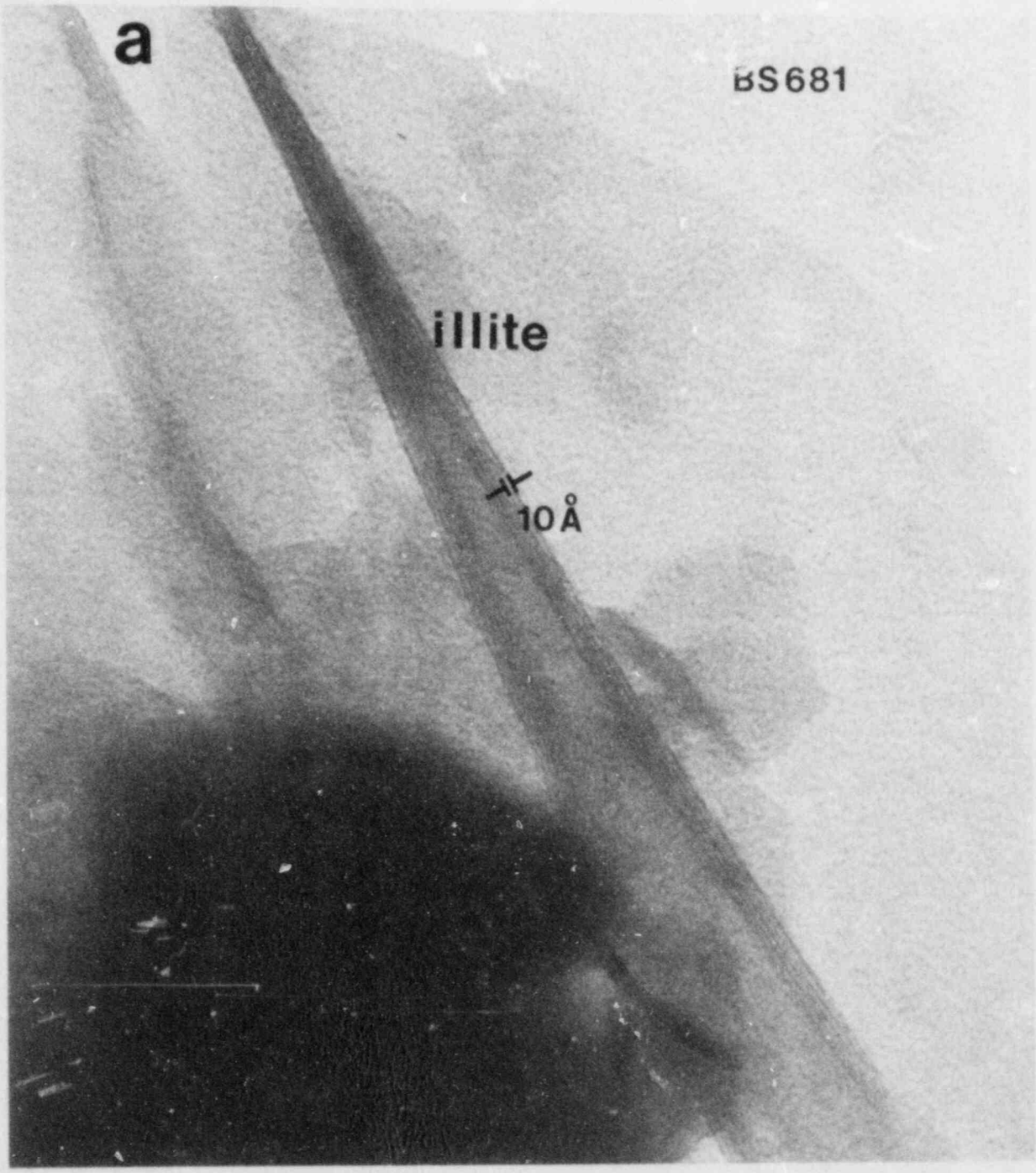

Figure 15a. A TEM image of a hydrothermally treated basalt sample at 360°C, 300 bars for 96.5 days. The figure shows lattice fringes of straight and continuous illite 001 layers (10 Å).

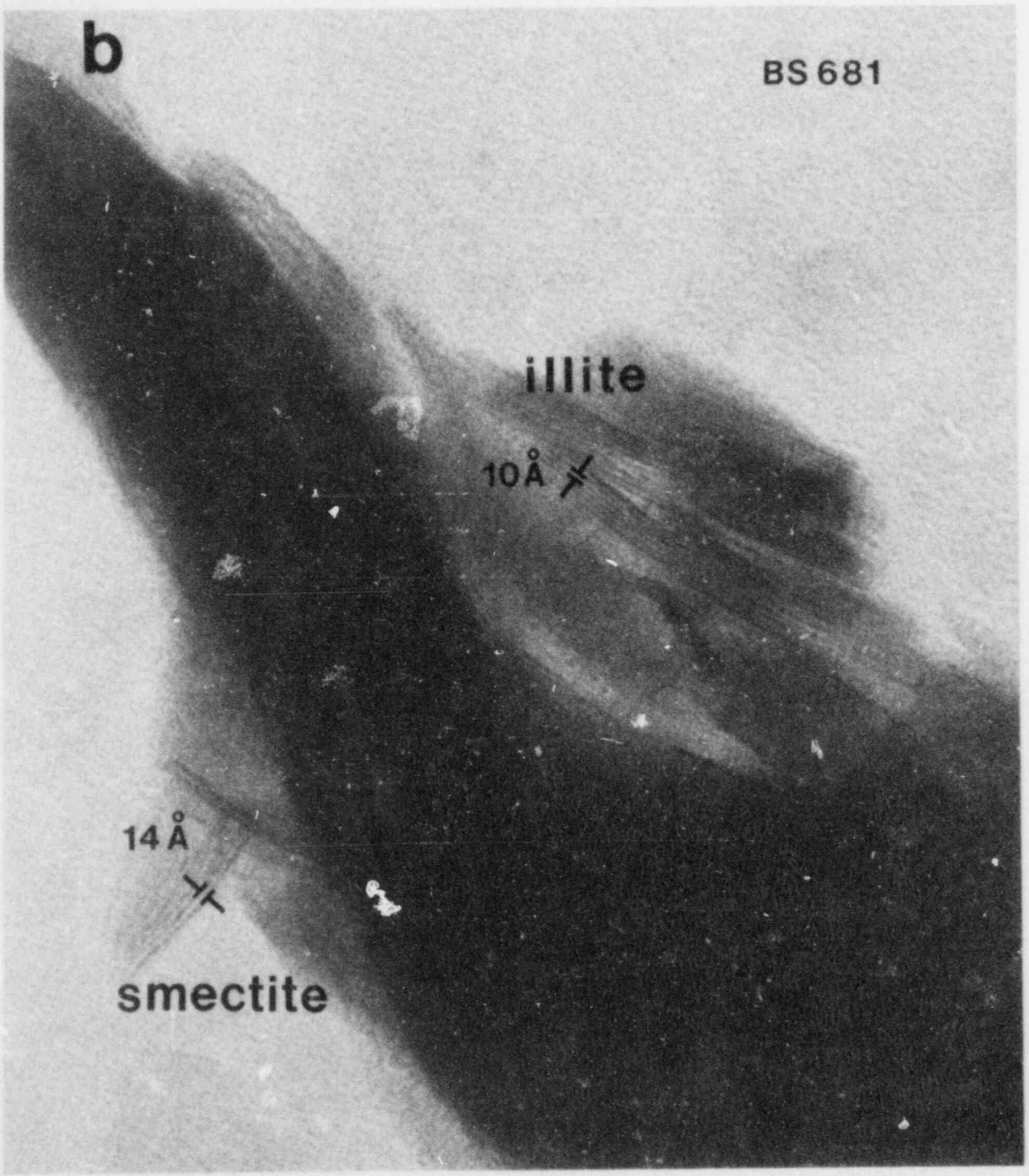

Figure 15b. A TEM image of the same sample as Figure 15a showing lattice fringes of 10 Å illite and 14 Å smectite layers. Illite layers are more regular and straight compared to smectite layers.

3.3.3.3 Geological Systems

Studies of diagenesis of sediments over the range of temperature (below 300°C) of the repository, focusing on the smectite/illite/muscovite transition, have been carried out emphasizing STEM/AEM techniques (all references to our work: Lee et al., 1982a, 1982b, 1983, 1984a, 1984b, 1984c; Lee and Peacor, 1983, 1984a; Ahn et al., 1983; Yau et al., 1983; Ahn and Peacor, 1984). Three sequences have been emphasized. These include an approximately 3000 m depth interval of Gulf Coast sediments and a transitional sequence of mudstone to slate in the Martinsburg Formation at Lehigh Gap, Pennsylvania. These sequences, when combined, represent a continuous sequence of diagenesis for temperatures up to approximately 250°C. As shown below, the changes in mineralogy apparently occur under closed system conditions; i.e., fluids are excluded by the impermeable clay matrix. By contrast, a sequence from the Salton Sea geothermal field represents a completely open system, with geothermal waters flowing through permeable sediments, with temperatures below approximately 300°C. These contrasting systems thus represent limiting cases in rock/fluid ratios relative to the repository conditions.

The changes that occur in the Gulf Coast diagenetic sequence were characterized by Hower et al. (1976). Smectite is the original detrital clay mineral at shallower depths. The major changes in mineralogy and chemistry which occur at the depth interval between 2000 and 3700 m are an increase in the illite proportion of mixed-layer I/S from 20 to 80%, a decrease of calcite from 20% to 0%, a decrease of K-feldspar to 0% and an increase of chlorite with increasing depth. However, the bulk chemical composition shows no major changes with depth except for a decrease in CaO concomitant with the decrease in calcite. On the other hand, the <0.1 μm fraction (virtually pure I/S) exhibits a large increase in K_2O, Al_2O_3 and a decrease in SiO_2, implying the reaction:

$$\text{smectite} + K^+ + Al^{3+} = \text{illite} + Si^{4+}.$$

The K and Al appear to be derived from the decomposition of K-feldspar (and mica) and the excess Si forms quartz. Below the 3700 m depth, no major changes in mineralogy and chemistry are observed.

TEM observations (Ahn, pers. comm.) using the same samples as in Hower et al. (1976) reveal the nature of the transitions. Transformation from smectite to illite in beginning stages at shallow depths occurs on a small scale. Illite layers appear as small domains (usually less than 100 Å, or 10 illite layers, in thickness) within smectite crystals (Fig. 16a). Smectite crystals are imperfect and irregular with a characteristic appearance of undulating and anastomozing layers with high concentrations of defects such as dislocations and general heterogeneities in both local chemistry and structure. Illite, in contrast, generally shows much more regular, straight and well crystallized structure layers. As the smectite to illite

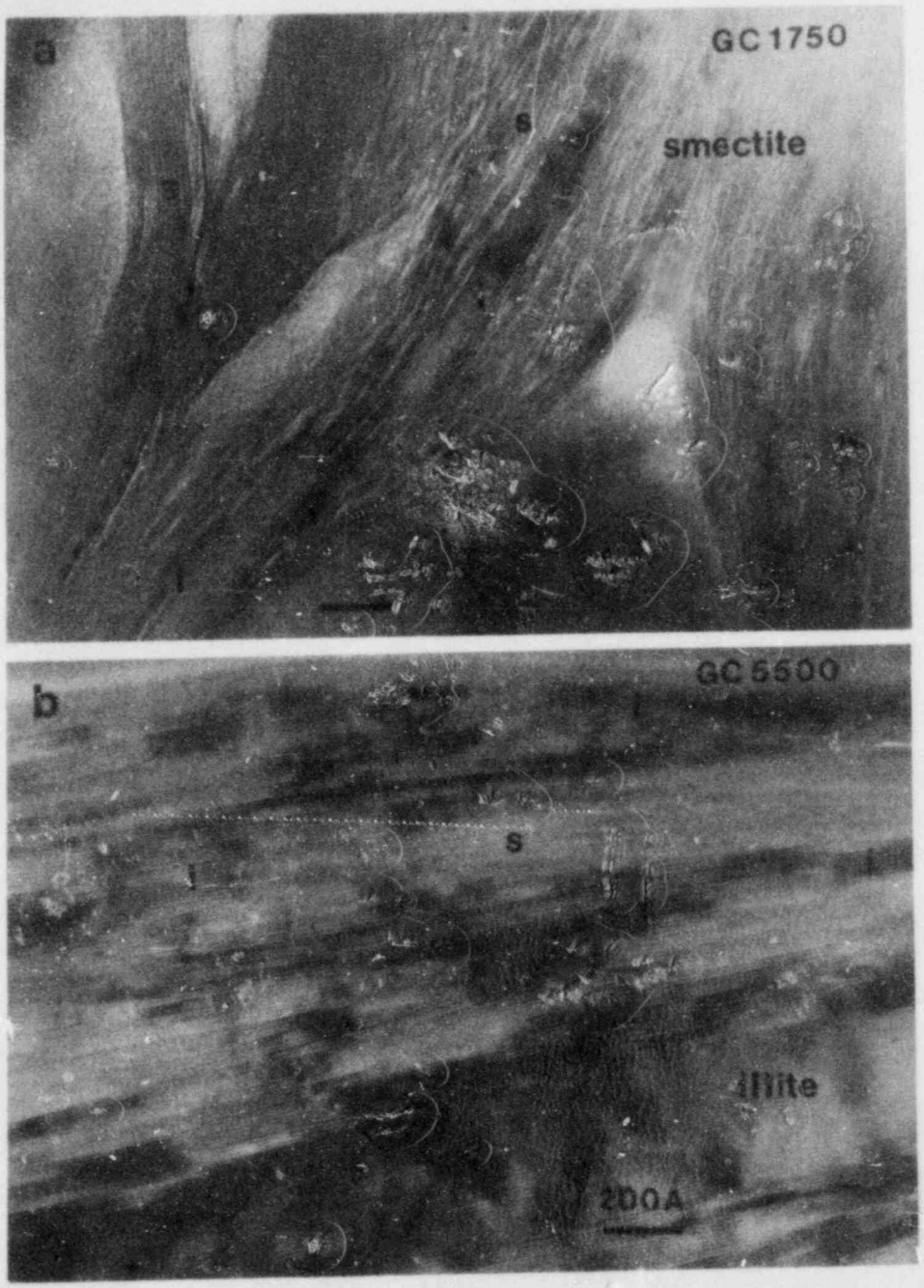

Figure 16. TEM lattice-fringe images of samples from Gulf Coast sediments at two different depths, (a) 1750 m and (b) 5500 m showing changes in smectite and illite layer proportions: (a) At 1750 m depth, smectite is dominant over illite. Smectite layers are characteristically very irregular and imperfect. Small packets of illite (i) occur within smectite. (b) At 5500 m depth, illite is the dominant mineral. The layers are relatively regular and well crystallized but show some imperfections along grain boundaries (packet boundaries) with mottled contrast feature. Smectite (s) is rare and shows very little contrast because it is easily damaged by the electron beam relative to illite. (photos from Lee et al., 1984a)

conversion proceeds in deeper sections, the domains of illite layers become thicker and longer and finally become dominant over smectite layers below 3700 m (Fig. 16b).

The Martinsburg Formation (Ordovician) at Lehigh Gap, Pennsylvania represents a diagenetic sequence whose least deformed rock corresponds to the deepest section of the Gulf Coast sequence (Wintsch, 1978; Lee et al., 1984a). The outcrop at Lehigh Gap displays a transition of rock type from mudstone to slate which is paralleled by a gradual development of slaty cleavage perpendicular to the original bedding (Holeywell and Tullis, 1975). The least deformed mudstone is at the contact with the overlying Shawangunk Formation. Illite and chlorite are the dominant clay-size minerals and no mixed-layer I/S is present in the outcrop. The Martinsburg Formation (approximately 4 km thick) is slate deformed by a tectonic event (post Silurian, after Epstein and Epstein, 1969). The occurrence of undeformed mudstone is due to a pressure shadow caused by the competent quartzitic Shawangunk Formation (Epstein and Epstein, 1969) and the release of strain by the fault (Wintsch, 1978). No major changes in bulk composition (Wintsch, pers. comm.) and in mineralogy (Lewis, 1980) occur across the entire sequence. XRD studies (Lewis, 1980) show that the mudstone to slate transition is associated with a transition of $1M_d$ illite toward well-crystallized, ordered muscovite.

STEM/AEM observations reveal the chemical, structural and textural changes in the clay minerals in three significant ways: 1) The change in illite polytypism ($1M_d$ to 2M) is paralleled by an increase in K and Al and a decrease in Si. The composition of illite in the slate is close to muscovite; 2) Illite layers in mudstone samples gener[illegible]ighly imperfect with small angle grain boundary-lik[illegible]es where structural defects (layer terminations [illegible]ocations) are concentrated (Fig. 17a). Such imperfect[illegible]crease in concentration as the transition to slate proceeds [illegible]. 17b); 3) Random interlayering between illite and chlorite occurs commonly in mudstones and intermediate samples but disappears in slate samples and changes to discrete packets of two different layers (Figs. 18a and 18b); 4) Kaolinite layers which occur, although only rarely, as packets interleaved with illite decrease in packet thickness and frequency with the mudstone to slate transition (Lee et al., 1984c). Chemical compositions of illite and chlorite analyzed by AEM are highly variable from one grain to another. This is probably in part due to a highly variable composition of their precursor (smectite).

The clay mineral rock-fluid reactions in the Gulf Coast sequence become apparent at a depth of approximately 2000 m and at the temperature of approximately 60°C (Hower et al., 1976). Most of the pore water had been expelled from the sediment by that depth (about 10% pore water remaining, after Burst, 1969) and the sediments were well lithified. Many of detrital minerals (calcite, mica, K-feldspar and most importantly smectite) underwent reactions under these changing conditions. Most of the components from the breakdown of the detrital minerals were actively redistributed within the system except Ca

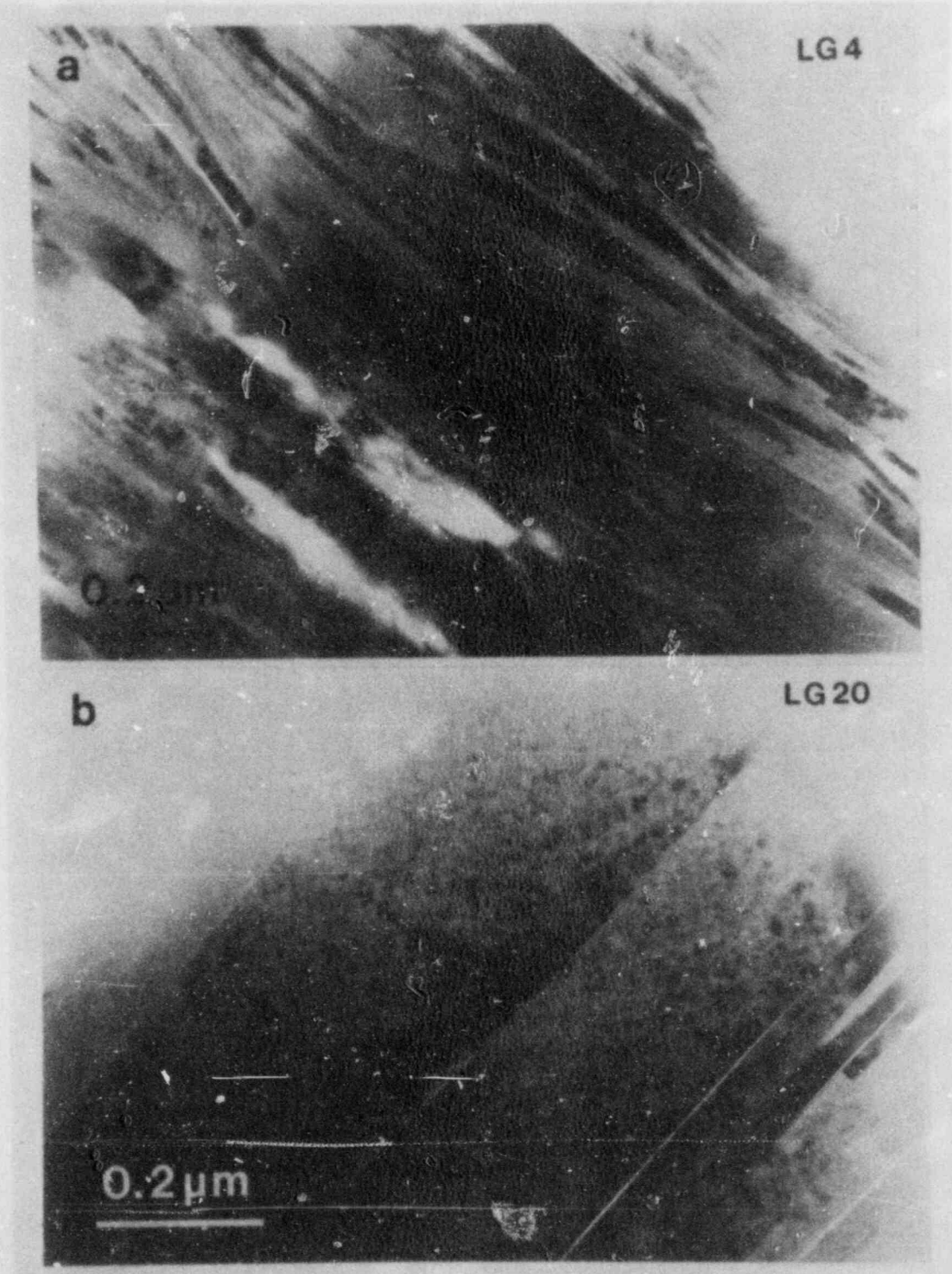

Figure 17. TEM images of samples from the Lehigh Gap outcrop showing changes in perfection of layer texture and structure in illite. Notice the increase in the thickness of layer packets and regularities along the packet boundaries from (a) mudstone near the Shawangunk-Martinsburg contact to (b) slate further (130 m) from the contact. There are parallel changes in composition, too (see text). (photos from Lee et al., 1984a)

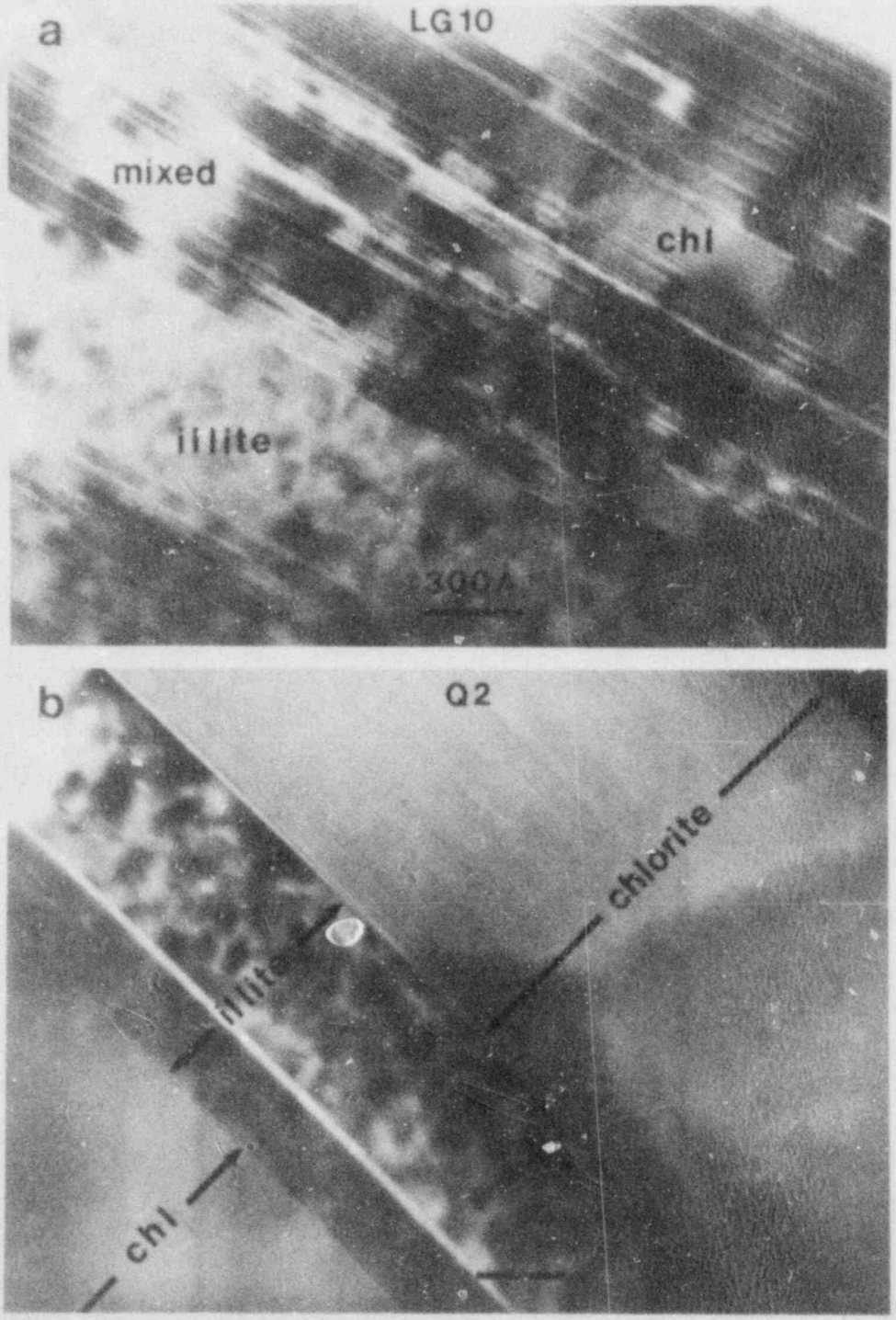

Figure 18. TEM lattice-fringe images of samples from the Lehigh Gap outcrop showing changes in illite-chlorite interlayering from (a) random interlayering in a sample closer to the Shawangunk-Martinsburg contact to (b) complete separation of the two minerals into well defined packets in slate samples. (photos from Lee et al., 1984b)

and water. Ca was completely expelled from the system while the pore water content decreased further (to around 5%) along with the interlayer water released by smectite dehydration. In a filtration experiment, Benzel and Graf (1984) showed that Ca passes through smectite membranes preferentially relative to Na. The K and Al from K-feldspar and mica react with smectite which is converted to illite and excess Si which forms quartz (Hower et al., 1976).

As the depth approaches 3700 m (approximately 110°C) conditions for the reactions are no longer favorable due apparently to lower permeability and lack of pore waters (about 5%, after Burst, 1969) relative to temperature conditions (110-170°C). At this stage, the reaction rate becomes too slow even in a geologic time scale (Burst, 1969). This is evidenced by the fact that most young diagenetic sequences (Tertiary) extend only to approximately 80% illite in mixed-layer I/S (Burst, 1969; Perry and Hower, 1970; Hower et al., 1976) while most Paleozoic sequences show no smectite or mixed-layer I/S (Velde and Hower, 1963; Maxwell and Hower, 1967). STEM and AEM data also indicate that the changes occur on a small scale and at a slow rate even in the depth interval with the active mineral reactions. Therefore, the systems have reached a point where reaction rate is so slow that no major change can be detected within 10-20 million years (Burst, 1969).

Compared to the Gulf Coast sediments, Lehigh Gap samples represent a higher degree of diagenesis with further dehydration evidenced by absence of smectite and lower Ca content (Wintsch, 1978) and by lack of changes in bulk chemistry (Wintsch, pers. comm.) and mineralogy (Lewis, 1980). From this and other evidence, it is inferred that the system was already closed at the time of deformation with a very low pore water content (around 5%, from Burst, 1969). Reactions in the Lehigh Gap system occurred very slowly on a local scale (only around 100's of Ångstroms: Lee et al., 1984c). Temperature in the sequence is estimated, although imprecisely, to have been 200-250°C (Epstein and Epstein, 1969; Lewis, 1980; Lee et al., 1984c), but isothermal throughout the outcrop (Lee et al., 1984c). Under these conditions, reactions in the Martinsburg Formation were promoted by tectonic compression to produce the regionally developed slaty cleavage. However, the reaction rates near the Martinsburg-Shawangunk contact were still too slow (due to a local lack of stress) to result in a transformation to slate and, as a consequence, a diagenetic sequence displaying a gradual transition from illite (mudstone) to muscovite (slate) was developed.

The Salton Sea geothermal field represents an extreme example of a diagenetic system. An unusually high geothermal gradient (over 300°C/km: Helgeson, 1968) and an actively circulating brine water (major elemental components, Cl, Na, K, and Ca: Muffler and White, 1969) promote reactions at shallow depths at an exceptionally rapid rate (Pliocene and Pleistocene sediments, after Muffler and Doe, 1968) compared to most other diagenetic systems (upper Cretaceous-lower Tertiary). Original detrital smectite transforms to mixed layer I/S with increasing

Figure 19. A TEM image of a sample from Salton Sea geothermal field (250 m depth) showing lath-shaped authigenic illite crystals. (Courtesy of Lancy Yau)

Figure 19

depth. In spite of their young age and shallow depth, the mixed-layer I/S goes through a complete conversion from 70% to 100% illite at around 250°C (at 500 m depth). However, with increasing depth, a second kind of illite increases in proportion (Fig. 19). This illite is authigenic; i.e., it forms by direct precipitation from circulating brines, as dramatically contrasting with the relatively passive conversion of smectite to illite in closed systems such as the Gulf Coast argillaceous sediments. TEM images show growing crystals, abundant pore space and other features compatible with massive chemical exchange through the medium of the circulating brines. Nevertheless, mixed-layer I/S extends to depths with temperatures of up to 200°C, and illite fails to convert to muscovite at temperatures up to 250°C.

In summary, these geological systems indicate the following relations concerning smectite/illite/muscovite transitions in relation to repository conditions:

(1) Argillaceous sediments such as Gulf Coast shales generally act as nearly closed systems; i.e., when compacted through burial, the clay fabric forms a closed network which effectively forms a barrier to fluid flow. Even at the highest levels of TEM resolution we fail to see pore space in such sediments.

(2) The smectite to illite to muscovite transitions are kinetically controlled, with active water flow through permeable rocks greatly increasing reaction rate. The effect may be more significant than that of temperature, although both factors are significant. For the Lehigh Gap transitions, temperature was constant (approximately 200-250°C) across the entire sequence for geological times. The entire range from illite to muscovite is still present, however. That is, even though smectite, I/S and illite are unstable relative to muscovite (given the necessary ions in solution) these phases may be retained in geological systems, with smectite or I/S retained up to 150 and 200°C, respectively and illite up to approximately 300°C.

(3) STEM studies show that the transitions involve three factors: a) Addition of K; b) Substitution of Al for Si; c) Reconstruction of entire layers or packets of layers of structure. That is, smectite does not transform to illite only by substitution of K. The Al/Si ratio and other structure bonds must be broken with at least small units of structure undergoing local solution/recrystallization. Such processes are inherently sluggish. They therefore require that the rate of smectite to illite transition is basically sluggish. This explains why unstable clays such as I/S may be retained at elevated temperatures even over geological time periods.

3.3.4 CONCLUSIONS

3.3.4.1 Characterization of Backfill Materials

All three potential backfill materials studied have been found to be extremely heterogeneous. The two clays, bentonite and illite, are heterogeneous in two ways: (1) The clay minerals are compositionally variable in both dioctahedral and trioctahedral components, and have variable structure and texture, as shown by TEM. (2) Additional mineral phases are present, making up a major part of the illite, in particular. The basalt is mineralogically heterogeneous by definition, but has the disadvantage of containing an interstitial glass phase which constitutes up to 25% of the rock. Furthermore, the glass is two-phase, one component being relatively K-rich.

Heterogeneity in phases causes groundwater/backfill systems to be complex in chemistry and properties, such that they cannot be modeled solely on the assumption of the presence of single mineral phase. Natural geologic systems are, therefore, especially significant as analogues because they are chemically, mineralogically and structurally similar.

As concluded below, all potential mineral phases are metastable and reactive in the backfill environment, with reaction states being dependent on kinetic factors. Because glass is far and away the least stable phase, and as it may contribute K^+ to reacting groundwater which may in turn affect such phases as smectite, its presence should be entirely avoided. The basalt should not be used as a backfill material. Rather, a diabase, which is mineralogically and chemically similar to the basalt but which contains no glass, should be used.

3.3.4.2 Analogous Geological Systems

Smectite (bentonite), when deposited in sediments and progressively buried by overlying sediments, is subjected to increasing temperature and reactions involving pore fluids, as postulated for a repository. It undergoes a continuous series of transformations to mixed-layer I/S, to illite and finally to muscovite. All except the latter are metastable phases. The degree of reaction is determined by kinetic factors.

Nevertheless, smectite is observed to commonly be preserved at temperatures up to approximately 150°C, mixed-layer I/S to 200°C and illite up to at least 250°C. This occurs despite the availability of pore solutions over geologic time periods, measured in millions of years.

The rate-determining factor is not substitution of K in smectite interlayer sites. The transformations involve Al/Si bond breaking and diffusion, with local reconstruction of crystal structures and are, therefore, sluggish. Metastable phases, therefore, persist in the geological environment. Data on synthetic conversion rates confirms these relations.

A critical factor in the geologic systems where phases are retained is that they apparently act as closed systems, being

largely impermeable to fluid flow. Even at the TEM level, pore space is not observed. This is caused by the presence of a high proportion of clay minerals forming, when compacted, a continuous structural network. Thus it is essential that backfill materials including clays have: (1) a high proportion (greater than 50%) of clay, (2) a low proportion of granular material (e.g., basalt) which must, in turn, be as fine-grained as possible. Large non-clay mineral grains interrupt the impermeable clay network, (3) a high degree of compaction.

3.3.4.3 Hydrothermal Experiments

All of our synthetic experiments which have taken place at 300°C or below have shown virtually no change. Only calcite dissolution and cation exchange in smectite have been observed. Dramatic changes occur at higher temperatures, however. These observations and those of other experimentors who observed changes at 300°C and below are consistent with the fact that all phases are metastable at all conditions, but that reaction progress is controlled by kinetic factors; e.g., cation exchange and calcite dissolution are processes with low activation energies that occur readily even near room temperature. However, reaction involving transitions in clay structures are sluggish. Data on the natural geologic systems are therefore critical in determining the effect of temperature, rock/water ratios and other factors affecting reaction kinetics.

The bentonite experiments, however, imply that Ca present in solution will buffer substitution of K in smectite and therefore retard transformation to illite. Addition of limestone to the backfill may give rise to sufficient Ca to retard transformation.

3.3.4.4. Additional General Conclusions

Because the transitions from smectite to mixed-layer I/S to muscovite involve phases which are metastable (except for muscovite) and because reactions are kinetically controlled, the rates of transition must be greater for the least transformed phases. Thus smectite is most reactive and illite least reactive. The phase chosen as a backfill material should therefore be as near to muscovite as possible, for any given repository temperature. Mixed-layer I/S (so-called Fithian illite) is significantly advanced in the transition sequence but still retains significant expansion properties, and should therefore be preferable to smectite. From the point of view of relative phase stabilities and reaction rates illite is preferable to mixed-layer I/S and bentonite (smectite) is the poorest choice. These preferences assume a repository temperature of 300°C, however. If temperatures could be maintained as low as 200°C, then reaction rates for mixed-layer I/S are nil, and smectite may even remain little changed. If clay minerals are used as backfill materials, every attempt should be made to minimize the temperatures to which they are subjected.

3.3.5 RECOMMENDATIONS

Our studies of the ultrastructure of argillaceous sediments in the Gulf Coast (closed system) and Salton Sea (open system) demonstrated the mechanism by which such sediments may be impermeable to fluid flow. The required network of clay minerals ("megacrystal") forms only where; (1) significant compaction occurs, coupled with recrystallization across parallel grain boundaries, (2) the size of the non-clay grains is not so large as to interrupt the clay network, (3) the proportion of non-clay minerals is not too high. Because the rates of reaction of metastable phases such as smectite are critically dependent on rock/fluid ratios, it is essential to minimize permeability by optimizing the above three parameters.

The temperatures up to which smectite, mixed-layer I/S and illite remain unreacted are (very approximately) 150, 200 and 300°C, respectively. Their detailed rates of reaction as a function of temperature and rock/fluid ratios are still not well known. Given data on permeabilities of actual clay-containing backfill materials, such rates should be determined as a function of temperature, using, for example, solutions of natural composition. Present, best estimates of reaction rates are from geological data but it is essential that realistic experimental values be obtained for the actual backfill material in a physical state of agglomeration (permeability) matching the actual repository material.

Furthermore, given the relative stabilities of smectite, mixed-layer I/S and illite, much improved estimates of the peak temperatures to which the backfill will be submitted must be obtained. The current figure (300°C) is a "guesstimate." If the actual peak temperature is significantly lower, then smectite becomes a viable backfill material. It is essential to refine the estimate of temperature variation with time.

The available thermochemical data on clay minerals is inaccurate and virtually useless for calculating phase relations, or rates of reactions. Models based on such data are questionable at best. Because reaction rates are so slow at the temperature conditions of the repository, the effects of change may not be clear even using STEM techniques applied to experimental materials from year-long experiments. Accurate thermochemical data on well characterized phases would permit calculation of phase relations which could then be used to supplement both the experimental and geologic parameters.

Our characterization using STEM/AEM techniques of both starting and product phases has permitted us to detect characteristics of starting materials and changes in those materials which are of great significance to repository properties. Such characterization has been lacking in many experiments involving backfill materials. Because conclusions regarding phases are useful only insofar as they reflect a specific material in a specific state, it is essential that complete characterization of materials be carried out, and that standard materials be used in all experiments; i.e., if a specific bentonite such as "Envirogel" is completely

characterized, some other material should not be utilized as it may be very different. Complete characterization up to the level of STEM/AEM analysis is essential.

3.3.6 PLANNED RESEARCH

All of the proposed backfill materials are metastable under the repository conditions. Reactions to products which are more stable are controlled by kinetic factors with reaction progress being time dependent. The short times (90 days) which have been used for the duration of our past experiments have not been sufficient to cause significant changes in the starting materials at repository temperatures. We are, therefore, currently carrying out a series of long term, one year experiments, at temperatures up to 300°C with variable rock/fluid ratios (Table 7). These experiments should provide optimum conditions for transitions in starting materials and provide quantitative data on the relative effects of temperature and fluid/rock ratio in promoting reaction rates. These materials will be characterized completely by STEM/AEM techniques to determine the extent of even the smallest transitions, which when extrapolated over the life of the repository, may significantly effect repository conditions. Experiments of one year duration are the longest that can reasonably be carried out. If changes are detected, they will provide a reasonable basis for extrapolations to longer times.

We are also carrying out experiments on basalt-bentonite mixtures (Table 7). Such a mixture is a prime candidate for a backfill material. Although our previous and present experiments provide data on those systems with a single starting material, this represents our initial attempt to extrapolate those data to more complex systems. Such a system has no natural geologic analogue, and experimental data are, therefore, especially significant.

Lastly, many of the experimental products which we have already processed are still only partially characterized; that is, detailed STEM/AEM data remains to be obtained for several experimental runs in order to determine the nature of transitions that may have occurred, but which were not detected by standard XRD and other techniques of characterization.

3.3.7 ACKNOWLEDGEMENTS

We thank Dr. Donald Alexander (U. S. Nuclear Regulatory Commission) for his enthusiastic encouragement and helpful suggestions during the course of this study. Valuable discussions with Dr. Martin Seitz and Dr. Rex Couture (Argonne National Laboratory) are appreciated. Thanks are due Dr. Lawrence Allard and his technical group (University of Michigan) for their efforts in maintaining the electron microanalytical facilities, and Mr. Jung-Ho Ahn, Mr. Carl Henderson, Ms. Susan Penoyar, and Dr. Alan Treiman for their assistance in various

Table 7. Hydrothermal experiments in progress.

Run No.	T (^{o}C)	R/F ratio	starting material	proposed time
BN571	300	0.86	bentonite	1 year
BN780	300	0.36		
BN282	300	0.20		
BN802	300	0.11		
BN384	200	0.57		
BN181	200	0.31		
BS570	300	0.92	basalt	
BS786	300	0.37		
BS284	300	0.22		
BS807	300	0.10		
BS388	200	0.57		
BS187	200	0.27		
IL572	300	0.95	Illite	
IL783	300	0.43		
IL281	300	0.20		
IL805	300	0.11		
IL389	200	0.81		
IL184	200	0.43		
BB-41	300	0.97	bentonite (25%) + basalt (75%)	5 months
BB-44	300	0.11		
BB-62	400	0.48		3 months
BB-69	400	0.17		

All experiments at 300 bars total pressure

parts of this research. Mr. Jung-Ho Ahn and Ms. Lancy Yau are gratefully acknowledged for providing their unpublished research data relating to natural systems.

3.3.8 REFERENCES

Ahn, J. H., Peacor, D. R. (1984) The TEM and AEM characterization of chlorite diagenesis in Gulf Coast argillaceous sediments. In submission to Clays Clay Miner.

Ahn, J. H., Lee, J. H., Peacor, D. R. (1983) Mineralogical and textural transitions in phyllosilicates during burial diagenesis of Gulf Coast shales (abstr.). Geol. Soc. Amer. Abstr. Progr., 15, 512.

Allard, L. F., Blake, D. F. (1982) The practice of modifying an analytical electron microscope to produce clean X-ray spectra. In: Heinrich (ed) Microbeam Analysis, 1982, San Francisco Press, 8-19.

Allpress, J. G., Hewat, E. A., Moodie, A. F., Sanders, J. V. (1972) n-beam lattice image. I. experimental and computed images from $W_4Nb_{26}O_{77}$: Acta Cryst., A28, 528-536.

Anderson, J. S. (1978) Lattice imaging by high resolution electron microscopy. The role of high resolution electron microscopy in solid state chemistry. Proc. Indian Acad. Sci., 87A, 295-329.

Apted, M. ..., Myers J. (1982) Comparison of the hydrothermal stability of simulated spent fuel and borosilicate glass in a basaltic environment. Rockwell Hanford Operations, RHO-RW-ST-38 P, 101 p.

Artru, P., Dunoyer de Segonzac, G., Combaz, A., Giraud, A. (1969) Variations d'origine sedimentaire et evolution diagenetique des caracteres palynologiques et geochimiques des Terres Noires jurassiques en direction de l'Arc Alpin (France, sud-set). Bull. Centre Rech. Pau-SNPA, 3, 357-376.

Artru, P., Gauthier, J. (1968) Evolution geometrique et diagenetique d'une serie miogeosynclinale (Lias inferieur a Berriasien) d'apres l'etude du sondage de Valvigneres (France sud-est). Bull. Centre Rech. Pau-SNPA, 2, 101-116.

Benzel, W. M., Graf, D. L. (1984) Studies of smectite membrane behavior: importance of layer thickness and fabric in experiments at 20°C. Geochim. Cosmochim. Acta, In press.

Bischoff, J. L., Dickson, F. W. (1975) Seawater-basalt interaction at 200°C and 500 bars: implications for origin of sea-floor heavy-metal deposits and regulation of seawater chemistry. Earth Planet. Sci. Lett., 25, 385-397.

Blake, D. F., Allard, L. F., Peacor, D. R., Bigelow, W. C. (1980) "Ultra-clean" X-ray spectra in JEOL JEM-100CX. Proc. Elect. Micro. Soc. Amer., 38th Meeting, 136-137.

Blake, D. F., Isaacs, A. M., Kushler, R. H. (1983) A statistical method for the analysis of quantitative thin-film X-ray microanalytical data. J. Micros., 131, Part 2, 249-255.

Blake, D. F., Peacor, D. R. (1981) Biomineralization in crinoid echinoderms: characterization of crinoid skeletal elements using TEM and STEM microanalysis. SEM/1981, III, 321-328.

Boles, J. B., Franks, S. G. (1979) Clay diagenesis in Wilcox Sandstones of southwest Texas: implications of smectite diagenesis on sandstone cementation. J. Sed. Petrol., 49, 55-70.

Bonatti, E. (1975) Metallogenesis at oceanic spreading centers. Ann. Rev. Earth Planet. Sci., 3, 401-431.

Burst, J. F., Jr. (1959) Postdiagenetic clay mineral environmental relationships in the Gulf Coast Eocene. Clays Clay Miner., Proc. 6th Natl. Conf., 327-341.

Burst, J. F., Jr. (1969) Diagenesis of Gulf Coast clayey sediments and its possible relation to petroleum migration. Amer. Assoc. Petroleum Geol. Bull., 53, 73-93.

Carrigy, M. A., Mellon, G. B. (1964) Authigenic clay mineral cements in Cretaceous and Tertiary sandstones of Alberta. J. Sed. Petrol., 34, 461-472.

Cliff, G., Lorimer, G. W. (1972) The quantitative analysis of thin metal foils using EMMA-4 -- The ratio technique. Proc. 5th Europ. Conf. Electron Micros. Inst. Physics, London, 140-141.

Cliff, G., Lorimer, G. W. (1975) The quantitative analysis of thin specimens. J. Micros., 103, 203-207.

Crovisier, J. L., Thomassin, J. H., Juteau, J., Eberhart, J. P., Touray, J. C., Baillif, P. (1983) Experimental seawater-basaltic glass alteration at 50°C: study of early developed phases by electron microscopy and X-ray photoelectron spectrometry. Geochim. Cosmochim. Acta, 47, 377-387.

Dunoyer de Segonzac, G. (1964) Les argiles du Cretace superieur dans le bassin de Douala (Cameroun): Problemes de diagenese. Bull. Serv. Carte Geol. Alsace Lorraine, 17, 287-310.

Dunoyer de Segonzac, G. (1969) Les mineraux argileux dans la diagenese; passage au metamorphisme. Mem. Serv. Carte Geol. Alsace Lorraine, 29, 320 p.

Dunoyer de Segonzac, G. (1970) The transformation of clay minerals during diagenesis and low-grade metamorphism: a review. Sedimentology, 15, 281-346.

Dunoyer de Segonzac, G., Artru, P., Ferrero, J. (1966) Sur une transformation des mineraux argileux dans les "terres noires" du bassin de la Durance: influence de l'orogenie alpine. C. R. Acad. Sci., Ser. D, 262, 2401-2404.

Eberl, D. (1978) The reaction of montmorillonite to mixed-layer clay: the effect of interlayer alkali and alkaline earth cations. Geochim. Cosmochim. Acta, 42, 1-7.

Eberl, D., Hower, J. (1976) Kinetics of illite formation. Geol. Soc. Amer. Bull., 87, 1326-1330.

Eberl, D., Hower, J. (1977) The hydrothermal transformation of sodium and potassium smectite into mixed-layer clay. Clays Clay Miner., 25, 215-227.

Epstein, J. B., Epstein, A. G. (1969) Geology of the Valley and Ridge province between Delaware Water Gap and Lehigh Gap, Pennsylvania. In: Subitzky, Seymour (ed.) Geology of selected areas in New Jersey and eastern Pennsylvania and guide book of excursions, New Brunswick, New Jersey, Rutgers Univ. Press, 132-205.

Eslinger, E. V., Savin, S. M. (1973) Oxygen isotope geothermometry of the burial metamorphic rocks of the Precambrian Belt Supergroup, Glacier National Park, Montana. Geol. Soc. Amer. Bull., 84, 2549-2560.

Ferguson, J. E. (1982) Inorganic Chemistry and the Earth. Pergamon Press, 400 p.

Foscolos, A., Kodama, K. (1974) Diagenesis of clay minerals from lower Cretaceous shales of northeastern British Columbia. Clays Clay Miner., 32, 319-336.

Frey, M. (1969) Die Metamorphose des Keupers vom Tafeljura bis zum Lukmaniergebiet. Beitr. Geol. Karte Schweiz., 137, 161 p.

Frey, M. (1970) The step from diagenesis to metamorphism in pelitic rocks during Alpine orogenesis. Sedimentology, 15, 261-279.

Gavrilov. A. A. and Alexandrova, V. A. (1968) Postsedimentation argillitization in Paleozoic clastic deposits of the southern Urals and northern Mugodzhars. Dokl. Acad. Sci. U.S.S.R., Earth Sci. Sect. (transl. from Dokl. Akad. Nauk S.S.S.R.), 182(5), 178-180.

Goldstein, J. I., Costley, J. L., Lorimer, G. W., Reed, S. J.

B. (1977) Quantitative X-ray microanalysis in the electron microscope. In: Johari (ed.) IITRI Chicago, Ill., 1, 315-324.

Hajash, A., Chandler, G. W. (1981) An experimental investigation of high-temperature interactions between seawater and rhyolite, andesite, basalt, and peridotite. Contrib. Miner. Petrol., 78, 240-254.

Helgeson, H. C. (1968) Geologic and thermodynamic characteristic of the Salton Sea geothermal system. Amer. J. Sci., 266, 129-166.

Hiltabrand, R. R., Farrell, B. E., Billings, G. K. (1973) Experimental diagenesis of Gulf Coast argillaceous sediment. Amer. Assoc. Ptroleum Geol. Bull., 57(2), 338-348.

Holeywell, R. C., Tullis, T. E. (1975) Mineral reorientation and slaty cleavage in the Martinsburg Formation, Lehigh Gap, Pennsylvania. Geol. Soc. Amer. Bull., 86, 1296-1304.

Hosterman, J. W., Wood, G. H., Jr., Bergin, M. G. (1970) Mineralogy of underclays in the Pennsylvania anthracite region. U.S. Geol. Surv. Prof. Pap., 700-C, 89-97.

Hower, J., Eslinger, E. V., Hower, M. E., Perry, E. A. (1976) Mechanism of burial and metamorphism of argillaceous sediment: 1. mineralogy and chemical evidence. Geol. Soc. Amer. Bull., 87, 803-810.

Humprhis, S. E., Thompson, G. (1978) Hydrothermal alterations of oceanic basalts by seawater. Geochim. Cosmochim. Acta, 42, 107-126.

Isaacs, A. M., Brown, P. E., Valley, J. W., Essene, E. J., Peacor, D. R. (1981) An analytical electron microscopic study of a pyroxene-amphibole intergrowth. Contrib. Miner. Petrol., 77, 115-120.

Karpova, G. V. (1966) On paragonite hydromicas in terrigenous rocks of the Great Donets Basin. Dokl. Akad. Nauk S.S.S.R., 171, 443-445.

Karpova, G. V. (1967) Muscovite hydromicas in coal-bearing polyfacies deposits. Lithol. Miner. Resourc. (transl. from Litol. Polezn. Iskop.), 1967, 688-697.

Karpova, G. V. (1969) Clay mineral post-sedimentary ranks in terrigenous rocks. Sedimentology, 13, 5-20.

Karpova, G. V., Timofeeva, Z. V. (1971) Post-sedimentational alteration of Aalenian rocks in the structural-facies complexes of the nothern Caucasus. Lithol. Miner. Resour.

(transl. from Lithol. Polezn. Iskop.), 5, 600-608.

Keene, J. B., Clague, D. A., Nishimori, R. K. (1976) Experimental hydrothermal alteration of tholeiitic basalt: resultant mineralogy and textures. J. Sed. Petrol., 46, 647-653.

Khitarov, N. I., Pugin, V. A. (1966) Behaviour of montmorillonite under elevated temperatures and pressures. Geochem. Int., 3, 621-626 (transl. from Geokhimiya, 7, 790-795).

Kirov, G. N., Pechigargov, V., Landzheva, E. (1979) Experimental crystallization of volcanic glasses in a thermal gradient field. Chem. Geol., 26, 17-28.

Kisch, H. J. (1974) Anthracite and meta-anthracite coal ranks associated with "anchimetamorphism" and "very-low-stage" metamorphism. I,II,III. Proc. K. Ned. Akad. Wet., Amsterdam, Ser. B, 77(2), 81-118.

Kisch, H. J. (1983) Mineralogy and petrology of burial diagenesis (burial metamorphism) and incipient metamorphism in clastic rocks. In: Larsen, Chilinger (eds.) Diagenesis in Sediments and Sedimentary Rocks, 2: Developments in Sedimentology, 25B, Elservier, 289-493.

Knipe, R. J. (1979) Chemical changes during slaty cleavage development. Bull. Miner., 102, 206-209.

Kossovskaya, A. G., Drits, V. A. (1970) The variability of micaceous minerals in sedimentary rocks. Sedimentology, 15, 81-101.

Kubler, B. (1964) Les argiles, indicateurs de metamorphisme. Rev. Inst. Fr. Petrol., 19, 1093-1112.

Kubler, B. (1967) La cristallinite de l'illite et les zones tout a fait superieures du metamorphisme. In: Etages Tectoniques. A la Baconniere, Neuchatel, Suisse, 105-121.

Larsen, G., Chilinger, G. V. (1983) Diagenesis in Sediments and Sedimentary Rocks, 2: Developments in Sedimentology, 25B, Elservier, 572 p.

Lee, J. H., Peacor, D. R. (1983) Intralayer transitions in phyllosilicates of the Martinsburg shale. Nature, 303, 608-609.

Lee, J. H., Peacor, D. R. (1984a) Ordered 1:1 24 Å interlayering of illite and chlorite: A TEM-AEM study. In submission to Clays Clay Miner.

Lee, J. H., Peacor, D. R. (1984b) The effect of diffusion on AEM

analysis for K and other elements. In preparation.

Lee, J. H., Ahn, J. H., Peacor, D. R. (1983) TEM study of textural changes in phyllosilicates through diagenesis to low temperature metamorphism (abstr.). 20th Ann. Meet., Clay Miner. Soc., Progr., 41.

Lee, J. H., Ahn, J. H., Peacor, D. R. (1984a) A TEM study of textural changes in layer silicates: Progressive changes through diagenesis and low temperature metamorphism. In submission to J. Sed. Petrol.

Lee, J. H., Peacor, D. R., Lewis, D. D., Wintsch, R. P. (1984b) Chlorite-illite/muscovite interlayered and interstratified crystals: A TEM/STEM study. In submission to Contrib. Miner. Petrol.

Lee, J. H., Peacor, D. R., Lewis, D. D., Wintsch, R. P. (1984c) Solution-recrystallization origin of the slaty cleavage in the Martinsburg Formation at Lehigh Gap, Pennsylvania. In submission to J. Struct. Geol.

Lee, J. H., Peacor, D. R., Wintsch, R. P. (1982a) TEM and AEM study of changes in dioctahedral micas during slaty cleavage development (abstr.). Trans. Amer. Geophy. Union, 63, 468.

Lee, J. H., Peacor, D. R., Wintsch, R. P. (1982b) TEM and AEM study of interlayering and along-layer transition in tri- and dioctahedral phyllosilicates (abstr.). Geol. Soc. Amer. Abstr. Progr., 14, 544.

Lewis, D. D. (1980) An investigation of the preferred orientation of phyllosilicates in the Martinsburg slate, Lehigh Gap area, Pennsylvania. Master's thesis, Indiana Univ., 96 p.

Logvinenko, N. V., Karpova, G. V. (1968) Stages of postdiagenetic alterations in rocks of coal-bearing formations. Int. Geol. Congr., Rep. 23rd Sess., Czechoslovakia 1968, Abstr., 238-239.

Lorimer, G. W., Cliff, G. (1976) Analytical electron microscopy of minerals. In: Wenk (ed.) Electron Microscopy in Mineralogy, Springer-Verlag, 506-519.

Ludwig, V. (1973) Zum Ubergang eines Tonschiefers in die Metamorphose: "Griffelschiefer" im Ordovizium von NE-Bayern. Neues Jahrb. Geol. Palaontol. Abh., 144, 50-103.

Maxwell, D. T., Hower, J. (1967) High-grade diagenesis and low-grade metamorphism of illite in the Precambrian Belt series. Amer. Miner., 52, 843-857.

Mottl, M. J., Holland, H D. (1978) Chemical exchange during hydrothermal alteration of basalt by seawater - I. experimental results for major and minor components of seawater. Geochim. Cosmochim. Acta, 42, 1103-1115.

Muffler, L. J. P., Doe, B. R. (1968) Composition and mean age of detritus of the Colorado River delta in the Salton Trough, southeastern California. J. Sed. Petrol., 38, 384-399.

Muffler, L. J. P., White, D. E. (1969) Active metamorphism of Upper Cenozoic sediments in the Salton Sea geothermal field and the Salton Trough, southeastern California. Geol. Soc. Amer. Bull., 80, 157-182.

Perry, E. A., Hower, J. (1970) Burial diagenesis in Gulf Coast pelitic sediments. Clays Clay Miner., 18, 165-177.

Perry, E. A., Hower, J. (1972) Late-stage dehydration in deeply buried pelitic sediments. Amer. Assoc. Petroleum Geol. Bull., 56, 2013-2021.

Powers, M. C. (1959) Adjustment of clays to chemical change and the concept of the equivalence level. Clays Clay Miner. 7, 309-326.

Powers, M. C. (1967) Fluid-release mechanisms in compacting marine mudrocks and their importance in oil exploration. Amer. Assoc. Petroleum Geol. Bull., 51, 1240-1254.

Roberson, H. E., Lahann, R. W., (1981) Smectite to illite conversion rates: effects of solution chemistry. Clays Clay Miner., 29, 129-135.

Roedder, E. W. (1978) Silicate liquid immiscibility in magmas and in the system K_2O-FeO-Al_2O_3-SiO_2: an example of serendipity. Geochim. Cosmochim. Acta, 42, 1596-1617.

Savage, D., Chapman, N. A. (1982) Hydrothermal behavior of simulated waste glass- and waste-rock interactions under repository conditions. Chem. Geol., 36, 59-86.

Seyfried, W. E., Bischoff, J. L. (1981) Experimental seawater-basalt interaction at 300°C, 500 bars, chemical exchange, secondary mineral formation and implications for the transport of heavy metals. Geochim. Cosmochim. Acta, 45, 135-147.

Singer, A., Muller, G. (1983) Diagenesis in argillaceous sediments. In: Larsen, Chilinger (eds.) Diagenesis in Sediments and Sedimentary Rocks, 2: Developments in Sedimentology, 25B, Elsevier, 115-212.

Spence, J. C. H. (1981) Experimental High-resolution Electron Microscopy. Monographs on the Physics and Chemistry of

Materials, Oxford University Press, 370 p.

Steiner, A. (1968) Clay minerals in hydrothermally altered rocks at Wairakei, New Zealand. Clays Clay Miner., 16, 193-213.

Teodorovich, G. I., Konyukhov, A. I. (1970) Mixed-layer minerals in sedimentary rocks as indicators of the depth of their catagenetic alteration. Dokl. Acad. Sci. U.S.S.R., Earth Sci. Sect. (transl. from Dokl. Akad. Nauk S.S.S.R.), 191, 174-176.

Teodorovich, G. I., Chernov, A. A., Kotel'nikov, D. D. (1967) Postsedimentation alteration of clayey material in sediments of the lower division of the Azerbaydzhan productive series. Dokl. Acad. Sci. U.S.S.R., Earth Sci. Sect. (transl. from Dokl. Akad. Nauk S.S.S.R.), 182, 152-155.

Velde, B., Hower, J. (1963) Petrographical significance of illite polymorphism in Paleozoic sedimentary rocks. Amer. Miner., 48, 1239-1254.

Weaver, C. E. (1959) The clay petrology of sediments. Clays Clay Miner., Proc. 6th Natl. Conf., 154-187.

Weaver, C. E. (1961) Clay minerals of the Ouachita structural belt and adjacent foreland. In: Flawn, Goldstein, King, Weaver (eds.) The Ouachita Belt. Univ. Texas Publ. 6120, 147-160.

Weaver, C. E. (1967) Potassium illite and the ocean. Geochim. Cosmochim. Acta, 31, 2181-2196.

Weaver, C. E., Beck, K. C. (1971) Clay-water diagenesis during burial: how mud becomes gneiss. Geol. Soc. Amer. Spec. Pap., 134, 96 p.

Weber, K. (1972a) Notes on determination of illite crystallinity. Neues Jahrb. Miner. Monatsh., 1972, 267-276.

Weber, K. (1972b) Kristallinität des Illits in Tonschiefern und andere Kristerien schwacher Metamorphose in nordöstlichen Rheinischen Schiefergebirge. Neues Jahrb. Geol. Palaeontol. Abh., 141, 333-363.

Wintsch, R. P. (1978) A chemical approach to the preferred orientation of mica. Geol. Soc. Amer. Bull., 89, 1715-1718.

Yau, L. Y. C., Lee, J. H., Peacor, D. R., McDowell, D. (1983) TEM study of illite diagenesis in shales of the Salton Sea geothermal field, California (abstr.). 20th Ann. Meet., Clay Miner. Soc., Progr., 42.

Yoder, H. S., Eugster, H. P. (1955) Synthetic and natural

muscovites. Geochim. Cosmochim. Acta, 8, 225-280.

Yoshida, T. (1973) Elementary layers in the interstratified clay minerals as revealed by electron microscopy. Clays Clay Miner., 21, 413-420.

4.0 ISOTOPE MIGRATION IN NATURAL SYSTEMS

Isotope migration studies are useful in nuclear waste management for characterizing the mobilities of radionuclides at actual waste disposal sites (Robertson et al., 4.1); bounding the mobilities of important radionuclides under a wide range of conditions (Simpson et al., 4.2); assessing and modeling the effects of long time periods on radionuclide mobility (Airey et al., 4.3); assessing and modeling the relationships between site mineralogy and radionuclide mobility (4.1 and 4.3); characterizing groundwater flow history and age (Davis et al., 4.4); and testing transport models (Carnahan et al., 5.1 and Peterson et al., 5.6). Because the goal in waste management is to isolate wastes from the "biosphere", one of the most obvious and important needs is to know the mobilities of radionuclides at proposed waste disposal sites. The most commonly used approach to characterize radionuclide mobility is to conduct laboratory tests on small samples taken from the field. Laboratory tests cannot be used successfully to predict the effects of long periods of time on radionuclide mobility because many geochemical reactions are too slow to have an effect on a laboratory test of mobility. Field conditions and processes such as flow and adsorption in a fractured system cannot be simulated adequately in the laboratory. Laboratory experiments provide incomplete and unrealistic tests of the limitation of models of site performance. For these and many other reasons studies of isotope migration in natural systems are needed in addition to laboratory studies.

The following discussion considers the relationship between isotope migration studies and performance assessment. One of the primary tools planned for use in licensing high and low level waste disposal sites is numerical performance assessment modeling. The DOE and NRC plan to use these models to demonstrate compliance (or non-compliance) with regulatory standards. Presumably applicants will provide model results to the NRC which show that proposed sites will comply with standards. The NRC will have to decide how much confidence it has in model predictions. How can the NRC assess model predictions? The NRC is using three procedures. First, models are being compared with other models and sensitivity studies are being conducted. Through this approach a greater understanding is gained of the models but this approach does nothing to test the models against actual field conditions. Second, models can be compared with laboratory results. This approach is very useful for evaluating the capability of a model to simulate individual processes but it cannot be used to evaluate whole systems. The only way to assess model predictions for a whole system is the third approach which is to compare model predictions with actual field conditions. Therefore, studies of isotope migration in natural systems are absolutely essential in developing and testing models of isotope migration which will be used in licensing waste disposal sites.

Isotope studies are also necessary for adequately characterizing site hydrology. In situ hydrologic testing is used for characterizing present day groundwater conditions but cannot provide essential information on flow over long periods of time. In order to characterize groundwater flow over long time periods, tracers of flow over long time periods are needed. Natural isotopic tracers (4.4) provide a means of characterizing large scale movement

of groundwater over the long periods of time of interest to high level waste management. The applicability and limitations of isotope hydrology methods is reviewed in Section 4.4 in detail.

Engineered systems performance evaluation can make use of isotopic studies of natural systems. The effectiveness of clays, zeolites and iron hydroxides, which are natural materials that could be emplaced in backfill or overpack for limiting long-term movement of water and radionuclides can be evaluated under realistic field conditions (Peacor et al., 3.3; Airey et al., 4.3).

Studies of the long-term migration of isotopes out of minerals provides information useful in assessing the performance of waste form materials (Phillip et al., 1981). Studies of the behavior of isotopes in natural systems provides information needed for understanding the performance of the individual components of waste repositories as well as for the behavior of integrated systems.

This section addresses only a small proportion of the issues that could be addressed by isotope migration studies. Some of the issues are addressed in other papers in this document. The papers by Wollenberg (5.4), Brookins (5.3), Peterson (5.6), and Dayal (5.2) which address areas of overlap between performance assessment and isotope migration could have been incorported into this section. Many of the issues must be addressed on a site specific basis by the site applicant. The research in this section has been developed solely to address NRC concerns.

The research program on isotope migration has been developed to: (1) assess the importance of long periods of time on radionuclide mobility (4.3); (2) assess the mobilities of a whole suite of radionuclides at a low level waste disposal site (4.1); (3) assess the mobilities of actinides in natural waters as a function of the concentration of common inorganic ligands (4.2) and; (4) to assess isotopic methods of dating and tracing long term movement of groundwater (4.4). These issues are being studied because they are major areas of uncertainty in radioactive waste management. Results of these efforts to date have shown that, a number of commonly used laboratory and numerical methods for evaluating radionuclide movement at a site are oversimplified or misleading. These investigations indicate that: (1) there are important long term processes that affect radionuclide mobility which are not readily assessed by laboratory studies; (2) the mobilities of low level waste radionuclides may be predicted very poorly based on batch tests and models using distribution coefficients; (3) organic complexation may cause columr tests and coupled hydrogeochemical models to be unrepresentative if it is not better understood (4.1); (4) the mobility of an actinide in natural waters may vary systematically as a function of the concentration of one ligand while mobility may be insensitive to other combinations of actinides and ligands (4.2); (5) C-14 groundwater dating methods cannot be extended much beyond 40,000 years because of in situ C-14 production; and (6) Cl-36 will be a very useful tool for characterizing waters older than 100,000 years (4.4).

REFERENCES

Airey, P. L., D. Roman, C. Golian, S. Short, T. Nightingale, and R. T. Lowson. 1984. "Radionuclide Migration Around Uranium Ore Bodies in the Aligator Rivers Region of the Northern Territory, Australia-Analogue of Radioactive Waste Repositories". In NRC Nuclear Waste Geochemistry '83. NUREG/CP-0052.

Brookin, D. G., M. T. Murphy, H. A. Wollenberg and S. Flexser. 1984. Geochemical and Strontium Isotopic Studies of Columbia River Basalts". In NRC Nuclear Waste Geochemistry '83. NUREG/CP-0052.

Carnahan, C. L., C. W. Miller, and J. S. Remer. 1984. "Verification and Improvement of Predictive Algorithms for Radionuclide Migration". In NRC Nuclear Waste Geochemistry '83. NUREG/CP-0052.

Davis, S. N., H. W. Bentley, and R. Zito. 1984. "Dating Ground Water: An Evaluation of its Use in the Assessment of HLW Repositories". In NRC Nuclear Waste Geochemistry '83. NUREG/CP-0052.

Daval, R., D. G. Scweitzer, and R. E. Davis. 1984. "Wet and Dry Cycle Leaching: Aspects of Releases in the Unsaturated Zone". In NRC Nuclear Waste Geochemistry '83. NUREG/CP-0052.

Peacor, D. R., E. J. Essene, J. H. Lee, and L. Kuo. 1984. "Long-term Stability of the Backfill-Host Rock System for High Level Waste Disposal: Experimental and Electron Microscopic Studies". In NRC Nuclear Waste Geochemistry '83. NUREG/CP-0052.

Peterson, S. R., R. J. Serne, A. R. Felmy, R. L. Ericson, K. M. Krupka and G. W. Gee. 1984. "Interactions of Acidic Solutions with Sediments: A Case Study". In NRC Nuclear Waste Geochemistry '83. NUREG/CP-0052.

Phillips, M. W., A. I. Kilinc, K. L. Chyi, J. W. Shade and E. L. Wegert. 1981. "Durability of Simulated Supercalcine and Ceramics at Geologic Storage Conditions". In NRC Nuclear Waste Geochemistry '83. NUREG/CP-0052.

Robertson, D. 1984. "Speciation and Transport of Radionuclides in Natural Environments." In NRC Nuclear Waste Geochemistry '83. NUREG/CP-0052.

Simpson, H. J., R. M. Trier, Y.-H. Li, and R. F. Anderson. 1984. "Field Experiment Determinations of Distribution Coefficients of Actinide Elements in Alkaline Lake Environments". In NRC Nuclear Waste Geochemistry '83. NUREG/CP-0052.

Wollenberg, H. A., D. G. Brookins, L. H. Cohen, S. Flexser, M. Abashian, M. Murphy, and A. E. Williams. 1984. "Uranium, Thorium and Trace Elements in Geologic Occurrences as Analogues of Nuclear Waste Repository Conditions". In NRC Nuclear Waste Geochemistry '83. NUREG/CP-0052.

4.1 SPECIATION AND TRANSPORT OF RADIONUCLIDES IN GROUNDWATER

D. E. Robertson
A. P. Toste
K. H. Abel
C. E. Cowan
E. A. Jenne
C. W. Thomas

Pacific Northwest Laboratory
Richland, Washington 99352

ABSTRACT

Studies of the chemical speciation of a number of radionuclides migrating in a slightly contaminated groundwater plume are identifying the most mobile species and providing an opportunity to test and/or validate geochemical models of radionuclide transport in groundwaters. Results to date have shown that most of the migrating radionuclides are present in anionic or nonionic forms. These include anionic forms of ^{55}Fe, ^{60}Co, ^{99m}Tc, ^{106}Ru, ^{131}I, and nonionic forms of ^{63}Ni and ^{125}Sb. Strontium-90 and a small fraction of the mobile ^{60}Co are the only cationic radionuclides which have been detected moving in the groundwater plume beyond 30 meters from the source. A comparison of the observed chemical forms with the predicted species calculated from modeling thermodynamic data and groundwater chemical parameters has indicated a good agreement for most of the radioelements in the system, including Tc, Np, Cs, Sr, Ce, Ru, Sb, Zn, and Mn. The discrepancies between observed and calculated solution species were noted for Fe, Co, Ni, and I. Traces of Fe, Co, and Ni were observed to migrate in anionic or nonionic forms which the calculations failed to predict. These anionic/nonionic species may be organic complexes having enhanced mobility in groundwaters. The radioiodine, for example, was shown to behave totally as an anion but further investigation revealed that 49-57% of this anionic iodine was organically bound. The groundwater and aqueous extracts of trench sediments contain a wide variety of organic compounds, some of which could serve as complexing agents for the radionuclides. These results indicate the need for further research at a variety of field sites in defining precisely the chemical forms of the mobile radionuclide species, and in better understanding the role of dissolved organic materials in groundwater transport of radionuclides.

4.1.1 INTRODUCTION

One of the major gaps in understanding the environmental behavior of the long-lived radionuclides associated with radioactive waste disposal is the lack of an adequate knowledge of the mechanisms by which these radionuclides may be mobilized and transported if groundwater intrusion of the disposal site occurs. Present methods for predicting the performance of a radioactive waste disposal site for isolating radioactive materials are, by necessity, based primarily upon geochemical and hydrological modeling. A number of geochemical models are available that predict soil solution species of radionuclides, the controlling solid phases, retardation on soils, and migration in groundwaters waters. However, these models are presently incomplete with respect to a number of key groundwater parameters, including dissolved organic materials, biologically mediated processes, and reaction kinetics. These parameters may play an important role in controlling the chemical speciation of radionuclides and their subsequent geochemical behavior and transport by groundwater. In order to provide greater confidence in predictive geochemical modeling and to identify needed areas of further field studies and model development, the present models need to be tested and verified at actual field sites where radionuclides are migrating in groundwaters. This paper describes work performed at a low-level waste disposal facility which has provided a natural laboratory environment for studying radionuclide migration in groundwater as a function of the physicochemical forms of the radionuclides.

4.1.1.1 Issues Addressed by This Research

Geochemical and hydrological modeling forms the basis for predicting the potential far-field migration of radionuclides from a waste disposal site in the event of containment failure and groundwater intrusion. To the degree possible, the accuracy

of these models needs to be tested under actual field conditions. The primary issues concerning the use of field sites for testing of geochemical models are as follows:

What are the limitations in the application of laboratory data for predicting radionuclide transport in natural systems?

How can information from natural systems be used to validate models?

To what extent will radionuclides be complexed by natural inorganic and organic ligands, and how does complexation affect mobility?

Consideration of these primary issues leads to the identification of secondary issues:

Which radionuclides tend to form mobile chemical species in groundwaters over a range of environmental conditions?

What are the physicochemical forms of the radionuclide species migrating in groundwaters?

What are the controlling mechanisms for the formation of mobile radionuclide species?

What are the stabilities of the mobile radionuclide forms, especially during changes in complexant content and in redox conditions of the groundwaters?

How do field observations of radionuclide mobility in groundwaters compare with predictions based on geochemical modeling?

What are the mechanisms by which important radionuclides are retarded by soils--sorption, precipitation, chemical transformation?

4.1.1.2 Background and Objectives

Several studies at field sites having contaminated groundwater plumes have shown enhanced mobility of various radionuclides beyond that predicted from hydrogeochemical modeling considerations (Coles and Ramspott, 1982; Cooper and McHugh, 1983; Killey, et al., 1984; Means, Crerar and Duguid, 1978;

Kirby, 1981). This unexpected mobility was due to the presence of organically complexed radionuclides or unique chemical forms which were relatively unretarded by surrounding soils. It is therefore essential that the mobile species of radionuclides and the factors contributing to their formation be identified so that more accurate assessments of their environmental behavior can be made.

The objectives of this research program are to utilize a slightly contaminated groundwater plume as a natural laboratory for: 1) identifying what specific physicochemical forms of the long-lived radionuclides are migrating; 2) determining the rates and mechanisms of radionuclide migration during groundwater transport; and 3) comparing the actual chemical species of radionuclides observed in the groundwater system with predicted species based on geochemical modeling. These studies are helping to provide a sound basis for understanding the mechanisms of groundwater transport of radionuclides, for testing geochemical models, and for identifying needed areas of further model development and field studies.

4.1.1.3 Scope of Research

The research conducted at this field site involves the application of large volume water sampling of a slightly contaminated groundwater plume for identifying the physicochemical forms of the migrating radionuclides. The determination of the charge forms (cationic, anionic, and nonionic forms) of a number of radionuclides are being made by pumping filtered groundwater through a series of dual beds of cation resin, anion resin, and activated aluminum oxide. More detailed studies of the chemical species of several radionuclides are also being conducted using a variety of chemical manipulations to identify the dissolved chemical forms and oxidation states of migrating radionuclides. Water samples are simultaneously collected for detailed measurements of temperature, pH, Eh, dissolved oxygen, alkalinity, DOC, major cations and anions, trace elements, and dissolved organic

constituents. Together with mineralogical analyses of soil cores collected within the groundwater plume, these data are being utilized to test the ability of geochemical modeling to adequately predict the solution species and behavior of radionuclides during migration in groundwaters.

4.1.2 METHODS

The disposal facility consists of an unlined basin and connecting trench which receives effluent water containing low levels of fission and activation products and trace amounts of transuranic radionuclides. The effluent water percolates through the soil, and a small fraction of it emerges at seepage springs located some 260 meters from the trench. The disposal basin and trench are very efficient in retaining most of the radionuclides, but trace amounts of a number of radionuclides existing in mobile chemical forms migrate in the groundwater from the trench to the springs. Three research wells have been installed at distances of 30, 46, and 73 meters from the trench to permit sampling of the groundwater between the trench and the springs. Soil samples collected from the saturated zones in these wells were subjected to particle sizing and mineralogical analysis. The soil textures at this facility typically consist of 77-80% as aggregate >2 mm, 17-21% sand, 0.3-2.2% silt, and 0.6-0.7% clay. The dominant minerals are quartz and feldspar which compose approximately 80% of the soils. Clay minerals consist of montmorillonite, kaolinite, and illite. Other trace minerals include amphibole, biotite, and calcite.

Water samples were collected from the disposal trench, two sampling wells, and the seepage springs for determining the chemical speciation of migrating radionuclides and for characterizing the chemistry of the trench water and groundwater.

The chemical speciation studies involve the identification of particulate, cationic, anionic, and nonionic forms of the

migrating radionuclides. A special sampling technique is utilized in which water is pumped directly from the trench, wells, and springs through assemblies containing membrane filters, cation and anion exchange resins and activated aluminum oxide beds. The details of this sampling procedure have been published elsewhere (Robertson, et al., 1983).

Briefly, 10 to 20 liters of trench water are pumped at a flow rate of about 0.5 to 1.0 liters/minute through a 0.4 micron Nuclepore membrane filter. The filtered water then passes directly through a 2.5 cm thick x 15 cm diameter bed of cation exchange resin (Dowex 50 x 8, H^+ form, 200-400 mesh), a 2.5 cm thick x 15 cm diameter bed of anion exchange resin (Dowex 1 x 8, Cl^- form, 200-400 mesh), and then through a 0.7 cm thick x 15 cm diameter bed of fine grained activated aluminum oxide. The filters remove the particulate forms of the radionuclides greater than 0.4 micron, the resins remove soluble cationic and anionic species, and the activated aluminum oxide removes nonionic species.

When sampling the wells and springs, larger versions of this assembly employing dual resin and aluminum oxide beds are used to sample much greater volumes of water, since the radionuclide concentrations are much lower. Typically, 50 to 100 liters of well water and 1000 to 5000 liters of spring water are pumped at a flow rate of 1 to 8 liters/minute through the larger assemblies.

Samples for complete chemical analyses of the trench, well, and spring waters were collected at the time of sampling for the radionuclides. The anions, cations, trace elements and parameters having a potential role in controlling the chemical speciation of the radionuclides were included in the analyses. Temperature, pH, Eh, dissolved oxygen, and alkalinity were measured onsite during the sampling process. Aliquots of 0.4 micron filtered water were preserved by freezing for later laboratory analyses of major anions by ion chromatography. For major cation and

trace element analyses, a separate aliquot of filtered water was acidified by adding 20 ml of concentrated Ultrex hydrochloric acid per liter of water. For the sulfide analyses, an inline filtered sample of water was collected in a glass bottle containing a sufficient quantity of an antioxidant preservative solution. Sulfide analyses were performed by a very sensitive polarographic technique. Another aliquot of filtered water was also collected and preserved by refrigeration for dissolved organic constituent analyses. The details of the procedures for the organic analyses have been published elsewhere (Toste, et al., 1983; Robertson, et al., 1983). Briefly, the waters or trench sediment aqueous extracts were extracted with chloroform to remove nonpolar organic compounds. The hydrophilic organic compounds in the purified aqueous extract were then concentrated by evaporation, methylated, extracted into chloroform and submitted for gas chromatography-mass spectrometry (GC-MS) analysis. The nonpolar organic fraction was likewise analyzed by GC-MS.

4.1.3 RESULTS

4.1.3.1 Physicochemical Speciation

The disposal basin/trench system has been very effective in removing most of the radionuclides in the discharged effluent water by sorption onto the soil. However, trace amounts of several radionuclides have been observed to migrate to the seepage springs.

The measurement of particulate, cationic, anionic, and nonionic forms of the radionuclides in the trench, well, and spring waters have shown that the migrating radionuclides are primarily those in anionic and nonionic forms. This group of mobile radionuclides includes isotopes of Co, Tc, I, Ru, Sb, Fe, and Ni. Table 1 gives a typical analysis of a number of the most abundant gamma-emitting radionuclides in trench, well, and spring waters. Although the trench water contains predominantly cationic species

TABLE 1

Chemical Speciation of Gamma-Emitting Radionuclides in Trench, Well and Spring Waters

	TRENCH - MANWAY #1 (1/26/83 @ 1400)				
RADIONUCLIDE	TOTAL pCi/l	% PARTICULATE	% CATIONIC	% ANIONIC	% NONIONIC
^{54}Mn	109,900	11.6	87.6	0.6	0.002
^{59}Fe	57,030	96.7	2.3	1.0	0.02
^{58}Co	3,670	23.0	76.3	0.5	<0.02
^{60}Co	49,330	58.5	41.3	0.1	0.03
^{95}Zr	11,230	90.6	3.0	6.0	0.4
^{95}Nb	21,580	58.2	33.7	7.9	0.06
^{99}Mo	121,200	1.2	1.1	97.7	<0.01
^{99m}Tc	17,930	<0.2	0.8	99.2	<0.01
^{103}Ru	4,140	74.0	12.2	12.6	1.2
^{106}Ru	1,440	>65	<14	<23	<0.4
^{124}Sb	1,355	60.9	0.8	34.7	3.6
^{125}Sb	344	<54	ND	98.0	2.0
^{140}Ba	38,990	14.2	85.8	<0.1	<0.1
^{140}La	113,880	63.6	36.3	0.1	<0.1
^{131}I	31,980	2.7	2.9	94.0	0.5
^{133}I	459,200	4.1	<0.05	95.5	0.4
^{137}Cs	16,100	0.1	99.9	<0.1	<0.1
^{144}Ce	7,010	~100	<4	<1	<0.06
^{154}Eu	670	~100	<3	<40	<0.1

	WELL #1 (1/27/83 @ 1430)				
RADIONUCLIDE	TOTAL pCi/l	% PARTICULATE	% CATIONIC	% ANIONIC	% NONIONIC
^{54}Mn	90.6	0.08	0.4	99.4	0.1
^{59}Fe	21.6	0.3	16.0	82.2	<1
^{58}Co	12.2	<0.2	8.2	90.2	1.1
^{60}Co	210	0.4	64.8	33.7	1.1
^{95}Zr	19.9	0.09	8.0	90.4	<0.5
^{95}Nb	118	0.08	1.9	97.5	0.3
^{99}Mo	13,590	0.2	0.7	99.0	<0.01
^{99m}Tc	2,400	0.2	<0.8	99.0	<0.01
^{103}Ru	300	0.3	11.7	86.7	1.2
^{106}Ru	324	<0.2	10.9	87.6	1.3
^{124}Sb	233	<0.2	0.5	91.0	9.0
^{125}Sb	102	0.2	1.0	83.2	15.6
^{140}Ba	40	1.5	<0.1	98.5	<0.1
^{140}La	<6	-	-	-	-
^{131}I	11,120	0.4	4.9	94.7	<0.1
^{133}I	21,740	0.5	<0.3	99.2	0.2
^{137}Cs	<1	-	-	-	-
^{144}Ce	<60	-	-	-	-
^{154}Eu	<50	-	-	-	-

	SPRINGS (1/31/83 @ 0900)				
RADIONUCLIDE	TOTAL pCi/l	% PARTICULATE	% CATIONIC	% ANIONIC	% NONIONIC
^{54}Mn	<0.1	-	-	-	-
^{59}Fe	<0.2	-	-	-	-
^{58}Co	0.28	<0.3	5.0	92.9	1.7
^{60}Co	62.2	0.2	44.9	50.9	4.0
^{95}Zr	<0.1	-	-	-	-
^{95}Nb	<0.1	-	-	-	-
^{99}Mo	48	<0.2	<12	>88	<0.3
^{99m}Tc	12	<0.1	<1	>99	<0.3
^{103}Ru	39.2	0.1	13.0	83.2	3.6
^{106}Ru	45.7	0.3	16.1	80.5	3.9
^{124}Sb	6.2	<0.2	<1.6	26.0	74.2
^{125}Sb	88.0	<0.05	0.6	23.3	76.1
^{140}Ba	<0.1	-	-	-	-
^{140}La	<0.5	-	-	-	-
^{131}I	182	0.4	5.6	92.3	1.5
^{133}I	7.2	<2	-	100	<8
^{137}Cs	<0.1	-	-	-	-
^{144}Ce	<0.4	-	-	-	-
^{154}Eu	<0.3	-	-	-	-

of ^{54}Mn, ^{59}Fe, ^{95}Nb, ^{140}Ba, ^{140}La, and ^{137}Cs, the cationic forms of these radionuclides have not been observed to migrate to the springs. The behavior of several of the more important radionuclides during the percolation of the effluent water through the soil bank is discussed below.

Cesium-137

Cesium-137 is the least mobile of the radionuclides studied to date. During all sampling periods, the ^{137}Cs in the trench water was present as a soluble cation. However, the ^{137}Cs was usually nondetectable in the well waters, and never detectable in the spring water samples. A decontamination factor (DF), calculated by dividing the radionuclide concentration in the trench water by the concentration in the well or spring water, gives a measurement of the radionuclide adsorption capacity afforded by the soil column between the trench and the wells and springs, respectively. Decontamination factors of $>1.6 \times 10^4$ to $>1.6 \times 10^5$ for the well water and spring water, respectively, were afforded by the soil column during the January 1983 sampling. The tenfold greater DF for ^{137}Cs at the springs is simply due to the fact that a tenfold larger water sample was taken at the springs, thereby improving the detection limit by an order of magnitude. The ^{137}Cs presumably exists in the trench water as Cs^+, and the principal retention mechanism on soils is expected to be cation exchange on the clay minerals (kaolinite, montimorillonite, and illite) present in these soils (Rai and Serne, 1978).

Iodine

Iodine-131 (8.04 days) can be a useful tracer of the long-lived ^{129}I (1.59×10^7 year), which has been shown to be mobile in slightly contaminated groundwaters (Barraclough, et al., 1981; Eddy and Wilbur, 1980). The radioiodine in the trench, well, and spring water occurs predominantly in soluble anionic forms. Further studies (Robertson, et al., 1983) have recently shown that about 42-48% of the soluble anionic ^{131}I is in the form of iodide (I^-), and about 49-57% occurs presumably as an organically bound anionic complex as shown in Table 2.

Table 2
Chemical Speciation of Radioiodine in
Trench, Well, and Spring Waters

Sample	Date	Chemical Forms of ^{131}I	% of Total
Trench Water	1/26/83	I^-	48
		IO_3^-	3
		Organic I	49
Well #1	1/27/83	I^-	46
		IO_3^-	2
		Organic I	52
Spring Water	1/31/83	I^-	42
		IO_3^-	1
		Organic I	57

The ^{131}I is relatively mobile in the groundwater, with DF's of 2.8 and 176 at Well #1 and the springs, respectively. The fraction of ^{131}I in the soluble anionic forms changes only slightly during transport from the trench to the springs, but it appears that a slight conversion of I^- to organic iodine occurs. About 3 to 5% of the total ^{131}I is taken up by the cation exchange resin during the sampling. It is not known if this is due to adsorption of a truly cationic or positively charged species or to reactions of the radioiodine with the organic matrix of the cation resin. The dominant form of iodine calculated from thermodynamic data would be I^- (Rai and Serne, 1978). The organically complexed iodine could not be predicted because of a lack of thermodynamic data for organic iodine compounds.

Cobalt-60

The ^{60}Co in the trench water is typically partitioned between particulate, cationic, and traces of anionic species. As the water moves from the trench to the springs, the selective uptake of the cationic ^{60}Co by the soil is clearly evident, resulting in trace amounts of anionic ^{60}Co being the predominant

form in the spring water. The DF's for the "total" ^{60}Co gradually increased in going from Well #1 to the springs, being 235 and 790, respectively. While the cationic ^{60}Co is reduced in concentration by a factor of 731 in going from the trench water to the springs, the anionic ^{60}Co is reduced by only a factor of 1.5. It appears that the anionic ^{60}Co is one of the most mobile species in this groundwater system. Predictions of chemical forms of cobalt based on thermodynamic data indicate that Co^{+2} would be the predominant solution species with a much smaller contribution from $Co(OH)^{+}$ (Rai and Serne, 1978). A possible form for the anionic ^{60}Co is $Co(OH)_3^{-}$, although this ion is predicted to exist at concentrations approximately 8 orders of magnitude lower than Co^{+2}. The discrepancy may be due to organically complexed ^{60}Co which would appear as a soluble anionic form in our separation scheme. Organically complexed anionic ^{60}Co has been observed to be quite mobile in a contaminated groundwater plume at the Chalk River Nuclear Laboratories (Cooper and McHugh, 1983; Killey, et al., 1984).

Cobalt-60 has been shown to be one of the few radionuclides to migrate in groundwaters from a variety of other low-level waste disposal sites (Means, et al., 1978; Barraclough, et al., 1981; Kirby, 1981; Eddy and Wilbur, 1980; Stone, 1982). This ubiquitous mobility may be related to the occurrence of the anionic cobalt species, possibly organic complexes.

Strontium-90

Strontium-90 measurements made in January, 1983 of trench, well, and spring water samples indicate that the dissolved cationic form is always predominant (see Table 3).

TABLE 3

PHYSICOCHEMICAL FORMS OF ^{90}Sr IN TRENCH, WELL AND SPRING WATERS
January, 1983

	pCi/liter		
	Trench Water	Well #1 Water	Spring Water
Particulate	425 ± 41	--	--
Cationic	6582 ± 740	16,485 ± 1870	1036 ± 117
Anionic	266 ± 25	71 ± 7	<0.1
Nonionic	47 ± 13	222 ± 3	0.45 ± 0.05

The ^{90}Sr concentration in Well #1 water (30 m from the trench) was actually higher than observed in the trench, suggesting that gradual dissolution of the soil-adsorbed ^{90}Sr inventory in the trench was occurring. The soil bank between Well #1 and the springs is effective in removing over 90% of the ^{90}Sr which migrates to Well #1, and a spring water concentration of 1036 pCi/ℓ was observed. The most probable form of the ^{90}Sr in these waters is Sr^{+2}, and ion exchange may be the principal mechanism of strontium adsorption on these soils (Rai and Serne, 1978).

Nickel-63

The physicochemical speciation and behavior of ^{63}Ni in this groundwater system is of interest because of its listing in 10 CFR 61 as a radionuclide of primary concern in low-level waste management. This concern is based on the long half-life of ^{63}Ni (100 yr) and the fact that it is an abundant radionuclide in nuclear power plant low-level wastes.

Therefore, a suite of water and soil samples collected in June, 1981, was analyzed for ^{63}Ni to determine its concentrations and physicochemical forms. Water from the trench and the springs was sampled using the system previously described. The ^{63}Ni taken up on the filters, resin, and Al_2O_3 was leached with hot

concentrated HCl, radiochemically separated, electrodeposited on stainless steel discs, and counted in a specially constructed anticoincidence shielded, low-level beta proportional counter. The results of these analyses are shown in Table 4.

TABLE 4

Nickel-63 Concentrations and Chemical Speciation
June, 1981

	Trench Water pCi/ℓ	% of Total
Particulate	199.6 ± 28	59.1
Cationic	107.4 ± 38.4	31.8
Anionic	16 ± 16	4.7
Nonionic	15 ± 15	4.4

	Spring Water pCi/ℓ
Cationic	<0.8
Anionic	<1.9
Nonionic	1.2 ± 0.2

The ^{63}Ni in the trench water was partitioned mainly between particulate and cationic forms. The cationic and anionic forms were nondetectable in the spring water, but a measurable fraction appeared to be in a nonionic form which was retained on the activated Al_2O_3. The total decontamination factor afforded by the soil column amounted to 280. The trench sediments contained 6-30 x 10^4 pCi/g of ^{63}Ni and this sediment-sorbed ^{63}Ni appears to be tightly bound. Possible forms of nickel which may be present in these oxygenated groundwaters are Ni^{+2}, $NiOH^-$ and $Ni(OH)_2$.

Ruthenium-103,106

Ruthenium-103,106 present in the trench waters is variably distributed between particulate, cationic, anionic, and nonionic species. During migration in the groundwater, the cationic $^{103,106}Ru$ is preferentially sorbed to the soil in comparison to

the anionic form(s). Once the $^{103,106}Ru$ reaches Well #1, the anionic form(s) in the well water generally accounts for about 80-90% of the total $^{103,106}Ru$. The relative amounts of cationic, anionic, and nonionic $^{103,106}Ru$ did not appreciably change during the ensuing transport to the springs. The overall DF's for Well #1 and the springs amounted to 14 and 106, respectively. However, the DF at the springs for the cationic species was 99, whereas the DF for the anionic forms was only 16. Based on the thermodynamic data, the predicted soluble anionic $^{103,106}Ru$ species that would be prevalent in an oxidizing groundwater environment would be RuO_4^-, RuO_4^{-2}, RuO_4° and $Ru(OH)_2^{+2}$ (Rai and Serne, 1978).

Antimony-125

Antimony-125 in the trench water is present primarily in a soluble anionic form, with a small fraction being present as a soluble nonionic species. During migration in the groundwater, the anionic ^{125}Sb was preferentially adsorbed onto the soil compared to the nonionic ^{125}Sb. At the springs the ^{125}Sb is typically partitioned as follows: 76% nonionic, 23% anionic, and only 1% cationic. The ^{125}Sb is very mobile in the groundwater at this site with DF's for "total" Sb species of only 3.4 and 3.9 at Well #1 and the springs, respectively. Much of the anionic ^{125}Sb appears to be forming in situ in the trench by desorption of the accumulated ^{125}Sb inventory present in the trench sediments, since the concentration of the anionic ^{125}Sb species in the groundwater actually increases substantially (7X) as the water moves from the trench to the springs. These experimental observations are in agreement with the predicted chemical forms estimated to be present in oxygenated groundwater, namely the nonionic species $HSbO_2^\circ$ and $Sb(OH)_3^\circ$ (Rai and Serne, 1978).

Niobium-95

Niobium-95 is a convenient tracer in this system for the much longer-lived ^{94}Nb. Niobium-94 is of concern in low-level

waste management because it is calculated to be a major constituent in aged neutron activated metal components of reactor pressure vessel internals. Based on the results to date in this groundwater system, the ^{95}Nb does not appear to be very mobile. In the trench water sampled in January 1983, the ^{95}Nb was partitioned as follows: 58% particulate, 34% cationic, and 8% anionic. In water from Well #1, most of the cationic ^{95}Nb had been removed by adsorption on the soil and the anionic ^{95}Nb accounted for 97.5% of the total (see Table 1). During the ensuing movement from Well #1 to the springs, the remaining anionic ^{95}Nb is removed by adsorption on the soil, and ^{95}Nb was not detectable in water from the springs. The DF factors for Well #1 and the springs amounted to 180 and >2 x 10^5, respectively. No predictions based on thermodynamic data of the chemical species of niobium occurring in groundwater have been published.

Iron-59

The ^{59}Fe is predominantly present in the trench water in a particulate form, and during the January, 1983 sampling the particulate ^{59}Fe accounted for 96.7% of the total (see Table 1). The soluble cationic and anionic species represented 2.3% and 1.0% of the total ^{59}Fe, respectively. Iron-59 has never been detected in the spring water, but a trace of it was found in Well #1 water partitioned as follows: 82.2% anionic, 16.0% cationic, and 0.3% particulate. The anionic ^{59}Fe did not migrate to the springs, and DF's for Well #1 and the springs amounted to 2.6 x 10^3 and >2.9 x 10^5, respectively.

For the January, 1983 samples, ^{55}Fe was removed from the filters, resins, and aluminum oxide with nitric acid, radiochemically purified, electrodeposited, and then counted on an intrinsic germanium detector. The results are shown in Table 5.

TABLE 5

Iron-55 Concentrations and Physicochemical Forms
January, 1983

	pCi/ℓ		
	Trench Water	Well #1 Water	Spring Water
Particulate	3270 ± 16	---	---
Cationic	5538 ± 22	8.01 ± 0.22	2.14 ± 0.06
Anionic	116 ± 0.1	1.96 ± 0.05	4.43 ± 0.18
Nonionic	40 ± 0.2	3.03 ± 0.07	<0.01

The ^{55}Fe behavior did not exactly duplicate that observed for ^{59}Fe. The ^{55}Fe was present in the trench, and at a much lower level in Well #1 water, mainly in a dissolved cationic state. In the spring water, the ^{55}Fe was the only iron radionuclide observed and was 67% anionic. The difference in speciation between the ^{55}Fe and the ^{59}Fe may be due to the differences in half-lives and their relative inventories in the trench sediments. The relatively short half-life of ^{59}Fe (45 d) does not permit its extensive accumulation in trench sediments and its presence in the trench water reflects fairly recent additions. In contrast, the ^{55}Fe (2.7 yr) inventory in the trench sediments must be much greater, allowing the ^{55}Fe more time to engage in possible dissolution processes which could result in somewhat different chemical forms compared to the ^{59}Fe.

Measurements of stable Fe(II) and Fe(III) in the trench waters during the January 1983 sampling gave concentrations of 6.1 and 84.9 μg/ℓ, respectively. The high concentration of iron in the trench water is undoubtedly due to corrosion of the steel piping which delivers the effluent water to the trench. It is possible that some of the Fe(III) may be present as colloidal material which passes the 0.4 μ filter used for filtering the water. In Well #1 and the 1/31/83 spring sample, the Fe(II) and Fe(III) concentrations were nondetectable at less than 2 μg/ℓ.

The trench and groundwater at this site is well-oxygenated and soluble Fe(II) is rarely observed in the well and spring waters. Thermodynamic calculations indicate that essentially all of the iron should exist as Fe^{+2} (Cowan, et al, 1983), which is not in agreement with the field observations. Organic complexation of the iron may be an important mechanism here.

Manganese-54

In the trench water the ^{54}Mn typically occurs primarily as cationic and particulate species (see Table 1). In the January 1983 sampling of Well #1, a trace of ^{54}Mn was detected, essentially all in an anionic form. The anionic ^{54}Mn did not migrate to the springs. The DF's for Well #1 and the springs amounted to 1.2×10^3 and $>1 \times 10^6$, respectively. The dominant solution species of manganese in this type of water is reported to be Mn^{+2}, with smaller amounts of $Mn(HCO_3)^+$ and $MnSO_4^\circ$ present (Morgan, 1967).

Other Radionuclides

A number of other radionuclides of lesser significance in the management of low level wastes are also present in this system. Cobalt-58 is a shorter-lived activation product formed by an (n,p) reaction with stable nickel. Its behavior relative to ^{60}Co, which is formed by an (n,Y) reaction with cobalt, is often slightly different. This may be due to its formation from different parent material, to kinetic differences, and to differences in half-lives which result in a much greater inventory of ^{60}Co in the trench sediments relative to ^{58}Co. If microbial or very slow geochemical processes are affecting the chemical speciation of the radiocobalt, then these effects would probably have a more pronounced effect on the longer-lived ^{60}Co.

Zirconium-95 is the precursor of ^{95}Nb and its behavior is somewhat similar. Zirconium-95 is present in the trench water mainly in particulate form, with the anionic form being the dominant soluble species. In Well #1, 90.4% of a trace amount of

^{95}Zr is in an anionic form. The ^{95}Zr has never been detected in the spring water, giving a DF of >1 x 10^5. Thermodynamic data (Rai and Serne, 1978) suggests that $Zr(OH)_5^-$ would be the dominant solution species with smaller amounts of $Zr(OH)_4^\circ$ and $Zr(OH)_3^+$, which would be in good agreement with the field observations.

Barium-140 is often present in the trench water and occurs primarily as a cation. A trace of ^{140}Ba was detected in an anionic form in Well #1. It has never been detected at the springs. Its short half-life does not make this an important radionuclide in waste management.

Several rare earth radionuclides, ^{140}La, ^{141}Ce, ^{144}Ce, and ^{154}Eu are present in the trench water, mainly in particulate forms. The rare earths could not be detected in well or spring waters, indicating efficient retention by the soil.

Antimony-124 exhibits behavior very similar to the longer-lived ^{125}Sb in the well and spring water. However, the ^{124}Sb appears to be associated with particulates in the trench water to a greater degree than the ^{125}Sb. This may be due to the fact that the ^{124}Sb is a relatively short-lived neutron activation product and the ^{125}Sb is a longer-lived fission product.

4.1.3.2 Chemistry of Trench and Groundwater

The chemistry of the trench water has occasionally been observed to be somewhat variable, with the pH ranging from about 7 to 9. Normally, the pH of the trench water is close to 8, and a typical analysis of the trench, well and spring waters is shown in Table 6. Despite the occasional variability of the trench water chemistry, the well and spring waters have exhibited a rather uniform chemistry during the sampling period of this study.

The trench, well and spring waters are well oxygenated as evidenced from the high positive Eh values, the nearly saturated dissolved oxygen content, and the complete absence of sulfide

TABLE 6 Chemical Composition of Trench, Well and Spring Waters, January 1983

Constituent	Trench 1/26/83	Well #1 1/27/83	Well #3 1/26/83	Spring 1/28/83	Spring 1/31/83
Temp. °C	21	18	18	20	20
pH	7.30	8.10	8.15	8.10	8.15
Eh (mv)	+405	+430	+355	+435	+385
Dissolved O_2 (mg/ℓ)	6.9	7.2	9.2	4.9	4.5
Alkalinity ($CaCO_3$ mg/ℓ)	38.0	54.9	52.8	57.5	57.7
DOC (mg/ℓ)	<1	<1	<1	<1	<1
Ca (mg/ℓ)	16.3	25.2	25.3	26.0	20.1
Mg (mg/ℓ)	4.0	4.2	4.2	4.3	4.8
Na (mg/ℓ)	1.68	1.70	1.70	1.99	2.17
K (mg/ℓ)	0.40	1.0	1.0	0.50	1.8
Sr (mg/ℓ)	0.081	0.093	0.093	0.094	0.12
SO_4^{-2} (mg/ℓ)	14.3	13.9	12.2	13.5	13.9
$S^=$ (polarographic) (mg/ℓ)	<0.003	<0.003	<0.003	<0.003	<0.003
S (total by ICP) (mg/ℓ)	5.6	5.1	5.1	5.4	4.6
NO_3^- (mg/ℓ)	9.2	13.2	8.2	12.5	13.2
NO_2^- (mg/ℓ)	2.5	<0.05	<0.05	<0.05	<0.05
F^- (mg/ℓ)	<0.15	<0.15	<0.15	<0.15	<0.15
PO_4^{-3} (mg/ℓ)	3.8	<0.2	<0.2	<0.2	<0.2
P (total by ICP) (mg/ℓ)	1.48	<0.1	<0.1	<0.1	<0.1
Cl^- (mg/ℓ)	0.90	0.87	0.70	0.83	0.87
Si (mg/ℓ)	1.8	4.4	4.4	2.9	8.2
Al (µg/ℓ)	<50	<50	<50	<50	<50
As (µg/ℓ)	<30	<30	<30	<30	<30
B (µg/ℓ)	10	10	10	10	10
Ba (µg/ℓ)	34	28	26	16	14
Co (µg/ℓ)	<10	<10	<10	<10	<10
Cr (µg/ℓ)	<10	<10	<10	<10	<10
Fe (total by ICP) (µg/ℓ)	110	<20	<20	<20	<20
Fe^{+2} (colorimetric) (µg/ℓ)	6.1	<2*	6.1*	3.6	<2
Fe^{+3} (colorimetric) (µg/ℓ)	84.9	<2*	5.9*	2.5	<2
Fe^{+2}/Fe^{+3}	0.067	-	1.03	1.44	-
Li (µg/ℓ)	<5	<5	<5	<5	<5
Mn (µg/ℓ)	<10	<10	<10	<10	<10
Mo (µg/ℓ)	<10	<10	<10	<10	<10
Ni (µg/ℓ)	<20	<20	<20	<20	<20
Se (µg/ℓ)	<100	<100	<100	<100	<100
Ti (µg/ℓ)	<10	<10	<10	<10	<10
V (µg/ℓ)	<5	<5	<5	<5	<5
Zn (µg/ℓ)	24	<10	<10	<10	<10

*Water pumped through stainless steel sampling device - probable contamination with iron.

ions. The major anions are HCO_3^-, $SO_4^=$ and NO_3^-, while the major cations are Ca^{++}, Mg^{++} and Na^+. The dissolved organic carbon content of the waters are low, usually about 1 to 3 mg/ℓ, or less.

4.1.3.3 Organic Characterization of Trench Sediment Extracts

Earlier analyses identified citrate as a major constituent of the hydrophilic fraction of the dissolved organic matter in the trench water (Robertson, et al., 1981). Since citrate is a potential complexing agent for a number of metal ions, an identification of the organic constituents in the trench sediments was performed. Sediments were sampled at three locations equally spaced along the trench, and these locations are referred to as Manways 2, 6, and 9.

Hydrophilic Organics

A variety of carboxylic acids was identified in the hydrophilic organic fraction of the trench sediments, generally at ppb levels (see Table 7). The sediment from Manway 6 was much richer in total acids (9609 ppb) compared to Manways 2 (482 ppb) and 9 (1630 ppb). Several classes of carboxylic acids are represented: tricarboxylic acids, dicarboxylic acids, monocarboxylic acids, oxygenated acids, and aromatic acids.

The least abundant of the carboxylic acids identified in the trench sediments are the tricarboxylic acids. Citric acid is the only species identified in this class. It was present in the sediments from Manways 2 and 6 at concentrations of 34 ppb and 159 ppb, respectively. Citric acid constitutes only 7% and 2% of the total carboxylic acids in Manways 2 and 6, respectively. In contrast, as reported earlier, citric acid was the major hydrophilic organic species (380 ppb) in a sample of the effluent water entering the trench (collected on 9/22/81). The latest data indicate that citric acid has not substantially accumulated in the trench sediments.

TABLE 7 Hydrophilic Organics in Trench Sediments

	CONCENTRATION (ppb)[c] IN DRIED SEDIMENT FROM MANWAYS		
	NO. 2	NO. 6	NO. 9
TRICARBOXYLIC ACIDS			
CITRIC ACID[d]	34	153	
DICARBOXYLIC ACIDS			
OXALIC ACID[d]	13	1971	347
MALONIC ACID[d]	8	903	141
MALEIC ACID[d]	3	375	31
SUCCINIC ACID[d]	33	1992	328
2-METHYL-SUCCINIC ACID[d]		94	
PENTANEDIOIC ACID[d]		282	
HEXANEDIOIC ACID[d]	3	193	34
HEPTANEDIOIC ACID[d]	20		
OCTANEDIOIC ACID[d]	41	592	67
NONANEDIOIC ACID[d]	91	587	163
CARBOXYLIC ACIDS			
TETRADECANOIC ACID[d]	3	65	34
HEXADECANOIC ACID[d]	49	292	55
OCTADECANOIC ACID[d]	45	190	39
OXYGENATED ACIDS			
2-HYDROXY-PROPANOIC ACID[d]		138	
3-HYDROXY-BUTANOIC ACID[d]	12		
4-METHOXY-BUTANOIC ACID[d]		16	
2-METHOXY-2-BUTENOIC ACID[d]	49		
4,4-DIMETHOXY-2-PENTENEDIOIC ACID[d]	21		
2-METHOXY-BENZOIC ACID[d]		274	80
2-OXO-PROPANOIC ACID[d]		10	3
4-OXO-PENTANOIC ACID[d]	2	169	39
AROMATICS			
BENZENEACETIC ACID[d]		222	79
FURANCARBOXYLIC ACID[d]		120	20
BENZOIC ACID[d]		362	45
DIMETHYL PHTHALATE	34	188	68
DIBUTYL PHTHALATE	21		
BENZALDEHYDE		96	14
2,6-PYRIDINECARBOXYLIC ACID[d]	92		
PYRIDINECARBOXYLIC ACID[d]		4	
NITROBENZOIC ACID[d,e]		115	
NITRO-HYDROXYBENZOIC ACID[d,e]		300	57

[a] METHYLATED, BF_3/METHANOL;
[b] SAMPLED ON 6/7/82;
[c] NO ENTRY INDICATES COMPOUND IS BELOW DETECTION LEVELS;
[d] METHYL ESTER;
[e] TENTATIVE IDENTIFICATION

The dicarboxylic acids are the most abundant class of acids identified in the trench sediments; 44% of the total acids in Manway 2; 73% in Manway 6; and 68% in Manway 9. In Manway 2, two of these species, oxalic and succinic acids, were present at ppm levels (1.97 ppm and 1.99 ppm, respectively). Some of the dicarboxylic acids are common metabolic intermediates in microbiota. Such acids are also formed by some bacteria via oxidation of monocarboxylic acids or alkanes, e.g., ω-oxidation of monocarboxylic acids (fatty acids).

The monocarboxylic acids identified in the trench sediments are considerably less abundant than the dicarboxylic acids; 20% of the total acids in Manway 2, 6% in Manway 6, and 8% in Manway 9. Of these species palmitic acid (hexadecanoic acid) was most abundant followed by stearic acid (octadecanoic acid). In an earlier analysis of spring water (collected on 9/22/81), palmitic and stearic acids were the major hydrophilic organic components, but at much lower levels (1.8 ppb and 2.3 ppb, respectively). Monocarboxylic acids, or fatty acids, such as palmitic and stearic acids are common metabolic intermediates and structural components of microbiota. They are also present in detergents, and this could be another source of these compounds.

The oxygenated carboxylic acids identified in one trench sediment include hydroxy-, methoxy-, and oxo-substituted acids. The concentrations of oxygenated acids are comparable to those of the monocarboxylic acids: 17% of the total acids in Manway 2 (vs. 20% for the monocarboxylic acids), 6% in Manway 6 (vs. 6%), and 7% in Manway 9 (vs. 8%). A probable source of these compounds is bacterial diagenesis of unoxygenated carboxylic acid and/or alkanes. Some bacteria, for example, oxidize alkanes to hydroxy-monocarboxylic acids.

Unlike the other classes of carboxylic acids, the concentrations of the aromatic acids in the sediments from the three Manways were roughly comparable: 11% of the total acids in Manway 2, 14% in Manway 6, and 17% in Manway 9. Perhaps the two com-

pounds of most interest are the two nitro-substituted benzoic acids we have tentatively identified, nitrobenzoic acid and nitro-hydroxygenzoic acid. The fragmentation patterns of the two species from the GC-MS analysis strongly suggest these two structures, but we are looking at the evidence more closely to confirm their identities.

Hydrophobic Organics

The organic content of the hydrophobic organic extract was easily the most complex of the extracts analyzed. The hydrophobic organic extract accounted for much of the total organic extracts of the sediments, specifically 52-68%. It was too complex to permit thorough GC and GC-MS analyses. Many of the organic species in this extract may actually be so nonvolatile that they are unchromatographable by GC and GC-MS. More chromatographic fractionation will be necessary before the hydrophobic organics can be exhaustively characterized. Nevertheless, some species could be identified. Alkanes, alkenes, alkynes, and elemental sulfur were identified in the hydrophobic organic extracts from all three trench sediments. The most notable observation about the hydrophobic organic extract, however, is that three cyclic sulfur species were identified in the extract from Manway 2: a five-membered ring compound, CHS_4, a six-membered ring compound, CH_2S_5; and a seven-membered ring compound, CH_2S_6. We are currently assessing whether or not such species can mediate radionuclide transport in soils.

4.1.4 CONCLUSIONS

The chemical speciation of a number of radionuclides migrating in a slightly contaminated groundwater plume is being investigated. It has been observed that the migrating radionuclides are mainly those that exist in anionic or nonionic forms. These include anionic species of ^{99}Tc, ^{131}I, ^{60}Co, ^{103} ^{106}Ru, and a nonionic form(s) of ^{125}Sb. The only exceptions are cationic forms of ^{90}Sr and a small fraction of the ^{60}Co which migrate from

the trench to the springs, a distance of about 260 meters. The other radionuclides which are present in the trench waters in predominantly cationic and particulate forms are efficiently retained by the soil in the immediate vicinity of the trench.

A comparison of the field observations of the physicochemical forms of the radionuclides at this site with predicted chemical forms based on thermodynamic data indicate that for most of the radionuclides rather good agreement between observed versus predicted chemical forms is achieved (see Table 8). Table 8 lists the elements having radionuclides which may be of concern to radioactive waste management, together with their charge-forms observed in trench and spring waters, and their relative mobilities in this groundwater plume. The predicted solution species were derived from activity-pH diagrams constructed from thermodynamic data (Rai and Serne, 1978), or by incorporation of water chemistry data similar to that in Table 6 into the MINTEQ geochemical model for calculating the solution species.

As shown in Table 8, good agreement between observed versus calculated charge-forms was achieved for Tc, Np, Cs, Sr, Ce, Ru, Sb, Zn, and Mn. The major discrepancies were noted for Co, I, Fe, and Ni. The anionic forms of Co and Fe, and the nonionic form(s) of Ni in the spring water were not predicted by the thermodynamic calculations and geochemical modeling. Also, the organic iodine species which behave like an anion and account for 49 to 57% of the total iodine were likewise unpredictable. The most likely explanation for these discrepancies would seem to be the role of organic complexation of the radioelements having the anomalous chemical forms.

For example, the anionic ^{60}Co species migrating in groundwaters at the Chalk River Nuclear Laboratories have been shown to be organically complexed (Killey, et al., 1984; Cooper and McHugh 1983). Also, traces of citrate, oxalate, and carboxylic acids have been observed in the trench waters and these ligands could complex with the Fe and Ni to form dissolved anionic species.

TABLE 8

COMPARISON OF FIELD OBSERVATIONS VS. PREDICTED SPECIES FOR CHEMICAL FORMS OF RADIONUCLIDES AT THE LOW LEVEL AQUEOUS WASTE DISPOSAL SITE

	FIELD OBSERVATIONS			
	TRENCH	SPRINGS	RELATIVE MOBILITY	PREDICTED SOLUTION SPECIES
Tc	ANIONIC	ANIONIC	HIGH	TcO_4^-
Np	CATIONIC	BD	LOW	NpO_2^+
I	ANIONIC (49% ORG.)	ANIONIC (57% ORG.)	HIGH	I^-
Cs	CATIONIC	BD	LOW	Cs^+
Sr	CATIONIC	CATIONIC	HIGH	Sr^{+2}
Ni	CATIONIC	NONIONIC	LOW	Ni^{+2}, $NiOH^-$, $Ni(OH)_2^o$
Co	90-99% CATIONIC	50-75% ANIONIC	HIGH	Co^{+2}
Ce	CATIONIC	BD	LOW	$Ce(OH)_2^+$
Ru	30-96% CATIONIC	80-93% ANIONIC	HIGH	$Ru(OH)_2^{+2}$, RuO_4^-, RuO_4^{-2}
Sb	VARIABLE	NONIONIC	HIGH	$HSbO_2^o$, $Sb(OH)_3^o$, $Sb(OH)_6^-$
Fe	50-70% CATIONIC	67% ANIONIC	LOW	Fe^{+2}
Zn	80-99% CATIONIC	BD	LOW	Zn^{+2}, $ZnHCO_3^+$, $ZnSO_4^o$ $ZnCO_3^o$, $ZnOH^+$, $Zn(OH)_2^o$
Mn	CATIONIC	BD	LOW	Mn^{+2}, $MnHCO_3^+$, $MnSO_4^o$

BD = LOWER THAN DETECTION LIMIT

The observed anionic forms of these radionuclides in the well and spring waters, which account for the mobile species, underscores the need for further research aimed at developing a better understanding of the role of natural and man-made organic ligands in complexing radionuclides and enhancing their mobility in groundwaters.

4.1.5 RECOMMENDATIONS

The work conducted at this site has identified several important research areas which need addressing to better understand the potential for radionuclide migration in groundwaters. One important area is the influence of organic materials in complexing radionuclides in a way which enhances their mobility. The unusual anionic species of ^{60}Co and ^{55}Fe, and the nonionic ^{63}Ni in the groundwater suggests that perhaps organic complexation has resulted in the occurrence of these forms. The organic iodine which behaves like an anion at this site further emphasizes the need for more complete studies of the occurrence and behavior of organoradionuclide complexes in groundwaters. Certainly, geochemical modeling needs to eventually include the effects of certain important dissolved organic compounds in groundwaters. These compounds need to be identified in field investigations at a variety of field sites. Also, the identification of radionuclide complexes with inorganic ligands (e.g., carbonate, hydroxide, or fluoride) need to be made.

Another important area needing further development is the coupling of improved geochemical models with appropriate hydrological models to provide realistic predictive radionuclide transport modeling capabilities. Both site specific and generic coupled models need to be better developed to predict radionuclide transport under a variety of environmental conditions.

A picture is beginning to emerge of a select group of radionuclides which appear to be mobile in several slightly contaminated groundwaters (e.g., Tc, Co, I, Ru, Sb). There is a need to

examine a number of sites where radionuclides are migrating in groundwaters to determine if generic mechanisms are responsible for these field observations. These mechanisms then need to be understood and applied to the performance objectives of commercial waste disposal sites for more realistic assessments of the potential transport of radionuclides from the sites by groundwater intrusion.

REFERENCES

Barraclough, J. T., B. D. Lewis, and R. C. Jensen, 1981. Hydrologic Conditions at the Idaho National Engineering Laboratory, Idaho. Emphasis: 1974-1978. IDO-22060, U. S. Geological Survey, Water Resources Investigation, Open File Report 81-526.

Coles, D. G. and L. D. Ramspott, 1982. Migration of Ruthenium-106 in a Nevada Test Site Aquifer: Discrepancy Between Field and Laboratory Results, Science 215: 1235-1237.

Cooper, E. L. and J. O. McHugh, 1983. Migration of Radiocontaminants in a Forested Wetland on the Canadian Shield: Nuclide Speciation and Arboreal Uptake. The Science of the Total Environment 28: 215-230.

Eddy, P. A. and J. S. Wilbur, 1980. Radiological Status of the Ground Water Beneath the Hanford Project. PNL-3346, UC-41, Pacific Northwest Laboratory, Richland, WA.

Killey, R.W.D., et. al., 1984. Subsurface Cobalt-60 Migration from a Low Level Waste Disposal Site, Environ. Sci. Tech. 18, 148-156.

Kirby, L. J. (ed.), 1982. Radionuclide Distribution and Migration Mechanisms at Shallow Land Burial Sites. NUREG/CR-2383, PNL-4067 RW, U. S. Nuclear Regulatory Commission, Washington, D.C.

Means, J. L., D. A. Crerar, and J. O. Duguid. Migration of Radioactive Wastes: Radionuclide Mobilization by Complexing Agents, Science 200: 1477-1481, June 30, 1978.

Morgan, J. J., 1967. Chemical Equilibria and Kinetic Properties of Manganese in Natural Waters. In: Principles and Applications of Water Chemistry, S. D. Faust and J. V. Hunter, Eds., John Wiley and Sons, Inc., New York.

Rai, D. and R. J. Serne, 1978. Solid Phases and Solution Species of Different Elements in Geologic Environments, PNL-2651, UC-70, Pacific Northwest Laboratory, Richland, WA.

Robertson, D. E., K. H. Abel, W. H. Rickard, and A. P. Toste, 1981. Influence of the Physicochemical Forms of Radionuclides During Migration in Groundwaters. Annual Progress Report for 1981. Prepared for the U. S. Nuclear Regulatory Commission by Pacific Northwest Laboratory, Richland, WA.

Robertson, D. E., A. P. Toste, K. H. Abel, and R. L. Brodzinski, 1983. Radionuclide Migration in Groundwater, NUREG/CR-3554, PNL-4773 RW, U. S. Nuclear Regulatory Commission, Washington, D.C.

Stone, J. A., 1982. Radionuclide Migration Studies at the Savannah River Plant LLW Burial Ground, a Humid SLB Site. In: Proceedings of the Fourth Annual DOE LLWMP Participants Information Meeting, August 31-September 2, 1982, Denver, CO.

Toste, A. P., L. J. Kirby, and T. R. Pahl, 1983. Role of Organics in the Subsurface Migration of Radionuclides in Groundwater. 185th National Meeting, American Chemical Society, Seattle, WA, March 20-25, 1983.

4.2 FIELD EXPERIMENT DETERMINATIONS OF DISTRIBUTION COEFFICIENTS OF ACTINIDE ELEMENTS IN ALKALINE LAKE ENVIRONMENTS

H. J. Simpson,
R. M. Trier,
Y.-H. Li, and
R. F. Anderson

Lamont-Doherty Geological Observatory of Columbia University

ABSTRACT

Transport calculations designed to simulate mobility in the far field of radionuclides released from a high level waste repository are very sensitive to the numerical values used to describe the extent of adsorption and/or desorption of particular nuclides. Groundwater radionuclide concentrations are often estimated from solubility calculations or from laboratory distribution coefficients. Field data on radionuclide concentrations in natural waters provide critical tests for the validity of numerical values employed for these radionuclide transport calculations.

Radionuclide concentrations of a number of elements (Am, Pu, U, Pa, Th, Ac, Ra, Po, Pb, Cs and Sr) have been measured in the water and sediments of a group of alkaline lakes in the western USA. These data demonstrate greatly enhanced soluble phase concentrations of elements with oxidation states of III, IV, V and VI as the result of carbonate complexing. Dissolved concentrations of isotopes of U, Pa, and Th in a lake with pH=10 and a total inorganic carbon concentration of 4×10^{-1} moles/l were greater than those in sea water (pH=8, $\Sigma CO_2=2\times10^{-3}$ moles/l) by orders of magnitude for ^{233}U, ^{238}U ($\sim10^2$), ^{231}Pa, ^{228}Th, ^{230}Th ($\sim10^3$) and ^{22}Th ($\sim10^5$). Concentrations of fallout $^{239,240}Pu$ in the more alkaline lakes were equivalent to effective distribution coefficients of $\sim10^3$, about a factor of 10^2 lower than in most other natural lakes, rivers, estuaries and coastal marine waters.

Measurements of radionuclides in natural systems are essential for assessment of the likely fate of radionuclides which may be released from high level waste repositories to groundwater. Laboratory scale experiments using tracer additions of radionuclides to mixtures of water and sediment yielded distribution coefficients which were significantly different from those derived from field measurements (10^1-10^2 lower for Po and Pu). Order of magnitude calculations from thermodynamic data of expected maximum U and Th concentrations, limited by pure phase solubilities, suggest that carbonate complexing can enhance solubility by many orders of magnitude in natural waters, even at relatively low carbonate ion concentrations. These calculations do not, however, accurately predict the natural system concentrations we measured. Thus neither laboratory tracer experiments nor calculations from thermodynamic pure-phase solubility data were able to adequately explain or predict measured field concentrations of soluble radionuclides.

4.2.1 Introduction

One of the most important factors governing the transport of radionuclides in aqueous environments is partitioning between aqueous phases and geological materials such as detrital particles. The propensity of a particular radionuclide to associate with solid phases, often expressed in terms of an effective distribution coefficient, K_d, has considerable influence on its transport rates and pathways in aquatic systems. Low values of K_d (i.e. $\leq 10^1$), defined here as the ratio of the activity of nuclide R per gram of dry solid material to the activity of nuclide R per ml of solution (A_R per gram solid/A_R per ml solution), imply behavior of radionuclides predominantly as soluble components with relatively little retardation of either diffusive or advective aqueous phase transport. In contrast, high values of K_d (i.e. 10^4-10^6) indicate substantial association with solid materials, and net aqueous phase transport by diffusion and advection at rates orders of magnitude slower than for low K_d radionuclides.

4.2.1.1 Issues addressed by this research

Some of the primary issues concerning the migration of radionuclides in the far field that we are examining include:

To what extent will radionuclides be complexed by natural inorganic and organic ligands?

How do numerical values of effective distribution coefficients of radionuclides in real natural water systems compare with those derived from small scale experiments?

How do numerical values of effective distribution coefficients of radionuclides in natural waters vary depending upon the oxidation state of a particular nuclide?

Which inorganic ions are most important in forming anion complexes with radionuclides in natural waters?

4.2.1.2 Background and Objectives

One method to help establish representative radionuclide distribution coefficients is through laboratory experiments using small amounts of solid and aqueous phases. The compositions of both phases can be readily varied in such experiments, and "end-members" such as specific clay minerals or manganese oxides and reagent NaCl solutions buffered at various pH levels can be used, as well as natural solid phases and solutions from representative environmental systems (Duursma and Bosch, 1970). Measurements of distribution coefficients in such experiments can be made rapidly and with considerable precision for a single equilibration by employing tracer activity levels of one or more radionuclides analyzed by gamma spectrometry (Schell and Sibley, 1982). These types of experiments can provide valuable insights into processes which are likely to be important in regulating effective distribution coefficients, but they are not sufficient by themselves to establish representative radionuclide behavior in real aqueous systems. Laboratory experiments restrict both the time and spacial scales involved in radionuclide behavior, and may inadvertently exclude some of the processes which are important in the situations of most relevance to management of radionuclides.

The data reported here consist primarily of measurements of natural and anthropogenic (fallout) radionuclides in the water and sediments of a group of natural lakes. These lakes can be viewed as a set of large-scale natural experiments from which the effective partitioning of radionuclides between water and solid phases can be observed. The time-scales of equilibration and spacial scales represented by these natural lakes are much greater than is feasible to employ in laboratory distribution coefficient measurements, and thus can provide valuable constraints on extrapolations of results from these latter experiments to the real systems of primary interest in waste management.

4.2.1.3 Scope of Research

Our efforts are directed towards obtaining data on radionuclide behavior in natural water systems which can provide critical information for testing of nuclide concentrations computed from thermodynamic models and small scale laboratory experiments. The systems we have studied initially provide information on radionuclide complexing by carbonate ions, which appear to be of considerable importance in enhancing the potential for nuclide transport. Field and laboratory work in progress will provide information on the effects of sulfate and chloride ions on radionuclide mobility.

4.2.2 Methods

The systems chosen for sampling are fairly large (most have surface areas of more than one hundred square kilometers), closed-basin, alkaline lakes located (Figure 1) in the western Great Basin physiographic province of the United States (California, Oregon and Nevada). This area is characterized by a series of structural basins with no exterior drainage to the ocean. Many of these interior drainage basins contain persistent saline lakes or playas which support ephemeral lakes during unusually wet periods. Some of these lakes, such as Great Salt Lake in Utah, have relative proportions of major ions similar to seawater, with chloride accounting for a large fraction (more than 90%) of the total anionic balance and inorganic carbon as bicarbonate and carbonate ions being minor constituents (less than 1% of total anion equivalents). Another group, which derive most of their supply of dissolved ions from weathering of silicate minerals followed by extensive evaporation of the resultant fresh water streams and springs to produce alkaline lakes (Hutchinson, 1957; Broecker and Walton, 1959; Jones, 1966; Garrels and MacKenzie, 1967; Simpson, 1970), have relative proportions of major ions quite different from seawater. This latter group, some of which have carbonate ion concentrations of more than 10^3 greater than in seawater, provides an ideal natural environment for establishing the effect of carbonate complexing on radionuclide mobilities.

We concentrated $^{239,240}Pu$, ^{238}U, ^{232}Th, ^{230}Th, ^{228}Th, ^{231}Pa, ^{210}Po, and ^{210}Pb from large samples in the field (80 to 240 liters) after filtration through glass fiber filters, by coprecipitation with $Fe(OH)_3$. The hydroxide precipitates were returned to the laboratory, and analyzed by chemical preparation and alpha spectrometry procedures frequently used in the field of chemical oceanography (Ku, 1968; Wong, 1971; Kaufman et al., 1973). Measurements of ^{238}U, ^{234}U and ^{233}Th were made on small samples (1-10 liters) after filtration, laboratory chemical preparation and alpha (^{238}U, ^{234}U) or beta (^{233}Th) counting. We measured ^{226}Ra by scintillation counting of its gaseous daughter product, ^{222}Rn. Cesium-137 was determined by γ-counting of an exchange resin used to

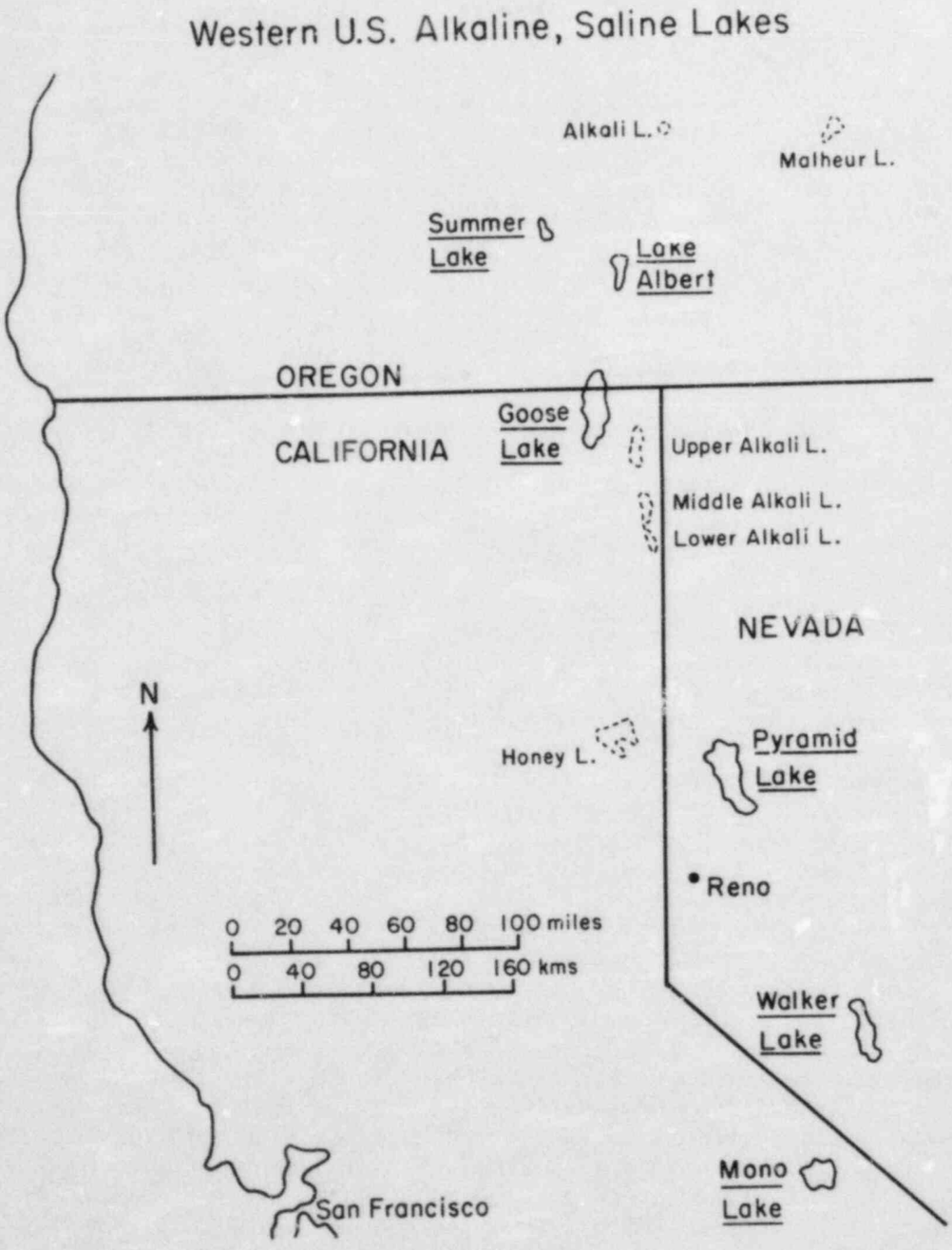

Figure 1: Locations of closed basin saline lakes in the Great Basin from which samples for radionuclide measurements were collected.

remove cesium from large samples (40-240 liters) and ^{90}Sr was determined by β-counting. Sediment samples were collected by coring, and analyzed at many depth intervals for the same nuclides discussed above.

4.2.3 Results

Chemical data for the major anion compositions of six alkaline lakes that we sampled, plus data for seawater, are given in Table 1 and Figure 2. Carbonate alkalinities ranged from $2x10^{1}$ to $7x10^{2}$ meq/l in the lakes, compared with 2.5 meq/l for seawater, and carbonate ion ranged from $<10^{1}$ to $2x10^{2}$ m mole/l, compared to $2x10^{-1}$ m mole/l for seawater. Concentrations of dissolved ^{238}U in the lakes ranged from 10^{1} to $2x10^{2}$ pCi/l, dissolved ^{232}Th from $<10^{1}$ to $7x10^{2}$ pCi/m^3, and fallour $^{239,240}Pu$ from $2x10^{-1}$ to $1x10^{-1}$ pCi/m^3 (Table 2). Sediment radionuclide concentrations in the alkaline lakes were not unusually high (Table 3).

Distribution coefficients of a number of radionuclides in six alkaline lakes are listed in Table 4, based on a large amount of data summarized in Tables 2 and 3. Uranium was very strongly complexed in all of the lakes ($K_d \sim 10^{1}$), and Am, Pu, Pa and Th had considerably higher water column concentrations ($K_d \sim 10^{3}$) than is typical of most natural waters (Simpson et al., 1980). Comparison of dissolved radionuclide concentrations in Mono Lake with data for seawater (Table 5) clearly indicate the importance of carbonate complexing for elements with oxidation states of IV to VI, and to a lesser extent for III.

Laboratory distribution coefficient measurements (sorption experiments) with Mono Lake water and sediments, while clearly demonstrating the importance of carbonate complexing, yielded K_d values for Pu and Po of $\sim 10^{1}$ and $\sim 10^{3}$, respectively. These values were stustantially lower than suggested by our field measurements ($\sim 10^{3}$ for Pu and $\sim 10^{4}$ for Po).

The soluble concentrations of the longest half-life nuclides of uranium and thorium in Mono Lake are $2x10^{-6}$ mole/l ^{238}U and $3x10^{-8}$ mole/l ^{232}Th (Table A-1), compared to $1x10^{-8}$ mole/l ^{238}U and $<3x10^{-13}$ mole/l ^{232}Th in seawater. Solubilities of actinide oxides are known to be very low ($\sim 10^{-54}$ for $MO_2(s)$), and thus dissolved concentrations of elements present in the +4 oxidation state would be expected to be very low. Based on one set of equilibria calculations (Table A-2), concentrations of U and Th as UO_2^{2+} and Th^{4+} which would coexist in the presence of $UO_2(OH)_2(s)$ and $ThO_2(s)$ would be of the order of 10^{-15} mole/l (pH=10) and 10^{-38} mole/l (pH=10), respectively. If the effects of hydroxide and carbonate complexes are included, the ratio of $UO_2(CO_3)_3^{4-}$ to UO_2^{2+} would be 10^{22} in Mono Lake; the ratio of $Th(CO_3)_5^{6-}$ to Th^{4+} in Mono Lake would be 10^{33} (Table A-2). Considering the very high ratio of complexed U or Th to uncomplexed species due to the strength of actinide carbonate complexes, the upper limit on total complexed U and Th in solution would essentially be defined by the total ligand concentration, divided by the mean number of ligands per complex. In the case of Mono Lake, with carbonate ion concentrations of $\sim 2x10^{2}$ m mole/l, the computed solubilities, based on pure-phase solid equilibration and the complexing effects of hydroxide and carbonate would be of the order of 10^{-2}-10^{-1} mole/l for U compared to values of 10^{-6} mole/l which we measured.

Table 1

Average Major Anion Composition of Alkaline Lakes

Lake	Chloride (meq/l)	Chloride (% of ΣAnions)	Sulfate (meq/l)	Sulfate (%of ΣAnions)	Carbonate Alkalinity (meq/l)	Inorganic Carbon (%of ΣAnions)	Total anions: $Cl^- + SO_4^= + HCO_3 + CO_3^=$ (meq/l)	Carbonate ion (mM)
Mono L.	595	39	268	18	650	43	1513	200
L. Abert	735	59	24	2	485	39	1244	160
Walker L.	74	41	53	29	54	30	181	20
Pyramid L.	59	68	6.3	7	22	25	87.3	(10)
Goose L.	66	54	6.6	5	50	41	122.6	20
Summer L.	150	34	27	6	270	60	447	40
Sea Water	550	95	28	5	2.5	0.4	580.5	0.2

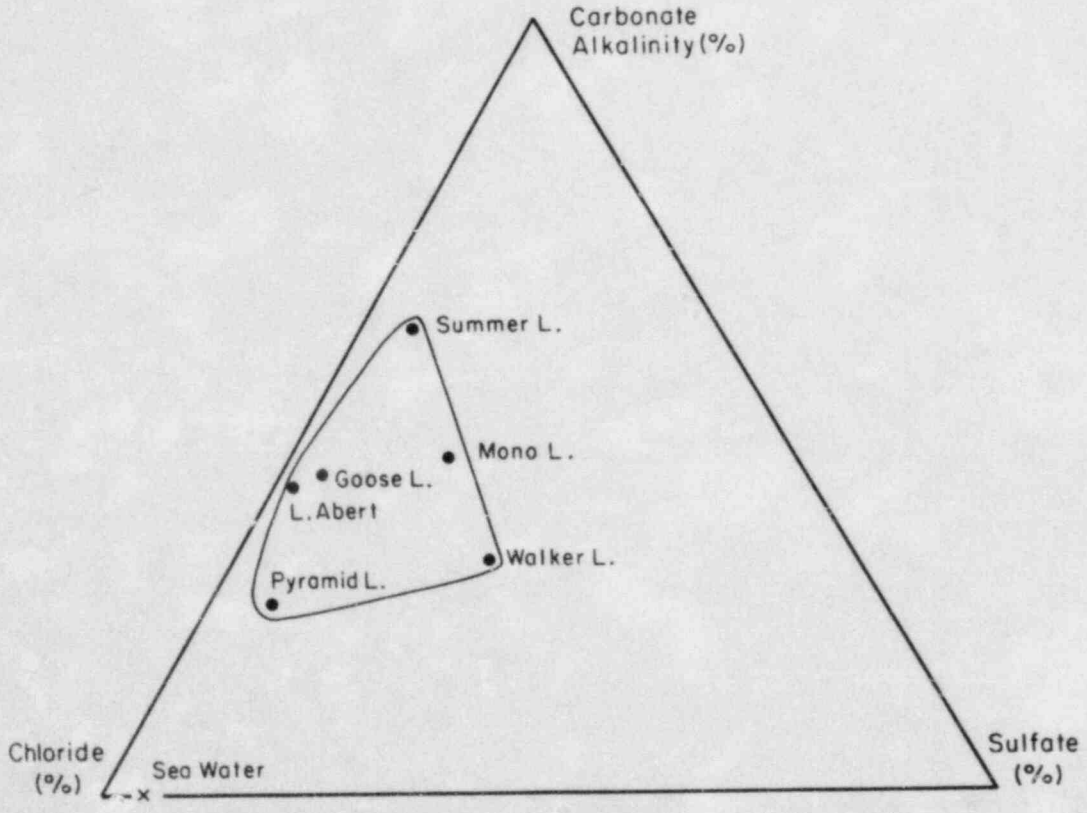

Figure 2: Relative concentrations of major anions, expressed as milliequivalents per liter, for high carbonate Great Basin Lakes.

Table 2

Summary of Dissolved Radionuclides in Alkaline Lakes

Nuclide	Mono L.	L. Abert	Walker L.	Pyramid L.	Goose L.	Summer L.
^{241}Am (pCi/m^3)	1.8	-	-	-	-	-
$^{239,240}Pu$ (pCi/m^3)	13	11	0.5	0.2	-	-
^{239}Pu (pCi/m^3)	0.54	0.42	(0.02)	(0.008)	-	-
^{238}U (pCi/1)	170	19	51	6	4	9
^{234}U (pCi/1)	230	47	72	12	9	15
^{231}Pa (pCi/m^3)	115	-	-	-	-	-
^{234}Th (pCi/1)	220	18	36	(0.6)	1.8	-
^{232}Th (pCi/m^3)	690	94	5	3	-	-
^{230}Th (pCi/m^3)	1330	130	8	4	-	-
^{228}Th (pCi/m^3)	790	110	(47)	9	-	-
^{227}Ac (pCi/m^3)	<2.7	-	-	-	-	-
^{228}Ra (pCi/m^3)	230	-	-	-	-	-
^{226}Ra (pCi/m^3)	420	40	200	25	20	-
^{210}Po (pCi/m^3)	105	185	7.7	-	-	-
^{210}Pb (pCi/m^3)	200	750	63	-	-	-
^{137}Cs (pCi/1)	2.0	-	0.13	0.14	-	-
^{90}Sr (pCi/1)	0.16	-	-	-		
HTO (T.U.)	70	35	93	45	-	-

Table 3

Summary of Sediment Radionuclides in Alkaline Lakes

Nuclide	Mono L.	L. Abert	Walker L.	Pyramid L.	Goose L.	Summer L.
^{241}Am (pCi/kg)	[7]	-	-	-	-	-
^{230,240}Pu (pCi/kg)	28	22	16	40	20	10
^{239}Pu (pCi/kg)	1.1	1.1	0.6	3	0.7	0.5
^{238}U (pCi/g)	2.4	1.1	2.7	1.4	0.1	0.2
^{234}U (pCi/g)	2.9	2.4	3.5	2.2	0.3	0.4
^{231}Pa (pCi/g)	[0.11]	-	-	-	-	-
^{234}Th (pCi/g)	[2.4]	[1.1]	[2.7]	[1.4]	[0.1]	[0.2]
^{232}Th (pCi/g)	0.5	0.2	1.4	0.4	0.2	0.3
^{230}Th (pCi/g)	0.7	0.2	1.5	0.5	0.3	0.3
^{228}Th (pCi/g)	0.4	0.2	1.3	0.4	0.3	0.3
^{228}Ac (pCi/g)	0.3	0.2	1.2	0.4	0.3	0.4
^{227}Ac (pCi/g)	[0.11]	-	-	-	-	-
^{228}Ra (pCi/g)	[0.5]	[0.2]	[1.4]	[0.4]	[0.2]	[0.3]
^{226}Ra (pCi/g)	[0.8]	[0.2]	[1.5]	[0.6]	[0.3]	[0.4]
^{214}Bi (pCi/g)	0.8	0.2	1.5	0.6	0.3	0.4
^{210}Po (pCi/g)	[0.8]	[0.2]	[1.5]	[0.6]	[0.3]	[0.4]
^{210}Pb (pCi/g)	[0.8]	[0.2]	[1.5]	[0.6]	[0.3]	[0.4]
^{137}Cs (pCi/kg)	150	1500	1800	1100	750	600
^{90}Sr (pCi/kg)	~1000	-	-	-	-	-
^{40}K (pCi/g)	16	15	16	12	9	17

Table 4

Ratio of Sediment to Dissolved Radionuclides
(expressed as $K_d = A_i$ per g sed./A_i per mil water)

Nuclide	Mono L.	L. Abert	Walker L.	Pyramid L.	Goose L.	Summer L.
^{241}Am	$4x10^3$	-	-	-	-	-
$^{239,240}Pu$	$2x10^3$	$2x10^3$	$3x10^4$	$2x10^5$	-	-
^{238}Pu	$2x10^3$	$3x10^3$	$3x10^4$	$4x10^5$	-	-
^{238}U	$1x10^1$	$6x10^1$	$5x10^1$	$2x10^2$	$3x10^1$	$2x10^1$
^{234}U	$1x10^1$	$5x10^1$	$5x10^1$	$2x10^2$	$3x10^1$	$3x10^1$
^{231}Pa	$1x10^3$	-	-	-	-	-
^{234}Th	[$1x10^1$]	[$6x10^1$]	[$8x10^1$]	[$2x10^3$]	[$6x10^2$]	-
^{232}Th	$7x10^2$	$2x10^3$	$3x10^5$	$1x10^5$	-	-
^{230}Th	$5x10^2$	$2x10^3$	$2x10^5$	$1x10^5$	-	-
^{228}Th	$5x10^2$	$2x10^3$	$3x10^4$	$4x10^4$	-	-
^{227}Ac	[$>4x10^4$]	-	-	-	-	-
^{228}Ra	$2x10^3$	-	-	-	-	-
^{226}Ra	$2x10^3$	$5x10^3$	$8x10^3$	$2x10^4$	$2x10^4$	-
^{210}Po	$8x10^3$	$1x10^3$	$2x10^5$	-	-	-
^{210}Pb	$4x10^3$	$3x10^2$	$2x10^4$	-	-	-
^{137}Cs	$8x10^1$	-	$1x10^4$	$8x10^3$	-	-
^{90}Sr	$6x10^3$	-	-	-	-	-

Table 5

Comparison of Dissolved Radionuclides in Mono Lake and Sea Water

Nuclide	Mono Lake (pCi/m³)	Surface Sea Water (pCi/m³)	Mono L./ Sea Water
^{241}Am (III)	1.8	2.23[a]	8
^{239,240}u (IV-VI)	13	1.4[b]	9
^{238}Pu (IV-VI)	0.54	0.056[b]	10
^{238}U (VI)	170,000	1,100[c]	150
^{234}U (VI)	230,000	1,300[c]	180
^{231}Pa (V)	115	0.1[d]	>1x10³
^{234}Th (IV)	(220,000)	800[e]	~250
^{232}Th (IV)	690	<0.008[f]	>8x10⁴
^{230}Th (IV)	1,330	<0.6[d]	>2x10³
^{228}Th (IV)	790	<0.4[g]	>2x10³
^{227}Ac (III)	<2.7	-	-
^{228}Ra (II)	230	20[h]	12
^{226}Ra (II)	420	40[i]	11
^{210}Po (IV)	105	30[j]	4
^{210}Pb (II)	200	50[i]	4
^{137}Cs (I)	2,000	120[k]	17
^{90}Sr (II)	160	80[l]	2
HTO (T.U.)	70	15[m]	5

a) Livingston and Bowen, 1976
b) Bowen et al., 1980
c) Ku et al., 1977
d) Moore and Sackett, 1964
e) Bhat et al., 1969
e) Kaufman, 1969; Moore, 1981
g) Knauss et al., 1978
h) Kaufman et al., 1973
i) Bruland et al., 1974
j) Bacon et al., 1976; Nozaki et al., 1976
k) ^{137}Cs to ^{90}Sr ratio assumed to be 1.5
l) Bowen et al., 1969
m) Roether; 1967

4.2.4 Conclusions

The data reported here for radionuclide concentrations in a group of alkaline lakes demonstrate clearly that effective solubilities of a number of nuclides with oxidation states of III to VI are substantially higher than in natural waters with lower carbonate in concentrations. In addition, the degree of solubility enhancement is proportional to carbonate ion concentration, especially for elements such as Th and Pu (Simpson et al., 1983). Concentrations of dissolved U and Th (10^{-6} - 10^{-8} mole/l) in the highest alkalinity lakes (0.5 - 0.7 eq/l of carbonate alkalinity) demonstrate substantial mobilities for elements with oxidation states of IV and VI in natural waters with appreciable carbonate ion concentrations. Although both laboratory distribution coefficient experiments and pure-phase thermodynamic solubility calculations clearly support the importance of carbonate complexing in enhancing actinide solubility, neither of these approaches is able to accurately predict or explain distribution coefficients based on field sample radionuclide concentration measurements. There is clearly no adequate substitute for such field data in assessing radionuclide transport pathways and rates for possible releases from a high level waste repository to groundwater.

4.2.5 Recommendations

Design and performance assessment of high-level radionuclide waste repository facilities requires consideration of a large set of complicated and interactive processes and components. Some of the most important elements of choice for appropriate sites and design strategies are the geologic and hydrologic environments to be used. Solid phase and groundwater chemical conditions, as well as groundwater movement rates in the vicinity of a waste repository will be very strongly influenced by both geologic and hydrologic conditions. Behavior of radionuclides in a variety of groundwater and environments can be computed on the basis of a variety of thermodynamic and laboratory simulation models to gain insights about important processes. In addition to these activities, however, it is important to accumulate sufficient information on radionuclide behavior in natural systems to provide direct indication of likely soluble phase nuclide concentrations in the far field for a number of geologic and hydrologic conditions. We recommend that a significantly larger research effort should be devoted to the study of radionuclide behavior in natural environments than is presently occurring. This effort is not presently being accomplished under the general category of "site characterization", and represents what should be a more important component of the national program in high level nuclear waste management.

4.2.6 Planned Research

The data reported here were obtained to provide information about the influence of carbonate complexing on radionuclide mobility in natural waters. We are currently analyzing water and sediment samples collected from high sulfate and high chloride environments to establish the effect of these anions on enhancing or reducing solubilities of radionuclides in natural systems. The field environments from which these samples were collected include evaporite deposit areas (gypsum or halite) in the USA (New York and New Mexico) and saline lakes in western Canada.

4.2.7 Acknowledgements

The data reported here represent considerable field and laboratory effort by a number of people in addition to the authors, including B. Deck, A. Herczeg and G. Mathieu of Lamont-Doherty Geological Observatory, D. Hammond from the University of Southern California and C. Olsen from Oak Ridge National Laboratory. The information summarized here is based on field work initiated at Mono Lake with financial support by the Department of Energy (E-2529) and expanded to include work at a number of other alkaline lakes with financial support by the Nuclear Regulatory Commission (NRC-04-81-217). Contribution number 0000 of Lamont-Doherty Geological Observatory.

4.2.8 References

Allard, B.; 1982. Solubilities of actinides in neutral or basic solutions, N. Edelstein (Ed.) Actinides in Perspective, Pergamon Press, Oxford, pp. 553-580.

Anderson, R. F., 1980. The marine geochemistry of thorium and protactinium. Ph.D. Thesis, Massachusetts Institute of Technology-Woods Hole Oceanographic Institution Joint Program in Oceanography, Woods Hole, Massachusetts. 287 pp.

Anderson, R. F., M. P. Bacon and P. G. Brewer, 1982. Elevated concentrations of actinides in Mono Lake. Science, 216: 514-516.

Bacon, M. P., D. W. Spencer and P. G. Brewer, 1976. 210Pb/226Ra and 210Po/210Pb disequilibria in seawater and suspended particulate matter. Earth Planet. Sci. Lett., 32: 277.

Bhat, S. G., S. Krishnaswami, D. Lal, Rama and W. S. Moore, 1969. 234Th/238U ratios in the ocean. Earth Planet. Sci. Lett., 5: 483.

Bowen, V. T., V. E. Noshkin, H. L. Volchok and T. T. Sugihara, 1969. Strontium-90; concentrations in surface waters of the Atlantic Ocean. Science, 1964: 825.

Bowen, V. T., V. E. Noshkin, . D. Livingston and H. L. Volchok, 1980. Fallout radionuclides in the Pacific Ocean: vertical and horizontal distributions, largely from GEOSECS stations. Earth Planet. Sci. Lett., 49: 411.

Broecker, W. S. and A. F. Walton, 1959. Re-evaluation of the salt chronology of several Great Basin lakes. Geol. Soc. Am. Bull., 31:411-419.

Bruland, K. W., M. Koide and E. D. Goldberg, 1974. The comparative marine geochemistries of lead-210 and radium-226. J. Geophys. Res., 79:3083.

Duursma, E. K. and C. J. Bosch, 1970. Theoretical, experimental and field studies concerning diffusion of radioisotopes in sediments and suspended particles of the sea. Part B: methods and experiments. Netherlands J. of Sea Res., 4: 395:469.

Garrels, R. M. and Mackenzie, F. T., 1967. Origin of the chemical composition of some springs and lakes. In: Equilibrium Concepts in Natural Water Systems (R. F. Gould, ed.). Amiercan Chemical Society, Advances in Chemistry, Series No. 67, Washington, D.C. pp. 222-242.

Hutchinson, G. E., 1957. A Treatise on Limnology, Vol. I. Geography, Physics and Chemistry. John Wiley and Sons, New York. 1015 pp.

Jones, B. F., 1966. Geochemical evolution of closed basin water in the western Great Basin. In: Second Symposium on Salt (J. L. Rau, ed.). Cleveland, Ohio, Northern Ohio Geological Society, Vol. 1, pp. 181-199.

Kaufman, A., 1969. The 232Th concentration of surface ocean water. Geochim. Cosmochim. Acta, 33: 717-724.

Kaufman, A., R. M. Trier, W. S. Broecker and H. W. Feely, 1973. Distribution of 228Ra in the world ocean. J. Geophys. Res., 78: 8827.

Knauss, K. G. T. L. Ku and W. S. Moore, 1978. Radium and thorium isotopes in the surface waters of the East Pacific and coastal southern California. Earth Planet. Sci. Lett., 39: 235.

Ku, T. L., 1968. Protactinium 231 method of dating coral from Barbados Islands, J. Geophys. Res., 73: 2271-2276.

Ku, T. L., K. G. Knauss and G. G. Mathieu, 1977. Uranium in the open ocean concentration and isotopic composition. Deep Sea Res., 24: 1005.

Langmuir, D. and J. S. Herman, 1980. The mobility of thorium in natural waters at low temperatures, Geochim. Cosmochim. Acta 44: 1753-1766.

Livingston, H. D. and V. T. Bowen, 1976. Americium in the marine environment-relationships to plutonium, in Environmental Toxicity of Aquatic Radio nuclides: Models and Mechanisms. Ann Arbor Science, Ann Arbor, Michigan. pp. 107-130.

Moore, W. S. and W. M. Sackett, 1964. Uranium and thorium series in equilibrium in seawater. J. Geophys. Res., 69: 5401.

Moore, W. S., 1981. The thorium isotope content of ocean water. Earth Planet. Sci. Lett., 53: 419.

Nozaki, Y., J. Thomson and K. K. Turekian, 1976. The distribution of 210Pb and 210Po in the surface waters of the Pacific Ocean. Earth Planet. Sci. Lett., 32: 304.

Roether, W. 1967. Tritium in Wasser Kreislauf. Ph.D. Thesis, University of Heidelberg, West Germany.

Schell, W. R. and T. H. Sibley, 1982. Distribution coefficients for radio-nuclides in aquatic environments, final summary of report. NUREG/CR-1869, Office of Nuclear Regulatory Research, U.S. Nuclear Regulatory Commission, Washington, D.C. 21 pp.

Simpson, H. J., 1970. Closed basin lakes as a tool in geochemistry. Ph.D. Thesis, Columbia University, New York. 325 pp.

Simpson, H. J. and T. Takahashi, 1973. Interstitital water studies, Leg 15 - chemical model of seawater and saline water. In: Initial Reports of the Deep Sea Drilling Project, 20, 877 (B. C. Heezen, I. D. MacGregor, eds.). U.S. Govt. Printing Office, Washington, D.C.

Simpson, H. J., R. M. Trier and C. R. Olsen, 1980. Transport of plutonium by rivers. In: Transuranic Elements in the Environment (W. C. Hansen, ed.). Technical Information Center/U.S. Department of Energy (DOE/TIC-22800). pp. 684-690.

Simpson, H. J., R. M. Trier, C. R. Olsen, D. E. Hammond, A. Ege, L. Miller and J. M. Melack, 1980. Fallout plutonium in an alkaline, saline lake. Science, 207: 1071-1073.

Simpson, H. J., R. M. Trier, J. R. Toggweiler, G. Mathieu, B. L. Deck, C. R. Olsen, D. E. Hammond, C. Fuller and T. L. Ku, 1982. Radionuclides in Mono Lake, California. Science, 216: 512-514.

Simpson, H. J., R. M. Trier and Y.-H. Li, 1983, Field experiment determinations of distribution coefficients of actinide elements in alkaline lake environments, Report to Nuclear Regulatory Commission, March 1983, 129 p.

Thurber, D., 1965. The concentration of some natural radioelements in the waters of the Great Basin. Bull. Volcanologique, 28: 1. Napoli, Italy, 1-7.

Wong, K. M., 1971. Radiochemical determination of plutonium in seawater, sediments and marine organisms. Anal. Chim. Acta, 56: 355.

4.2.9 Appendix

Table A-1

Mono Lake U and Th Concentrations

$^{238}U = 170$ pCi/l

Conversion to molar units:

$$2.22 \frac{dpm}{pCi} \times 5.26\times10^{5} \frac{min}{Yr} \times \frac{4.51\times10^{9} yr}{1n2} \times \frac{1 \text{ mole}}{6.02\times10^{23} \text{ atoms}}$$

$$= 1.26\times10^{-8} \times \frac{pCi}{1} = \frac{mole}{1}$$

$$^{238}U = 1.7\times10^{2} \frac{pCi}{1} \times 1.26\times10^{-8} = \underline{2.1\times10^{-6} \text{ mole/l}}$$

$^{232}Th = 690$ pCi/m^3

Conversion to molar units:

$$2.22 \frac{dpm}{pCi} \times 5.26\times10^{5} \frac{min}{Yr} \times \frac{1.39\times10^{10} Yr}{1n2} \times \frac{1 \text{ mole}}{6.02\times10^{23} \text{ atoms}} \times \frac{10^{-3} m^3}{1}$$

$$= 3.89\times10^{-11} \times pCi/m^3 = mole/1$$

$$^{232}Th = 6.9\times10^{2} \frac{pCi}{m^3} \times 3.89\times10^{-11} \quad \underline{2.7\times10^{-8} \text{ mole/l}}$$

Table A-2

Uranium and Thorium Solubility Calculations for Mono Lake[a]

		U	Th
Assumed solubility limiting species		$UO_2(OH)_2(s)$	$ThO_2(s)$
Solubility product (K_s)		10^{-23}	10^{-54}
$\log[UO_2^{2+}]=(\log K_s+28.0-2pH)$		10^{-15} mole/l (pH=10)	--
$\log[Th^{4+}]=(\log K_s+56.0-4pH)$[b]		--	10^{-38} mole/l (pH=10)
$UO_2^{2+}+3CO_3^{2-} \rightleftharpoons UO_2(CO_3)_3^{4-}(\beta_3)$[c]	10^{24}		--
$Th^{4+}+5CO_3^{2-} \rightleftharpoons Th(CO_3)_5^{6-}(\beta_5)$[c]		--	10^{37}
U(VI) complex/UO_2^{2+}-Mono Lake[d]	10^{22}		--
Th(IV) complex/Th^{4+}-Mono Lake[d]	--		10^{33}

[a] Most of the calculations summarized in this table are based on results from Allard, 1982.

[b] Values of $[Th^{4+}]$ tabulated were computed from the expression shown in this table (taken from Allard, 1982.) Another calculation of ThO_2 solubility suggests ΣTh(IV) concentrations of $\sim 10^{-14}$ mole/l above pH=8, including hydrolysis effects but not carbonate ion (Langmuir and Herman, 1980).

[c] These complexes were chosen to illustrate representative actinide carbonate complex constants for Mono Lake, based on personal communications with Prof. I. Grenthe, Royal Institute of Technology, Stockholm, Sweden.

[d] Mono Lake water contains total carbonate ion concentrations of 2×10^{-1} mole/l (Simpson and Takahashi, 1973).

RADIONUCLIDE MIGRATION AROUND URANIUM ORE BODIES IN THE ALLIGATOR RIVERS REGION OF THE NORTHERN TERRITORY, AUSTRALIA - ANALOGUE OF RADIOACTIVE WASTE REPOSITORIES

P.L. Airey, D. Roman, C. Golian, S. Short, T. Nightingale, R.T. Lowson, Australian Atomic Energy Commission, Lucas Heights Research Laboratories, Sutherland, NSW 2232

B.G. Davey, D. Gray
Department of Soil Science, University of Sydney
Sydney, NSW 2600

ABSTRACT

Appropriate geochemical analogues may be used to reduce the uncertainties in predicting the long-term transport of actinides, radium and fission products from laboratory adsorption and hydrological data. In this study the migration of uranium series nuclides within, and down-gradient of ore bodies in the Alligator Rivers uranium province of the Northern Territory of Australia is described. A mathematical framework has been developed to permit calculation of the rate of leaching or deposition of uranium and radium between defined zones of the ore bodies, and the rate of loss of the nuclides due to groundwater transport and surface erosion.

A detailed study has been made of the distribution of uranium, thorium and radium isotopes within various minerals comprising the weathered ore assemblage. Uranium and thorium concentrate principally in the iron minerals and radium in the clay-quartz phases. Substantial disequilibria are observed, which are attributed to a combination of α-recoil and chemical effects. Evidence of the relative lability of iron phases is presented.

The transport of uranium series nuclides in groundwater intersecting the deposits has been investigated. Down-gradient of the Ranger One deposit, the maximum retardation factor of uranium is 250. The role of colloids in groundwater transport is being studied. Uranium is transported principally in solution. There appears to be an equilibrium between 'solute' and 'particulate' uranium. These investigations are being extended to thorium.

Extensions of the analogue to include iodine-129, technetium-99, neptunium-237 and plutonium-239 are planned. A conceptual framework has been developed and some field work undertaken in collaboration with the University of Arizona.

1. INTRODUCTION

In this project, a geochemical analogue approach is used in an attempt to understand the scientific principles whereby observations made over laboratory time-scales can be used to predict rates of transport of radionuclides over thousands or even tens of thousands of years. The redistribution of radionuclides within, and their migration down-gradient of, a number of deposits in the Alligator Rivers Uranium Province of the Northern Territory of Australia are being studied (Figure 1). Progress has been detailed in reports to the US Nuclear Regulatory Commission[1,2] and presented at scientific meetings.[3,4]

Uranium ore deposits are appropriate analogues of high-level radioactive waste repositories (HLWR) because the long-term migration of some members of the decay series (e.g. ^{226}Ra) need to be considered in site assessment. In addition, other significant transuranic elements and fission products (e.g. ^{237}Np, ^{239}Pu, ^{129}I and ^{99}Tc) can be incorporated into the analogue as technological advances make routine environmental measurements possible.

The Northern Territory deposits are particularly suited to this work. Most intersect the surface and well-defined weathered zones between 10 and 30 m thick overlay the uranium-bearing microgneiss, schist and silicified carbonates from which they were derived. An estimate can be made of the rate of evolution of the weathered profile. This provides a basis from which to calculate a time-scale for the distribution of uranium series nuclides throughout the near-surface zone. Correlations may therefore be established between the following parameters : the distribution of radionuclides within the ore, the groundwater hydrology and the laboratory leaching and sorption experiments. A schematic representation of the geochemical analogue approach is shown in Figure 2.

The ore samples are represented by a matrix hosting a suite of radionuclides M, and associated either with natural or 'synthetic' groundwater. Three important relationships are illustrated :

1. The relationship between the groundwater chemistry and the distribution of radionuclides through the ore sample. This is fundamental to the understanding of the mechanism of mobilization of radionuclides and sub-surface transport.

2. The relationship between leaching experiments and the distribution of radionuclides through the ore sample. These experiments may contribute to the interpretation of laboratory observations in terms of the sample geochemistry which has evolved over geological time.

3. The relationship between the sorption experiments and the matrix composition.

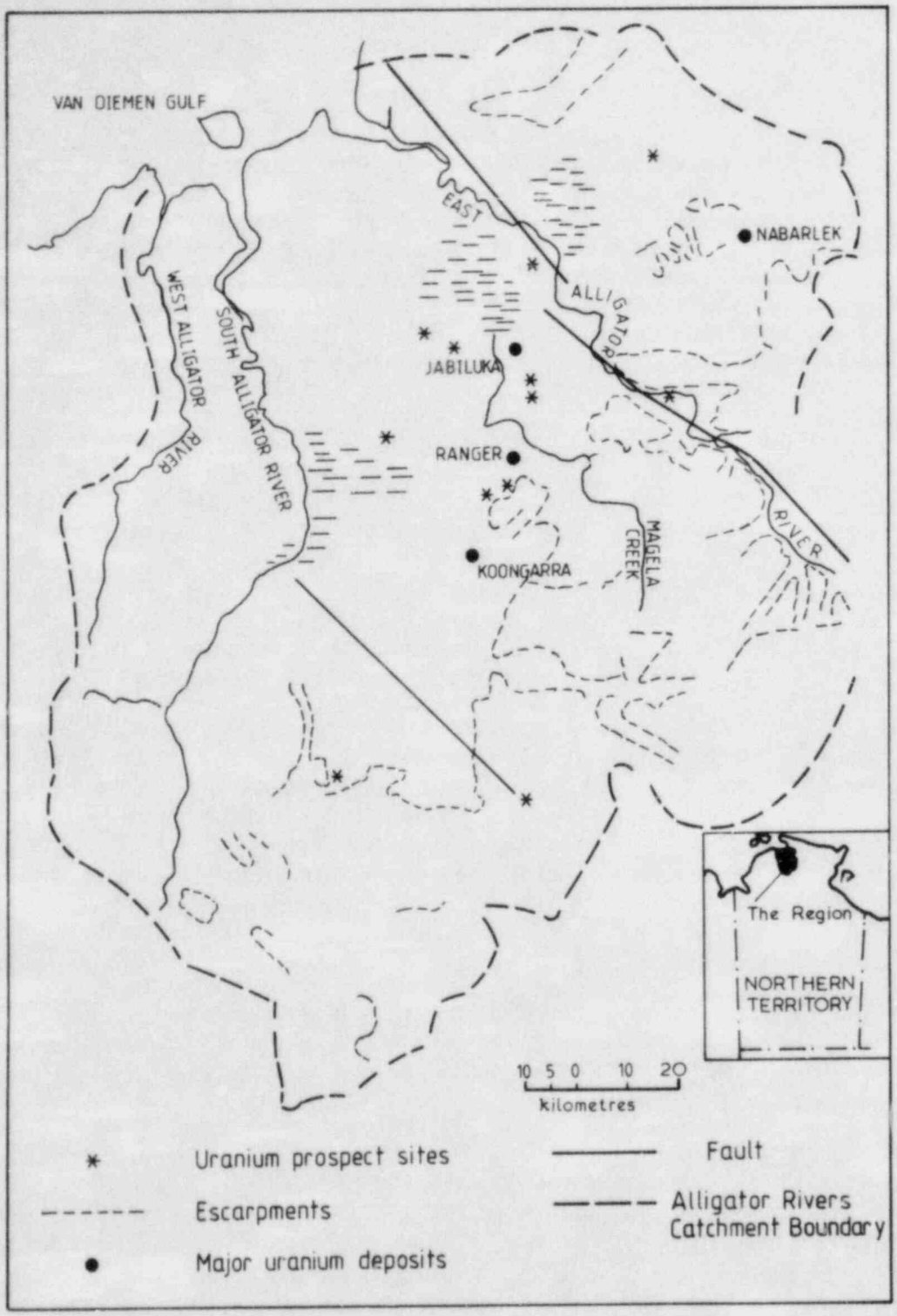

Figure 1

The Location of the Principal Uranium Ore Bodies and Prospects in the East Alligator River Area of the Northern Territory of Australia

In the uranium ore body, it may be possible to study these relationships for selected transuranic and fission product elements as well as for the uranium series nuclides. It is of course important to relate the findings from the geochemical analogue to the proposed repository site. As illustrated in Figure 2, parallel relationships 1 to 3 can normally be obtained using the ubiquituous uranium series nuclides. To predict the transport behaviour of ^{237}Np, ^{239}Pu, ^{99}Tc and ^{129}I, correlations with the uranium, thorium and radium properties established from the geochemical analogue study would need to be applied.

2. METHODOLOGY

2.1 Geochemical Modelling

A mathematical model has been developed to describe the gross features of the redistribution of uranium and radium within the upper sequences of the uranium deposits. It has enabled the calculation of a time frame for the evolution of the weathered zone, from which an estimate of the elapsed time since weathering is made for each sample. The model is useful in interrelating leaching, deposition and erosion parameters between one deposit and another, and in providing a quantitative assessment of possible extensions to the analogue.

2.2 Properties of Ore Samples

The geochemical model describes only the gross features of the near-surface zones of the uranium deposits. Model output needs to be interpreted by more detailed studies of the ore samples.

2.2.1 Mineralogy. X-ray diffraction techniques are used to study the mineralogy. Special attention is paid to iron minerals on which a substantial proportion of uranium and thorium is adsorbed and which comprise a significant fraction of groundwater particulates.

2.2.2 Selective Phase Separation. Sequential extraction techniques have been applied to the separation of identifiable phases from the weathered ore. If it is assumed that the co-extracted uranium series nuclides are uniquely associated with the separated phase, this is a powerful technique for studying their distribution throughout the samples. These distributions, particularly the $^{234}U/^{238}U$ ratio differences, may reflect the the time which has elapsed since weathering and may provide a basis for correlating laboratory observations with the output of the geochemical model.

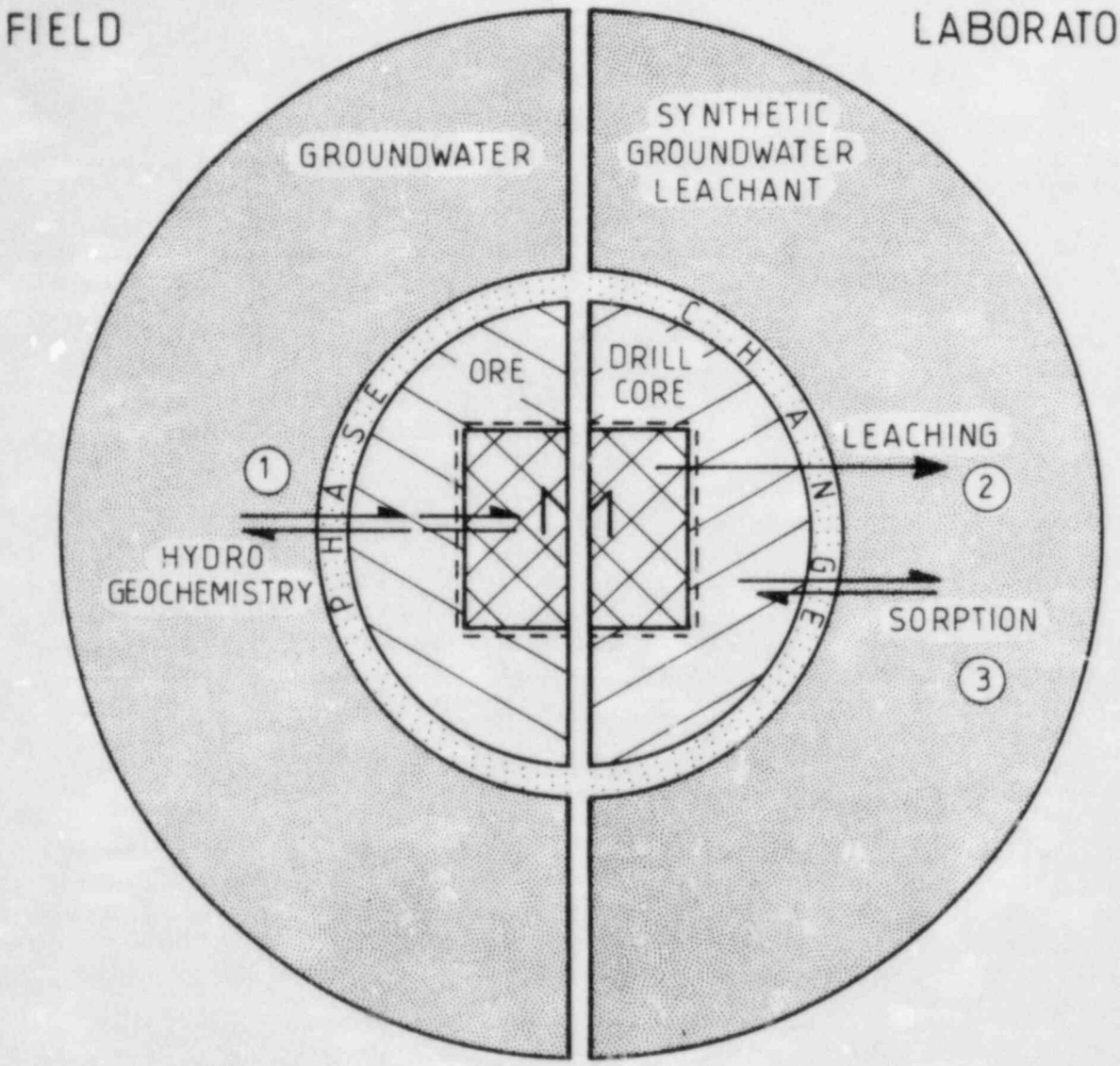

Figure 2

Schematic Representation of the Geochemical Analogue Approach. The relationship between field observations and laboratory studies is shown. The central portion of the diagram shows the solid phase which comprises the rock matrix and a suite of radionuclides M; the outer portion represents the aqueous phase. The relationships 1, 2 and 3 are discussed in the text. In the ore body M consists of the uranium series nuclides and a number of transuranic and fission product elements; at a repository site, M would include only the uranium series.

2.3 Laboratory Sorption/Leaching Studies

As the establishment of relationships 2 and 3 (Figure 2) is crucial to achieving the aims of the project, a systematic set of laboratory sorption/leaching experiments is planned.

As yet, only batch experiments with uranium have been attempted. Synthetic groundwater under both oxidizing and reducing conditions is used and care taken to disturb the samples as little as possible before the experimert. As indicated in Section 1, sorption and leaching experiments are conceptually different. The former reflects the short-term uptake of uranium; the latter, the net effect of the processes of redistribution of uranium through the ore after weathering.

There are clear advantages of running both classes of experiment simultaneously on the same sample. An isotope not found in nature, ^{236}U, is added to the aqueous phase and ^{234}U:^{236}U:^{238}U ratios are measured both in solution and on the substrate. The ^{236}U distribution coefficient monitors sorption; the corresponding ^{234}U and ^{238}U parameters reflect leaching. Other members of the uranium series may be similarly studied.

2.4 Groundwater Studies

Groundwater is the principal means of sub-surface transport of uranium series nuclides. Isotope hydrology techniques have been used to study the cumulative transport of water over thousands of years. Attempts are being made to quantify the relative roles of solution and colloidal transport of uranium and thorium.

2.5 Extension of the Analogue

As pointed out in Section 1, the analogue may be extended to include other transuranic elements and fission products. Plans are under way to measure ^{129}I, ^{239}Np, ^{239}Pu and ^{36}Cl within and, in some cases, down-gradient of the ore deposits. Details are presented in Section 4.

2.6 Application to a Repository Site

Analogous studies on host rock associated with an HLWR site could be made (Figure 2). As pointed out in Section 1, extrapolation to transuranic and fission product nuclides may be possible if the corresponding data for the geochemical analogue is available.

3. EXPERIMENTAL RESULTS

3.1 Geochemical Model

An open system uranium series model has been developed to allow quantitative assessment of radionuclide redistribution within the ore body.[1,2] The upper sequences of the Ranger One, Jabiluka One, and Nabarlek deposits have been classified into four zones :

Zone I - Zone of leaching; unsaturated in the dry season.
Zone II - Permanently saturated within the weathered rock.
Zone III - A transition zone between weathered and unweathered rock.
Zone IV - Unweathered crystalline rock.

A schematic representation is shown in Figure 3. Some evidence for the validity of the classification is obtained from the similarity of $^{230}Th/^{234}U$ profiles in the upper sequences of each of the three deposits (Figure 4).

Mathematically, the model finds values of the following variables which are consistent with the experimental data :

(i) the rate of leaching (or deposition) of uranium;
(ii) the rate of advance of the weathering front (assumed to be equal to the rate of surface erosion); and
(iii) the $^{234}U/^{238}U$ disequilibria caused by leaching.

The model has recently been generalized in two ways :

(i) the assumption of linear leaching or deposition has been removed, and both are now considered normal first order processes; and

(ii) a procedure has been developed to assess the sensitivity of the calculated parameters to experimental uncertainties.

A number of significant results have been derived from the model. For instance, it has been calculated that the rate of leaching (or deposition) is in the range 0 to 1 percent per thousand years with many values between 0.3 and 0.6. Vertical redistribution of uranium is at least two orders of magnitude greater than removal by the horizontal component of groundwater flow. Second, the model has estimated rates of surface erosion in the range 0.01 and 0.2 m per 1,000 years with many values between 0.03 and 0.06. These data are consistent with an independent estimate that the base level erosion rate in the Ranger area is about 0.1 m/100 years.[5]

Further work on the global model is proceeding in two directions. First, an attempt is being made to reconcile the observed erosion rates with what is known of the evolution of the land-

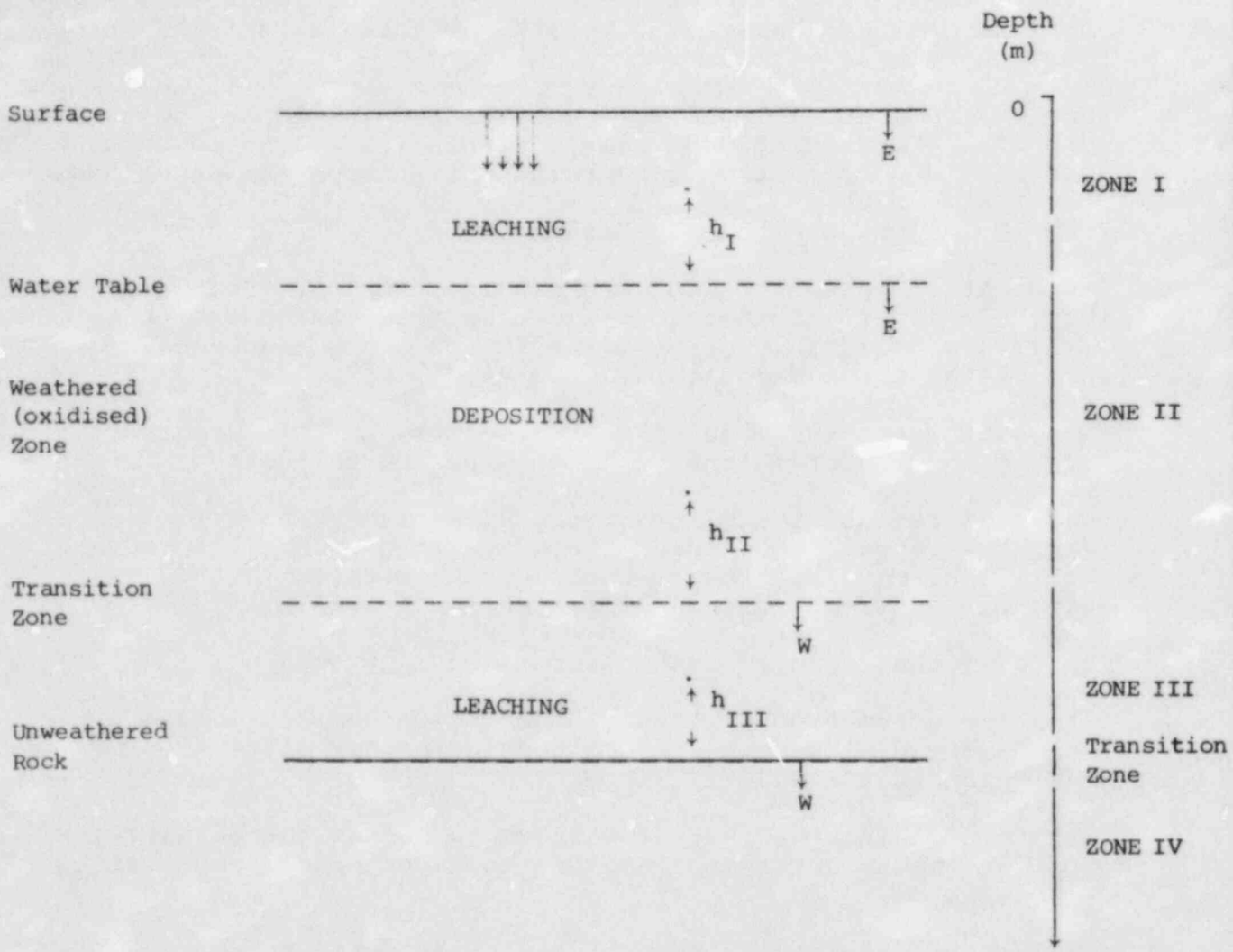

Figure 3

Schematic Representation of the Four-Zone Model

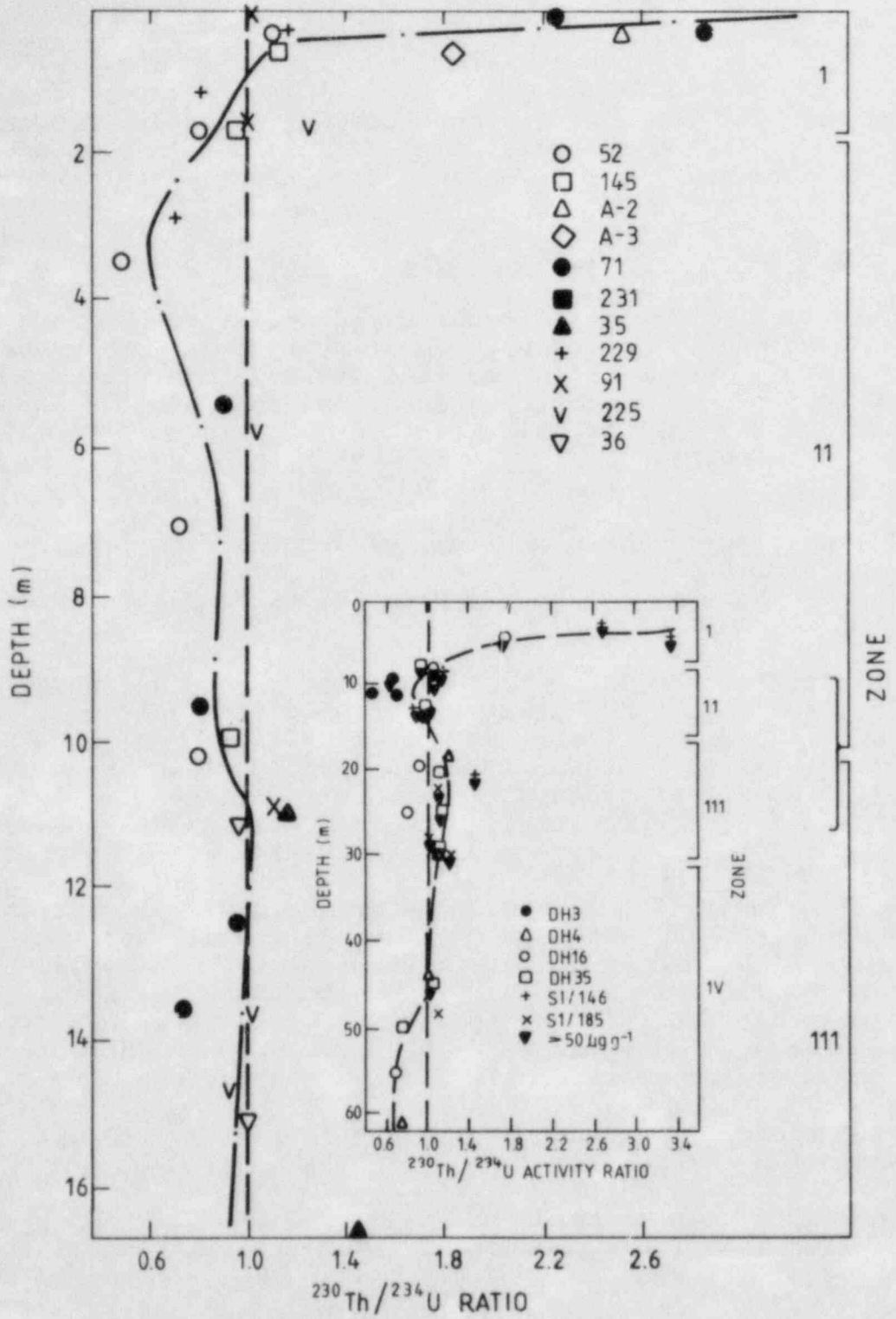

Figure 4

Composite Illustration of the Variation with Depth of the $^{230}Th/^{234}U$ Ratios for the Nabarlek Drill Holes Listed in the Key.
The three-zone classification is illustrated. The analagous variation for Ranger One and Jabiluka One deposits is shown as an insert.

scape since the Tertiary period. Second, progress is being made towards correlating the model with N.J. Rosholt's uranium trend model[6] developed for the dating of Quaternary sediments.

3.2 Distribution of Uranium Series Nuclides in Ore Samples

A contination of X-ray diffraction and selective phase separation techniques is being used to study systematically the distribution of uranium series nuclides through the weathered ore of the upper sequences of the Ranger One and Jabiluke One deposits. Particular attention has been paid to core S1/146 from the Ranger deposit.

3.2.1 Mineralogy. The mineralogy of samples from depths of 2.7 m, 4.0 m, 9.1 m, 13.1 m, 14.6 m and 21.0 m within the S1/146 core of the Ranger One deposit was investigated using X-ray diffraction analysis.

The results for the 2.7 - 13.1 m samples are shown in Tables 1 and 2. At 2.7 m, the system is mainly quartz-kaolinite, with some smectite and little mica. Low levels of iron oxide as hematite are also present. This is a red mottled zone. Below this (4.0 m, 9.1 m) is a pallid zone with little iron, low quartz and high clay content. The major clay minerals are kaolinite and smectite. Mica content increases down the profile.

The 13.1 m and 14.6 m samples have higher quartz levels (~50%), and increased mica content. Major clay minerals are mica and kaolinite with some smectite and vermiculite. These samples contain the iron oxide goethite in which there is isomorphous replacement of aluminium in some of the iron positions (~15%). The samples also show the rock fabric. The unweathered rock (21.0 m) contains quartz, chlorite and muscovite.

The mineralogy is consistent with the following description of the weathering process :

1. Decomposition of chlorite and muscovite, forming vermiculite as a first product, with smectite and kaolinite as the ultimate products.

2. Release of iron during decomposition, which is deposited as goethite.

3. Mobilization of iron as Fe^{2+}; upward movement causing formation of the pallid zone.

4. Re-deposition of iron near the surface as hematite, following oxidation of Fe^{2+} to Fe^{3+}.

Table 1

Mineralogy of Samples from S1/146 Drill Core (Ranger One)

Depth (m)	T.O.C. * %	Quartz %	<2 μm %	Clay Mineralogy (<2 μm fraction)			
				Kaolinite	Mica	Smectite	Vermiculite
2·7	0·08	35	40				
4·0	0·03	10	70				
9·1	0·03	30	45				
13·1		50	35				low

* carbon content

Table 2

Iron Mineralogy of Samples from S1/146 Drill Core (Ranger One)

Depth (m)	Colour	Hematite	Goethite	Magnetic Component %
2.7	Red	Present	N.D.	0.5
4.0	White	Low	?	0.6
9.1	White	N.D.	Low	2.0
13.1	Yellow	N.D.	Present	1.0

N.D. = not detectable

3.2.2 Selective Phase Separation. A combination of chemical and X-ray diffraction techniques is used to refine sequential leaching techniques for selective phase separation. An outline of procedures is given in Table 3.

The $^{234}U/^{238}U$ and $^{230}Th/^{234}U$ activity ratios from various extracts from the S1/146 core are illustrated in Figures 5 and 6 respectively. The percentages of uranium and thorium in the phases are also shown. Interestingly a large proportion of these elements is associated with the iron minerals even though the total iron is less than 4 percent of the dry weight. It is only possible to make qualitative comments on isotopic fractionation at this stage.

$^{234}U/^{238}U$ activity ratios. The clay-quartz fractions are all enriched in ^{234}U. This may be due largely to the recoil effect accompanying the α-decay of ^{238}U which causes the daughter to be ejected a distance of about 200 Å. The ^{234}U has a greater statistical probability of lodging in the clay/quartz phases since they comprise about 95 percent of the dry mass. An additional factor may be needed to explain the large discrimination observed in the 13.1 m sample. An explanation has been proposed in terms of the kinetics of the weathering process, further details of which are given in the Second Annual Report.(2)

$^{230}U/^{234}U$ activity ratios. As with uranium, thorium concentrates in the iron phases; the percentage of thorium varies from 75 to 96. Of particular interest are the $^{230}Th/^{234}U$ activity ratios in amorphous iron, which is considered to be the primary site of adsorption of metal ions from groundwater. In the 2.7 and 4.1 m samples, the activity ratios are high owing to the leaching of uranium; in the 9.0 and 13.1 m samples, the values are less than unity as a consequence of net uranium deposition in the pallid zone (Figure 6). The $^{230}Th/^{234}U$ ratios vary by more than a factor of 10.

By contrast, the $^{230}Th/^{238}U$ activity ratios in the crystalline iron phase show little variability; the average value for the four samples is 2.45±0.7. The $^{230}Th/^{234}U$ activity ratios are slightly more constant (2.3±0.4). It is tentatively assumed that the ratios are chemically controlled during crystallization of the secondary iron phase. Since radiogenic decay processes tend to lead to secular equilibrium, the high activity ratio would only be maintained if chemical control were re-established over time-scales commensurate with the half-life of ^{230}Th (75 200 y). Thus, crystalline iron phases must be labile, at least over these time-scales. It is generally accepted that ions from groundwater are not readily exchangeable with crystalline iron.

Radium. The radium data for core S1/146 are listed in Table 4. There is a significantly larger fraction of ^{226}Ra than uranium in the clay-quartz phase. More significantly, the ^{226}Ra is in excess of the parent ^{230}Th. Apart from the 13.1 m sample

Table 3

Sequential Extraction Techniques for Selective Phase Separation

No. (Figure)	Extractant	Conditions	Comment
1	0.1M NH_4Cl	24 h shake	removes ion-exchangeable and soluble salts (secondary mineralization)
2	Tamms acid oxalate 0.2M ammonium oxidate; 0.2M oxalic acid, pH 3.25	4 h shake ambient temp. in dark	amorphous and weakly crystalline iron, aluminium and manganese minerals
3	sodium dithionite sodium citrate sodium bicarbonate	shake for ½ h at 80°C, repeat	extracts well crystallized secondary iron oxides
4	5% sodium carbonate	shake for 16 h at ambient temp.	removes residual amorphous alumina and silica
5	digest with HF, HNO_3, $HClO_4$; fuse residue with Na_2O_2		extracts U, Th from resistate quartz and silicate minerals

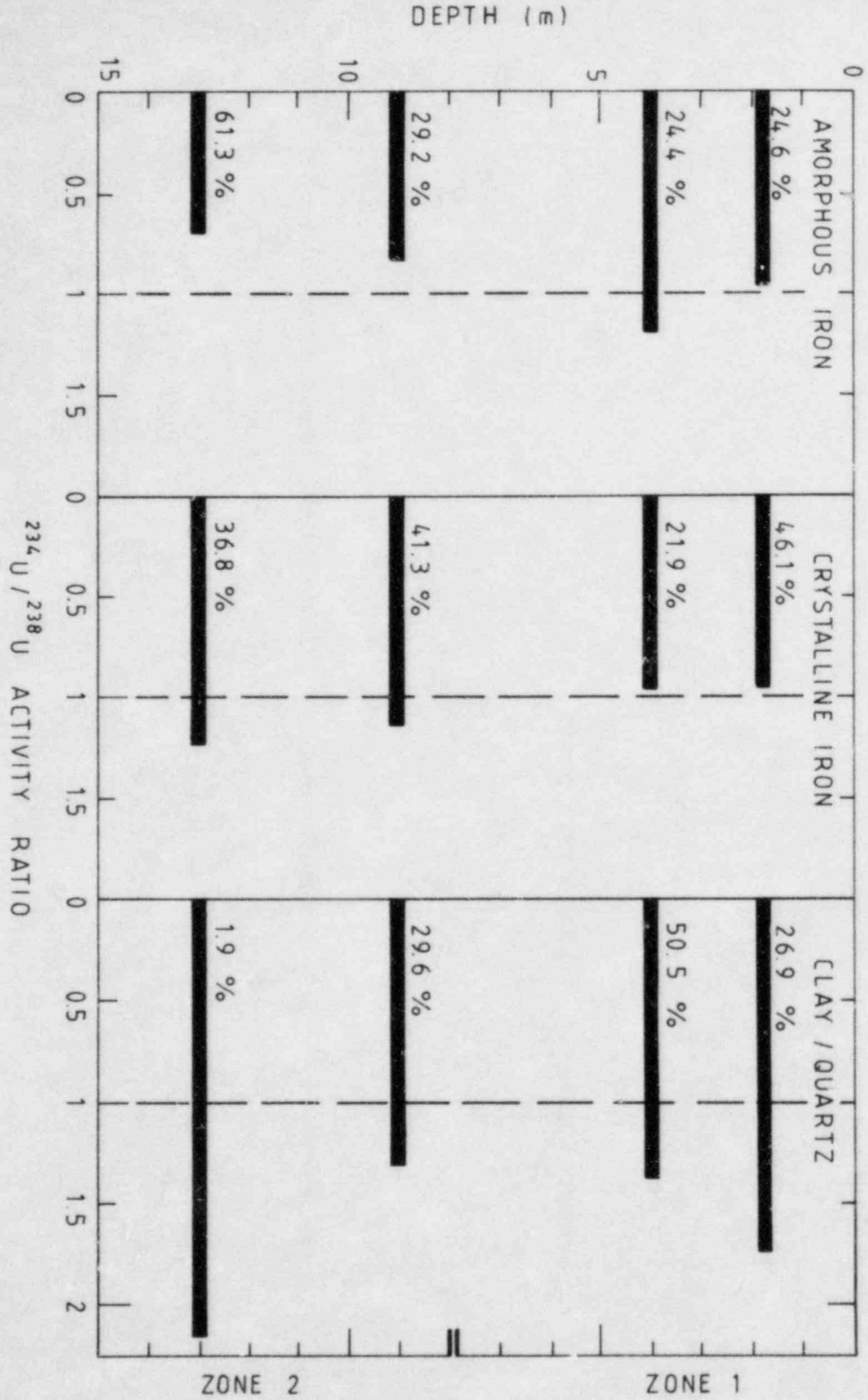

Figure 5

Variation of the $^{234}U/^{238}U$ Activity Ratios in Selectively Extracted Phases from Samples from the S1/146 Core of the Ranger One Ore Body. (a) amorphous iron, (b) crystalline iron, (c) clay and quartz phases.

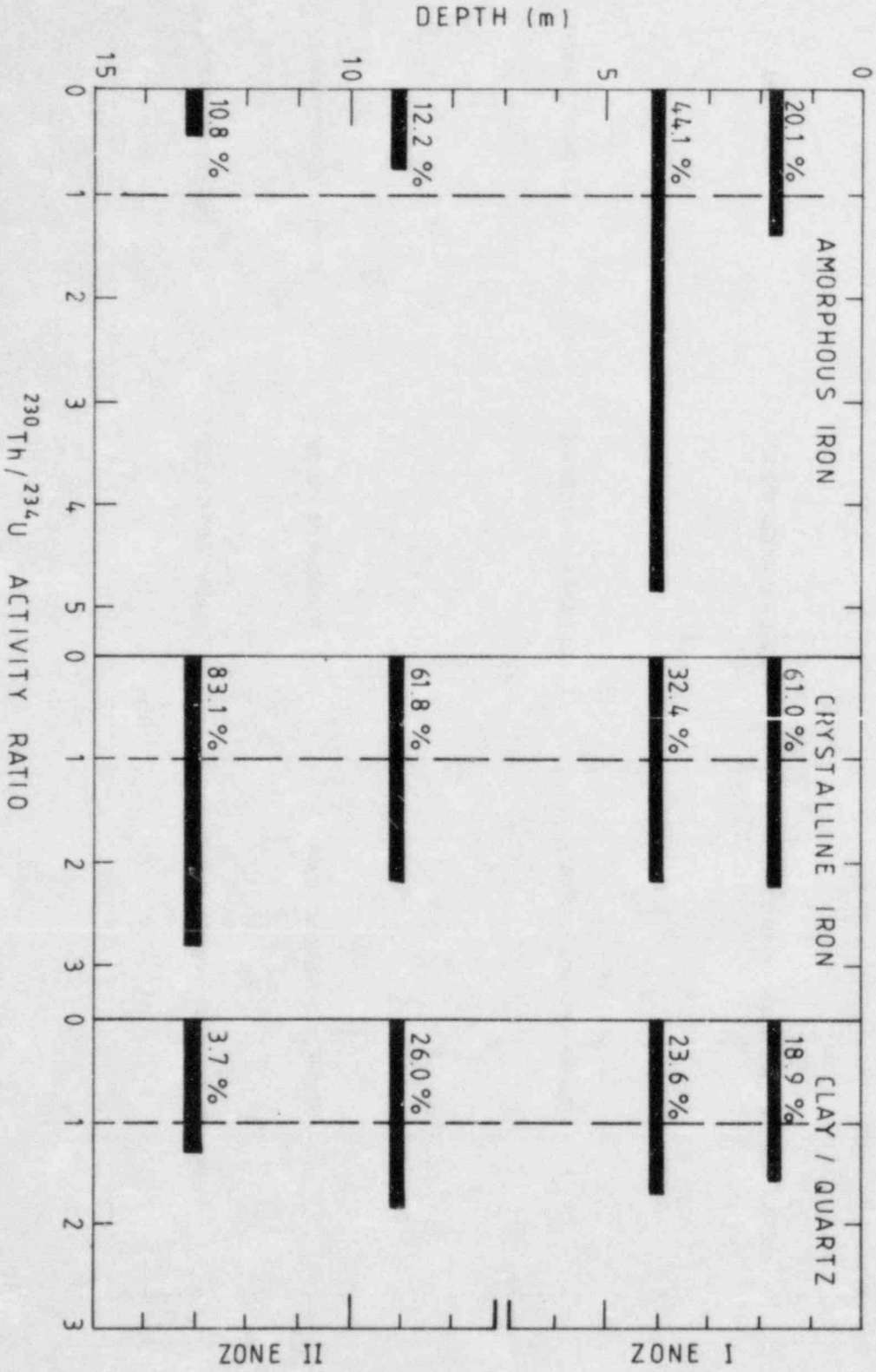

Figure 6

Variation of the $^{230}Th/^{234}U$ Activity Ratios in Selectively Extracted Phases from Samples from the S1/146 Core of the Ranger One Ore Body. (a) amorphous iron, (b) crystalline iron, (c) clay and quartz phases.

which, for reasons mentioned above, is considered anomalous, the excesses are not large and can be readily explained in terms of either recoil effects or preferential isomorphous substitution into the clay lattice. As with ^{234}U, recoil ^{226}Ra tends to lodge in the clay/silica phase.

3.2.3 Relevance of the Studies to the Long-term Prediction of Radionuclide Transport. Care must be taken when relating these findings to the prediction of the long-term migration of allogenic radionuclides. The uranium series elements measured in this study are essentially authigenic. They are generated *in situ* by radioactive decay, or released by the weathering process. However, a number of factors are relevant :

(i) There is evidence that the amorphous iron (managanese and aluminium) is the phase primarily involved in the sorption of metal ions from groundwater solution.(2b) However, a substantial proportion of uranium and thorium is associated with secondary crystalline iron phases. Since it appears that the amorphous and crystalline iron phases are exchangeable, at least over time-scales commensurate with the half-life of ^{230}Th, a mechanism exists for the long-term retardation of radionuclide transport.

$$M(\text{solution}) \rightleftharpoons M\text{-Fe(amorphous)} \rightleftharpoons M\text{-Fe(crystalline, largely inaccessible to groundwater)}$$

(ii) Some radionuclides which have particular relevance to HLWR siting assessment (e.g. ^{226}Ra) are formed by decay over time-scales of thousands to tens of thousands of years. Under the conditions being investigated, a significant fraction of the recoil radium would be ejected into the clay-quartz and hence be largely inaccessible to the groundwater. The large differences between $^{234}U/^{238}U$ ratios in the solid and aqueous phases provide evidence for groundwater inaccessibility.

3.3 Adsorption/Desorption Studies

3.3.1 Batch Adsorption Experiments. As noted in Section 2.3, a series of simultaneous sorption/leaching experiments is being run. Uranium-236 added to the aqueous phase is used to monitor sorption; uranium-238 levels reflect leaching from the ore. The batch technique has been chosen initially to enable a large number of variables to be studied concurrently. The aqueous phase comprises a synthetic groundwater determined from the analysis of a large number of samples from the Ranger area. Problems in pH stability have been overcome by using the WATEQ

Table 4

^{226}Ra Levels and $^{226}Ra/^{230}Th$ Activity Ratios in Phases Separated from S1/146 Ranger One

Depth	Total Uranium (µg/g)	Clay/Quartz		Other Phases (predominantly Fe)	
		^{226}Ra*	$^{226}Ra/^{230}Th$	^{226}Ra	$^{226}Ra/^{230}Th$
2.7	47.2	38.7	1.47	26.8	0.33
4.0	84.3	74.3	1.03	36.3	0.33
9.1	35.6	43.0	2.31	<1	<0.03
13.1	352	74.7	5.5	173.4	0.42

* Unit - disintegration min^{-1} g^{-1}

Table 5

Synthetic Groundwater Composition

Jabiru

Component	Concentration (mg L^{-1})
SiO_2	38.7± 4.5 (a)
Na^+	11.5± 1.8
K^+	3.2± 0.6
Ca^{2+}	11.5± 1.6
Mg^2	16.8± 2.4
Cl^-	9.5± 1.6
SO_4^{2-}	4.2± 0.9
HCO_3	143.0±12.0

(a) Uncertainties quoted to a 95% confidence level.

aqueous equilibrium program[8] to adjust the composition and avoid supersaturation. The composition chosen is given in Table 5. Redox potentials were controlled chemically. Oxidizing conditions were created by adding 100 ppm of hydrogen peroxide to the solution and maintaining the concentration; reducing conditions were established by using freshly boiled distilled water to make up the solutions, dosing with 0.1 g hydroxylamime hydrochloride, and maintaining a nitrogen blanket over the stock solutions and adsorption cells. The dominant uranium solutes comprise a complex mixture, as shown below :

pH 5.5 "oxidizing" UO_2^+, UO_2OH^+, $UO_2\ Si\ (OH)_3^+$, $UO_2CO_3^\circ$

pH 5.5 "reducing" $U(OH)_4^\circ$, $U(OH)_5^-$

pH 8.5 "oxidizing" $(UO_2)_3(OH)_5^+$, $UO_2(CO_3)_3^{4-}$, $UO_2(CO_3)_2^{2-}$

pH 8.5 "reducing" $U(OH)_5^-$

The S1/146 4.0 m sample was used in the initial experiment. At the end of 14 days, solid and liquid phases were separated by centrifugation at 3500 rev/min for one hour, the supernate was passed through a 0.45 μm filter, and the activity ratio ^{236}U: ^{238}U measured.

The data are expressed as distribution coefficients, are listed in Table 6. Two useful observations may be made :

(i) The distribution coefficients Rd of ^{238}U (leaching) based on the total uranium content of the ore, are considerably greater than those of ^{236}U (sorption). If the two coefficients were intrinsically equal, observed differences between the two uranium isotopes would reflect the fact that much of the ^{238}U is inaccessible to the groundwater. Under oxidizing conditions, the ratio of the distribution coefficients (Table 6) is close to the fraction of uranium associated with amorphous iron oxide (0.244). This is further evidence that only the uranium associated with the amorphous iron is in equilibrium with the groundwater.

(ii) Under reducing conditions, the Rd factors increase due to the formation of the less soluble U(IV) species. A corresponding decrease is observed in the Rd (^{236}U)/Rd (^{238}U) ratio, possibly indicating that much more of the ^{238}U than the ^{236}U is inaccessible to the groundwater. This effect may be due to the partial dissolution of the more labile amorphous iron following reduction to the ferrous state.

It is useful to compare the data listed in Table 6 with those quoted in the literature. Borovec[9] found that at pH 6 clay minerals have adsorption coefficients ranging from 50 for kaolinite to 10^3 for montmorillonite in the sequence kaolinite

Table 6

Fourteen Day Sorption/Leaching Experiments

Sample : 4.0 m S1/146, Ranger One

Mass of sample : 2.00 g
Volume of aqueous phase : 100 mL
Sample preparation : crushed to -100 B.S. mesh size with rotary mill
Uranium content : 84.3 μg g^{-1}
$^{234}U/^{238}U$ activity ratio : 1.19±0.04

Experimental Conditions (1)	^{236}U : R_d of adsorption	^{238}U : R_d of desorption (2)	$\frac{R_d(^{236}U)}{R_d(^{238}U)}$
pH 5.5, 'oxidizing'	2.2x10	9.9x10	0.22
pH 5.5, 'reducing'	4.2x10	3x10	0.13
pH 8,5, 'oxidizing'	4.2x10	2x10	0.21
pH 8.5, 'reducing'	8.1x10	7x10	0.11

(1) See section 3.

(2) Values are rounded to one significant figure if the standard deviation associated with measurements exceeds 10 percent.

<illite <montmorillonite. Values for humic acids ($\sim 10^4$), Fe(III) oxyhydroxides (10^6), amorphous $Ti(OH)_4$ (10^5-10^6), peat (10^4-10^5), limonite (10^4), and fine-grained natural goethite (10^3) have also been measured. Because of the complexity of the synthetic groundwater, comparison with model experiments should be treated with caution.

3.3.2 Effect of Recoil on Distribution Coefficients. It is necessary to establish experimentally whether the α-recoil process effects the distribution coefficients for the following reasons :

(i) It is currently proposed the observed $^{234}U/^{238}U$ and $^{230}Th/^{234}U$ fractionation between the chemically separated phases of the weathered ore is due to daughter product migration induced by α-recoil. A detailed understanding of this phenomenon is needed to establish the relationship between the distribution of radionuclides throughout the sample, and the results of laboratory sorption and leaching experiments (relationships (2) and (3), Figure 2)

(ii) One of the most significant nuclides, ^{226}Ra, is formed by α-recoil in significant amounts in the geologic medium over the time-scales of interest.

The aim of this experiment is to compare the distribution coefficients of ^{226}Ra and ^{224}Ra (the daughter product of ^{228}Th) between the water and dilute suspensions of montmorillonite, kaolinite and illite. Solutions of ^{226}Ra and ^{228}Th (from which ^{224}Ra has been separated) are added to the clay suspensions. Conditions are chosen to ensure that the ^{228}Th is almost entirely adsorbed on the clay. After the ^{224}Ra (half-life 3.6 d) has reached equilibrium, the $^{224}Ra/^{226}Ra$ ratios in the solution and on the clays are measured. Since ^{224}Ra is formed by decay on the clay surface, the relative distribution coefficients are a measure of the effect of α-recoil on adsorption coefficients. The data are listed in Table 7. The α-recoil appears to increase the adsorption coefficient by a factor of about two. Presumably, the effect of recoil is to eject a proportion of the daughter ^{224}Ra into less accessible sites in the lattice.

3.4 Radionuclide Migration in Groundwater

3.4.1 Nabarlek Groundwater Study.

Evidence for a two-component system

Samples for isotopic assay are collected from the wells at Nabarlek shown in Figure 7. The water is filtered through 0.45 μm membrane filters to separate particulates. In this

Table 7

The Effect of α-recoil on Radium Adsorption Coefficients

Volume of suspensions - 100 mL
Total ^{226}Ra added to each suspension - 4700 dpm
Total ^{228}Th added to each suspension - 4736 dpm
pH - 7.5

Suspension	Loading mg/mL	% activity in 'solution' (1)(2)			$\rho = \frac{R_d}{R_{r_d}}$ (3) (eqn 8)	ϕ_a
		^{226}Ra	^{228}Th	^{224}Ra		
Montmorillonite (4)	119	4.6	2.4	2.4	2.0	0.5
Illite	103	15	14	7.5	2.0	0.5
Kaolinite	137	1.5	0.7	0.7	2.0	0.5

(1) The ^{226}Ra, ^{228}Th solutions in this experiment were added on 15 September; the $^{224}Ra/^{226}Ra$ assay was undertaken between 30 September and 11 October 1982.
(2) Dissolved, i.e. 'non-filterable' activity was estimated by passing a one millilitre aliquot through a 0.2 μm membrane filter.
(3) The values of ρ are slight under-estimates, as no attempt has been made to correct for the small fraction of radium-224 formed from the dissolved thorium-228.
(4) Sodium forms of the clays were prepared.

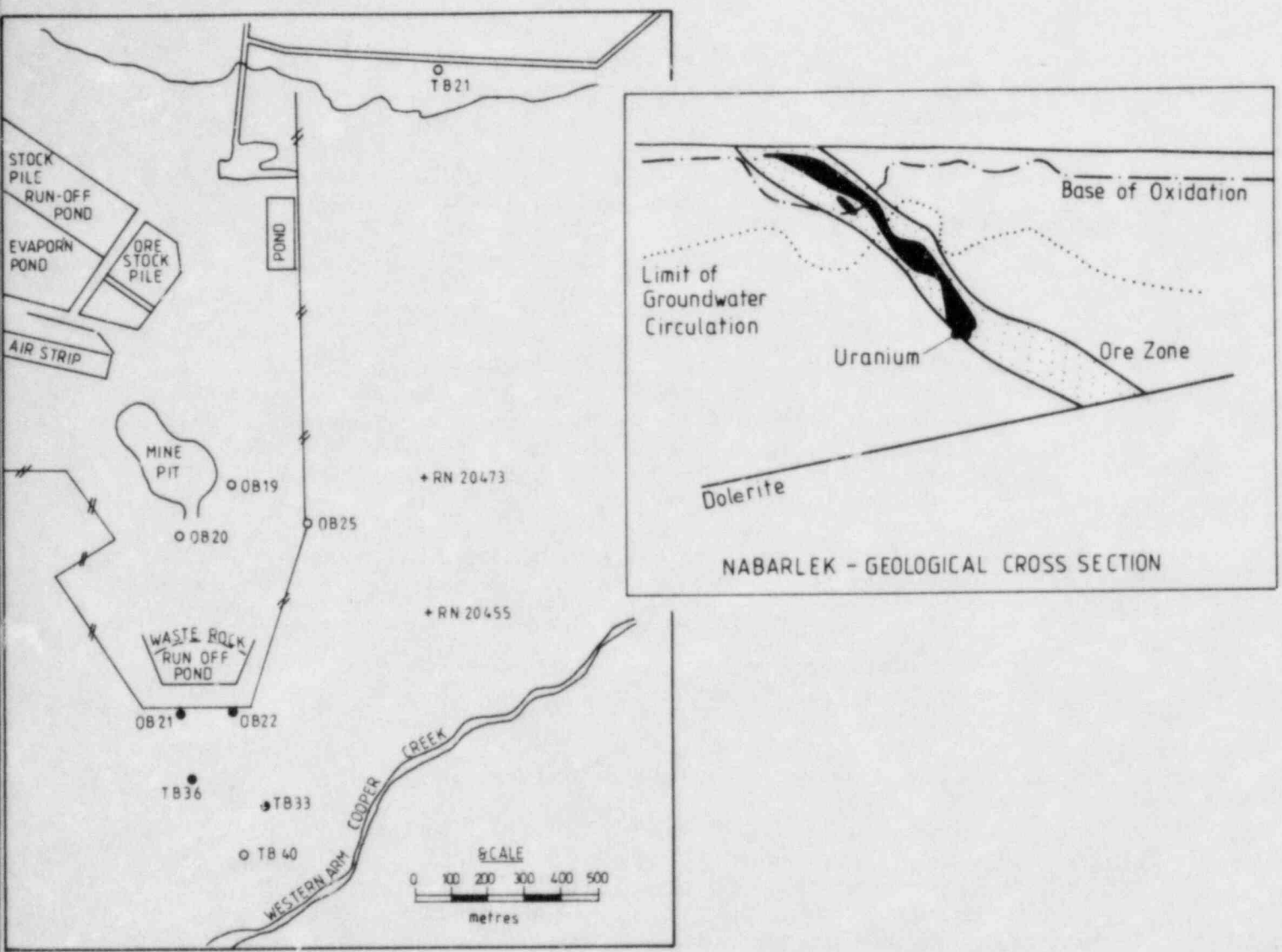

Figure 7

Location of the Sampling Wells at Nabarlek.
Insert : general geological cross-section

system, material passing through the filter is considered to be in 'solution'. The variation of $^{234}U/^{238}U$ activity ratios with uranium concentration is shown in Figure 8 and is plotted against the reciprocal of the uranium concentration in Figure 9. With the exception of TB40, the relationship is linear, which confirms that, down-gradient of the ore body, the uranium content of the groundwater can be rationalized in terms of a two-component system :

Component 1 is the uranium dissolved in groundwater intersecting the deposit. It is characterized by a relatively high uranium concentration, and a $^{234}U/^{238}U$ activity ratio close to unity.

Component 2 is the uranium dissolved in local recharge water. It has a low concentration but a high activity ratio.

Evidence for transport by groundwater particulates

The particulates separated from the groundwater by filtering were assayed for ^{238}U, ^{234}U and ^{230}Th. The results are given in Table 8. Between 0.8 and 11 percent of the uranium in these samples was associated with the 0.45 µm particulates; the corresponding fraction for thorium varied between >0.22 (22 percent) and >5.7.

The significance of these data in establishing a basis for predicting long-term transport depends on answers to the following questions :

(i) Are the radionuclides absorbed on the particulates in equilibrium with the solution?

(ii) If not, what is the relative rate of *transport* of particulates to solute radionuclide?

Evidence is presented in Figure 10 that the 'solute' and 'particulate' uranium are in equilibrium. Except for well TB40, the $^{234}U/^{238}U$ ratios for the two components fall close to the isotopic equilibrium line. Similar evidence could not be found for thorium because of the extremely low levels. A systematic investigation of this important question is planned. Should thorium-230 on the particulates *not* be in isotopic equilibrium with the solute, it will be necessary to determine the ratio of the rates of transport: ^{230}Th (particulate)/^{230}Th (solute). This will involve an estimation of the particulate to groundwater velocity ratio. In addition, it is hoped to establish the thorium and uranium levels for particles in the range 0.05 to 0.45 µm.

3.4.2 Geochemical Estimates of Uranium Retardation Factors. The aim of much of the laboratory adsorption isotherm work is the calculation of retardation factors (i.e. interstitial

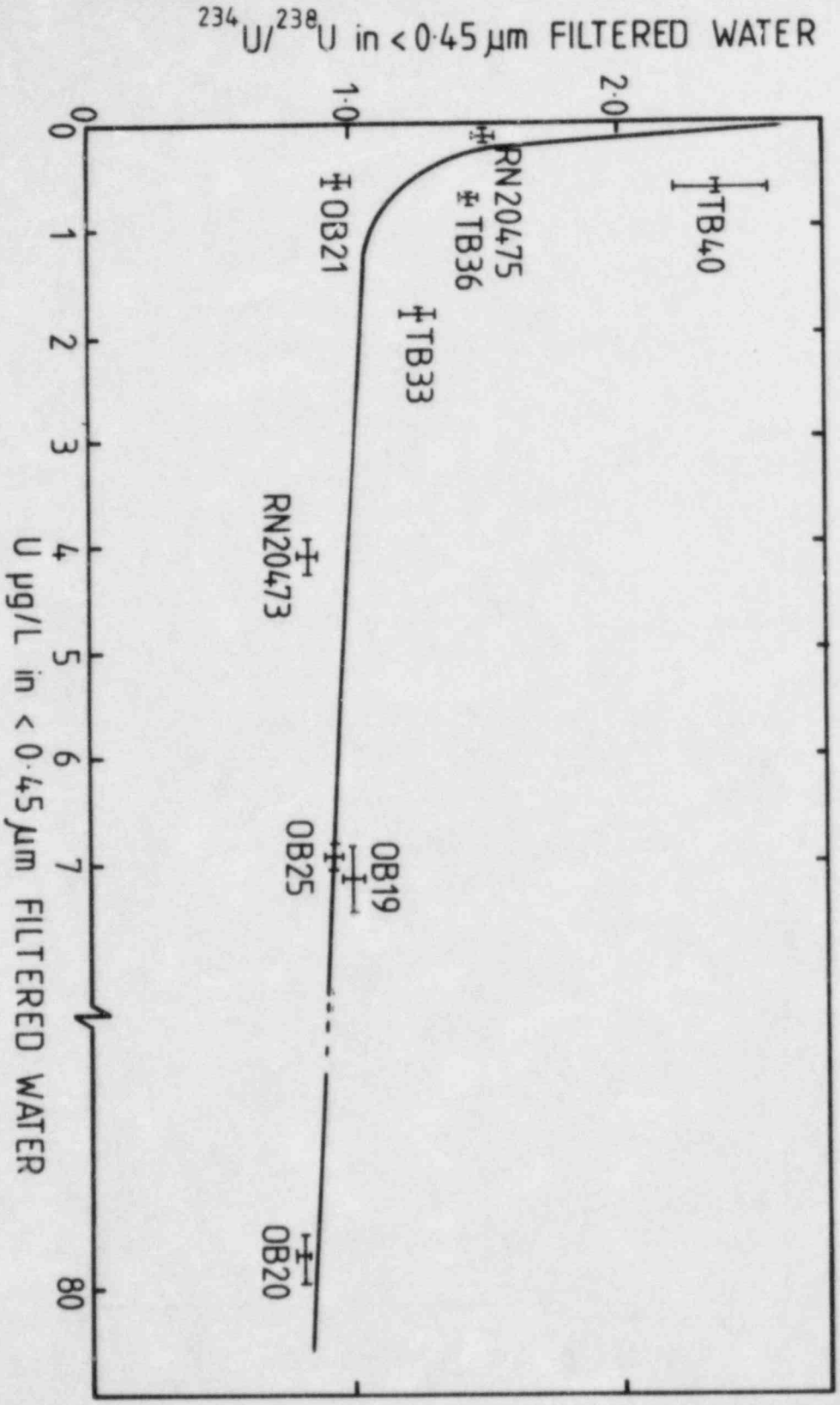

Figure 8

Variation of the $^{234}U/^{238}U$ Ratios with the Groundwater Uranium Concentration - Nabarlek.

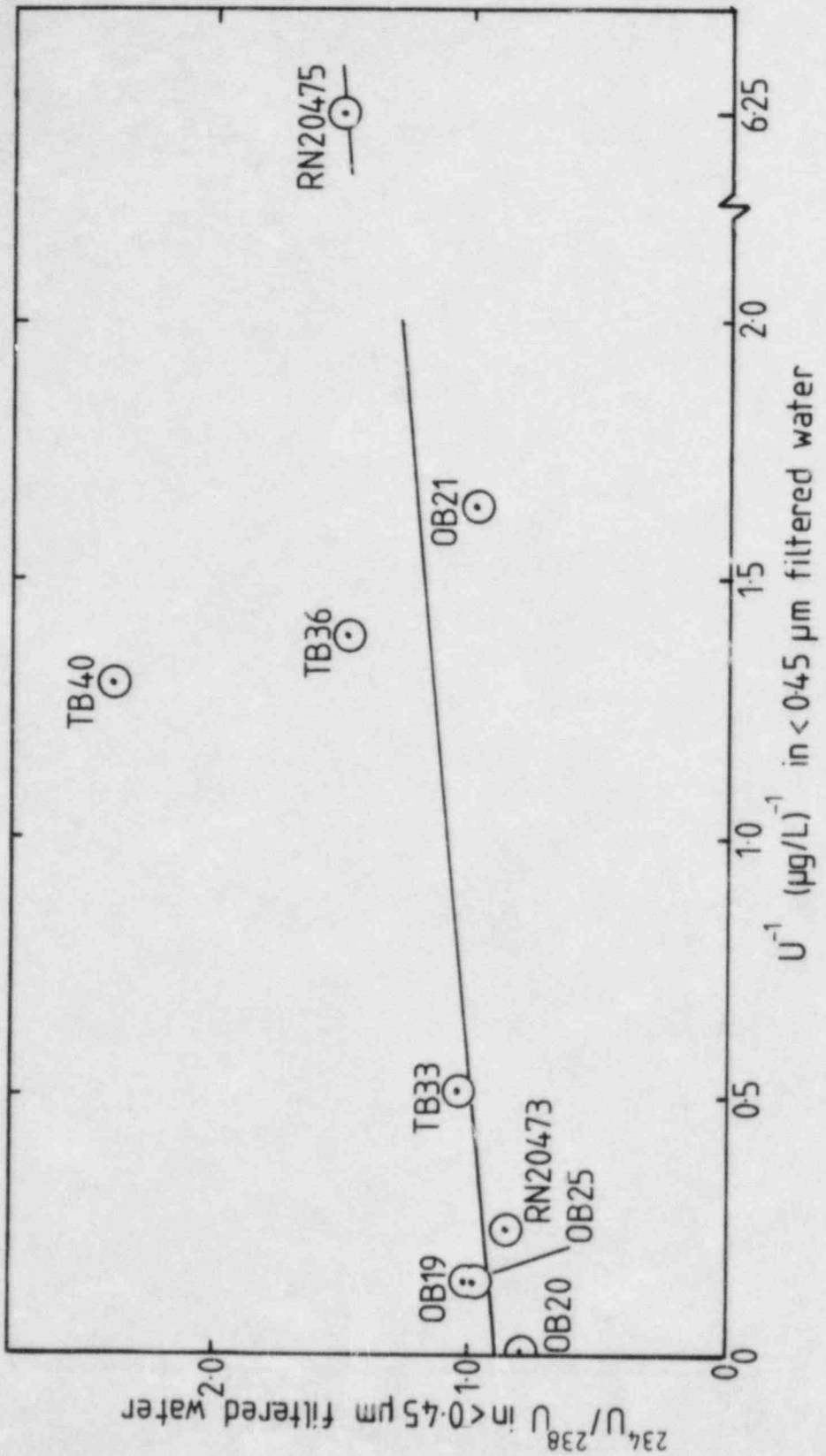

Figure 9

Variation of the $^{234}U/^{238}U$ Ratios with the Reciprocal of the Uranium Concentration - Nabarlek.

Table 8

Distribution of Uranium and Thorium between Nabarlek Groundwater and Particulates

Location (Bore No.)	Uranium $\mu g\ L^{-1}$ in <0.45 µm filtered water	$^{234}U/^{238}U$ in <0.45 µm filtered water	$^{230}Th/^{234}U$ in <0.45 µm filtered water	Uranium $\mu g\ L^{-1}$ in >0.45 µm particulates	$^{234}U/^{238}U$ in >0.45 µm particulates	$^{230}Th/^{234}U$ in >0.45 µm particulates	^{238}U in >0.45 µm/ ^{238}U in <0.45 µm	^{230}Th in >0.5 µm/ ^{230}Th in <0.5 µm	K_d
OB 19	7.13±0.32	1.05±0.05	BDL	ND	ND	ND	ND	-	-
OB 20	77.32±2.6	0.80±0.02	<0.0045	2374±51	0.79±0.06	0.75±0.10	3.05×10^{-2}	>5.7	0.15
OB 21	0.61±0.03	0.97±0.09	<0.06	ND	ND	ND	ND	-	-
OB 25	6.96±0.14	0.97±0.02	BDL	54.5±3.3	1.37±0.12	0.25±0.04	0.78×10^{-2}	>2.8*	0.7
TB 33	1.81±0.05	1.22±0.02	0.04±0.02	57.7±11.5	1.63±0.18	TBD	3.2×10^{-2}	-	3
TB 36	0.72±0.03	1.44±0.06	<0.02	27.5±1.6	1.66±0.14	0.11±0.02	3.8×10^{-2}	>0.22	4
TB 40	0.74±0.03	2.40±0.11	0.02±0.01	69.9±3.9	1.02±0.17	1.04±0.19	9.4×10^{-2}	>2	1.4
RN 20473	4.11±0.17	0.84±0.04	0.014±0.003	189±7	0.94±0.05	0.42±0.11	4.6×10^{-2}	>1.5	5
RN 20475	0.16±0.01	1.50±0.06	BDL	17.7±1.0	1.34±0.13	0.39±0.14	11.3×10^{-2}	>3.9*	10

BDL = Below Detection Limit

ND = Not Determined

TBD = Yet to Be Determined

* Assume DL 0.01

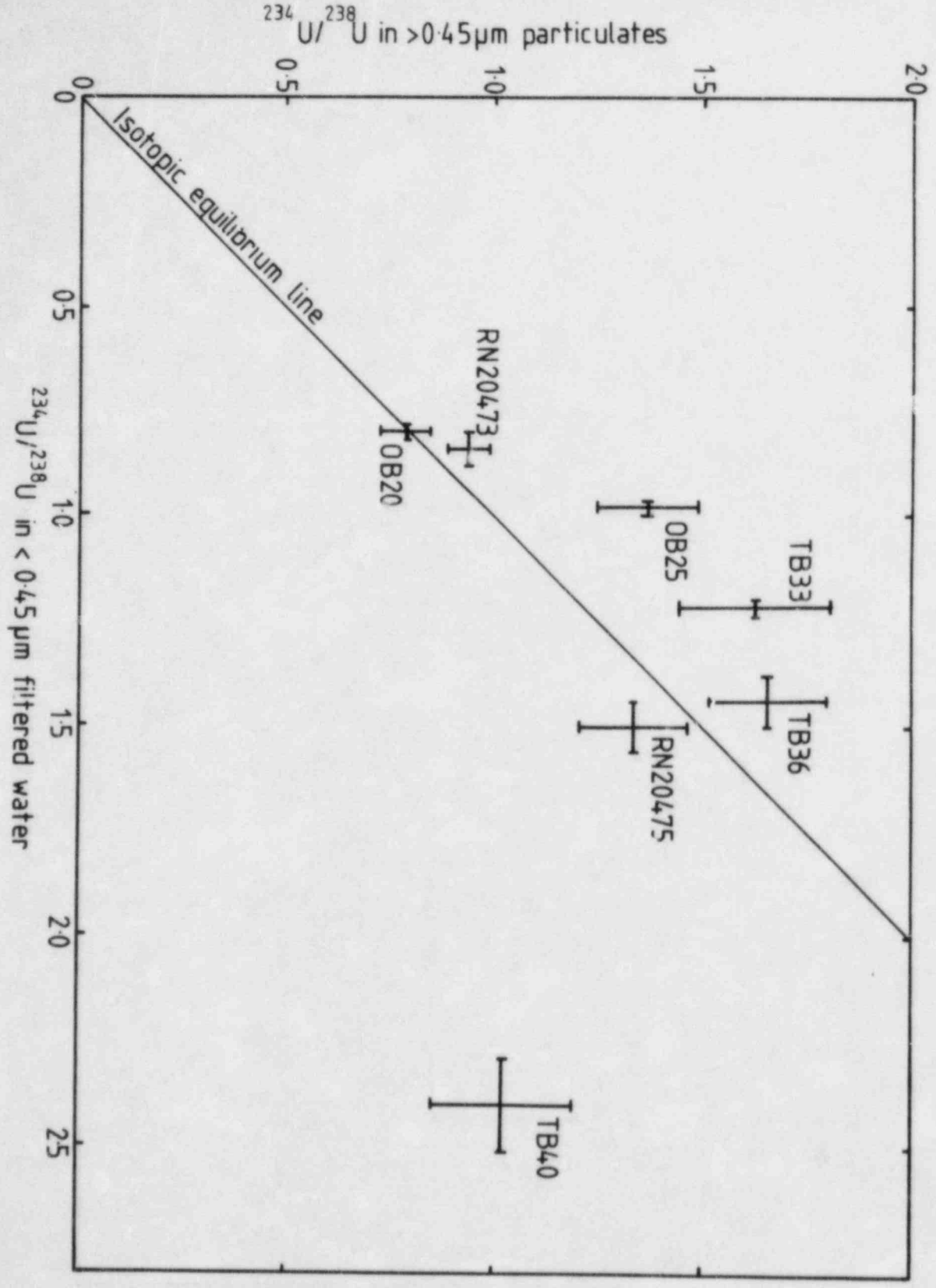

Figure 10

Relationship between the $^{234}U/^{238}U$ ratios in particulates and in the groundwater sampled from Nabarlek.

groundwater to radionuclide velocity ratios) which are valid over long periods of time. Independent estimates of the uranium parameters can be obtained from a systematic study of the isotope hydrology down-gradient of ore bodies. Two examples are cited :

Ranger One. The $^{234}U/^{238}U$ ratios in groundwater close to the Ranger One deposit have values near unity. They increase with distance up to 4 km down-gradient due to mixing with infiltrating water with a high activity ratio. Further down-gradient, there is no environmental isotope evidence for local recharge. The $^{234}U/^{238}U$ ratios return to secular equilibrium due to a combination of radiogenic decay and possibly exchange with the host rock. Assuming that decay is the dominating process, the maximum retardation factor was 250. Groundwater velocities were found using carbon-14 dating techniques.

Carizzo aquifer, Texas. Qualitatively similar, but more convincing, data from the Carizzo aquifer have recently been published.(9) "At distances from 0 to about 20 km where the Carizzo is oxidizing and uranium dissolution is occurring, $^{234}U/^{238}U$ activity ratio values AR of 1.0±0.3 are found. Between 20 and 33 km, uranium concentrations drop dramatically and AR values as high as 9 occur. Below 33 km, low dissolved uranium persists, accompanied by a regular decrease of AR towards secular equilibrium of 1." The systematic decrease in the activity ratios is interpreted in terms of ^{234}U decay. Uranium retardation factors of 30 were calculated from groundwater velocities using carbon-14 dating techniques. Since the Carizzo is a relatively homogeneous sandstone aquifer of known porosity and density, the retardation factor was interpreted as a K_d factor of 6. Clearly, an independent estimate of this parameter would be useful.

4. EXTENSIONS TO THE ANALOGUE

In Section 2.5, it was noted that the analogue should be extended to incorporate nuclides that are more relevant to the solution of long-term HLW storage problems than just of the uranium series. These include the transuranic elements ^{237}Np, $^{241,243}Am$ and $^{238-240,242}Pu$, and the fission products $^{135,137}Cs$, ^{126}Sn, ^{99}Tc and ^{129}I. Technological advances have allowed some of these nuclides to be included into the analogue. Using accelerator mass spectrometry, ^{129}I and ^{36}Cl can be measured at levels of 3×10^6 and 6×10^5 atoms respectively, with a 10 percent precision. With state-of-the-art mass spectrometry, the detection limit for ^{239}Pu and ^{237}Np is about 10^7 atoms.

4.1 Iodine-129

Iodine-129 is a long-lived isotope (half-life 15.9×10^6 y) generated by the spallation of atmospheric xenon or by uranium fission. It will be assumed initially, that there are no complications due to 'weapons test' iodine-129.

In the geochemical model described in Section 3.1 it is assumed that the weathered zone is essentially in a steady state, the downward advance of the weathering front being balanced by surface erosion. From this hypothesis, it appears that the residence time of material in the weathered zone is of the order of hundreds of thousands of years. As this period is short compared with the half-life of the isotope, only a small amount of ^{129}I was formed subsequent to weathering. The weathering process should lead to the mobilization and transport of ^{129}I out of the area of the deposit. A discontinuity of ^{129}I levels would therefore be expected across the transition zone between the oxidized and reduced regions. Measurements will be made of the levels of the isotope in groundwater down-gradient of the deposit to complement measurements on the drill core.

This simple picture is likely to be complicated by the presence of 'weapons test' iodine-129. The seasonally oscillating water table may possibly disperse the isotope over a substantial fraction of the weathered zone. As 'weapons test' chlorine-36 ought to behave similarly, analysis of the $^{129}I/^{36}Cl$ profile should lead to an estimate of the relative contribution from the two resources. If 'weapons test' ^{129}I dominates, it will be useful to establish its distribution through the mineral phases comprising the ore assemblage. Whether or not the 'weapons test' source dominates, it will be possible to study the distant field migration provided groundwater is collected from wells known to have no environmental tritium.

4.2 Neptunium-237

Neptunium-237 is a long-lived transuranic element (half-life 2.14×10^6 y). It will be included in the analogue in a similar way to ^{129}I. If the nuclide is mobile, it should leach from the profile following weathering; if it is immobile it should be retained within the weathered zone. Of particular interest would be to measure the $^{237}Np/^{129}I$ ratios systematically and hence establish mobility differences.

4.3 Plutonium-239

Interpretation of ^{239}Pu data is complicated by the fact that the half-life is comparable to the residence time of material in the weathered zone. A systematic study of the $^{239}Pu/^{36}Cl$ may be useful, since the generation of both nuclides is initiated by thermal neutron activation, hence the initial distribution functions can be interrelated.

5. CONCLUSIONS

1. Appropriate geochemical analogues can be used to study the scientific bases for the prediction of the long-term transport of radionuclides. Uranium deposits are useful analogues of high-level radioactive waste repositories. Not only do they comprise a local high concentration of uranium series nuclides but also the potential exists for investigating the mobility of the transuranic elements ^{237}Np, ^{239}Pu and the fission products ^{99}Tc and ^{129}I.

2. A large proportion of the uranium and thorium is associated with the amorphous and crystalline iron phases of the weathered sequences of the ore body. The uranium in the amorphous iron appears to be associated with the groundwater. Substantial uranium and thorium isotopic fractionation exists between the various phases, due to a combination of recoil and chemical effects. Radium tends to concentrate in the clay/quartz phases.

3. Sorption/leaching studies provide indirect evidence that, over short time-scales, uranium is adsorbed from solution on to the amorphous iron. It is also shown that radium formed by α-recoil on clay particles has a higher distribution coefficient than that adsorbed from solution.

4. There are early indications that groundwater colloids may be significant in the transport of thorium-230. On the other hand, uranium appears to migrate largely in solution. Under appropriate conditions, uranium retardation factors can be calculated from systematic observations of $^{234}U/^{238}U$ ratios in groundwater down-gradient of uranium deposits. Examples are cited.

6. REFERENCES

1. Airey, P.L., Roman, D., Golian, C., Short, S., Nightingale, T., Lowson, R.T. and Calf, G.E. (1982). Radionuclide Migration around Uranium Ore Bodies - Analogue of Radioactive Waste Repositories. USNRC Contract NRC-04-81-172.
   (a) Annual Report 1981-82, AAEC Report C29.
   (b) Quarterly Report No. 5, AAEC Report C34.
   (c) Quarterly Report No. 6, AAEC Report C37.

2. Airey, P.L., Roman, D., Colian, C., Short, S., Nightingale, T., Lowson, R.T., Calf, G.E., Davey, B.G., Grady, D. and Ellis, J. (1983). Radionuclide Migration around Uranium Ore Bodies - Analogue of Radioactive Waste Repositories. USNRC Contract NRC-04-81-172.
   (a) Quarterly Report No. 7, AAEC Report C38.
   (b) Annual Report 1981-82, AAEC Report in preparation.

3. Airey, P.L. (1982). The Transport of Uranium Series Nuclides Down-gradient of Ore Bodies in the Alligator Rivers Uranium Province. Proc. Scientific Workshop on Environmental Protection in the Alligator Rivers Region, Jabiru, May 1983, Vol. 1 (Office of the Supervising Scientist, Darwin) pp.19-1 to 19-7.

4. Airey, P.L., Golian, C., Nightingale, T., Roman, D. and Short, S. (1983). Groundwater Induced Migration of Uranium and its Daughter Products in the Vicinity of the Ranger No. 1 Ore Body. Proc. Aust. Water and Wastewater Association Int. Specialist Conference on Water Regime in Relation to Milling, Mining and Waste Treatment including Rehabilitation with Emphasis on Uranium Mining, Paper 18, Darwin, September 1983.

5. Duggan, K. (1983). Geomorphic Response to Development in the Alligator Rivers Region. Proc. Scientific Workshop on Environmental Protection in the Alligator Rivers Region, Jabiru, May 1983, Vol. 1 (Office of the Supervising Scientist, Darwin) paper 21.

6. Rosholt, J.N. (1980). Uranium Trend Dating of Quaternary Sediments, US Geological Survey Open File Report 80-1087.

7. Pearson, F.J. Jr, Norohne, C.J. and Andrews, R.W. (1981). Mathematical Modelling of the Distribution of Natural ^{14}C, ^{234}U and ^{238}U in a Regional Groundwater System. Proc. Radiocarbon Conference, Seattle.

8. Truesdell, A.H. and Jones, B.F. (1974). WATEQ, a computer program for calculating chemical equilibrium of natural waters. J. Res. US Geol. Survey 2, 233.

9. Borovec, Z. (1981). The adsorption of uranyl species by fine clay. Chem. Geol. 32, 45-58.

DATING OF GROUND WATER
AN EVALUATION OF ITS USE IN THE ASSESSMENT OF HLW REPOSITORIES

STANLEY N. DAVIS, HAROLD W. BENTLEY, AND RICHARD ZITO

Department of Hydrology and Water Resources
University of Arizona
Tuscon, Arizona 85721

ABSTRACT

Dating of ground water is potentially useful in the evaluation of the hydrogeologic hazards associated with proposed repositories for high-level radioactive waste in the following ways: (1) Identification of areas of static ground water where regional migration of radionuclides should be minimal; (2) Help with the calibration of numerical transport models; (3) Estimation of water velocities; (4) Help with the prediction of future natural changes in the chemistry of ground water; (5) Help with the interpretation of the Pleistocene history of a region which will have a bearing on the development of hazards not related directly to ground water.

Methods judged to be most useful for dating water are hydrodynamic calculations, the use of atmospherically derived radionuclides, and the measurement of the accumulated products of the decay of certain radionuclides. Thus far, the most useful atmospherically derived radionuclide is chlorine-36 with a half-life of about 3×10^5 years. Water as old as 1.5×10^6 years can be dated, but corrections for the subsurface production of small amounts of chlorine-36 must be made for most water older than about 8×10^5 years.

Natural levels of iodine-129 in ground water have been measured for the first time as a result of our research. Iodine-129, with a half-life of 1.6×10^7 years, is potentially useful in dating and tracing some waters older than 5×10^6 years. Further study is needed, however.

INTRODUCTION

The Nature of Water Ages

Dating of ground water is potentially the most useful hydrogeologic tool in assessing the long-term hazards that could arise from the movement of radionuclides away from a repository for high-level radioactive waste. If ground water in the region surrounding a proposed repository is uniformly very old, say more than 4×10^6 years, and generally beyond most dating methods, then future movement of radionuclides in the ground water under natural conditions would simply not be a major problem. Investigations of such a region should then be focused on the potential future effects of ground-water pumping, the drilling of exploration holes, and other human activities. If dating indicates younger water which varies systematically in age from one area to another, then the dating of water from extensive aquifers will help a) to calibrate numerical transport models, b) to calculate ground-water velocities and directions, c) to estimate the effects of megadispersion, d) to predict future changes in water quality, and e) to understand the history of the water and, consequently, the variables which have worked together to determine the present chemical characteristics of the water.

The age of ground water is the length of time that ground water has been isolated from the surficial portion of the hydrologic cycle such as from atmospheric transportation, glaciers, rivers, and lakes. Actually, this definition is almost too simplistic to be useful unless water flows

as one-dimensional piston flow, a condition which is not even approximated very commonly in nature. What we are really measuring is some complex function of water age because various forms of mixing will always be present, both within the undisturbed aquifer as well as within the bore holes and wells. Although as a convenience the terms "water age" and "dating water" will be used, the fact should be kept in mind that, in a strict sense, all water samples if analyzed thoroughly in the laboratory bear the chemical imprint of at least some mixing.

The collection of water from widely separated sampling points together with the use of multiple methods of dating which measure different spans of time should be always employed in field investigations of ground-water ages. In this way, the effects of large-scale mixing, or megadispersion, can commonly be identified. This dispersion is the real concern rather than some hypothetical water age. It is the filament of ground water moving well ahead of other filaments of water which will carry the first radioactive contaminants to the biosphere. This disparity in transport velocities can be detected in natural systems by the use of multiple dating techniques. For example, if water samples have no significant tritium nor carbon-14 yet chlorine-36 concentrations indicate water ages of 3×10^5 years, this is reassuring and would suggest that all the water is at least 5×10^4 years old and most water is much older. Evidence for the rapid transportation of natural radionuclides would be lacking. On the other hand, if tritium dating suggests 50-year-old water, carbon-14 dating indicates 2,000-year-old water, and chlorine-36 suggests 2×10^5-year-old water, then, unless mixing has

taken place in a well or bore hole, vast differences of water velocities are suggested.

Scope of Research

The objective of our project was to evaluate the various methods which could be of possible use to date ground water. For those methods which have been developed extensively, the evaluation was confined to a literature review. For certain basic questions, a limited amount of field testing, laboratory measurements, and analytical calculations were undertaken. For three potential methods of dating, original developmental research was undertaken. The three methods were chosen because they had promise of positive results within a reasonable period of time.

The nine basic methods for dating ground water which were considered were:

1) Hydrodynamic equations using Darcy's law and an expression of continuity.
2) Decay of radionuclides which have entered the water when it was in contact with the atmosphere. Examples of radionuclides would be ^{3}H, ^{14}C, ^{32}Si, ^{36}Cl, ^{39}Ar, and ^{81}Kr.
3) Accumulation of stable products of radioactive disintegration. An example would be ^{4}He.
4) The degree of disequilibrium between radionuclide pairs. Examples would be $^{234}U/^{238}U$ and $^{129}I/^{238}U$.

5) Time-dependent changes in the structure of molecules in water such as the racemization of amino acids.

6) The degree of chemical disequilibrium among various components dissolved in, or in contact with, ground water. Examples might be certain sluggish chemical processes such as the dissolution of silica or the oxygen isotope disequilibrium between the sulfate ion and the surrounding water.

7) Correlation of paleoclimatic indicators with the known chronology of past climates. Paleoclimatic indicators considered were ^{18}O, ^{2}H, Cl^{-}, and the noble gases.

8) The presence or absence of ions in the ground water which can be correlated with past geologic events which have been dated previously. Examples would be chloride related to ancient sea water in a marine terrace or dissolved solids leached from a historical lava flow.

9) Anthropogenic compounds found in ground water. Examples are ^{3}H, ^{85}Kr, TCE, and Freons.

Each of the methods listed above has certain difficulties associated with its application. Because ^{14}C and ^{3}H have been applied widely in hydrogeologic studies to date ground water, two potential problems were given a high priority in our work. These were: the extent of subsurface (nonatmospheric) production of ^{3}H and ^{14}C and the definition of $^{13}C/^{12}C$ ratios necessary for determining ^{14}C ages in arid regions. The work on subsurface

production has been most fruitful and has an underlying importance in much of our work.

New methods deemed suitable for development were dating by the use of ^{36}Cl, ^{129}I, and dissolved noble gases as climatic indicators. These methods and their development constituted a major part of our research and will be central to much of the following discussion.

SUBSURFACE PRODUCTION OF RADIONUCLIDES

Introduction: Because water dating for the purpose of studying the safety of nuclear repositories would press tritium and carbon-14 methods to their theoretical limits, the possible importance of subsurface production was considered. Normally, natural tritium and carbon-14 are considered to originate only in the earth's atmosphere through the interaction of cosmic radiation with various gases. If this were true, then even the smallest concentrations of these radionuclides would be important in indicating the rapid migration and mixing of a small but important amount of ground water within a region saturated with water which in general is much older. However, several potential sites of production exist for tritium, carbon-14, and other "atmospheric" radionuclides. The extent of this production, therefore, is a critical factor to be evaluated for the general purpose of hydrologic studies related to radioactive waste isolation.

In general, natural subsurface production is most important near the land surface where cosmic radiation is still effective and near large concentrations of uranium and thorium. The importance in water dating varies greatly with the radionuclide considered. In our studies, we have estimated the relative importance to be as follows with the radionuclide having the most subsurface production given first:

^{129}I, ^{39}Ar, ^{36}Cl, ^{3}H, ^{14}C, ^{32}Si, and ^{81}Kr.

Radionuclides from Spontaneous Fission: Spontaneous fission of uranium-238 will produce some radionuclides directly. Ternary fission will produce some tritium but at levels below direct detection. The only direct product of interest in possible dating which we have measured is iodine-129. This probably is the most important source of natural iodine-129 in the subsurface and will be discussed further in a later section.

Neutron Capture: Capture of thermal neutrons is probably the most important reaction giving rise to "atmospheric" radionuclides in the subsurface. Some of these reactions are listed below:

$Li^{6}\ (n,\alpha)^{3}H$

$C^{13}\ (n,\gamma)^{14}C$

$N^{14}\ (n,p)^{14}C$

$Cl^{35}(n,\gamma)^{36}Cl$

$K^{39}\ (n,p)^{39}Ar$

At the ground surface, neutrons which are produced from various interactions between primary and secondary cosmic radiation and atmospheric gases will produce the largest number of "atmospheric" radionuclides. The neutrons which come from the atmosphere and enter the subsurface, however, will primarily affect the first few tenths of a meter. Penetration below a meter can be neglected.

Neutrons can also be produced by muons which are secondary cosmic ray particles which penetrate much deeper into the subsurface than the neutrons from the atmosphere. Below about 50 meters, the production of neutrons is

dominated by (α,n) reactions where the α particles come mostly from the decay of the primordial radionuclides uranium-238, thorium-232, and uranium-235. Under special conditions, samarium-147 may contribute up to about 2% of the α particles.

Natural spontaneous fission of uranium-238 will also produce some neutrons, but generally only 5 to 15 percent of the total in the subsurface beyond the effects of muon penetration. If concentrated uranium ore is considered, some neutrons are also produced by naturally induced fission of uranium-235.

Calculated Neutron Densities: Fiege et al. (1968) measured the (α,n) reactions for a large number of light elements exposed to thermal neutrons. These data together with a knowledge of concentrations of uranium and thorium, the spontaneous fission half-life of uranium-238, and the neutron adsorption cross sections of the elements in the solid matter under study allowed Fiege and coworkers to calculate the subsurface production of neutrons from both (α,n) reactions and spontaneous fission. We have followed Fiege's method as further modified and described by Zito et al. (1982) and Andrews and Kay (1983) using chemical analyses listed in Tables 1 and 2. Results of our calculations are shown in Table 3.

Field Measurements of Thermal Neutrons: Because of the approximate nature of our calculations and because of the very small number of published studies

bearing on subsurface neutron densities, we undertook direct measurements of thermal neutrons in the subsurface. A helium-3 proportional counter with appropriate electronics was used (Kuhn, 1983) to measure thermal neutrons at various depths in different geologic materials. Counts were made with and without cadmium shielding in order to discriminate against other sources of the signals. Measurements at each location took several hours to complete because of the low neutron densities and the length of time needed to accumulate sufficient counts. Field counts were converted into neutron densities by a method outlined by Kuhn (1983) and are presented in Table 3.

TABLE I

Major Constituents in Samples

Constituent	Sample Number					
	1	2	3	4	5	6
	Concentrations in percent					
SiO_2	55.7	71.3	56.0	10.6	72.7	72.8
Al_2O_3	16.0	8.8	15.5	1.3	12.7	11.9
CaO	4.0	4.1	4.7	29.5	1.2	2.2
MgO	3.4	3.3	5.1	19.5	0.7	0.7
Na_2O	3.3	0.5	0.8	0.0	2.9	1.3
K_2O	3.3	3.6	2.5	0.04	4.8	5.3
Fe_2O_3	6.9	2.4	7.3	0.7	3.2	1.6
MnO	0.1	0.04	0.08	0.6	0.05	0.02
TiO_2	1.0	0.7	0.8	0.04	0.33	0.75
P_2O_5	0.3	0.1	0.2	0.03	0.09	0.22
CO_2	6.0	5.7	7.2	37.0	1.2	2.5

TABLE 2

Minor and Trace Constituents in Samples

Constituent	Sample Number					
	1	2	3	4	5	6
	Concentrations in MG/KG					
Li	58	28	32	7	15	30
B	25	50	50	10	75	50
Cl	200	<50	50	50	<50	100
Sm	7.9	4.5	3.6	1.1	4.9	12.0
Gd	6.6	3.9	2.9	1.4	4.3	13.0
U	4.0	3.4	0.6	1.3	3.6	2.9
Th	8.3	7.9	2.4	0.7	14.0	15.0
Cr	80	80	10	0	50	30
Rb	120	130	60	0	190	130
Sr	320	150	250	40	260	170
Zn	300	180	120	0	160	250

TABLE 3

Measured and Calculated Thermal Neutrons

Description of Measurement Site. Number corresponds to Tables 1 and 2	Depth of Measurements (M)	Thermal Neutrons in N/CM^3Yr	
		Calculated	Field Measurement
1. Test hole in granite near Oracle, Az.	11	31±3	116±21
2. Patagonia mine, highly altered limestone near Patagonia, Az.	31	19±2	42±8
3. Superior mine, conglomerate, at Superior, Az.	1385	5.5±0.6	1.1±0.2
4. Superior mine, limestone, at Superior, Az.	1385	5.8±0.5	7.8±1.4
5. Well in alluvium, Tucson, Az.	21	34±5	53±9.5
6. San Manuel mine, altered granite, at San Manuel, Az.	638	28±3	33±5.9

Interpretation of Table 3: Despite the differences between calculated and measured neutron densities shown in Table 3, we consider that the agreement between the two sets of values is excellent in view of the large number of approximations necessary to obtain the numbers listed. Differences shown are probably due to two primary reasons. First and most important, measurements taken at a shallow depth are almost certainly affected by neutrons produced by muon interactions. Muons, which are energetic secondary cosmic ray particles of small mass, can penetrate several hundred meters into the earth but more than 50% react within the upper 10 to 20 meters of the earth. At a depth of 300 meters, neutrons produced by muon reactions should be about at the lower limits of our method of detection. The second major source of error comes from the rock sampling process. Owing to limitations of time and resources, only grab samples were used for the chemical analyses of the rocks near the locations where neutrons were counted. Local variations of uranium and thorium concentrations must be large near some of the locations.

CORRECTION OF CARBON-14 DATES BY RATIOS OF STABLE CARBON ISOTOPES

Introduction: Because of the complex chemistry of bicarbonates in natural waters, the "original" carbon-14 content of water is difficult to reconstruct. The ratios of the two stable isotopes of carbon (masses 12 and 13) vary considerably in nature and their ratios are widely used to help reconstruct the geochemical history of the ground water and to estimate the original amount of carbon-14 introduced into the system. Lack of data on the carbon-13/carbon-12 ratios in arid climates prompted a study of this problem in order to better understand the uncertainty of carbon-14 dating in regions similar to Tucson, Arizona. The following description is abstracted from a report by Parada et al. (1983).

The total dissolved inorganic carbon in the typical aquifers originates in part from the soil CO_2 and in part from dissolution of carbonates in the soil zone and in the aquifer. The ^{14}C content of soil CO_2 is usually close to 100% modern; solid carbonate in the subsurface commonly contains no ^{14}C. To correct for the dilution of modern carbon in ground water, several chemical and/or isotopic models have been proposed (Ingerson and Pearson, 1964; Tamers, 1975; Mook, 1976; Fontes and Garnier, 1979; Wallick, 1973). All models, except that of Tamers, require data on the stable isotopic composition of soil CO_2.

The principal mechanisms producing soil CO_2 are plant respiration through roots and decomposition of organic matter. Precipitation of carbonate minerals also produces CO_2. The stable isotopic composition of soil

CO_2 is related to the photosynthetic pathway of the vegetation cover. Plants with different photosynthetic pathways have different $^{13}C/^{12}C$ ratios. Most plants in humid temperate areas follow the Calvin, or C_3, pathway and $\delta^{13}C$ values for soil CO_2 in these areas range from -22‰ to -27‰ (Galimov, 1966; Rightmire, 1978a; Reardon, Allison, and Fritz, 1979). Tropical and desert areas may, in addition to C_3 type plants, support plants that photosynthesize via C_4 (Hatch-Slack) or CAM pathways and consequently the $\delta^{13}C$ values for soil CO_2 in these areas vary more than in temperate and humid areas. $\delta^{13}C$ values ranging from -12‰ to -23‰ have been reported in the literature (Rightmire, 1978b; Kunkler, 1979; Wallick, 1973; Fritz, et al., 1978; Lerman, 1972) for soil CO_2 from desert or semi-desert environments. Wallick (1973) analyzed the ^{13}C content of five soil CO_2 samples in the Tucson basin and found values ranging from -12‰ to -18‰ with a mean of -15.1‰. He pointed out the possibility that the lighter (more negative) values were influenced by lighter atmospheric CO_2 produced by burning of fossil fuels. He suggested a mean of about -12‰ as a reasonable value for soil CO_2 in the Tucson basin.

Nature of the Study: The purpose of our study was to determine (1) the average $\delta^{13}C$ value of soil CO_2 in semiarid environments with vegetation similar to that of Tucson, and (2) the influence of vegetation and seasonal factors on $\delta^{13}C$ values of soil CO_2. Soil gas collection sites chosen are in or near assumed recharge areas for the Tucson basin aquifer.

Ninety-one soil gas samples were collected at three long-term sites in the Tucson area from July 1980 to June 1981 to determine the extent of seasonal variations and the influence of vegetation on the $\delta^{13}C$ and CO_2 concentration of soil gases. Variations were observed in both $\delta^{13}C$ and CO_2 concentrations. The highest CO_2 concentrations, up to 1.3% at 60 cm depth, were observed during March and April; the lowest, 0.1% CO_2 at 12 cm depth, were observed during the winter months. The $\delta^{13}C$ values vary by about 5‰ during the sampling period. The lowest ^{13}C contents were found in early spring and summer. Part of the $\delta^{13}C$ variation is due to exchange with an atmospheric CO_2. Other causes could be decomposition of organic matter with different isotopic composition and different decay rates and/or to a seasonal displacement of the period of maximum activity among different varieties of plants. The mean $\delta^{13}C$ for samples at the long-term sites was about -18‰.

In addition, fifteen soil gas samples were collected in the bottom of washes which are the assumed recharge areas of the Tucson aquifer. Both CO_2 and ^{13}C concentrations showed changes with time and location. High concentrations of CO_2 of up to 4.8% were found. The mean $\delta^{13}C$ for these samples was about -20‰. A major source of CO_2 in the riverbeds is believed to be decomposition of organic matter carried out by the runoff water during the periodic flooding of the washes.

Significance of the Study: Previous work had suggested a $\delta^{13}C$ value of soil gas of -12‰ for the region studied (Wallick, 1973). Large seasonal and spacial variations, however, were not taken into account. A more reasonable value might be as high as -20‰ if most recharge takes place through stream channels. The resultant errors in not using the correct values is emphasized. For the ground water in the Tucson basin and the actual ratios given above, both Mook's and Fontes' models give infinite ages. Ingerson and Pearson's model, however, gives a reasonable value of several thousand years. In the Ingerson and Pearson model, a difference of 4‰ in $\delta^{13}C$ in the older water gave an age difference of almost 3,000 years.

PALEOCLIMATIC CORRELATIONS

Introduction: Several constituents in ground water give either direct or indirect indications of original water temperatures or general climatic conditions during the time when the water infiltrated into the subsurface. At least three general approaches can be used to reconstruct these past climates. The most common method uses the $^{2}H/^{1}H$ and $^{18}O/^{16}O$ ratios in water to infer storm patterns, evapotranspiration, and past temperatures. A second method uses the concentrations of noble gases in water also to infer paleotemperatures. A third method uses the chloride content of ground water to interpret ancient rates of evapotranspiration and/or positions of ancient shorelines.

Once climatic trends as interpreted from the ground-water data are established, they can be matched with the known chronology of climatic fluctuations back to about 200,000 years before present. This method, of course, is not precise and may even be misleading unless abundant regional data are available. Notwithstanding many shortcomings of the method, the simple fact that ground water may have recharged at a time when average surface temperatures were distinctly different than at present is a valuable bit of information which, when combined with other dating methods, may provide information on ground-water ages.

Only the possible use of noble gases will be discussed in this paper.

Noble Gases: The use of concentrations of noble gases in water to reconstruct temperatures at the time of ground-water recharge was first demonstrated by Sugisaki (1961) who used argon concentrations in recent water recharged from a river. Later, Mazor (1972) extended this idea to the use of other noble gases to reconstruct temperatures of much older waters. Phillips (1981) has reviewed the entire problem of trying to reconstruct paleotemperatures from noble gas data. He presented a number of equations which provided corrections for sample contamination as well as supersaturation of the original ground water. However, the equations require the analyses of dissolved Ne, Ar, Kr, and Xe for each water sample which are only available from a very limited number of special studies.

The key to the use of noble gases for paleotemperature reconstructions is the fact that the solubilities of the different noble gases in water are temperature-dependent and each noble gas has a unique temperature-concentration relationship. Inasmuch as the gases do not react chemically with the aquifer, are adsorbed only to a very minor extent, and normally stay in solution, the imprint of the original temperature during the recharge of the aquifer should remain in the ground water. Phillips has estimated that, with good quality gas analyses, these temperatures might be reconstructed with an accuracy of about 0.5°C.

Obvious difficulties exist with the use of noble gases. Sample collection is not routine. Most important, wells or springs which do not have atmospheric contamination or effervescing natural gas must be used. Also,

ordinary sample containers will not be satisfactory. We have had an apparent success in using about three meters of copper tubing through which the ground water is passed as it comes out of the well. Both ends of the tube are clamped tightly with special clamps prior to transportation to the laboratory. Another fundamental problem is related to the interpretation of the data. If infiltration of water takes place well above the water table, this water as it moves through the unsaturated zone will come into equilibrium with "soil" gases which may be quite different in composition and temperature from the surface atmospheric gases which are assumed to control the noble gas concentrations. Thus paleotemperature calculations will not give direct information concerning temperatures at the land surface which are the temperatures keyed into the chronology.

We are continuing our studies with analyses of noble gases in samples from the Great Artesian Basin of Australia. Thus far, results show that reconstructed paleotemperatures are generally reasonable but that the accuracy of the method may not allow chronological reconstructions based only on noble gases. One interesting and hydrologically important conclusion is that dissolution of gases has not taken place under atmospheric pressures but at pressures well above atmospheric. This same phenomenon has been observed widely in studies of noble gases in ground water in South Africa. The reason for the excess pressure probably relates to capillary effects in trapped soil gas during recharge events.

CHLORINE-36

Introduction: Three isotopes of chlorine, with masses of 35, 36, and 37, have been identified in natural materials. The common stable isotopes (35 and 37) have a ratio of chlorine-37/chlorine-35 of 0.32 which is almost constant in natural materials, thus indicating that the distribution of the unstable isotope, chlorine-36, is probably not affected measurably by natural fractionation processes. This fact, together with the fact that the natural distribution of the ionic form of the element in water is rarely affected by sorption, precipitation, or mineral dissolution means that chlorine-36 is a potentially useful radionuclide for age dating of ground water. Also, its half-life of 3.01×10^5 years makes it ideal for older waters.

A major problem in the application of ^{36}Cl to geological studies has always been the combination of a low natural abundance with a long half-life, resulting in a very low specific activity. Chlorine-36 activity in natural samples ranges from 10^{-5} to 10 disintegrations per minute per gram chloride (equivalent to 1.36×10^{-16} to 1.36×10^{-10} atoms $^{36}Cl/Cl$), with most samples near the lower end of the range. The activity of sea salt and bedded salt is even lower than 10^{-5} dpm per gram chloride. The history of ^{36}Cl application is, therefore, closely related to analytical developments.

Analytical difficulties were largely overcome by the recent work of David Elmore and Harry Gove at the Nuclear Structure Research Laboratory

at the University of Rochester who developed chlorine-36 analysis by the application of tandem accelerator mass spectrometry (TAMS) (Elmore et al., 1979). This mass spectrometic approach is a radical departure from the direct counting procedures previously used and combines the advantages of great sensitivity (down to 5×10^{-16} $^{36}Cl/Cl$) with small sample size (10 mg of chloride). With this instrument, all natural samples (with the exception of marine salts) are now within the range of analysis.

Field Studies of Chlorine-36 in Ground Water: Several field studies of chlorine-36 in ground water have been outlined by Bentley et al. (1983). As far as we know, thus far all the completed hydrogeologic studies of ground-water samples using modern analytical techniques have been by the University of Arizona team with the analyses being done at the University of Rochester under the direct supervision of David Elmore. However, several laboratories are currently developing similar capabilities for chlorine-36 analyses so that such studies should be almost routine within another decade.

We have taken multiple samples from a number of ground-water systems, the most important of which are the Carrizo aquifer in Texas, the Milk River aquifer in Alberta, the Fox Hills aquifer in North Dakota, the Tajo basin in Spain, and the Great Artesian Basin of Australia. Although anomalies exist and correspondence between hydrodynamic ages and chlorine-36 ages is not perfect, the data obtained are reasonable. Of all the studies undertaken, the Great Artesian Basin was the most complete and it also yielded the best results.

The Great Artesian Basin covers about 1.7×10^6 km^2 in northeastern Australia, about one-fifth of the continent. It is one of the largest artesian aquifer systems in the world. The physical hydrology of the basin has been described by Habermehl (1980) and the isotope hydrology by Airey et al. (1979). The basin contains a multiple aquifer system in Triassic, Jurassic, Cretaceous, and Tertiary sandstones.

The aquifers are recharged around the margin of the structural basin and discharge in the south-central portion, near Lake Eyre. The study was conducted along two flowlines extending from a recharge area on the western flanks of the Great Dividing Range, northeast of Charleville, west and southwest to Innamincka, in South Australia. The study area and the distribution of the $^{36}Cl/Cl$ ratio in the "J" aquifer are illustrated in Figure 1. The $^{36}Cl/Cl$ ratio decreases smoothly from the recharge area in the direction of flow and can be contoured consistently.

The chloride concentrations along these flowlines in the "J" aquifer are relatively constant. There is no consistent increase in chloride which would indicate subsurface sources. Ground-water ages were therefore calculated using a simple decay equation. The $^{36}Cl/Cl$ ratios in the recharge area show little variation, ranging from about 95×10^{-15} to 125×10^{-15} in waters younger than 2×10^4 years. These isochrons are relatively evenly spaced and indicate ground-water velocities which are reasonable given the known hydraulic parameters of the system.

Isochrons calculated by the Australian Bureau of Mineral Resources digital simulation model of the Great Artesian Basin model, GABHYD (Figure 2), are quite close to those determined by us on the basis of chlorine-36.

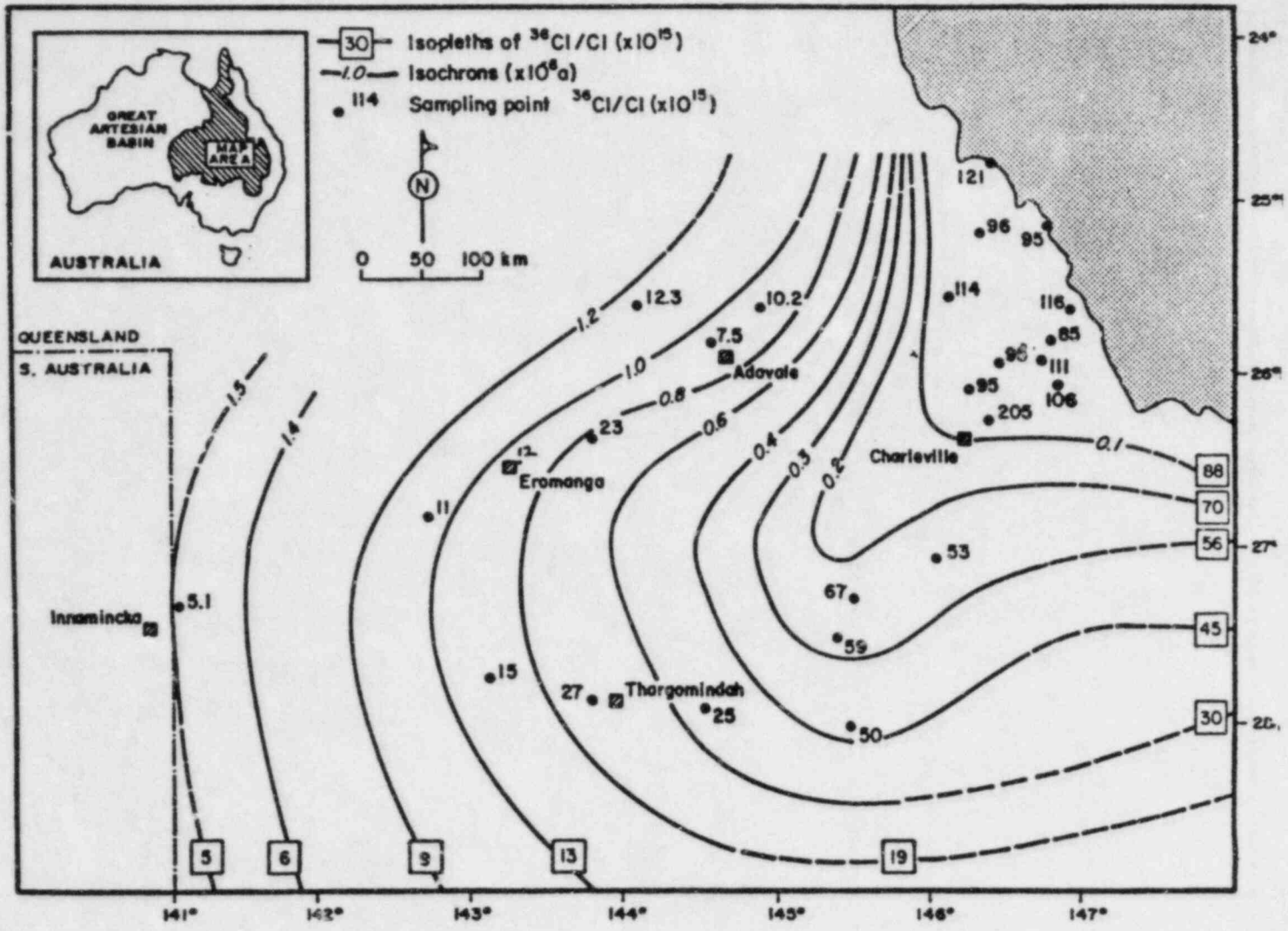

Fig. 1 Ratios of chlorine-36 to total chlorine and isochrons based on chlorine-36.

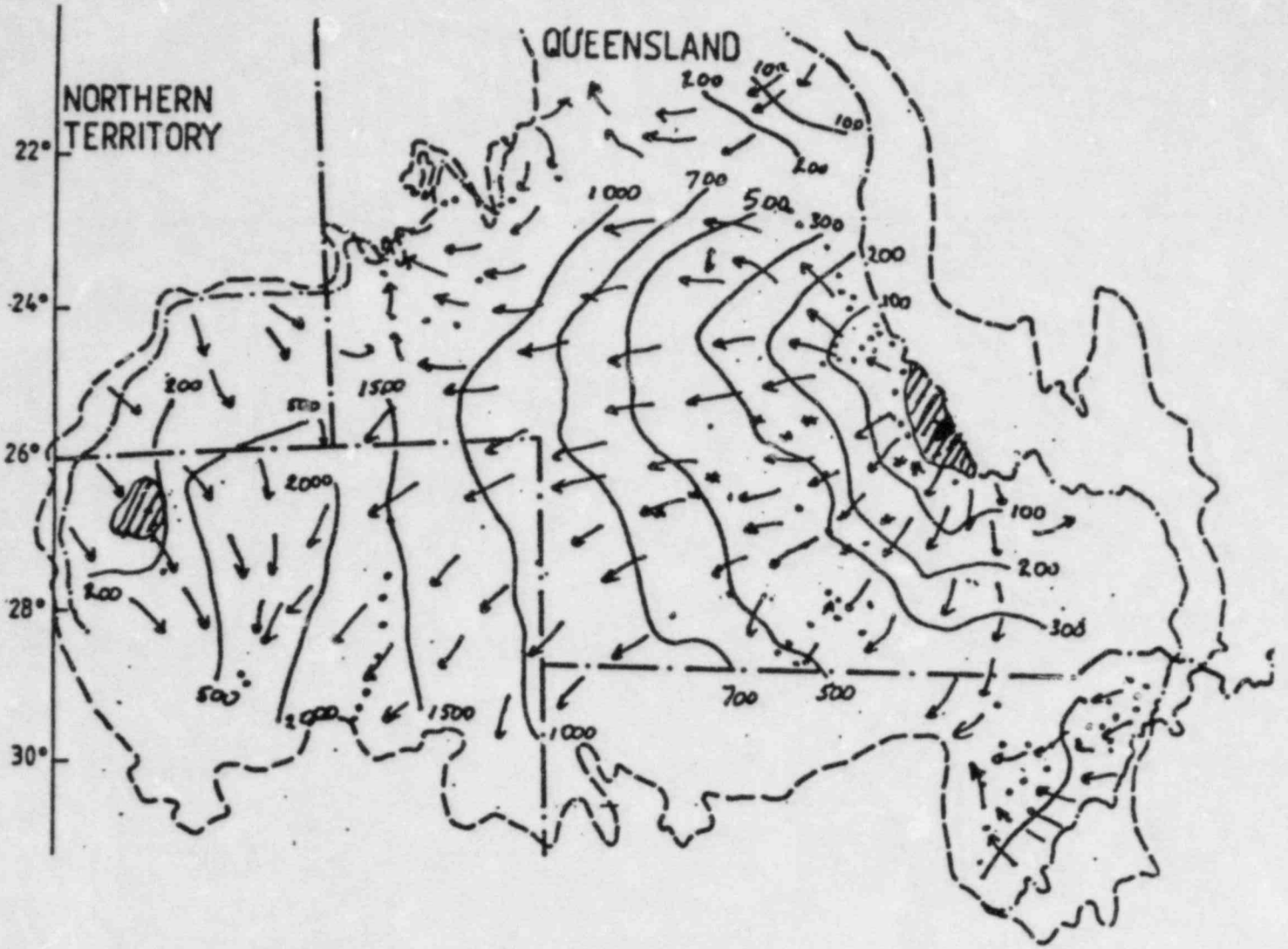

Fig. 2 Hydraulic isochrons calculated from the 1880 potentiometric surface. The area shaded is that with significant levels of carbon-14.

Thus, this work strongly suggests that chlorine-36 can be useful in dating old ground water in large aquifers.

Limitations of Chlorine-36 Dating: Several limitations must be kept in mind when working with chlorine-36 dating. Most important is the establishment of the initial concentration of chlorine-36. This can be accomplished by two methods. First, by taking the total chloride from precipitation (dry plus wet contributions) and dividing it by the predicted fallout of chlorine-36 from natural atmospheric production, a very generalized map of chlorine-36 atoms/total chlorine atoms can be constructed (Figure 3). Another method is to sample young ground water in the intake area of an aquifer and assume that chlorine-36 input into the intake area has been constant with time. Both methods assume that cosmic-ray production has been constant during the past 2×10^6 years and that the input of stable chlorine has also been constant. Both assumptions are certainly not true in a strict sense, but we consider the errors introduced by these assumptions to be less than 50 percent. Theoretically, sampling the young water in the aquifer may be superior because near surface, muon-related production is also included in the initial concentrations. Also, the young water sample allows a study of absolute chlorine-36 concentrations as well as chlorine-36/total chlorine ratios.

Another limitation of chlorine-36 dating is imposed by a significant subsurface production. This production produces a small residual chlorine-36 concentration in which chlorine-36/stable chlorine ratios $\times 10^{15}$

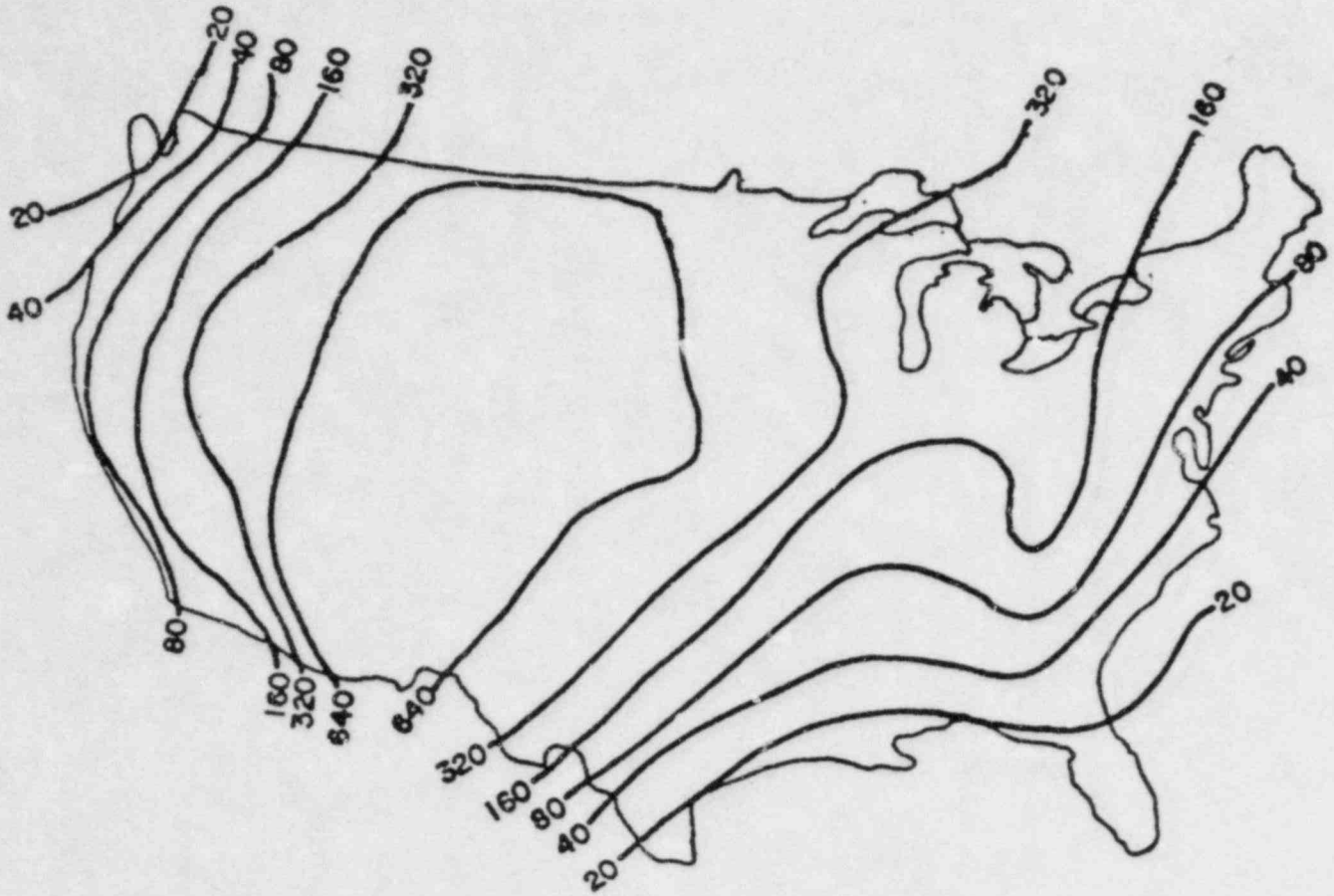

Fig. 3 Calculated $^{36}Cl/Cl$ ($\times 10^{15}$) ratios of prebomb ground water.

may vary from about 4 for quartz sandstone to about 30 for granite. Much higher values are possible, however, for rocks with uranium and thorium enrichment. This production limits the total span of ground-water which can be dated to about 1×10^6 years for granitic rocks and about 2×10^6 years for a quartz-sandstone aquifer.

A third limitation is the necessity of understanding something of the hydrogeologic system before interpreting the data. This, of course, is also true of any dating method. Some problems which may be encountered are the addition of dead chloride from adjacent aquifers and the presence of chlorine-36 which originated in the testing of nuclear devices in the Pacific. Where present in recent waters, "bomb pulse" chlorine-36 is a distinctive sharp signal with concentrations characteristically much higher than background values.

Other Potential Uses of Chlorine-36: Although not strictly related to ground-water dating, a number of other potential uses of chlorine-36 deserve mention. Three of these are listed below.

(a) A tracer for recent water. The "bomb pulse" was much sharper and relatively larger than the tritium pulse. Also, it will not decay in the near future. The application to hydrology is almost identical to tritium but in many ways superior.

(b) A possible indicator of ion filtration in natural systems. Chloride commonly increases downdip in aquifers. An increase in nonradioactive chloride without an increase in chlorine-36 would indicate the addition of chloride from a connate source or

exceptionally slow-flowing water with ion filtration effects. If both increase together in a rapidly flowing system, ion filtration is suggested.

(c) A tracer for old chloride. Ocean water and natural rock salt have very low chlorine-36 concentrations relative to the total chloride present. On the other hand, all old ground water in contact with normal aquifers will have significant concentrations of chlorine-35. The recent addition of chloride from sea-water intrusion or from the dissolution of subsurface salt can, therefore, be detected by the presence of chlorine-36/total chlorine ratios below the present limits of detection.

IODINE-129

Introduction: Natural production of the radionuclide iodine-129 occurs largely as a result of two fundamentally different processes. One is by spallation reactions induced by high energy cosmic radiation interacting with xenon in the atmosphere and with cesium, barium, and some of the rare earth elements in solid materials. The other natural process is through fission of uranium. A very small amount may also be produced by a neutron capture on tellurium. Natural concentrations are very low and until recently have been measured primarily in meteorites, lunar rocks, and uranium-rich samples. The first analyses of natural levels of iodine-129 in potable ground water were made in early 1983 by Dr. David Elmore and June Fabryka-Martin on samples collected and concentrated by Ms. Fabryka-Martin, Dr. Harold Bentley, Dr. Fred Phillips, and Dr. Peter Airey. The potable water was from the Great Artesian Basin of Australia. A number of brine samples collected by Ms. Fabryka-Martin were also analyzed by Dr. Elmore and Ms. Fabryka-Martin.

Potential Importance of Iodine-129: The half-life of iodine-129 is 1.6×10^7 years. This, together with the fact that it is very mobile in the hydrosphere, suggests that studies of iodine-129 may yield useful information concerning the age of extremely old water. In many aquifers, particularly in rocks with high to moderately high uranium contents, the natural background concentrations in precipitation will probably be lower than the final subsurface concentrations after equilibrium has been

reached with the aquifer materials. If this proves true, dating of water as old as 5×10^7 years may be possible with a disequilibrium method.

Another potential use of iodine-129 is to help with the studies of the movement of other trace constituents in ground water downgradient from uranium ore deposits. These studies, which bear directly on the understanding of the potential migration of radionuclides from a repository for high-level radioactive wastes, require tracers for the hydrologic system. Iodine-129 is potentially a natural inbuilt tracer. Also, iodine-129 will probably be a useful index of the total amount of fission products which would be present. Lastly, iodine-129 is itself of some concern as a possible health hazard, and the understanding of its mode of migration is important.

To study the dispersion of anthropogenic iodine-129, an accurate measurement of the natural background concentrations of iodine-129 are needed. Present studies we are conducting will help with this task.

Because iodine-129 has such a long half-life, it can serve as a built-in tracer for ground water. Natural iodine-129/iodine-127 ratios at equilibrium should vary from about 9×10^{-14} to about 7×10^{-12} (Fabryka-Martin, 1983). These ratios should be distinctive enough to enable the tracing of very slowly moving ground water which migrates from an aquifer of one lithology to an aquifer of another lithology.

Work in Progress: At the present time, samples of iodine from Australian ground water are being studied. Two general types of samples are involved.

One is a series of samples taken downgradient from a uranium ore body. The other is a series of samples from the Great Artesian Basin. These groups of samples were chosen because the hydrogeologic and isotopic characteristics of these systems are well defined and were being studied for related purposes.

Iodine-129/iodine-127 ratios from ground-water samples measured thus far range from 5×10^{-13} for water near the recharge zone to 7×10^{-12} for old water which may come from deeper zones in the Great Artesian Basin.

Work to be Completed: The most important task is to understand the iodine-129 distribution in meteoric waters of recent origin prior to the injection of anthropogenic iodine-129 into the hydrosphere. This will involve looking at samples from ground water which are from well-defined aquifers where mixing of recent surface waters has not taken place.

The present method of iodine collection uses an anion exchange resin which removes iodine from several hundred liters of water in the field. As analytical sensitivity of the TAMS system improves, field sampling procedures can also be made less cumbersome.

A large number of field samples are needed to verify what we believe to be theoretically reasonable assumptions about the hydrochemistry of the iodine, the rate of production of iodine-129 from natural fission, and the relative importance of the "atmospheric" component.

REFERENCES CITED

Airey, P.L., Calf, G.E., Campbell, B.L., Hartley, P.E., Roman, D., Habermehl, M.A., 1979, Aspects of the isotope hydrology of the Great Artesian Basin, Australia, In: Isotope Hydrology, 1978, Interna. Atomic Energy Agency, Vienna, Vol. 1, p. 205-217.

Andrews, J.N., and Kay, R.L.F., 1982, Natural production of tritium in permeable rocks, Nature, 298: 361-363.

Elmore, D., Fulton, B.R., Clover, M.R., Marsden, J.R., Gove, H.E., Naylor, H., Purser, K.H., Kilius, L.R., Beukens, R.P., Litherland, A.E., 1979, Analysis of ^{36}Cl in environmental water samples using an electrostatic accelerator, Nature, 277, 22-25.

Fabryka-Martin, J., 1982, The value of ^{129}I measurements in assessing salt-dome hydrology: In Annual Report on NRC contract 04-78-272 for the period Dec. 1, 1981 through Nov. 30, 1982, University of Arizona, p. 71-109.

Feige, Y., Oltman, B.G., Kastner, J., 1968, Production rates of neutrons in soils due to natural radioactivity, J. Geophys. Res., 73: 3135-3142.

Fontes, J.C., and Garnier, J.M., 1979, Determination of the initial ^{14}C activity of the total dissolved carbon -- a review of the existing models and a new approach: Water Resour. Res., 15(2): 399-413.

Fritz, P., Hennings, C.S., Suzuki, O., and Salati, E., 1978, Isotope hydrology in northern Chile. In: Isotope Hydrology 1978. Int. At. Energy Agency (I.A.E.A.), Vienna, p. 525-543.

Galimov, E.M., 1966, Carbon isotopes in soil CO_2. Geochem. Int., 3: 889-898.

Habermehl, M.A., 1980, Hydrogeology of the Great Artesian Basin, BMR J of Aust. Geol. Geophy, 5, 9-38.

Ingerson, E., and Pearson, F.J., 1964, Estimation of age and rate of motion of ground water by the C-14 method. In: Recent Researches in the Fields of Hydrosphere, Atmosphere and Nuclear Geochemistry, Sugarawa Festival Volume, Maruzen, Tokyo, p. 263-283.

Kuhn, M.W., 1984, Subsurface neutron production and its impact on ^{36}Cl groundwater dating, M.S. thesis, 35 pp., Univ. of Arizona.

Kunkler, J.L., 1969, The sources of carbon dioxide in the zone of aeration of the Bandelier Tuff, near Los Alamos, New Mexico. U.S. Geol. Surv. Prof. Pap. 650B, p. B185-B188.

Lerman, J.C., 1972, Soil CO_2 and ground water: carbon isotopes compositions. In: T.A. Rafter and T. Grant-Taylor (Editors), Proc. 8th Int. Conf. on Radiocarbon Dating. R. Soc. N.Z., Wellington, p. D93-D105.

Mazor, E., 1972, Paleotemperatures and other hydrological parameters deduced from noble gases dissolved in groundwaters, Jordan Rift Valley, Israel, Geochim. Cosmochim. Acta, 36, 1321-1336.

Mook, W.G., 1976, The dissolution-exchange model for dating groundwater with ^{14}C. In: Interpretation of Environmental Isotope and Hydrochemical Data in Groundwater Hydrology. Int. At. Energy Agency (I.A.E.A.), Vienna, p. 212-225.

Parada, C.B., Long, A., and Davis, S.N., 1983, Stable-isotope composition of soil carbon dioxide in the Tucson basin, Arizona, U.S.A.: Isotope Geoscience, Vol. 1, p. 219-236.

Phillips, F.M., 1981, Noble gases in ground water as paleoclimatic indicators, Ph.D. dissertation, 189 p., Univ. of Arizona.

Reardon, E.J., Allison, G.B., and Fritz, P., 1979, Seasonal, chemical, and isotopic variations in soil CO_2 at Trout Creek, Ontario. J. Hydrol., 43: 355-371.

Rightmire, C.T., 1978a, Seasonal variations of P_{CO_2} and ^{13}C content of soil atmosphere. Water Resour. Res., 14(4):691-692.

Rightmire, C.T., 1978b, Changes in formation gas composition and isotope content as indicators of unsaturated-zone chemical reactions related to recharge events. In: Isotopes in Hydrology, Int. At. Energy Agency (I.A.E.A.), Vienna, p. 711-732.

Sugisaki, R., 1961, Measurement of effective flow velocity of ground water by means of dissolved gases, American J. Sci., 259, 144-153.

Tamers, M.A., Ronzani, C., Scharpenseel, H.W., 1969, Naturally occurring chlorine-36, Atompraxis, 15, 433-437.

Wallick, E.I., 1973, Isotopic and chemical considerations in radiocarbon dating of ground water within the arid Tucson basin, Arizona. Ph.D. Thesis, University of Arizona, Tucson, Arizona.

Zito, R., Donahue, D.J., Davis, S.N., Bentley, H.W., and Fritz, P., 1980, Possible subsurface production of carbon-14: Geophys. Res. Lett., 7, 235-238.

Appendix

Published Reports, Theses, and Dissertations Completed in Connection with Research Sponsored by NRC.

Theses and Dissertations
Department of Hydrology and Water Resources
University of Arizona, Tucson, Arizona 85721

Alweis, S.J., 1981, Possible subsurface production of carbon-14 in ground water: M.S. Thesis.

Bitner, M.J., 1983, The effects of dispersion and mixing on radionuclide dating of ground water: M.S. Thesis.

Brinkman, J.E., 1981, Water age dating of the CorrizoSand: M.S. Thesis.

Fitzwater, P.L., 1981, Age and movement of ground water in the Madison Limestone, northeastern Wyoming: M.S. Thesis.

Parada, C.B., 1981, Isotopic composition of soil carbon dioxide in the Tucson basin: M.S. Thesis.

Phillips, F.M., 1981, Noble gases in ground water as paleoclimatic indicators: Ph.D. Dissertation.

Swanick, G.B., 1982, The hydrochemistry and age of the water in the Milk River Aquifer, Alberta, Canada: M.S. Thesis.

Trotman, K.N., 1983, Thermonuclear chlorine-36 in arid soil: M.S. Thesis.

PUBLISHED REPORTS

Phillips, F.M., and Davis, S.N., 1979, Noble gases in groundwater as paleoclimatic indicators: Am. Geophys. Union, EOS, v. 40, no. 46, p. 830.

Zito, R., Donahue, D.J., Davis, S.N., Bentley, H.W., and Fritz, P., 1980, Possible subsurface production of carbon-14: Geophysical Research Letters, v. 7, no. 4, p. 235-238.

Bentley, H.W., and Davis, S.N., 1980, Isotope geochemistry as a tool for determining regional ground-water flow: Proceedings, Office of Nuclear Waste Isolation, Battelle Memorial Inst., ONWI-212, p. 35-41.

Bentley, H.W., and Davis, S.N., 1980, Feasibility of ^{36}Cl-dating of very old ground water: Am. Geophys. Union, EOS, v. 61, no. 17, p. 230.

Bentley, H.W., and Davis, S.N., 1980, ^{36}Cl as a ground-water dating tool and environmental tracer: Am. Geophys. Union, EOS, v. 61, no. 48, p. 1192.

Bentley, H.W., and Davis, S.N., 1981, Applications of AMS to hydrology, in Symposium on accelerator mass spectrometry, edited by W. Kutschera: Argonne Nat. Lab. ANL-PHY-81-1, p. 193-227.

Davis, S.N., 1981, Water dating and regional ground-water studies: Geol. Soc. Am., Abstracts with Programs, v. 13, no. 7, p. 437.

Davis, S.N., and Bentley, H.W., 1982, Dating groundwater, a short review in Nuclear and chemical dating techniques: Am. Chemical Soc. Symposium Series No. 176, p. 187-222.

Davis, S.N., 1982, Isotopes useful for hydrologic studies of arid regions: Geol. Soc. America, Abstracts with Programs, v. 14, no. 4, p. 158.

Zito, R.R., Davis, S.N., Bentley, H.W., and Kuhn, M.W., 1982, Water dating and radionuclide production by subsurface neutrons: Geol. Soc. America, Abstracts with Programs, v. 14, no. 7, p. 653.

Bentley, H.W., Phillips, F.M., Davis, S.N., Gifford, S., Elmore, D., Tubbs, L.E., and Gove, H.E., 1982, Thermonuclear Cl-36 pulse in natural water: Nature, v. 300, no. 23, p. 737-740.

Davis, S.N., Bentley, H.W., Phillips, F.M., and Elmore, D., 1983, Use of cosmic-ray produced radionuclides in hydrogeology (Abstract): Amer. Geophys. Union, EOS, v. 64, no. 18, p. 283.

Bentley, H.W., Davis, S.N., Swanick, G., Elmore, D., and Gove, H., 1983, ^{36}Cl in the Milk River aquifer, Alberta: Groundwater dating and verification of ion filtration (Abstract): 1983 AGU Spring Meeting Program, Amer. Geophys. Union, p. 49.

Airey, P., Bentley, H.W., Davis, S., Phillips, F., and Elmore, D., 1983, ^{36}Cl investigation of the Great Artesian Basin, Australia: 1983 AGU Spring Meeting Program, Amer. Geophys. Union, p. 49.

Parada, C.B., Long, A., and Davis, S.N., 1983, Stable-isotopic composition of soil carbon dioxide in the Tucson basin, Arizona, U.S.A.: Isotope Geoscience, v. 1, p. 219-236.

5.0 GEOCHEMICAL MODELLING AND PREDICTION

One of the main objectives of DOE and NRC research is to provide information that can be used in performance assessment analyses to determine whether high level wastes can be safely disposed in proposed deep geologic systems. Guidance for the assessment of safety is provided by NRC technical criteria (10 CFR 60) and EPA draft environmental release standards. (40 CFR 191). The regulations will require a quantitative assessment of cumulative releases of specific toxic radionuclides to the accessible environment over a period of 10,000 years post repository closure. The analyses will consider waste package life, the effect of waste emplacement and heat on performance of the geologic system, source term characteristics of the radionuclides released from the waste package to the near-field and from the near-field to the far-field, and retardation of the nuclides relative to the flow of ground water between the waste package and the accessible environment. In order to numerically simulate and predict the migration of HLW radionuclides the important geochemical interactions between radionucludes, water, waste package, backfill, and host rock must be considered. At present, the interactions and controlling mechanisms are not adequately understood to permit development of a reliable and verifiable repository systems analysis (Carnahan et al., 5.1). However, recent advances in modeling the behavior and mobility of chemical species in thermally perturbed geothermal systems are encouraging (Tsang et al., 1984).

The research reported in the following papers on geochemical modeling and prediction is intended to provide the NRC with a capability to assess (1): whether transport models proposed by DOE for licensing adequately account for the significant geochemical processes and interaction (Carnahan et al., 5.1); (2) which experimental and observational data are required to implement identified geochemical processes as algorithms in models (e.g., Apps, 2.1; Silva and Nitsche 2.3; Dayal et al., 5.2); and (3) which approaches are best suited for the verification of numerical simulation of radionuclide transport (Seitz et al., 5.5; Peterson et al., 5.6).

Carnahan et al. (5.1) recommend that the development of an ability to predict the performance of nuclear waste repositories reliably, will depend on close interaction between laboratory and field investigators and developers of predictive codes. The codes used by Carnahan et al. (5.1) were used to simulate carefully controlled laboratory experiments conducted by Seitz et al. (5.5) with little initial success. However, through the collaborative effort the model was improved and additional data required by the model was collected. The mechanistic models used by Carnahan et al. were also compared to empirical models using K_d values to simulate ion transport in field studies. They found that if the concentration of the ion of interest is comparable to the concentrations of major, exchanging ions or if a number of sorptive sites is a function of pH, then a constant K_d model is not adequate to simulate the chemical transport process (for more details see Carnahan et al., 5.1). Therefore, Carnahan et al. conclude that "experimental programs for measurement of k_D values should be redirected toward identification of chemical mechanisms influential in waste transport, identification of aqueous and sorbed species involved in the mechanisms, and measurement of thermodynamic and chemical-

kinetic data associated with species and mechanisms. These efforts should include characterization of solid phases active in chemical reactions during waste transport. Many of these important data are currently lacking, but are required for development and application of a capability to predict repository performance."

Scaling factors can add an additional level of complexity to the simulation of transport in natural field systems. Peterson et al. (5.6) were able to successfully model solid-phase reactions that control the concentrations of major solution species. The MINTEQ code successfully predicted gypsum and jarosite precipitation and concentrations of several macroconstituents (e.g., Ca, SO_4, Al, Fe, and Mn) in uranium mill tailings ponds. Lack of success in predicting trace metal concentrations in the mill tailings case is attributed to a failure of the model used to account for other important mechanisms such as adsorption. Peterson et al. (5.6) conclude that geochemical modeling methodology coupled with the laboratory and field studies should be applicable to a range waste management problems.

REFERENCES

Apps, J. 1984. "Hydrothermal Evolution of Repository Groundwaters in Basalt." In NRC Nuclear Waste Geochemistry '83. NUREG/CP-0052.

Carnahan, C. L., C. W. Miller, and J. S. Remer. 1984. "Verification and Improvement of Predictive Algorithms for Radionuclide Migration." In NRC Nuclear Waste Geochemistry '83. NUREG/CP-0052.

Dayal, R., D. G. Schweitzer, and R. E. Davis. 1984. "Wet and Dry Cycle Leaching: Aspects of Releases in the Unsaturated Zone." In NRC Nuclear Waste Geochemistry '83. NUREG/CP-0052.

Peterson, S. R., R. J. Serne, A. R. Felmy, R. L. Erickson, K. M. Krupka and G. W. Gee. 1984. "Interactions of Acidic Solutions with sediments: A Case Study. In NRC Nuclear Waste Geochemistry '83. NUREG/CP-0052.

Seitz, M. G., G. F. Vandergrift, D. L. Bowers, and T. S. Gerding. 1984. "Effect of Aged Waste Package and Aged Basalt on Radioelement Release." In NRC Nuclear Waste Geochemistry '83. NUREG/CP-0052.

Silva, R. J. and H. Nitsche. 1984. "Thermodynamic Properties of Chemical Species of Waste Radionuclides." In NRC Nuclear Waste Geochemistry '83. NUREG/CP-0052.

Tsang, C. F. 1984. "Investigation of Coupled Interactions in Geothermal and Hydrothermal Systems for the Assessment of HLW Isolation - Panel Report." Conducted under FINB-3046, United States Nuclear Regulatory Commission.

U. S. Environmental Protection Agency, 1981, "Working Draft No. 20, Environmental Protection Agency, 40 CFR 91, Environmental Standards and Federal Radiation Protection Guidance for Management and Disposal of Spent Nuclear Fuel, High-Level and Tansuranic Radioactive Waste," U.S. EPA, Washington, D.C.

U. S. Nuclear Regulatory Commission, 1983, "Disposal of High-Level Radioactive Wastes in Geologic Repositories, Technical Criteria," Federal Register, v. 46, No. 120, pp. 28194-282229.

5.1 VERIFICATION AND IMPROVEMENT OF PREDICTIVE ALGORITHMS FOR RADIONUCLIDE MIGRATION

C. L. Carnahan, C. W. Miller, and J. S. Remer
Lawrence Berkeley Laboratory
University of California
Berkeley, California 94720

ABSTRACT

This research addresses issues relevant to numerical simulation and prediction of migration of radionuclides in the environment of nuclear waste repositories. Specific issues investigated are the adequacy of current numerical codes in simulating geochemical interactions affecting radionuclide migration, the level of complexity required in chemical algorithms of transport models, and the validity of the "constant-k_D concept" in chemical transport modeling. An initial survey of the literature led to the conclusion that existing numerical codes did not encompass the full range of chemical and physical phenomena influential in radionuclide migration. Studies of chemical algorithms have been conducted within the framework of a one-dimensional numerical code that simulates the transport of chemically reacting solutes in a saturated porous medium. The code treats transport by dispersion/diffusion and advection, and equilibrium-controlled processes of interphase mass transfer, complexation in the aqueous phase, pH variation, and precipitation/dissolution of secondary solids. Irreversible, time-dependent dissolution of solid phases during transport can be treated. Mass action, transport, and sorptive site constraint equations are expressed in differential/algebraic form and are solved simultaneously. Simulations using the code show that use of the constant-k_D concept can produce unreliable results in geochemical transport modeling. Applications to a field test and laboratory analogs of a nuclear waste repository indicate that a thermodynamically based simulator of chemical transport can successfully mimic real processes provided that operative chemical mechanisms and associated data have been correctly identified and measured, and have been incorporated in the simulator. Success in the development of an ability to reliably predict the performance of nuclear waste repositories will depend on close interaction and coordination of effort between experimenters and developers of predictive codes.

5.1.1 INTRODUCTION

Prediction of the rates of migration of radionuclides in ground water moving through engineered barriers and host rocks surrounding underground repositories for nuclear waste is

essential to the assessment of the ability of a repository to meet standards for performance. The hydrogeological and geochemical processes that could influence the rates of migration may operate over times spanning many thousands of years and are difficult, if not impossible, to study in real-time laboratory and field experiments. Therefore, recourse is made to numerical simulations of these processes and their spans of time in order to predict, as accurately as possible, the total amounts and the concentrations of radionuclides that might be transported from waste repositories to the accessible environment. Only in this way can the potential hazard to public health and safety arising from nuclear waste repositories be quantified and evaluated.

5.1.1.1 Issues Addressed by This Research

The principal issues concerning our abilities to numerically simulate, and thus to predict, the migration of radionuclides in a repository environment are:

> What geochemical interactions between radionuclides, water, backfill, and host rock must be considered in order to achieve reliable simulations and predictions?
>
> What experimental and other observational data are required to implement identified geochemical processes as algorithms in simulators of radionuclide transport?
>
> How can the results of numerical simulations of radionuclide transport be verified?

This task addresses these principal issues and, in particular, certain specific issues necessary for their resolution. The specific issues are:

> Are currently applied numerical codes adequate to simulate geochemical interactions affecting radionuclide migration?
>
> What level of complexity is required in chemical algorithms of transport models to adequately predict radionuclide migration?
>
> Under what conditions, if ever, is the use of the constant distribution coefficient (k_D) valid in describing sorption and retardation of radionuclides?

5.1.1.2 Background and Objectives

In general, two methods have been used to simulate transport

of chemically reactive solutes.

One method is based on the plate theory of chromatography and uses codes that calculate equilibrium, closed-system distributions of chemical species sequentially with transport algorithms in a two-step procedure. This method was used, for example, by Routson and Serne (1972), Ahlstrom, Foote, Arnett, Cole, and Serne (1977), Grove and Wood (1979), and Strickert, Friedman, and Fried (1979). Applications of this method can be differentiated by the manner in which they attempt to account for transport by dispersion/diffusion. Thus, Ahlstrom et al. (1977) used a random walk procedure, while Grove and Wood (1979) solved the nonreacting convective-dispersive transport equation.

The second method is a one-step procedure that consists of solving a system of equations simultaneously describing chemical reactions and convective-dispersive transport with interphase mass transfer. In its simplest form, exemplified by the work of Holly and Fenske (1968), the method assumes uncoupled equilibrium exchange of noncompeting solutes, each with a constant k_D value; in this case, the system of simultaneous equations reduces to a set of independent, linear, partial differential transport equations, one for each exchanging solute. In its more advanced form, exemplified by the work of Rubin and James (1973) and Valocchi, Street, and Roberts (1981), the method is more soundly based on chemical and thermodynamic principles and leads to a system of simultaneous, nonlinear, partial differential equations coupled to a set of mass action equations. This approach appears to have produced the greatest degree of success in matching experimental laboratory and field data.

Various models have focused on particular physical or chemical phenomena identified to be influential in chemical transport. In general, however, models existing at the beginning of this work did not incorporate complete descriptions of the entire set of chemical phenomena known to affect rates of chemical migration. More particularly, existing models that incorporated individual chemical processes suffered from omission of other possibly significant processes, and the reliability of predictions made by these models was, at best, difficult to assess. Thus, there was an apparent need for a transport model capable of incorporating the essential set of chemical processes necessary for adequate understanding and prediction of migration of radionuclides.

The study described here addressed two objectives.

The first objective was to evaluate existing transport models with regard to their treatment of chemical processes affecting rates of movement of radionuclides in flowing ground water. The results of work toward this objective, briefly summarized in the preceding paragraphs, have been presented in

detail by Miller, Benson, and Carnahan (1982).

The second objective was to determine the necessity to include specific chemical processes in models used to predict radionuclide transport, and the level of complexity needed to describe the chemical processes. This objective has been approached by adding chemical algorithms to an existing computer code and observing the effects of including, omitting, and combining algorithms that describe individual chemical processes on computed histories of radionuclide migration.

5.1.1.3 Scope of Research

Because the primary emphasis in this research was the study of chemical algorithms, the numerical simulator used as a research tool was based on a very simple fluid flow model. The flow model is one-dimensional and assumes constant fluid velocity, diffusion, and dispersion. However, considerable effort has been spent on coupling the chemical algorithms to the fluid transport algorithm in as chemically and thermodynamically rigorous a manner as possible.

The more advanced form of the one-step approach was used in the simulator of chemical transport, CHEMTRN, used in this work. This allows simulation of the transport and chemical reactions of both major and minor chemical species and evaluation of the effects of major species on the transport of minor species, including radioactive species. The chemical equilibrium algorithms included in CHEMTRN are complexation in the aqueous phase, sorption of simple ions and complexes by either ion exchange or surface complexation, dissociation of water, and reversible precipitation/dissolution of solid phases. A nonequilibrium algorithm for the simulation of irreversible dissolution of solid phases during transport is included also.

5.1.2 CHEMICAL AND MATHEMATICAL BASES OF THE SIMULATOR, CHEMTRN

5.1.2.1 Chemical Equations

To simplify solution of the transport equations for a given chemical system, a set of basis species $A_j^{n_j}$ is defined, where n_j is the ionic charge of the species. This set consists of the minimum number N_b of species necessary to define all species present, either through equilibrium mass action relations or through nonequilibrium rate expressions.

Thermodynamic activities of basis species, $[A_j^{n_j}]$, and of complexes in the aqueous phase, $[C_i^{n_i}]$, (where n_i is the ionic charge of the complex) are approximated by the relations

$$[A_j^{n_j}] = \gamma_j m_{bj} \tag{1}$$

and

$$[C_i^{n_i}] = \gamma_i m_{ci}, \tag{2}$$

where γ_j and γ_i are activity coefficients and m_{bj} and m_{ci} are mass concentrations of basis species and complexes, respectively, in moles per dm^3 of aqueous phase. Activity coefficients are approximated using a modification of the Davies equation given by Stumm and Morgan (1970, p. 83, footnote),

$$\log_{10} \gamma_h = -\frac{1}{2} n_h^2 \left(\frac{\sqrt{I}}{1+\sqrt{I}} - 0.3I \right), \tag{3}$$

where subscript h represents either i or j. I is the ionic strength defined by

$$I = \frac{1}{2} \left(\sum_{j=1}^{N_b} n_j^2 m_{bj} + \sum_{i=1}^{N_c} n_i^2 m_{ci} \right), \tag{4}$$

and N_C is the number of complexes in the aqueous phase. The activities of water and of uncharged complexes are assumed to be unity.

Chemical reactions for the formation of complexes $C_i^{n_i}$ and precipitates G_k from basis species $A_j^{n_j}$ are written

$$\sum_{j=1}^{N_b} a_{ij} A_j^{n_j} \rightleftarrows C_i^{n_i} \qquad \text{R1}$$

and

$$\sum_{j=1}^{N_b} s_{kj} A_j^{n_j} \rightleftarrows G_k, \qquad \text{R2}$$

where a_{ij} and s_{kj} are stoichiometric reaction coefficients, which are zero for basis species that do not participate in a given reaction. Under the assumption of chemical equilibrium the mass action relation for the formation of a complex is then

$$K_i = \frac{[C_i^{n_i}]}{\prod_{j=1}^{N_b} [A_j^{n_j}]^{a_{ij}}}, \tag{5}$$

where K_i is the thermodynamic equilibrium constant. Similarly,

the mass action relation for the dissolution of a precipitate is

$$K_k = \prod_{j=1}^{N_b} [A_j^{n_j}]^{a_{kj}}, \tag{6}$$

where K_k is the thermodynamic solubility product of the solid phase G_k. Activities of solid phases are assumed to be unity.

Interphase mass transfer of basis species and charged complexes by cation exchange takes place by reactions of the type

$$n_2 B_1^{n_1}(aq) + n_1 \overline{B}_2 \rightleftarrows n_2 \overline{B}_1 + n_1 B_2^{n_2}(aq), \tag{R3}$$

where $B_i^{n_i}(aq)$ denotes a positively charged species (basis or complex) in the aqueous phase and $\overline{B}_i$ denotes the sorbed component. Assuming chemical equilibrium, the mass action relation for this reaction is

$$K_{eq} = \frac{[\overline{B}_1]^{n_2}[B_2^{n_2}]^{n_1}}{[\overline{B}_2]^{n_1}[B_1^{n_1}]^{n_2}}. \tag{7}$$

Activities of sorbed components are approximated by assuming that they can be described by an ideal-solution model in which

$$[\overline{B}_j] = \frac{\overline{m}_j}{\overline{m}_T}, \tag{8}$$

where $\overline{m}_j$ is the concentration of species j in the sorbed phase and $\overline{m}_T$ is the total concentration in the sorbed phase. $\overline{m}_T$ is given by

$$\overline{m}_T = \sum_{j=1}^{\overline{N}_b} \overline{m}_{bj} + \sum_{i=1}^{\overline{N}_c} \overline{m}_{ci}, \tag{9}$$

where $\overline{N}_b$ is the number of sorbed basis species and $\overline{N}_c$ is the number of sorbed complexes. The concentrations of sorbed components are expressed as moles per dm^3 of the aqueous phase. The number of surface sites available for cation exchange is a constant characteristic of the sorbent, and is measured by the cation exchange capacity (CEC). In the CHEMTRN code, the number of equivalents of available sites per dm^3 of aqueous phase, N_s, is assumed constant and is given by

$$N_s = \sum_{j=1}^{\overline{N}_b} n_j \overline{m}_{bj} + \sum_{i=1}^{\overline{N}_c} n_i \overline{m}_{ci}. \tag{10}$$

The treatment of interphase mass transfer by surface complexation used in CHEMTRN is based on the electrical double layer site-binding model developed by Davis, James, and Leckie (1978). In this case, the surface electrical charge is not necessarily conserved and both cations and anions can be sorbed. Thus a neutral surface site denoted by SOH can dissociate to give a negatively charged site SO^-:

$$SOH \rightleftarrows SO^- + H_s^+, \qquad \text{R4}$$

where the subscript s denotes that the hydrogen ion is located at the so-called "surface plane". SOH can react with H^+ at the surface plane to give a positively charged surface complex SOH_2^+:

$$SOH + H_s^+ \rightleftarrows SOH_2^+. \qquad \text{R5}$$

This surface complex can react with an anion such as Cl^- to form a formally neutral surface complex:

$$SOH_2^+ + Cl_\beta^- \rightleftarrows SOH_2^+Cl^- \qquad \text{R6}$$

The subscript β denotes the plane where the chloride ion is located when it forms a complex with the surface site. Finally, a SOH site can react with a bivalent cation such as Sr^{2+} to form a charged surface complex:

$$SOH + Sr_\beta^{2+} \rightleftarrows SO^-Sr^{2+} + H^+. \qquad \text{R7}$$

The CHEMTRN code treats only those surface complexation reactions involving a single site; reactions involving two or more sites must be simulated by the ion exchange algorithm.

Thermodynamic equilibrium constants for reactions R4--R7 are formed in the usual manner. Following the discussion by Davis, James, and Leckie (1978), the activity of a species B^n in the s or β plane is related to its activity in the bulk solution by

$$[B_p^n] = [B^n] \exp\left(-\frac{ne\psi_p}{kT}\right), \qquad (11)$$

where ψ_p is the change of electrical potential when the species moves from the bulk solution to the plane denoted by p, k is the Boltzmann constant, T is the absolute temperature, and e is the electronic charge.

Irreversible dissolution of a solid phase along the path of transport is treated in the following way. A stoichiometric equation is written for dissolution of one mole of the solid such that the reactants and products consist of the solid and basis species only. Given a rate of dissolution of the solid expressed

as moles per dm^3 of aqueous phase per unit time, the stoichiometric equation determines rates of production or consumption of each basis species. These rates are specified as part of the input data for each basis species, and are added or subtracted at each finite difference node during the solution procedure. It is noted that this method does not account for changes of dissolution rates caused by changes of aqueous phase composition.

5.1.2.2 Transport Equations

Basis species and complexes are transported by advection with velocity v and by hydrodynamic dispersion (mechanical dispersion plus molecular diffusion) with dispersion coefficient D. W_j, the total concentration of a component A_j in the aqueous phase, is defined by

$$W_j = m_{bj} + \sum_{i=1}^{N_c} a_{ij} m_{ci}, \tag{12}$$

and $\overline{W}_j$, the total concentration of component A_j in sorbed phases, is defined by

$$\overline{W}_j = \overline{m}_{bj} + \sum_{i=1}^{\overline{N}_c} a_{ij} \overline{m}_{ci}. \tag{13}$$

Then, if N_p precipitates are present, the mass balance for component A_j is expressed by

$$\left(\frac{\partial}{\partial t} + v\frac{\partial}{\partial x} - D\frac{\partial^2}{\partial x^2}\right) W_j = -\frac{\partial}{\partial t}\overline{W}_j - \frac{\partial}{\partial t}\sum_{k=1}^{N_p} s_{kj} m_{pk} + d_j, \tag{14}$$

where m_{pk} is the equivalent, aqueous-phase concentration of a compound removed by reversible precipitation (negative values of m_{pk} correspond to addition of the compound by reversible dissolution) and d_j is the incremental concentration of A_j added per unit time by irreversible dissolution of a solid phase. The number of unknowns equals $N_b + \overline{N}_b + N_c + \overline{N}_c + N_p$. There are N_b transport equations having the form of (14). The mass action relations, (5), provide N_c equations. N_p equations are provided by (6). There are $\overline{N}_b + \overline{N}_c - 1$ mass action relations for ion exchange or surface complexation having the form of (7), and one site-constraint equation, (10). The activity coefficients are given by (3) and (4), and $\overline{m}_T$ is given by (9). These equations are sufficient to determine the m_{bj}, $\overline{m}_{bj}$, m_{ci}, $\overline{m}_{ci}$, and m_{pk}.

5.1.2.3 Boundary Conditions

The CHEMTRN simulator accepts either constant-flux or constant-concentration boundary conditions. Semi-infinite systems are simulated by imposing outer boundary conditions at a distance large enough that they do not noticeably perturb solutions computed at inner nodes, in the region of interest.

5.1.2.4 Method of Solution

The transport equations (14) are discretized in space and time to give a set of finite difference equations which are solved simultaneously with the algebraic equations given in the preceding sections. The Newton-Raphson method is used for the solution, and special techniques are used for precipitation and the treatment of pH changes. A detailed description of the method of solution has been given by Miller and Benson (1983).

5.1.3 APPLICATIONS AND RESULTS

In this section we discuss applications of the CHEMTRN simulator to an investigation of the validity of the constant-k_D concept, to a field experiment in which the principal chemical process acting during transport was multicomponent ion exchange, and to simulations of laboratory experiments on the sorption of neptunium on basalt surfaces. Simulations of systems involving reversible precipitation and surface complexation have been discussed by Miller (1983) and by Miller and Benson (1983).

5.1.3.1 Validity of the Constant-k_D Concept

Transport of contaminants in ground water often has been simulated under the assumption that the solid/fluid distribution coefficient (k_D) for a chemical species is constant throughout its transport path. Increasingly, this assumption is being questioned (e.g., Reardon, 1981).

It can be shown that the k_D of an exchanging ion depends on the exchange capacity of the sorbent, the concentration(s) of other exchanging ion(s), and the ionic strength of the aqueous phase (e.g., Miller and Benson, 1983). If these quantities change during transport, then it must be expected that the k_D will change also. This situation will occur when the concentrations of exchanging ions in the aqueous phase are comparable. On the other hand, if the concentration of the ion of interest is very small relative both to the concentration of the supporting electrolyte and the cation exchange capacity, then the k_D for this ion will be independent of its concentration.

Figure 1 shows the results of simulations by CHEMTRN when competition for sites on the sorbent affects sorption of cations. The aqueous phase initially contained 10^{-4} M Na^+, 10^{-5} M Ca^{2+}, 10^{-8}M Sr^{2+}, 4.5 x 10^{-5} M CO_3^{2-}, and 3 x 10^{-5} M Cl^-, where M has the units moles per dm^3. At the inner boundary, the concentration of Sr^{2+} was maintained slightly in excess of 10^{-5} M. The k_D calculated for Sr^{2+} was 5000 initially and 2000 at the inner boundary. For comparison with the CHEMTRN results, Figure 1 also shows the results obtained when the sorption of Sr^{2+} is assumed to follow a constant-k_D model with k_D equal to 2000. It is seen that the latter model predicts a slower rate of movement of Sr^{2+} than is predicted when competition for sorptive sites is accounted for.

In some situations the constant-k_D model can give acceptable results even though the value of k_D varies during transport. Figure 2 shows concentrations of Sr^{2+} computed by CHEMTRN for the system used above, but with a much smaller concentration of Ca^{2+}. In this case the Sr^{2+} exchanges primarily with Na^+, and the amount of the latter that is displaced from the sorbent by ion exchange does not change the composition of the aqueous phase enough to affect the value of k_D significantly. Results computed using a constant value of k_D equal to 2000 agree closely with the results computed by CHEMTRN.

In general, the results of simulations of transport with multicomponent ion exchange and surface complexation done with CHEMTRN show the following. If the major ion content of ground water remains unaltered during transport and if the sorbed concentration of a trace ion is small relative to the exchange capacity of the sorbent, then a constant-k_D model could be used to simulate the transport of the trace ion. However, the k_D value used would have to be measured or calculated for exactly the conditions postulated to exist in the chemical transport system. On the other hand, if the concentration of the ion of interest is comparable to the concentrations of major, exchanging ions or if the number of sorptive sites is a function of pH, then a constant-k_D model is not adequate to simulate the chemical transport process.

5.1.3.2 Simulation of a Field Experiment

CHEMTRN was used to simulate a field experiment in which treated municipal waste water was injected into a shallow aquifer in the Palo Alto (California) Baylands region. During the period of injection, water samples were collected at several observation wells and were analyzed for their chemical composition. Also, tests were performed to evaluate physical characteristics of the aquifer. The test has been described and results of measurements have been given by Valocchi, Street, and Roberts (1981).

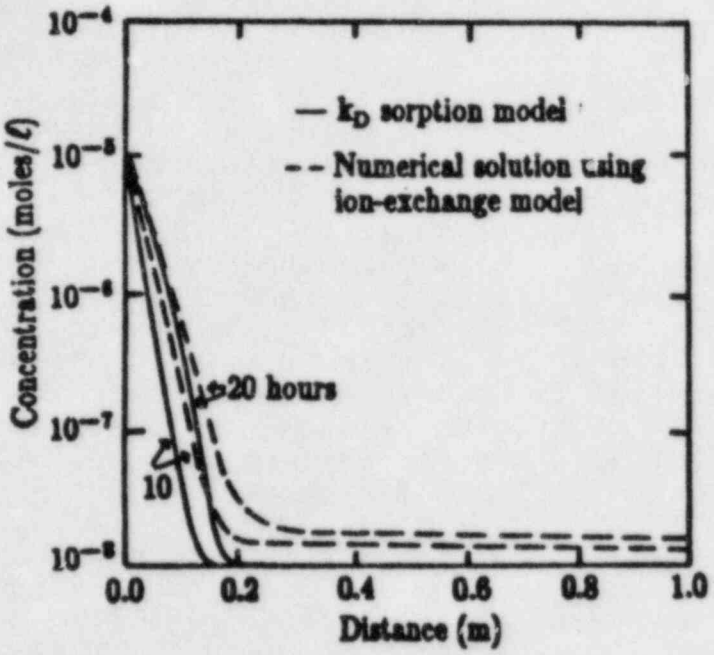

Fig. 1: Comparison of ion-exchange model with a constant-k_D sorption model when changes in background electrolyte concentrations are important.

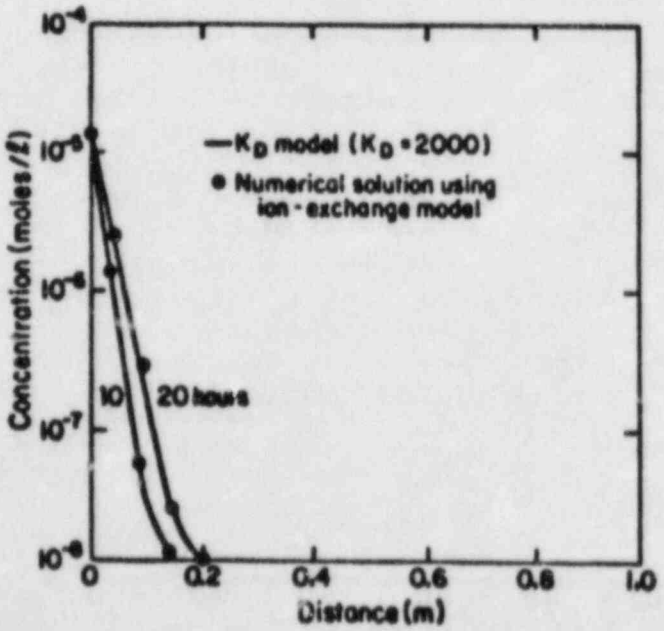

Fig. 2: Comparison of ion-exchange model with a constant-k_D sorption model when changes in background electrolyte concentrations are not important.

The initial composition of ground water at observation well S23, 16 m from the injection well, was 1990 mg/dm^3 Na^+, 444 mg/dm^3 Ca^{2+}, 436 mg/dm^3 Mg^{2+}, and 5700 mg/dm^3 Cl^-. The waste water was injected at an average rate of 21 m^3/hour and had an average composition of 216 mg/dm^3 Na^+, 85 mg/dm^3 Ca^{2+}, 12 mg/dm^3 Mg^{2+}, and 320 mg/dm^3 Cl^-. The aquifer thickness was 2 m, the density of the solid matrix was 2500 kg/m^3, the cation exchange capacity was 0.1 equivalent/kg, and the porosity was 0.25. Measured selectivity coefficients (expressed in the mole fraction convention used in CHEMTRN) were 1.0 for Ca^{2+} replacing Na^+ and 0.65 for Mg^{2+} replacing Na^+. (Valocchi et al., 1981)

A CHEMTRN simulation was done for the composition of the fluid arriving at well S23 as a function of time since the start of injection. The chemical mechanism simulated was ion exchange between Na^+, Ca^{2+}, and Mg^{2+}. Radial flow was assumed with the fluid velocity v at a distance r from the injection well proportional to $Q/(2\pi b\phi r)$, where Q is the rate of injection, b is the aquifer thickness, and ϕ is the porosity. The dispersion coefficient used was approximately 1.3v; about 20 percent of this value is attributable to numerical dispersion.

Figures 3-6 are comparisons between measured and simulated histories of concentrations of Ca^{2+} and Mg^{2+} at well S23. In each figure the solid curves are the "best fit" simulations, and the discrete points are the measured values. The dashed curves are results of simulations using values of fluid velocity, density of exchange sites in units of sites/dm^3 of aqueous phase, and selectivity coefficients at the extrema of their ranges of uncertainty. These ranges were estimated from uncertainties in the reported data. Examination of Figures 3-6 shows that the "best fit" simulations provide very good matches to the measured concentration histories and are within the ranges of uncertainty of the parameters used.

5.1.3.3 Simulation of a Laboratory Experiment

Experiments with laboratory analogs of the BWIP site are being conducted at Argonne National Laboratory (Seitz, Gerding, Vandegrift, Bowers, and Fried, 1982). In an experiment, synthetic ground water is pumped through basalt chips and bentonite, contacts a glass frit containing radionuclide tracers which simulates a glass waste form, flows through more bentonite, and then flows through the fissure in a split basalt core before leaving the apparatus. In several experiments the basalt core was removed after periods of time varying from 90 to 150 days, and the surface of the fissure was scanned radiometrically to detect residual ^{237}Np. The results of three such measurements are shown in Figure 7.

The data in Figure 7 show, generally, a plateau region near

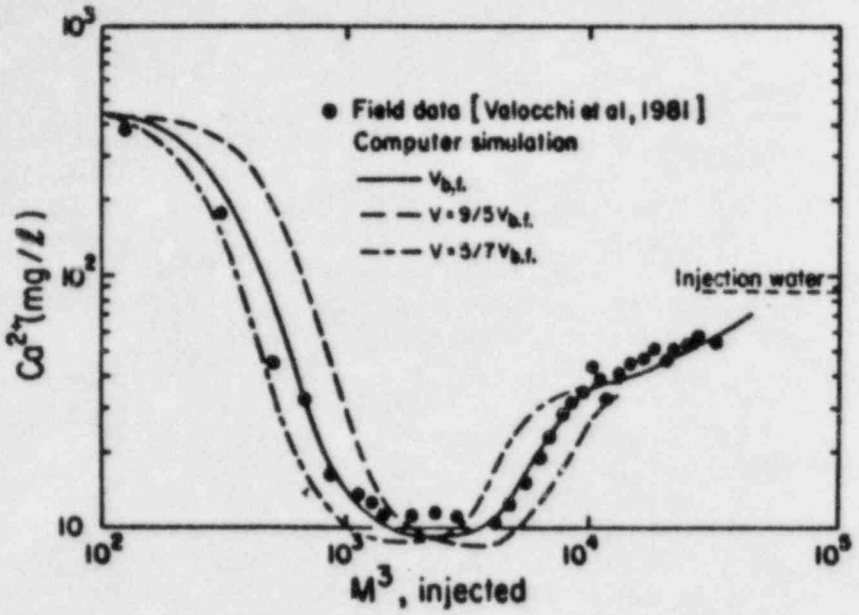

Fig. 3: Effects on numerical simulations of varying fluid velocity about the best-fit value ($v_{b.f.}$).

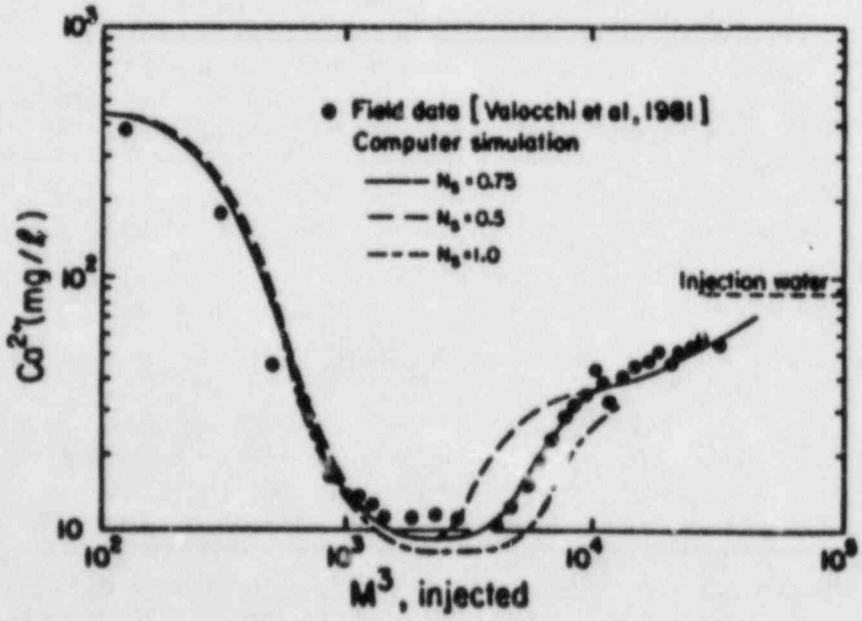

Fig. 4: Effects on numerical simulations of varying cation exchange capacity about the best-fit value (N_s=0.75).

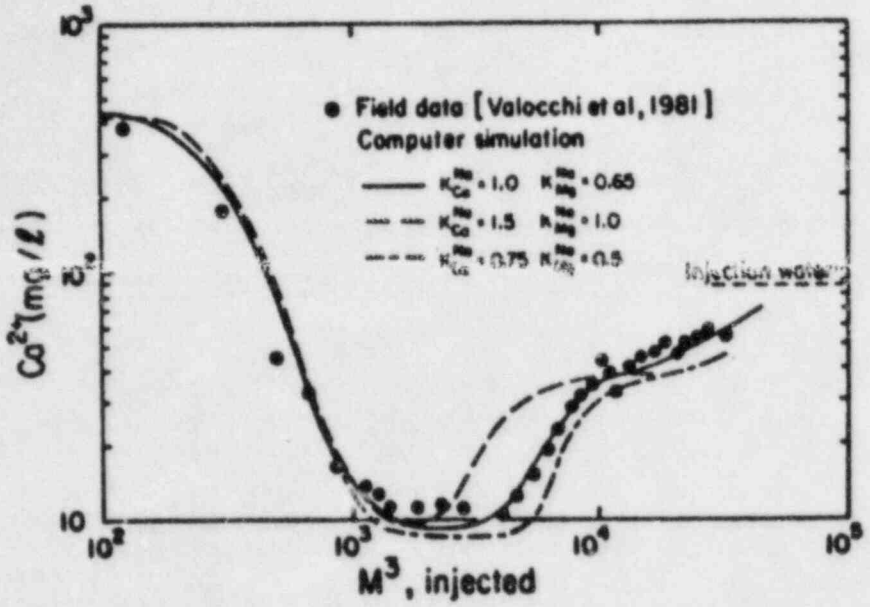

Fig. 5: Effects on numerical simulations of varying equilibrium exchange constants about the best-fit values (K_{Ca}^{Na}=1.0, K_{Mg}^{Na}=0.65).

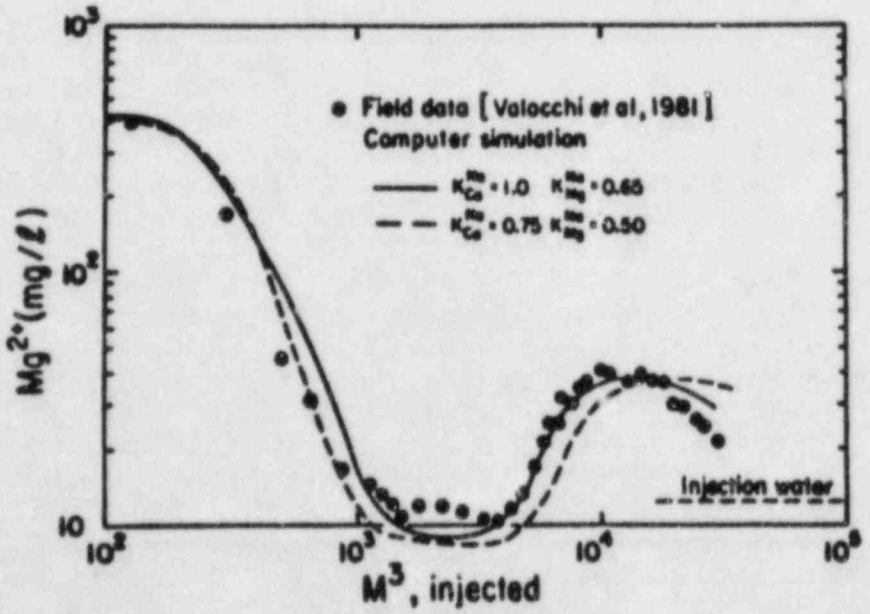

Fig. 6: Effect on numerical simulations of varying equilibrium exchange constants from the best-fit values (K_{Ca}^{Na}=1.0, K_{Mg}^{Na}=0.65).

the inlet to the rock face. (Fluctuations in this region are attributed to variations of the flow rates.) The plateau merges into a diffuse leading edge as distance from the inlet increases. These sorbed-phase distributions are similar to distributions resulting from ion-exchange equilibria between previously sorbed cations and a different, incoming cation (in this case a positively charged neptunium species) being transported in the fluid phase. Therefore, we attempted to simulate the experimental data using this mechanism of transport with interphase mass transfer. It should be noted, however, that the chemical mechanisms actually operating to produce the distributions observed in these experiments have not been identified.

Details of the analog experiments, including the composition of the simulated ground water, have been given by Seitz et al. (1982). The total concentration of neptunium entering the system was approximately 1.5×10^{-8} M. The total carbonate content of the ground water was 1.26×10^{-3} M, the concentration of Na^+ was 1.36×10^{-2} M, and the pH was 10. Published thermodynamic data (Benson and Teague, 1980; Nitsche and Edelstein, 1982) indicate that the neptunium species present under these conditions are the oxo cation of neptunium(V), NpO_2^+, and its complexes NpO_2OH^0, $NpO_2HCO_3^0$, $NpO_2CO_3^-$, and $NpO_2(CO_3)^{5-}$, the last being the dominant species. Preliminary calculations of distributions of species by the CHEMTRN code showed that ion exchange reactions of Ca^{2+} and Mg^{2+} and complexation with SO_4^{2-} and F^- were not significant influences in the simulations. The transport of neptunium with sorption on the rock surface was then simulated by ion exchange between NpO_2^+ and Na^+ and complexation of NpO_2^+ in the aqueous phase to form the tris(carbonato) complex. The formation constant of this complex has been reported to be 2×10^{16} M^{-3} (Nitsche and Edelstein, 1982). The cation exchange capacity of the basalt was assumed to be 0.02 equivalent/kg, as reported by Barney (1980) for Umtanum basalt. Equilibria between CO_3^{2-}, HCO_3^-, and $H_2CO_3^0$ were included in the simulations.

Unknown quantities were the equilibrium constant for the ion-exchange reaction between NpO_2^+ and Na^+, and the linear velocity of the fluid phase through the fissure in the basalt core. We assumed a velocity of 0.088 m/day (32 m/year), based on data reported by Seitz et al. (1982), for the second analog experiment. This experiment was terminated at 150 days, and from the data in Figure 7 we estimated that in this time the midpoint of the leading edge of the sorbed neptunium distribution had migrated 0.072 m from the inlet. Under the assumption of constant retardation (which is approximately valid under the conditions of this part of the analog experiments), we calculated a retardation factor of 180 for neptunium. When the complexation of NpO_2^+ in the aqueous phase is accounted for, this value of retardation requires that the equilibrium constant for $NpO_2^+(aq)$ replacing sorbed Na^+ by ion exchange be equal to 7.2×10^{11}.

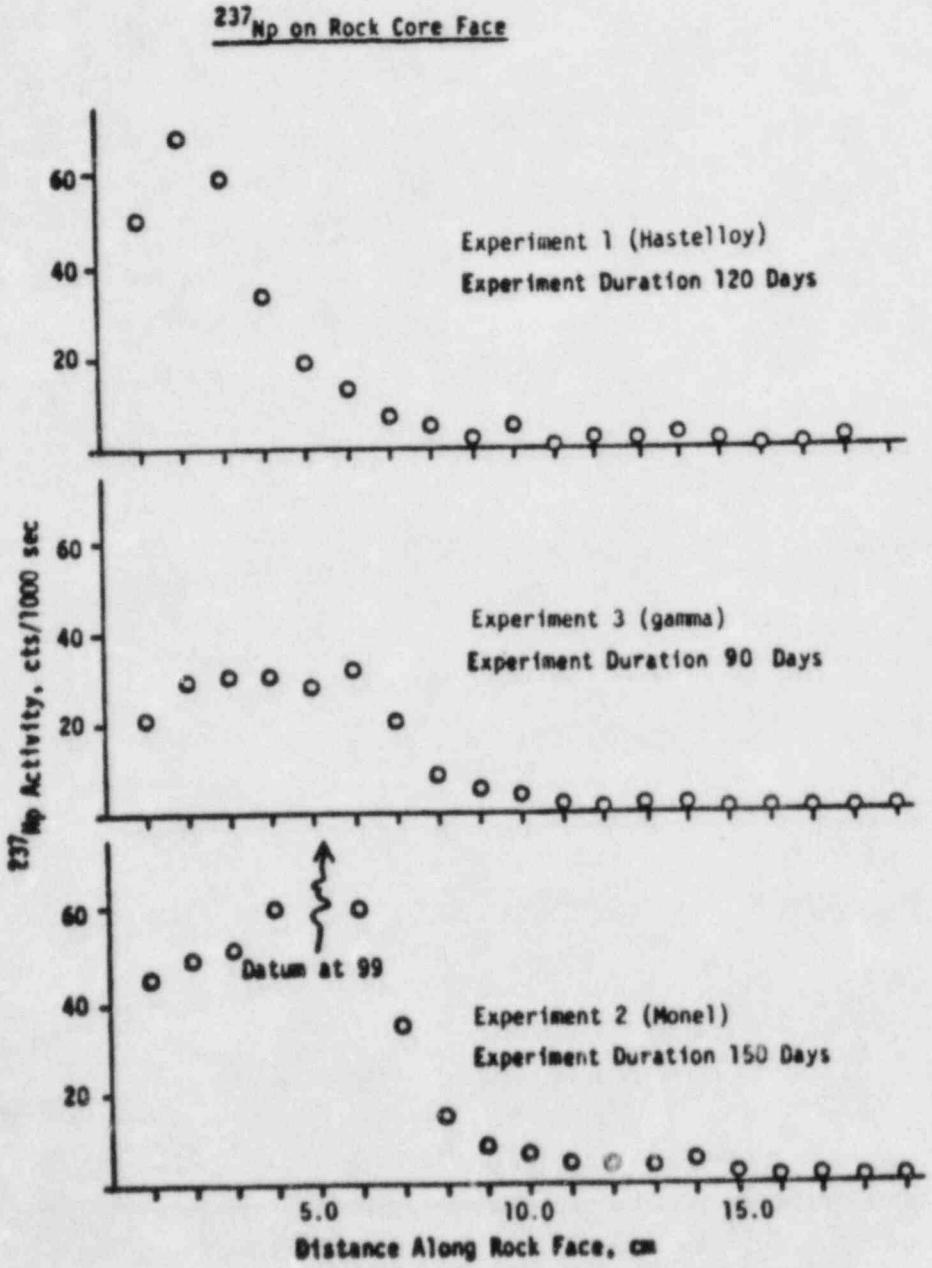

Fig. 7: Neptunium Distribution on the Surface of Split Basalt Cores from Three Analog Experiments. (Reproduced from Seitz et al., 1982)

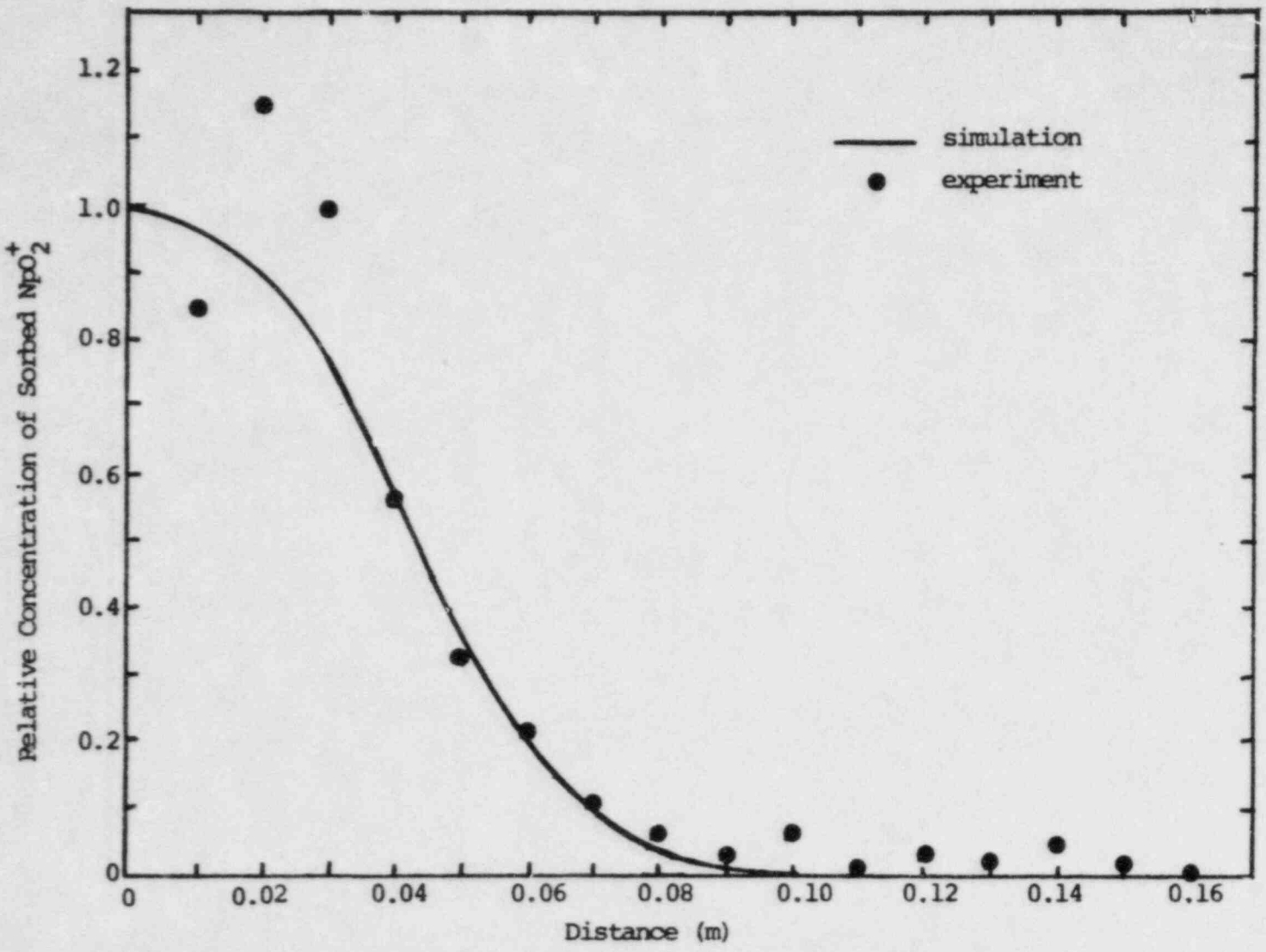

Fig. 8: Concentration of sorbed NpO_2^+ relative to sorbed concentration at inlet for Analog Experiment 1 at 120 days and fluid velocity of 0.066 m/day.

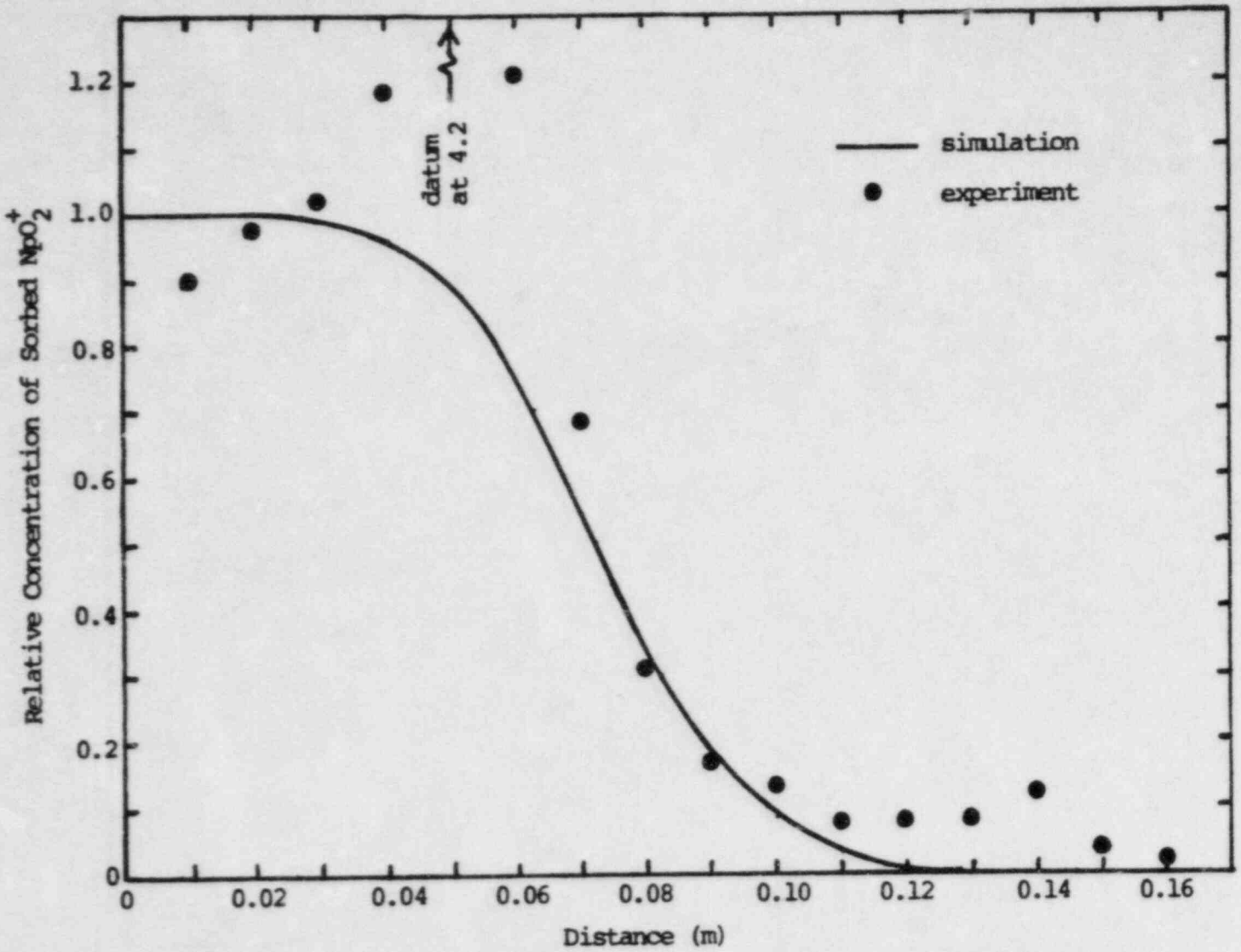

Fig. 9: Concentration of sorbed NpO_2^+ relative to sorbed concentration at inlet for Analog Experiment 2 at 150 days and fluid velocity of 0.088 m/day

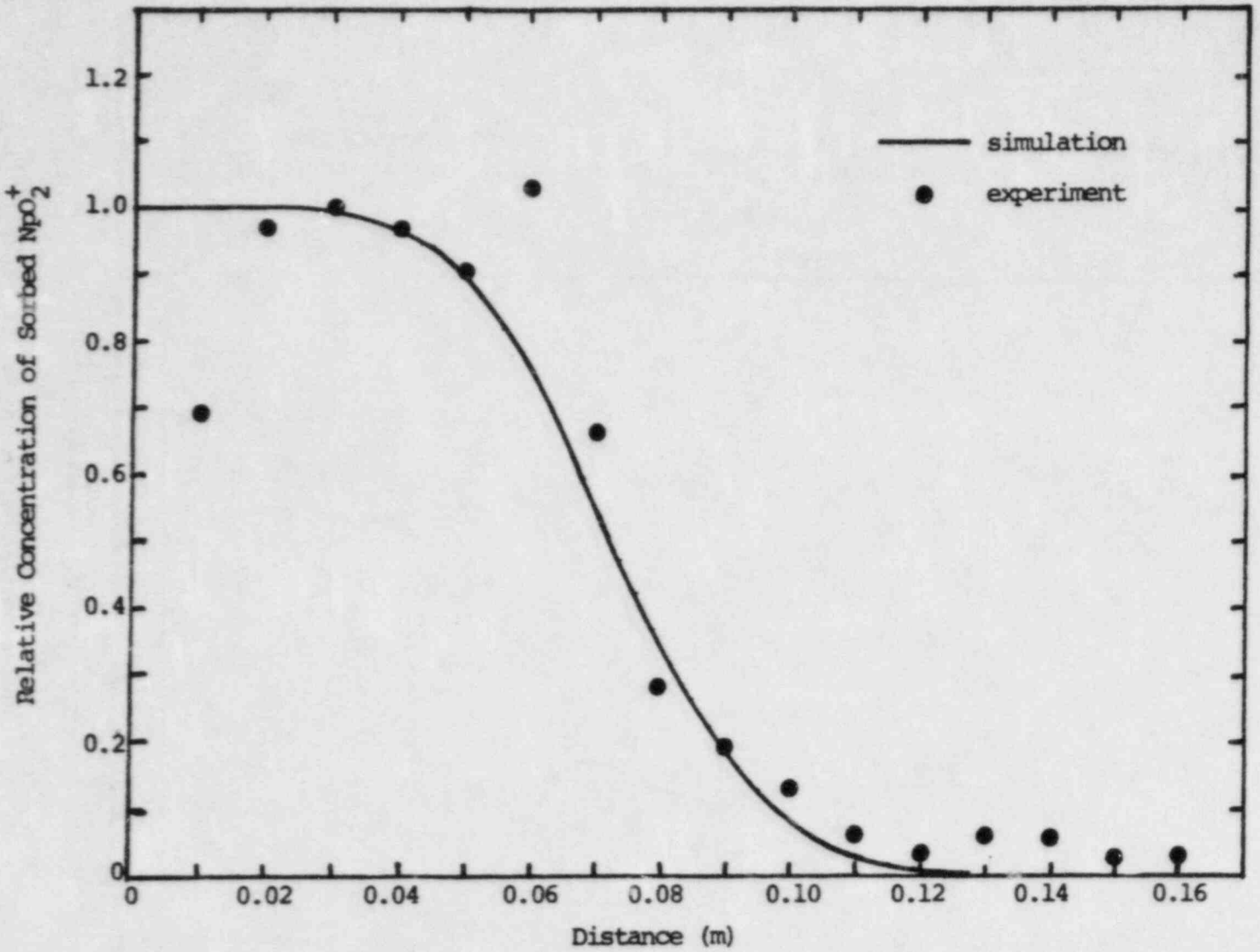

Fig. 10: Concentration of sorbed NpO_2^+ relative to sorbed concentration at inlet for Analog Experiment 3 at 90 days and fluid velocity of 0.153 m/day.

This value was used in all simulations of the analog experiments.

The results of the simulations are shown in Figures 8--10, where relative concentrations of sorbed neptunium are plotted against distance from the inlet at the times of termination of each experiment. To facilitate comparison with the experimental data, computed concentrations of sorbed NpO_2^+ are expressed as ratios to the concentrations at the inlet, and similar normalizations were done to the experimental data. (Estimated inlet "concentrations" for data points in experiments 1, 2, and 3 were 62, 52, and 32 counts per 1000 seconds, respectively.) The computed distributions correspond to linear flow velocities of 0.066, 0.088, and 0.153 m/day and diffusion coefficients of 1.4×10^{-6}, 1.2×10^{-6}, and 1.9×10^{-6} m^2/day for experiments 1, 2, and 3. Agreement between simulations and experimental data is reasonably good at the leading edges of the distributions.

It must be noted that considerable uncertainty exists about the chemical mechanisms producing the observed distributions. In the numerical simulations, two critical items of information -- the velocity of the fluid through the fissure and the equilibrium constant for the assumed ion-exchange reaction -- were not known and were adjusted to make the simulations match the data. Independent evaluation of these quantities would permit evaluation of the validity of the mechanisms assumed in these simulations. We cannot eliminate the possibility that other chemical mechanisms such as nonequilibrium reactions, surface complexation of anionic species, precipitation, and heterogeneous electron-transfer reactions may have produced or contributed to the observed distributions. Until the correct mechanisms have been identified unequivocally by appropriate experiments, numerical simulations based on plausible, but hypothetical, mechanisms must be regarded as speculative at best. Furthermore, given a correct mechanism, numerical simulations will remain speculative until reliable values of all chemical and physical parameters associated with the mechanism have been obtained experimentally.

5.1.4 CONCLUSIONS

The results of simulations with several chemical algorithms in the simulator CHEMTRN, presented here and also previously by Miller (1983) and Miller and Benson (1983), identify a minimum set of requirements that should be imposed on geochemical transport codes considered for use as part of an assessment of the performance of a nuclear waste repository. Specifically, the assumption of a constant distribution coefficient (k_D) for interphase mass transfer cannot be relied upon to adequately account for changes of chemical composition of major, minor, or trace chemical components of ground water in the vicinity of a repository. A higher level of chemical complexity is required.

This includes using thermodynamic equilibrium constants for all chemical reactions, using nonideality corrections via activity coefficients, accounting for changes in ionic strength, accounting for finite exchange or sorptive capacity of the solid phase and competition for sorptive sites among aqueous species, accounting for complexation of aqueous species, the ability to compute variations of pH, the ability to account for precipitation/dissolution equilibria of secondary solid phases, and the ability to simulate both equilibrium and nonequilibrium processes.

In addition, systems with variable oxidation potential require algorithms for electron-transfer reactions, and significant precipitation or dissolution will require the ability to simulate changes of flow velocity caused by decreases or increases of permeability. These effects have not been included in the present version of the CHEMTRN simulator, but are regarded as necessary components of an adequate chemical transport code.

These requirements for adequacy in numerical simulations of geochemical transport imply corresponding needs for chemical, thermodynamic, kinetic, and mineralogical data to be used as input to chemical algorithms. These data include identities of reaction mechanisms and the species participating in them, solubilities of solid phases and identities of the species in equilibrium with them, and thermodynamic equilibrium constants for both homogeneous and heterogeneous chemical reactions involving species that are influential on migration of nuclear waste. Unfortunately, practically all of the measurements of k_D values made over the past fifteen to twenty years are useless as input to thermodynamically based chemical algorithms.

5.1.5 RECOMMENDATIONS

The following recommendations are based on the findings and conclusions of this research effort, and are directed to the objective of improving the ability to assess long-term performance of nuclear waste repositories.

Use of the k_D concept in models of waste transport should be abandoned. This concept has little, if any, chemical and thermodynamic contents and can produce misleading results if applied uncritically. It should be replaced by thermodynamically based chemical algorithms that describe experimentally identified chemical mechanisms.

Experimental programs for measurement of k_D values should be redirected toward identification of chemical mechanisms influential in waste transport, identification of aqueous and sorbed species involved in the

mechanisms, and measurement of thermodynamic and chemical-kinetic data associated with species and mechanisms. These efforts should include characterization of solid phases active in chemical reactions during waste transport. Many of these important data are currently lacking, but are required for development and application of a capability to predict repository performance.

Conceptual and numerical models of reactive chemical transport should be extended to include collateral processes (hydrothermal, thermochemical, thermomechanical) that are coupled both mathematically and thermodynamically to chemical reactions, fluid flow, and solute transport. Only in this way can a comprehensive description of the entire repository system and its evolution in time and space be developed.

Our research during the past several years has made us keenly aware of the necessity for close interaction between those investigators making measurements in the field or laboratory, and those attempting to develop the ability to predict the behavior of the complex chemical systems anticipated to exist at a nuclear waste repository. Each group can, and should, provide guidance and input to the other. Communication between the two groups and coordination of their activities is vital to the successful development of an ability to reliably assess the performance of a repository.

5.1.6 PLANNED RESEARCH

Future research in this program will include extension of chemical algorithms to include nonequilibrium reversible and irreversible reactions and electron-transfer reactions. Chemical algorithms will be combined with broadly based thermohydromechanical simulators and the range of phenomena covered will be extended to include thermodynamic coupling among transport processes. These efforts will have the objective of providing more comprehensive predictors of repository evolution and performance.

5.1.7 ACKNOWLEDGEMENT

We are grateful to Drs. Martin Seitz and George Vandegrift of Argonne National Laboratory for providing us with data and guidance relevant to the laboratory analog experiments.

5.1.8 REFERENCES

Ahlstrom, S. W., Foote, H. P., Arnett, R. C., Cole, C. R., and Serne, R. J., 1977. Multicomponent Mass Transport Model, Battelle Pacific Northwest Laboratories report BNWL-2127.

Barney, G. S., 1980. Sorption studies, in Smith, M. J., et al., Engineered Barrier Development for a Nuclear Waste Repository in Basalt: An Integration of Current Knowledge, Rockwell Hanford Operations report RHO-BWI-ST-7, p. 2-329 - 2-331.

Benson, L. V., and Teague, L. S., 1980. A Tabulation of Thermodynamic Data for Chemical Reactions Involving 58 Elements Common to Radioactive Waste Package Systems, Lawrence Berkeley Laboratory report LBL-11448, 97 p.

Davis, J. A., James, R. O., and Leckie, J. O., 1978. Surface ionization and complexation at the oxide/water interface I. computation of electrical double layer properties in simple electrolytes, Journal of Colloid and Interface Science, vol. 53, p. 480-499.

Grove, D. B., and Wood, W. W., 1979. Prediction and field verification of subsurface-water quality changes during artificial recharge, Lubbock, Texas, Ground Water, vol. 17, p. 250.

Holly, D. E., and Fenske, P. R., 1968. Transport of dissolved chemical contaminants in ground-water systems, in Eckel, E. B., ed., Nevada Test Site, Memoir 110, Geological Society of America, p. 171-183.

Miller, C. W., 1983. Toward a comprehensive model of chemical transport in porous media, Materials Research Society Symposia Proceedings, vol. 15, p. 481-488.

Miller, C. W., and Benson, L. V., 1983. Simulation of solute transport in a chemically reactive heterogeneous system: model development and application, Water Resources Research, vol. 19, p. 381-391.

Miller, C. W., Benson, L. V., and Carnahan, C. L., 1982. Verification and improvement of predictive models for radionuclide migration, in Geochemical Assessment of Nuclear Waste Isolation, Report of Activities during Fiscal Year 1981 to the Nuclear Regulatory Commission, Lawrence Berkeley Laboratory report LBID-429 (Revised), p. 128-175.

Nitsche, H., and Edelstein, N., 1982. Formation Constants for the NpO_2^+-Carbonate System, Lawrence Berkeley Laboratory

report LBL-14344, 8 p.

Reardon, E. J., 1981. K_d's -- can they be used to describe reversible ion sorption reactions in contaminant migration?, Ground Water, vol. 19, p. 279-286.

Routson, R. C., and Serne, R. J., 1972. One-Dimensional Model of the Movement of Trace Radioactive Solute through Soil Columns: the Percol Model, Battelle Pacific Northwest Laboratories report BNWL-1918.

Rubin, J., and James, R. V., 1973. Dispersion-affected transport of reacting solutes in saturated porous media: Galerkin method applied to equilibrium-controlled exchange in unidirectional steady water flow, Water Resources Research, vol. 9, p. 1332-1356.

Seitz, M., Gerding, T., Vandegrift, G., Bowers, D., and Fried, S., 1982. Laboratory analog program, in Steindler, M. J., et al., Fuel Cycle Programs Quarterly Progress Report, October-December 1982, Argonne National Laboratory.

Strickert, R., Friedman, A. M., and Fried, S., 1979. ARDISC (Argonne Dispersion Code): Computer Programs to Calculate the Distribution of Trace Element Migration in Partially Equilibrating Media, Argonne National Laboratory report ANL-79-25.

Stumm, W., and Morgan, J. J., 1970. Aquatic Chemistry, Wiley-Interscience, New York.

Valocchi, E. J., Street, R. L., and Roberts, P. V., 1981. Transport of ion-exchanging solutes in ground water: chromatographic theory and field simulation, Water Resources Research, vol. 17, p. 1517-1527.

5.2 WET AND DRY CYCLE LEACHING: ASPECTS OF RELEASES IN THE UNSATURATED ZONE

R. Dayal, D. G. Schweitzer and R. E. Davis
Brookhaven National Laboratory
Upton, NY 11973

ABSTRACT

The NRC criteria of containment and controlled release for a HLW repository have in the past been addressed by leaching and radionuclide release experiments that correspond to repository flooding or temporally independent saturation. Both high-level waste repository and low-level waste burial sites can be expected to experience unsaturated conditions. We have considered aspects of radionuclide release from low-level waste forms subjected to wet/dry cycles, simulating burial in the unsaturated zone. Some preliminary results of cesium and strontium release are presented, showing that the processes occurring during the unsaturated period of the wet/dry cycle can have a profound effect on the overall release of radionuclides, especially strontium. Significantly lower releases of Sr-85 were observed in comparison with Cs-137 from resin/cement waste forms subjected to cyclic wet/dry leach conditions. Cesium release when considered as a function of the actual immersion time (total length of the wet periods of wet/dry cycles) remains relatively constant, irrespective of the varying lengths of dry spans. The observed cesium release is also comparable to that based on an IAEA-type leach test, which represents continuously saturated leach conditions. In contrast, the strontium release is significantly lower and exhibits a systematic decrease with increasing length of dry period. The observed differences in their release behavior can be attributed to different mechanisms by which these radionuclides are mobilized and transported from the bulk matrix into the leachant. The results indicate further that IAEA-type leach tests give conservative estimates of the actual release observed under partially saturated conditions. This finding, together with the observed dependence of radionuclide release on the nature of the wet/dry cyclic leaching a waste form is subjected to, indicates that extreme variability can be expected in the rate and extent of solute formation (source term) under partially saturated conditions in the field.

5.2.1 Introduction

Radionuclide containment and controlled release for a high-level waste (HLW) repository or a low-level waste (LLW) burial site are determined, to a large extent, by the characteristics of the waste package. Among the rate-limiting components of the waste package, the waste form plays an important role in controlling radionuclide release. As a result, numerous studies

have focused on radionuclide release and leaching experiments on both HLW and LLW forms using the IAEA-type leach tests which correspond to a flooded repository or a temporally saturated condition at a LLW burial site. Although these studies have produced a wealth of data on waste form leaching under continuously saturated conditions, it is often difficult to apply such leach data to actual field burial conditions.

One of the important field conditions that has not been given much attention in leaching studies is the effect of alternate wet/dry cycles (cyclic saturated/unsaturated conditions) on radionuclide release. LLW burial sites and HLW buried in the unsaturated zone can be expected to experience such cyclic wet/dry leaching conditions, as characterized by the passage of wetting fronts of varying length and frequency. Other important rate-controlling factors are solubility limitations and the role of barriers such as sediment or crushed host rock on radionuclide release.

The main objective of this investigation is to develop a geochemical data base on solute formation in the unsaturated or partially saturated zone. The data base will aid the NRC in the licensing and regulation of low level waste disposal sites. Recognizing the limitations of the IAEA or ANS 16.1 test procedures and the potential significance of cyclic saturated/unsaturated leaching conditions, we recently initiated a research program to compare the leachabilities of LLW forms based on IAEA-type test and wet/dry cyclic test. Some preliminary leach data have also been generated, showing the effects of solubility constraints, leachant flow rate, and the presence of a sediment barrier on waste form leachability (Dayal, R., 1983a,b,c). Although this study is directly concerned with radionuclide release from LLW forms under field burial conditions, we believe that some of the geochemical processes identified as controlling radionuclide release are probably similar to those expected to operate in a HLW repository.

In this paper, we present the preliminary results of Cs-137 and Sr-85 release from low-level cation exchange resin/cement waste forms subjected to alternate wet/dry cycles, simulating unsaturated or partially saturated leaching conditions. Although preliminary in nature at this time, a discussion of the differences in the release behavior of Cs-137 and Sr-85 is presented. Of particular interest is strontium release behavior as a function of varying lengths of dry periods in the wet/dry cyclic leaching experiments.

5.2.2 Issues Addressed by This Research

1. Lack of a geochemical data base on solute formation in the unsaturated zone for modeling radionuclide transport at shallow land burial sites.

2. Lack of generic data for the standard ANS 16.1 leach test on the leaching characteristics of solidified waste forms during long term leaching and on the effective release mechanisms as affected by radionuclide type and the nature of wet/dry leaching conditions.

3. The limitations of leach data based on IAEA or ANS 16.1 test procedures which represent continuously saturated leaching conditions in predicting release under actual field burial conditions.

4. The need for data on the effects of cyclic saturated/unsaturated leaching conditions on radionuclide release from waste forms. How is radionuclide release affected by changing the frequency and length of the wet/dry cycles?

5. Lack of knowledge of the mechanisms by which different radionuclides are mobilized and transported in the bulk matrix of a waste form. Specifically, what geochemical processes occur during the unsaturated period and how do they control the overall release of radionuclides?

6. Uncertainty in the degree of conservatism in radionuclide release observed under continously saturated leach conditions (IAEA or ANS 16.1 test procedures) compared to cyclic wet/dry leaching conditions, characterizing passage of wetting fronts of varying length and frequency.

5.2.3 Experimental

The simulated waste form consisted of cation exchange resin (IRN-77), loaded with Cs-137 and Sr-85 as tracers, and solidified in Portland Type I cement. The test specimens were right cylinders with a nominal dimension of 5 x 10 (diameter x height, in cm). All test specimens were made in triplicate. A detailed description of the preparation of simulated resin waste and of the solidification procedure is given elsewhere (Dayal, R., 1983c; Morcos, N., 1982a).

The cyclic wet/dry leach testing of waste forms involved the following steps. Briefly, a test specimen was placed in a porous medium contained in a column. To minimize the sorption of leached radionuclides, an inert material [high density Polyethylene (PE) beads] was selected for porous medium. The specimen was surrounded on all sides by a 2-inch-thick layer of PE beads. Deionized water was used as a leachant, with the total volume of leachant being 10 times the exposed surface area of the specimen during the wet period. The various wet/dry cycles used in the leaching experiments are given in Table 1. The wet period of the total wet/dry experimental cycle is kept constant

at one day, while the dry period is varied from one day in Experiment B to six days in Experiment M. It should be noted that "dry" period does not mean that the waste form is indeed dry, free of water. In actuality, the waste form retains sufficient moisture from the preceding rinse cycle to remain wet. In an experimental sense, dry period simply refers to the period during which no water is added to the bead column. Wet and dry cycles correspond to unsaturated and saturated conditions of the medium surrounding the test specimen, although the waste form remains saturated during the entire length of a wet/dry cycle. All experiments were conducted at ambient room temperature. A detailed description of these experiments is given elsewhere (Morcos, N., 1982b).

Table 1. Experimental conditions for wet-dry cyclic leach testing of resin/cement waste forms.

Experiment Code	Leachant	Cyclic Period (Days)		
		Wet	Dry	Total
B	Deionized Water	1	1	2
D	Deionized Water	1	2	3
L	Deionized Water	1	4	5
M	Deionized Water	1	6	7

5.2.4 Results and Discussion

The cumulative fractional release (CFR) of radioactivity from a test specimen can be expressed as

$$CFR = \Sigma a_n / A_o$$

where Σa_n = total amount of radioactivity leached from the specimen in cumulative leach time and A_o = amount of radioactivity present initially in the specimen. The CFR plots display cumulative fractional releases of Cs-137 and Sr-85 as a function of total elapsed leach time (Figure 1).

A comparison of the CFR plots shown in Figure 1 indicates that the release behavior of strontium is significantly different from that of cesium. In addition, the overall strontium release in a given length of time is much lower. For example, only 7% of the initial amount of Sr present in the test specimen is released in Experiment B in a period of 175 days, whereas ~40% of Cs release is observed under identical experimental conditions and in the same length of time. Other Experiments (D, L, and M) also show relatively lower releases for Sr.

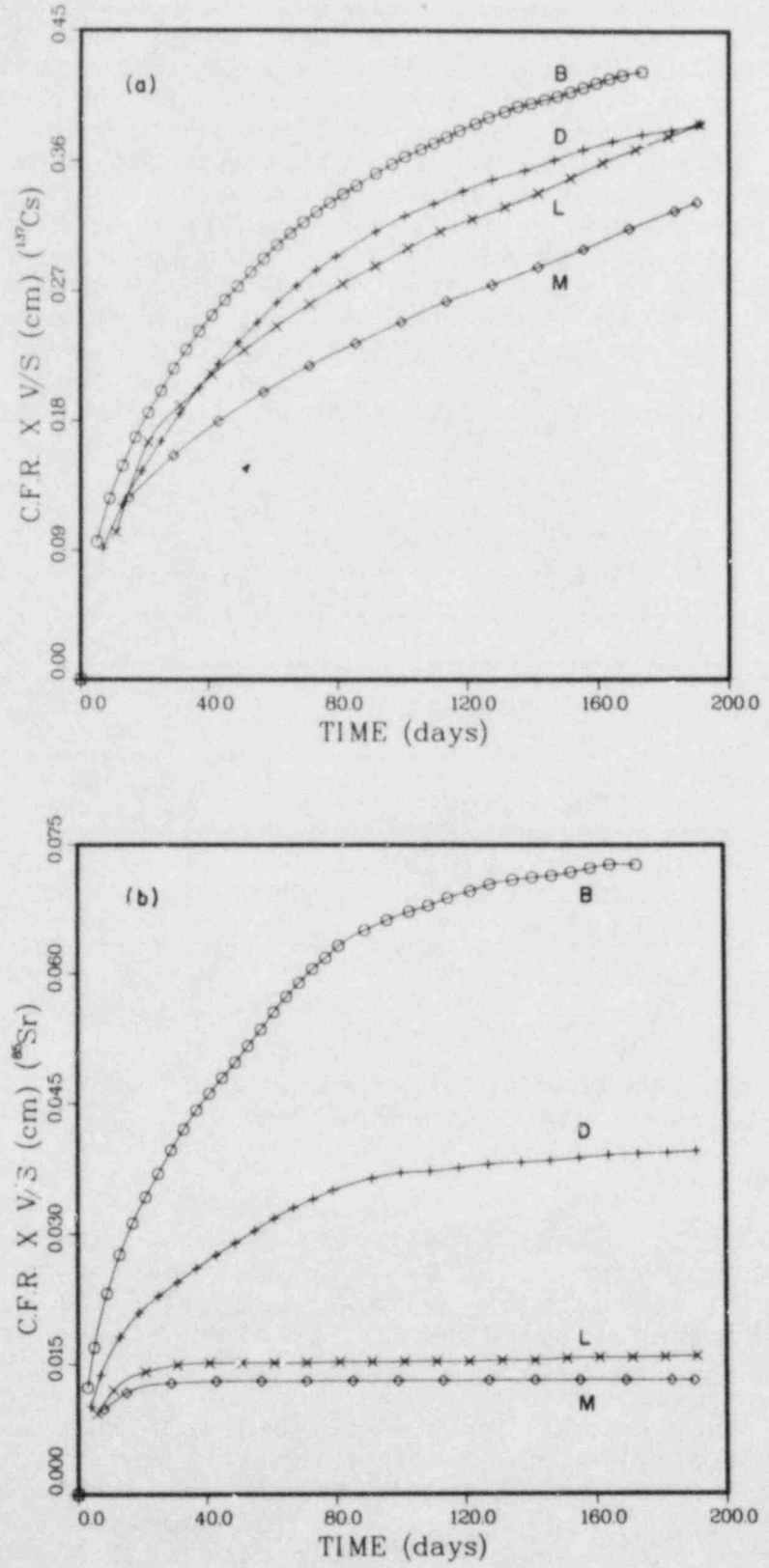

Figure 1. Normalized cumulative fractional releases of Cs-137 (a) and Sr-85, (b) as a function of total experimental time in Experiments B, D, L, and M.

The preferential release of Cs, relative to Sr, can be attributed to the differences in their degrees of retention in the cementitious matrix of the waste form. The retention and releases of Cs from ion-exchange resins are reasonably well understood processes. The Cs is readily released by water containing divalent and trivalent cations such as Ca^{2+} and Al^{3+} but it is not easily released in deionized water. This is also supported by observations in our laboratory where significantly greater releases of Cs are observed when both unsolidified and solidified resins are leached with synthetic groundwater as opposed to deionized water (Arora, H., 1983a; Morcos, N., 1982a). When resins containing Cs are mixed with cement, the water required to obtain an acceptable matrix quickly develops a pH of about 10-12 and contains relatively large concentrations of Ca^{2+} and Al^{3+}. Experiments performed at BNL (Morcos, N., 1982a; Colombo, P., 1979) in this research program show that appreciable amounts of Cs are relatively rapidly released from the resins and remain in the excess water required for the cement to set.

In general, it is known that Cs is not readily incorporated into cement mineral structures. Appreciable quantities of Cs are likely to be deposited in the pores and on cement mineral surfaces along with that remaining on the resin surfaces. It is also likely that different Cs compounds with different solubilities occur in the cement resin matrix.

The mobilization and transport of Cs into the leachant will consequently depend on several processes, viz., desorption from cement mineral surfaces, ion exchange from resins, possible ion exchange in cement minerals itself, differential solubilities of the different Cs compounds, etc. The diffusion and bulk movement of leachant through the matrix should, in turn, depend on the porosity, tortuosity, permeability and internal surface tension in the cement resin matrix. Clearly, the effective diffusivity obtained from the analyses of leach data through any diffusion model is a complex average of many poorly defined processes (Dayal, R., 1983c).

In the case of Sr, however, the release behavior is different. Several calcium and strontium minerals are known to exhibit diadochic substitution, where small amounts of strontium can substitute for calcium in calcium minerals. Therefore, during the curing process, it is likely that some removal of Sr from resin occurs by ion exchange and the released Sr is subsequently incorporated in hydrated calcium silicate or hydroxide phases present in the cementitious matrix. In such a case, the release of Sr from a cementitious resin waste form can be attributed primarily to three processes: ion-exchange of Sr^{2+} from resin, dissolution of the sparingly soluble calcium silicate and hydroxide minerals, and subsequent diffusion of the released Sr through the matrix. Consequently, one would expect the rate of Sr release into the leachant to be much lower than that of Cs.

The incremental fractional release (IFR) data on Cs and Sr in Experiments B, D, L, and M indicated significantly higher initial releases followed by gradually decreasing incremental releases. Further examination of these data suggested a high degree of scatter in the IFR values for the first two or three wet cycles. In contrast, relatively consistent IFR values were observed for most subsequent immersions, irrespective of the length of dry period of one to six days. Elevated radionuclide release during initial immersion periods may be attributed to a "washing-off" effect from surface related processes, not representative of the bulk matrix. The initially rapid surface-controlled release followed by diffusion-controlled release have been identified as principal release mechanisms for Cs-137 from cement waste forms (Dayal, R., 1983c; Godbee, H. W., 1980; Moore, J. G., 1977).

Figure 2 displays the CFR data for cesium and strontium for different immersion periods (total lengths of the wet cycles) plotted as a function of the length of dry cycle (the period during which the surrounding medium remains unsaturated) in each experiment. The initially high surface related releases have not been considered in the plots. Also presented in Figure 2 is the cesium release data, based on a modified IAEA test, which represents continuously saturated conditions. The CFR plot in Figure 2a shows that cesium release is governed by the actual immersion time rather than the total elapsed experimental time, indicating that cesium migration via diffusion in the bulk matrix is negligible during dry spans of up to six days. Compared to these release data, a comparable CFR value is observed for Cs based on the modified IAEA leach test. This comparison indicates further that Cs release is governed primarily by the length of the saturated period and that unsaturated periods of up to six days have no significant effect on Cs release. However, a comparison of Cs releases observed in total elapsed experimental periods (wet plus dry periods) in Experiments, B, D, L. and M with that observed based on the IAEA leach test in the same period (Dayal, R., 1983c) shows clearly that the IAEA leach data represent conservative estimates of the actual Cs release from a waste form subjected to cyclic wet/dry leach conditions.

An examination of the cumulative strontium release plot in Figure 2b indicates that its overall release behavior is significantly different from that of cesium. Unlike the cesium release behavior, the display in Figure 2b shows varying amounts of Sr release depending on the experiment type, with Experiment M (longest dry span) exhibiting the minimum release in a given immersion time.

Figure 2b shows further a systematic trend of decreasing Sr release with increasing length of the dry cycle. For example, in an immersion period of 28 days, a CFR of 4%, observed in the one-day dry cycle experiment, drops by more than an order of

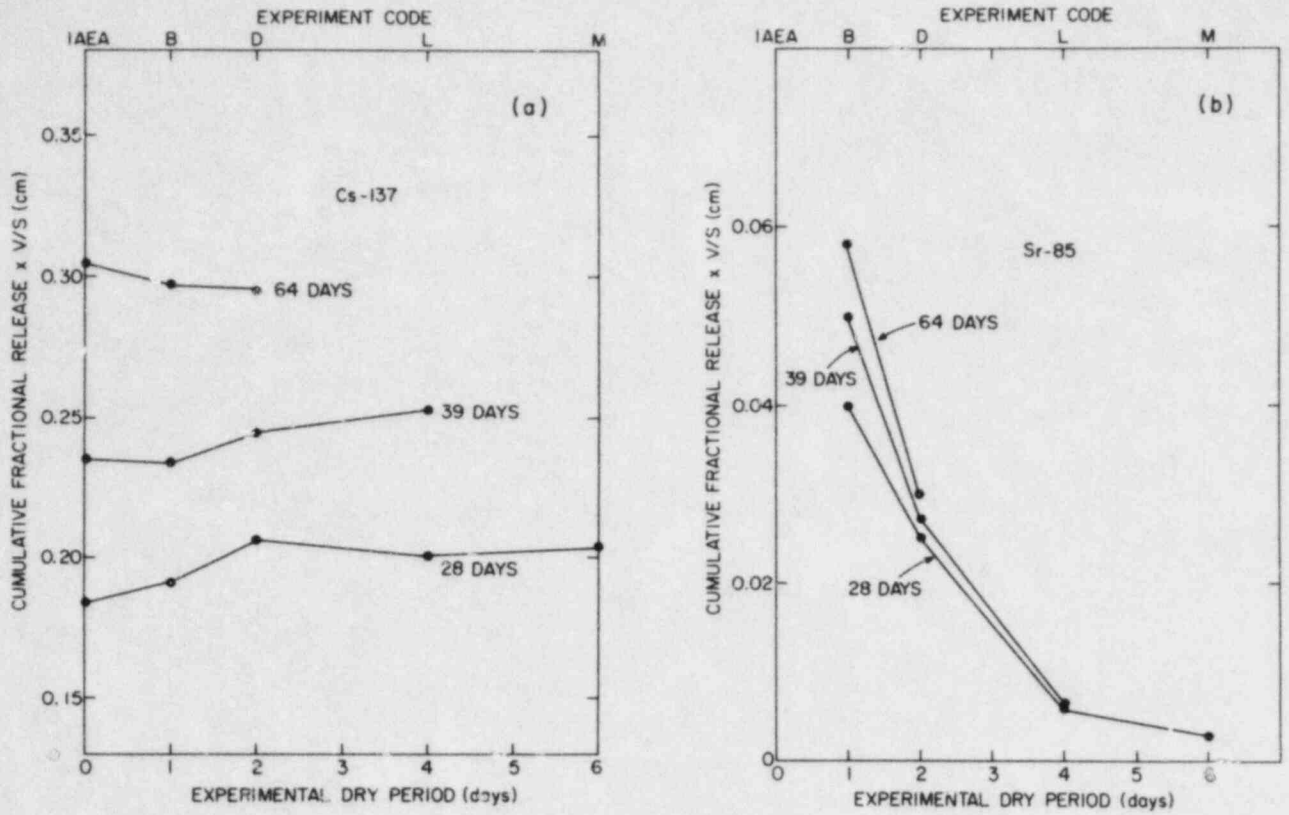

Figure 2. Normalized cumulative fractional releases of Cs-137 (a) and Sr-85 (b) as a function of experimental dry periods in Experiments B, D, L, and M. The release data are shown for total immersion periods of 28, 39, and 64 days. The continuously saturated conditions under modified IAEA testing correspond to a dry period of zero.

magnitude in the six-day dry cycle experiment. In the case of Cs, however, no such trend was observed. The cesium CFR values remain relatively constant, irrespective of the lengths of dry periods in Experiments B, D, L, and M.

The observed differences in the cumulative fractional releases of Cs and Sr as a function of total immersion time are also reflected in their effective diffusivity (D_e) values calculated from the CFR data. The apparent diffusion coefficient values, given in Table 2, include the retardation effects of tortuosity, sorption, and reaction in the waste form matrix. As shown in Table 2, the calculated diffusivities for cesium do not vary significantly from one experiment to another. The Cs diffusivity values are also comparable to that based on IAEA-type leach test (Dayal, R., 1983c), which represents a continuously saturated leach condition. In contrast, the diffusivity values for Sr exhibit a systematic decrease from $\sim 10^{-9}$ cm^2/s for one-day dry cycle Experiment B to $\sim 10^{-14}$ cm^2/s for six-day dry cycle Experiment M. Furthermore, a comparison of the diffusivity values for Cs and Sr for the same experiment shows that the Sr values are consistently lower.

Table 2. Effective diffusivities of Cs and Sr in resin/cement matrix[a].

Experiment	Dry Period (Days)	D_e (cm^2/s)[b] Sr	Cs
B	1	8.9×10^{-10}	2.6×10^{-8}
D	2	3.1×10^{-10}	3.4×10^{-8}
L	4	4.4×10^{-14}	2.6×10^{-8}
M	6	8.6×10^{-15}	2.6×10^{-8}
IAEA	0	[c]	1.6×10^{-8}

[a] Based on the relationship $(\Sigma a_n/A_o)(V/S) = 2(D_e/\pi)^{1/2} \times (\Sigma t_n)^{1/2}$, where D_e is the effective diffusivity and Σt_n, the total immersion time. The initially rapid release and the release observed at extended periods were not considered in these calculations (Dayal, R., 1983c; Arora, H., 1983b).

[b] Includes the retardation effects of tortuosity, sorption, and reaction in the bulk matrix.

[c] Data not available.

We believe that the differences observed in the Cs and Sr release from waste forms subjected to varying wet/dry cycles can be explained as follows. Mobilization and transport of Sr involves ion exchange of Sr from resin, leaching from the

cementitious matrix during wet periods and subsequent diffusion of the leached Sr into the leachant. In contrast to Cs, the Sr release involves an additional rate-controlling dissolution step. Consequently, the observed release rate of Sr is much lower than that of Cs.

Decreasing amounts of Sr release with increasing length of dry periods in the cyclic leaching experiments may be a result of redistribution of Sr between resin and the cement matrix in the saturated waste form. This appears to happen during the curing process; the exchangeable Sr^{2+} on resin is replaced by Ca^{2+} to be subsequently incorporated in the hydrated calcium silicate and hydroxide phases in the cement matrix, which are relatively less soluble. Therefore, the longer the dry period, the greater the extent of curing. McDaniel, E. W. and others (1982) and Moore, J. G. and others (1977) observed lower releases of Sr from cement grout samples cured for longer time periods. In a sense, the six-day dry period in which the medium surrounding the sample is unsaturated may, for the sample itself, represent a wet curing time of ∿170 days (total experimental period, excluding 28 one-day rinses). Experiments with shorter dry periods represent shorter curing times. For example, the curing time in Experiment B (one-day wet, one-day dry) would correspond to half of the total experimental time, that is, ∿90 days. Therefore, the observed dependence of decreasing Sr release with increasing length of the dry cycle can be explained by the varying lengths of wet curing periods which are a direct function of the experimental dry periods.

Cesium transport to the leachant is primarily controlled by diffusion, resulting in a surface-depleted zone. There are three major classes of diffusion effects that can occur in waste forms that are being depleted of radionuclides by leaching. For a given size, the diffusion in the bulk can be fast compared to the surface depletion, it can be slow, or it can be comparable to the depletion by leaching. In the first case (for example, tritium) the concentration of the species being leached will be uniform through the bulk of the solid and the release rate at the beginning of the $n+1^{th}$ wet period should be comparable to the leach rate at the end of the n^{th} wet period (assuming no changes in the surfaces with drying). This would also be expected if diffusion in the bulk were slow enough during the dry period so that the surface concentration gradients were not appreciably reduced. In the situation where bulk diffusion and surface depletion rates were comparable, the magnitude of the leach rate at the beginning of a wet cycle would be greater than the magnitude of the leach rate at the end of the prior wet cycle, because of enrichment of the radionuclide depleted surface during the dry spans. Depending upon the size of the pulse, the frequency and the duration, specific radionuclides may be released for short times at rates that temporarily exceed NRC criteria in terms of controlled release for a HLW repository or Leachability Index for a LLW form.

Based on an effective diffusivity of 10^{-8} cm^2/s for Cs in a resin/cement matrix, our calculations indicate that ∿12 days are required for Cs to traverse a diffusion path length of ∿1 cm in the saturated waste form matrix. Experiments, involving longer dry periods, are in progress to determine whether episodic release of Cs will occur during a rinse cycle, following a long dry cycle, as a result of replenishment of the depleted surface zone.

5.2.4 Conclusions

Significantly lower releases of Sr-85 were observed in comparison with Cs-137 from resin/cement waste forms subjected to cyclic wet/dry leach conditions. Cesium release when considered as a function of the actual immersion time (total length of the wet periods of wet/dry cycles) remains relatively constant, irrespective of the varying lengths of dry spans. The observed cesium release is also comparable to that based on the IAEA-type leach test, which represents continuously saturated leach conditions.

In contrast to cesium release, the strontium release is significantly lower and exhibits a systematic decrease with increasing length of the dry period. This is also reflected in the effective diffusivity values, which vary from ∿10^{-9} cm^2/s in one-day dry period experiment to ∿10^{-14} cm^2/s in six-day dry period experiment. Cesium, on the other hand, has an effective diffusivity on the order of ∿10^{-8} cm^2/s, regardless of the length of the dry period in the cyclic leaching experiments.

The observed differences in their release behavior can be attributed to different mechanisms by which these radionuclides are mobilized and transported from the bulk matrix into the leachant. In the case of cesium, diffusion is the principal release mechanism. Ion-exchange of cesium from the resin and dissolution of cesium compounds are too rapid to be rate-controlling. Strontium, on the other hand, gets incorporated in the cement matrix during curing of the waste form. Consequently, release of strontium involves leaching of the matrix and subsequent diffusion of the leached strontium into the leachant. Because of an additional rate-controlling, dissolution step, the observed release rate of strontium is much lower than that of cesium.

Decreasing amounts of Sr release with increasing length of dry periods may be due to differences in wet curing times of different wet/dry leaching experiments. The longer the period of the dry cycle, the greater is the curing time. For example, in the six-day dry cycle experiment, the wet curing time corresponds to ∿170 days, whereas in the one-day dry cycle experiment the total wet curing time is approximately 90 days. Therefore, it appears that the observed dependence of decreasing Sr release

with increasing length of the dry cycle can be attributed to increased wet curing of the waste forms during long dry periods of the experiments.

5.2.5 Recommendations

In addition to the known variability in the intrinsic properties of low level waste forms, there are important extrinsic variables, associated with the disposal environment, such as the composition, quantity, and flow rate of subsurface water interacting with the waste form, and the underlying sediment. In the unsaturated zone, the waste form/water interactions are likely to be dominated by the quantity and residence time of accumulated water in a trench, trench hydrodynamics such as stagnant versus well-drained conditions, and the frequency, duration and periodicity of wetting fronts.

Previous work at BNL has shown that the intrinsic properties of waste forms are very important in terms of determining the nature and extent of radionuclide release under a given set of experimental conditions. Preliminary results of more recent work at BNL in NRC-sponsored research programs (A-3027, A-3042) show that extrinsic variables such as the type of leaching conditions (leach rate-limiting vs solubility-limiting; varying leachant residence time as controlled by varying leachant renewal frequency; periodic wetting followed by a dry period of variable frequency and length) and the presence of a sediment barrier can cause significant variability in the nature and rate of radionuclide release.

Recognizing these uncertainties in leach data and that the commonly used IAEA and ANS 16.1 leach test procedures do not provide information on waste form leaching behavior under anticipated field conditions, there is a need for a broader data base on waste form leachability and for bounding the uncertainties to increase confidence in the leach data. It is only through the development of a generic data base that one can use laboratory leach data to extrapolate to field conditions and time scales in order to evaluate leach behavior of a waste form under anticipated field conditions.

Generic studies involving the investigation of the leaching characteristics of solidified low level waste forms are recommended. We propose that further research be carried out to elucidate the role of extrinsic variables on the leach behavior of waste forms with time. Long term leaching experiments should be conducted to establish the rate-controlling mechanisms by which different radionuclides are mobilized and transported in the waste form matrix subsequently to being released to the leachant. Of further interest is to determine whether the release mechanisms change with time.

In order to bound the uncertainties in radionuclide release from a given waste form, two types of release limits should be determined for the radionuclides of concern: (a) the solubility-limiting release under static or very low flow rate conditions; (b) the leach rate-limiting release under high flow conditions. The resultant upper and lower bounds will provide conservative estimates of the release under a range of flow conditions. Subsequently, the effect of periodic wetting fronts, simulating a range of climatic conditions ranging from arid to humid, should be investigated to obtain more realistic release data. Experiments should be designed to provide mechanistic data on the release behavior of different radionuclides under unsaturated conditions.

In order to bound uncertainties in radionuclide release as affected by radionuclide type and form, experiments should be conducted to investigate the leach behavior of the most and the least leachable radionuclides. For example, tritium is known to behave conservatively and its release from a waste form under a given set of leaching conditions is likely to provide a conservative bound of waste form leachability. On the other hand, elements such as cobalt or strontium, which precipitate out as separate mineral phases or coprecipitate with certain minerals in the cementitious matrix of the waste form, involve dissolution as the principal rate-controlling mechanism, with the resultant release being relatively very small. Therefore, proper selection of radionuclides such as H-3 (not immobilized in the matrix and hence diffusion is rate-controlling) and Co-60 (immobilized in the matrix minerals and hence dissolution is rate-controlling) can be used to bound uncertainties in radionuclide release from a given waste form, as affected by radionuclide type.

Further experiments are recommended to investigate the effect of a sediment barrier on radionuclide release from a waste form.

5.2.6 Acknowledgments

The authors thank all who participated in the project; in particular, H. Arora for his significant contribution. We would also like to thank G. Searles and M. McGrath for their patience and skill in typing the manuscript.

5.2.7 References

Arora, H. and R. Dayal, "Properties of Radioactive Wastes and Waste Containers, Quarterly Progress Report, October-December 1982," BNL-NUREG-32498, 1983a.

Arora, H. and R. Dayal, "Properties of Radioactive Wastes and Waste Containers, Quarterly Progress Report, April-June 1983," BNL-NUREG-33522, 1983b.

Colombo, P. and R. M. Neilson, Jr., "Properties of Radioactive Wastes and Waste Containers, First Topical Report," NUREG/CR-0619, BNL-NUREG-50957, 1979.

Dayal, R. and H. Arora, "Source Term Studies at Shallow Land Burial Sites, Quarterly Progress Report, April-June 1983," BNL-NUREG-33520, 1983a.

Dayal, R. and H. Arora, "Source Term Studies at Shallow Land Burial Sites, Quarterly Progress Report, July-September," BNL-NUREG-33822, 1983b.

Dayal, R., H. Arora and N. Morcos, "Estimation of Cesium-137 Release From Waste/Cement Composites Using Data From Small-Scale Specimens, Topical Report," BNL-NUREG-51690, 1983c.

Godbee, H. W., E. L. Compere, D. S. Joy, A. H. Kibbey, J. C. Moore, C. W. Nestor, O. U. Anders and R. M. Neilson, Jr., "Applications of Mass Transport Theory to the Leaching of Radionuclides From Waste Solids," Nuclear and Chemical Waste Management 1, 29-35, 1980.

McDaniel, E. W., M. T. Morgan, J. G. Moore, H. E. Devaney and L. R. Dole, "Strontium Leachability of Hydrofracture Grouts for Sludge-Slurries," ORNL/TM-8198, 1982.

Moore, J. G., H. W. Godbee and A. H. Kibbey, "Leach Behavior of Hydrofracture Grout Incorporating Radioactive Wastes," Nuclear Technology 32, 39-52, 1977.

Morcos, N., R. Dayal and A. J. Weiss, "Properties of Radioactive Wastes and Waste Containers, Status Report, October 1980-September 1981," NUREG/CR-2617, BNL-NUREG-51515, 1982a.

Morcos, N. and R. Dayal, "Properties of Radioactive Wastes and Waste Containers, Quarterly Progress Report, January-March 1982," BNL-NUREG-31412, 1982b.

5.3 GEOCHEMICAL AND STRONTIUM ISOTOPIC STUDIES OF COLUMBIA RIVER BASALTS

D. G. Brookins and M. T. Murphy
University of New Mexico

H. A. Wollenberg and S. Flexser
Lawrence Berkeley Laboratories
Berkeley, California

Abstract

A rhyodacite intrudes the Wanapum basalt and is exposed in a quarry along the Hood River, Oregon. Since the rhyodacite is different geochemically from the basalt, and was intruded at a high temperature, then this site can be used to evaluate the effects of the intrusion on the basalt. In such a study we assume the intrusive rock is a high temperature heat engine, and that cooling may be by convection, conduction, or both. Contact effects of the intrusion are not pronounced in the basalt, and are restricted to minor recrystallization within one meter of the contact, and to possibly some minor fracture filling. Traverses were made from the rhyodacite into the basalt, and samples at closely spaced intervals were analyzed for K, U, Th by field and laboratory gamma spectrometry and by neutron activation analysis for some 35 elements. Separate aliquots were analyzed by isotope dilution to inspect Sr isotopic variations. The chemical studies do not indicate migration of any elements from the rhyodacite into the basalt, nor for any in-basalt or in-rhyodacite migration. Despite a pronounced chemical gradient between the rocks, each has remained a closed, isochemical system. The Sr isotopic studies indicate that the rhyodacite possesses $Sr(87/86) = 0.70407 \pm 0.00008$ while the intruded basalts possess $Sr(87/86) = 0.7052 \pm 0.0002$. Even in samples of the contact, with intermingled rhyodacite and basalt, each rock preserves its own characteristic Sr(87/86) signature, thus again attesting to the closed system conditions. We conclude for this natural experiment that the Wanapum basalt is not readily penetrated by elements from a high temperature, molten source.

Samples from the Grande Ronde basalt, including the Umtanum member, have been analyzed for their mineralogy and Sr isotopic composition. All samples are from drill core some 15 km from the BWIP exploratory shaft. These samples have been studied in order to address the problem of genesis of the fracture filling minerals encountered in the basalt at depths equal or close to that of the proposed repository horizon. Fracture filling minerals may be the consequence of deuteric mineralization, essentially at the time of crystallization of the basalt, or to much younger fracture filling due to infiltration of the rocks by meteoric waters, or to both. Should the fracture filling minerals indicate the presence of meteoric water, then this poses serious questions about the ability of the basalts to be impervious to such infiltration. We have addressed this problem by use of Sr isotopic systematics. Basically, the problem is one of mixing of two finite reservoirs, each with different total Sr and with markedly different Sr(87/86) ratios. Despite some local variations, Sr(87/86) ratios in the Grande Ronde basalt vary between 0.7050 to 0.7062, while meteoric waters in

the surface environments typically vary between 0.7084 to 0.7110. These ratios can be measured on any given sample to ± 0.00003, hence any mixing of the two reservoirs is easily detected. Our measurements confirm the Sr(87/86) ratios for the Grande Ronde basalt, with an average of 0.7055. Analyses of fracture filling minerals, which consist of clinoptilolite, chabazite, other zeolites, minor Ca-plagioclase, and calcite, range from 0.7052 to 0.7063 and average 0.7057. These data confirm that the Sr in the fracture filling minerals has been derived from the Grande Ronde basalt, and that there is no evidence for mixing of meteoric-derived Sr with basalt Sr.

5.3.1 Introduction - General

Work on analogues and related topics has been useful in addressing many of the problems of nuclear waste management. Many of these studies have dealt with various igneous rocks, dikes in bedded salts, and so on, but few have dealt with problems somewhat restrictive to basalts such as the site rocks at BWIP.

We have chosen to investigate two problems related to the BWIP area. The first of these deals with the fracture filling minerals from a drill hole some 10 km from the BWIP exploratory shaft. These fracture filling minerals have been studied in order to determine if meteoric waters have penetrated vertically through the basalts, in which case the fracture filling minerals should have a chemistry and/or isotopic component which reflects the meteoric input. This research is necessary as most of the commentary on the role of vertical water flow at Hanford is speculative, and this study allows quantitative estimation of how much, if any, meteoric water has moved vertically through the basalts. A combined assessment of the fracture filling minerals and their host basalts by isotopic and trace element study has been carried out. The results are of importance to the licensing of the BWIP site.

In addition, the fate of radionuclides hypothetically released from a buried HLW canister can be indirectly evaluated by examination of a siliceous (rhyodacite) dike which cuts the Wanapum basalt in the southern part of the Columbia River basalt province. Use of isotopic and trace element chemistry allows a quantitative assessment of elemental mobility in the vicinity of the dike-basalt contact. This study will provide information concerning elemental retardation from breached HLW canisters to the licensing process.

5.3.1.1 Analytical Methods

The analytical work was carried out at the University of New Mexico (UNM), Lawrence Berkeley Laboratory (LBL), and the Los Alamos National Laboratory (LANL). The strontium isotopic analyses were carried out at UNM using a Nier-design NUCLIDE 1290 solid source mass spectrometer. All $^{87}Sr/^{86}Sr$ ratios are precise to ± 0.0000_3 (two sigma) and normalized to $^{86}Sr/^{88}Sr = 0.1194$. Four runs of Eimer and Amend standard $SrCO_3$ yielded $^{87}Sr/^{86}Sr = 0.7080_3$, in exact agreement with the accepted value for this standard. The gamma spectrometer determination of K, U, Th was carried out at LBL, and the data are accurate to ± 2% of the reported values. The instrumental neutron activation analyses (INAA) were carried out at LANL through one of us (DGB) at UNM. The details of the INAA methodology are given by (8). This method allows some 31 elements

to be determined, most with high precision. No special loading techniques are used, but large (4 cm^3 vials) samples are used.

Part A--Sr isotopic and trace element study of Hanford site fracture filling minerals.

5.3.2 Introduction

A topic of some concern is whether or not waters can percolate vertically through the rocks at the BWIP site. Flow in well defined horizontal, interbed units is well known, but vertical flow has not been fully investigated. Since vertical fractures are common, it is possible that some waters could penetrate the basalts and move normal to the horizontal flow layers. To investigate this, we have chosen to examine the chemistry and isotopics of minerals found in the fractures. These minerals may have originated earlier in the basalt history, i.e., deuteric, and this would be manifested in the chemistry and isotopic composition of the basalt. Alternately, they may have formed late in the basalt's history, in which case their chemistry may be a reflection of material deposited from percolating waters. Thirdly, they may represent a mixing of the basalt and groundwater reservoirs. We choose to examine this important problem by determining the strontium isotopic composition of the various reservoirs, supported by other chemical studies. In this fashion we have carefully investigated the origin of the strontium and other trace elements in the fracture filling minerals. To date, waters from surface or subsurface reservoirs at Hanford have not been provided for analysis, although we plan to run these as soon as they are available. Our conclusions on the strontium isotopic work are therefore qualitative to semi-qualitative at best, but the results can be directly applied to the source of the strontium in the fracture filling minerals.

5.3.2.1 Mixing of Two Sr Reservoirs

When two reservoirs, each of different total Sr and ($^{87}Sr/^{86}Sr$) ratios, are mixed, the mixing equation can be expressed as follows:

$$\left\{\frac{^{87}Sr}{^{86}Sr}\right\}_m = \left\{\frac{^{87}Sr}{^{86}Sr}\right\}_i \left\{\frac{Sr_i f}{Sr_m}\right\} + \left\{\frac{^{87}Sr}{^{86}Sr}\right\}_j \left\{\frac{Sr_j(1-f)}{Sr_m}\right\} \quad (1)$$

or:

$$\left\{\frac{^{87}Sr}{^{86}Sr}\right\}_m = \left[\frac{Sr_i Sr_j \left\{\frac{^{87}Sr}{^{86}Sr}\right\}_j - \left\{\frac{^{87}Sr}{^{86}Sr}\right\}_i}{Sr_m(Sr_i - Sr_j)}\right] + \left[\frac{Sr_i \left\{\frac{^{87}Sr}{^{86}Sr}\right\}_i - Sr_j \left\{\frac{^{87}Sr}{^{86}Sr}\right\}_j}{Sr_i - Sr_j}\right] \quad (2)$$

where the subscripts are: m = mixture; i, j = different reservoirs; f = fraction of component i. The above equation (2) is that of a hyperbola with coordinates of $(^{87}Sr/^{86}Sr)_m$ and Sr_m of the form:

$$\frac{^{87}Sr}{^{86}Sr_m} = \frac{a}{Sr_m} + b \quad (3)$$

where a and b are constants specified by the concentrations and $^{87}Sr/^{86}Sr$ ratios of Sr in components i and j. It is convenient to plot $(^{87}Sr/^{86}Sr)_m$ versus $1/Sr_m$ in order to transform the hyperbola into a straight line with coordinates in $^{87}Sr/^{86}Sr$ and 1/Sr. Numerous examples where this relationship has been used are presented in (5). From equation (1), the fraction of component i mixed with component j can be estimated.

In the case of fracture filling minerals in Grande Ronde basalts, these minerals will contain Sr with at least the isotopic signature of its source. Total Sr contents may vary somewhat differently, as the partitioning of Sr between phases may vary. Hence use of the mixing model (above) is limited in that, based on measurement of $(^{87}Sr/^{86}Sr)_m$, the corresponding estimate of Sr_m may or may not be close to the actual value based on mixing of Sr_i with Sr_j. Yet the isotopic measurements are so sensitive that any large amount, or even relatively small amounts, of an extraneous reservoir Sr mixed with basalt Sr will be readily apparent.

5.3.2.2 Discussion

The trace element data for the Hanford fracture filling materials and host basalts are given in Tables 1 and 2, and the strontium isotopic data for basalts and fracture filling materials are given in Table 3. The mineralogy of the fracture filling materials is given in Table 4.

The mineralogy of most of the fracture filling materials consists of a mixture of zeolite, primarily clinoptilolite, with quartz, although four samples contain phillipsite and six samples contain low cristobalite. Illite and erionite were identified in only two samples. A more complete mineralogical description of the secondary minerals in the basalts is given by (7). Some of the fracture filling mineral assemblages contain cristobalite, and the presence of this mineral alone precludes a low temperature origin. The stability of the zeolites, especially clinoptilolite and phillipsite, coupled with quartz, cannot unequivocally be used in the same fashion as all these minerals can form at low temperatures. However, when zeolites form at low temperatures due to the interaction of waters percolating through rocks with the rocks, the chemistry of the waters is reflected in the zeolites. Hence these minerals are useful for tracing the source material responsible for their formation.

The trace element data are interesting to compare to average basalts and continental stream waters for selected elements as shown in Table 5. It is apparent that the fracture filling trace element data are much more consistent with the basalt values than the stream water samples, especially when elemental ratios are considered for selected elements. It is noted (4) that many Columbia River basalts yield K/Rb values near 250 - 400, whereas other data show that the K/Rb ratio for average stream water is commonly in excess of 1000. The K/Rb ratio of the fracture filling samples is 217. In the case of Th/U, the average basalt ratio is 2.7 and the ratio in stream waters is 1. The fracture filling materials yield 3.27. Similarly, the fracture filling Rb/Sr ratio is 0.175, moderately close to basalt values of 0.279, and very different from stream water average of 0.016. Other elemental pairs such as Co/Sc, Sc/Fe,

Co/Mn also indicate an affinity of fracture filling material with basalt and no apparent affinity with stream water values nor with average ground water values from the Hanford area (2). In the site characterization for BWIP (2), some analyses of various ground waters are given. The values for Sr, Cr, Co, Fe, Mn are in moderately good agreement with the values for average waters given by (3) as shown in Table 3; and they are quite different by orders of magnitude, from typical basalt values (Table 3).

The strontium isotopic studies of Hanford basalts from drill hole DC-6 (Table 2) also support a lack of major stream water component in the fracture filling minerals, The $^{87}Sr/^{86}Sr$ ratios for basalt-fracture filling pairs are plotted in Figure 1, and it is seen that there is only a very small difference between individual pairs, while there is some real isotopic difference between different parts of the basalt as a function of depth. This variation in strontium isotopic composition has been noted by others (See discussion in (4)). One of the fracture filling samples, however, yields a value of $^{87}Sr/^{86}Sr = 0.0789$ (Sample 3436) which is significantly higher than it's host basalt (0.7057). Petrographic examination indicates this sample to contain small amounts of xenocrysts, which probably accounts for the high Sr isotopic value (See also (4)). This sample will be studied in detail to resolve this matter. The petrography and trace element work do not indicate any water-derived secondary minerals in the sample.

Waters from surface streams and from groundwaters have not yet been made available for study. As a result, we can only use the strontium mixing model developed earlier in this report as a qualitative tool. Strontium data for several western streams have been given by (1), and, with caution, his results can be used for testing the model. Assuming values of 60 ppb Sr for average streams, and $^{87}Sr/^{86}Sr = 0.709$, the data for the fracture fillings is compatible with derivation from a large amount of basalt (95%) and no more than 5% water. Further, the supporting trace element data argue that the actual surface water component is probably near zero, although we readily admit the specific waters must be tested to verify this.

The rare earth element plots for the individual Hanford fracture filling minerals (Figures 2 and 3) are very similar to REE/CHON plots for Columbia River basalts, and quite dissimilar from REE/CHON plots for waters. In Figures 2 and 3, a REE/CHON curve for the average of 282 continental basalts (noted as basalt composite), from (6) is given for comparison with the REE/CHON curves for the fracture filling minerals. The similarity of the curves is striking, and attests to the probable derivation of the REE from the host basalt as opposed to derivation from percolating waters. While data for stream waters are few, most are characterized by patterns close to average shale, with a pronounced negative Eu anomaly and, often, a mild Ce negative anomaly. Yet the data in Figures 2 and 3 show no negative Eu and/or Ce anomaly and, in fact, are parallel to the basalt patterns. This information also supports a source for the REE found in the fracture fillings to be the host basalt, as a stream source would not only yield much lower REE content but also a very different REE/CHON distribution. We estimate no more than 1 to 2% water-derived REE in the fracture fillings.

Part B--Geochemical Study of Wanapum Basalt, Oregon

5.3.3 Introduction

The Columbia River Basalts have been intensively studied in conjunction with the BWIP project. Despite the large number of such studies, detailed investigation of certain facets of the project have not previously been examined. Specifically, how elements may mobilize in the presence of a heat sink has not been examined, nor have certain, refined chemical and isotopic studies been undertaken to fully explore the origin of fracture filling minerals in the rocks.

In the case of an analogue for a heat sink, an area near the Hood River, Oregon was chosen where a siliceous rock, a rhyodacite dike, is intrusive into the Wanapum basalt. The chemical gradients for many elements between the two rock types is pronounced, and it is our purpose to investigate the elemental behavior in the vicinity of the intrusive contact to test for elemental migration. These studies can, with caution and proper scaling, be applied to hypothetical buried radwaste, and allow estimates of the amount of radionuclide migration from this buried waste.

5.3.3.1 Analogue Studies

Sites were identified in the Pacific Northwest where intrusive rocks cut basalt of the Columbia River plateau. The Wind River quarry near Wind Mountain in the Columbia River Gorge, Washington, provides samples of large (meter-scale) xenoliths of basalt in diorite - quartz diorite, and samples were obtained of fractured and unfractured rock, centimeters and decimeters away from contacts between these rock types. At a second site, the Robin Hood quarry on the East fork of the Hood River, Oregon, a rhyodacite dike cuts basalt of the Frenchman Springs member of the Wanapum Formation.

The samples of flood basalt and intruding rocks from the Columbia Gorge and Hood River sites were analyzed for radioelement contents by laboratory gamma spectrometry. At the Wind Mountain quarry, a basalt xeonlith in contact with quartz diorite was sampled on a centimeter scale, near and away from the contact, and two samples were obtained of the quartz diorite. Variations in radioelement contents are plotted in Figure 4. The apparent depletion of U and Th in basalt at the contact indicates that assimilation of basaltic material occurred with intrusion of the quartz diorite. The U, Th, and K contents of the basalt xenolith at Wind Mountain are considerably lower than those of basalt farther from the quartz diorite contact at Shellrock Mountain on the opposite side of the Columbia River. There is greater contrast in radioelement contents of basalt and quartz diorite at Shellrock Mountain than at the basalt xenolith/quartz diorite contact zone at the Wind Mountain quarry, also supporting the assumption of assimilation of components of the basalt by the quartz diorite at Wind Mountain.

Results of laboratory gamma spectrometric analyses of the sample set from the Robin Hood quarry on the East fork of the Hood River are listed on Table 6, and the distribution of U and Th contents plotted on Figure 5. This occurrence is considered to be more analogous to waste repository conditions than the sites

in the Columbia Gorge, because of the sharp contrast in radioelements between the rhyodacite dike and the basalt.

5.3.3.2 Strontium Isotope Investigations for Analogues Study

Samples from the rhyodacite dike intrusive into Wanapum basalt from a quarry along the Hood River, Oregon have been analyzed. One objective in studying these samples is to examine the rhyodacite - basalt contact zone, and for some distance in both rocks away from the contact, to determine if there has been any chemical or isotopic exchange between them caused by the thermal regime present at the time of intrusion.

Samples of rhyodacites and basalts, from the Hood quarry site have been analyzed for their Sr isotopic composition and trace element content. If chemical and/or isotopic exchange has taken place between such different rock reservoirs, then, if initial Sr isotopic composition is different in each, mixing of the two will be obvious. In the case of the Hood quarry samples, the rhyodacites yield $^{87}Sr/^{86}Sr$ ratios of $0.7040_7 \pm 0.0000_8$ while the basalts average 0.7052 ± 0.0002. These data argue against any transfer of Sr from either reservoir into the other, a situation similar to that observed earlier for U and Th. Neutron-activation analytical data (INAA) also show this trend. Sample no. RQ-4a, rhyodacite from the immediate contact zone, shows a slightly high $^{87}Sr/^{86}Sr$ value of 0.7043, yet the basalt sample from the same zone (RQ5) yields 0.7052 and is apparently not depleted in 87-Sr. Sample Rq 9 yields 0.7054, which is higher than the average of 0.7052, yet the source of this excess ^{87}Sr cannot be from the rhyodacite as its ratio is too low (i.e. near 0.704). The data are shown in Table 7 and Figure 6. Details of Sr mixing models are given in Brookins et al., (this volume), Faure (1977), and in part in Carlson et al. (1981).

5.3.3.3 Trace Element Studies: Hood Quarry Samples

Instrumental neutron activation analysis (INAA) of the Hood quarry samples, as shown in Table 8, show trends similar to U and Th (Figure 5). Alkali and alkaline earth elements are similar to K (Table 6 data), and Cr, Ni, Co, Sc, Fe, Ta, Zr like U, Th. The REE show different distribution patterns in the dacite and basalt, and no perturbations in the contact zone samples.

5.3.4 Conclusions - Part A

In the licensing process attention is given to many topics, including radionuclide migration and to hydrologic integrity of the repository rocks. Our studies allow us to reach the following conclusions:

1. Strontium isotopic signatures of fracture filling minerals are essentially identical to their host basalt. The model for Sr mixing between reservoirs of different total and isotopic Sr is a powerful tool for investigating the origin of such fracture filling.

2. REE/CHON plots indicate that the rare earth elements (REE) in the fracture filling minerals have been derived from their host basalts.

3. The INAA data for numerous trace elements indicate that the fracture filling minerals have obtained their chemistry from a basalt source.

4. If water flowing vertically through the basalt had caused the precipitation of the secondary minerals noted, the chemistry of the minerals would reflect this water. This is not the case.

5. Studies of similar fracture filling minerals from the newly proposed BWIP repository horizon should be undertaken.

5.3.5 Conclusions - Part B

In the licensing process attention is given to many topics, including radionuclide migration and to hydrologic integrity of the repository rocks. Our studies allow us to reach the following conclusions:

1. The strontium isotopic characteristics of both the intrusive and intruded rocks from Hood quarry are preserved. These is no evidence for strontium isotopic disturbance or redistribution due to the emplacement of the rhyodacite dike into Wanapum basalt.

2. The studies of Th, U, K and other elements, most with pronounced chemical gradients between the rhyodacite and basalt, show that no elemental transfer has taken place across the contact.

3. Use of the rhyodacite as a heat engine as analogue for buried radwaste indicates that, for the natural conditions encountered during rock intrusion, radionuclide migration is not likely through solid rock.

5.3.6 Recommendations

The results of our studies have led us to the following recommendations.

1. Trace element and Sr isotope studies of fracture filling and other secondary minerals at the BWIP site may unequivocally demonstrate whether or not vertical flowing waters have penetrated the BWIP rocks. Special attention should be given to secondary smectites, which have not been studies by these means to date. This same approach can also be used for NTS rocks.

2. When secondary smectites and zeolites are made available for study, these should also be subjected to laboratory experiments, mainly cation exchange, to determine if the readily exchangeable sites contain Sr of an isotopic composition slightly different from, or identical to, either source waters (for groundwaters) or basalt.

3. Some secondary minerals contain potassium. It may be possible to separate these and determine their ages by the K-Ar method. This would answer the question as to whether these minerals are truly deuteric or very young.

5.3.7 Planned Research

1. Continuation of characterizing and testing of fracture filling and other secondary minerals from BWIP site rocks. These studies, ongoing, include:

   a. Sr isotopic composition of basalt and the secondary minerals.
   b. Trace element abundance and distribution in all samples.

2. Detailed Sr isotopic and selected trace element study of surface waters, groundwaters from identified aquifers, and waters from basalts proper (from drill holes).

3. Leaching studies of secondary minerals to see if:

   a. Surface layers are enriched in a different suite, or same suite-different abundances, of trace elements.

   b. Cation exchange experiemnts to determine the nature (and source) of radiogenic ^{87}Sr.

   c. Leaching of whole rock basalt samples to see if calcite in selected samples represents a meteoric source or not.

4. Integration of the BWIP site studies into a larger program of natural analogues.

5. Preparation of a document addressing the application of the analogue work to problems of licensing.

6. Expansion of the work to include samples from the NTS and bedded and dome salts under consideration for HLW repository studies.

5.3.8 Acknowledgments

We wish to acknowledge support by Lawrence Berkeley Laboratory and by the University of New Mexico, as well as partial financial support from the U.S. Nuclear Regulatory Commission. Laboratory and/or field assistance was provided by Steve Flexser, LBL, and M. S. Abashian, R. K. Matheney, H. A. Vogler, and P. S. Fridlund, UNM. Mr. S. Garcia, Los Alamos National Laboratory, kindly arranged for some samples to be run by neutron activation analysis.

References

1. G. W. Brass, the source of marine strontium and the $^{87}Sr/^{86}Sr$ ratio in the sea throughout Phanerozoic time: Unpub. Ph.D. dissertation, Yale Univ., 160 pp. (1973).

2. D. G. Brookins, M. T. Murphy, and H. A. Wollenberg, Strontium isotopic study of fracture filling minerals in the Grande Ronde Basalt, Washington: In Scientific Basis for Nuclear Waste Management, VII (G. L. McVay, Ed.), in press.

3. R. W. Carlson, G. W. Lugmair, and J. D. Macdougall, Geochim. Cosmochim. Acta 45, p. 2483-2500 (1981).

4. Department of Energy, Site characterization report for the Basalt Waste Isolation Project: U.S. Dept. Energy Rpt. DOE/RL 82-3, vol. 1 (1982).

5. J. I. Drever, The geochemistry of natural waters: Prentice-Hall Pub. Co.,NJ, 388 p. (1982).

6. G. Faure, Principles of Isotope Geology (Wiley-Interscience, New York, 1977), 460 p.

7. L. A. Haskin, M. A. Haskin, F. A. Frey, and T. R. Wildeman, Relative and absolute terrestrail abundances of the rare earths: In Origin and Distribution of the Elements (Pergamon Press, New York, 1968), p. 889-912.

8. C. W. Myers, and S. M. Price, Geologic studies of the Columbia Plateau: A Status Report (RHO BWI-ST 4, 1979).

9. M. M. Minor, W. K. Hensley, M. M. Denton, and S. R. Garcia, An automated activation analysis system: 1981 Int. Conf. on Modern Trends in Activation Analysis (Univ. Toronto, June 15-19, 1981), 12 p.

5.4 URANIUM, THORIUM AND TRACE ELEMENTS IN GEOLOGIC OCCURRENC AS ANALOGUES OF NUCLEAR WASTE REPOSITORY CONDITIONS

H. A. Wollenberg[a], D. G. Brookins[b], L. H. Cohen[c], S. Flexser[a], M. Abashian[b], M. Murphy[b] and A. E. Williams[c]

ABSTRACT

Contact zones between intrusive rocks and tuff, basalt, salt and granitic rock were investigated as possible analogues of nuclear waste repository conditions. Results of detailed studies of contacts between quartz monzonite of Laramide age, intrusive into Precambrian gneiss, and a Tertiary monzonite-tuff contact zone indicate that uranium, thorium and other trace elements have not migrated significantly from the more radioactive instrusives into the country rock. Similar observations resulted from preliminary investigations of a rhyodacite dike cutting basalt of the Columbia River plateau and a kimberlitic dike cutting bedded salt of the Salina basin. This lack of radionuclide migration occurred in hydrologic and thermal conditions comparable to, or more severe than those expected in nuclear waste repository environments and over time periods of the order of concern for waste repositories.

Our attention is now directed to investigation of active hydrothermal systems in candidate repository rock types, and in this regard a preliminary set of samples has been obtained from a core hole intersecting basalt underlying the Newberry caldera, Oregon, where temperatures presently range from 100 to 265°C. Results of mineralogical and geochemical investigations of this core should indicate the alteration mineralogy and behavior of radioelements in conditions analogous to those in the near field of a repository in basalt.

---

a. Lawrence Berkeley Laboratory,
b. University of New Mexico,
c. University of California, Riverside

5.4.1 INTRODUCTION

Prediction of the long-term performance of a nuclear waste repository requires evidence from natural occurrences in candidate rock types. Principle questions that need to be addressed pertinent to the long-term isolation of radioactive waste are:

1) What is the capability of radionuclides to migrate from a breached waste package into and through the disturbed zone, and into and through the groundwater system in crystalline, tuffaceous and basaltic rock and salt?

2) Which radionuclides are most likely to migrate and to what extend do they migrate?

3) What is the composition of material lining and filling fractures and vugs? Was it formed early in the emplacement of the host rock or is it the result of present-day or recent circulation of ground water?

4) What changes will occur in the composition and the properties of rock and fluids in the near field in response to heating by the radioactive waste?

In this paper we describe analogue investigations focused on issues 1, 2 and 4. A companion paper in this volume by Brookins et al. (1983) emphasizes issue 3.

The Oklo occurrence in Gabon (Maurette, 1978) demonstrated that U and its daughters and fission products have been retained in host-rock argillaceous sandstone within tens of meters of the site of a naturally fissioning "reactor" for ~ 1.8×10^9 years. Many other occurrences can be investigated in which rocks or veins with relatively high concentrations of these elements are in direct contact with host rock similar to rocks presently considered as candidates for waste repositories. These occurrences include both U and Th veins in crystalline rock, and contact zones between intrusive rocks containing relatively high abundances of U, Th, and trace elements, and crystalline rock, tuff, basalt and salt. In most cases, the conditions of intrusion resulted in temperatures considerably higher than those considered appropriate for waste isolation (temperatures of dikes or large igneous bodies generally exceed 1000°C at time of intrusion, and cooling may occur over periods of millions of years, depending on the conductive or convective thermal regimes set up in the intrusives and country rocks). However, at stages in the cooling history, temperatures at contact zones reach the range expected in the near-field of a respository, and upon cooling, hydrologic regimes are established that are maintained for periods that match or exceed periods of concern for repository environments. Thus, investigation of these contact zones

-- particularly the distribution of elements that accompanied the thermal episodes associated with and following intrusion, and the distribution of elements that may have resulted from the long-term operation of hydrologic systems -- is valid in considering their application as analogues to conditions in the near- and mid-field regions of repository environments.

Another aspect of geologic analogue considerations that bears investigation is the changes in the mineralogy of near-field host rocks that may accompany the thermal effects of introduction of nuclear waste. Present-day active hydrothermal systems where temperatures are similar to those expected in rock close to waste canisters in a repository (100 to over 250°C) may provide analogues of the expected alteration in host rock minerals. The effects of long-term high temperatures on the structural properties of near-field repository rock may be best assessed by sampling and testing rock from these hydrothermal temperature zones. Comparison of samples from heated and cooler zones will also disclose the effects of a convective thermal hydrologic regime on radio-and trace-element distributions.

Recent studies of these topics include work on contacts between intrusives and carbonate and crystalline country rock (Papike et al., 1983) supported primarily by the U.S. Dept. of Energy, and the work reported here, supported to date by the U.S. Nuclear Regulatory Commission.

In this report we first summarize work on two occurrences of contrasting character: a contact zone between a Tertiary intrusive and Precambrian gneiss where conductive thermal conditions prevailed, and a contact zone between a Tertiary monzonite stock and tuff where inception of a strong circulating hydrothermal system accompanied intrusion. Preliminary findings at contacts between relatively radioactive dikes cutting basalt and salt are also briefly described, as is a present-day circulating hydrothermal system that provides an analogue occurrence at expected near-field repository temperatures in basalt.

5.4.2 CRYSTALLINE ROCK:

5.4.2.1 The Eldora Stock - Idaho Springs Formation Contact Zone

In considering igneous intrusions as analogue occurrences, the intrusive body is treated as a heat engine, chemically different from the intruded rocks. A high-temperature intrusive which took 10^5 - 10^6 years to crystallize and cool represents an extreme-case scenario for possible elemental transfer from intrusive into intruded rocks while the rocks are heated. Study of U, Th, the lanthanides, Rb-Sr geochronology, stable oxygen isotope distribution, and various other elements in the intruded rocks as a function of distance from the contact permits an assessment of elemental transfer

due to the intrusion. Such a study also permits assessment of any elemental redistribution that may have occurred subsequent to cooling of the intrusion. As an analogue of waste isolation conditions in crystalline rock, we obtained samples from the contact zone between the 58-million-year-old Eldora Stock and Precambrian gneiss of the Idaho Springs Formation, Colorado, where previous geochronologic, mineralogic, geochemical and heat-flow modeling studies were well documented (Hart et al., 1968). Our samples were collected from the stock and from the Idaho Springs Formation at the contact and at increasing distances to 7.5 km from the contact, (Figure 1) following a traverse essentially identical to that used by Hart et al., (1968).

The fresh stock rocks range in composition from monzonite to granodiorite. As described by Hart et al. (1968), the stock crystallized from a magma temperature of 780°C under a water load of 2km. The rocks now exposed were never at depths greater than 1 km. The rocks of the Idaho Springs Formation consist predominantly of alternating felsic- and mafic rich plagioclase-hornblende gneiss with occasional secretion pegmatites. The age of the Idaho Springs Formation is approximately 1.5-1.6 billion years, and the rocks were regionally metamorphosed approximately 1.4 billion years ago, at which time the pegmatites were injected. These "sweat" pegmatites filled the fractures and formed the veinlets that appear in the gneiss. Because of their more complex history, elemental variations due to pre-stock emplacement thermal events in the gneiss must be carefully deciphered before attempting to interpret the stock-induced effects at 58 million years ago.

Samples from the stock, and of felsic, mafic and pegmatitic phases of the Idaho Springs Formation, were taken along the aforementioned traverse. Samples from another site near Antelope Creek, Colorado (southwest portion of Figure 1) of both stock and Idaho Springs Formation were also taken for comparative purposes. Splits of the samples were used for thin section preparation, laboratory gamma spectrometry, fission track radiography, Rb-Sr and K-Ar geochronologic study, neutron activation analysis (NAA), and for stable oxygen isotopic analysis. The petrography was carried out at both the University of New Mexico (UNM) and Lawrence Berkeley Laboratory (LBL), radiography and gamma spectrometry at LBL, the Rb-Sr work at UNM, the stable oxygen isotope analyses at the University of California at Riverside, and the NAA analyses at the Los Alamos National Laboratory. Descriptions of the samples and results of chemical analyses are tabulated in the second annual report of this project (LBL), 1982).

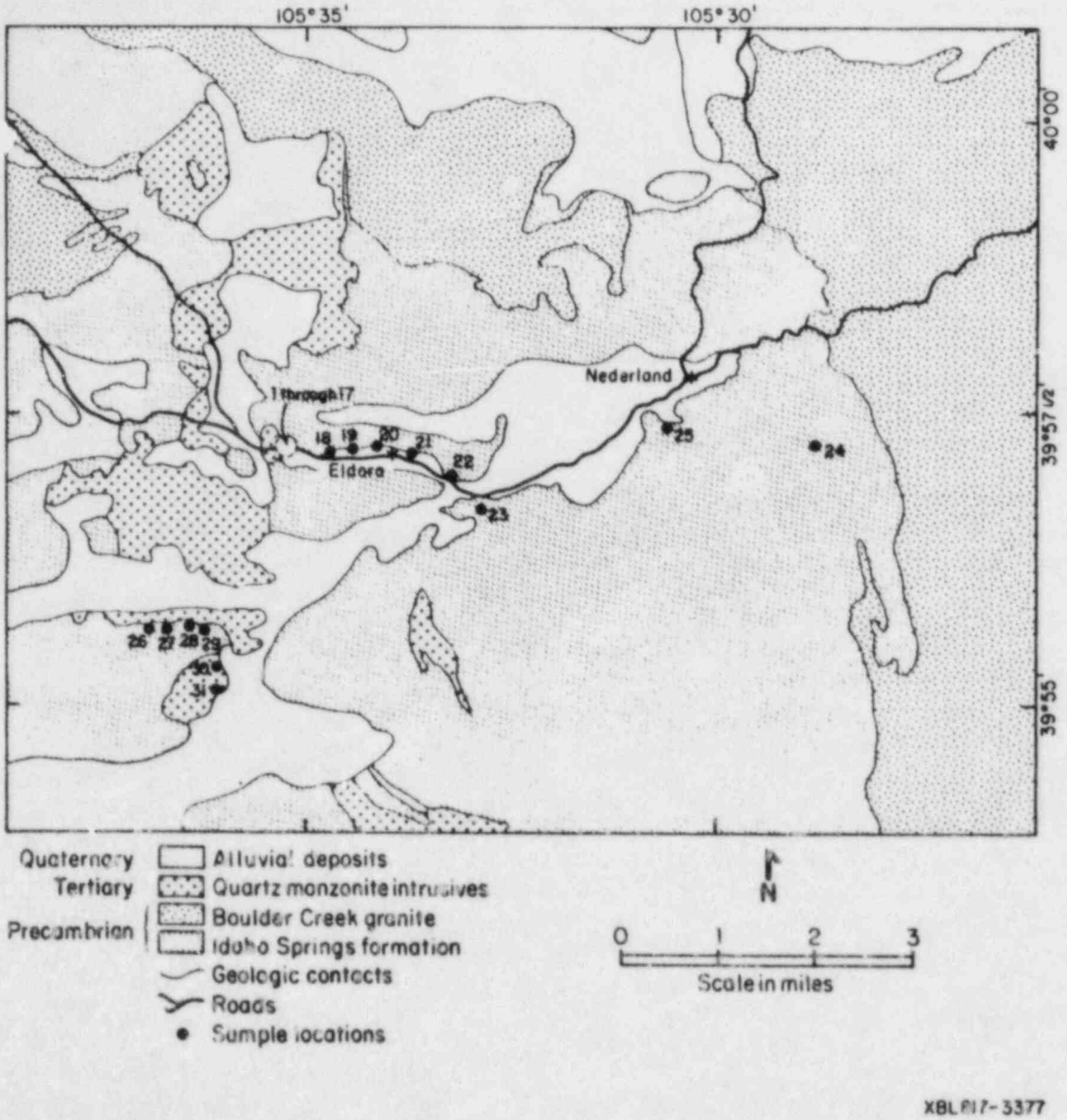

Figure.1. Simplified geologic map (after Hart, et al., 1968) showing sampling locations in the Eldora Stock-Idaho Springs Formation, Colorado. XBL 817-3377.

The previously reported Rb-Sr, K-Ar, U, and Th-Pb radiometric ages and other data (Simmons and Hedge, 1978; Hart et al., 1968) are of value in allowing essential heat models for the Eldora stock to be calculated. In brief, the stock is known to be steep-to-vertical on the sides, the heat distribution about the stock fairly uniform based on radiogenic Ar, Sr and Pb behavior in minerals, and the isotherm corresponding to the orthoclase-microcline transition (a maximum of 400°C) is considered to be 300-800 m from the contact (Hart et al., 1968). The model advocated by these workers is that of a "brick" with large vertical extent downwards, its thickness equal to the average E-W outcrop extent of the stock and its length equal to the average N-S extent of the stock. The model is based on the assumption that cooling is solely by conduction. This model has been shown to best explain the isotopic variations as a function of distance from the contact. Most of these early studies were aimed at behavior of specific minerals, and whole rock samples were not investigated for element abundances other than for a Rb-Sr date (a whole-rock isochron date of 1.4 to 1.6 billion years). Radiogenic Rb from the stock was shown to be confined to within 3 m of the contact, and in this zone there is petrographic evidence for infiltration of the Idaho Springs Formation by fluids from the stock.

The loss of radiogenic ^{40}Ar from minerals as a function of distance in the gneiss from the contact was well documented by Hart et al. (1968), who also related estimated temperatures and apparent radiometric ages to distance from the contact. We corroborated these apparent ages by K-Ar determinations on biotite, hornblende and feldspar from varying distances, and confirmed that the ages of minerals from various whole-rock samples are more thoroughly reset near the contact than away from it. In addition, Rb-Sr whole-rock ages were determined on samples obtained at, near, and removed from the contact. The whole-rock isochron age is 1.5+0.1 billion years, in close agreement with earlier work by Simmons and Hedge (1978). The Rb and Sr analyses also indicated that there was no gain of these elements in the Idaho Springs Formation from the Eldora stock except possibly within the 1-to-3 m contact zone where some mixing of magmatic fluids with the metamorphic rocks occurred.

To further investigate the matter of closed versus open system conditions, as well as to address the problem of conductive versus convective cooling, trace element and stable isotopic analyses of the samples used for Rb-Sr whole-rock geochronology were carried out. The rare earth/chondrite ratio versus rare-earth atomic number distribution plot is shown in Fig. 2. Samples 1a and 1b are from fresh stock material and samples 2 and 3 from stock-plus-metamorphic rocks in the 1-to 3 m contact zone. These four curves are all similar and show pronounced enrichment of the light rare earth elements (LREE). Curves 5a and 6a are from mafic units of the Idaho Springs

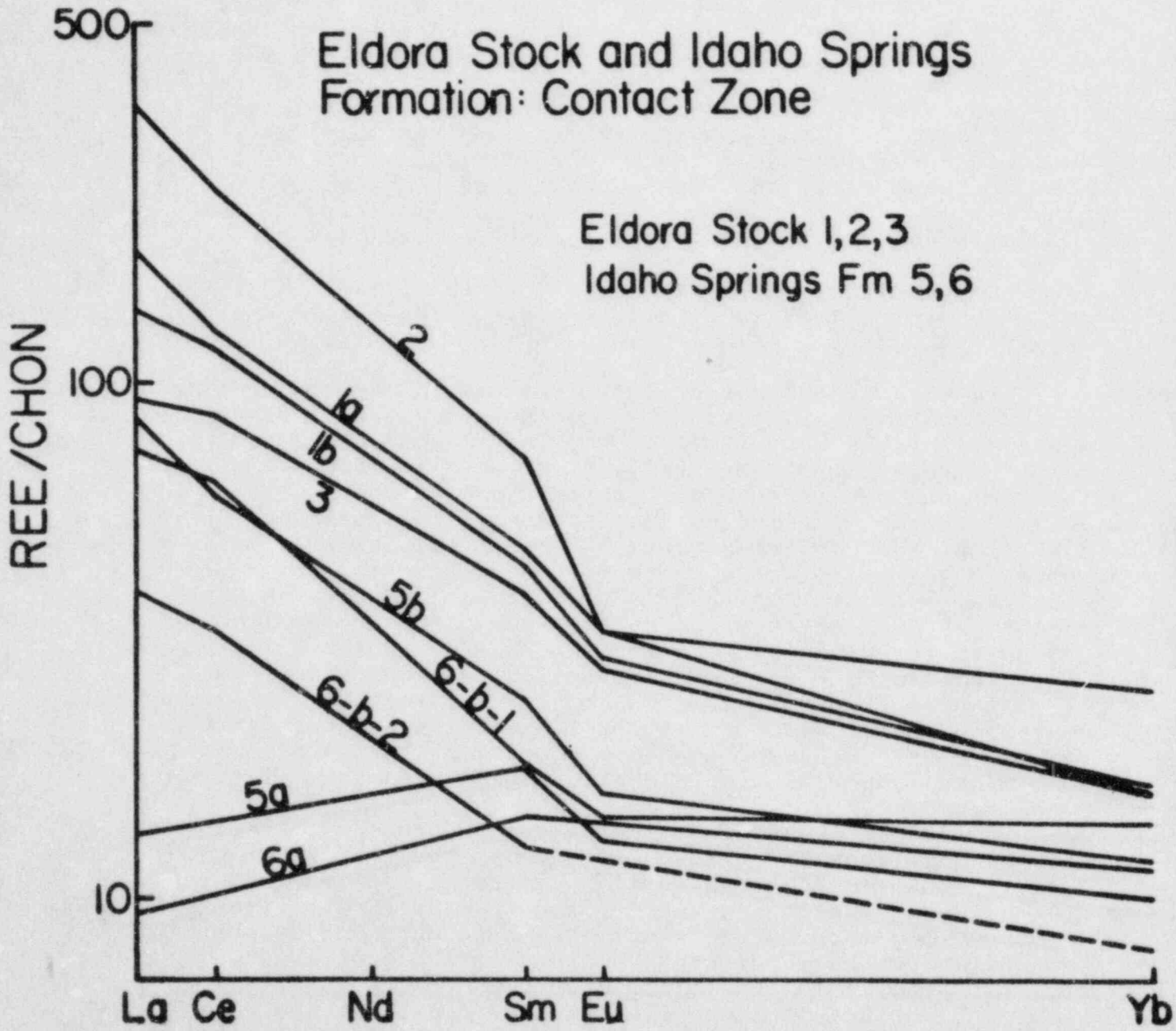

Figure 2. Rare earth element distribution plots for Eldora stock (Nos. 1a, 1b), Idaho Springs Formation (5a, 5b, 6a, 6b), and mixed samples (2, 3).

Formation, whereas curves 5b, 6b-1 and 6b-2 are from felsic units. The LREE are depleted in the mafic units but enriched in the felsic units; this behavior is noted not only for these samples taken 20-to-25 m from the contact (nos. 5, 6), but also for samples taken 2,500 m from the contact where resetting of K-Ar mineral systematics due to heat from the contact is not noted. Our interpretation of these data is that some REE partitioning between mafic and felsic rocks took place during the Precambrian regional metamorphism mentioned earlier. Open system conditions apparently existed at that time as evidenced by the formation of secretion pegmatites, some of which are enriched in Eu whereas others are depleted, especially when adjacent to mafic units.

The stable oxygen isotopic data show a distinct contrast between the Eldora stock and the Idaho Springs Formation. Del ^{18}O values for the stock and stock-metamorphic mixes (in the contact zone) are confined to a relatively narrow range (~8.0-9.0 o/oo) compared with those of the Idaho Springs Formation (~7.5-11.5 o/oo). This indicates essentially closed system conditions for oxygen in the intruded rocks and no exchange of oxygen between the stock and the Idaho Springs Formation. In turn, this implies a lack of hydrothermal convective cooling, usually accompanied by hydrothermal solutions, (Parmentier and Schedl, 1981) and cooling by conduction appears most likely.

The location and abundance of uranium near and away from the contact were determined by fission track radiography and gamma spectrometry (Flexser and Wollenberg, 1981). It was found that the occurrence of uranium is controlled predominantly by primary accessory minerals, both in the stock and in the Idaho Springs Formation. These accessories are zircon, sphene, monazite, allanite, opaque minerals, and an unidentified highly uraniferous mineral present only in the Eldora intrusive (Figure 3.) Secondary migration of uranium due to the intrusion of the stock has occurred, but on a small scale and only within a few meters of the contact. There is no indication of systematic enrichment or depletion in uranium, in either country rock or stock, as a function of distance from the contact. Migration of uranium is probably due to local redistribution from the accessory minerals by diffusion; there is no evidence to suggest that transport of uranium by circulating hydrothermal solutions in fractures played a significant role.

In summary, at the time of intrusion of the Eldora Stock and following its intrusion, the rocks of the Idaho Springs Formation were of low porosity and permeability, and the numerous fracture fillings and veinlets are prestock in age. In the 0-3m zone at the contact, there was mixing of some fluids from the Eldora stock due to infiltration into cracked and deformed parts of the Idaho Springs Formation accompanying

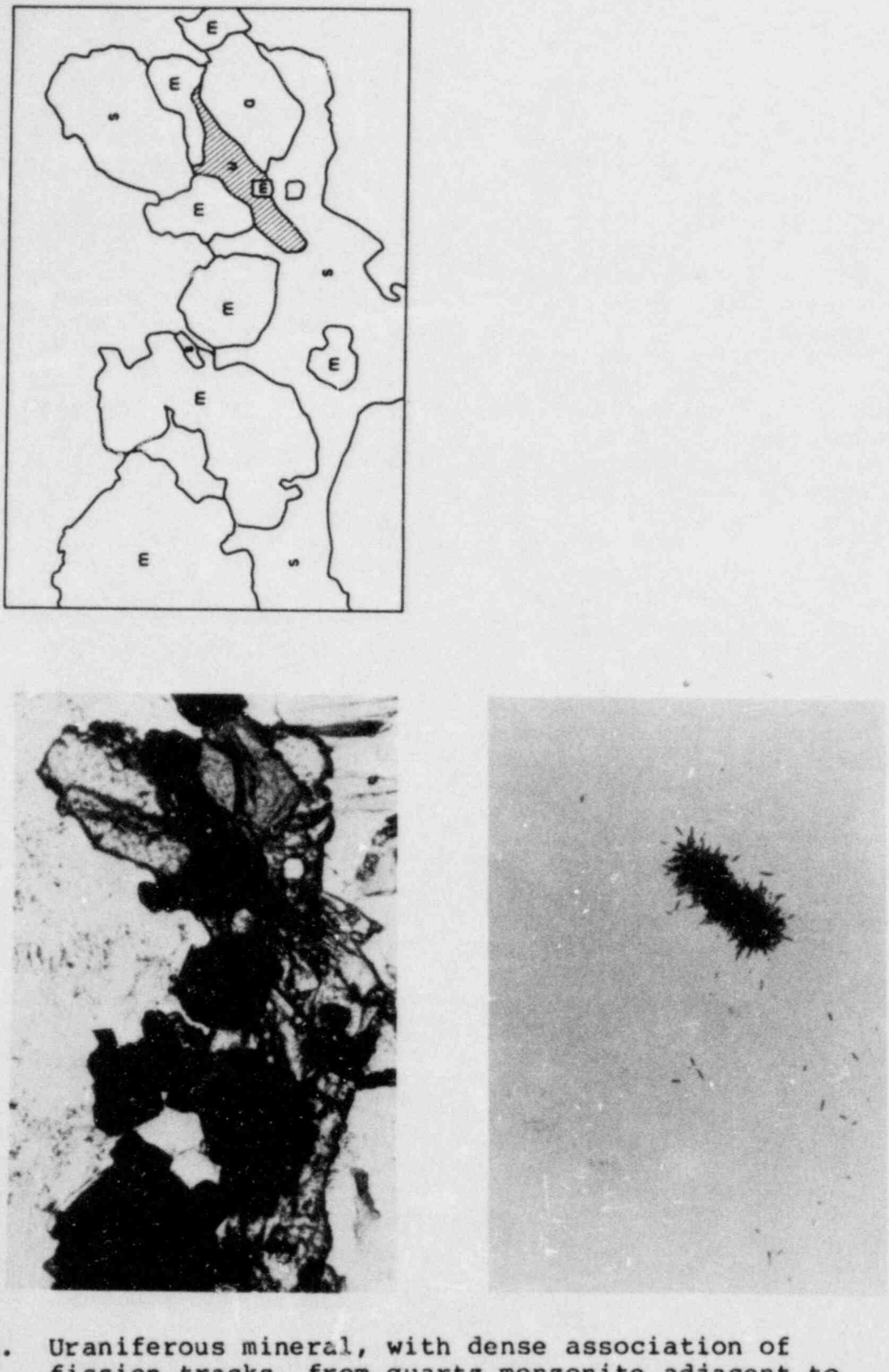

Figure 3. Uraniferous mineral, with dense association of fission tracks, from quartz monzonite adjacent to contact with country rock. Sparser fission tracks are associated with sphene. Plane-polarized light. (u-uraniferous mineral; s-sphene; m-magnetite: a-allanite; d-diopside; h-hematite. Lighter areas are feldspars and quartz).

emplacement. With the exception of this zone, closed system conditions, over the 10^5 to 10^6 years of stock crystallization and cooling, are demonstrated by the geochemical data. The data also indicate that subsequent to intrusion and cooling of the stock, there has been no appreciable migration or redistribution of elements within the gneiss over the zone investigated. If rocks of the Idaho Springs (or equivalent) formation were to be used for the storage of radioactive waste, especially when one considers the very small volume of canisters and their lower temperatures, breaching of canisters would probably result in only meter-scale migration of radionuclides. In this respect, we consider rocks of the character of the Idaho Springs gneiss suitable for storage of radioactive waste.

5.4.2.2 Uranium Veins at Marysvale, Utah

Examination of the distribution and abundance of uranium in and away from veins at Marysvale, Utah (Shea, 1982) also points out the excellent retentivity of this element by crystalline rock. Here the country rock is predominantly a quartz monzonite stock, emplaced in a volcanic terrane 23 million years ago and subsequently intruded by granite at 20 m.y. Both intrusives host uranium veins, emplaced as recently as 10 million years ago. Fission-track radiography disclosed that uranium moved only a few cm at most from veins containing up to 10% U; the movement was primarily by diffusion in microcracks and around grain boundaries. This occurrence adds to the evidence from the Eldora-Idaho Springs investigation that some crystalline rock terranes have excellent characteristics for the retention of radionuclides.

5.4.3 TUFF: The Alamosa River Stock - La Jara Tuff contact zone

As described in the preceeding section, at Eldora, Colorado there was apparently no circulating hydrothermal system accompanying or subsequent to the intrusion of quartz monzonitic magma into a Precambrian crystalline terrane. In contrast, the presence of strong hydrothermal circulation in tuffaceous rock in response to the intrusion of the Alamosa River stock near Platoro, Colorado was evident from oxygen isotope ratios measured by Williams (1980) on samples collected over a broad region. Based on this evidence, we have investigated the contact zone and areas away from the contact between the stock and the intruded rocks -- the La Jara member of the Treasure Mountain tuff, and the Summitville andesite -- primarily to determine if radioelements and fission-product-analogue trace elements moved from the monzonite into the tuff or andesite, or moved within the tuff, in response to the circulating hydrothermal system.

The Platoro caldera complex encompasses the Summitville and Platoro calderas and the Alamosa River stock. The stock, of monzonitic composition, was emplaced at 29.1 $\pm$ 1.2 MYBP

into predominantly andesitic volcanics forming and filling caldera structures (Lipman, 1975). The La Jara is predominantly a densely welded and devitrified ash flow tuff primarily of phenocryst rich quartz latite, ejected by an explosive event at 29.8 ± 1.2 MYBP.

Based on analyses of oxygen isotope ratios in 260 minerals and whole rock samples from the Alamosa River stock region, Williams (1980) suggested that the heat from the stock and other small intrusions, which range in age from 28 to 22.6 my (Lipman, 1975), initiated extensive hydrothermal circulation. A roughly concentric aureole of $\delta^{18}O$ depletion was noted around the south and east margins of the stock, with depletion enhanced along two major faults, attesting to the importance of fracture permeability in the circulation of this system. Temperatures of the hydrothermal system were estimated by Williams (1980) to have been in the range 250-370°C.

For our studies, samples from the Alamosa River stock area were collected at several locations as shown in Figure 4. A detailed traverse was made across the intrusive-tuff contact, as well as regional traverses in the tuff and in the andesite away from the stock, and samples were analyzed by neutron activation and fission-track methods to determine the distribution of radio- and trace elements.

Thin-section petrography shows that alteration of the tuff related to the monzonite contact has affected both the phenocrysts and the interstitial matrix. The progression of alteration starts within 60m of the contact with the development of calcite, intergrown with the fine quartz-feldspar mosaic of the matrix. Within 40 m of the contact chlorite and sericite appear in the matrix, as well as stringers and overgrowths of quartz which increase in abundance and coarseness toward the contact. Epidote also becomes a common matrix alteration within 12 m of the contact. Phenocryst alteration in the tuff more than 60 m from the contact is mainly confined to biotite, which is partly altered to fine opaque grains and sphene. Closer to the contact, pyroxene grains are altered to an opaque mineral, probably magnetite, and within 30 m of the contact biotite grains have been reduced to mere streaks of fine opaque grains, with associated epidote and sphene.

The distribution of uranium in rocks of this contact zone, represented by a traverse at Telluride Mountain (Figure 4), was examined by fission-track radiography. Uranium in the monzonite is mainly confined to minute accessory grains (probably zircon) which occur most typically in grains of potassium feldspar. Uranium also occurs, though more rarely, with altered mafic grains in monzonite close to the contact, and is probably associated there with very fine sphene. In contrast to the monzonite, the tuff rarely contains uranium-bearing accessory grains. Instead, U in the tuff usually occurs in low concentrations in the fine feldspar-quartz intergrowth comprising the matrix between phenocryst grains.

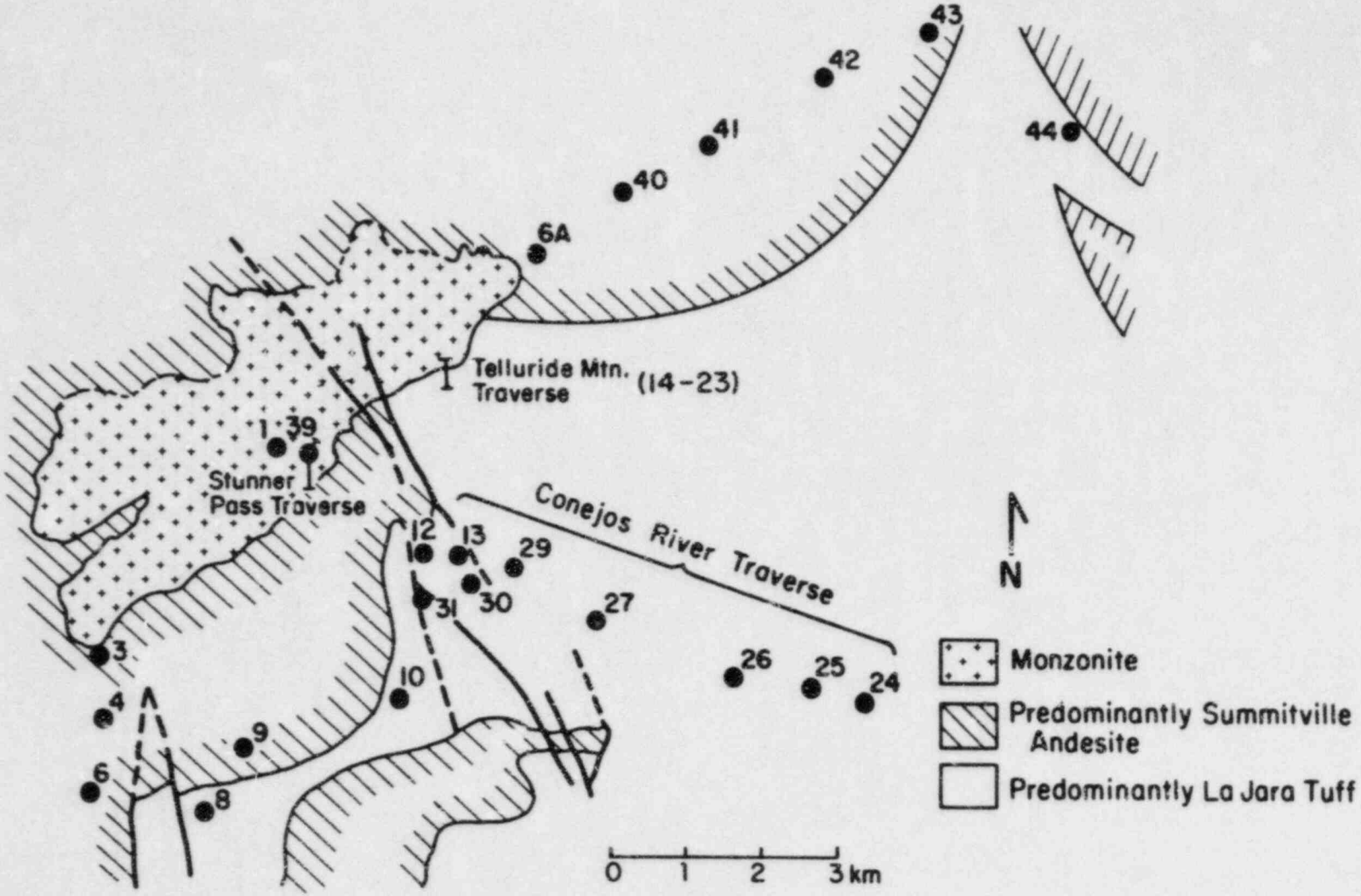

Figure 4. Simplified geologic map of the Platoro area, showing sampling traverses in monzonite, tuff and andesite.

The actual contact between monzonite and tuff, identifiable in thin sections, is marked by a dense intergrowth of epidote and lesser sphene. Uranium is often associated there with sphene, but is otherwise absent from the contact. The contact is also cut by fine hematite-filled fractures extending into adjacent tuff and monzonite. Uranium does not appear to be asociated with these fractures within the immediate contact zone or on either side of the contact.

Results of neutron activation analyses of some trace elements in samples of monzonite and tuff from the meter-scale traverse across the contact at Telluride Mountain comprise Figure 5. Strong contrasts between monzonite and tuff are evident, with higher contents of Cs, Rb, Sc, V, Fe, Th, U and Co in the monzonite. On the 10-meter scale of sampling, there are suggestions of gradients in Cs, Th and Co in the tuff, with abundances of these elements increasing towards the contact. In general, the elements studied with the exception of Cs, Th and Co, show no evidence for migration between the stock and intruded rocks. These observations, together with petrographic investigation (Wollenberg et al., 1983), indicate that elemental distributions in the rocks appear to be mineralogically controlled, and local whole-rock chemical variations reflect mineralogical variations. On a broader scale, analyses of samples from a regional traverse (Figure 6), extending several kilometers from the contact, indicate that there are no apparent chemical gradients to match the regional gradients in whole-rock $\delta^{18}O$ in the La Jara tuff.

The effects of alteration on trace element abundances are illustrated by plotting their variations against those of thorium (Figure 7a, b, and c). Strongly altered tuff is enriched in Cs, Sr, and Rb and depleted in La and Fe relative to the less altered tuff. Alteration effects are less apparent in the monzonite, though altered samples are high in Th and relatively low in La and Fe. The general high degree of correlation between U and Th, irrespective of degree of alteration and distance from the contact, contrasts with the lack of correlations between Th and both Sr and Cs. Weak correlations with Th hold (in all but the strongly altered samples) for Rb and La, and for Fe in tuff and monzonite. These observations suggest that Sr and Cs were relatively mobile in response to alteration, while La, Rb, and Fe were less affected, and U and Th were essentially unaffected by alteration, and thus were relatively immobile.

An epidotized breccia zone at the contact between the monzonite and La Jara tuff was sampled in detail. The breccia samples were divided into a dark green, epidote-rich sample (14a) and an epidote-poor sample (14b). The stock sample, 15, was collected two meters from the contact. The epidote-rich sample possesses a low total REE content (Figure 8). The epidote-poor sample shows a pattern very similar to that of the monzonite. When compared to all other data, the tuffaceous,

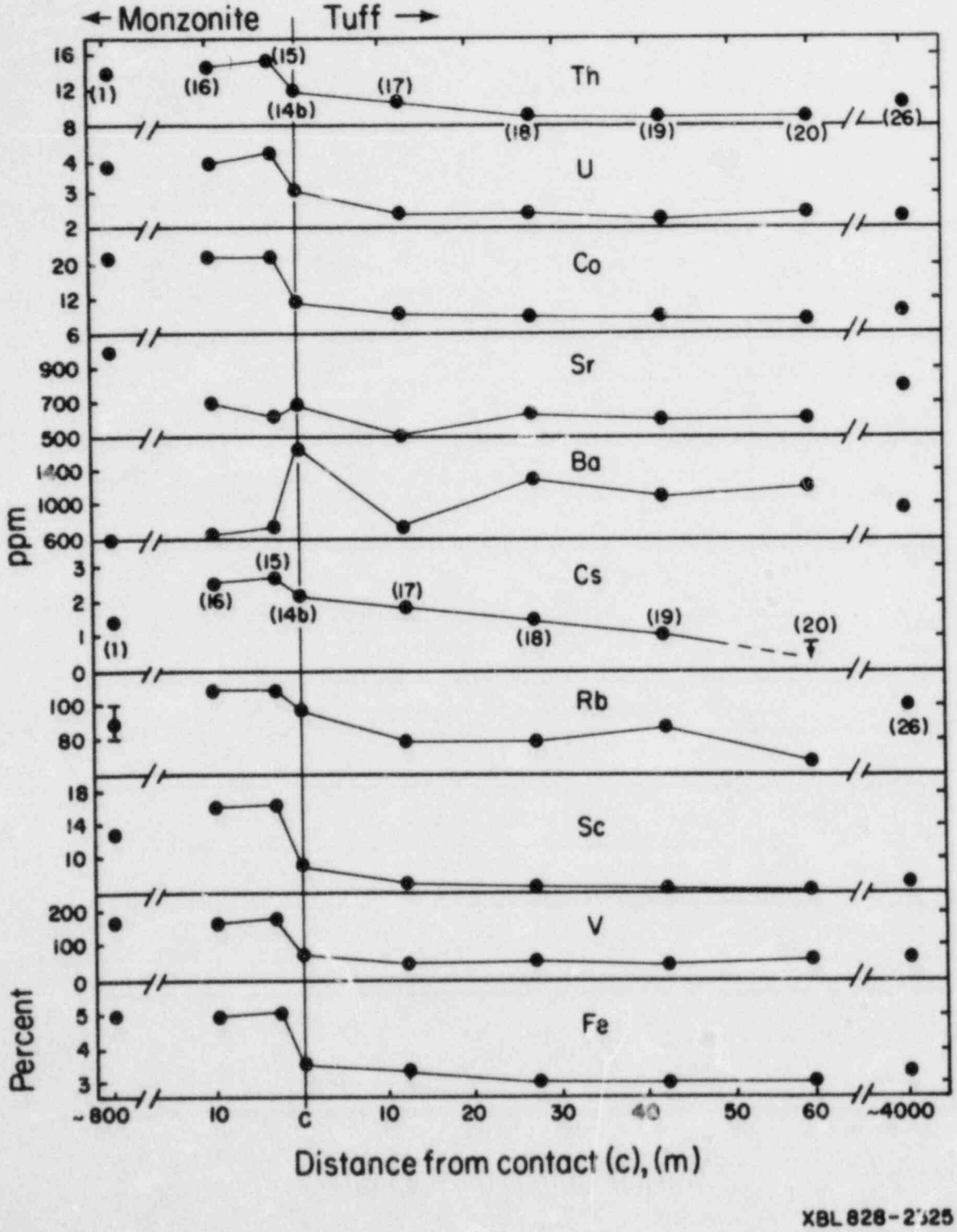

Figure 5. Element variations across the contact between monzonite and tuff, Telluride Mountain traverse.

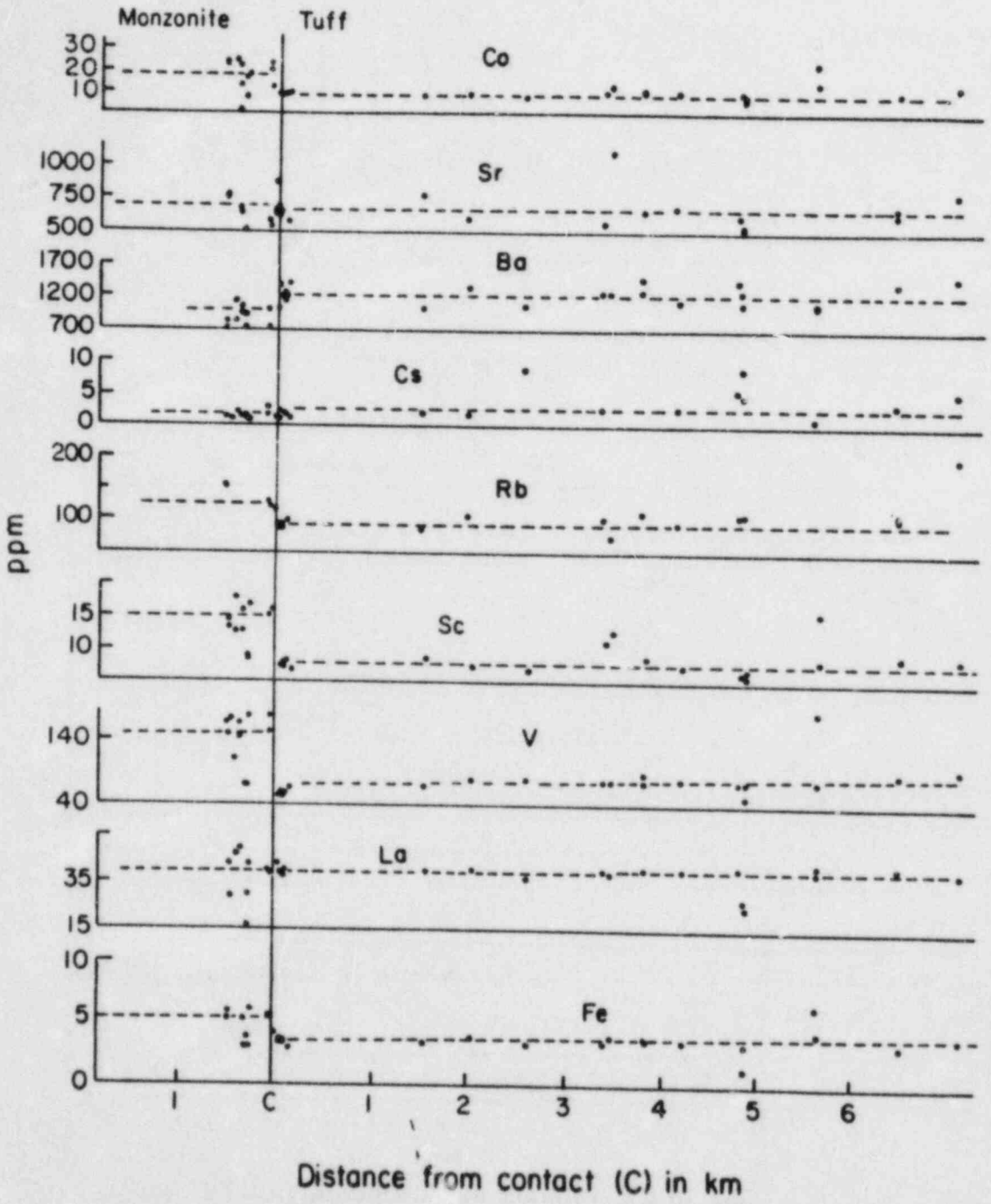

Figure 6. Element variations with distance from the contact between monzonite and tuff, Platoro region, Colorado.

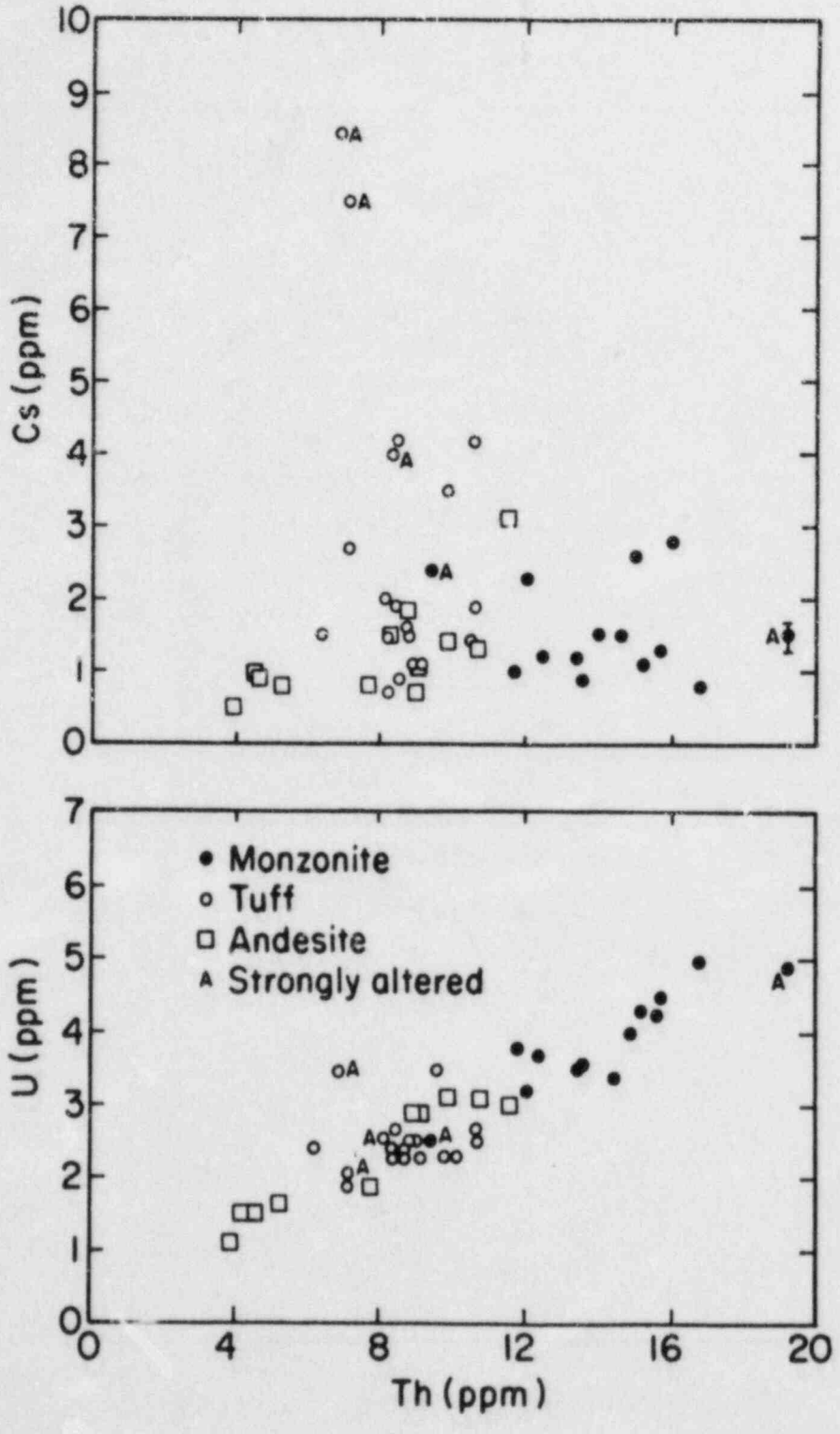

Figure 7a. Cesium and uranium versus thorium in strongly altered and less altered tuff, monzonite and andesite of the Platoro caldera.

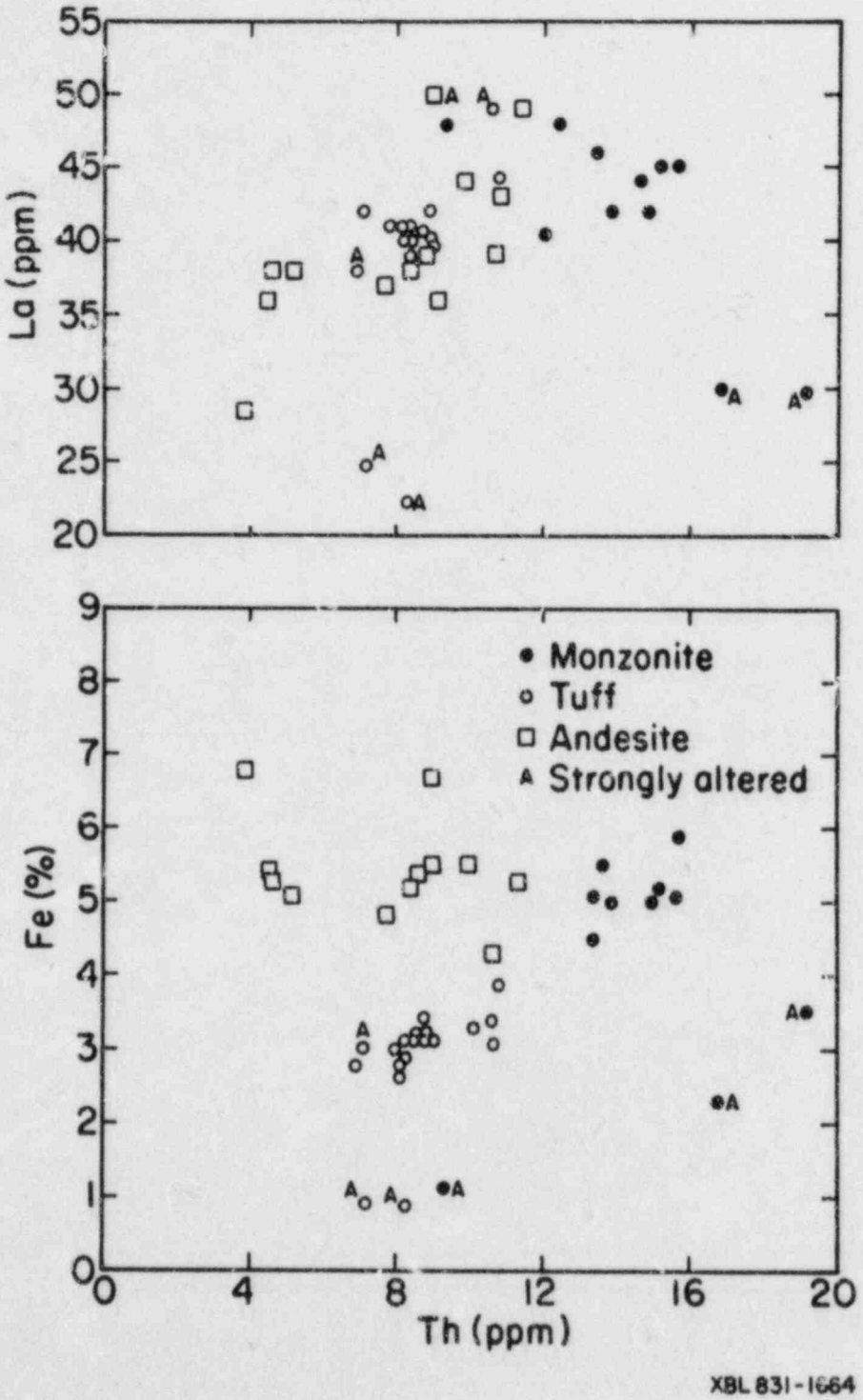

Figure 7b. Lanthanum and iron versus thorium in strongly altered and less altered tuff, monzonite and andesite of the Platoro caldera.

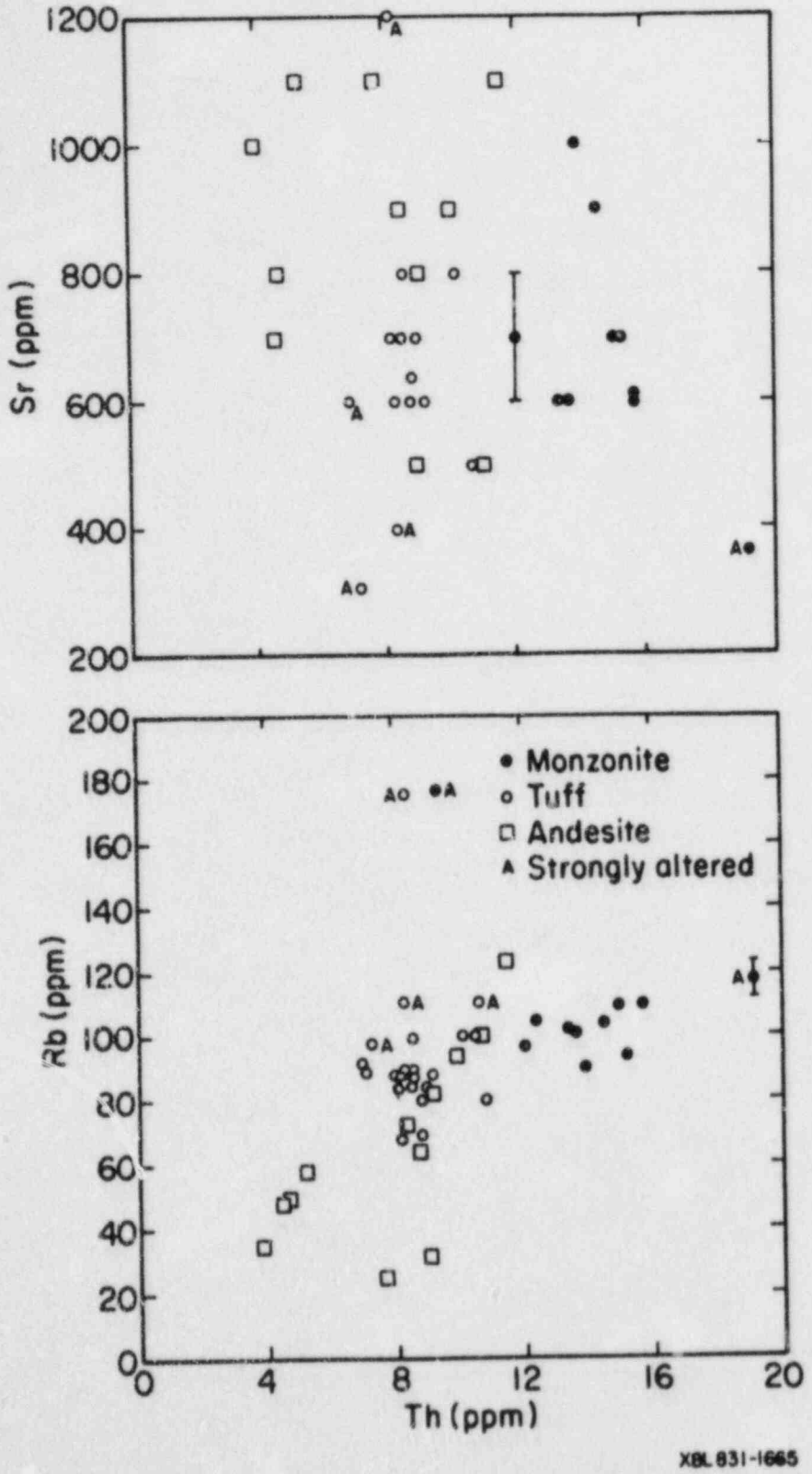

Figure 7c. Strontium and rubidium versus thorium in strongly altered and less altered tuff, monzonite and andesite of the Platoro caldera.

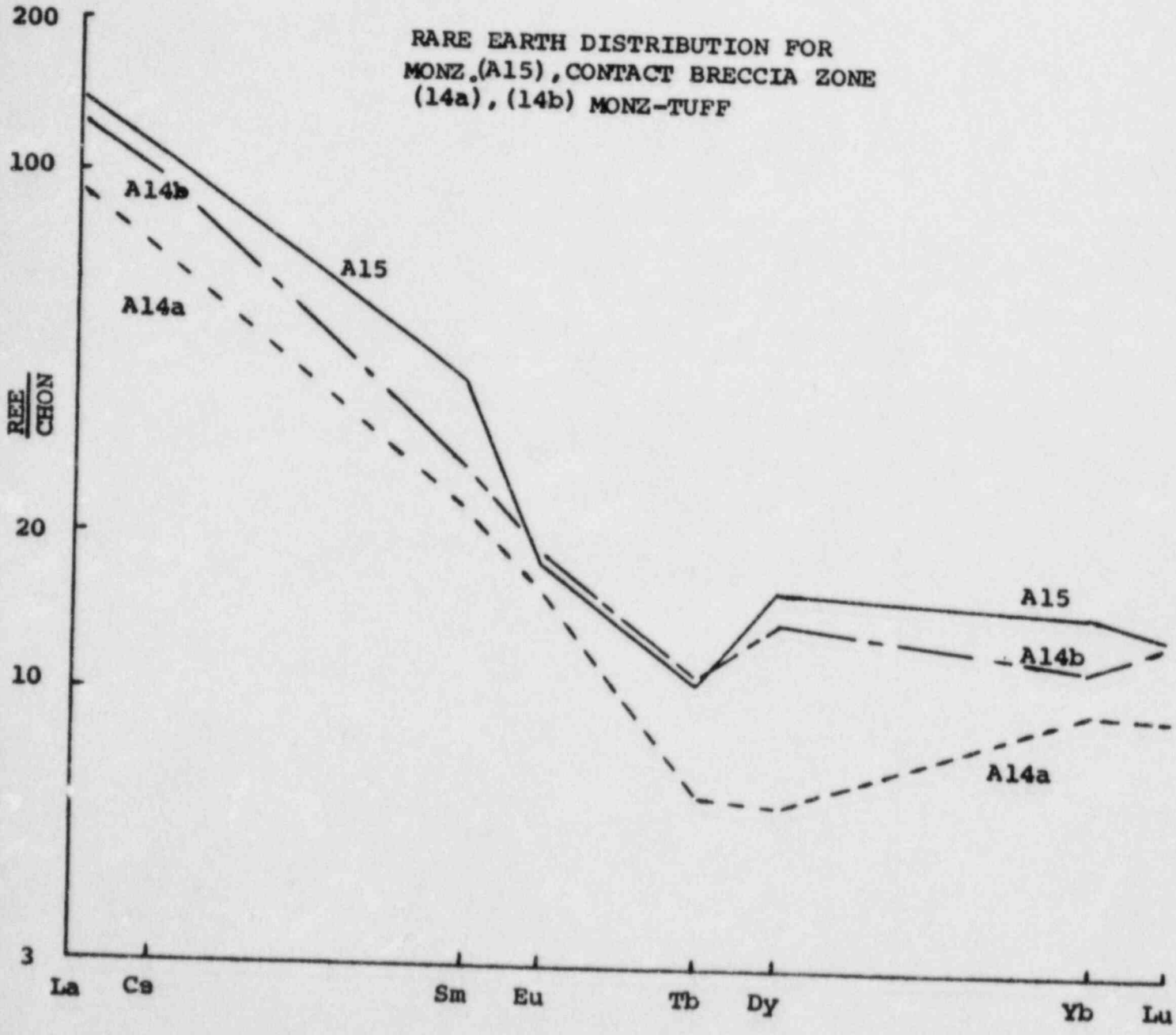

Figure 8. Rare earth distribution for monzonite (A15), contact breccia zone (14a), (14b) monzonite-tuff.

epidote-rich sample is depleted in REE, and this may be due to the effect of the intrusion, hydrothermal activity or other factors.

Oxygen isotope data, obtained for samples from the Telluride Mountain traverse show a broad variation of $\delta^{18}O$ values of the tuff, ranging from + 0.8 °/oo to 3.6 °/oo in the zone within 60 m of the contact. Values in the monzonite within 10 m of the contact are +2 °/oo. The general degree of depletion in the monzonite and in the tuff is consistent with previous data (Williams, 1980). However, the ^{18}O depletion does not, on the scale examined in the Telluride Mountain traverse, show any consistent gradient away from the intrusive in the tuff. Local fracture permeability variations appear to control the variations observed in the ^{18}O depletion of any specific sample. Although rock samples from the Telluride Mountain traverse are quite variable in $\delta^{18}O$, they are all significantly depleted relative to normal igneous rock. Water-rock mass ratios greater than 0.1 are implied for even the least ^{18}O-depleted samples. The samples lowest in $\delta^{18}O$ indicate water/rock values greater than 0.3.

Conclusions with regard to the Platoro occurrence are:

- The oxygen isotopic studies show the effect of extensive hydrothermal activity on the intruded rocks, as well as the host tuffaceous and flow rocks.

- Convective cooling has been demonstrated for the Alamosa River Stock.

- The distribution of U, Th, REE, V, K, and Ti in each rock is apparently unaffected by the intrusion or is the result of complete homogenization by the hydrothermal circulation. This is true also for Rb, Sr, and other elements, although for some of these elements there is no strong chemical gradient between the rocks. U and Th are essentially immobile with alteration, in comparison with other trace elements.

- Within ten meters of the contact, some elements show evidence for contact zone mobility.

- Both monzonite and tuff have essentially retained their bulk chemistry during and after intrusion.

- The absence of discernible large-scale elemental migration between the monzonite and tuff, even in a convective system, supports continued assessment of such rocks for nuclear waste repository consideration.

5.4.4 SALT

The migration of radio- and trace elements into salt in response to intrusion of a dike and over long time periods following its cooling may be analogous to migration of radionuclides in the near-field of a breached canister in a salt repository. Investigation of the abundance and contents of fluid inclusions in the salt may also be definitive in assessing the thermal and chemical effects of the dike. Potential analogue occurrences include a lamprophyre dike cutting the evaporite sequence of the Delaware Basin in southeastern New Mexico, a basaltic dike transecting salt of the Zechstein, West Germany, and Permain kimberlitic dikes cutting upper Silurian salt beds of Salina Basin in northwestern New York.

Gamma spectrometric measurements of a set of samples obtained of the basaltic dike, of Miocene age, and salt of the Zechstein indicated appreciable radioelement contents of the dike (U = 2.1 ppm, Th = 7.6 ppm), while radioelement contents of the salt at and away from the contact are below detectability limits. A similar situation was observed in a set of samples of kimberlite dikes (U = 1.5-1.9 ppm, Th = 11.7-12.6 ppm) and salt obtained from underground exposures at the Cayuga mine, New York (Figure 9). Preliminary investigation of fluid inclusions in salt samples from the Cayuga mine by D.K. Smith (1983) indicates that their homogenization temperatures exceeded 380°C.

The Cayuga set remains to be examined in more detail petrographically, and selected samples of salt and dike analyzed for trace elements by neutron activation techniques. More samples will be prepared for examination of fluid inclusions, their abundance and configuration, and analyses of their contents.

Preliminary data then suggest that U and Th have not migrated appreciably from the dikes into salt, either in response to injection of the dikes or over the tens to hundreds of millions of years subsequent to their cooling.

5.4.5 BASALT

Investigations of natural analogues in basalt include a contact zone between a rhyodacite dike and a Columbia River Basalt flow, comparison of strontium isotope ratios of fracture-filling and rock matrix minerals in the Grande Ronde Basalt (the subject of the companion paper by Brookins et al., 1983), and the petrology and geochemistry of samples from a geothermal system at Newberry, Oregon where temperatures presently span the range of those expected in the near field of a repository. This latter study is described below.

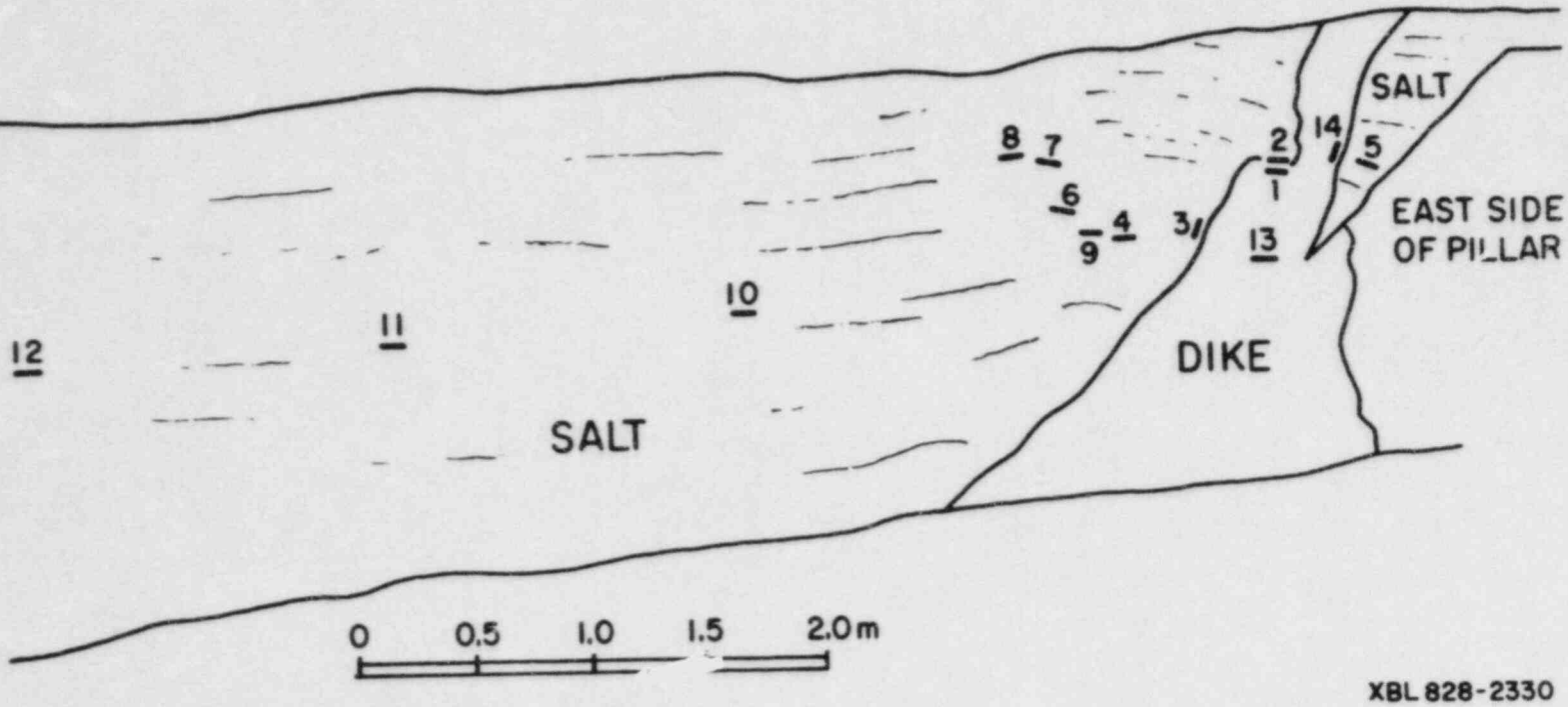

Figure 9. Sketch profile (from photographs) of the south face of a pillar in the Cayuga Salt Mine, New York, showing the locations of samples of the salt and the intruding kimberlite dike.

5.4.5.1 Newberry, Oregon: A Present-day Hydrothermal System

A set of samples of andesitic basalt, from a hydrothermal regime where temperatures range from 150 to 265°C, was obtained from core from a 950m deep hole drilled by the USGS in the Newberry Caldera, Oregon (Macleod and Sammel, 1982). Saturated rock at these temperatures may be analogous to conditions in the near-field of a repository, within a few hundred years following emplacement of radioactive waste.

Twenty-four samples from the U.S. Geological Survey's core repository in Vancouver, Washington were selected from the lower 200 m of the hole, encompassing andesitic basalt that exhibits varying degrees of brecciation and alteration. The alteration mineral assemblage in the basalt was preliminarily documented by Keith and Barger (1983) and is shown in Figure 10. The generally straight temperature gradient in the lower portion of the hole suggests conductive thermal conditions, so that, as expected at the Hanford Reservation, the Newberry basalt flows are low-permeability layers that inhibit vertical fluid flow. Some horizontal fluid flow probably occurs along flow-top breccia zones, indicated by the strongly altered brecciated zones in the core.

Preliminary whole-rock gamma spectrometric analyses of U, Th and K in core from the lower 200 m of Newberry 2 are plotted in Figure 11. A general decrease of U and Th with increasing depth in the basalt is evident, and appears to be independent of the degree of alteration. This decrease may be attributed to more prevalent oxidizing conditions at depth, evidenced by the increasing scarcity of sulfide minerals and appearance of sulfates. However, a definitive explanation for this variation awaits detailed petrography to determine more accurately the alteration mineralogy; radiography to determine the mineral association of these elements; and, ultimately, analysis of fluid samples to determine Eh and pH conditions at depth. Neutron activation analyses will also more accurately disclose the distribution of radio- and fission-product-analogue elements and their association with alteration minerals and temperature zones. The sample set also remains available to examine an analogue of the effects of exposure to high temperature on the structural properties of basalt in the near-field of a repository.

5.4.6 CONCLUSIONS and RECOMMENDATIONS

Geochemical investigations of contact zones where stocks have intruded gneiss and tuff indicate that U, Th, and some trace elements have not migrated appreciably from the intrusive rock, either in response to the intrusions, or over long time periods subsequent to the intrusions. Examination of the occurrences of U veins in granite and of dikes cutting basalt and salt, although preliminary, also suggests that there has been no appreciable migration of radioelements from the

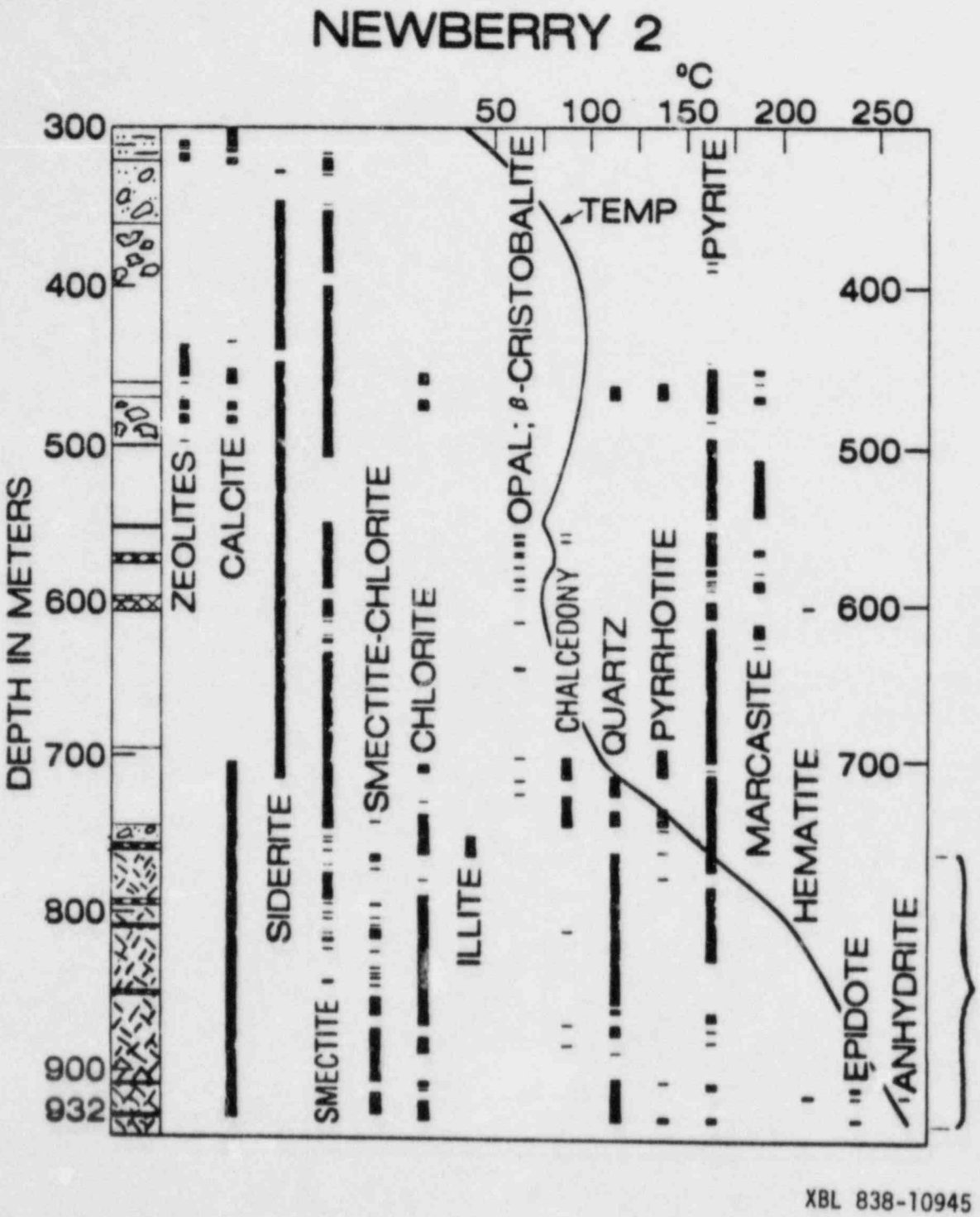

Figure 10. Preliminary observations of the mineralogy in the Newberry 2 hole (Keith and Barger, 1982). The bracketed basaltic zone in the bottom portion of the hole indicates the extent of our samples.

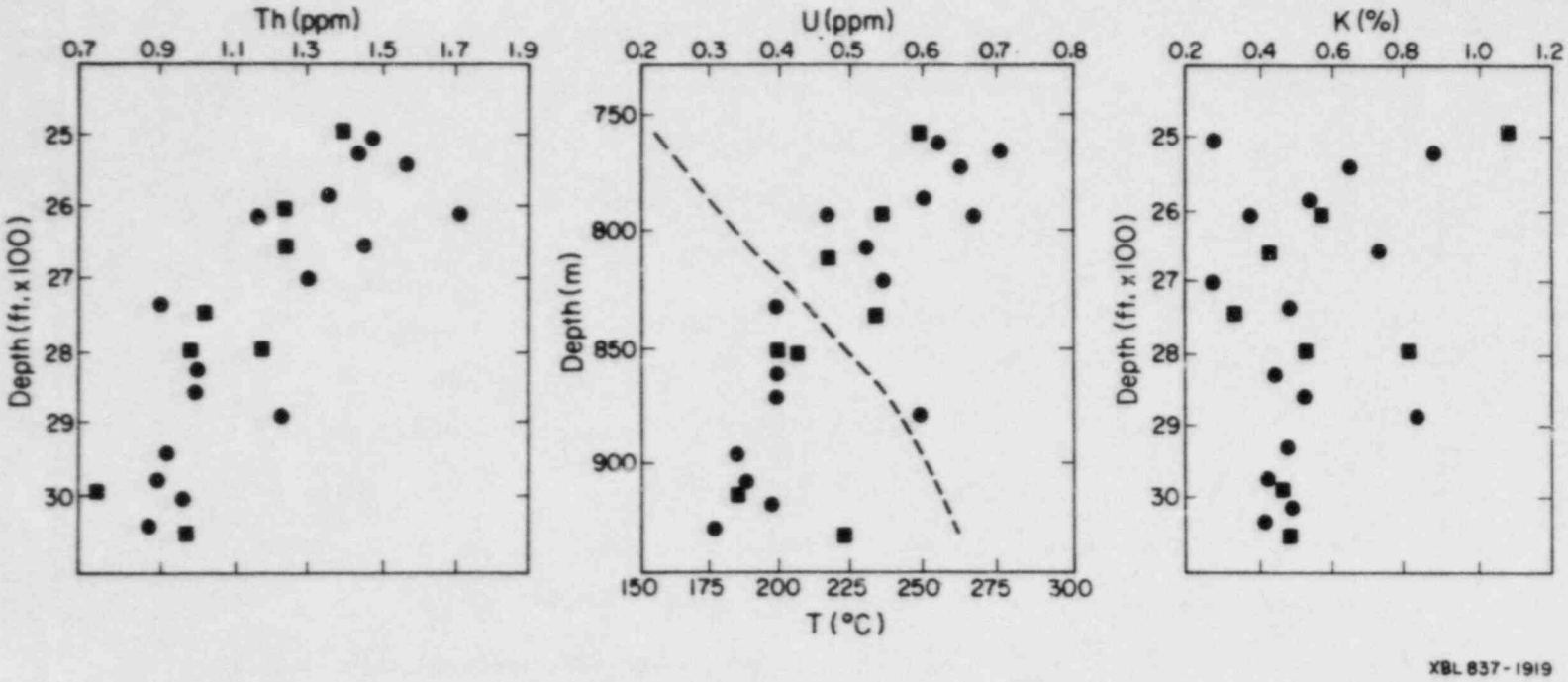

Figure 11. Variation with depth of radioelements in basalt of the Newberry 2 core. The most strongly altered samples are designated by squares. The dashed line is the temperature gradient determined by bottom-hole measurements during drilling (Macleod and Sammel, 1982).

intrusives into these host rocks. The lack of migration of U and Th is due partly to their principal location in the accessory minerals of the intrusive rocks investigated. This lends credence to suggestions that waste forms modeled after these minerals would successfully retain actinide elements over time spans exceeding those of concern to repositories. Lack of migration of radio- and fission-product-analogue elements also attests to the capabilities of the rock types studied to retard the movement of these elements under conditions comparable to or more stringent than those expected for waste repositories. Therefore, this also lends encouragement to consideration of these rock types as candidate hosts for repositories.

Continuing investigation of basalt and instigation of studies of tuff and granitic rock in present-day active hydrothermal systems where temperatures approximate those expected in the near-field of a repository, would disclose the distribution of elements, mineralogy, and mechanical characteristics of these rocks in conditions analogous to the repository environments.

ACKNOWLEDEMENTS

We thank R. Kuhn and W. Holser for providing samples from the Kalibergwerke Mine, and T.E.C. Keith and N. Macleod who provided preliminary data and arranged for us to obtain samples from the Newberry-2 collection.

REFERENCES

Brookins, D.G., Cohen, L.H., Wollenberg, H.A., and Abashian, M.S., "Radwaste Storage in Crystalline Rocks: A Natural Analog," International Atomic Energy Agency Symp. on Migration in the Terrestrial Environment of Long-Lived Radionuclides from the Nuclear Fuel Cycle (July 1981).

Brookins, D.G., Murphy, M.T., Wollenberg, H.A. and Flexser, S., "Geochemical and Strontium Isotopic Studies of Columbia River Basalts," this volume, 1983.

Flexser, S. and Wollenberg, H.A., "The distribution of uranium in and near the contact zone between the Tertiary Eldora Stock and the Precambrian Idaho Springs formation, Colorado;" Lawrence Berkeley Lab. Report LBL 14974 (1981).

Hart, S.R., Davis, G.L., Steiger, R.H., and Tilton, G.R., "A Comparison of the Isotopic Mineral Age Variations and Petrologic Changes Induced by Contact Metamorphism" in Radiometric Dating for Geologists, Interscience Publishers, N.Y. p. 73-100 (1968).

Keith, T.E.C. and Barger, K.E., "Hydrothermal alteration in core from Drill Hole Newberry 2, Oregon;" Trans. Amer. Geophys. Union (EOS) (abstract), v. 63, no. 45, p. 1128 (1982).

LBL, "Geochemical Assessment of Nuclear Waste Isolation," report of activities during the fiscal year 1981; Lawrence Berkeley Laboratory Report, LBID-429, (1982).

Lipman, P.W., "Evolution of the Platoro Caldera Complex and related volcanic rocks, southesastern San Juan Mountains, Colorado;" U.S. Geol. Serv. Professional Paper 852 (1975).

Macleod, N.S., and Sammel, E.A., "Newberry Volcano, Oregon, a Cascade Range geothermal prospect," California Geology, November, 1982, p. 235-244 (1982).

Maurette, M., "Fossil nuclear reactors," Ann. Rev. Nucl. Sci., 26: p. 319-350, (1976).

Papike, J.J., Shearer, C.K., Simon, S.B., Laul, J.C. and Walker, R.J., "Pegmatite/Wallrock interactions, Black Hills, South Dakota: natural analogs for radionuclide migration": Trans., Amer. Geophy. Union (EOS), V. 64, p. 351 (abstract), (1983).

Parmentier, E.M. and Schedl, A. "Thermal Aureoles of Igneous Intrusions: Some Possible Indications of Hydrothermal Convective Cooling," J. Geol. 72, 1-22 (1981).

REFERENCES (Continued)

Shea, M., "Uranium migration at Marysville, Utah: a natural analog for radioactive waste isolation," MS. Thesis, University of California, Riverside, 120 p. (1982).

Simmons, E.C. and Hedge, C.E., "Minor-Element and Sr-Isotope Geochemistry of Tertiary Stocks, Colorado Mineral Belt," Contr. Mineral. Petrol. 67, 379-396 (1978).

Smith, D.K., Heating and freezing stage experiments, University of California, Riverside, (private communication, 1983).

Williams, A.E., "Investigation of oxygen-18 depletion of igneous rocks and ancient meteoric-hydrothermal circulation in the Alamosa River Stock region," Colorado; Ph. D. Thesis, Brown University, (1980).

Wollenberg, H., Flexser, S., Brookins, D., Abashian, M., Cohen, L. and Williams, A., "Geologic Systems as Analogues for long-term radioactive waste isolation," Task 5 in Geochemical Assessment of Nuclear Waste Isolation; report of activities during fiscal year 1982 to the Nuclear Regulatory Commission; Lawrence Berkeley Laboratory Report, LBL-16045, 1983.

5.5 EFFECT OF AGED WASTE PACKAGE AND AGED BASALT ON RADIOELEMENT RELEASE*

M. G. Seitz, G. F. Vandegrift, D. L. Bowers, and T. J. Gerding

Argonne National Laboratory, Argonne, IL 60439

Abstract

Results of experiments are described that combine backfill, radioactive waste, and repository host rock in a single flowing groundwater stream in a manner analogous to a hydraulic breach of a waste repository. The experimental design is used to identify the chemical interactions that would occur if repository components were breached by flowing water.

The result of most significant to issues of repository safety was that uranium, neptunium, and plutonium were found to move more rapidly through repository components that were altered to represent aging than through fresh materials. Two other parameters studied experimentally, the metal alloy used in the apparatus and an ionizing radiation field imposed on the experimental apparatus, had little or no measurable effect on radioactive element transport by flowing water.

Inasmuch as the alteration of the repository materials represents aging in an actual repository, it is concluded that changes with age will detrimentally affect the ability of a repository to isolate uranium, neptunium, and plutonium. Because these elements have long-lived radioactive isotopes in nuclear waste, the long-term performance is a major issue regarding the safety of a repository in basalt for nuclear waste.

5.5.1 Introduction

Disposal of radioactive waste in geologic formations may offer a practical method of permanently isolating the waste from the biosphere. For such disposal, solidified nuclear waste is surrounded by multiple barriers such as a metal canister and backfill, which isolate the radioactive waste. The flow of groundwater that would be allowed by the disruption of these barriers is the most credible mechanism that may jeopardize the safety of a waste repository. But even if groundwater infiltrates these barriers, then dissolves radioactive elements in the solid waste, and eventually transports

*Work supported by the U.S. Nuclear Regulatory Commission under Contract FIN A-2230.

the radioactivity into fissures and pores of the surrounding rock, the radioelements could react with the rock and again become immobile. Thus, the geologic formation itself is considered a barrier to the radioelements. So, both man-made barriers and the geologic formation could prevent the dispersal of radioactivity into the biosphere.

The detailed technical understanding of the possible retention of radioactivity by all these barriers is not simple. In a comprehensive description of the performance of the repository, there are enormous numbers of solution and sorbed species that participate in the chemical processes of dissolution, complexation, ion exchange, sorption, and precipitation. Reactions involving the chemical species are kinetically controlled and, thus, depend on groundwater flow rate. The reactions occur in the radiation and thermal fields that are centered on the waste itself. Moreover, the reactions change as the repository ages. Since the performance of a repository even after thousands of years is important for the safe disposal of the nuclear waste (Nuclear Regulatory Commission), the understanding of the long-term performance of the repository is also needed.

5.5.1.1 Issues Addressed by This Research

The general issues addressed in this work are:

1. Can we identify the interactions between repository components of most importance to repository safety under the conditions of the experiments. By corollary, can we demonstrate that some interactions are not important to issues of repository safety?

2. Do laboratory systems studies efficiently contribute to our understanding of safety issues related to repository performance?

3. Can we evaluate, using laboratory systems studies, commonly followed practices of repository design with regard to safety issues?

The specific issues addressed by the research are:

1. Do different metal alloys that are proposed for canisters of nuclear waste effect radioelement migration and hence repository safety?

2. Does radiolysis of groundwater solution produced experimentally effect radioelement migration and, hence, repository safety?

3. Does alteration of repository components such as is expected upon aging of a repository degrade repository performance or improve repository performance as commonly stated?

4. What concepts and measurements (of solubility products, leach rates, adsorption ratios, etc.) are sufficient to describe radioelement migration in systems with flowing groundwater?

5. Are experimental programs undertaken to support repository development properly designed to address the subject of repository safety?

In addition to these issues, a very specific goal of the work was to establish sets of data on radioelement migration collected under accurately measured conditions of temperature, water flow, water composition, etc. The data from this program would be useful in verifying predictions from computer codes of radioelement migration. This last goal of the work could be realized independently of whether or not the research uncovered new insight to the treatment of radioelement dispersal from a repository breached by flowing groundwater.

5.5.1.2 Background and Objectives

Much experimental work to evaluate the potential for dispersal of radioactivity has focused on a single process such as the leaching of solid nuclear waste or the adsorption of radioactivity by rock. Each process studied is very complex and merits individual scrutiny. Other fundamental studies have resulted in measurements of thermodynamic properties of solids and solutions. These measurements allow predictions to be made of chemical reactions in many geologic systems.

In contrast to these approaches of dissection and analyses, experiments have been run that combined various components in environments that might be expected in a waste repository. Since the flow of groundwater is the most credible mechanism to jeopardize the safety of a waste repository, one approach has been to use flowing groundwater to link components in experiments. Some studies have combined solid radioactive waste and repository host rock in flowing groundwater (Avagadro, A.; Seitz, M. G., 1981 a,b). The work was done with naturally fractured samples of impermeable rock (Seitz, M. G., 1981 a), as well as with permeable rock. The movement of radioelements were measured directly in these experiments, with the results of interactions on radioelement movement clearly apparent.

For example, the concentrations of a radioelement leached from the waste form were seen to effect directly the movement of that radioelement through rock (Seitz, M. G., 1981 b).

Other studies using flowing water have concentrated on the leaching of waste glass (Coles, D. G.; Strachen, D.) in distilled water or on bicarbonate solutions moving at differing flow rates. Studies have been performed of rock-water interactions in recirculating groundwaters subjected to a thermal gradient (Charles, R. W.). This latter technique, originally developed to study alteration in recirculating hydrothermal systems, is applicable to the general understanding of alteration in the thermal gradients that would surround a waste repository.

In another approach to systems studies, materials have been combined in autoclaves and subjected to elevated temperatures to cause them to react (Bischoff, J. L.; McCarthy, G. J.; Savage, D.; Scheetz, B. E.; Shade, J. W., 1980, 1982). Solution compositions and solid reaction products are monitored with time and temperature to gain an understanding of the progression of reaction products in the repository environment. These studies have focused on changes in major element compositions with the work on radioelements being directed to uranium (Scheetz, B. E.; Shade, J. W., 1982). In other studies of this type, the compatibility of repository components such as canister metals and groundwaters have been investigated using apparatus built in an autoclave (Bradley, D. J.).

In the work presented here, backfill, radioactive waste, and repository host rock are coupled in a flowing groundwater stream in a manner analogous to a breach of a waste repository (Vandegrift, G. F.). Using the experiments, we hoped to identify the chemical interactions important to migration that occur when repository components are combined. The phenomena leading to significant mobilization or retention of radioactive elements, once identified, could then be studied in detail in more conventional experiments.

The experimental program examined a waste repository in basalt. Bentonite mixed with basalt was considered as the backfill and borosilicate glass as the nuclear waste form.

5.5.1.3 Scope of Research

The experimental program is intended to identify the important processes that could lead to substantial dispersal of radioelements in flowing groundwater. The experimental design is of a simple, well defined system in which radioelement migration is measured directly. These measurements

are compared to predictions of radioelement migration obtained from results of simpler experiments and from calculations of computer-based models. Differences found in the comparisons can signal processes important to migration that have not been considered in simple tests or in calculations of radioelement migration. So, the results of this experimental program are intended to be used with other experimental and analytical approaches to gain understanding of radioelement migration.

Relationships between the results reported here and behavior expected in an actual repository can be complex. Specifically, no single scaling factor is intended to relate experimental results to repository behavior since a single correlation between experiment and repository parameters does not apply to all phenomena. However, measured parameters such as radioelement concentrations, distances of radioelement migration, and groundwater compositional changes can all be projected to conditions expected in a repository.

5.5.2 Methods

A schematic of the apparatus for these experiments is shown in Fig. 1. In an experiment, groundwater is pumped at a rate of 0.5 mL/h through the system so that it passes through the first vessel, which contains basalt chips, bentonite, and the nuclear waste form; then through the second vessel, which contains more bentonite and basalt chips; and then through a narrow basalt fissure in the third vessel. At this flow rate, water moves through the first and second vessels at a linear flow rate of 30 m/yr and through the basalt fissure at a rate of ~500 m/yr. The flow is maintained 30 days prior to the introduction of the radioactive waste to allow the groundwater and solids to adjust chemically. The apparatus is maintained at a temperature of 90°C, which is 40°C hotter than the ambient temperature of the Umtanum flow considered for the waste repository (Table 5-30, Rockwell Hanford Operations).

Solutions are collected continuously at the outlet of the core for the five month duration of the experiment, with the exception of intermittent sampling taking place at the outlets of the first and second vessels. These solutions are analyzed for stable and radioactive constituents. After termination of the experiment, the apparatus is dissassembled and materials are analyzed to determine the chemical and mineralogical changes and the distributions of radioelements that were leached from the waste form.

5.5.2.1 Analytical Methods

Water compositions were analyzed by emission spectroscopy, ion chromatography, and acid-base titrations. Uranium concentrations were measured by laser fluorescence spectrometry;

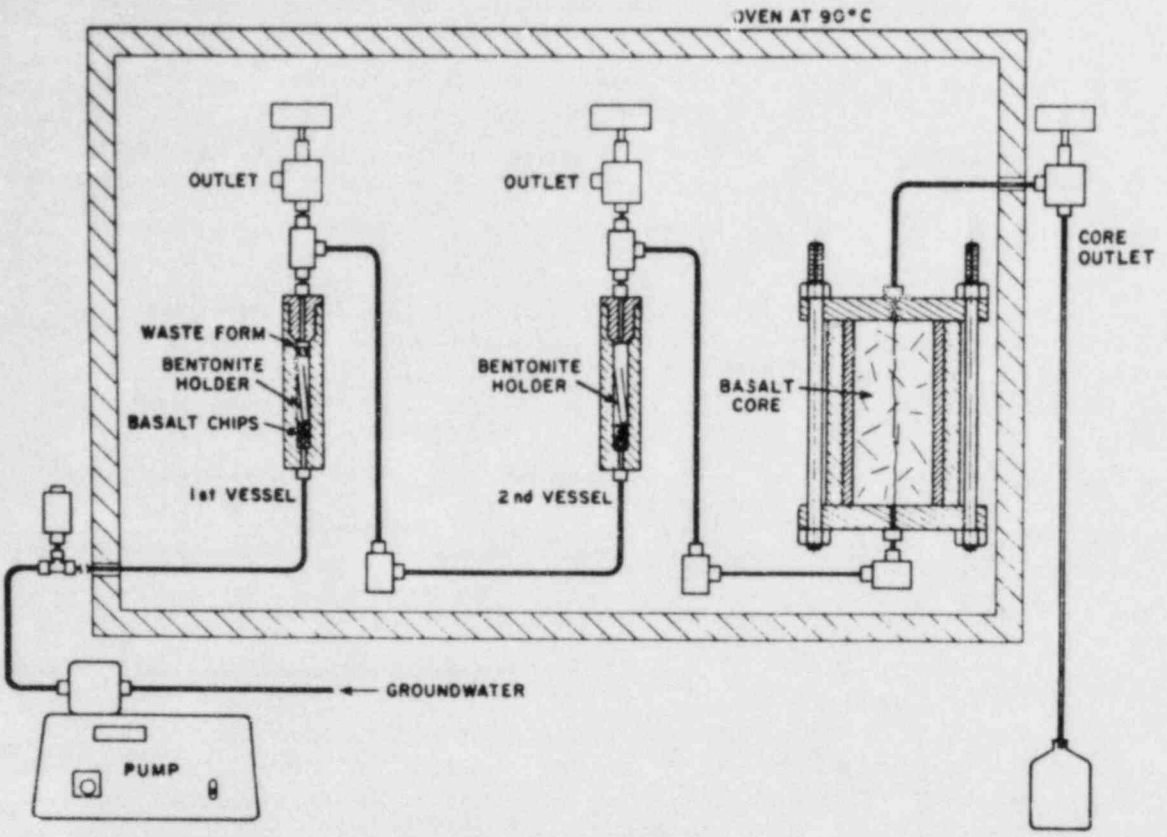

Fig. 1. Schematic of the experimental apparatus.

radioisotopic concentrations were determined by gamma- and alpha-counting analyses. Because of the high dissolved solid content (830 mg/L) of the eluant water, ^{239}Pu and ^{237}Np were separated from the dissolved solids by hexone extraction prior to analysis by alpha counting (Steindler, M. J., 1982). Analyses were performed on both filtered (0.1-μm pore size filters) and unfiltered water samples to determine characteristics of the suspended materials.

The bentonite and rock samples were subjected to elemental analyses by microprobe, X-ray diffraction analyses, and radioactivity-counting analysis, and were examined by optical microscopy.

5.5.2.2 Experiments

The initial two experiments were run to test if constructing the apparatus from different metal alloys would affect the results. A third experiment was performed in a gamma-radiation field (0.2 to 1.1 x 10^5 rad/h) to examine if changes in waste-form leaching and solution speciation would lead to substantially different behavior of the leached radioelements.

The fourth, fifth, and sixth experiments were performed with hydrothermally-altered materials to examine whether alteration, such as could occur upon aging of the repository components, would substantially modify the migration of the radioelements.

5.5.2.3 Experimental Materials

The water used in these experiments was prepared to represent the composition of groundwater from Well DC-6, Grande Ronde Formation, which samples water primarily from 200 m below the Umtanum unit on the U.S. DOE Hanford site (Gephart, R. E.). The water contains 830 mg/L total dissolved solids with sodium, chloride, sulfate, carbonate, bicarbonate, and silica the major constituents. Five other constituents, calcium, magnesium, potassium, borate, and fluoride, are present in lesser amounts and make up the balance, with the water having a pH of 10.1 at 25°C.

For the experiments, the water is sparged and stored under nitrogen gas to limit oxygen and CO_2 pickup. Prior to being pumped into the apparatus, the water was sparged with nitrogen bubbled through a chromous chloride solution to remove oxygen (computed to be below 1×10^{-20} M O_2, Seitz, M. G., 1979). The lowering of dissolved oxygen in water is not intended to determine the oxidation states of solutes in the water that dissolve from the solid waste or the rock. Rather, by reducing the oxygen in the water we allow the redox characteristics of the waste glass and rock to control oxidation states.

The rocks were taken from the Pomona flow in the vicinity of the Near Surface Test Facility at the Hanford, Washington, site. The Pomona flow consists of high-magnesium basalt (~7.0 wt % MgO, Ames, L. L.) and occurs at a depth of 250 m at the reference location for the proposed repository (Figure 6-1, Rockwell Hanford Operations).

Basalt cores were cut from the interior of rocks supplied by personnel of the Basalt Waste Isolation Project, were ground to size (6.83-cm diameter by 14.60-cm long, weighing ~1545 g), and were split to provide a flow path for the water. (The two halves of the core were held 0.017 cm apart by two strips of gold ribbon.)

Backfill in waste disposal may serve as a primary chemical barrier to radioelement migration. Bentonite mixed with crushed basalt has been proposed as one material to serve this function (Coons, W. E.; Turcotte, R. P.), and was used as the backfill in these experiments. Five grams of basalt having a surface area of ~30 cm^2 was used in each holder with bentonite. The bentonite is a source clay, SWy-1, of the Clay Mineral Society. It is primarily sodium smectite with albite, quartz,

mica, calcite, amorphous silica, aluminum oxide, and iron oxides as minor phases (Van Olphen, H.). The sample is from the Newcastle Formation (Cretaceous), Crook County, State of Wyoming.

The solid radioactive waste was prepared by mixing eight radioelements (^{241}Am, ^{238}U, ^{237}Np, ^{133}Ba, ^{141}Ce, ^{152}Eu, ^{137}Cs, ^{85}Sr) as dried oxides or chlorides with crushed frit of the 76-68 borosilicate waste glass. The frit was melted under argon gas at 1050°C for six hours, cooled, then annealed at 500°C before being cut into wafers with average weight of 0.4 g and average dimensions of 1.1 x 0.90 x 0.13 cm. The product was found to consist mostly of glass with ~0.8% by volume chromite, 0.2% by volume bubbles, and a tiny amount (~1 x 10^{-4}%) metal, possibly palladium or ruthenium. The alpha-active radioelements were uniform on a microscopic scale, with uranium in the oxidized (+6) valence state.

Materials of construction of vessels, tubing, and couplings for each experiment were either Hastelloy C-276* or Monel-400†.

5.5.2.4 Hydrothermal Alteration of Materials

Three fissured basalt cores and bentonite were altered by placing them in an autoclave with water and gas at ~320°C for 27 to 60 days. Each of the cores was run with either air or argon as specified in Table 1. The rock cores were found to have reacted with the water and formed secondary minerals (quartz, anthophyllite, scapolite, sericite, and zeolites) on their surfaces.

The bentonite used in three of the experiments was altered hydrothermally by placing 6 g of bentonite, 6 g of water solution, and ~0.003 g of air in four sealed stainless steel vessels and heating two vessels for 30 days and two vessels for 60 days at a temperature of 320°C. The altered bentonite was grey in color (as opposed to the yellow starting material) and formed clods that did not disperse in flowing water. Analyses by X-ray diffraction of the bentonite revealed no changes in mineralogy due to this treatment.

The borosilicate waste glass was hydrothermally altered in saturated steam and air. Two glass wafers were suspended in a 35.6-mL Hastelloy C-276 autoclave to which was added 10 mL of water solution. After being heated at 340°C for 17 days, the

*Trademark of the Cabot Corporation. Hastelloy C-276 contains 59% nickel, 17% molybdenum, 15% chromium, and 4% tungsten by weight.

†Trademark of Huntington Alloys. Monel-400 contains 66.5% nickel, 31.5% copper, 1.2% iron, 1.0% manganese, 0.2% carbon, and 0.2% silicon by weight.

Table 1. Conditions for alteration of three fissured rock cores. Each alteration run contains a rock core of ~1545 g and 1 L of water solution.[a]

Alteration Run	Gas	Temperature (°C)	Time at Temperature (d)	Materials for Use in Experiment No.
1	Air, 350 mg	320	30	4
2	Air, 350 mg	320	60	5
3	Argon, 490 mg	325	27	6

[a]The 2-L autoclave was made of Hastelloy C-276 alloy.

autoclave was cooled and disassembled. The glass had substantially altered with a green hydrated layer having formed from about half the original volume of the glass. The hydrated layer broke away from the unreacted substrate of one glass wafer. Analyses revealed no radioactivity in the condensed phase, indicating that the radioactive waste glass was not contacted by liquid water.

The altered samples were stored at room temperature in humidified chambers prior to their use in the experiments.

5.5.3 Results

5.5.3.1 Changes in Solution Composition

Water traversing the experimental apparatus underwent compositional changes that depended upon whether the materials had been altered or not. The greatest changes in solution composition were found using the as-received bentonite; the as-prepared waste glass, and the freshly fissured basalt (experiments 1, 2, and 3). In these experiments, most of the change in solution composition occurred when the water contacted the fissured core of basalt (Vandegrift, G. F.). No change in major constituents of the water were attributed to leaching of the radioactive waste glass. None are expected (Steindler, M. J., 1983) based on analyses of leach data obtained from continuous flow tests (Coles, D. G.; Strachen, D.). The results of the first three experiments can be summarized as follows.

Water exiting the apparatus was found to exhibit increased levels of calcium (from an initial ~1.5 to 46 mg/L) and magnesium (~0 to 14 mg/L) and decreases levels of sodium

(315 to 220 mg/L). Changes in other cations and changes in anions were noted as well. Generally, the largest changes in chemical composition occurred initially, during the conditioning period. Smaller, but still substantial, changes from the initial composition persisted as the experiments progressed.

The changes in composition of the water from experiments 4, 5, and 6 with the hydrothermally altered materials were quite limited, with calcium, magnesium, and sodium levels unchanged after 90 days of water flow. Changes noted were increases in potassium and total carbonate plus bicarbonate in the exiting water (Vandegrift, G. F.). These results indicate a chemical compatibility of the water with the altered basalt surfaces suggesting that the altered basalt is similar, chemically, to the naturally aged fissured surfaces of the basalt.

5.5.3.2 Migration of Radioelements

Migration of radioelements leached from the radioactive waste glass and transmitted by the flowing water was determined from analyses of the solutions and solid materials obtained from the experiments.

Analyses of solutions from the first, second, and third experiments showed cesium, europium, barium, uranium, neptunium, and plutonium to have moved in detectable quantities downstream from the radioactive waste glass. Because none of the neptunium activity was removed when the solutions were filtered, neptunium was concluded to be in solution rather than in colloidal form. In contrast, a substantial amount (~50%) of plutonium in some solutions was removed by filtering. The level of plutonium associated with particulate was lower the further downstream the solutions were collected. In addition, the overall concentration of plutonium decreased with distance away from the waste forms.

In contrast to the strong removal of plutonium, little adsorption of neptunium occurred upon passage of the water through the bentonite. Similarly, uranium is not removed from solution by bentonite.

Both plutonium and neptunium and, to some extent, uranium, are removed from solution upon passage through the rock core. This is illustrated in Table 2, which shows concentrations of actinides in solutions before and after passage of the solutions through the rock cores. Higher concentrations of plutonium and lower concentrations of neptunium were seen from the radioactive waste when leached in an ionizing radiation field. This effect for plutonium had been noted in previous leach tests (Nash, K. L., 1982; 1983).

Table 2. Actinide concentrations at the inlet and outlet of the fissured basalt core.

Experiment		Plutonium (10^{-11} mol/L)	Neptunium (10^{-9} mol/L)	Uranium (10^{-9} mol/L)
1	inlet	1.2	15	149
	outlet	$\leq$0.02	0.08	40
2	inlet	0.3	14	114
	outlet	$\leq$0.02	0.2	47
3	inlet	16	2.2	31
	outlet	0.003	$\leq$0.003	2.5
4[a]	inlet[b]	89	109	2560
	outlet	41	67	1660
5[a]	inlet[b]	128	120	3000
	outlet	105	120	2730
6	inlet[b]	3.0	2.4	50
	outlet	0.5	0.8	22

[a]Plutonium, neptunium, and uranium concentrations decreased significantly with time throughout the course of experiments 4 and 5. These values are near the maximum values.

[b]This sample was from the outlet of vessel 1, but is expected to be similar to a sample collected at the inlet to the core.

The data in Table 2 for the first three experiments indicate the strong retention of both plutonium and neptunium by the fissured rock surfaces. The neptunium distribution on the rock cores, as illustrated in Fig. 2 for one experiment, shows that the neptunium is removed upon its contact with the initial third of the rock.

In contrast to results from the first three experiments, the results from the latter experiments with hydrothermally altered materials indicate that substantially higher concentration of plutonium, neptunium, and uranium are dissolved from the hydrated waste glass (experiments 4 and 5). Moreover, a greater fraction of the leached uranium, neptunium, and plutonium pass through the altered rock cores (experiments 4, 5, and 6). This behavior is in contrast to that for cesium, which is substantially removed from solution by the altered rock. (Solution from experiment 4 contained a concentration

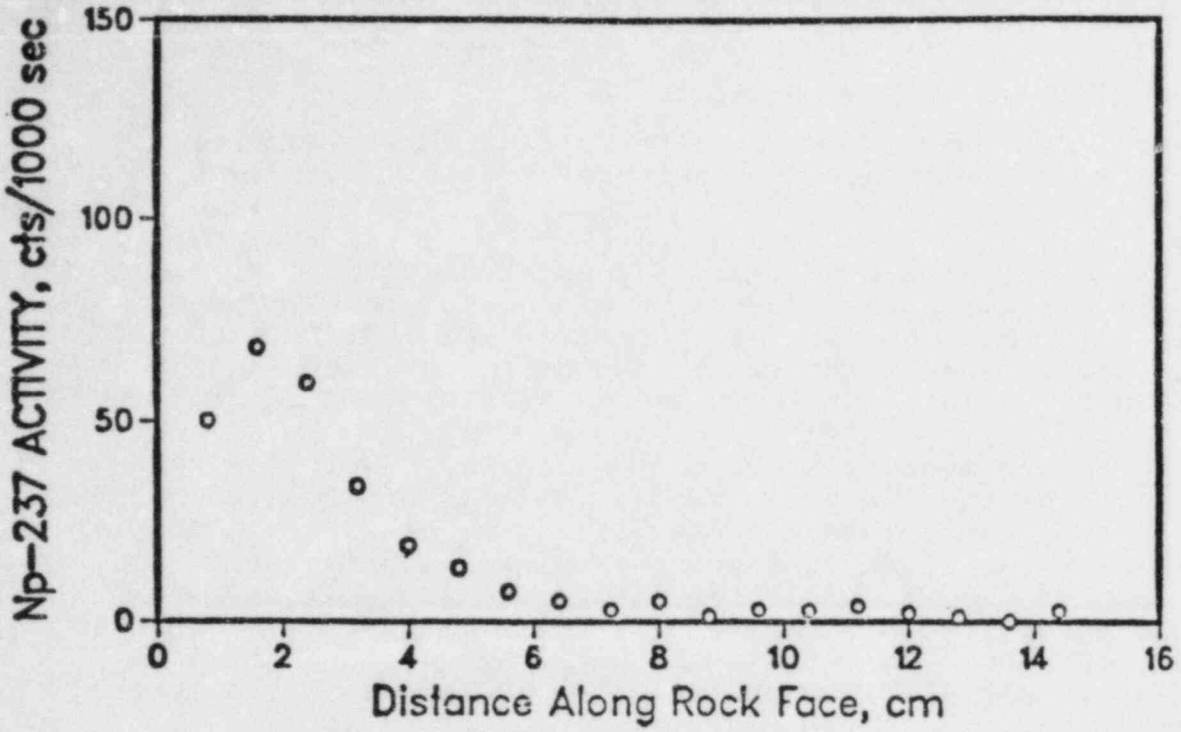

Fig. 2. Distribution of neptunium along the face of the basalt fissure from the first experiment. Water inlet to the fissure is on the left, outlet is at 14.6 cm.

of 7.2×10^{-14} M radioactive cesium at the inlet to the rock core and a concentration of $0 \pm 0.4 \times 10^{-14}$ M at the outlet of the rock core.)

5.5.3.3 Relationship of Hydrothermal Alteration to Aging

Laboratory treatments of repository materials were selected in this work to reproduce the major effects of aging of the materials in a nuclear waste repository. By the treatments, materials were prepared for use in experiments to explore the performance of an aged repository.

The aging that will occur after emplacement of waste in a nuclear waste repository involves many processes, such as devitrification, hydration, dissolution, radioelement transmutation, radiolysis, radiation damage, and chemical reaction.

Aging depends on the compositions of the materials (chemicals added to the waste, the backfill that is ultimately used, etc.) and is influenced by open-system variables (groundwater flow rate, groundwater composition, etc.) which may be influenced by the rock (e.g., the composition of groundwater may be controlled by reaction with rock). Aging of repository materials also depends on the size and geometry of breaches of

the waste package. Responding to so many variables, the materials may acquire any one of many possible different aged conditions.

Different aged conditions may exist simultaneously in a repository containing hundreds of waste canisters. The practice in this program was to produce the modifications of repository materials that were thought to be most significant in terms of radioelement release and migration.

The aging process selected for the solid waste in this work was hydration in water vapor. This is expected to be the most common aging process for solid waste because the durable, essentially leak-free containers (canister and overpack) and clay barrier envisioned in repository designs will exclude most of the water. Some water for hydration may exist in the sealed containers or diffuse through holes in the barriers. Hydration would be the dominant aging process in a repository built in unsaturated sediments (Winograd, I. J.).

Factors that affect the hydration of glass are temperature, time at temperature, water-vapor pressure, glass composition, and vapor species other than water. The relation of hydration to time and temperature has been studied for obsidian (Ericson, J. E.; Ewing, R. C.; Friedman, I.; Tombrello, T. A.), reviewed by the U.S. Nuclear Regulatory Commission (Barkatt, A.), and can be approximated by the relationship,

$$k = Ae^{-E/RT} \qquad (1)$$

where k is the amount of hydration (μm^2/1000 yr), A is a constant, E is the activation energy of the hydration process (cal/mol), R is the gas constant (cal/mol·K), and T is temperature (K).

The thickness, d, of the hydration layer is given by

$$d = (kt)^{1/2} \qquad (2)$$

where t is the time in units of 1000 years. These relationships incorporate (in the values selected for A and E) the effects of water-vapor pressure and glass composition, both of which are known to affect the amount of hydration. In these analyses, water is assumed to be the only important vapor species.

To simulate a repository condition using our present understanding, it is necessary to assume that the above relationships are valid, to ignore the effect of water pressure, and to use data obtained for obsidian (which are the best data we have for this analysis). When this is done, the value adopted for A is 1×10^{16} μm^2/1000 yr and for E is 2×10^4 cal/mol (Tombrello, T. A.).

If the aging conditions in a repository are assumed to include water vapor at a temperature of 100°C for 1000 yr, the hydrated layer is estimated to attain a thickness of 150 μm. This thickness is comparable to that produced by the hydrothermal treatment incorporated in this program. However, this calculated thickness could vary between 17 and 320 μm/1000 yr on the basis of the full range of known values for A and E [A ranging from 1.4×10^{15} to 1.8×10^{16} μm^2/1000 yr and E ranging from 19,200 to 20,700 cal/mol (Friedman, I.)]. Given the uncertainty in the thickness of the hydration layer, consideration of a more detailed thermal history for a repository does not appear to be warranted. This analysis is consistent with known behavior of waste glasses where a hydration thickness of 150 μm would be predicted for the waste glass SRL-131 (Bates, J. K., 1982 a,b).

Recent fracture surfaces of basalt (within and surrounding a recently constructed repository) will age in the hydrous and thermal environments of the waste repository. Fracture surfaces will age primarily by reactions with groundwater. The approach used for the laboratory modification of basalt surfaces to represent aging was hydrothermal treatment of fresh basalt surfaces in water formulated to represent the composition of water from the Grande Ronde formation. The laboratory aging would be comparable to that expected to occur in a repository that quickly becomes saturated with groundwater.

A great deal of information on the alteration of Pasco Basin basalts by groundwater, meteoritic water, and humidity is presented in several reports (Ames, L. L.; Benson, L. V., 1978; 1979; 1980; Teague, L. S.) that could be used as a guide to the alteration products expected in a repository. Unfortunately, the specific conditions under which the basalts were altered are poorly not known. As might be expected from the variety of conditions leading to alteration, there are great differences in alteration products from place to place. These observations substantiate the viewpoint that many aged conditions of a material are possible and that any aged condition is a result of the particular environment to which the material was subjected.

Although bentonite may not alter to different minerals in a basaltic environment, it may be modified in other ways. Temperatures at the interface of the canister and engineered barrier may be as high as 300°C (Taylor, C. L.). The hydrothermal treatment used for the engineered barrier did not change the mineralogy of the clay but did alter its physical and chemical properties in a fashion that was readily observable from its interaction with flowing water.

Because the temperature of 320°C used in the hydrothermal treatment is not substantially higher that expected in a

repository (300°C), it would be reasonable to assume that the results using laboratory-altered bentonite might have relevance to its performance upon aging.

5.5.3.4 Overall Results

In a series of six experiments, the influences of apparatus, ionizing radiation, and hydrothermal alteration of the repository materials on the migration of eight radioactive elements in nuclear waste were examined. Migration of the radioactive elements was found not to be measurably changed by the use of either of the alloys, Hastelloy C-276 or Monel-400, as a material of construction for the apparatus. Because these alloys differ substantially in composition, the results indicate that neither alloy affected the chemical properties of dissolved radioelements.

The dissolution of plutonium from radioactive waste glass was found to be enhanced and the dissolution of neptunium was found to be depressed by ionizing radiation. The species leached in a radiation field interacted with bentonite and basalt measurably the same as species leached in the absence of radiation. This result suggests that no radioelement species produced by radiolysis migrate differently than species formed in the absence of radiation.

The largest effects observed from the series of experiments were the greatly enhanced dissolution of plutonium, neptunium, and uranium from hydrated waste and the movement of these leached species through bentonite and basalt that were hydrothermally altered to simulate aging of the repository materials.

The oxidation states of the actinide elements, plutonium, neptunium, and uranium, are initially those in the simulated waste glass. The oxidation states can change upon reaction with the ferrous-ferric redox couple in the water and the ferrous ion on the rock surfaces (Jacobs, G. K.). At the pH range of 8 to 10, the ferrous ion would reduce higher oxidation states to Np(IV), Pu(IV), and U(IV) (Apted, M. J.; Duffy, C. J.; Moody, J. B.; Rydberg, J.). This is most likely still true with the complexants, e.g., the CO_3^{2-} and F^-, that are present in the groundwater.

5.5.4 Conclusions

Of the three parameters investigated experimentally, alloy of construction of the apparatus, ionizing radiation field, and altered conditions of the repository components, the altered conditions of the repository components were found to have the most substantial influence on the migration of radioactive elements dissolved from the waste glass. Inasmuch as the alterations represent changes that may occur upon aging

of the repository, the ability of a repository for nuclear waste to isolate many radioactive elements is concluded to degrade with time due to aging of the repository system.

5.5.5 Recommendations

The most striking behavior seen in these experiments is that plutonium and neptunium moved more rapidly through hydrothermally altered basalt than through freshly fractured basalt. While this behavior can be understood in terms of reduction of the radioelements at the basalt surface (Meyer, R. E.) the behavior is contrary to that predicted from the generally accepted trend that sorption of radioelements increases with extent of alteration of basalt (Barney, G.S.; Deutsch, W. J.). This trend is valid for elements such as cesium and strontium and is due to the increased surface and cation exchange capacity of the altered basalt. However, the extrapolation to other radioelements, specifically those radioelements that are sensitive to reduction, is not valid. The major recommendation from this work is that safety assessments of a repository in basalt should consider the enhanced mobility of plutonium and neptunium that is expected with age. Moreover, greater attention needs to be given, in general, to the consequence of aging of a waste repository. An additional recommendation would be that assumptions used to predict radioelement migration be checked experimentally. Experiments that measure radioelement movement, such as those described here, give results that can be compared directly to those predicted in models of radioelement migration. The experimental approach is flexible and can be used to investigate many repository configurations in both saturated and unsaturated rock.

5.5.6 Planned Research

Experimental studies of repository systems are planned to investigate the movement of radioelements from waste solids through saturated and unsaturated tuff. This work will examine issues of repository safety with regard to developments for a nuclear waste repository at the Nevada Test Site.

5.5.7 Acknowledgments

Much of the work reported here was performed by personnel at Argonne National Laboratory other than the authors. A. M. Essling, E. A. Huff, and F. L. Williams of the Analytical Chemistry Laboratory performed the analyses of stable elements in solution. M. J. Steindler reviewed the ongoing work and contributed to the technical content of the program. The secretarial work was directed by L. J. Jensen, who was ably

assisted by R. T. Riel. R. B. Keener edited the manuscript. The authors thank these people for their contributions and the many others of the Chemical Technology Division, headed by L. Burris, who contributed to the success of this program.

We also thank M. J. Smith of the Basalt Waste Isolation Program, who graciously supplied us with rock samples and kept us informed of progress in designing waste packages.

5.5.8 References

Ames, L. L., "Hanford Basalt Flow Mineralogy," PNL-2847, 1980.

Apted, M. J., and J. Meyer, "Comparison of the Hydrothermal Stability of Simulated Spent Fuel and Borosilicate Glass in a Basaltic Environment," Rockwell-Hanford Operations Report RHO-BW-ST-38P, 1982.

Avagadro, A., C. N. Murray, and A. DePlano, "Transport through Deep Aquifers of Transuranic Nuclides Leached from Vitrified High-Level Wastes," in C. J. M. Northrup, (ed.) Scientific Basis for Nuclear Waste Management, Vol. 2, p. 665-671, Plenum Press, NY (1980).

Barney, G. S., "Radionuclide Reactions with Groundwater and Basalts from Columbia River Basalt Formations," Rockwell Hanford Operations Report RHO-SA-217, 1981 (also conference 8106119-1, Northwest Regional ACS Meeting, Bozeman, MT, June 17, 1981).

Bates, J. K., L. J. Jardine, and M. J. Steindler, "Hydration Aging of Nuclear Waste Glass," Science, 218:51, 1982 a.

Bates, J. K., L. J. Jardine, and M. J. Steindler, "The Hydration Process of Nuclear Waste Glass: An Interim Report," Argonne National Laboratory, ANL-82-11, 1982 b.

Barkatt, A., "Review of Chemical Stability of Glasses: Dissolution Mechanisms, Test Evaluations, and Applications to Radioactive Waste Fixation," Final Report, NRC Contract No. 04-78-25, 1980.

Benson, L. V., et al., "Basalt Alteration and Basalt-Waste Interaction in the Pasco Basin of Washington State," Lawrence Berkeley Laboratory, LBL-8532, 1978.

Benson, L. V., and L. S. Teague, "A Study of Rock-Water-Nuclear Waste Interactions in the Pasco Basin, Washington," Lawrence Berkeley Laboratory, LBL-9677, 1979.

Benson, L. V., C. L. Carnahan, and M. Che, "A Study of Rock-Water-Nuclear Waste Interactions in the Pasco Basin, Washington, Part II. Preliminary Equilibrium-Step Simulations of Basalt Diagenesis," Lawrence Berkeley Laboratory, LBL-9677, 1980.

Bischoff, J. L. and W. E. Seyfried, Jr., "Hydrothermal Chemistry of Seawater from 25° to 350°C," Am. J. Sci. 278, p. 838-860, 1978.

Bradley, D. J., D. G. Coles, F. N. Hodges, G. L. McVay, and R. E. Westerman, "Nuclear Waste Package Materials Testing Report: Basaltic and Tuffaceous Environments," Battelle Pacific Northwest Laboratory, PNL-4452, 1983.

Charles, R. W. and G. K. Bayhurst, "Sentinel Gap Basalt Reacted in a Temperature Gradient," Los Alamos National Laboratory, LA-9481-MS, 1983.

Coles, D. G., R. W. Mersing, J. Rego, H. C. Weed, and B. W. Buddemeir, "A Leaching Study of PNL 76-68 Glass Beads Using the LLNL Continuous-Flow Method and the PNL Modified IAEA Method: A Final Report," Lawrence Livermore National Laboratory, UCID-19492B, 1982.

Coons, W. E., E. L. Moore, M. J. Smith, J. D. Kasu, "The Functions of an Engineered Barrier System for a Nuclear Waste Repository in Basalt," Rockwell Hanford Operations, RHO-BWI-LD-23, 1980.

Deutsch, W. J., E. A. Jenne, and K. M. Krupka, "Solubility Equilibria in Basalt Aquifers: The Columbia Plateau, Eastern Washington, U.S.A.," in G. W. Bird and W. S. Fyfe (eds.) Geochemistry of Radioactive Waste Disposal, Chem. Geol., 36:15-34, 1982.

Duffy, C. J., and A. E. Ogard, "Uranite Immobilization and Nuclear Waste," Los Alamos National Laboratory, LA-9199-MS, February 1982.

Ericson, J. E., "Prehistoric Exchange Systems in California: The Results of Obsidian Dating and Tracing," Thesis, UCLA, 1977.

Ewing, R. C., and R. F. Haakes, "Naturally Occurring Glasses: Analyses for Radioactive Waste Forms," Pacific Northwest Laboratory, PNL-2776, 1979.

Friedman, I., and W. Long, "Hydration Rate of Obsidian," Science, 191:347, 1976.

Gephart, R. E., R. C. Arnett, R. G. Baca, L. S. Leonhart, F. A. Spane, Jr., "Hydrologic Studies within the Columbia Plateau, Washington: An Integration of Current Knowledge," Table III-45, Rockwell Hanford Operations, RHO-BWI-ST-5, 1979.

Jacobs, G. K., and M. J. Apted, "Eh-pH Conditions for Groundwater at the Hanford Site, Washington: Implications for Radionuclide Solubility in a Nuclear Waste Repository Located in Basalt," EOS, Trans. Am. Geophys. Union, 62:1065, 1981.

McCarthy, G. J., W. B. White, R. Roy, B. E. Sheetz, S. Komareni, D. K. Smith, and D. M. Roy, "Interactions between Nuclear Waste and Surrounding Rock," Nature (London), 273, p. 217-219, 1978.

Meyer, R. E., W. D. Arnold, and F. I. Case, "Valence Effects on Sorption," U.S. Nuclear Regulatory Commission, Status of NRC Sponsored Research on Waste Management Geochemistry, this report, 1984.

Moody, J. B., "Radionuclide Migration/Retardation Research and Development Technology Status Report," U.S. Department of Energy, ONWI-321, March 1982.

Nash, K. L., S. Fried, A. M. Friedman, N. Susak, P. Rickert, J. C. Sullivan, D. P. Karim, and D. J. Lam, "The Effect of Radiolysis on Leachability of Plutonium and Americium from 76-101 Glass," in S. V. Topp, (ed.) Scientific Basis for Nuclear Waste Management, North Holland Press, New York, p. 661, 1982.

Nash, K. L., S. Fried, A. M. Friedman, N. Susak, P. Rickert, and J. C. Sullivan, "Radiation Effects in Solution and on the Solid Liquid Interface," Nucl. Technol. 60:257, 1983.

Nuclear Regulatory Commission, "Disposal of High-Level Radioactive Wastes in Geologic Repositories Technical Criteria," 10 CFR Part 60, Final Rule, Federal Register, Vol. 48, No. 120, Rules and Regulations, June 21, 1983.

Rockwell Hanford Operations, "Rockwell Hanford Operations Site Characterization Report for the Basalt Waste Isolation Project," DOE/RL 82-3, 1982.

Rydberg, J., "Groundwater Chemistry of a Nuclear Waste Repository in Granite Bedrock," Lawrence Livermore National Laboratory, UCRL-53155, September 1981.

Savage, D., and N. A. Chapman, "Hydrothermal Behavior of Simulated Waste Glass and Waste-Rock Interactions Under Repository Conditions," in G. W. Bird and W. S. Fyfe (eds.), Geochemistry of Radioactive Waste Disposal, Chem. Geol., 36:59-86, 1982.

Scheetz, B. E., S. Komareni, D. K. Smith, C. A. F. Anderson, S. D. Atkinson, and G. J. McCarthy, "Hydrothermal Interactions of Simulated Nuclear Waste Glass in the Presence of Basalt," in C. J. M. Northrup (ed.), Scientific Basis for Nuclear Waste Management, 2, Plenum Press, New York, p. 207-214, 1980.

Seitz, M. G., P. G. Rickert, S. M. Fried, A. M. Friedman, and M. J. Steindler, "Studies of Nuclear-Waste Migration in Geologic Media," Argonne National Laboratory, ANL-79-30, 1979.

Seitz, M. G., "Repository-Analog Experiments of Nuclear Waste Leaching and Migration," Proceedings of the International Symposium on the Migration in the Terrestrial Environment of Long-Lived Radionuclides from the Nuclear Fuel Cycle, IAEA-SM-257, 1981 a.

Seitz, M. G., and M. Seliga, "A Study of the Migration of Leached Radionuclides in a Natural Fissure of Granite Rock," Jarderna Energie, 27:399, 1981 b.

Shade, J. W., and D. J. Bradley, "Initial Waste Package Interactions Tests," Battelle Pacific Northwest Laboratory, Richland, WA, Status Report PNL-3559, 1980.

Shade, J. W., "Release Kinetics and Alteration of Waste Glass in Crystalline Rocks Systems," in G. W. Bird and W. S. Fyfe (eds.), Geochemistry of Radioactive Waste Disposal, Chem. Geol., 36:103-121, 1982.

Steindler, M. J., et al., "Fuel Cycle Programs Quarterly Progress Report, April-June 1982," Section IV, Argonne National Laboratory, ANL-82-58, 1982.

Steindler, M. J., et al., "Fuel Cycle Programs Quarterly Progress Report, October-December 1982," Section VI, Argonne National Laboratory, ANL-83-19, 1983.

Strachen, D., personal communication to G. F. Vandegrift, Argonne National Laboratory, November 1982.

Taylor, C. L., G. J. Anttonen, et al., "Borehole Plugging of Man-Made Accesses to a Basalt Repository," Rockwell Hanford Operations, RHO-BWI-C-49, 1979.

Teague, L. S., "Secondary Minerals Found in Cores DS2 A1 and DS2 A2 Taken from the Grande Ronde Basalt Formation, Pasco Basin Washington," Lawrence Berkeley Laboratory, LBL-10387, 1980.

Tombrello, T. A., "Weathering of Natural Glasses," in High-Level Radioactive Solid Waste Forms, Proc. Conf., Denver, Colorado, U.S. Nuclear Regulatory Commission, NUREG-CP-0005, 1978.

Turcotte, R. P., J. W. Wald, and R. P. May, "Devitrification of Nuclear Waste Glasses," in C. J. Northrup (ed.) Scientific Basis for Nuclear Waste Management, Vol. 2, Plenum Press, 1980.

Vandegrift, G. F., D. L. Bowers, T. J. Gerding, S. M. Fried, C. K. Wilbur, and M. G. Seitz, "The Interaction of Groundwater and Basalt Fissure Surfaces and Its Effect on the Migration of Actinides," ACS Symposium on Geochemical Behavior of Disposed Radioactive Waste, Seattle, Washington, March 20-25, 1983.

Van Olphen, H., and J. J. Frigiat, Data Handbook for Clay Materials and Other Non-Metallic Minerals, Pergamon Press, New York, 1979.

Winograd, I. J., "Radioactive Waste Disposal in Thick Unsaturated Zones," Science, 212:1457, 1981.

5.6 INTERACTIONS OF ACIDIC SOLUTIONS WITH SEDIMENTS: A CASE STUDY

S. R. Peterson
R. J. Serne
A. R. Felmy
R. L. Erikson
K. M. Krupka
G. W. Gee

Pacific Northwest Laboratory
Richland, Washington 99352

ABSTRACT

A methodology is presented for investigating the chemical interactions of acidic solutions with sediments. This approach illustrates how geochemical modeling can be used, in parallel with characterization data for sediments from field and laboratory experiments, to derive a composite description of the solution/sediment interactions. The MINTEQ geochemical computer code was used to predict solid-phase reactions that might occur when acidic solutions contact neutral sediments which, in turn, may control the concentrations of certain dissolved components. Results of X-ray diffraction analysis of laboratory samples of sediments that have been contacted with acidic uranium mill tailings solutions suggest gypsum and jarosite precipitated. These same mineralogical changes were identified in sediment samples collected from a drained uranium mill evaporation pond (Lucky Mc mine in Wyoming) with a 10-year history of acid attack. Geochemical modeling predicted that these same phases and several amorphous solids not identifiable by X-ray diffraction should have precipitated in the contacted sediments.

An equilibrium conceptual model consisting of an assemblage of minerals and amorphous solid phases was then developed to represent a sediment column through which uranium mill tailings solutions were percolated. The MINTEQ code was used to predict effluent solution concentrations resulting from the reactions of the tailings solution with the assemblage of solid phases in the conceptual model. The modeling predictions were compared to the measured column effluent concentrations, and hypotheses were formed as to the probable mechanisms controlling the migration of selected contaminants. The conceptual model successfully predicted the concentrations of several of the macro-constituents (e.g., Ca, SO_4, Al, Fe, and Mn), but was not successful in modeling the concentrations of trace elements. The lack of success in predicting the observed trace metal concentrations suggests that other mechanisms, such as adsorption, must be included in future models. The geochemical modeling methodology coupled with the laboratory and field studies should be applicable to a variety of waste disposal problems.

5.6.1 INTRODUCTION

Disposal of uranium mill tailings is likely the most difficult technical challenge presently faced in solving the nuclear waste problem (Cunningham 1978). The technical challenge lies in adequately handling massive volumes of leachable, low level radioactive wastes, which exceed the amount of any other wastes generated in the nuclear fuel cycle. The quantity of uranium mill tailings in the United States is approximately 1.8×10^8 metric tons and this amount is expected to double by the year 2007 (Oak Ridge National Laboratory 1983).

The seepage of acidic leachate from disposed tailings is potentially hazardous at sites where wastes are disposed in impoundments with high permeability and low-acid neutralizing capacitites, or with small distances between the tailings and existing water tables. In Canada, the Elliot Lake and Bancroft areas have had the water quality adversely affected by the migration of tailings solution (Brown et al. 1981) and in the United States, contamination of surface and/or ground water has also occurred [e.g., Cannon City, Colorado (Cotter); Ford, Washington (Dawn Mining); Gas Hills, Wyoming (Union Carbide)]. Details of these occurrences are described in a Mineral Resources Waste Management Team report (1980).

5.6.1.1 Issues Addressed by This Research

To better understand such water quality degradation, our program has used experimental and computer modeling techniques to assess the long-term environmental impact of leachate movement from uranium mill tailings impoundments. Specifically, laboratory experiments and geochemical computer codes were used to evaluate the migration potential of selected contaminants (both radioactive and toxic elements) from uranium mill tailings leachate in contact with sediments and geologic liner materials.

The principal issues addressed by our experimental and geochemical modeling study are:

What are the short- and long-term mineralogical and hydrological changes that occur when acidic tailings solutions contact sediments?

Which contaminants will migrate from uranium mill tailings impoundments?

What are the sediment/solution interactions that attenuate movement of contaminants?

If the contaminants do move, what will be their concentrations in the migrating solution and in the groundwater systems?

The specific issues discussed in this document are:

Can laboratory and geochemical modeling techniques be used to simulate chemical processes that occur in the field?

Can a conceptual chemical model be used to predict the concentrations of selected contaminants that result from tailings solutions reacting with a sediment column?

5.6.1.2 Background and Objectives

Crim et al. (1979) measured increases in the permeability of montmorillonite clays subjected to extended contact with an acidic (pH < 1) tailings solution. These changes in permeability varied by more than two orders of magnitude, but tended to increase most dramatically after the pH of the effluent dropped below 4 (from an initial value near 8). Gee et al. (1980a,b) and Peterson et al. (1982) studied the effects of extended contact of acidic tailings solution (pH = 2) on the permeability of native clays from Morton Ranch mine in central Wyoming. Their results indicate the permeability of the clays gradually decreased with time during contact periods extending up to 3 years. Because the clay material exhibited little physical evidence of deterioration, they partly attributed the decreases in permeability to the precipitation of iron and aluminum solid phases and possibly of secondary clay minerals stable at pH < 3. In addition, Relyea and Martin (1982) reported dramatic (up to three orders of magnitude) decreases in permeability after contacting highly calcareous soils with acidic tailings solutions. They also attributed the decrease in permeability to the precipitation of solid phases. Langmuir and Riese (1981) predicted that amorphous ferric hydroxide would begin to precipitate around pH 2 in uranium mill tailings. This precipitation, as a slime, was thought to help reduce seepage away from the tailings impoundments.

Ion-speciation and solid-phase solubility calculations have been extensively used to gain a better understanding of the geochemical processes controlling the chemical composition of natural waters. Several computer codes have been utilized to perform these calculations. Some of the more recent programs include MINEQL (Westall et al. 1976), PHREEQE (Parkhurst et al. 1980), WATEQ3 (Ball et al. 1981), and MINTEQ (Felmy et al. 1983). Several such computer programs have been successfully used to evaluate possible solid-phase controls on solution composition (Nordstrom et al. 1979, Gang and Langmuir 1974, Peterson and Krupka 1981, Peterson et al. 1982, and Deutsch et al. 1982). Geochemical modeling involving ion-speciation and solubility calculations (Peterson and Krupka 1981; Peterson et al. 1982) was used to verify if precipitation of solid phases in laboratory permeability columns was thermodynamically possible, and if so, what solids would be expected to precipitate. The results of the modeling efforts were then compared to mineralogical characterization studies performed on laboratory and field samples.

Little work, however, has been done in using geochemical computer codes to predict the aqueous phase compositions of solutions resulting from inter-

action with an assemblage of solid phases in a flow-through system. During such chemical interactions, one or more solid phases may dissolve and thermodynamically more stable solid phases precipitate as the solution composition changes. The new assemblage of solid phases can then be reacted with a new volume of influent solution and the process repeated.

A hypothesized assemblage of solid phases can be used to represent heterogeneous geologic materials, which are permitted to dissolve or precipitate in response to changes in the aqueous media. This conceptual model, in conjunction with the MINTEQ geochemical code, is then used to simulate the contact of a specified solution with these geologic materials. The resultant compositions of the aqueous phase and the change in mass of each solid phase in the assemblage are calculated as successive pore volumes of solution interact with the solid phase assemblage.

5.6.1.3 Scope of Research

A system consisting of uranium mill tailings solution, of low pH and high dissolved solids, in contact with clay sediments was chosen as a test for our predictive modeling study. In this system, precipitation/dissolution of solid phases is expected to be the dominant mechanism controlling the concentrations of several dissolved constituents. The contaminant concentrations predicted by our conceptual model were compared to experimental data from laboratory flow-through columns; the mineral phases predicted from the solution/mineral interactions were similarly compared to laboratory studies and to field samples from an inactive tailings pond.

5.6.2 MATERIALS AND METHODS

The mineralogical alteration of sediments caused by contact with acidic tailings solution was evaluated from laboratory column experiments (Uziemblo et al. 1981, Peterson et al. 1982) and a study of field soil samples (Erikson and Sherwood 1982). The laboratory experiments involved the flow of Highland Mill tailings solution through Morton Ranch clay sediment for an 838-day period.

Table 1 lists the physical and chemical properties of the clay sediment obtained at the Morton Ranch mine in Wyoming. These materials were characterized using standard soil testing procedures as outlined in Black (1965a,b). Details of the experimental set-up and methodology can be found in Gee et al. (1980a), Peterson et al. (1982), Serne et al. (1983), and Peterson et al. (1983).

The compositions of the tailings solutions used as influent for the column experiments are given in Table 2. The Highland Mill tailings solutions were taken from the Exxon Highland Mill in Wyoming. In general, the major cationic constituents were analyzed by inductively coupled plasma emission spectroscopy and the concentrations of trace elements were determined by graphite-furnace atomic absorption. Anionic components were

TABLE 1. Characterization of the Morton Ranch Clay Sediment

Water Content (g/g) (%) (after air drying)	4.10
Particle Density (g/cm^3)	2.72
Particle Size Distribution (wt%)	
Sand (50-2000 μm)	12.0
Silt (2-50 μm)	54.0
Clay (<2 μm)	34.0
pH of Saturated Paste	8.2
Eh of Saturated Paste (volts)	+0.406
EC of Saturated Extract (mmhos/cm)	0.70
Organic Matter (g/g) (%)	1.44
$CaCO_3$ (g/g) (%)	0.3[a]
Cation Exchange Capacity (CEC) (meq/100 g)	31.6

[a] Average of eight measurements.

analyzed by ion chromatography and titration; X-ray and γ-ray radioanalytical techniques were used to measure radionuclide activities. A combination glass electrode was used to measure the pH of the tailings solutions and soil. The redox potential (e.g., Eh) of the solution was measured using a combination platinum-reference electrode. The pH and Eh values of the tailings solutions were determined on filtered (0.45 μm membrane) samples.

The interaction of Morton Ranch clay sediments and Highland Mill tailings solution was studied in the laboratory using permeability and vacuum extractor columns. The permeability column was packed with the sediment from Morton Ranch to 96% of maximum compaction as determined by a standard compaction test (Black 1965a). This resulted in a bulk density of 1.76 g/cm^3 for the sediment in this column. The permeability column was leached with the Highland Mill (H.M.) tailings solution (H.M. #1 in Table 2).

The vacuum extractor columns were packed with sediment from Morton Ranch to a density of 1.25 g/cm^3. The material in the vacuum extractor

TABLE 2. Composition (in mg/ℓ) of Highland Mill (H.M.) Tailings Solutions Used in Permeability and Vacuum Extractor Columns

Constituent	H. M. Tailings Solution #1 (used in permeability column)	H. M. Tailings Solution #2 (used in vacuum extractor columns)
Li	0.9	0.48
B	0.19	0.19
HCO_3/CO_3	0.0	0.0
NO_3	16.5	8.5
F	4.0	4.0
Na	343	364
Mg	690	440
Al	600	396
Si	234	255
P	30	6.8
SO_4	12,850	9,100
Cl	97	330
K	40	<3
Ca	537	483
V	10.6	10.6
Cr	2.7	1.5
Mn	64	43
Fe	2,215	560
Co	<1	1
Ni	3.0	1.7
Cu	2.3	1.3
Zn	8.4	3.9
As	3.50	0.45
Se	0.6	1.18
Sr	15.7	6.6
Mo	0.35	<0.05
Cd	0.04	0.04
Sb	<1	<1
Ba	<0.05	<0.05
La	ND[a]	5.0
Pb	<0.05	<0.04
U	40.0	7.2
pH	1.8	2.19
Eh(mV)	910	750

(a) ND - not determined.

columns was packed to a lower density than that in the permeability column to speed the movement of solution through the columns. The vacuum extractor experiments are described in Serne et al. (1983), and used solution H.M. #2

in Table 2 as a leachate. The contaminant concentrations found in the effluent solutions from these columns were compared to the modeling predictions.

At the conclusion of the experiments, the sediment column was dissected into five sections and the mineralogy of each section identified. In addition, sediment samples were collected to a depth of 60 cm below the bottom of an evaporation pond at the Lucky Mc Mill in Wyoming, which had been in contact with acidic mill tailings solution for approximately 10 years.

The mineralogy of all sediment samples was determined from bulk and/or clay-sized fractions using powder X-ray diffraction techniques. The clay-sized fraction of the sediments was separated from the bulk samples by sedimentation (Jackson 1956, 1979). X-ray diffractograms were obtained using CuKα radiation. The mineralogy of the field sediment samples from the Lucky Mc Mill was determined as a function of depth below the pond bottom. Mineralogical alteration of the sediments caused by reaction with the acidic leachates was evaluated by comparing diffractograms of contacted and uncontacted sediments.

5.6.3 COMPUTER MODELING

The development of geochemical codes and their application to aqueous geochemical systems has been described in the reviews of Jenne (1981) and Mercer et al. (1981) and the compilation of geochemical modeling papers in Jenne (1979).

For the modeling calculations discussed in this paper, the MINTEQ geochemical code (Felmy et al. 1983) can be considered as having three parts: 1) a speciation submodel, 2) a solubility submodel, and 3) a mass transfer submodel. The calculations completed by each submodel, in turn, are dependent on the thermodynamic and reaction data stored in MINTEQ's thermodynamic data base. The sources of thermodynamic data in MINTEQ are described in Truesdell and Jones (1974), Ball et al. (1980, 1981), and in Krupka and Jenne (1982).

The speciation submodel first calculates the activities for the uncomplexed and complexed cationic, anionic, and neutral species and the distribution of these species among their redox states for a given water composition. Activities of individual aqueous species are corrected for ionic strength using the extended Debye-Huckel equation with two adjustable parameters (Truesdell and Jones 1974) or the Davies equation (Davies 1962, Ball et al. 1980).

After calculating the aqueous speciation, the solubility submodel then determines if the solution is at equilibrium with any of the minerals and other solids (including amorphous solids) in the MINTEQ thermodynamic data base. The solubility submodel calculates ion activity products (AP) from the activities of the aqueous species and the reaction stoichiometries for

solids contained in the MINTEQ data base. These activity products (AP) are then compared to the equilibrium solubility products (K) stored in MINTEQ for these same solids, to test the assumption that certain of the dissolved constituents in the aqueous solution are in equilibrium with particular solid phases. Saturation indices [log (AP/K)] are calculated to determine if the aqueous solution is at thermodynamic equilibrium [log (AP/K) = 0], oversaturated [log (AP/K) > 0], or undersaturated [log(AP/K) < 0] with respect to a certain solid phase. If a solution is computed to be at equilibrium with a particular solid, then it is possible that the solid is precipitating or dissolving at a sufficient rate for it to control the concentration of certain of its constituents in that solution. If an aqueous solution is calculated to be oversaturated with respect to a certain solid phase, then it is inferred that kinetic and/or mineralogical factors prevent precipitation of the solid phase at a sufficient rate to significantly affect the concentration of dissolved constituents in the solution.

The results from the solubility submodel are then used by the mass transfer submodel of MINTEQ. If the solubility submodel indicates that a given solution is oversaturated with respect to a solid phase considered in the conceptual chemical model of the system, the mass transfer submodel will "precipitate" that solid phase until the solution is at equilibrium [i.e., log (AP/K) = 0] with the solid. MINTEQ keeps track of the mass of precipitated material. If the solubility submodel computes a solution to be undersaturated with regard to a particular solid phase in the chemical model of the system, the MINTEQ mass-transfer submodel will "dissolve" that solid until solution equilibrium is achieved with respect to the solid, or until the finite mass of solid is completely dissolved.

The interaction of the acidic tailings solution with the clay sediment material was simulated by reacting incremental pore volumes of solution (H.M. Tailings Solution #2 in Table 2) with a hypothetical assemblage of solid phases, i.e., our conceptual model of the system. The solid phase assemblage consisted only of solids which could readily dissolve from the sediments or precipitate from solution. This was especially important because each pore volume of solution in the vacuum extractor columns was in contact with the sediments for only 16 hours. Because the MINTEQ computer code assumes a 1-liter volume of solution, the initial column pore volume of solution was multiplied by a scalar to convert a pore volume of solution to 1 liter of solution. The mass of solid in the column was then multiplied by this same scalar.

The solid phases included in the conceptual chemical model, their thermodynamic data, and the sources of these data are given in Table 3. Two of the most important criteria for selection of these solid phases were: 1) the rate of attainment of equilibrium of the solid with the solution, and 2) availability of accurate thermodynamic data for the solid. The rate of attainment of equilibrium was evaluated by reviewing the experimental literature. If these data were unavailable, the solid was considered if it had been identified as having formed under conditions similar to those present in these experiments. The only solid phase used in the chemical model to represent the sediment before contact with the acidic tailings

TABLE 3. Summary of Solids Considered in the Conceptual Chemical Model

Solid	Reaction	$\log K^{o}_{r}$, 298	Reference
Jurbanite	$Al^{3+} + 6H_2O + SO_4^{2-} \rightleftarrows AlOHSO_4 \cdot 5H_2O + H^+$	3.80	Nordstrom, D. K. 1982
Basaluminite (A)[a]	$4Al^{3+} + SO_4^{2-} + 15H_2O \rightleftarrows 10H^+ + Al_4(SO_4)(OH)_{10} \cdot 5H_2O$	-23.98	Nordstrom, D. K. 1982
$Al(OH)_3$(A)	$Al^{3+} + 3H_2O \rightleftarrows Al(OH)_3(A) + 3H^+$	-10.38	Truesdell, A. H. and B. F. Jones 1974
Gypsum	$Ca^{2+} + SO_4^{2-} + 2H_2O \rightleftarrows CaSO_4 \cdot 2H_2O$	4.60	(b)
Calcite	$Ca^{2+} + CO_3^{2-} \rightleftarrows CaCO_3$	8.48	Plummer L. N. and E. Busenberg 1982
$Fe(OH)_3$(A)	$Fe^{3+} + 3H_2O \rightleftarrows Fe(OH)_3(A) + 3H^+$	-4.891	Truesdell, A. H. and B. F. Jones 1974
Siderite	$Fe^{2+} + CO_3^{2-} \rightleftarrows FeCO_3$	10.55	Truesdell, A. H. and B. F. Jones 1974
Pyrochroite	$Mn^{2+} + 2H_2O \rightleftarrows 2H^+ + Mn(OH)_2$	-15.088	Ball et al. 1980
Rhodochrosite	$Mn^{2+} + CO_3^{2-} \rightleftarrows MnCO_3$	10.585	Johnson, K. S. 1982

(a) A = amorphous
(b) Letter from D. K. Nordstrom, U.S.G.S, Menlo Park, CA, to E. A. Jenne, Battelle Pacific Northwest Laboratories, Richland, WA, dated February 6, 1981.

solution was calcite ($CaCO_3$); the mass of calcite being determined from the carbonate analyses of the sediment (Table 1). The other solids shown in Table 3 were allowed to precipitate if they became oversaturated during the modeling simulation. The folowing constituents were included in the conceptual aqueous model: aluminum, calcium, carbonate, chloride, fluoride, iron, manganese, sodium, sulfate, and magnesium.

5.6.4 RESULTS AND DISCUSSION

Peterson et al. (1982) observed a decrease in permeability with time in laboratory permeability columns contacted with acidic uranium mill tailings solutions. These decreases in permeability were partially attributed to pore plugging resulting from the precipitation of minerals and amorphous solids. Other possible contributors to the decreases in permeability are examined in Peterson et al. (1982). In the first phase of this study (Peterson and Krupka 1981, Peterson et al. 1982), geochemical modeling (ion-speciation and solubility computations) was used to verify if this precipitation was thermodynamically feasible, and if so, to predict which solids would be expected to precipitate. The predicted solids were then compared to minerals observed in a laboratory permeability column and in sediment from the evaporation pond at the Lucky Mc mine. The objective of the second phase of our study was to predict the changing solution concentrations of selected contaminants as uranium mill tailings solutions flowed through sediments.

5.6.4.1 Phase 1: Model-Predicted Solids versus Observed Solids

X-ray Diffraction Analysis

The uncontacted sediments consist of a mixture of sand, silt and clay. The minerals identified in the uncontacted Morton Ranch clay sediments are feldspar [$(K,Na,Ca)(Al,Si)_4O_8$], illite [$K(Al,Mg,Fe)_2(Si,Al)_4O_{10}(OH)_2(H_2O)$], quartz ($SiO_2$), and smectite [$(Na,Ca)_{0.33}(Al,Mg)_2Si_4O_{10}(OH)_2 \cdot nH_2O$]. These minerals were also identified in the uncontacted Lucky Mc alluvium. However, the Lucky Mc alluvium is strongly calcareous (U.S.NRC 1977) and, in addition, contains calcite ($CaCO_3$), dolomite [$(Ca,Mg)(CO_3)_2$] and gypsum ($CaSO_4 \cdot 2H_2O$). The total carbonate content of this native alluvium is estimated to be approximately 20% (Erikson and Sherwood 1982). No carbonate minerals were detected in X-ray diffractograms of Morton Ranch clay liner.

The permeability column was dissected after approximately 18 pore volumes of Highland Mill tailings solution (solution 1 in Table 2) had flowed through the Morton Ranch clay liner over a period of 838 days. The extracted sediment was split into five sections perpendicular to the column axis; each section was 0.9 cm thick.

The sediment samples from the Lucky Mc mill were collected to a depth of 60 cm while the evaporation pond was temporarily drained. The sediment

profile was distinctly stratified with depth, based on color of the soil and measurement of the soil pH of the saturated pastes.

The results of the mineralogical studies (Uziemblo et al. 1981, Erikson and Sherwood 1982, and Peterson et al. 1982) suggest similar mineralogical alterations occurred in the laboratory column experiments and at the Lucky Mc field site. For example, the mineralogical changes with depth at the Lucky Mc site are schematically illustrated in Figure 1. The sample designations assigned to the field sediment samples are based on the location and depth from the pond bottom, the locations and abbreviations used are layered surface (LS), red sand (RS), 7400, northeast corner (NEC), and pipeline (P). The widths of the bars in Figure 1 indicate, qualitatively, the relative increase or decrease in proportions of the various minerals as estimated from the peak intensities on the diffractograms. The shallower field samples (LS, RS, 7400) are characterized by the complete dissolution of carbonates (calcite, dolomite) and the precipitation of two sulfates, jarosite, and gypsum. Gypsum and jarosite were also identified as precipitates in the laboratory permeability column experiment. Although gypsum was present in the uncontacted Lucky Mc sediment, the number of X-ray peaks detected and the major peak intensities for gypsum significantly increased in the contacted samples. This suggests the formation of gypsum in the contacted soils in addition to that present in the uncontacted Lucky Mc sediment. Moreover, the X-ray diffraction data also indicate gypsum continues to form throughout the depth profile of the Lucky Mc evaporation pond (Figure 1) and throughout the permeability column.

Jarosite, however, is most concentrated in the shallower sediment from the Lucky Mc site (Figure 1, LS sample) where the sediment and tailings solution coexist at low pH (~3.0). The relative proportion of jarosite to the other detected minerals decreases with depth below the evaporation pond as the soil pH increases to 5.0 (7400 sample). Jarosite was not detected in deeper samples where the soil pH was > 5.0. A similar trend was noted in the column experiments (Peterson et al. 1982) in which jarosite was identified only in the two sections of soil nearest the influent end of the column.

The silicate minerals smectite, illite, kaolinite, quartz and feldspar are present in both the uncontacted Lucky Mc and Morton Ranch soils and are also identified in all of the contacted samples. This suggests the silicate minerals in the two sediments were not dissolved to a large extent, when reacted with acidic tailings solutions over the time frame of the laboratory experiment (838 days) and operation of the evaporation pond at the Lucky Mc mill (10 yr). The dissolution of carbonates and precipitation of secondary sulfate minerals (gypsum and jarosite), however, are the dominant processes occurring in the sediments contacting acidic tailings solutions. The general agreement between the mineralogical data from the laboratory and field results implies that field processes can be successfully simulated in the laboratory.

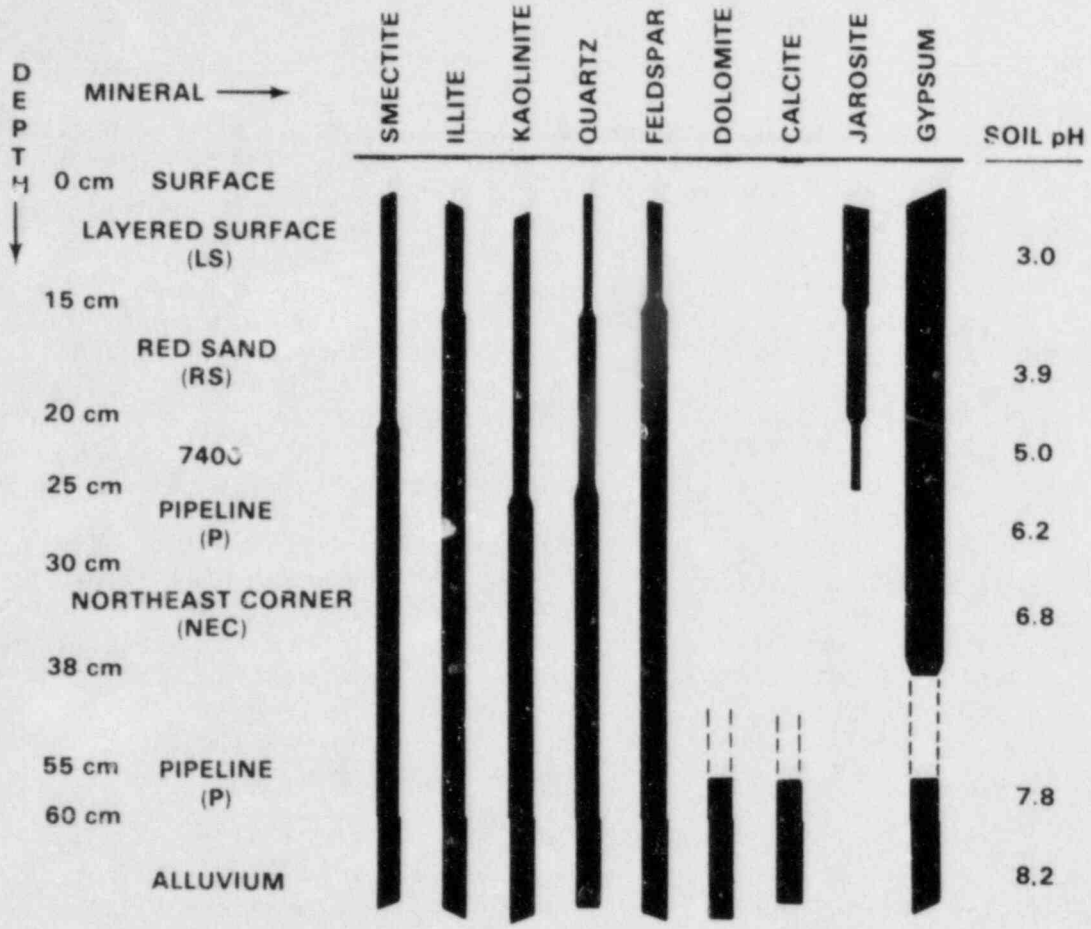

FIGURE 1. Mineralogical and Soil pH Profile as a Function of Depth Beneath Evaporation Pond, Lucky Mc Site, Gas Hills, Wyoming

Geochemical Modeling

The solubility controls calculated using the MINTEQ code for effluent solutions from the permeability column are in good agreement with solid phases identified by X-ray diffraction analysis (Peterson et al. 1982). Ion speciation and solubility calculations indicated that the effluent solutions were in apparent equilibrium with the solid phases $Fe(OH)_3(A)$, $Al(OH)_3(A)$, celestite ($SrSO_4$), anglesite ($PbSO_4$), gypsum, and alunite [$KAl_3(SO_4)_2(OH)_6$]. Thus, the modeling results suggest that these solids could be precipitating and/or dissolving rapidly enough to control the concentrations of certain of their dissolved components.

The geochemical computer code computed all column effluent solutions, resulting from the interaction of H.M. tailings solution with the sediments to be oversaturated with respect to K-, Na-, and H-jarosites [$KFe_3(SO_4)_2(OH)_6$, $NaFe_3(SO_4)_2(OH)_6$, $HFe_3(SO_4)_2(OH)_6$, respectively]. These

ion-speciation solubility calculations indicate the possibility of jarosite precipitation in these columns, though the attainment of equilibrium appears to be inhibited by kinetic and/or other constraints.

These results illustrate how geochemical modeling can be used, in parallel with mineralogical characterization techniques performed on laboratory and field samples, to identify the chemical reactions that are occurring in the uranium mill tailings/sediment system. The identification of jarosite and gypsum confirm the geochemical modeling predictions that these minerals formed when uranium mill tailings solutions contacted these sediments. In addition, modeling predicted the precipitation of several solids that could not be identified by X-ray diffraction because of the amorphous nature of some of these solids or the limited amount of material that precipitated.

A conclusion drawn from the first phase of our work is that the geochemical modeling predictions and laboratory experiments were capable of simulating mineralogical changes that occurred in the field. Thus, the theoretical modeling predictions, laboratory experimental work, and field studies are complementary.

5.6.4.2 Phase 2: Comparisons of Column Effluent Compositions with Model Predictions

To accomplish the objectives of phase two of our study, a conceptual chemical model was formulated to represent the passage of reacting incremental pore volumes of tailings solution through the sediments. The predicted concentrations of contaminants were then compared to the experimental data at each pore volume. Results will be discussed for aluminum, manganese and calcium to demonstrate the utility of this approach for our system. In the results presented here, the pH and Eh were fixed at the observed values for each pore volume. Additional modeling results are discussed in Peterson et al. (1983).

Aluminum

Three aluminum solids (Table 3) were considered in the chemical model of the system: amorphous aluminum hydroxide [$Al(OH)_3$(A)], amorphous basaluminite [$Al_4(SO_4)(H_2O)_{5}H_2O$(A)], and jurbanite ($AlOHSO_4 \cdot 5H_2O$). The predicted aluminum concentrations [moles/ℓ, molarity (M)] obtained by using these solids as solubility controls for aluminum are represented by the square symbols in Figure 2. The predicted aluminum concentrations closely follow the experimental concentrations (triangle symbols) in the first five pore volumes having high pH values but do not show the large increase in aluminum concentrations observed in the latter pore volumes for the experimental system. One explanation for the depressed values of the predicted aluminum concentrations in the latter pore volumes is due to the calculated precipitation of jurbanite. Jurbanite is the most thermodynamically stable solid phase (of the three considered) at these latter pore volumes, but could not be precipitating at a sufficient rate to significantly affect the concentration of dissolved aluminum.

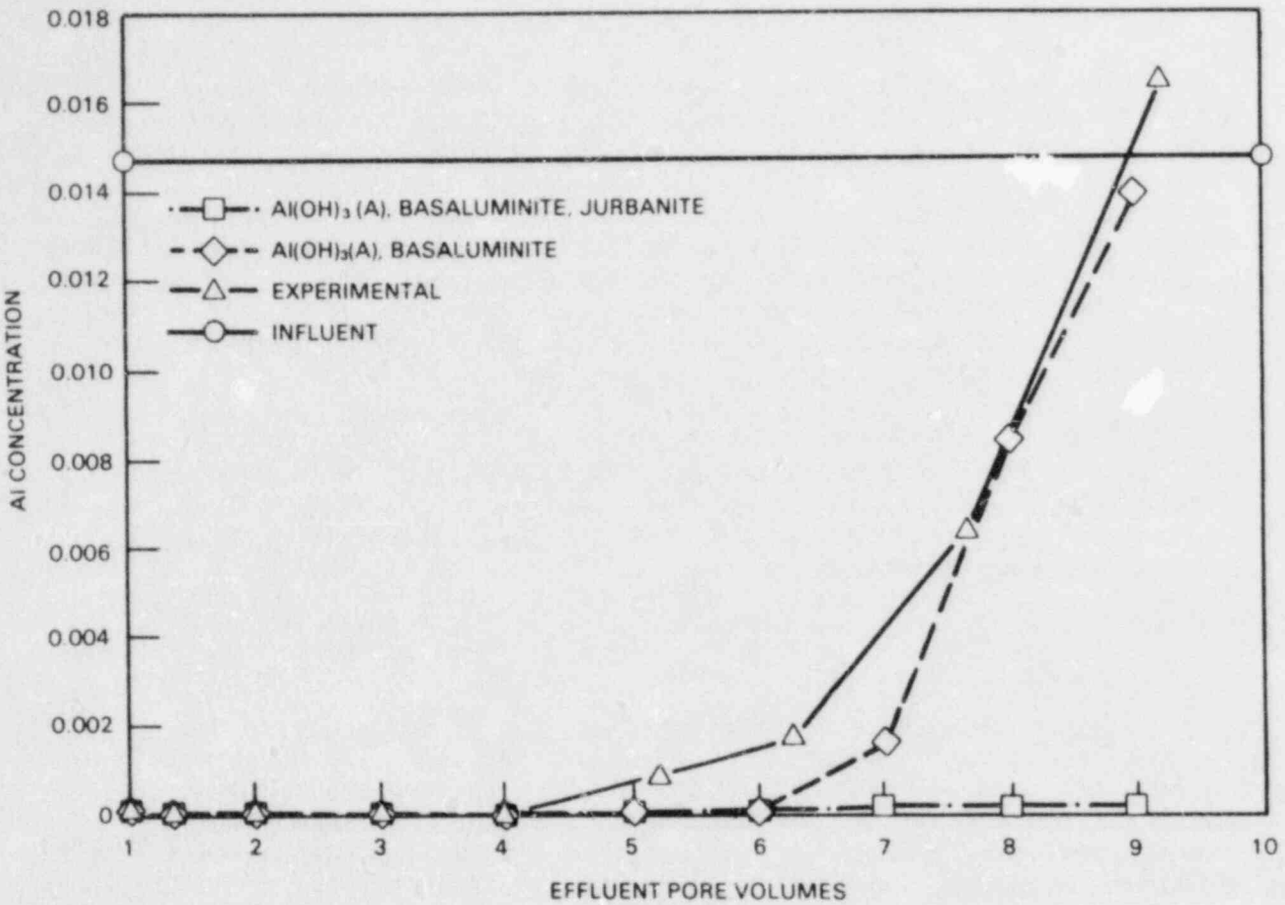

FIGURE 2. Predicted and Experimental Aqueous Aluminum Concentrations (M) with Measured pH and Eh Values

Therefore, jurbanite was excluded from our second chemical model of the aluminum system because of possible kinetic constraints. The second aluminum model contained only amorphous aluminum hydroxide and amorphous basaluminite as potential solubility controls for the dissolved aluminum concentrations. In these modeling results, amorphous aluminum hydroxide precipitates in the first pore volume and basaluminite precipitates in pore volumes 2 through 9. The predicted aluminum concentrations are extremely close to the experimental results. Thus, a chemical model consisting of amorphous aluminum hydroxide and amorphous basaluminite provides an accurate model of the experimentally observed aluminum concentrations for the tailings solution/sediment system. Formation of amorphous basaluminite is supported by Nordstrom (1982), who concluded that amorphous basaluminite is likely to precipitate from acid sulfate solutions and may persist for long periods of time.

Manganese

Predicted versus experimental manganese concentrations are shown in Figure 3. Rhodochrosite was the only manganese solid predicted to precipitate of those manganese solids considered in the chemical model (see Table 3). In the chemical model, rhodochrosite precipitated in the first three pore volumes, began to dissolve at pore volume four, and completely redissolved at pore volume five. After the fifth pore volume, predicted manganese concentrations fell to the influent values. The experimental values show the same general trends as the predicted values, i.e., lower concentrations than the influent values at early pore volumes, higher than influent values at intermediate pore volumes, and concentrations that decrease towards the influent values at latter pore volumes.

Therefore, a chemical model that included the precipitation and dissolution of rhodochrosite, was able to predict the manganese concentration trends that were observed in the experimental data. The predicted manganese concentrations, however, did not exactly match the observed effluent curve.

Calcium

The chemical model included calcite and gypsum as possible solubility controls for calcium.

The predicted and experimental concentrations of calcium are shown in Figure 4. The predicted calcium concentrations are always less than the experimental concentrations; this is exactly opposite of the pattern predicted for sulfate concentrations. In the first pore volume, the predicted calcium concentration is 0.01 molar lower than the experimental value, and the predicted sulfate concentration approximately 0.01 molar higher than the experimental value. Thus, in both cases, the activity product of gypsum is being satisfied. Ion exchange or desorption of calcium from the sediments would not increase the predicted aqueous calcium concentration because the calcium released from the sediments would precipitate as calcite and gypsum in the chemical model.

Another possible explanation for the differences between the modeling and experimental systems is that the calcium carbonate phase actually present in the sediments was more soluble than end-member calcite. The high magnesium concentrations in the column effluents suggest the possible presence of a magnesium-substituted calcite. Magnesian calcites have a greater solubility than pure calcium carbonates (Thorstenson and Plummer 1977). The substitution of a magnesian calcite, for a pure end-member calcite, into the chemical model allowed us to predict the initial high concentrations of calcium that were observed in the experimental system. The dissolution of dolomite has been considered in other modeling studies of these systems (Peterson et al. 1983). The calcium-sulfate system demonstrates the ability of geochemical modeling to test the adequacy of proposed mechanisms and to suggest additional plausible mechanisms.

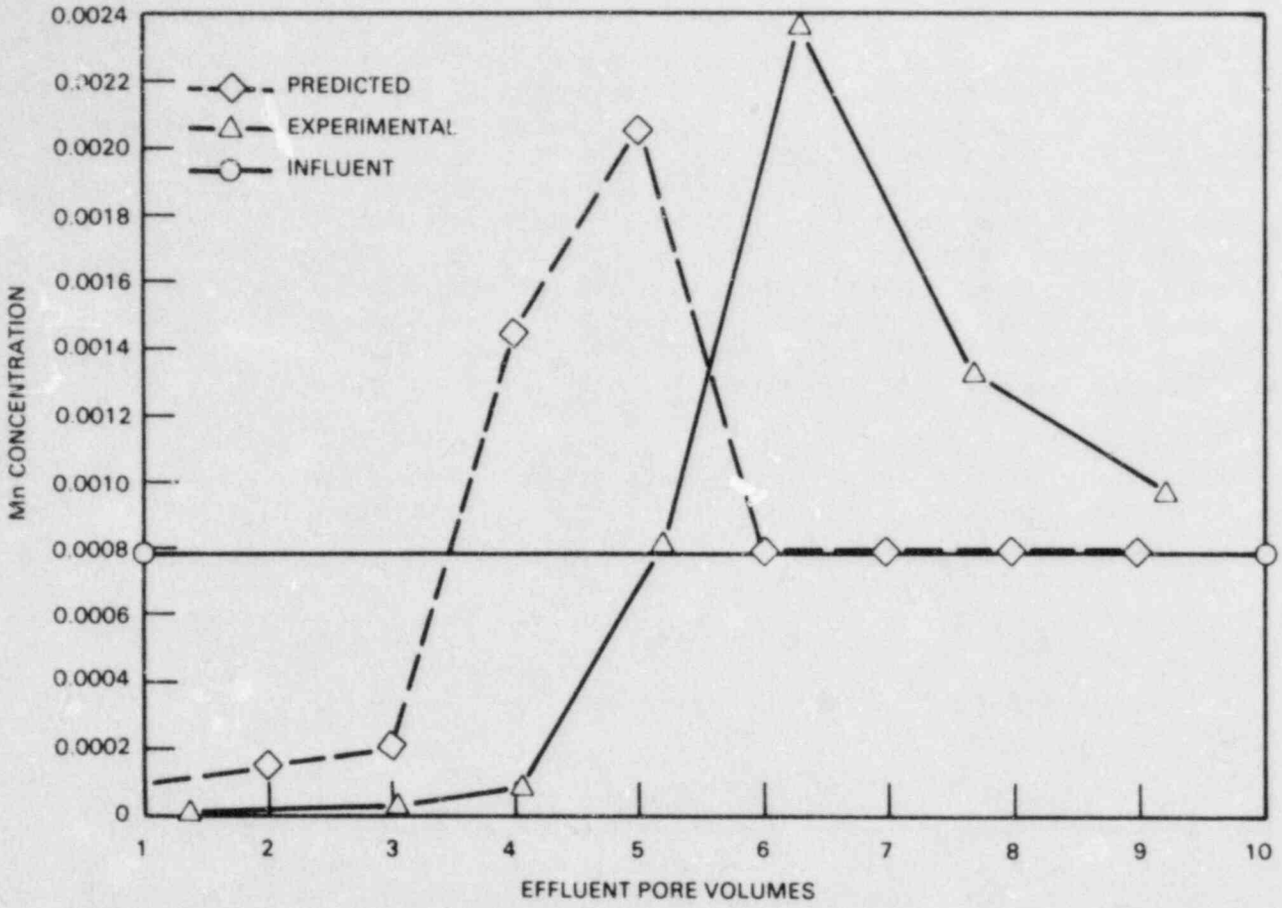

FIGURE 3. Predicted and Experimental Manganese Concentrations (M) with Measured pH and Eh

5.6.5 CONCLUSIONS

Decreases in permeability noted in permeability columns were partially attributed to the precipitation of solid phases which plugged the pores of sediments. Geochemical modeling predicts, and X-ray characterization confirms, that precipitation of solids from solution is occurring in the acidic tailings solution and sediment interactions studied. X-ray diffraction identified gypsum and an alunite-group mineral, such as jarosite, as having precipitated after acidic tailings solutions reacted with clay liners and sediments. Geochemical modeling predicted that these same phases should be precipitating, along with several amorphous solids not identifiable by X-ray diffraction. The same mineralogical changes observed in the laboratory sediment columns were found at a drained evaporation pond with a 10-year history of acid attack. The observed minerals were also predicted, from geochemical (thermodynamic) modeling, to form upon neutralization of the acidic tailings solutions by the contacted

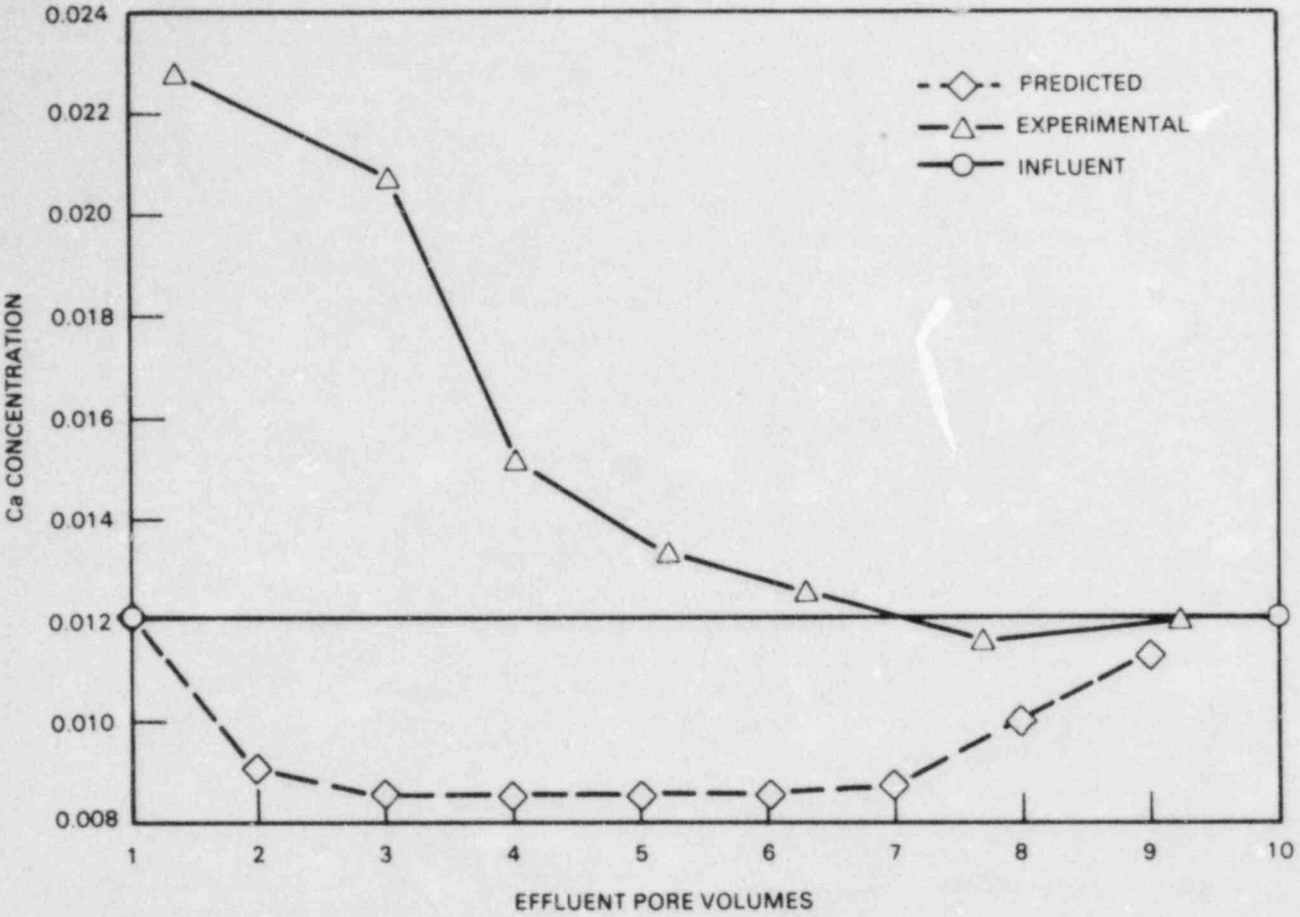

FIGURE 4. Predicted and Experimental Aqueous Calcium Concentrations (M) with Measured pH and Eh Values

sediments. This approach illustrates how geochemical modeling can be used, in parallel with mineralogical characterization techniques performed on laboratory and field studies, to delineate the chemical reactions that may change the permeability of liner materials.

Aqueous/sediment interactions are extremely complex. Predictive geochemical modeling was effective in unraveling some of the predominant mechanisms controlling the concentrations of certain dissolved constituents. The geochemical modeling can be used to quantitatively evaluate: 1) the accuracy of theorized chemical models of complex aqueous/sediment interactions, and 2) the predominant reactions affecting the composition of the aqueous phase.

The precipitation/dissolution reactions considered in the conceptual model were capable of predicting the column effluent concentrations of several major constituents in the tailings solutions (e.g., SO_4, Ca, Al, Mn, and Fe; Peterson et al. 1983). Sulfate concentrations in the column effluents were generally one to two orders of magnitude above the secondary

drinking water standards established by the U.S. Environmental Protection Agency. The conceptual model was able to predict these elevated concentrations. No solubility controls, however, were identified for the majority of the trace constituents. Many trace constituents appear to be controlled by adsorption on and/or coprecipitation with ferric oxyhydroxide solids (Serne et al. 1983). More work, namely incorporation of trace metal adsorption reactions, is necessary to predict the migration of other contaminants from uranium mill tailings solution. The geochemical modeling approach coupled with laboratory and field studies should be applicable to a variety of waste disposal problems.

5.6.6 RECOMMENDATIONS AND PLANNED RESEARCH

Additional characterization of sediments using techniques such as electron microprobe analysis, X-ray fluorescence and scanning electron microscopy needs to be completed on the field samples that were collected at the Pathfinder (Lucky Mc) evaporation pond. The soil profiles have already been characterized by X-ray diffraction and by radionuclide counting procedures to develop a profile of the mineralogy and radionuclide content with depth. Only crystalline minerals comprising approximately 5% or more of the sediments are capable of being identified by X-ray diffraction. The results to date have agreed with modeling predictions based on thermodynamic considerations and with laboratory experiments. The additional characterization techniques would: 1) allow trace element profiles to be identified, and 2) provide insight into how and with what minerals and solid phases the trace elements tend to be associated. These characterization techniques could also potentially identify precipitated solid phases (e.g., amorphous phases) that could not be identified by X-ray diffraction. This would allow further corroboration of the laboratory and geochemical modeling predictions and provide additional insight into the ability of our laboratory and modeling tools tc predict chemical reactions that will occur in the sediments at the field sites.

The conceptual model was unsatisfactory when used to predict the concentrations of selected trace elements (Peterson et al. 1983). Generally, the column effluent solutions were undersaturated relative to trace-element solid phases in the MINTEQ thermodynamic data base. Data developed through laboratory and field studies lead us to believe that we can empirically quantify the migration of trace elements though we were unable to make satisfactory predictions based on this initial attempt at developing a theoretical construct. The concentrations of many trace elements (e.g., Se, As, Mo, and Cd) appear to be controlled by adsorption on and/or coprecipitation with ferric oxyhydroxide solids. Several adsorption models of the hydrous oxide water surface have been formulated (Davis and Leckie 1978, Hohl and Stumm 1976) and have shown considerable success in modeling the adsorption of trace metals onto hydrous oxides. In addition, stability constants for the reaction of several trace metals with iron oxyhydroxides have also been published in the literature (Davis and Leckie 1978, Leckie et al. 1980, Balistrieri and Murray 1982). Thus, it appears that the chemical model presented here, which can estimate the mass of precipitated

iron oxyhydroxide by means of our solid phase assemblage, can be expanded to predict the adsorption of several trace metals onto the surface of iron oxyhydroxides. These thermodynamic adsorption constants could be utilized over a wide range of environmental conditions unlike empirical Kd's that are often measured for specific combinations of groundwater/sediment conditions.

5.6.7 ACKNOWLEDGEMENTS

This study was funded by the U.S. Nuclear Regulatory Commission as part of the Uranium Recovery Research Program at Pacific Northwest Laboratory. We wish to thank M. E. Dodson, A. W. Lautensleger, W. J. Martin, M. J. Mason, B. E. Opitz, D. E. Rinehart, D. R. Sherwood and J. M. Tingey (all of the Pacific Northwest Laboratory) for their help in performing the necessary experiments, collecting field samples and analyzing the sediments and tailings solutions. Special thanks are given to G. F. Birchard, NRC Office of Research, Waste Management Branch in Silver Spring, Maryland, for the guidance and encouragement that he has provided over the duration of this project.

5.6.8 REFERENCES

Balistrieri, L. S., and J. W. Murray. 1982. "The Adsorption of Cu, Pb, Zn, and Cd on Goethite from Major Ion Seawater." Geochimica et Cosmochimica Acta 46:1253-1265.

Ball, J. W., D. K. Nordstrom and E. A. Jenne. 1980. Additional and Revised Thermochemical Data and Computer Code for WATEQ2 - A Computerized Chemical Model for Trace and Major Element Speciation and Mineral Equilibria of Natural Waters. U.S. Geologic Survey, Water Resources Investigations WRI-78-116, 109 pp.

Ball, J. W., E. A. Jenne and M. W. Cantrell. 1981. WATEQ3: A Geochemical Model with Uranium Added. U.S. Geol. Survey, Open File Report 81-1183.

Black, C. A. 1965a. Methods of Soil Analysis. Part 1. Physical and Mineralogical Properties Including Statistics of Measurement and Sampling. American Society of Agronomy, Monograph 9.

Black, C. A. 1965b. Methods of Soil Analysis. Part 2. Chemical and Microbiological Properties. American Society of Agronomy, Monograph 9.

Brown, J. R., W. S. Fyfe, F. Murray and B. I. Kronberg. 1981. "Immobilization of U-Th-Ra in Mine Wastes." Can. Min. J., 102(3):71-76.

Crim, R. G., T. A. Shepherd and J. D. Nelson. 1979. "Stability of Natural Clay Liners in a Low pH Environment," Proceedings of the Second Symposium on Uranium Mill Tailings Management. Civil Engr. Dept. Colo. State Univ., Ft. Collins, Colorado, p. 41-53.

Cunningham, R. E. 1978. "Issues on Management, Stabilization and Environmental Impacts of Uranium Mill Tailings." In Proceedings of the OECD-NEA Seminar on Management, Stabilization and Environmental Impact of Uranium Mill Tailings, pp. 13-17, OECD, Paris.

Davies, C. W. 1962. Ion Association. Bitterworths Pub., Washington D.C., 190 pp.

Davis, J. A., and J. O. Leckie. 1978. "Surface Ionization and Complexation at the Oxide/Water Interface: II. Surface Properties of Amorphous Iron Oxyhyroxide and Adsorption of Metal Ions." J. Colloid Interface Sci., 67:90-107.

Deustch, W. J., E. A. Jenne and K. M. Krupka. 1982. "Solubility Equilibria in Basalt Aquifers: The Columbia Plateau, Eastern Washington, U.S.A. Chemical Geology 36:15-34.

Erikson, R. L., and D. R. Sherwood. 1982. "Interaction of Acidic Leachate with Soil Materials at Lucky Mc Pathfinder Mill, Gas Hills, Wyoming." Proceedings of the Fifth Symposium on Uranium Mill Tailings Management. Civil Engr. Dept. Colorado State University, Ft. Collins, Colorado, p. 335-351.

Felmy, A. R., D. C. Girvin and E. A. Jenne. 1983. MINTEQ: A Computer Program for Calculating Aqueous Geochemical Equilibria, Final Project Report Under EPA Contract 68-03-3089.

Gang, M. W., and D. Langmuir. 1974. "Controls on Heavy Metals in Surface and Ground Waters Affected by Coal Mine Drainage: Clarion River - Redbank Creek Watershed, Pennsylvania." In Proceedings of Fifth Symposium on Mine Drainage Research, pp. 39-63. Coal and the Environment Technical Conference, October 22-24.

Gee, G. W., A. C. Campbell, D. R. Sherwood, R. G. Strickert and S. J. Phillips. 1980a. Interaction of Uranium Mill Tailings Leachate with Soils and Clay Liners. NUREG/CR-1494. National Technical Information Service, Springfield, Virginia.

Gee, G. W., A. C. Campbell, B. E. Opitz and D. R. Sherwood. 1980b. "Interaction of Uranium Mill Tailings Leachate with Morton Ranch Liner and Soil Material," Proceedings of the Third Symposium on Uranium Mill Tailings Management. Civil Engr. Dept. Colorado State University, Ft. Collins, Collorado, p. 333-352.

Kohl, H., and W. Stumm. 1976. "Interaction of Pb^{2+} with Hydrous γ-Al_2O_3." J. Colloid Interface Sci. 55(2):281-288.

Jackson, M. L. 1956. Soil Chemical Analysis--Advanced Course. Published by the author, Dept. of Soils, Univ. of Wis., Madison, Wisconsin.

Jackson, M. L. 1979. Soil Chemical Analysis--Advanced Course. 2nd Edition, 11th Printing. Published by the Author, Madison, Wisconsin.

Jenne, E. A. (Ed.). 1979. Chemical Modeling in Aqueous Systems - Speciation, Sorption, Solubility, and Kinetics. ACS Symposium Series 93, American Chemical Society, Washington, D.C.

Jenne, E. A. 1981. Geochemical Modeling: A Review. PNL-3574, Pacific Northwest Laboratory, Richland, Washington.

Johnson, K. S. 1982. "Solubility of Rhodochrosite ($MnCO_3$) in Water and Seawater." Geochimica et Cosmochimica Acta 46:1805-1809.

Krupka, K. M., and E. A. Jenne. 1982. WATEQ3 Geochemical Model: Thermodynamic Data for Several Additional Solids. PNL-4276, Pacific Northwest Laboratory, Richland, Washington.

Langmuir, D., and A. C. Riese. 1981. "Geochemical Modelling of Radionuclides and Chemical Species Transport in Subsurface Waters: Application to Uranium Mill Tailings," p. A-34, Canadian Geological Meeting, Calgary, Maryland.

Leckie, J. O., M. M. Benjamin, K. Hayes, G. Kaufman, and S. Altman. 1980. Adsorption/Coprecipitation of Trace Elements from Water with Iron Oxyhydroxide. EPRI CS-1513 Project 910-1. Edison Power Research Institute, Palo Alto, California.

Mercer, J. W., C. R. Faust, W. J. Miller and F. J. Pearson, Jr. 1981. Review of Simulation Techniques for Aquifer Thermal Energy Storage (ATES). PNL-3769, Prepared by Geotrans, Inc. (Herndon, VA) and INTERA Environmental Consultants, Inc. (Houston, TX) for Pacific Northwest Laboratory, Richland, Washington.

Mineral Resources Waste Management Team, University of Idaho. 1980. Overview of Ground Water Contamination Associated with Six Operating Uranium Mills in the U.S., University of Idaho, Moscow, Idaho.

Nordstrom, D. K., E. A. Jenne and J. W. Ball. 1979. "Redox Equilibria of Iron in Acid Mine Waters." In Chemical Modeling in Aqueous Systems. E. A. Jenne (ed.), ACS Symposium Series No. 93:51-79.

Nordstrom, D. K. 1982. "The Effect of Sulfate on Aluminum Concentrations in Natural Waters: Some Stability Relations in the System Al_2O_3-SO_3-H_2O at 298 K." Geochimica et Cosmochimica Acta 46:681-692.

Oak Ridge National Laboratory. 1983. Spent Fuel and Radioactive Waste Inventories, Projections, and Characteristics. DOE/NE-0017/2. NTIS Springfield, VA.

Parkhurst, D. L., D. C. Thorstenson and L. N. Plummer. 1980. PHREEQE - A Computer Program for Geochemical Calculations. U.S. Geological Survey, Water Resources Investigations 80-96, 210 pp.

Peterson, S. R., and K. M. Krupka. 1981. "Contact of Clay Liner Materials with Acidic Tailings Solution. II. Geochemical Modeling." Proceedings of the Fourth Symposium on Uranium Mill Tailings Management, Civil Engr. Dept., Colorado State University, Ft. Collins, Colorado, p. 609-626.

Peterson, S. R., R. L. Erikson, and G. W. Gee. 1982. The Long Term Stability of Earthen Materials in Contact with Acidic Tailings Solutions. NUREG/CR-2946 (PNL-4463), Pacific Northwest Laboratory, Richland, Washington.

Peterson, S. R., A. R. Felmy, R. J. Serne and G. W. Gee. 1983. Predictive Geochemical Modeling of Interactions Between Uranium Mill Tailings Solutions and Sediments in a Flow-Through System: Model Formulations and Preliminary Results. NUREG/CR-4782 (PNL-4782), Pacific Northwest Laboratory, Richland, Washington.

Plummer, L. N., and E. Busenberg. 1982. "The Solubilities of Calcite, Aragonite and Vaterite in CO_2-H_2O Solutions Between 0 and 90°C, and an Evaluation of the Aqueous Model for the System $CaCO_3$-CO_2-H_2O." Geochimica et Cosmochimica Acta 46:1011-1040.

Relyea, J. F., and W. J. Martin. 1982. "Evaluation Inactive Uranium Mill Tailings Sites for Liner Requirements: Characterization and Interaction of Tailings, Soil and Liner Materials." Proceedings of the Fifth Symposium on Uranium Mill Tailings Management. Civil Engr. Dept., Colorado State University, Ft. Collins, Colorado, p. 507-519.

Serne, R. J., S. R. Peterson and G. W. Gee. 1983. Laboratory Measurements of Contaminant Attenuation of Uranium Mill Tailings Leachates by Sediments and Clay Liners. NUREG/CR-3124 (PNL-4605), Pacific Northwest Laboratory, Richland, Washington.

Thorstenson, D. C., and L. N. Plummer. 1977. "Equilibrium Criteria for Two-Component Solids Reacting with Fixed Composition in an Aqueous Phase-Example: The Magnesian Calcites." Amer. J. Sci. 277:1203-1223.

Truesdell, A. H., and B. F. Jones. 1974. "WATEQ, A Computer Program for Calculating Chemical Equilibria of Natural Waters." U.S. Geol. Survey J. Res. 2:233-248.

U.S. Nuclear Regulatory Commission (U.S.NRC). 1977. Final Environmental Statement Related to Operation of Lucky Mc Gas Hills Uranium Mill. NUREG-0357, National Technical Information Service, Springfield, Virginia.

Uziemblo, N. H., R. L. Erikson and G. W. Gee. 1981. "Contact of Clay Liner Materials with Acidic Tailings Solution. I. Mineral Chacterization." Proceedings of the Fourth Symposium on Uranium Mill Tailings Management. Civil Engr. Dept., Colorado State University, Ft. Collins, Colorado, p. 597-608.

Westall, J. C., J. L. Zachary and F. M. M. Morel. 1976. "MINEQL: A Computer Program for the Calculation of Chemical Equilibrium Composition of Aqueous Systems." Tech. Note 18, Dept. of Civil Engineering, Massachusetts Institute of Technology, Cambridge, Massachusetts.

NRC FORM 335 (6 83)

U S NUCLEAR REGULATORY COMMISSION

BIBLIOGRAPHIC DATA SHEET

1 REPORT NUMBER (Assigned by TIDC, add Vol No., if any)

NUREG/CP-0052

2 Leave blank

3 TITLE AND SUBTITLE

NRC Nuclear Waste Management Geochemistry '83

4 RECIPIENT'S ACCESSION NUMBER

5 DATE REPORT COMPLETED

MONTH: April | YEAR: 1984

6 AUTHOR(S)

D.H. Alexander and G.F. Birchard, Editors

7 DATE REPORT ISSUED

MONTH: May | YEAR: 1984

8 PERFORMING ORGANIZATION NAME AND MAILING ADDRESS (Include Zip Code)

Division of Health, Siting and Waste Management
Office of Nuclear Regulatory Research
U.S. Nuclear Regulatory Commission
Washington, D.C. 20555

9 PROJECT/TASK/WORK UNIT NUMBER

10 FIN NUMBER

11 SPONSORING ORGANIZATION NAME AND MAILING ADDRESS (Include Zip Code)

Division of Health, Siting and Waste Management
Office of Nuclear Regulatory Research
U. S. Nuclear REgulatory Commission
Washington, D. C. 20555

12a TYPE OF REPORT

Conference Proceedings

12b PERIOD COVERED (Inclusive dates)

August 30 - 31, 1983

13 SUPPLEMENTARY NOTES

14 ABSTRACT (200 words or less)

This document summarizes papers and panel discussions presented at the Office of Nuclear Regulatory Research sponsored conference on "Nuclear Waste Management Research on Geochemistry of HLW Disposal". The conference was held at the United States Geological Federal Center in Reston, Virginia on August 30-31, 1983. The purpose of the meeting was to present results from NRC sponsored research and to identify regulatory research issues which need to be addressed prior to licensing a high level waste repository. Important summaries of technical issues and recommendations are included with each paper. The issues reflect areas of technical uncertainty addressed by the NRC Research program in geochemistry. The objectives of the NRC Research Program in geochemistry are to provide a technical basis for waste management rulemaking, to provide the NRC Waste Management Licensing Office with information that can be used to support sound licensing decisions, and to identify investigations that need to be conducted by DOE to support a license application.

15a KEY WORDS AND DOCUMENT ANALYSIS

15b DESCRIPTORS

16 AVAILABILITY STATEMENT

Unlimited

17 SECURITY CLASSIFICATION (This report)

Unclassified

18 NUMBER OF PAGES

19 SECURITY CLASSIFICATION (This page)

Unclassified

20 PRICE

$

UNITED STATES
NUCLEAR REGULATORY COMMISSION
WASHINGTON, D.C. 20555

OFFICIAL BUSINESS
PENALTY FOR PRIVATE USE, $300

FOURTH-CLASS MAIL
POSTAGE & FEES PAID
USNRC
WASH. D.C.
PERMIT No. G-67